UNIVERSITÁ DEGLI STUDI DI ROMA "LA SAPIENZA"

Dipartimento di Chimica e Tecnologie del Farmaco

PhD program in Molecular Design and Characterization for the Promotion of Health and Well-being: From Drug to Food

XXXVII cycle

Synthesis of biologically important heterocyclic compounds via transition metal-catalyzed and SuFEx click reactions

PhD Student:

Karim Ullah

Tutor:

Prof. Giancarlo Fabrizi

Triennio 2021/2024

Table of Contents

Acknowledgment

Firstly, I would like to extend my heartfelt appreciation to my supervisor, **Prof. Giancarlo Fabrizi**, for giving me the opportunity to pursue a Ph.D. in his research group. I am deeply grateful for all the skills and knowledge I have gained under your supervision. Thank you for your encouragement, support, and enthusiasm over the last three years. I am also extremely grateful to the **Sapienza University of Rome** for providing the funding for my Ph.D.

I am also deeply grateful to **Prof. Antonella Goggiamani** and **Dr. Antonia Iazzetti** for their invaluable advice and assistance during the experimental work. Your insights and support have been instrumental in the successful completion of my research. Thank you for your guidance and for always being willing to help.

I am profoundly indebted to **Prof. Wim M. De Borggraeve** for the opportunity to conduct research in his research group, MoldesignS, during six-month research stay. The skills, knowledge, and experience gained during my time at KU Leuven have been invaluable. Thank you for your encouragement and support during the stay at KU Leuven. I am also grateful to **KU Leuven** for hosting me as a visiting researcher and for the support provided throughout my stay.

A special thanks to all past and present members of our research group, including Dr. Andrea Fochetti, Dr. Andrea Serraiocco, Dr. Federico Marrone, Dr. Francesco Cairone, Dario Allevi, Stefano Dessalvi, Daniele Brighenti, Elisa Verdiglione, Roberta Zoppoli, Riccardo Donato, Luca Palazzo, Yuri Gazzilli, Andrea Serrafini, Flavia Borrelli, and Marzia Patta. Your support and collaboration have been greatly appreciated over these three years.

I would like to extend my special thanks to **Dr. Joachim Demaerel** and **Armir Zogu** for their invaluable assistance and encouragement with my experimental work during the stay at KU Leuven. Additionally, I am grateful to my colleagues at MoldesignS: Reza Kordnezhadian, Lauren Voets, Qingqing You, Kexin Su, Stefanos Spanopoulos, Eva Daenens, Julia Wens, Carlotta Borgarelli, and Tim Balcaen. Your support and camaraderie made my time at KU Leuven both rewarding and enjoyable.

Finally, I wish to express my deepest gratitude to my family for their unwavering support and encouragement throughout this journey. **To my parents**, your love, sacrifices, and belief in me have been the cornerstone of my success. Your constant support has provided me with the strength and motivation to persevere through the challenges of this Ph.D. study. **To my siblings**,

your encouragement and understanding have been invaluable. Thank you for being my steadfast support system and for sharing this accomplishment with me.

“Reactivity isn’t everything; it's the only thing”

K. B. Sharpless

Summary

Heterocyclic compounds are a highly important class of organic compounds due to their large number of applications in pharmaceuticals, biology, agrochemicals, industry, biotechnology, and material chemistry. The synthesis of heterocyclic compounds has always been a fundamental topic for chemistry research. Among them, indoles, benzofurans, quinolines, azepines and triazoles play a major role since they are part of many natural products and biologically active compounds. Indeed, recent studies have confirmed the involvement of molecules containing these structural motifs in a diverse array of biological processes, thereby exerting modulatory effects on various cellular actions. In this context, the primary goal of organic and medicinal chemists is to develop novel synthetic strategies for accessing challenging structures and small heterocycles. Among the many known chemical processes, organometallic catalysis, in particular that mediated by palladium, copper and sulfur-fluorine exchange (SuFEx) reactions occupy a place of absolute importance for the following reasons. Palladium (Pd) catalysis represented a huge leap forward in heterocycle chemistry, paving the way toward a variety of compounds, once inaccessible. CuAAC reaction introduced the regioselective synthesis of 1,4-disubstituted 1,2,3-triazole under mild reaction conditions. SuFEx chemistry enables the efficient and selective formation of S–F bonds under mild conditions, facilitating the synthesis of diverse sulfur-containing compounds with high functional group compatibility.

Integrating these synthetic approaches enhances the efficiency and diversity to synthesize biologically relevant compounds. For instance, Pd-catalyzed cross-coupling reactions and C–H or C–X activation can introduce key functional groups, while click chemistry can modularly connect molecular scaffolds. SuFEx chemistry can establish specific functionalities or modify existing groups selectively. Overall, the combination of Pd-catalyzed, click, and SuFEx chemistry provides a powerful toolkit for the synthesis of biologically important moieties, enabling the rapid and efficient generation of diverse chemical libraries for drug discovery and development.

This PhD thesis investigates the synthesis of biologically significant heterocycles, focusing on these advanced methodologies as primary strategies. The research aims to elucidate their utility and efficacy in creating heterocyclic compounds with potential biological relevance, contributing to synthetic chemistry's advancement and novel compound development for drug discovery and biomedical applications.

Chapter 1 provides an overview of catalytic reactions, including Pd-catalyzed cross-coupling, C–H activation, and CuAAC, introducing SuFEx as an innovative synthetic methodology.

Chapter 2 outlines the primary objective of synthesizing biologically significant heterocycles through transition-metal catalyzed reactions, click chemistry, exploring novel SuFEx hubs and their applications.

Chapter 3-5 focus on synthesizing heterocyclic fused 1,2,3-triazoles using click chemistry and Pd-catalyzed intramolecular C–H activation, demonstrating efficient methodologies for building these compounds.

Chapter 6 presents novel approaches for synthesizing azepine- and oxepine-fused 1,2,3-triazoles *via* sequential click chemistry and Pd-catalyzed annulation, highlighting high yields and broad functional group tolerance.

Chapter 7 provides a gold-catalyzed protocol to obtain functionalized 3*H*-pyrrolo [1,2,3-*de*] quinoxalines from suitable substituted *N*-alkynyl indoles. The mild reaction conditions were revealed to be compatible with different functional groups, including halogen, alkoxyl, cyano, ketone, and ester, allowing the isolation of title compounds with yields from good to high. A reaction mechanism has been proposed, and theoretical calculations have been provided to rationalize the final step of the hypothesized reaction mechanism.

Chapter 8 presents a straightforward assembly of polysubstituted 1,2-dihydro-3*H*-pyrrolo[1,2-*a*]indol-3-ones through a domino Pd-catalyzed reaction of indol-2-ylmethyl acetates with 1,3-dicarbonyl derivatives. The key role of the features of the 1,3-dicarbonyls on the reaction outcome has been explored. The employment of 2-methylcyclohexan-1,3-dione as the dicarbonyl source could allow further challenging indole nucleus functionalization.

Chapter 9 is about the synthesis of silver pentafluorooxosulfate ($AgOSF_5$) as a viable SuFEx hub with reactivity equal to SOF_4. The AgF_2-mediated oxidation of $SOCl_2$ gives rise to the hexacoordinate $AgOSF_5$ adduct, which in contact with primary amines produces sulfurimidoyl fluorides in high yields. In addition, this workflow is fully extendable to the trifluoromethyl homologue, $AgOSF_4CF_3$, and we propose the use of $AgOSF_4X$ salts as a general route to azasulfur SuFEx electrophiles from commercial starting materials.

Chapter 10 presents a new method for the facile preparation of aryl–IF_4 compounds using KF and ex situ generated chlorine gas within a two-chamber reactor setup. Notably, the process

stands out for its simplicity by omitting the use of specialized equipment and generating less chemical waste than the previously reported works. While demonstrating high efficiency at room temperature, the novel approach provides access to a diverse array of products with moderate to excellent yields.

List of Abbreviations

δ	Chemical shift
μ	Dipole moment
1,10-Phen	1,10-Phenanthroline
ABP	Activity-based probe
ABPP	Activity-based protein profiling
AFs	Aryl fluorosulfates
Ar	Aryl
b.p	Boiling point
CuAAC	Copper(I)-catalyzed azide-alkyne cycloaddition
CuI	Copper(I) iodide
CuBr	Copper(I) bromide
CuOAc	Copper(I) acetate
CsOAc	Caesium acetate
d	Doublet in NMR spectroscopy
DCE	1,2-Dichloroethane
DCM	Dichloromethane
dd	Doublet of doublets in NMR spectroscopy
DMF	*N*,*N*-dimethylformamide
DMSO	Dimethyl sulfoxide
DMEDA	*N*,*N'*-Dimethylethylenediamine

equiv.	Equivalents
EtOAc	Ethylacetate
Et_3N	Triethylamine
HRMS	High Resolution-mass spectroscopy
HPLC	High-performance liquid chromatography
IR	Infrared
J	Couplings constant in NMR spectroscopy
K_2CO_3	Potassium carbonate
m	Multiplet in NMR spectroscopy
Me	Methyl
MeCN	Acetonitrile
m.p.	Melting point
MS	Mass Spectrometry
NMR	Nuclear Magnetic Resonance
Nu	Nucleophile
OMe	Methoxyl
Ph	Phenyl
ppm	Parts per million
Pd_2dba_3	Tris(dibenzylideneacetone)dipalladium(0)
$Pd(OAc)_2$	Palladium(II) acetate
$PdCl_2[p(o\text{-}tolyl)_3]_2$	Dichlorobis(tri-o-tolylphosphine)palladium(II)

$PdCl_2(PPh_3)_2$	Palladium(II)bis(triphenylphosphine) dichloride
$Pd(MeCN)_2Cl_2$	Bis(acetonitrile)dichloropalladium(II)
$Pd(dppf)Cl_2$	1,1′-Bis(diphenylphosphino)ferrocene]dichloropalladium(II)
q	Quartet
qd	Quartet of doublets
R_f	Retention factor
rt	Room temperature
SuFEx	Sulfur (VI)-fluoride exchange
t	Triplet
TFA	Trifluoroacetic acid
THF	Tetrahydrofuran
TLC	Thin layer chromatography

Chapter 1. Introduction

1.1 Pd-Catalyzed Reactions

Cross-couplings reactions and/or inter- intra-molecular C–H activation is one of the most versatile and useful tools for carrying out organic syntheses. Indeed, transition metal catalysts are essential for facilitating these reactions, and Pd-based catalysts have prominently featured in this domain. Their versatility and efficacy have made them dominant in the field thus far. Pd is a second-row transition metal characterized by a moderately large atomic size, that significantly influences its chemical properties. In fact, Palladium has 10 electrons in the valence shell and typically exists in the 0 and +2 oxidation states (with a relatively narrow gap between them); for this reason, one-electron or radical processes are rare whereas two electron oxidation and reduction are favored and reversible. Coupled with the ready formation of coordinatively unsaturated species of 16 or even less electrons providing one or more empty coordination sites, Pd can indeed provide simultaneously at least one each of empty and filled nonbonding orbitals. Thus, it can be understood why Pd can readily participate to concerted reactions with low activation energies. The most important consequence of these characteristics is the high affinity for nonpolar π-compounds, such as alkynes, alkenes and even arenes. Moreover, it can also form σ bonds with nonbonding electron donors such as amines, imines, nitriles, phosphines, phosphites, and various other N, P, S, O containing donors. Furthermore, Palladium is relatively unreactive toward many functionalities, such as aldehydes, ketones, esters, amides, as well as nitro and cyano groups permitting to have a wide generalization of the procedures.

Pd salts or complexes, preformed or generated *in situ* upon addition of a ligand, are commonly employed as sources of Pd for cross-coupling and related reaction: palladium (II) species are preferred since they are more stable. Such compounds are reduced *in situ* to palladium (0) which enter the catalytic cycle. This interconversion between the two oxidation states, as stated earlier, is kinetically easy in either direction or results to be a favorable factor rather than a limitation.

Although the mechanisms for the various Pd-catalyzed reactions differ in some detail, they conform to the general catalytic cycle (Scheme 1.1).

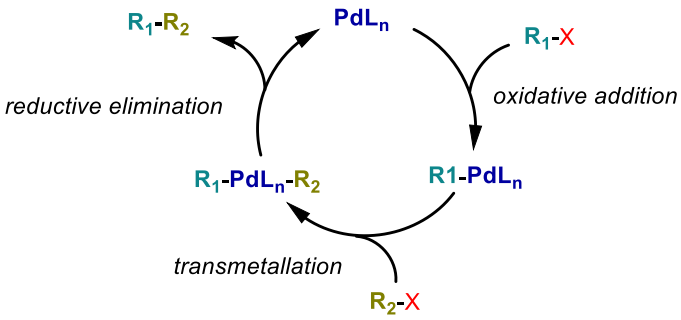

Scheme 1.1. Catalytic cycle for Pd-catalyzed cross-coupling reactions

Several Pd-catalyzed reactions related to cross-couplings (e.g., Heck reactions, Buchwald-Hartwig couplings, direct arylations) share with cross-couplings at least the initial steps of the catalytic cycle and are consequently influenced to a large extent by the same factors governing cross-couplings. As shown in the scheme 1.1, Pd catalysts and Pd-containing intermediates in a catalytic cycle itself must be regenerated to allow the effectiveness of the catalytic cycle: for this purpose there are different kinds of reagents that can reduce Pd(II) to Pd(0) species or provide reverse oxidation. It is interesting to highlight the fact that the majority of Pd-catalyzed reactions are initiated by Pd(0) species, which then undergo a series of Pd(0)–Pd(II) redox processes, and that most of the Pd(II) initiated reactions do involve reduction of Pd(II) species to Pd(0) species; furthermore, in many of these reactions the Pd(0) species must be externally oxidized to regenerate the external Pd(II) catalyst with oxidating agents such as O_2, CuCl, quinones and peroxides.

Historically, the use of Pd metal as catalyst for these reactions is as old as the reactions themselves: indeed, in the early 70s, the independent and almost concurrent discoveries by Mizoroki[1] and Heck[2] showed that coupling reactions between aryl, benzyl and styryl halides were catalyzed by Pd(II) catalysts and set the stage for the now named Mizoroki-Heck reaction. From that moment, different research groups focused on the development of new synthetic strategies to form C–C bonds taking advantage of this reactivity: Sonogashira used alkynes instead of alkenes for cross-coupling reactions with aryl halides;[3] Stille, on the other hand, initiates the use of organometallic reagents as nucleophile by using organostannane compounds for the Pd-catalyzed coupling reaction with aryl halides, however, the toxic nature of tin compounds limited their large-scale use;[4] as an alternative to tin reagents, less toxic organometallic compounds such as organozinc and organoaluminium was used by Negishi in the coupling reaction generating a mild and highly selective transmetallation agent that can tolerate a variety of functional groups;[5] Kumada used organomagnesium reagents for transmetallation,[6] although the highly reactive Grignard reagent also restricted their application to a selection of

functionalities;[7] Suzuki developed boron-based organometallic reagents for coupling reactions with aryl halides,[8] generating a non-toxic and practical alternative that can be used under mild reaction conditions (Scheme 1.2)

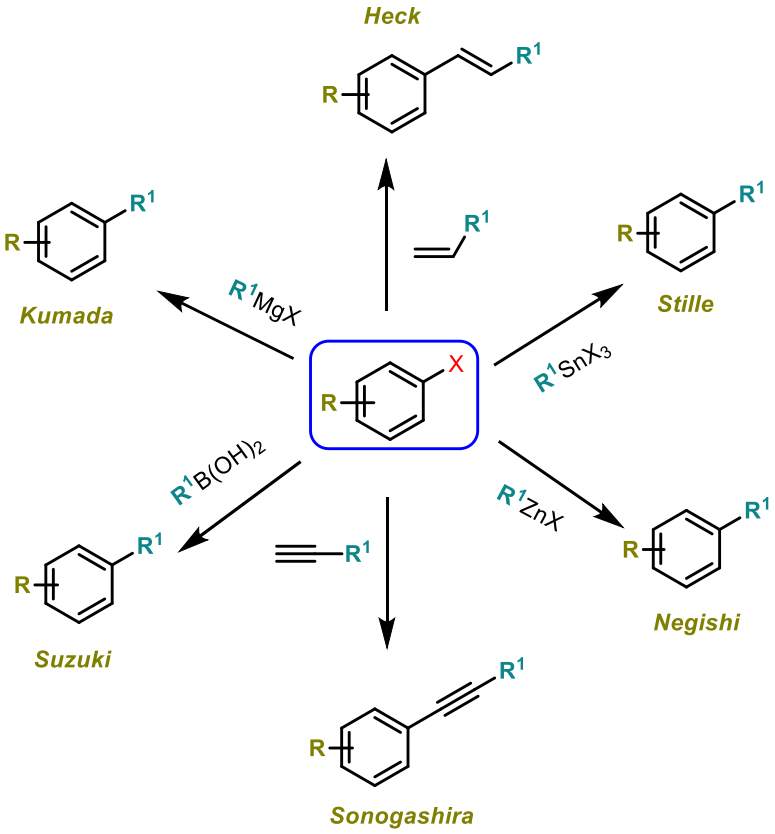

Scheme 1.2. Overview of key Pd-catalyzed cross-coupling reactions

1.1.1 Organo-Palladium complexes and their ligands

Pd(0) complexes tend to exist as coordinatively saturated 18-electron tetrahedral d^{10} complexes, but they can readily dissociate into coordinatively unsaturated 16 or less-electron d^{10} species. On the other hand, Pd(II) complexes tend to exist as coordinatively unsaturated 16-electron square planar d^8 complexes. Although they are reluctant to form coordinatively saturated 18 electron five-coordinated d^8 complexes, such complexes are kinetically readily accessible, and they can serve as transient intermediates in ligand substitution. Pd(II) d^8 complexes may also undergo substitution by dissociative processes, which must involve 14 or less-electron species as transient intermediate. In all these processes, the crucial requirement is the coordinative unsaturation or the presence of one or more valence-shell empty orbitals as Lewis acidic sites. For these reasons, the electronic and steric nature of the ligand and the coordination number of Pd influence strongly the two rate determining steps of the cross-coupling reactions (oxidative addition and reductive elimination, view scheme 1.1). Furthermore, the rate and equilibrium of ligand substitution is

strongly affected by the nature of the incorporated ligand, especially its nucleophilicity or basicity and by the electrophilicity or acidity of the leaving ligands. Until the mid-1990s, PPh_3 (see, Figure 1.1) was the most widely used ligand for Pd-catalyzed coupling reactions; then Fu's pioneering report in 1998 on the use of sterically hindered, electron-rich trialkylphosphine ligands such as $P(t\text{-}Bu)_3$ and PCy_3 (see, Figure 1.1) demonstrated the possibility of using less reactive organic chlorides as coupling partners in Pd-catalyzed cross-coupling reaction,[9] facilitating the formation of C–C bond between more challenging substrates, such as aryl chlorides, under mild reaction conditions.[10] Two of the most commonly used Pd(0) complexes are the commercially available $Pd(PPh_3)_4$, unstable in air and light sensitive, and $Pd_2(dba)_3$ (dba= dibenzylideneacetone), whose storage and manipulation is quite easier than $Pd(PPh_3)_4$. In the $Pd_2(dba)_3$ complex each palladium is coordinated with three olefinic double bonds. The most common way of preparing catalyst systems is mixing *in situ* a Pd precursor with a ligand: since dba is a weaker ligand than phosphines, $Pd_2(dba)_3$ represents the ideal source of Pd(0) to use for this purpose, because it easily undergo a ligand exchange reaction with a variety of phosphines (Scheme 1.3).

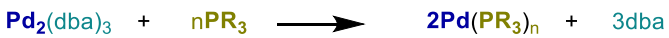

Scheme 1.3. Synthesis of Pd-phosphine complexes

In literature, there are some cases of ligand-free reactions, but ligands are required not only to generate soluble Pd catalysts, but also to influence the course of the reaction as well: indeed, Pd activity could be modulated by using phosphines with specific steric and electronic characteristics. In particular, the ligands can bear one or two sites of coordination, being named respectively mono- or bidentate and can have a massive or minimum steric hinderance. Recently, the discovery of new electron-rich ligands, such as $P(t\text{-}Bu)_3$ or N-heterocyclic carbene ligands, as well as Buchwald-type phosphines, has facilitated the emergence of Pd-catalyzed reactions involving aryl chlorides and alkyl halides. Some important examples of mono- and bidentate phosphines are shown in Figure 1.1.

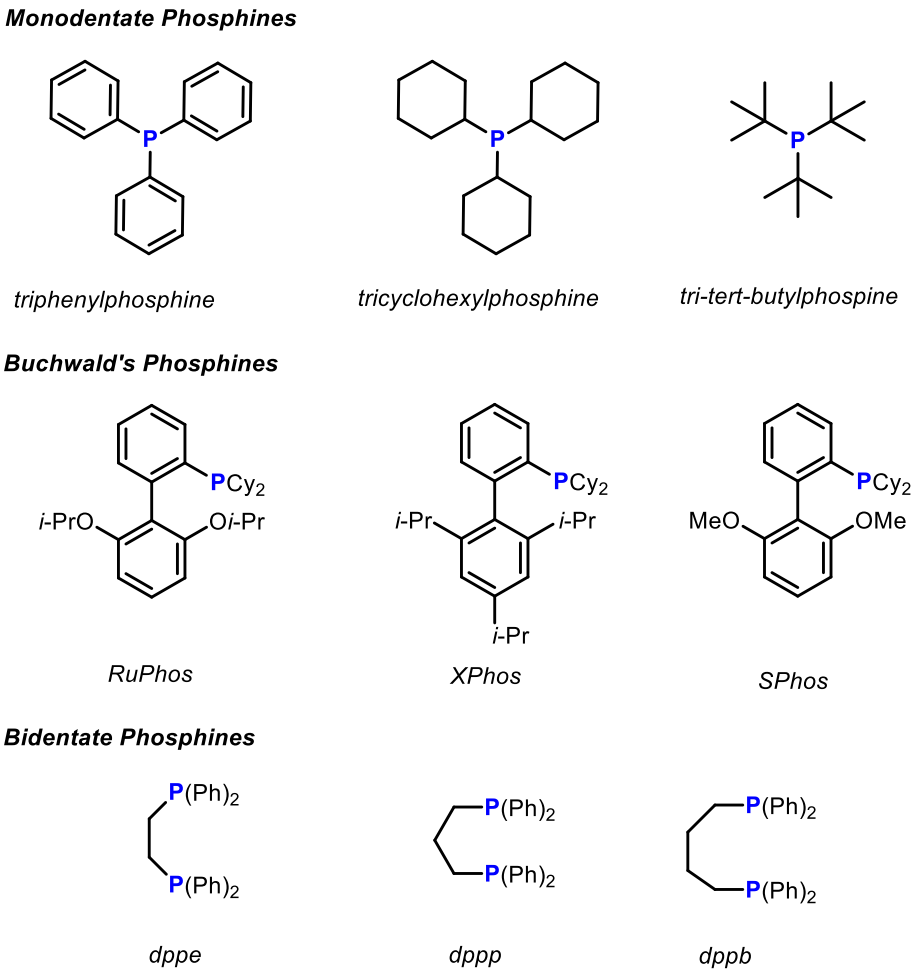

Figure 1.1. Classification of phosphine ligands used in catalysis

The most commonly used commercially available Pd(II) salts are $PdCl_2$ and $Pd(OAc)_2$, very often utilized as phosphines complexes such as $PdCl_2(PPh_3)_2$, $Pd(OAc)_2(PPh_3)_2$, typically formed *in situ* combining Pd(II) salts with PPh_3. Pd(II) salts tend to react with electron-rich compounds such as alkenes and alkynes, as well as arenes due to their electrophilic properties. Typical reaction of Pd(II) salts with alkenes or alkynes afford π-complexes. Pd(0) complexes instead usually have nucleophilic character. Most of the catalytic processes based on their utilization involve, in the initial step, their reaction with a variety of covalent polar and non-polar single bonds such as H–H, N–H, O–H, C–H, C–O, as well as C–X (halogen); the latter is most employed. Pd(II) salts produce palladation intermediates when reacting with arenes, basically through an electrophilic substitution reaction. These palladation intermediates can give rise to homocoupling reactions, acetoxylation reactions, or, in the presence of alkenes, vinylic substitution reactions.[11] In many Pd(II)-catalyzed reactions, Pd(II) species are reduced to Pd(0) species at the end of each cycle. Hence, the presence of oxidants such as Cu(II) salts and MnO_2 are required to make the reaction catalytic with respect to Pd(II).

Here, the focus lies on the exploration of the most renowned Pd-catalyzed coupling reactions, aiming to elucidate the reaction's nature, conditions, and catalytic pathways.

1.1.2 Heck reaction

The Heck reaction consists of the formation of a new C–C bond between an aryl/vinyl halide or triflate and an alkene, in the presence of a base and catalytic amount of Pd; since aryl/vinyl group substitutes a hydrogen atom, this reaction is known as vinylic substitution (Schem 1.4).

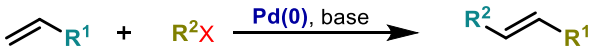

Scheme 1.4. General Heck reaction

The general mechanism of Heck reaction, as depicted in Scheme 1.5, the catalytically active species is a 14-electron complex, PdL_2, commonly generated *in situ* either from a Pd(0) complex or by reduction of relatively inexpensive Pd(II) acetate or chloride. The first step of mechanism is oxidative addition of an aryl halide RX to the Pd(0) complex, forming a σ–alkenyl or σ–aryl–Pd(II) complex *cis*-$RPdXL_2$. Ligands used in the Heck reaction can include monodentate[12] bidentate phosphines and 1,10- phenanthroline derivatives.[13] Next, a carbopalladation or a migratory step which produces new σ–C–Pd and σ–C–C bond. The elimination of HPdX occur only after an internal rotation around the σ bond as it requires a β-hydrogen atom to be oriented *synplanar* respect to the halopalladium to allow the agostic interaction between palladium and hydrogen which stabilizes the complex, so Heck reaction results stereospecific. After that alkene product and $L_2Pd(H)X$ are produced, the presence of a base is necessary in order to transform the $L_2Pd(H)X$ into the starting $L_2Pd(0)$ complex and close the catalytic cycle. Then, there is a carbopalladation or a migratory step which produces new σ–C–Pd and σ–C–C bond. Typical bases used in the Heck reaction are tertiary amines (Et_3N, iPr_2NEt, etc.) or acetate or carbonate bases (AcONa, K_2CO_3, etc.).

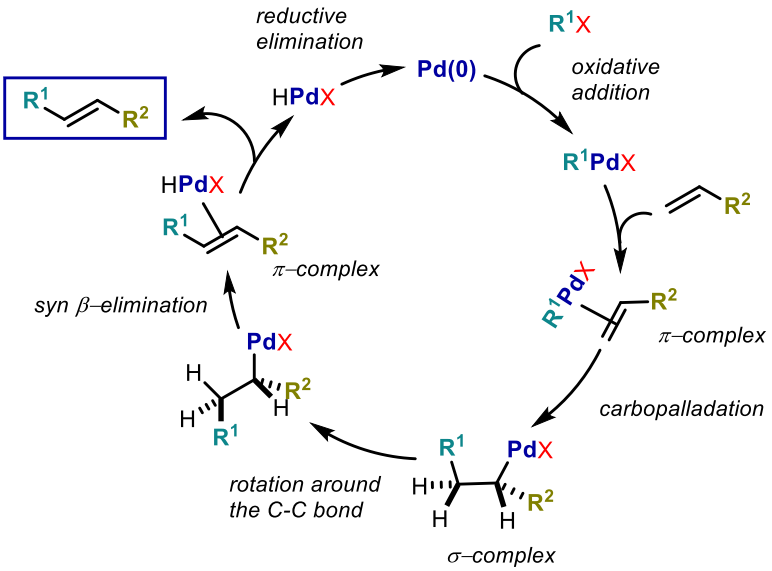

Scheme 1.5. General mechanism of Heck reaction

Heck reaction is reported to be a high regioselective reaction[14] using procedures that allow the coordination-insertion process *via* dissociation of the ligand.

A further achievement was the discovery that Heck reactions are greatly accelerated in the presence of quaternary ammonium salts ("Jeffery" conditions: $Pd(OAc)_2$, K_2CO_3, *n*-Bu_4NX, DMF). In these conditions iodoarenes and iodoalkenes can be coupled to alkenes at room temperature. The role of the quaternary ammonium salt is to stabilize the formation of palladium nanoparticles, preventing the precipitation of palladium (0) as palladium black. The nature of the leaving group greatly affects the reaction rate: aryl iodides react faster than bromides, and aryl chlorides are notoriously unreactive unless special catalysts or ligands and elevated temperatures are used to enhance the reaction rate. This has been taken to indicate that the oxidative addition of the haloarene to Pd(0) is the rate-determining step. This reaction can be catalyzed by palladium complexes with or without phosphine ligands (phosphine assisted *vs* phosphine-free catalysis). A primary role of phosphine ligands is to support palladium in its zero-oxidation state in the form of stable PdL_4 or PdL_3 species. The phosphine-assisted approach is the classical and well-established method which gives excellent results in most cases, but, for economical and chemical reasons, research was addressed in seeking for something else: in fact, phosphine ligands are expensive, toxic, and unrecoverable. In large- scale applications on industrial and semi-industrial scale, the phosphines might be a more serious economic burden than even Pd itself, which can be recovered at any stage of production or from wastes. The chemical reason is lower reactivity of fully ligated complexes of palladium, the main result of which is the need for higher loads of catalyst to achieve appropriate rates of reaction and therefore further aggravation of procedure

cost. Both underligated and phosphine-free catalysis are opposite to the phosphine-assisted conservative methodology. It relies not on the intrinsic stability of properly ligated isolable complexes, but rather on making zerovalent palladium species run for life within the Heck catalytic cycle or die as inactive black sediments. Underligated Pd(0) species (the term underligated means that a given palladium complex bears less strongly bonded ligands than is required to form a stable complex) are intrinsically unstable to survive outside of the cycle but are likely to have higher reactivity; therefore, their stationary concentration in a catalytic system is much lower. Unlike phosphine- assisted systems which are based on thoughtful design and knowledge of intimate details of coordination chemistry, phosphine- free systems are not so predictable yet. The primary reduction of Pd(II) to Pd(0) is most likely accomplished by phosphine in the phosphine assisted catalytic cycles. The reduction is assisted by hard nucleophiles, of which the most common are hydroxide and alkoxide ions, water, and acetate ion, though in special cases even fluoride in the presence of water can play the role.

In phosphine-free systems, the primary reduction of Pd(II) can be effected by amines, if these are used as base, or olefin. It is interesting to note that neither Et_3N nor olefin have any detectable influence on the reduction rate in the presence of phosphine. Still, it is well-known that in the absence of phosphine, olefins are oxidized by Pd(II) via the first turn of a Waker-type catalytic cycle. This process may be a serious yield-decreasing factor in the reactions with high initial loads of palladium salts in phosphine-free systems if the olefin is taken in an equimolar amount respect to the electrophilic substrate (that is the by-default case in the intramolecular Heck cyclization).

Nevertheless, over the following decades, a vast number of groups would demonstrate the high functional-group tolerance and wide applicability of this reaction system. Equally significant, powerful intramolecular variants[15] appeared from numerous laboratories, especially in natural-product synthesis, which has been perhaps most decisively demonstrated by Overman.[16] In addition, the construction of quaternary stereocenters in an intramolecular fashion,[17] coupled with the development of asymmetric versions,[18] would afford the Mizoroki–Heck reaction a unique place in the arsenal methods available to synthetic chemists.

1.1.3 Sonogashira cross-coupling reaction

Until the mid-1970s, the field of acetylene coupling was dominated by the use of copper salts as catalysts. However, in 1975 the Pd-catalyzed coupling of acetylenes with aryl or vinyl halides was concurrently disclosed by the group of Sonogashira (Scheme 1.6).[19]

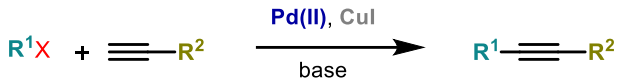

Scheme 1.6. General Sonogashira cross-coupling reaction

This protocol is based on the addition of copper salts as cocatalysts thus accelerating the coupling reaction and enabling performance of the alkynylation at room temperature.

As to the catalyst system, Pd(II) salts, in particular $PdCl_2(PPh_3)_2$, are most commonly used as source of Pd(0) species. Copper(I) iodide revealed a particularly effective co-catalyst. The use of additives such as Bu_4NI was found to provide beneficial results in some cases. Tertiary and secondary amines are usually employed as bases.

The copper-cocatalyzed Sonogashira reaction is believed to take place through two independent catalytic cycles, as shown in scheme 1.7, where a tertiary amine is represented as base, with other amines or inorganic bases performing similarly. The Pd-cycle is based on fast oxidative addition of R^1–X (R1= aryl, hetero-aryl, vinyl; X= I, Br, Cl, OTf) to the catalyst. This is classically thought to be 14-electron $Pd(0)L_2$, formed by reduction of different Pd(II) complexes using ligands and solvents that can reduce Pd(II) species typically via-complexation-dehydropalladation-reductive elimination.

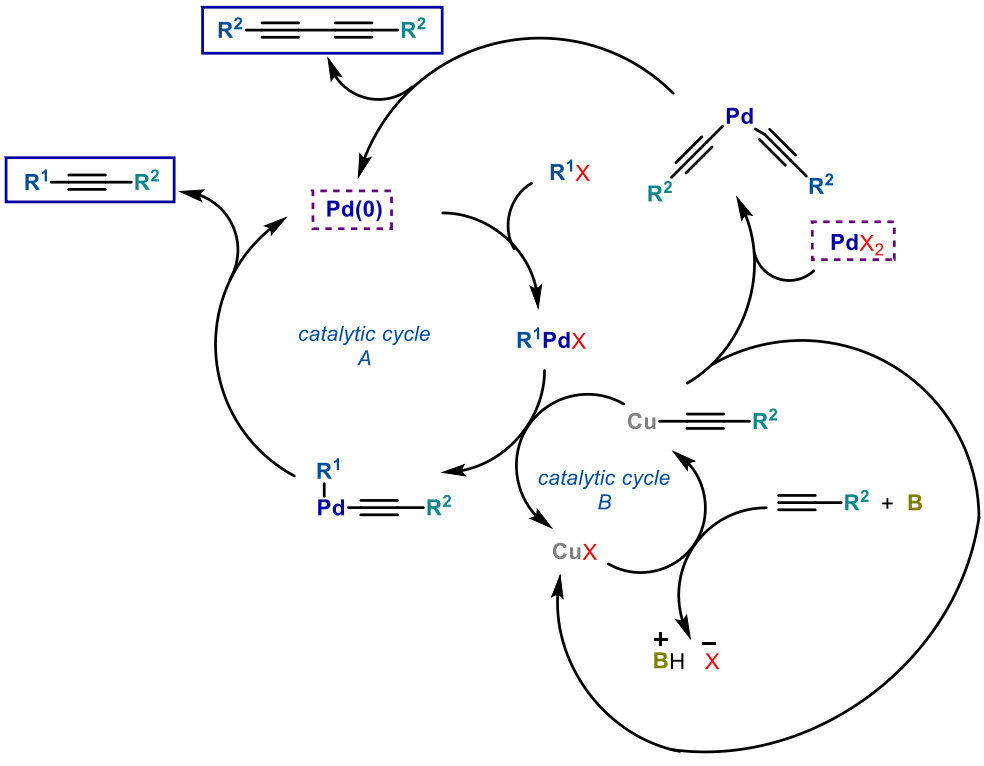

Scheme 1.7. General mechanism of Sonogashira cross-coupling reaction

It is important to underline that the high functional-group tolerance of the Sonogashira method places this reaction in a premium position as a late-stage coupling in the synthesis of complex molecules and natural products.[20]

1.1.4 Suzuki cross-coupling reaction

In 1979 Suzuki reported the Pd-catalyzed cross-coupling (see, Scheme 1.8) between 1-alkenylboranes and aryl halide.[8b] In general the Suzuki cross-coupling involves the reaction of organic halides or triflates with organoboranes under basic conditions.

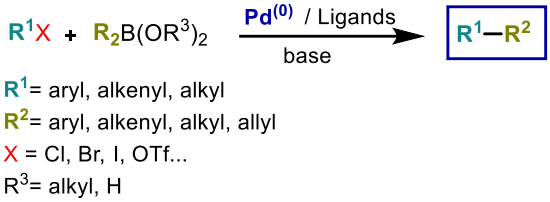

Scheme 1.8. General Suzuki cross-coupling reaction

The Suzuki-Miyaura protocol has developed into an extremely powerful and general method for the formation of C–C bonds, thanks to its advantageous features such as stable and easily handled organoboron starting materials, mild reaction conditions, and facile removal of less-toxic inorganic byproducts.

It has to be pointed out that the mechanism of the Suzuki reaction has not been fully established,[21] but, by analogy with related processes, the coupling is believed to proceed through a catalytic cycle involving three steps (Scheme 1.9): (1) the oxidative addition of the carbon electrophile to the zerovalent and unsaturated PdL_2, where L is normally a phosphine ligand such as PPh_3, (2) the transmetallation of a nucleophilic carbon from boron to the $R'PdXL_2$, and (3) the rapid reductive elimination of the cross-coupling product with the regeneration of the PdL_2 catalyst.

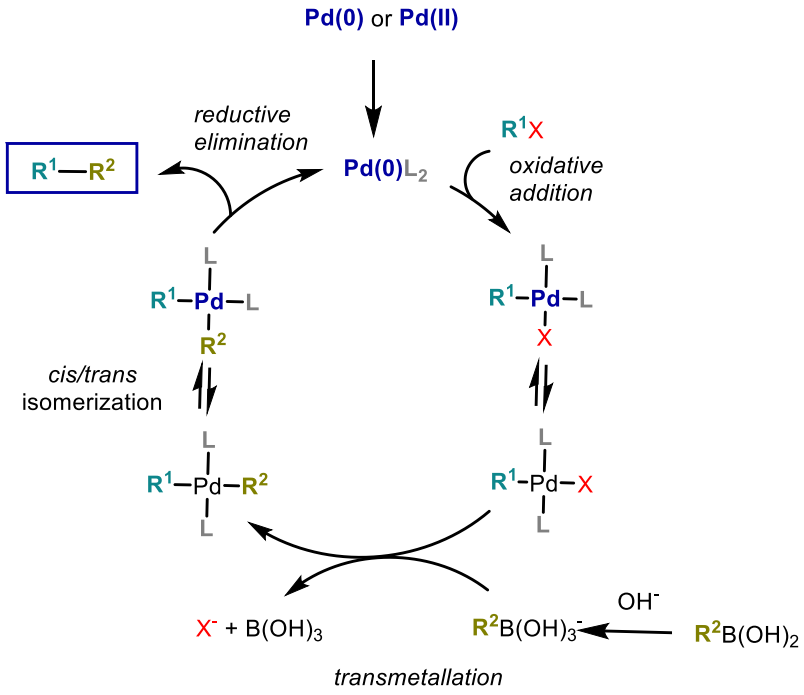

Scheme 1.9. General mechanism of Suzuki cross-coupling reaction

A determining factor in the Suzuki–Miyaura reaction is the base employed: in fact, organoboron compounds are highly covalent in character and do not undergo transmetallation readily in absence of a base. One of the most representative examples of the key role of the base in the outcome of the Suzuki–Miyaura coupling originates from Kishi's investigation on the total synthesis of Palytoxin:[22] in this work, the use of thallium hydroxide as base makes the reaction complete, essentially on mixing of the reagents. Although effects may not be as dramatic as this on a routine basis, such examples have elegantly shown the importance of base source as well as the synthetic power of the Suzuki–Miyaura reaction. Moreover, as in others Pd-catalyzed reaction, relative reactivity of leaving groups is I^- > OTf^- > Br^- > Cl^-. Then, isomerization to the *cis* complex is required before reductive elimination can occur. Relative rates of this step from Pd(II) complexes: aryl–aryl > alkyl–aryl > n-propyl-n-propyl > ethyl–ethyl > methyl–methyl.

The most commonly used catalytic system is $Pd(PPh_3)_4$, but other Pd sources have been used including Pd(II) pre-catalysts that are reduced to the active Pd(0) *in situ* (e.g. $Pd_2(dba)_3$ + PPh_3, $Pd(OAc)_2$ + PPh_3 and $PdCl_2(dppf)$).

"Ligand-free" conditions using $Pd(OAc)_2$ have also been developed. Side reactions often associated with the use of phosphine ligands (phosphonium salt formation and aryl-aryl exchange between substrate and phosphine) are thus avoided.

In conclusion, the hallmark of the Suzuki-Miyaura coupling was the demonstration that activation of organometallic component as the boronate (referred to as “ate” complex) could allow the coupling of organometallic reagents unable to undergo transmetallation under standard conditions.

1.1.5 Tsuji-Trost reaction

In the early 1960s, Tsuji discovered the reaction (see, Scheme 1.10) between π-allylpalladium chloride with malonate and acetoacetate as carbon nucleophiles to give allylmalonate and allylacetoacetate; this is the first example of C–C bond formation mediated by a Pd complex.[23] Tsuji-Trost reaction is the Pd-catalyzed substitution of allylic leaving groups by carbon nucleophiles, *via* π-allylpalladium intermediates. The π-allylpalladium complex is formed through oxidative addition of various allylic compounds to Pd(0). This electrophilic complex evolves through the attack of a *soft* nucleophile, regenerating Pd(0) and closing the catalytic cycle (Scheme 1.10). In particular, first, the palladium coordinates to the alkene, forming a η_2-π-allyl-Pd(0)-complex. The next step is oxidative addition in which the leaving group is expelled with inversion of configuration to form η_3-π-allyl-Pd(II) complex. The attack of the nucleophile specie to the allyl group regenerates the η_2-π-allyl-Pd(0) complex. In the last step, a reductive elimination occurs regenerating the active catalytic species and the alkene product.

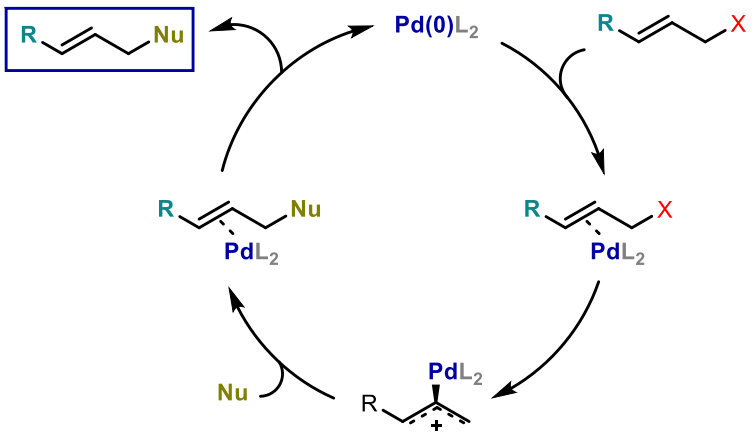

Scheme 1.10. General mechanism of Tsuji-Trost reaction

Many sources of allylic leaving groups are used for Pd-catalyzed reactions, with some differences in their specific reactivities: allylic alcohols are poor substrates, but their esters, typically acetates or carbonates, are highly reactive. In addition, allylic phosphates, allylic nitro compounds,[24] and sulfones[25] are used for allylation. Regarding the nucleophiles employed, *soft* carbon

nucleophiles with two EWGs groups, such as ester, ketone, aldehyde, nitro, sulfone, and nitrile, are allylated smoothly. An interesting aspect of this reaction is its stereochemistry, that has been studied extensively using substituted 2-cyclohexenyl acetate and results to be dependent on the nature of the nucleophiles employed:[26] the formation of the π-allylpalladium complex proceeds by an *anti*-attack of Pd(0) and, consequently, by inversion. The subsequent nucleophilic attack may involve an *anti*-attack, as it is the case with soft nucleophiles. Thus, an overall retention of configuration is observed (Scheme 1.11, a). With hard nucleophiles, such as organometallic compounds, the reaction proceeds via a transmetallation step followed by reductive elimination. This reaction pathway leads to an overall inversion of configuration (Scheme 1.11, b).

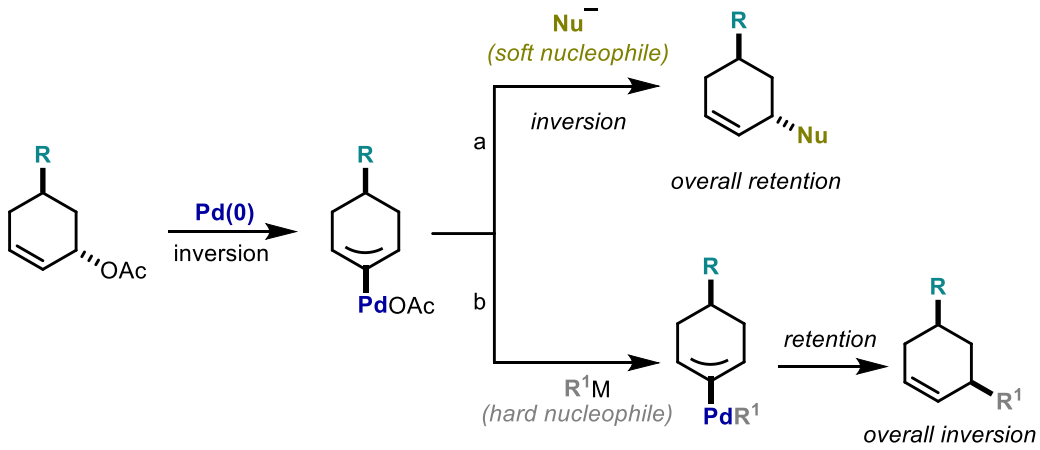

Scheme 1.11. Stereochemical outcomes of a Pd(0)-catalyzed reaction showing pathways leading to a) inversion or b) retention of configuration, with different ligand coordination steps.

Another important feature of this reaction is the regioselectivity: in fact, the substitution usually occurs at the less substituted side with high regioselectivity.

In 1977, Trost reported the first asymmetric transformation, which marked his contribution to this field.[27] The so called Trost asymmetric allylic alkylation (Trost AAA) is a potent instrument especially for the synthesis of complex natural products and scientists often took advantage of these features. The ligand plays a major role in the enantioselectivity: the types of ligands employed followed three general concepts in design: creating chiral space with an array of groups from primary stereogenic centers;[28] electronic desymmerization on the donor atoms of the ligand where different bond lengths on each side of the chiral space promote differential reactivity at each terminus;[29] attaching a tether to coordinate the incoming nucleophile.[30] In the AAA reaction, good enantioselectivity at the nucleophile and electrophile and diastereoselectivity with respect to both has been achieved with soft carbon nucleophiles on

cyclic and acyclic electrophiles. Thanks to this method, many natural products and drugs have been synthesized such as pentobarbital[31] and (-)-anatoxin-A (Scheme 1.12).[32]

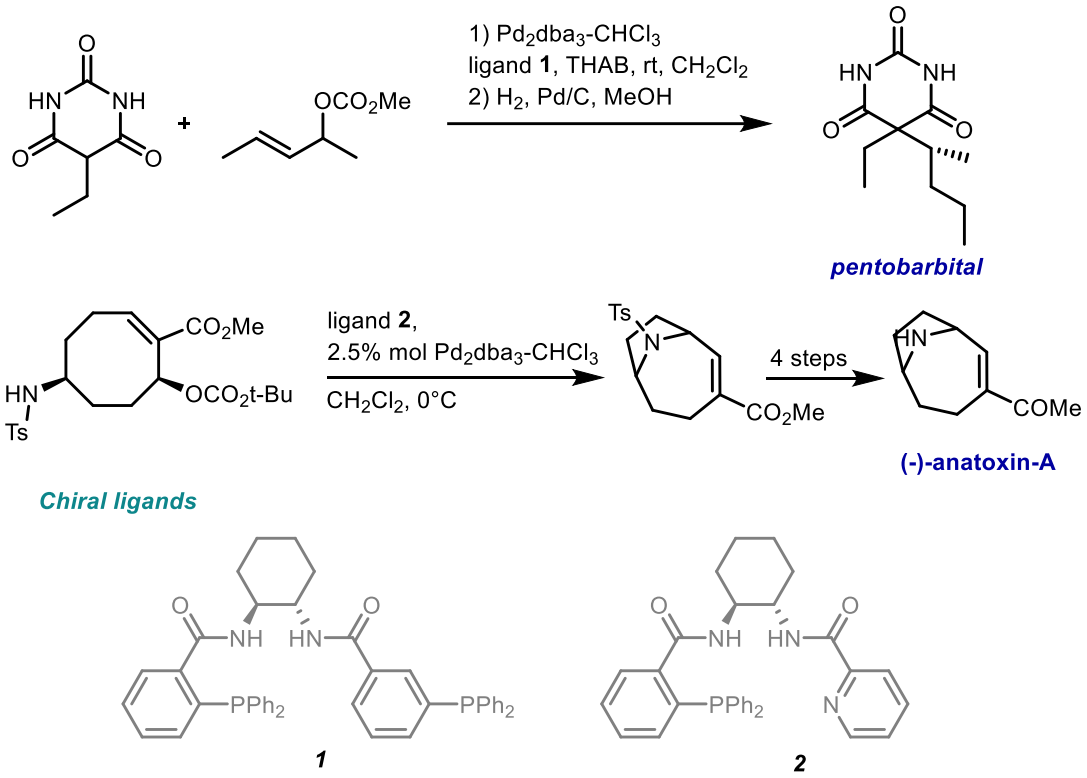

Scheme 1.12. Pd-catalyzed reactions employing chiral ligands for the synthesis of pentobarbital and (-)-anatoxin-A, highlighting the role of ligand design in stereoselective transformations

Eventually, over the years, the scope of Tsuji-Trost reaction has been extended to other nucleophiles: indeed, since the first reported AAA reaction with *N* nucleophiles by Trost group,[28] alkyl-amines, azides, amides, imides, and heterocyclic amines have all been employed as nucleophiles *via* cyclic and acyclic, hindered and unhindered π-allyl complexes as intermediates in catalytic cycles; also sulfonamides,[33] heterocyclic amine[34] and sulfur nucleophiles[35] can been used and resulted to be exceptionally versatile starting materials for the Tsuji-Trost reaction.

1.1.6 C–H activation or direct arylation

In the past few decades, synthetic chemists have been actively modifying organic synthetic pathways to avoid using hazardous chemicals and develop more streamlined methods to achieve desired outcomes. In this context, transition metal-catalyzed C–H bond functionalization for C–C bond formation has emerged as a promising area in organic synthesis.[36] Specifically, reactions involving Pd-catalyzed activation of sp^2 or sp^3 C–H bonds of arenes or alkenes have been

extensively explored.[37] Moreover, successful applications of the C–H activation strategy on readily available substrates have been reported using various metals besides Pd catalysts.[38]

1.1.6.1 C–H activation reaction

The C–H activation reaction marks an evolution in cross-coupling reactions, enabling direct manipulation of C–H bonds without the need for prior functionalization or modification. This methodology involves rendering the typically stable and inert C–H bond reactive, a feat accomplished through the use of transition metals as catalysts (Scheme 1.13).

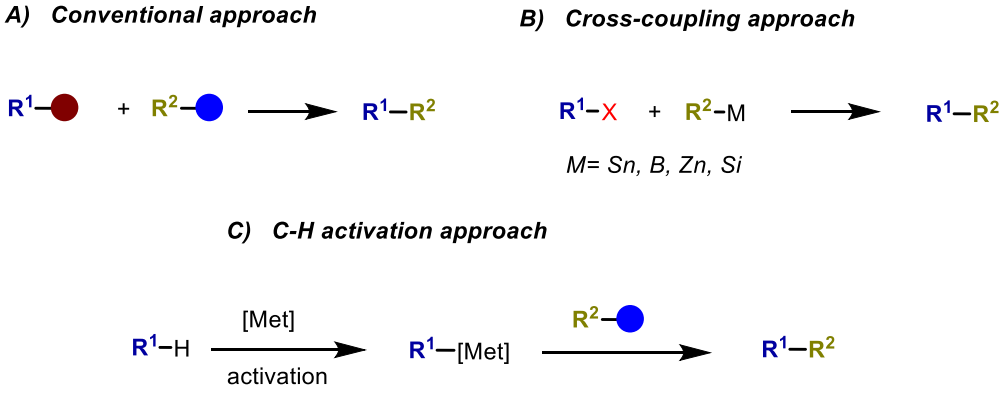

Scheme 1.13. Different approaches for C–H activation

One of the initial reports on biaryl formation *via* double C–H activation described the oxidative cross-coupling of simple arenes (Scheme 1.14, A), published by Lu and colleagues in 2006.[39] Following this, You and Xia conducted a direct arylation (*via* double C–H activation) of simple arenes with ferrocenyl oxazolines in the presence of a stoichiometric amount of $Pd(OAc)_2$ (Scheme 1.14, B).[40]

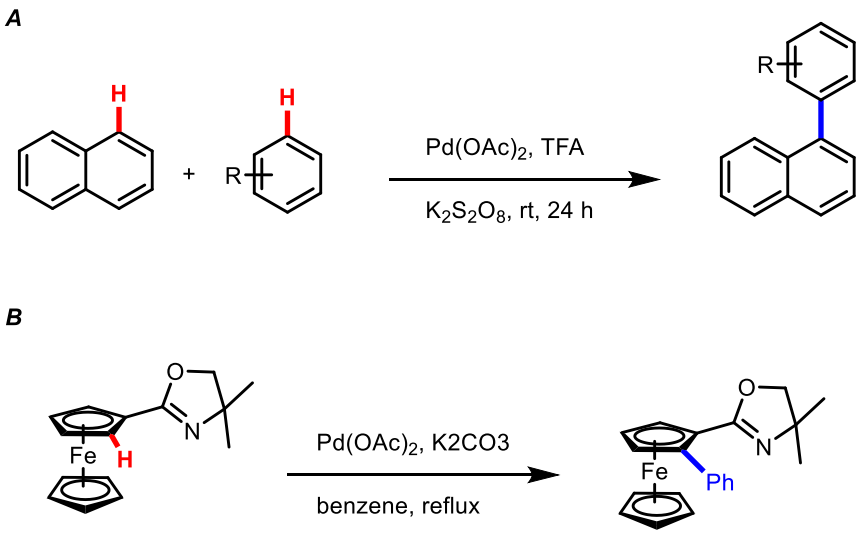

Scheme 1.14. Pd-catalyzed oxidative cross-coupling

Building on these groundbreaking studies, in 2007, the Fagnou group achieved a significantly more practical and selective aryl–H-aryl–H cross-coupling. They applied their methodology to the reaction of unactivated arenes with N-alkyl indoles, achieving yields of up to 84% (Scheme 1.15). Fagnou's Pd-catalyzed oxidative cross-coupling enabled access to both C-3 and C-2 arylindoles by varying the terminal oxidant, using $Pd(TFA)_2$ as a catalyst, and employing catalytic amounts of 3-nitropyridine and cesium carbonate. The authors also noted that changing from N-acetyl indole to N-pivalyl indole played a significant role in the selectivity of the reaction (Scheme 1.15).[41]

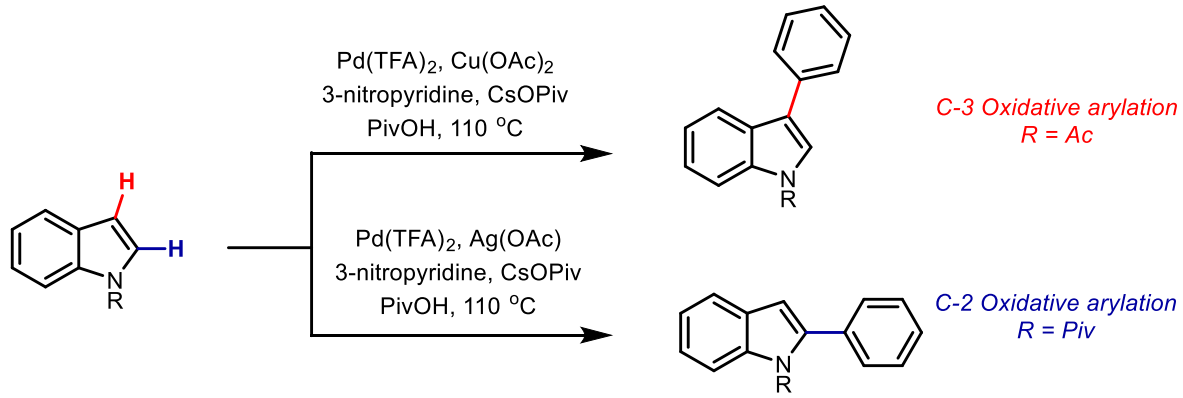

Scheme 1.15. Fagnou's aryl–H-aryl–H cross-coupling

In 2008, Fagnou and colleagues reported an intramolecular Pd-catalyzed oxidative biaryl synthesis under air using pivalic acid as the reaction solvent. This methodology was applied in the synthesis of three naturally occurring carbazole products: Murrayafoline A, Mukonine, and Clausenine (Scheme 1.16, A). Subsequently, Shi and co-workers made significant strides towards more sustainable routes to biaryls. In 2012, they reported the first Pd-catalyzed dual C–H activation of benzophenones to form fluorenone derivatives via oxidative dehydrogenative cyclization (Scheme 1.16, B). Excellent yields and functional group compatibility were achieved.[42]

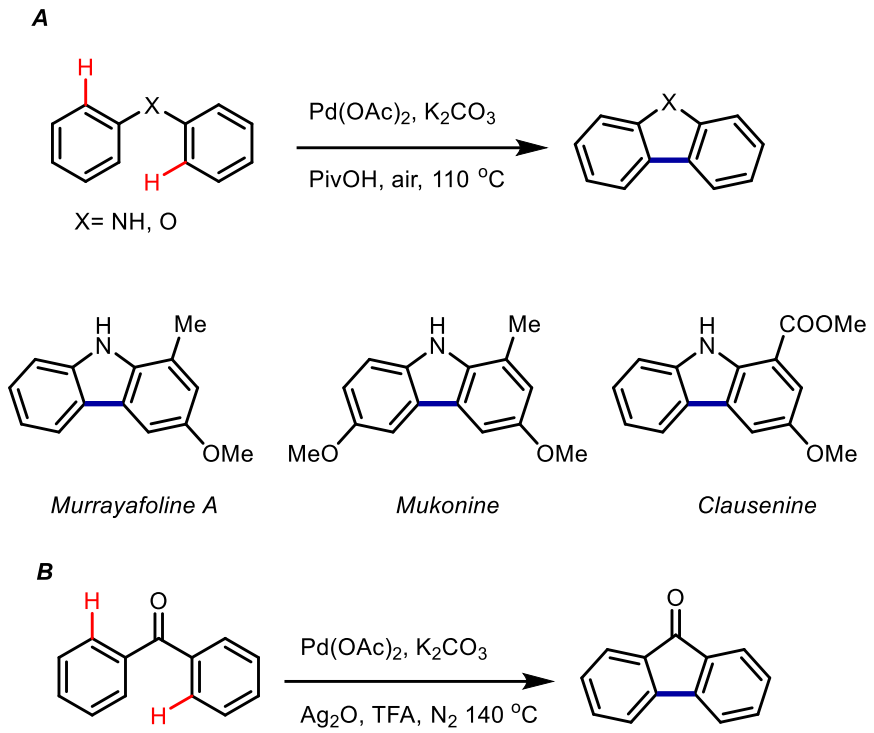

Scheme 1.16. Fagnou's intramolecular Pd-catalyzed oxidative biaryl synthesis

1.2 The Click Chemistry Concept

In 2022, the Nobel Prize in Chemistry was awarded by the Royal Swedish Academy of Sciences to Carolyn R. Bertozzi, Morten Meldal, and K. Barry Sharpless for their pivotal contributions to click chemistry and bioorthogonal chemistry. Over the past two decades, these foundational concepts have been closely associated and have played a significant role in driving numerous important discoveries. Whether utilized independently or in combination, these methodologies have had a profound impact on the field of chemistry and have brought about substantial benefits for humanity.

1.2.1 Click chemistry

Definition
A set of powerful, selective and modular "blocks" that work reliably in both small and largescale applications.

In 2001, K. Barry Sharpless and his colleagues Hartmuth C. Kolb and M.G. Finn published an influential article introducing the concept of Click Chemistry titled "Diverse Chemical Function from a Few Good Reactions."[43] The article demonstrated how complex and useful molecules

could be rapidly synthesized using a modular approach that relied on a small number of highly reliable reactions. The term "click" was coined as an analogy to the sound made when two sides of a buckle click together. In this context, the two sides of the buckle represent two small molecules that, after a simple "click" reaction, efficiently form more complex compounds.

The priority criteria for ideal click chemistry include modularity and wide scope. Subsequently, strict and specific requirements must be met:

- Readily available starting materials and reagents.
- Simple reaction conditions: no solvent or an easily removable solvent; ideally oxygen- and water-tolerant.
- Efficient procedure: high thermodynamic driving force (>20 kcal/mol) and rapid completion.
- Easy work-up: resulting compounds should be easily isolated via non chromatographic methods such as crystallization or distillation.
- Ideal results: high yields; production of harmless waste that can be removed without chromatography; high selectivity and stereospecificity for a single product (but not necessarily enantioselective); stability of the product under physiological conditions.[43]

It is noteworthy that among cycloaddition reactions, the Huisgen 1,3-dipolar cycloaddition of azides and alkynes, first discovered by Huisgen in 1963, stands out as the "cream of the crop."[44] This is attributed to the ease of installation and the inertness of both alkynes and azides. However, this cycloaddition was somewhat overlooked for decades due to its requirement for high temperature. Additionally, issues arise with structural certainty, particularly when terminal alkynes are used, leading to mixtures of 1,4- and 1,5-disubstituted 1,2,3-triazoles, sometimes in a 1:1 ratio (Scheme 1.17). In 2001, interest in this cycloaddition was revived with the development of the Cu(I)-catalyzed azide-alkyne cycloaddition (CuAAC).

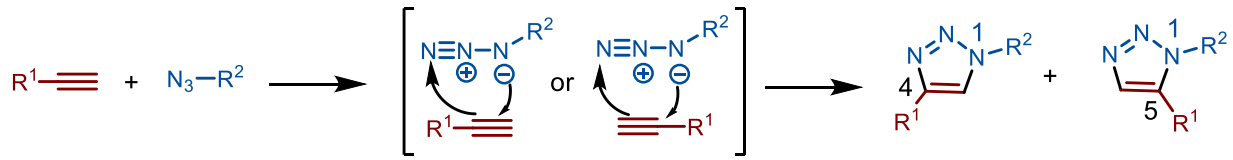

Scheme 1.17. General scheme of click chemistry

1.2.2 Cu(I)-catalyzed azide-alkyne cycloaddition (CuAAC)

In 2001, Meldal and Tornøe introduced a highly mild and efficient method for incorporating the 1,2,3-triazole pharmacophore into peptides.[45] According to their findings, in the presence of Cu(I) catalysis, the 1,4-substituted 1,2,3-triazole could be obtained as the only regioisomer on solid-phase at 25°C with high yields ranging from 80% to 95% (Scheme 1.19 A).

Almost simultaneously, in 2002, CuAAC was independently introduced by Sharpless, Rostovtsev, and their colleagues.[46] Instead of directly employing a Cu(I) salt, they generated Cu(I) *in situ* by reducing a Cu(II) salt with a reducing agent such as ascorbate. This modification improved the reaction in terms of cost and catalyst purity. Notably, this Cu-catalyzed reaction exhibited a broad scope and proceeded with good yields, predominantly yielding the 1,4-disubstituted 1,2,3-triazole product (Scheme 1.18 B).

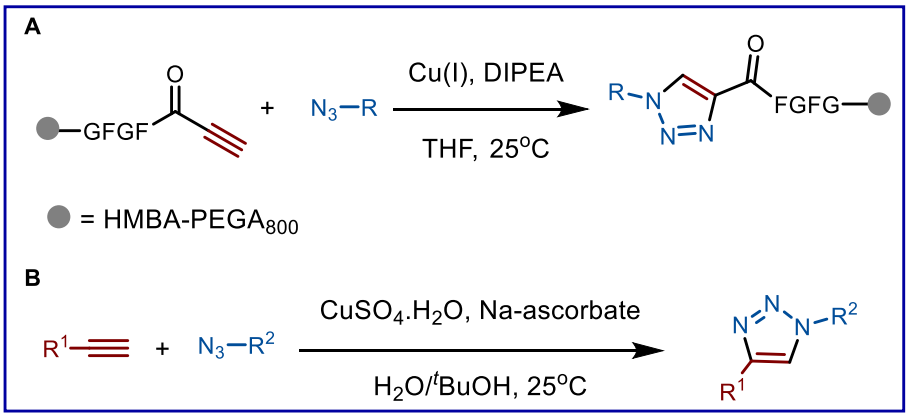

Scheme 1.18. CuAAC reaction by A) Meldal and Tornøe B) Sharpless

Furthermore, Sharpless and colleagues proposed a stepwise mechanism for CuAAC in the early stages.[47] In this mechanism, the *in situ*-generated Cu(I) forms a π complex with the triple bond of a terminal alkyne, leading to the formation of the well-known intermediate Cu(I) acetylide (Scheme 1.19 A). However, studies by Fokin and co-workers revealed that monomeric Cu acetylide complexes are not reactive towards organic azides unless an exogenous Cu catalyst is added. Moreover, crossover tests employing isotopically enriched external Cu sources demonstrated the equivalence of the two Cu atoms during the cycloaddition steps, confirming the stepwise nature of carbon-nitrogen bond formation (Scheme 1.19 B).[48]

Cu(I) has demonstrated remarkable catalytic activity, accelerating the cycloaddition reaction by 107 times.[47] Furthermore, triazole formation is largely unaffected by the steric or electronic properties of the substituents on either of the two reactants, although a terminal alkyne is

necessary. Typically, the reaction is completed within hours at room temperature in various solvents, including alcohols and water, without the need for an organic co-solvent. Moreover, while most experiments are conducted at pH levels close to neutral, the catalysis appears to function effectively over a wide range of pH levels.

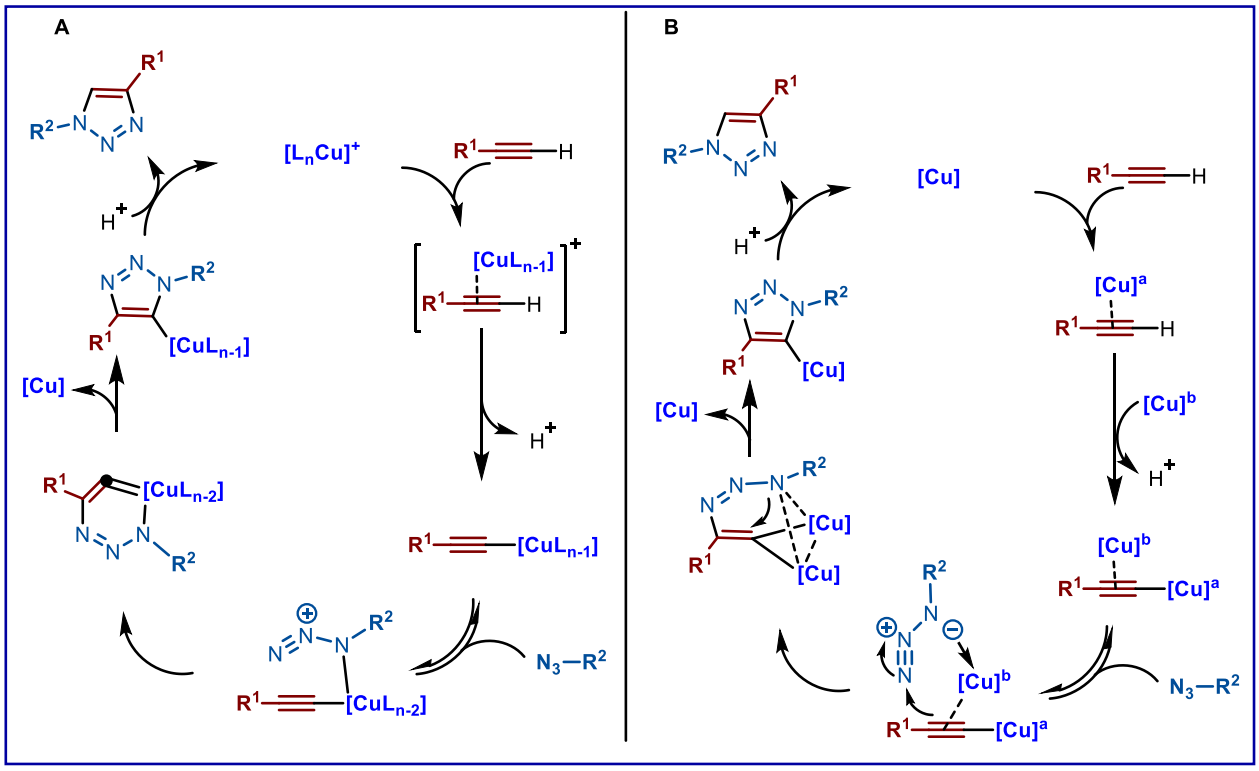

Scheme 1.19. CuAAC mechanism by A) Sharpless B) Fokin and co-workers

1.2.3 Heterocyclic fused 1,2,3-triazole

[1,2,3]-Triazolo-heterocycles are structurally diverse systems that belong to the novel 1,2,3-triazole family. The triazole structure serves as a bioisostere mimic of the amide bond, exhibiting similar spatial, structural, and electronic characteristics.[49] Additionally, the triazole moiety mimics other functional groups and displays secondary interactions, establishing it as a privileged pharmacophore.[50] Due to its drug-like properties, triazoles have been investigated for a wide range of activities including anti-Alzheimer, anti-cancer, anti-tubercular, anti-convulsant, anti-bacterial, anti-leishmanial, neuroprotective, anti-diabetic, anti-plasmodial, and anti-malarial activities, among others.[51] Fused triazoles can be accessed by intramolecular azide-alkyne cycloaddition (IAAC) reactions,[52] sequential multicomponent reaction or one-pot domino reaction and metal catalyzed intramolecular C–H activation or intramolecular Heck reaction or direct arylation (Scheme 1.20).[53]

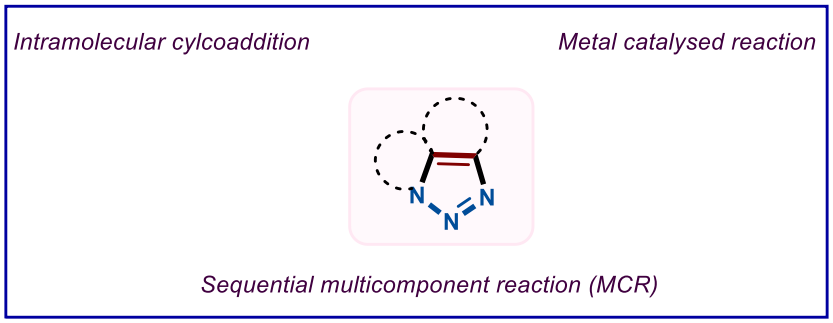

Scheme 1.20. General overview of different approaches for the synthesis of fused 1,2,3-triazole

1.2.4 Functionalization of 1,4-disubstituted 1,2,3-triazoles

Various methods have been employed for the synthesis of compounds containing the triazole motif. Among these, 1,4-disubstituted 1,2,3-triazoles are frequently functionalized using transition metal-catalyzed cross-coupling reactions, direct arylations, and Heck reactions.

In 2005, Wu[54] conducted a study on a regioselective intermolecular Heck reaction. This reaction involved combining 5-iodo-1,2,3-triazoles with monosubstituted alkenes under modified ligand-free Jeffrey conditions.[55] The outcome of the reaction was the exclusive or predominant formation of the *E*-isomer of the alkene in the product. Remarkably, various functional groups present in the reactants were well-tolerated, demonstrating the versatility and applicability of the method (Scheme 1.21).

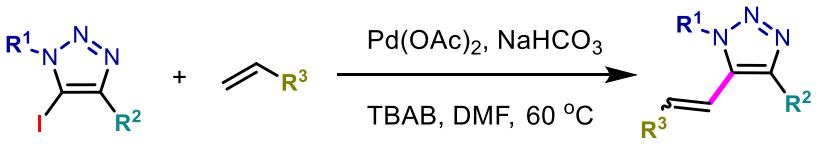

Scheme 1.21. Intermolecular Heck reaction involving a triazole substrate

Gevorgyan[56] presented an efficient method for synthesizing fully decorated 1,2,3-triazoles. The synthesis involved a direct Pd-catalyzed C–5 arylation reaction with aryl bromides (Scheme 1.22).

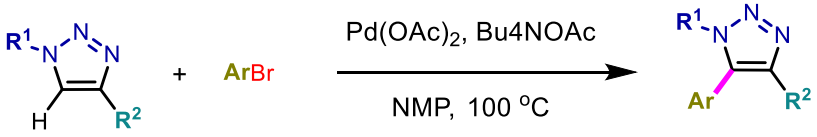

Scheme 1.22. Intermolecular Pd-catalyzed C–H activation

In the subsequent year, Ackermann[57] reported a one-pot multicomponent synthesis, employing CuI to consecutively facilitate two catalytic transformations: a CuAAC reaction and a C–H functionalization to synthesize multi-substituted 1,2,3-triazoles (Scheme 1.23).

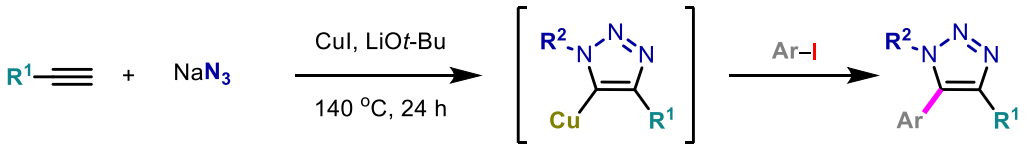

Scheme 1.23. Cu-catalyzed sequential reaction

In 2010, Ackermann[58] introduced a novel methodology focused on Pd-catalyzed intramolecular dehydrogenative direct arylation of 1,2,3-triazole. This innovative approach enables the synthesis of tri- and tetracyclic fused 1,2,3-triazole structures, representing a significant expansion in the scope of accessible triazole derivatives (Scheme 1.24).

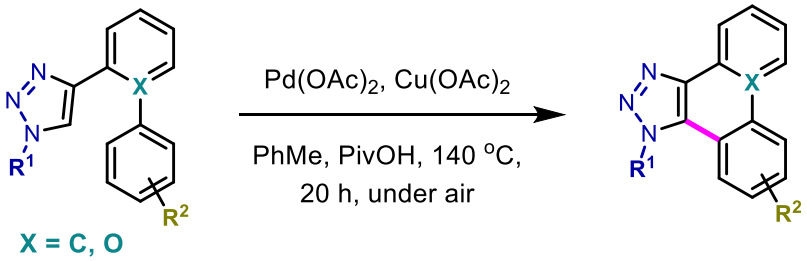

Scheme 1.24. Pd- catalyzed intramolecular C–H activation with triazole

R.V. Anand[59] developed a Cu-catalyzed one-pot approach for synthesizing 1,2,3-triazole-fused tricyclic heterocycles. This innovative tandem approach entails the 1,6-conjugate addition of Me_3SiN_3 to *o*-alkynylated *p*-quinone methides, followed by an intramolecular [3+2]-cycloaddition reaction (Scheme 1.25).

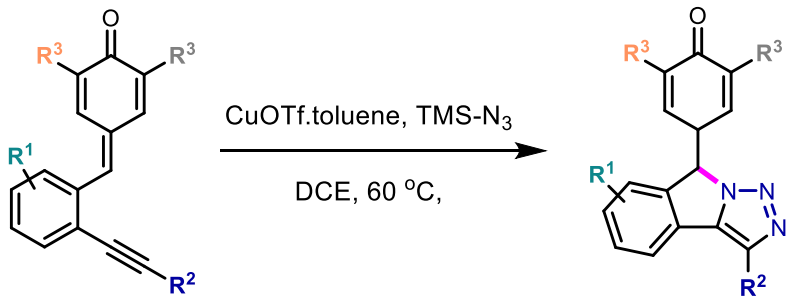

Scheme 1.25. Cu-catalyzed one-pot approach

A practical Cu-catalyzed multicomponent reaction has been developed by A.X. Wu[60] for the synthesis of 1H-[1,2,3]triazolo[4,5-c]quinoline derivatives using commercially available 2-bromobenzaldehydes, aryl methyl ketones, and sodium azide. This innovative protocol integrates consecutive base-promoted condensation, [3+2] cycloaddition, Cu-catalyzed S_NAr (substitution nucleophilic aromatic), and denitrogenation cyclization sequences. Preliminary mechanistic studies indicate that $CuBr_2$ serves as a multifunctional catalyst to facilitate and streamline this domino process (Scheme 1.26).

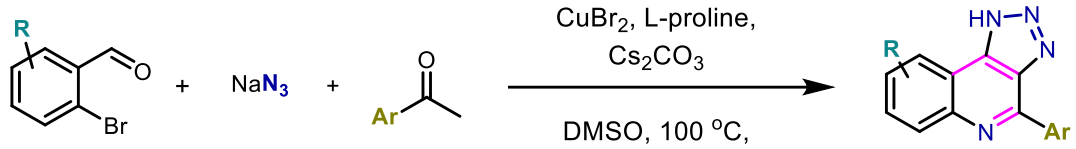

Scheme 1.26. Cu-catalyzed multicomponent reaction

1.2.5 Biological applications of triazole

The triazole ring, comprising both 1,2,3-triazole and 1,2,4-triazole, has garnered significant interest from researchers owing to its unique physicochemical characteristics. These attributes render it an attractive heterocycle for drug design, offering a less lipophilic option compared to the phenyl ring, or substituting heterocycles like homologous azines. Additionally, the triazole ring can mimic diverse functional groups such as amides and esters, further enhancing its utility in medicinal chemistry.[61] The synthesis of 1,2,3-triazole *via* click chemistry holds particular significance as it serves as a versatile connector to link two pharmacophore fragments.[62] Moreover, owing to their distinctive pKa characteristics, both 1,2,3-triazole and 1,2,4-triazole serve as versatile ligands for transition metal complexes and nonmetal organic catalysts, facilitating the formation of C−C bonds and commonly employed as precursors for carbonyl compounds.[63] The unique structural attributes of triazole enable diverse noncovalent interactions with various biological targets, demonstrating its dual capacity as both a hydrogen bond donor (HBD) and a hydrogen bond acceptor (HBA).[64] The inherent physicochemical properties of triazole and its fused homologues render them indispensable in the design of bioactive heterocycles.

Out of 1197 small molecule drugs introduced into the U.S. market from 1983 to 2012, only 13 featured the 1,2,4-triazole moiety. Conversely, just two drugs containing 1,2,3-triazole were FDA-approved during this period (Figure 1.2).[65] By 2020, the number of small molecule drugs incorporating the 1,2,4-triazole structure had risen by five, while those containing 1,2,3-triazole

increased by one.[66] As of 2023, three additional small molecule drugs containing the 1,2,4-triazole structure were approved, along with one more drug containing 1,2,3-triazole.[67] These statistics encompass small molecule drugs containing benzotriazole moieties as well. Notably, among the structurally related compounds, 1,2-dihydro-3H-1,2,4-triazol-3-one and 4H-benzo[*f*][1,2,4]-triazolo[4,3-*a*][1,4]diazepine are prominent.[65]

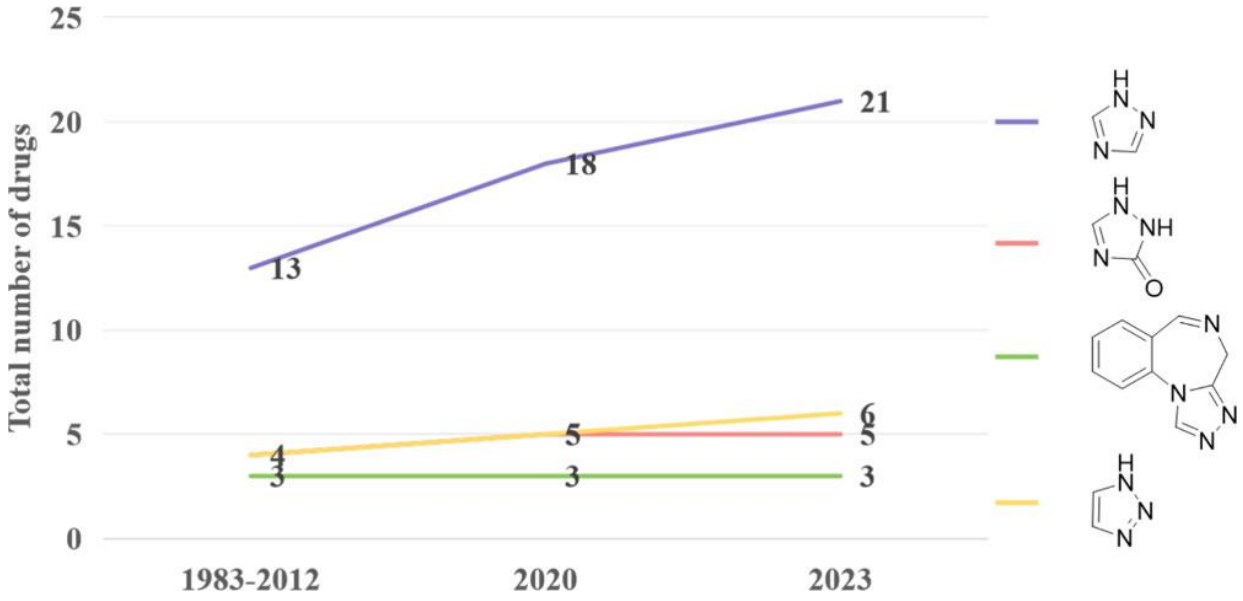

Figure 1.2. Graph of FDA-approved drugs containing triazole in different years

Both 1,2,4-triazole and 1,2,3-triazole have attracted attention in drug design, with 1,2,4-triazole playing a particularly pivotal role. It serves as a key pharmacophore widely utilized in the design of small molecule inhibitors, including antifungal agents and aromatase inhibitors.[68] In FDA-approved drug structures, 1,2,3-triazole is frequently employed in dual orexin receptor antagonists (DORAs) used for the treatment of insomnia. Examples of such drugs include daridorexant and suvorexant.[69] 1,2,3-Triazole is preferred in drug synthesis because of its facile synthetic methods, especially with the widespread utilization of "click" chemistry and bioorthogonal coupling reactions in medicinal chemistry. Notably, 1,2,3-triazole serves as a crucial linker in drugs through "click" chemistry.[70] Efforts have been undertaken to address the limitations of traditional small molecule inhibitors through the design of proteolysis targeting chimeras (PROTACs) and hydrophobic tagging (HyT) degraders, as well as peptide−drug conjugates (PDCs) incorporating 1,2,3-triazole linkers via "click" chemistry.[71] Some agents containing 1,2,3-triazoles and 1,2,4-triazoles approved for clinical treatment are shown in (Scheme 1.27).

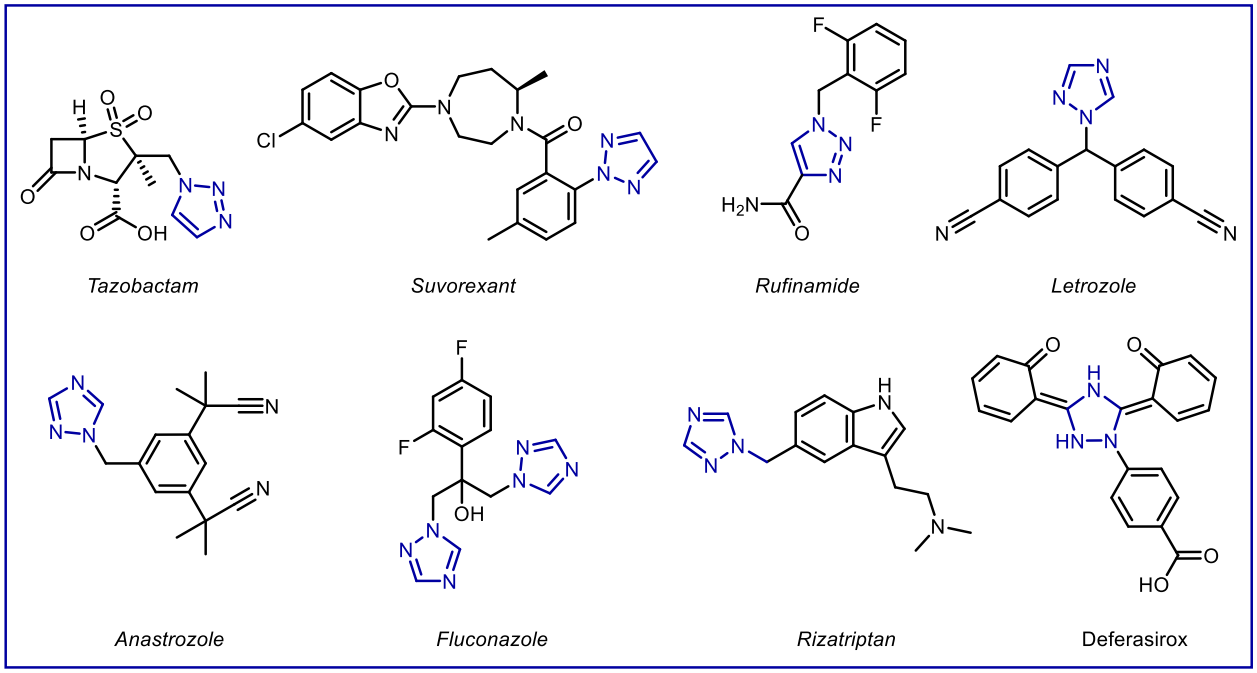

Scheme 1.27. Existing FDA-approved drugs containing triazole

1.3 Sulfur(VI) Fluoride Exchange Chemistry (SuFEx)

In 2014, K. B. Sharpless and their colleagues introduced sulfur(VI) fluoride exchange (SuFEx) as a next-generation click reaction.[72] SuFEx represents a rebirth of classical chemical methods, embodying a powerful methodology for establishing robust linkages with extensive tolerance towards diverse functional groups, all while operating in metal-free settings, ensuring unparalleled reliability.

In contrast to the typical sulfur(VI)–chloride bond with an approximate bond dissociation energy of around 45 kcal/mol,[73] sulfur(VI)–fluorides exhibit a notably higher bond dissociation energy, approximately 80 kcal/mol,[73-74] rendering them considerably resistant to hydrolysis and capable of withstanding a wide array of conditions commonly encountered in chemical reactions. The sleeping sulfur(VI)–fluoride bond is typically activated through the introduction of a hydrogen proton (H^+) and/or a silyl group (R_3Si^+), while the SuFEx linkage process can be expedited with the inclusion of tertiary amines (Scheme 1.28).

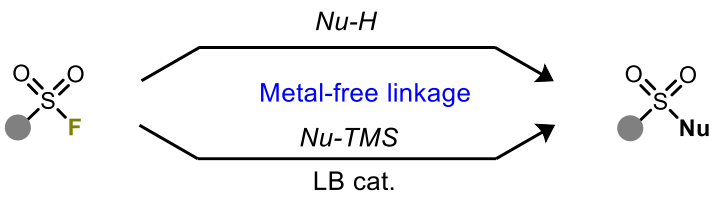

Scheme 1.28. Classic SuFEx reaction.

1.3.1 SuFEx hubs and their molecular linkage

SuFEx hubs, also known as SuFExable 'molecular plugins,' encompass molecules featuring the pivotal S–F bond. These hubs act as pivotal connecting nodes, facilitating the formation of diverse linkages (such as S–O, S–N, and S–C) around a central sulfur core, thereby enabling the construction of intricate molecular architectures. To date, numerous research groups have established the potential of SuFEx hubs such as sulfonyl fluorides (R–SO_2F), sulfuryl fluoride (SO_2F_2),[75] thionyl tetrafluoride (SOF_4),[76] ethenesulfonyl fluoride (CH_2=CH–SO_2F),[77] thiazyl fluoride (NSF_3)[78] (Scheme 1.29)

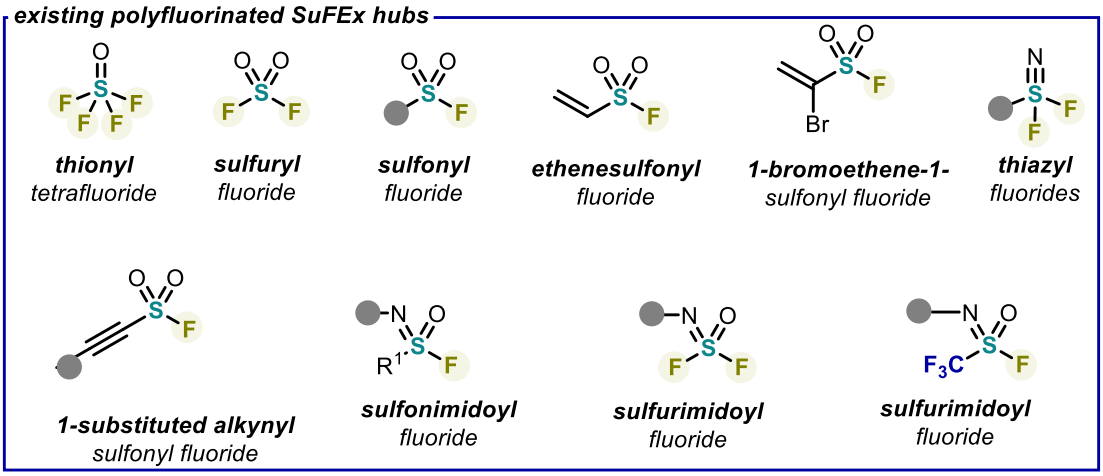

Scheme 1.29. Existing SuFEx hubs used in SuFEx chemistry

These "molecular plugins" collectively facilitate the efficient and selective establishment of connections around the Sulfur(VI) core within the realm of SuFEx Click Chemistry. Through this capability, SuFEx chemistry has unlocked a plethora of applications within the domain of synthetic chemistry, broadening the scope of feasible synthetic pathways and enabling the synthesis of diverse molecular structures with precision and efficiency.[79]

1.3.2 Possible mechanisms of SuFEx reactions

Despite the growing utility of the SuFEx reaction as a click chemistry tool, there remains a necessity for continued investigation into its underlying mechanism. In 2020, Luy and Tonner conducted a pivotal study utilizing a model SuFEx reaction, specifically the interaction between methanesulfonyl fluoride and methylamine. Through the application of density functional theory (DFT), they elucidated that the SuFEx reaction mechanism can be comprehended as an S_N2-type

reaction. Additionally, their findings indicated that enhancing the nucleophilicity of the primary amine through the addition of a base could substantially reduce the reaction barrier[80] (Scheme 1.30, A).

Furthermore, the research conducted by the Zuilhof group delved into the mechanistic intricacies of the sulfonimidoyl fluoride SuFEx reaction. By examining the chirality of both substrates and products, they aimed to differentiate between S_N1 and S_N2 pathways as well as addition/elimination mechanisms[81] (Scheme 1.30, B). Notably, the absence of racemization observations suggests that the S_N1 mechanism is unlikely. Instead, when employing a suitable nucleophile, both addition–elimination and S_N2 mechanisms emerge as the most widely acknowledged pathways. Importantly, both mechanisms yield stereospecific products.

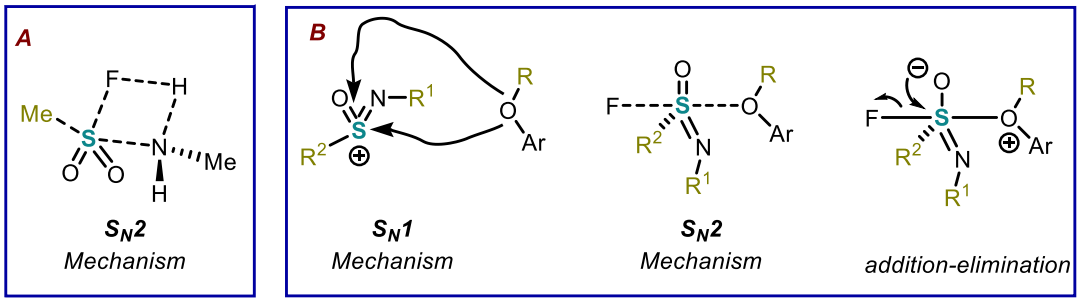

Scheme 1.30. Possible mechanisms of SuFEx reactions: S_N1, S_N2 and addition-elimination

To ascertain the more likely mechanism between the two, several factors need consideration. The ultimate determination hinges on various aspects such as the cumulative influence of leaving groups (LG), substituents attached to the sulfur atom, solvent properties, nucleophiles, among others, as demonstrated in prior studies on substitution reactions involving disulfides.[82] While this research succeeded in discarding one of the three proposed mechanisms, achieving a comprehensive understanding remains challenging. Nevertheless, three key facts have been substantiated:

1. The distinctive capacity of fluoride ion (F^-) to transition from a robust covalent bond to a leaving group, facilitated by interactions with 'H^+' and/or 'R_3Si^+', is pivotal to the reactivity observed in SuFEx reactions.
2. Incorporating silyl activated groups could enhance the reliability of SuFEx reactions in metal-free environments while potentially decreasing the need for base loading, because of the thermodynamics of the Si–F bond (with a bond-dissociation energy (BDE) of 135 kcal mol^{-1}).[81]

3. Typically, SuFEx reactions are catalyzed by a Lewis base amine,[83] such as DBU, BEMP, and BTMG in conjunction with the silicon additive hexamethyldisilazane HMDS[84]. Alternatively, bifluoride salts[85], or other catalysts, such as $Ca(NTf_2)_2$[86], and the combination of 1-hydroxybenzotriazole with 1,1,3,3-tetramethyldisiloxane (HOBt/TMDS)[87], may also be employed.

1.3.3 SuFEx chemistry application

1) Application in Synthetic methodology

In addition to the development of SuFExable hubs, numerous reports have emerged highlighting new techniques for incorporating SuFEx functionality into a diverse array of molecular scaffolds. Sharpless, Wu, and co-workers were the first to report a Heck–Matsuda cross-coupling approach between ethene sulfonyl fluoride (ESF) and arenediazonium tetrafluoroborate salts, resulting in the formation of β-arylethenesulfonyl fluorides (Scheme 1.31A).[88] The β-aryl ESF products retain an activated C=C bond, making them versatile bifunctional connectors that can be further functionalized through conjugate addition pathways and/or SuFEx transformations.

Alongside the rapid advancement of SuFEx chemistry as a technology for creating molecular connections, there has been a notable expansion in methodologies aimed not only at synthesizing S–F bond-containing substrates but also at developing these compounds as reagents in their own right. While this approach deviates from the core 'molecular plugin' concept of SuFEx, the development of these valuable methodologies and transformations has only been made possible by the emergence of the SuFEx reaction family.

This area of research was further expanded by Doyle and co-workers with the development of 2-pyridinesulfonyl fluoride, known as “PyFluor”, as a reagent for the deoxyfluorination of alcohols. As with conventional SuFEx reactions, strong amidine or guanidine bases such as DBU or MTBD were employed, albeit in super-stoichiometric quantities. This approach leads to the rapid formation of an intermediate sulfonate species, which gradually reacts with free fluoride ions to produce alkyl fluorides in good to excellent yields (Scheme 1.31B).[89] Furthermore, a modified version of PyFluor, labeled with radioactive ^{18}F, was demonstrated to be an effective reagent for incorporating the radioactive label into molecules, achieving this with short reaction times (Scheme 1.31C and D).[89]

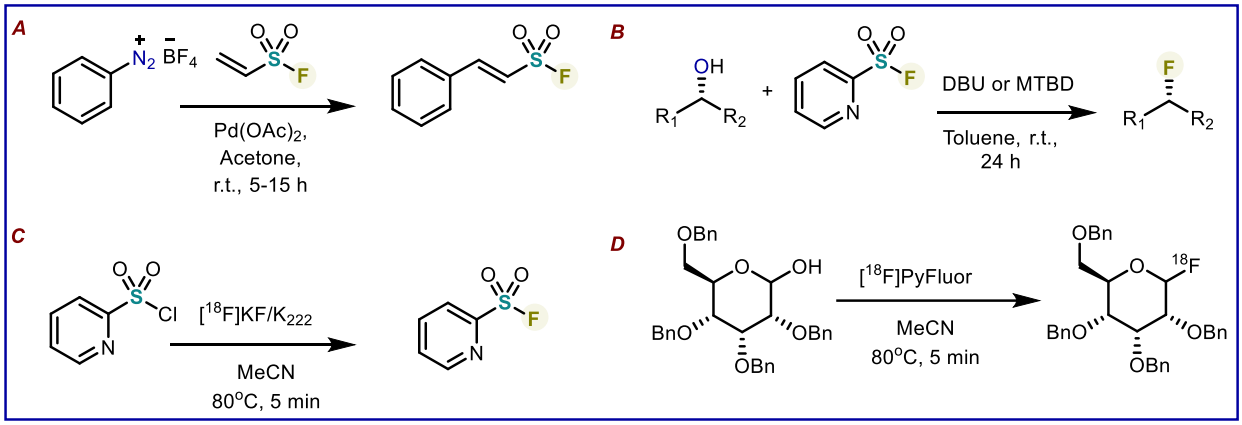

Scheme 1.31. Different SuFEx reactions used in synthetic methodologies

2) **Bio-SuFEx: applications of SuFEx click chemistry in chemical biology and drug discovery**

The exchange of sulfur–fluoride bonds to form covalent linkages has long been appreciated in chemical biology—with reports of aryl sulfonyl fluorides being employed as electrophilic probes from as early as the 1950's. Myers and Kemp's pioneering work on sulfonyl fluoride inhibition of proteases, followed by Fahrney and Gold's work on serine protease inhibitors are seminal contributions.[90] Unlike more reactive electrophilic groups such as acrylamides, vinyl sulfones, and fluorophosphonates, S–F-based probes tend to be comparatively unreactive.[91] Activation of their S–F centers typically rely on the assistance of nearby amino acid sidechains. Despite this lower inherent reactivity, S–F-based probes have been successfully used to target active residues such as serine, tyrosine, lysine, threonine, histidine, and cysteine.

Among the SuFEx hubs mentioned earlier, sulfonyl fluorides (SFs, $–SO_2F$), aryl fluorosulfates (AFs, $–OSO_2F$), and sulfuramidimidoyl fluorides (SAFs, $–N=S(O)(NR_1R_2)F$) have emerged as novel warheads in ABPP, representing a new generation of probes.[92] In contrast to other ABPs, these SF-containing modulators facilitate covalent modification of protein pockets without specifically targeting cysteines. This feature complements the "beyond-cysteine"[93] approaches and significantly broadens applicability across the proteome. Additionally, one of the most intriguing characteristics of SuFEx is its proximity-driven reactivity. In essence, SuFEx reagents remain inert until their fluoride groups are activated by binding pockets through appropriate solvation.[94] In the realm of ABPP, SFs were initially designed to covalently react with a range of residues, including serine,[95] tyrosine,[96] and lysine.[97] Subsequently, the focus shifted primarily to lysine residues.[98] More recently, the SAFs, introduced by the groups of Sharpless and Kelly, emerged as an imino analogue of SFs. These SAFs possess comparable click

properties to SFs but offer an additional "handle" at the nitrogen atom for modifying chemical properties (Scheme 1.32).

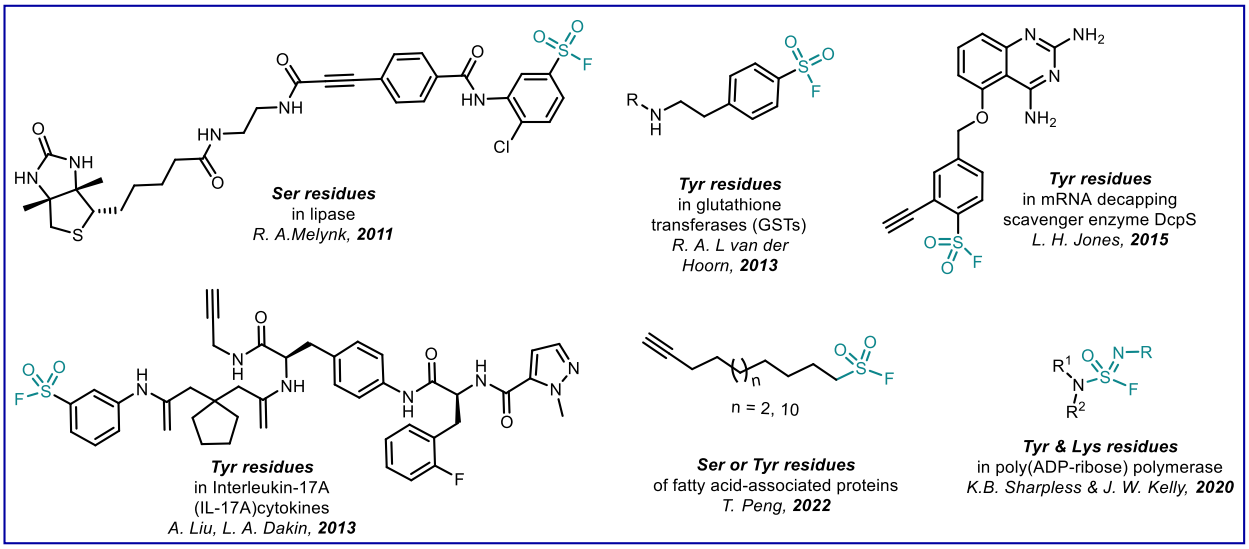

Scheme 1.32. SF-based probes used in ABPP

A pioneering study by Wu and co-workers demonstrated the utility of SuFEx click chemistry as a valuable tool for late-stage functionalization (LSF) of bioactive molecules.[99] Over the past decade, LSF has become an increasingly important technique, allowing for the rapid diversification of drug-like molecules at the later stages of synthesis. This approach aims to enhance both the physical and pharmacokinetic properties of the compounds, contributing to the overall optimization of drug candidates. Wu's team utilized SO_2F_2 to convert a panel of NIH-approved anticancer drugs into their fluorosulfate derivatives directly in a 96-well plate, enabling a direct comparison of their biological activity with that of the parent compounds (Scheme 1.33). Screening a library of 39 compounds, three aryl fluorosulfates exhibited enhanced anticancer activity. Notably, the fluorosulfate derivative of combretastatin A4 showed a remarkable 70-fold increase in potency against the colon cancer cell line HT-29.

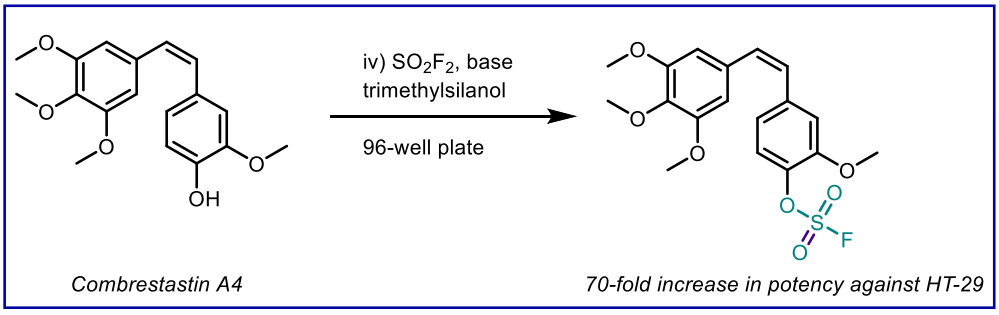

Scheme 1.33. SuFEx click chemistry as a late-stage functionalization (LSF)

More recently, the groups of Sharpless and Wolan introduced an innovative approach for discovering SuFExable small molecule covalent medicines using 'sleeping beauty' probes.[100] Their research highlighted the unique properties of sulfur fluorides as covalent warheads, particularly their remarkable ability to selectively and rapidly form covalent bonds with properly folded protein targets, while showing minimal reactivity towards their denatured counterparts (Scheme 1.34A).

The team screened a focused library of 105 randomly selected compounds from a principal collection of over 1000 in-house synthesized sulfur fluoride compounds against human neutrophil elastase (hNE). The compounds were categorized based on their sulfur fluoride functional groups. Among them, benzene-1,2-disulfonyl fluoride (177) was identified as a covalent modifier of hNE, exhibiting an IC50 of 3.3 μM. X-ray crystallography of the covalent protein-drug complex revealed that the inhibition mechanism involved the sulfonylation of Ser195 by the sulfonyl fluoride group (Scheme 1.34B). Further optimization of the hit compound through SuFEx chemistry led to the discovery of two new compounds with superior activity and selectivity compared to the parent compound. These include 2-fluorosulfonylphenyl triflone, with an IC50 of 1.1 μM, synthesized using Moses's late-stage SuFEx trifluoromethylation protocol, and 2-fluorosulfonylphenyl fluorosulfate, which exhibited an IC50 of 0.24 μM and demonstrated over 833-fold selectivity against the homologous neutrophil serine protease, cathepsin G.[85]

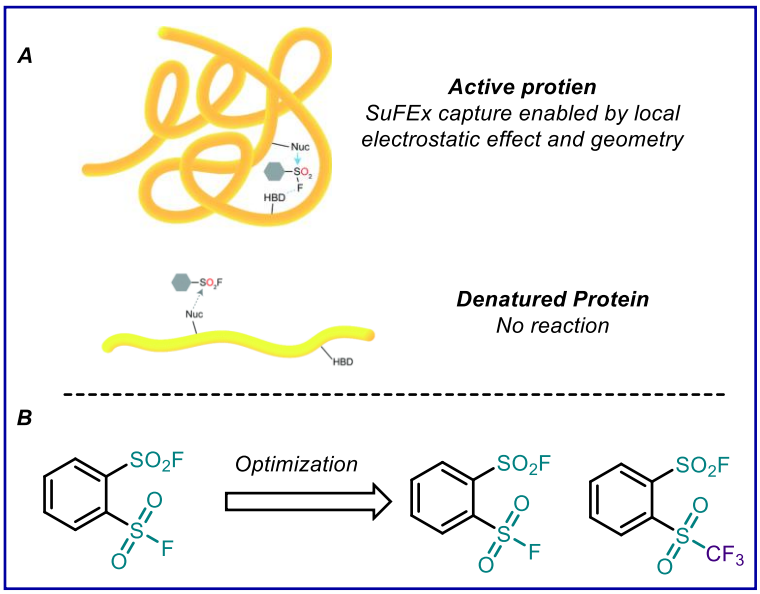

Scheme 1.34.A) SuFExable small molecules as 'sleeping beauty' probes B) Library of sulfur fluoride compounds against human neutrophil elastase (hNE)

In 2018, the group of Sharpless, Wilson, and Kelly introduced an "Inverse Drug Discovery (IDD)" strategy as a complement to the ABPP method, focusing on AFs as an example.[101] This innovative approach involved the use of a combination of chemical and proteomic techniques to identify proteins selectively modified by AFs containing an alkyne substructure. Subsequently, bioinformatics tools were employed to predict the functional consequences of these modifications. While ABPP typically utilizes simple, highly reactive probes to target specific enzyme classes, the IDD approach demonstrated that moderately complex probes with less reactive functional groups could form conjugates with a group of proteins possessing distinct functions capable of binding and reacting with the probe. Furthermore, by modifying the aromatic scaffold to which the electrophilic group is attached, different sets of proteins in the human proteome could be targeted. Through the integration of chemical, proteomic, and computational methodologies, researchers can identify and prioritize potential drug targets, thereby expediting the drug discovery process and potentially leading to the development of more effective and targeted therapies.

Chapter 2. This Thesis

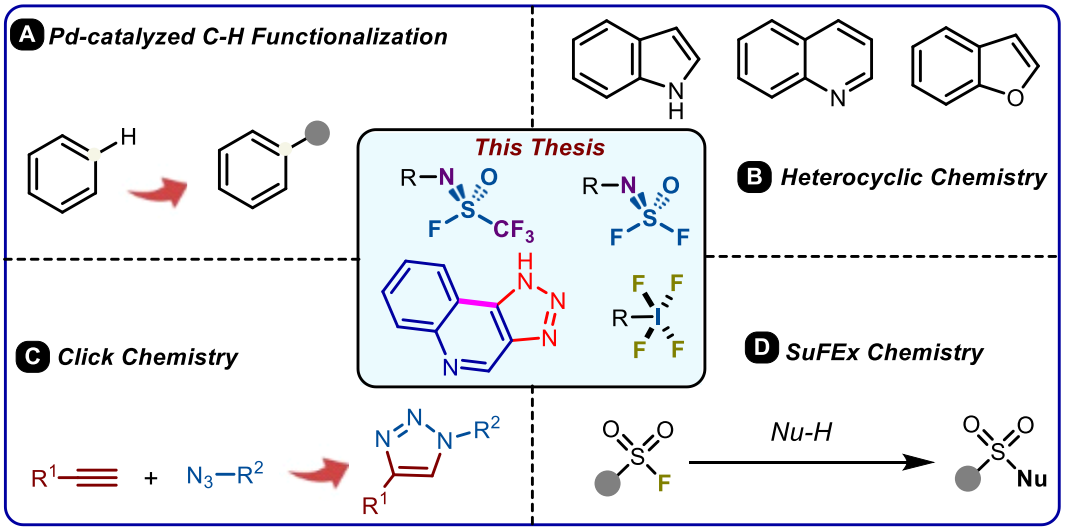

This thesis delves into the synthesis of biologically significant heterocyclic compounds, the development of SOF_4-gas-free SuFEx hubs, and the synthesis of hypervalent fluoroiodane compounds (IF_4).

Objectives of the Thesis:

1. **Synthesis of Novel 1,2,3-Triazole-Fused Heterocyclic Compounds:**
    - Utilize cutting-edge synthetic methodologies, including Pd-catalyzed intramolecular C–H activation, one-pot domino reactions, to develop novel 1,2,3-triazole-fused heterocycles.
2. **Development of SOF_4-Gas-Free SuFEx Hubs:**
    - Revolutionize the SuFEx (Sulfur Fluoride Exchange) reaction by designing SOF_4-gas-free hubs, thereby streamlining the process and making it more accessible for widespread application in research laboratories.
3. **Synthesis of Hypervalent Fluoroiodane Compounds (IF_4):**
    - Pioneer the synthesis of novel fluorinated reagents, specifically hypervalent fluoroiodane compounds (IF_4), to serve as versatile intermediate for fluorination processes in advanced organic synthesis.

A short summary to heterocycles

Why heterocycles? Why has Nature chosen these ring systems as a foundation for so many of her life processes? And why have organic chemists focused so much effort on understanding and synthesizing these materials? One reason is that heterocyclic rings (i.e. those containing atoms other than carbon) are present in the majority of known natural products, contributing to enormous structural diversity. In addition, they often possess significant biological activity. Medicinal chemists have leveraged this feature as a crucial factor in the development of most small molecule drugs use today. Indeed, a 2014 study found that nearly 60% of all FDA-approved drugs in this category incorporate a nitrogen heterocycle. Oxygen and sulfur heterocycles are also well represented.

Heterocycles represent a vast and diverse group of organic compounds, both naturally and synthetic, with a wide range of molecular structures and biological activities. Their unique physical and chemical properties, coupled with their significant bioactivities, make them the most extensive and varied family of organic compounds. These compounds play a crucial role in the biochemistry, structure, and function of all classes of living organisms and are integral to synthetic applications such as drugs, agrochemicals, herbicides, materials, ligands, and catalysts. They are also pivotal in the production of polymers, organic light-emitting diodes (OLEDs), and molecular wires. Consequently, heterocycles have a profound impact on numerous fields of research, including organic synthesis, medicinal chemistry, chemical biology, analytical chemistry, materials science, and catalysis.[65a, 102]

A notable subgroup of heterocycles is the benzo-fused heterocycles, where a heterocyclic ring is fused with a benzene ring. These compounds are widespread in both natural products and synthetic molecules, exhibiting remarkable structural diversity and a wide range of biological activities, such as antimalarial, antibacterial, anticancer, antidiabetic, antiviral, anti-HIV, anti-inflammatory, antianaphylactic, antimicrobial, and antifungal properties.[103] Due to these diverse biological activities, many benzo-fused heterocycles are considered privileged structures in medicinal chemistry. Figure 1 highlights some of the most significant examples of these compounds.

Among the various classes of heterocyclic compounds, nitrogen-containing heterocycles (N-heterocycles) are the most prevalent. Their significance as key structural units in FDA-approved small-molecule drugs are well-documented. A survey by Paul and Kumar provides statistical evidence of this, showing that 88% of small molecule drugs approved by the FDA between 2015 and 2020 contain one or more N-heterocyclic units.[104] Oxygen-containing heterocycles (O-

heterocycles) are the second most common type found in FDA-approved pharmaceuticals.[105] Although less common than their nitrogen and oxygen counterparts, sulfur-containing heterocycles (S-heterocycles) fused with benzene rings are also valuable core fragments in commercial drugs and drug candidates.[104]

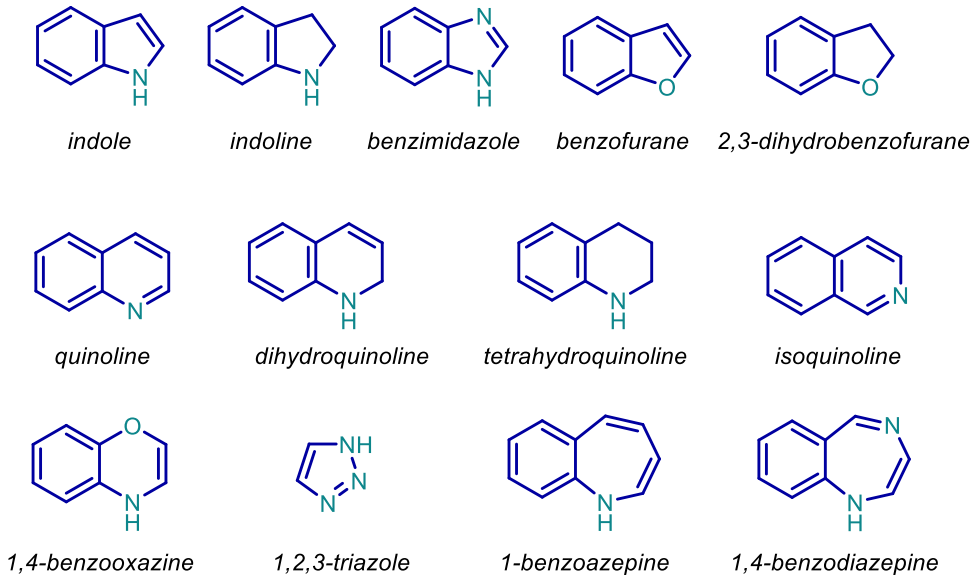

Figure 1. Selected examples of benzo-fused heterocycles

Fused heterocyclic compounds, where two or more rings share common atoms, represent an important and fascinating class of compounds within organic chemistry. The fusion of a heterocycle with another ring, such as a benzene ring, often leads to enhanced structural complexity and unique electronic properties, resulting in improved biological activity. The presence of these fused systems can lead to more efficient interactions with biological targets, making them key components in pharmaceuticals, agrochemicals, and other biologically active molecules. Here are examples of commercially available pharmaceuticals containing fused heterocyclic compounds. **Clopidogrel** (Figure 2, a) contains a fused thieno-tetrahydropyridine bicycle. Clopidogrel is indicated for use as an anticoagulant to lower the risk of stroke, blood clots, and postmyocardial infarction, and was first approved in 1997. Primarily marketed as an antipsychotic drug for the treatment of schizophrenia, **aripiprozole**, (Figure 2, b) contains a dihydroxyquinolinone fused-ring heterocycle tethered to an *N*-phenylpiperazine ring via an *n*-butyl chain. Another example is **atorvastatin**, (Figure 2, d) has the highest molecular weight at 463.55 g/mol, but still is comfortably within the desired mass for pharmaceuticals. The central functionality is a fully substituted pyrrole ring, including a para-fluorophenyl functionality. **Esomeprazole** (Figure 2, e) is an anti-ulcer medication that inhibits the functionality of the proton pumps in the stomach. **Esomeprazole** consists of a sulfoxide-coupled benzimidazole and trisubstituted pyridine. **Alprazolam** (Figure 2, c) is in a class of medications called

benzodiazepines, used to treat anxiety disorders and panic disorders (sudden, unexpected attacks of extreme fear and worry about these attacks). **Trapidil** (Figure 2, f), a platelet-derived growth factor antagonist, was originally developed as a vasodilator and anti-platelet agent and has been used to treat patients with ischemic coronary heart, liver, and kidney disease.

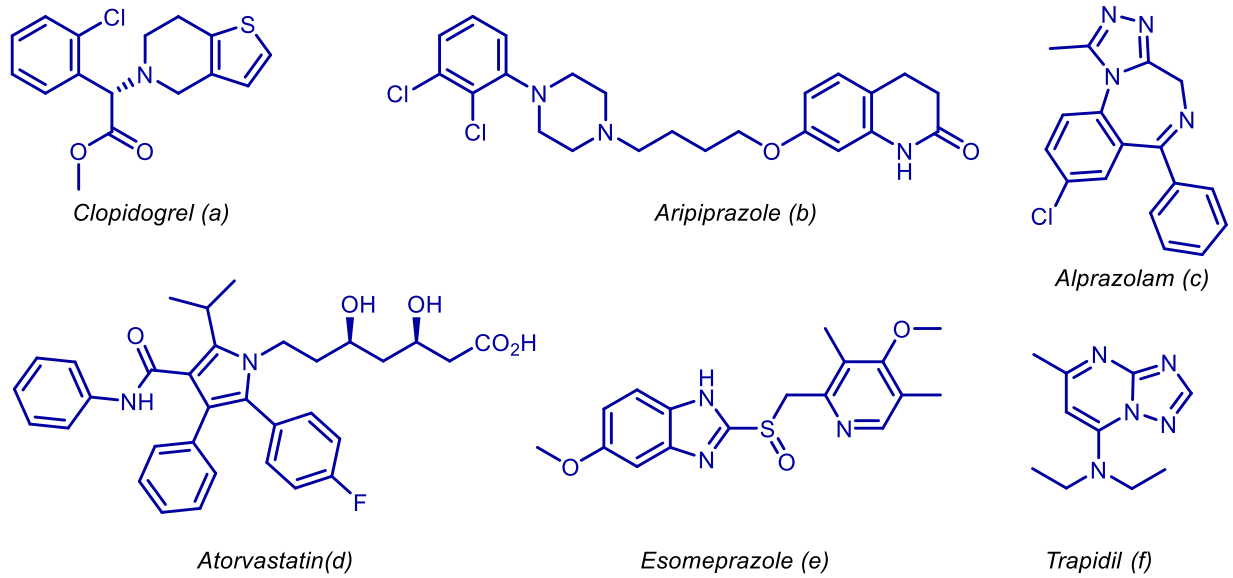

Figure 2. Heterocyclic compounds in drug discovery

The immense significance and widespread occurrence of heterocycles have made the efficient and rapid synthesis of these compounds a top priority. This challenge has fueled generations of synthetic chemists, inspiring the development of general, practical, and efficient strategies to construct these complex structures. Historically, few classes of compounds have stimulated as much synthetic innovation as heterocycles. As new target heterocycles continue to emerge daily, the field is not diminishing; rather, it is evolving towards more focused and challenging research endeavors. In particular, the development of new or enhanced synthetic methodologies that enable the rapid production of a diverse array of functionalized heterocycles remains a critical area of interest in modern drug discovery.

Within the broad category of heterocycles, the 1,2,3-triazole ring has emerged as one of the most prominent and widely studied structures due to its biological relevance and robust synthetic utility. The 1,2,3-triazole core is characterized by its nitrogen-rich five-membered ring, which imparts exceptional stability and unique electronic properties, such as high polarity and resistance to metabolic degradation. These features make 1,2,3-triazoles particularly attractive for drug development, where they have demonstrated a broad spectrum of biological activities, including anticancer, antiviral, antibacterial, and antifungal properties.

Fusing the triazole ring with other heterocyclic systems not only increases molecular complexity but also enhances the biological properties of the resulting compounds. The fusion can stabilize the molecules, promote stronger interactions with biological targets, and lead to compounds with superior pharmacokinetic profiles. The exploration of novel 1,2,3-triazole fused heterocycles is, therefore, a key area of research in drug discovery and development.

The synthesis of novel 1,2,3-triazole fused heterocyclic compounds involves a strategic approach that incorporates three crucial synthetic steps: 1) propargylation, 2) CuAAC (Copper-catalyzed Azide-Alkyne Cycloaddition), and 3) intramolecular C–H activation. Each of these steps plays a key role in the efficient construction of complex, functionalized 1,2,3-triazole fused heterocycles (Scheme 1).

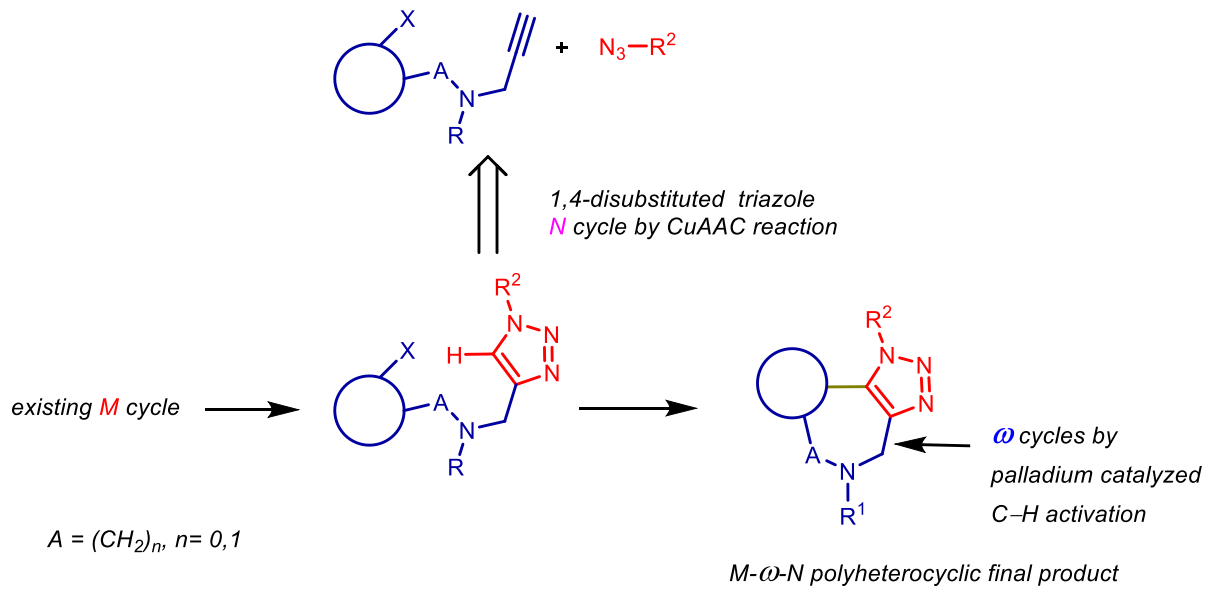

Scheme 1. General scheme of 1,2,3-triazole fused heterocycles

Propargylation: The synthesis begins with the propargylation of a precursor molecule. Propargylation refers to the introduction of a propargyl group (–$CH_2C{\equiv}CH$) into the substrate, which serves as a crucial handle for the subsequent CuAAC reaction. The propargylation step is typically accomplished by reacting an appropriate nucleophile (such as an amine or alcohol) with a propargyl halide or propargyl ester. This step sets up the alkyne moiety necessary for the copper-catalyzed cycloaddition that follows. Propargylation is an important first step as it introduces the functional group that facilitates the cycloaddition, enabling the formation of the triazole ring in the next stage.

CuAAC: In the second step, the alkyne introduced in the propargylation step reacts with an organic azide under CuAAC conditions to form a 1,4-disubstituted 1,2,3-triazole ring. CuAAC is a highly efficient, regioselective, and versatile reaction, often referred to as “click chemistry”

due to its simplicity and reliability. This cycloaddition reaction is crucial for constructing the 1,2,3-triazole core, which is central to the structure and functionality of the target fused heterocyclic compounds. The mild reaction conditions and high functional group tolerance of CuAAC allow for the synthesis of a wide range of triazole derivatives, making this a critical step in the overall synthetic route.

Intramolecular C–H activation: The final step in the synthesis involves intramolecular C–H activation, which facilitates the cyclization necessary to form the fused heterocyclic system. In this process, a C–H bond within the molecule is selectively activated and functionalized to form a new carbon-carbon or carbon-heteroatom bond, closing the ring and generating the fused triazole-heterocycle. C–H activation provides access to a variety of complex, highly functionalized fused heterocycles that would be challenging to synthesize through traditional methods.

The next four chapters, as illustrated in Scheme 2, focus on the synthesis of 1,2,3-triazole fused heterocyclic compounds using advanced synthetic methodologies. These chapters delve into the detailed exploration of each key step in the synthesis process, providing a comprehensive understanding of the strategies employed to construct these complex molecules.

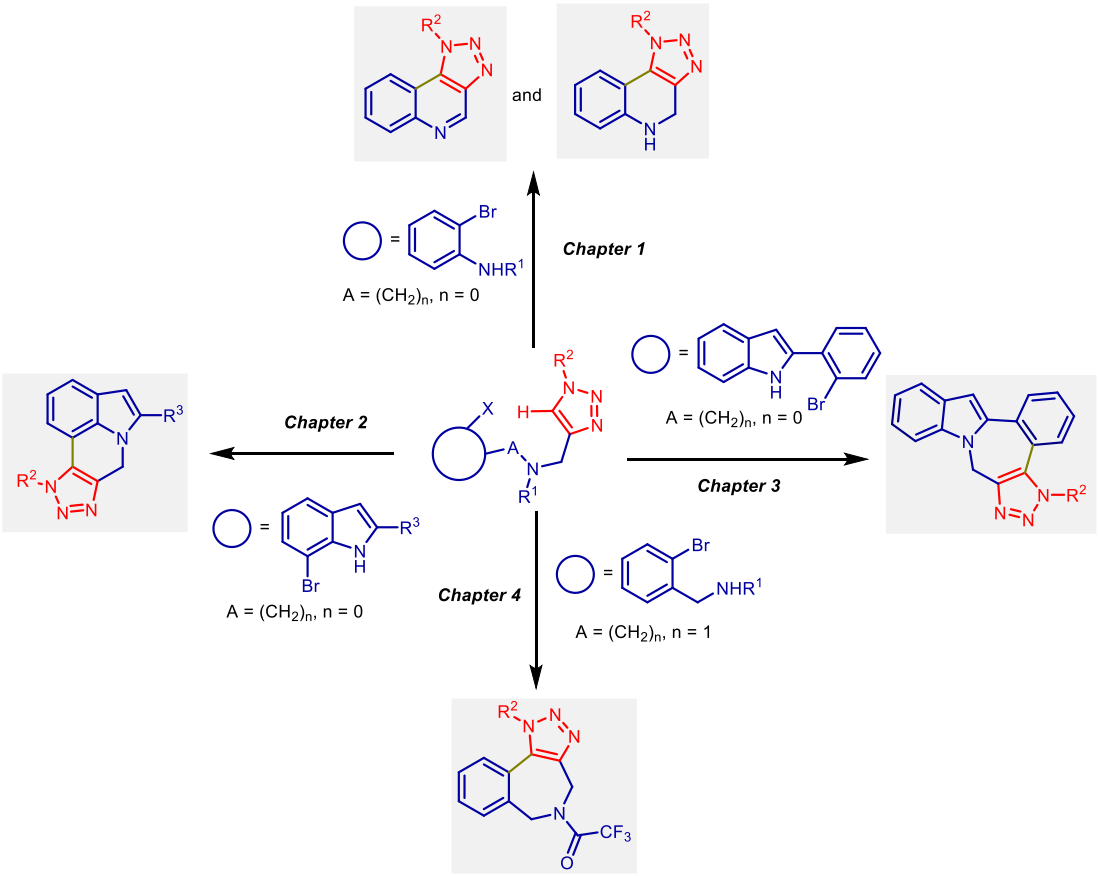

Scheme 2. Overview of next four chapters.

Chapter 3. Cu/Pd-catalyzed controlled intramolecular C–H annulation for the synthesis of quinoline or dihydroquinoline fused-1,2,3-triazole

3.1 Introduction

Heterocycles represent the most general structural moiety in many natural and synthetic bioactive compounds.[106] Among them, nitrogen-containing heterocyclic compounds are one of the most significant heterocycles, as they are privileged scaffolds possessing interesting biological, physicochemical, and pharmaceutical features.[107] In N-heterocycles, quinolines are one of the most significant heterocycles with intriguing biological activities.[108] Organic compounds with quinoline as a core structure have drawn extensive interest due to their broad range of applications in material science and biologically important activities such as anticancer, antioxidant, antimalarial, and antioxidant.[109] On the other hand, 1,2,3-triazoles are important N-heterocyclic scaffolds with a wide range of applications in organic synthesis, polymer science, materials science, and the pharmaceutical industry.[48, 110] The discovery of Cu(I)-catalyzed [3+2]-cycloaddition of azides with alkynes (CuAAC), the so-called “Click Chemistry”, by Nobel laureates K.B. Sharpless and M. Mendal has sparked renewed interest in the 1,2,3-triazole scaffold. "Click chemistry" describes the ease of the CuAAC reaction under mild conditions, which allows it to circumvent the challenges of low regioselectivity and high reaction temperature. [111]

Fused polycyclic heterocycles are the structurally most prevalent motifs in organic chemistry, with extensive applications.[112] 1,2,3-triazole-fused polycyclic heterocycles have been widely utilized as core structures in pharmaceutical targets and biologically active substances.[113] Recent reports indicate that triazole-fused polycyclic compounds possess effective serine protease inhibitory effects,[114] antibacterial activities,[115] GPR109A agonists,[116] cardiovascular agents, and promising anticancer activity.[117] In this context, 1,2,3-triazoles fused with quinolines are particularly interesting structures containing both quinoline and triazole systems.[118]

C–H activation/functionalization transformed the way that organic chemists approached the synthesis of target molecules. Interestingly, C–H activation is the most powerful approach towards C–C bond and C–X bond formation and one of the most viable tools for the synthesis of complex targets.[119] Transition-metal-catalyzed cyclization of C(sp^2) –H bonds through direct coupling with C–C multiple bonds an attractive and powerful motive because of their high efficiencies in the building of cyclic complex moieties, which play an important role in modern

organic chemistry.[120] In particular, the palladium (Pd) ability to activate the C–H bonds has been extensively utilized in organic synthesis.[121] In this context, our group has done a lot of work on palladium-catalyzed C–H functionalization, Heck coupling, Suzuki–Miyaura coupling, Tsuji–Trost allylation, and Buchwald–Hartwig amination reactions.[122]

As illustrated by several reports describing the synthesis of quinoline fused-triazoles, in particular, 1*H*-[1,2,3]triazolo[4,5-*c*]quinolines are a kind of structurally distinct triazole-fused heterocycle that contains both quinoline and 1,2,3-triazole frameworks. Due to the excellent therapeutic potential of quinoline and 1,2,3-triazole, it is assumed that this class of fused heterocycles may feature as a promising skeleton for the development of new chemical therapeutic agents. Nevertheless, only a few studies on synthetic methodologies for the synthesis of novel 1*H*-[1,2,3] triazolo[4,5-*c*] quinolines have been reported. Therefore, it is still an intriguing and desirable challenge to design and assemble this structurally novel class of fused N-heterocycles from readily available materials using an efficient and controlled catalytic methodology. For instance, in 2013, Chen and coworkers described the CuO-promoted tandem S_NR and cyclization of (*E*)-3-(2-bromoaryl)-1-arylprop-2-en-1-ones and sodium azide (Scheme 1A).[123] Later in 2018, Elangovan developed an oxidative azide-olefin [3+2] cycloaddition of organic azides with 2-hydroxychalcones and 2-nitrochalcones, followed by Fe/AcOH-mediated intramolecular reductive cyclization of 4-benzoyl-5-(2-nitrophenyl)-1,2,3-triazoles (Scheme 1B).[124] In 2020, Hu group developed a tandem TBAF-catalyzed intermolecular azide-alkyne cycloaddition (AAC) of β-(2-aminoaryl)-α,β-ynones and trimethylsilyl azide ($TMS–N_3$), followed by intramolecular dehydration annulation reaction (Scheme 1C) .[125]

Inspired by the aforementioned works, we set out to design flexible and powerful routes for the faster, easier, more efficient, and more controlled synthesis of quinolines or dihydroquinoline fused-1,2,3-triazoles through C–H bond annulation. We herein report, Cu/Pd-catalyzed an efficient and controlled two pathways for the synthesis of structurally diverse fused polycyclic quinolines, such as [1,2,3]triazolo[4,5-*c*]quinoline (3.3) or 4,5-dihydro-[1,2,3]triazolo[4,5-*c*]quinoline (3.4), via intramolecular C–H annulation (Scheme 1D). The synthesis consists of copper azide-alkyne cycloaddition (CuAAC) to synthesize the 1,2,3-triazole precursors, followed by Pd-catalyzed intramolecular ring closure/annulation to get our desired products (3.3 or 3.4) in good to excellent yield.

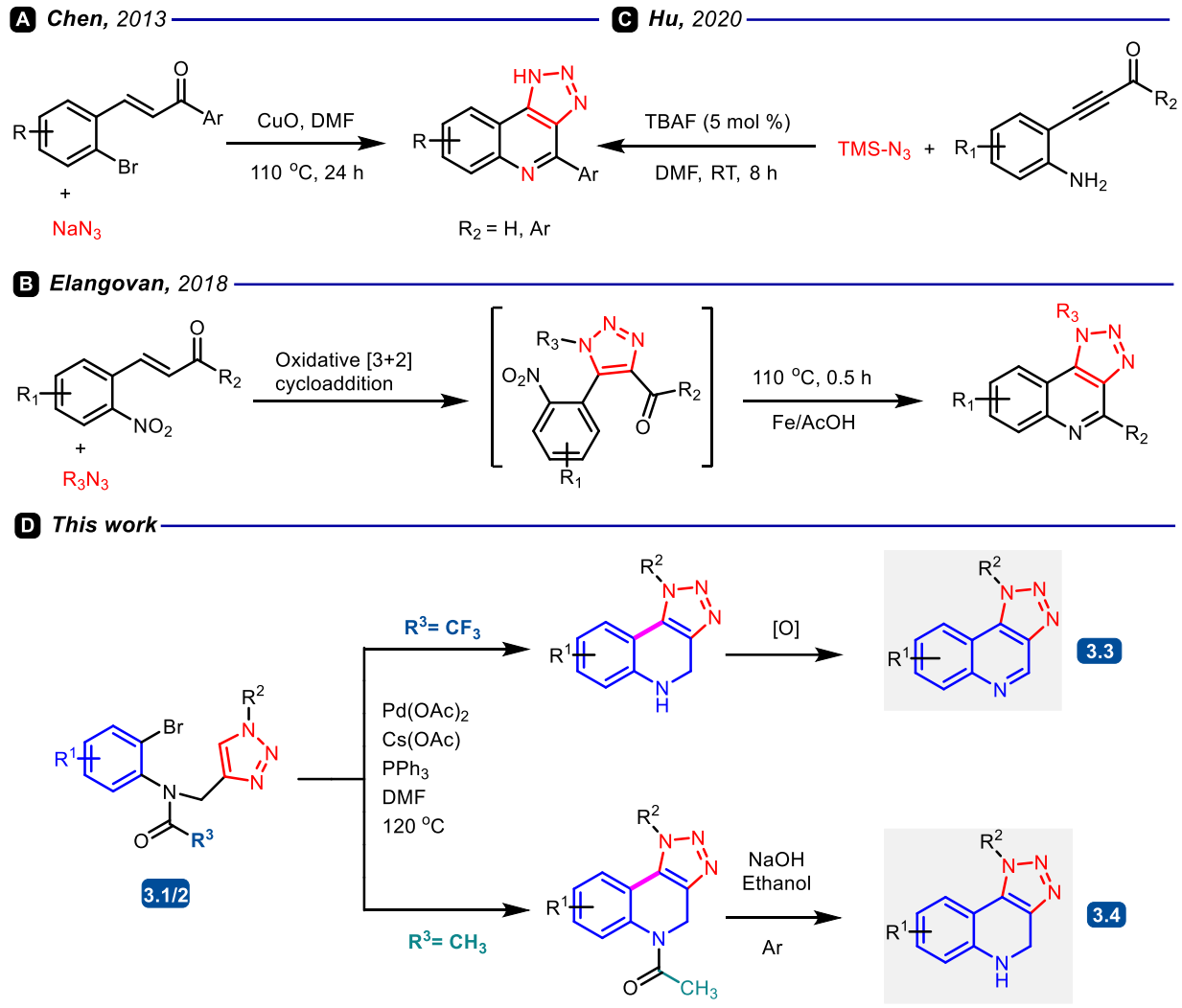

Scheme 3.1. Previous works and present work

3.2 Results and Discussion

At the outset, we commenced our investigations for the preparation of 1-benzyl-1*H*-[1,2,3]triazolo[4,5-*c*]quinoline (3.3a), N-((1-benzyl-1*H*-1,2,3-triazol-4-yl)methyl)-N-(2-bromophenyl)-2,2,2-trifluoroacetamide (3.1a) was chosen as a model substrate to optimize the intramolecular C–H activation/annulation. The substrate (3.1a) was synthesized from N-(2-bromophenyl)-2,2,2-trifluoro-N-(prop-2-yn-1-yl)acetamide and azide *via* the CuAAC reaction (*see supporting information*). The C–H activation failed to occur for substrate 1a using $Pd_2(dba)_3$, base (K_2CO_3), and XPhose as a ligand in dry dioxane at 120°C (Table 3.1, entry 1). Gratifyingly, the reaction proceeds to give the desired product as a mixture of 3.3a and 3.4a in a combined 68% yield by using $Pd(OAc)_2$, PPh_3, and CsOAc in dry DMF (Table 3.1, entry 2). Encouraged by this promising result, we thoroughly investigated various reaction parameters to further improve the combined yield. We then assessed several solvents and temperatures, and we obtained the combined yields of 3.3a and 3.4a in 63, 53, 51, and 43%, respectively (Table 3.1,

entries 3-6). Interestingly, we obtained 3.3a and 3.4a in a high combined yield of 85% using DMSO as a solvent (Table 3.1, entry 7). The efforts were then turned toward obtaining the particular desired product 3.3a. We then investigated by utilizing an oxygen supply as a mediator for the conversion of 3.4a in the same reaction to obtain 3.3a. Encouragingly, we found that the oxygen atmosphere worked efficiently to afford the particular desired product 3.3a in excellent yield of 95% (Table 3.1, entry 8). Other types of solvents were also screened; however, it demonstrates that their capacity for the reaction is lower (Table 3.1, entries 9-11). To our delight, $Pd(OAc)_2$, PPh_3 and CsOAc in dry DMSO and then an oxygen source were demonstrated to be the most efficient optimized conditions to afford 3.3a compound with an excellent yield of 95% (Table 1, entry 8).

Table 3.1. Optimization of the Reaction Conditions. [a, b]

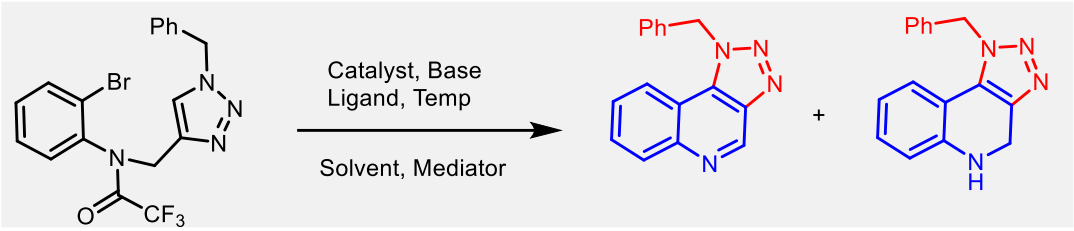

3.1a *3.3a* *3.4a*

Entry	Catalyst	Ligand	Base	Mediator	Solvent	Temp °C	Time	Yield[c] (%)	
								3.3a	**3.4a**
1	$Pd_2(dba)_3$	XPhos	K_2CO_3	-	Dioxane	120	12 h	-	-
2	$Pd(OAc)_2$	PPh_3	CsOAc	-	DMF	120	0.5 h	12	56
3	$Pd(OAc)_2$	PPh_3	CsOAc	-	DMF	100	1h	45	18
4	$Pd(OAc)_2$	PPh_3	CsOAc	-	DMF	80	3 h	38	15
5	$Pd(OAc)_2$	PPh_3	CsOAc	-	DMF	60	6 h	25	26
6	$Pd(OAc)_2$	PPh_3	CsOAc	-	MeCN	80	12 h	12	31
7	$Pd(OAc)_2$	PPh_3	CsOAc	-	DMSO	120	0.5 h	24	61
8	**$Pd(OAc)_2$**	**PPh_3**	**CsOAc**	**[O]**	**DMSO**	**120**	**1 h**	**95**	**-**
9	$Pd(OAc)_2$	PPh_3	CsOAc	[O]	DMF	120	1 h	65	-
10	$Pd(OAc)_2$	PPh_3	CsOAc	[O]	Dioxane	120	12 h	-	-

11	$Pd(OAc)_2$	PPh_3	CsOAc	[O]	MeCN	120	1 h	30	-

[a]Reaction Conditions: 1a (0.25 mmol), catalyst (5 mol%), base (2 equiv.,) Ligand (20 mol %), solvent (2 ml), [O]; [b]Reactions performed under argon atmosphere; [c]Isolated yield

The substrate scope was investigated to demonstrate the versatility of this intramolecular C–H annulation under the optimized reaction condition (Table 3.1, entry 8). A variety of substrates with different R^1 and/or R^2 substituents were subjected to the optimized reaction conditions, as summarized in Table 3.2. The intramolecular C–H annulation was versatile and showed broad scope, wherein diverse functional groups on R^1 and/or R^2 were tolerated. According to the screening, various R^1 and/or R^2, including benzyl, electron-rich (halogens) and an electron-donating group (Me and OMe) participated in C–H annulation, and displayed similar reaction activity, and offered good to excellent yields from 72 to 95 % (3.3a-3l). However, if halogen (Br) is attached at the R^2 (*pera*) position, it is challenging to obtain the desired product (3.3m). Whereas, if substrate (3.1) attached to strong electron withdrawing group (CF_3) at R^1 (3.3n), showed moderate yield 61%. Notably, C–H annulation and oxidation required an extended reaction time for strong electron withdrawing group.

Table 3.2. Substrate Scope of Compound 3.[a,b]

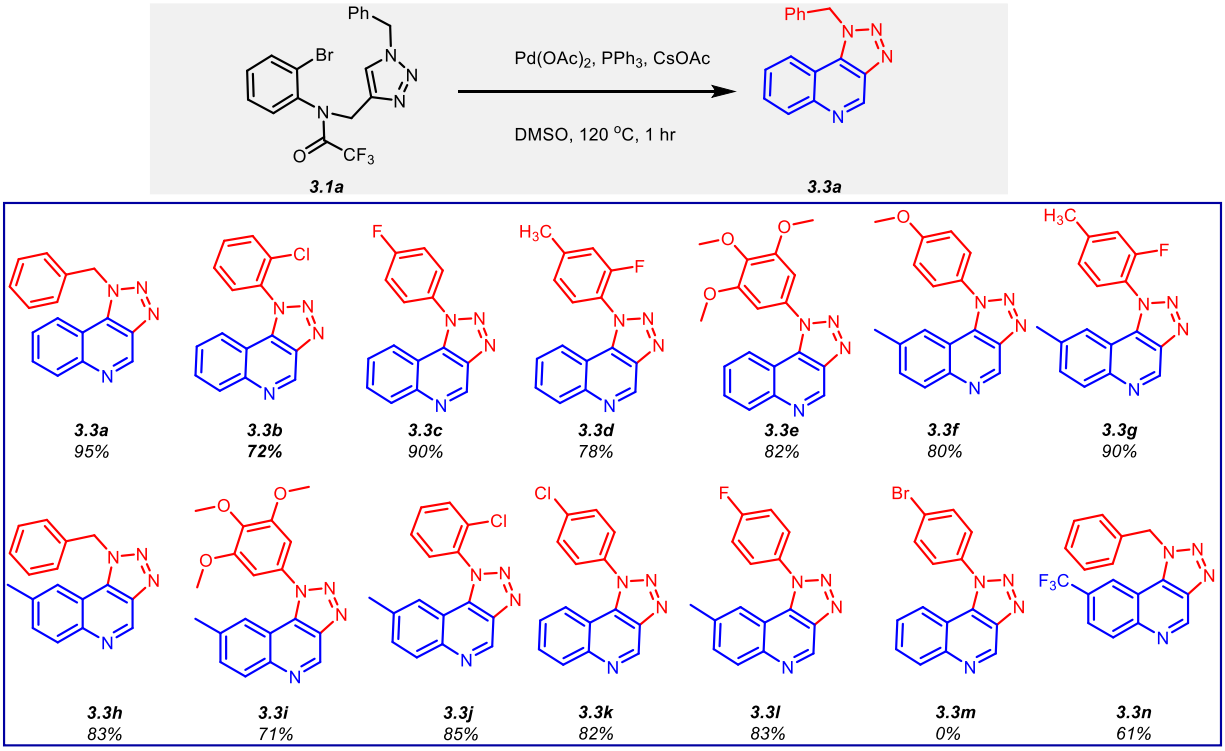

[a]Reaction Conditions: 1a (0.25 mmol), catalyst (5 mol%), base (2 equiv.,) Ligand (20 mol %), solvent (2 ml), [O], [b]Isolated yield

We questioned where it could be possible to carry out CuAAC and C–H annulation using copper in a one-pot. We performed the reaction on substrate 3.1a in the presence of CuI (20 mol%), 1,10-phen (20 mol%), and K_2CO_3 (2 equiv.) in DMSO at 120 °C (Scheme 3.2 A). Unfortunately, the reaction didn't proceed to give the desired product 3.3a. Subsequently, the newly developed pathway was applied to the gram scale to further strengthen this reaction more attractive in terms of synthetic applicability. Two selected reactions were carried out for C–H annulation under the optimized reaction conditions, and the final products (3.3a, 3.3k) were isolated 60 and 56% respectively **(**Scheme 3.2 B).

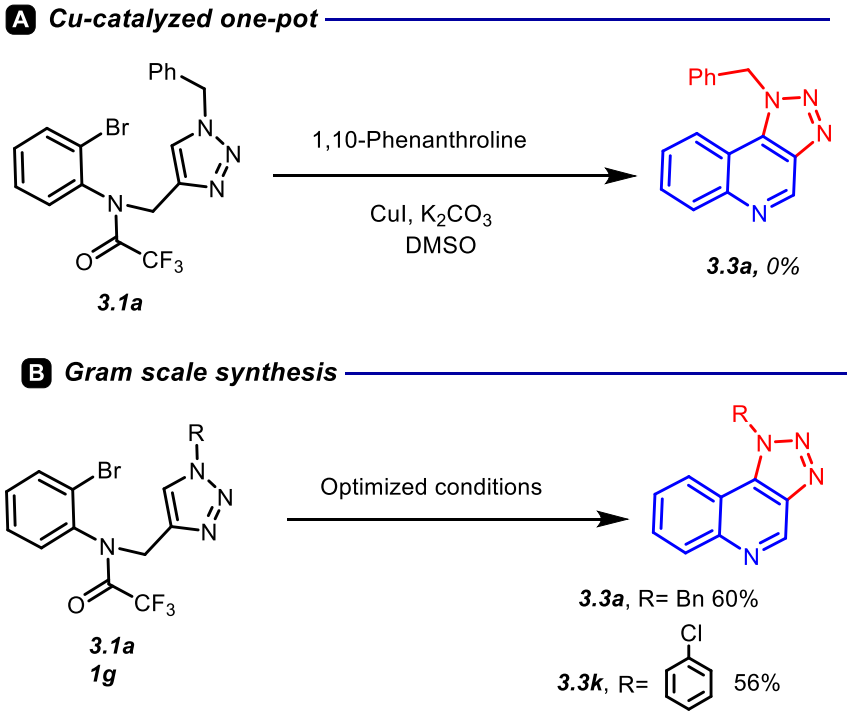

Scheme 3.2. One pot synthesis and scale up synthesis

The effective pathway for the synthesis of 1-(3,4,5-trimethoxyphenyl)-4,5-dihydro-1H-[1,2,3]triazolo[4,5-c]quinoline (3.4b) was then investigated. N-(2-bromophenyl)-N-((1-(3,4,5-trimethoxyphenyl)-1H-1,2,3-triazol-4-yl)methyl)acetamide (3.2) was chosen as a model substrate to optimize the C–H annulation. Using the same optimized reaction conditions as in substrate 3.1a, we successfully obtained the N-acetamide-dihydroquinoline fused-1,2,3-triazole (3.5) with an excellent yield of 89% and confirmed the structure by NMR and mass (*see supporting information*). Finally, we obtained the desired product 3.4b with a 95% yield by hydrolyzing compound 3.5 using NaOH and ethanol (1:1) (Scheme 3.3 A). In the second pathway, after the completion of C-H activation, simple extraction was carried out without further purification, following the reaction with NaOH and ethanol (1:1) to obtain the desired

product 3.4b in a 91% yield (scheme 3.3 B). The final pathway utilized a one-pot reaction to successfully obtain the desired product 3.4b with an excellent yield of 96% (scheme 3.3 C).

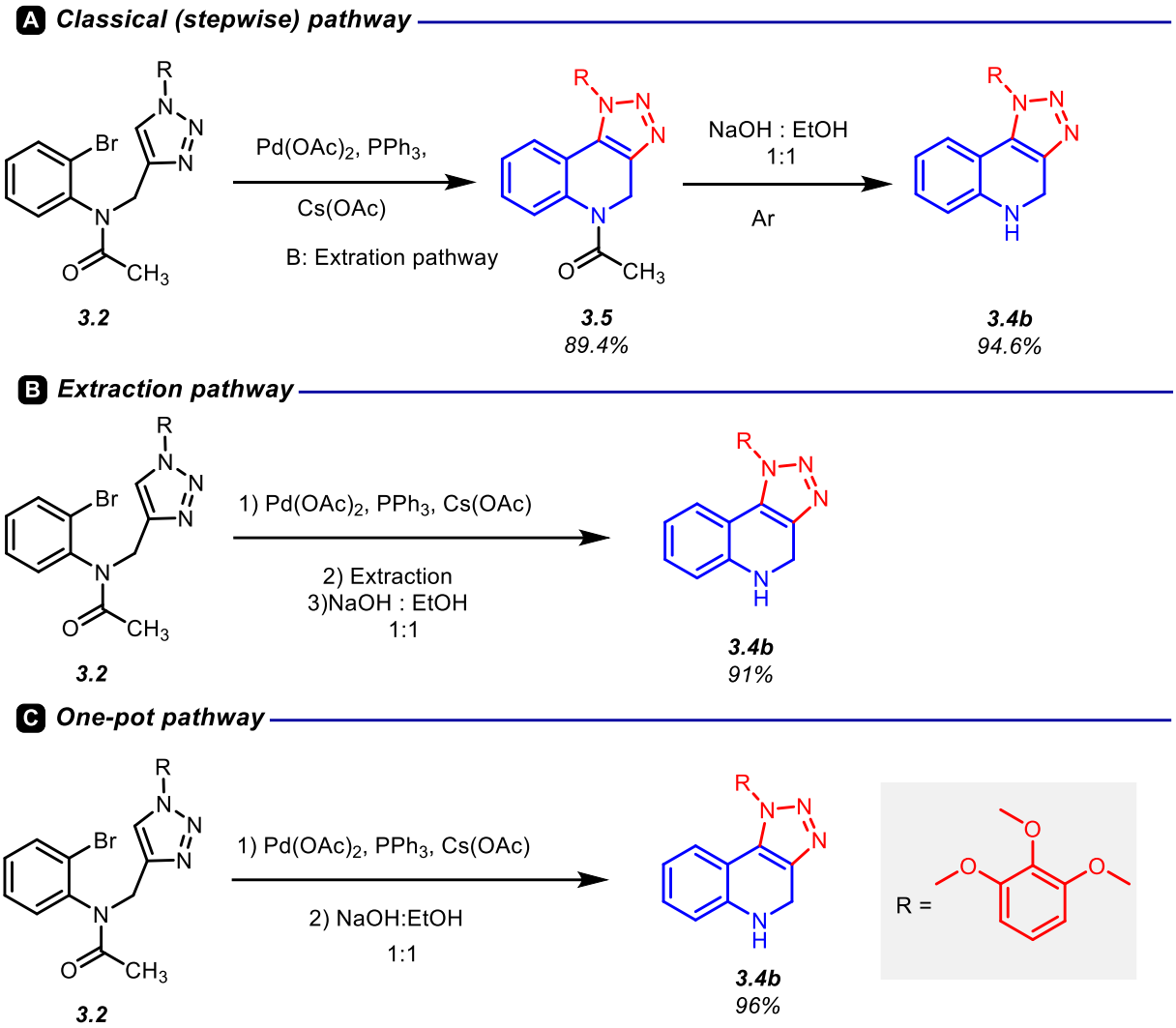

Scheme 3.3. Different pathways for the synthesis of 3.4b

To demonstrate the efficiency and generality of the C–H annulation of the one-pot pathway, a wide range of N-((H-1,2,3-triazol-4-yl)methyl)-N-(2-bromophenyl)acetamide (3.2) were examined under the optimized reaction conditions. Generally, substrates (3.2) with various R^1 and/or R^2 substituents were compatible with the reaction conditions, and the desired products were afforded in high to excellent yields. The electronic factor does not play any significant role in C–H activation/annulation. If substrate (3.2) was either attached to benzyl, an electron-donating group (Me and OMe) or a moderate electron-withdrawing group (F and Cl) in R_1 and/or R^2 displayed similar reaction activity, and corresponding products (3.4a-3.4h) were obtained in good to excellent yields (77-96%). The scope of a one-pot reaction is well illustrated with variously substituted substrates (3.2) at R^1 and/or R^2.

Table 1. Substrate Scope of Compound 3.4.[a,b]

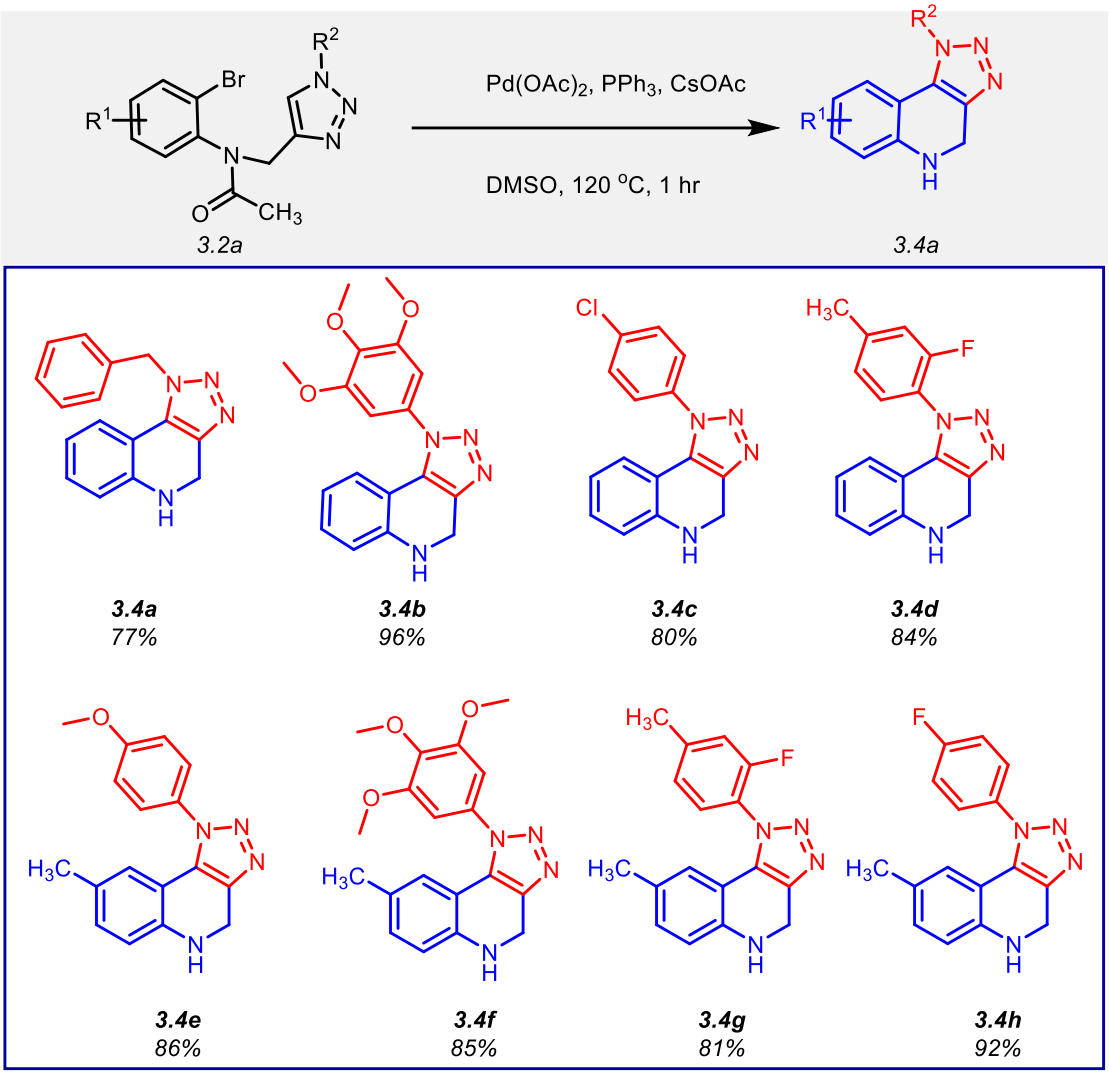

[a]Reaction Conditions: 1a (0.25 mmol), catalyst (5 mol%), base (2 equiv.,) Ligand (20 mol %), solvent (2 ml), [O], [b]Isolated yield

Post-synthetic Modifications

Further post-synthetic modifications of the synthesized moieties were explored to illustrate the synthetic utility and application prospects of this reaction. Post-synthetic modification of synthesized compounds 3.3k and 3.3j was carried out by using different Pd-catalyzed reactions, including the Suzuki reaction, the Buchwald reaction, nucleophilic aromatic substitution (S_NAr) and reduction with formate anion. As shown in the scheme 3.4, the compound 3.3k was treated with various boronic acid derivatives using $Pd(OAc)_2$, XPhose in dioxane at 100 °C. Gratifyingly, we obtained the desired products 3.6a, 3.6b, and 3.6c in excellent yields of (86%, 95%, 85%) respectively. The Buchwald coupling proceeded smoothly to afford the desired compound 3.7 in 51% yield. Further compound 3.3k participated in Pd-catalyzed selective reduction of the C–Cl,

led to the desired product 3.8 in good yield. The product 3.9 was obtained in a 65% yield by the nucleophilic aromatic substitution (S_NAr) reaction of compound 3.3j with $NaOCH_3$.

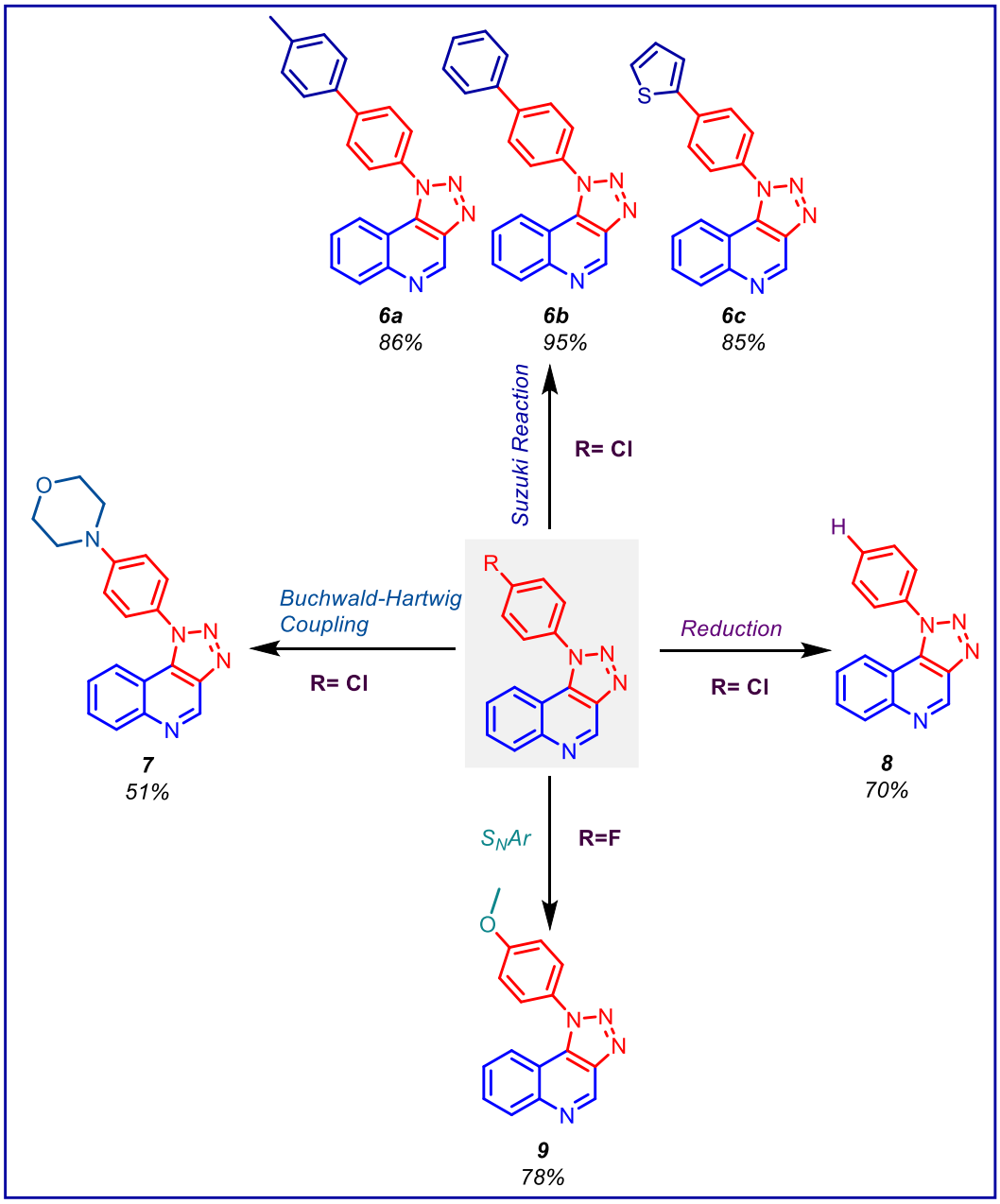

Scheme 3.4. Post-synthetic modifications

Based on literature reports,[126] the plausible mechanism for the synthesis of desired products 3.3 and 3.4 can be rationalized (Scheme 3.5). First, the active Pd (0) is presumably generated *in situ* during the reaction from $Pd(OAc)_2$. The initial step involves the oxidative addition of 3.1/2 to active Pd (0) to form an intermediate, aryl palladium species (A), followed by the intramolecular electrophilic aromatic substitution or direct arylation to afford the crucial Pd (IV) intermediate (B). In the next step, dissociation of H^+Br^- through Cs(OAc) produces the seven-member palladacycle intermediate (C). Pd (0) was finally regenerated to continue the catalytic cycle after

the reductive elimination of intermediate (C) from Pd (II), followed by oxidation in the context of trifluoroacetamide derivatives. These derivatives hydrolyze under reaction conditions and are oxidized directly using an oxygen balloon. In contrast, acetamide derivatives do not undergo hydrolysis during the reaction. The hydrolysis of acetamide derivatives is achieved through treatment with NaOH/MeOH (1:1), yielding the desired products 3.3 and 3.4, respectively.

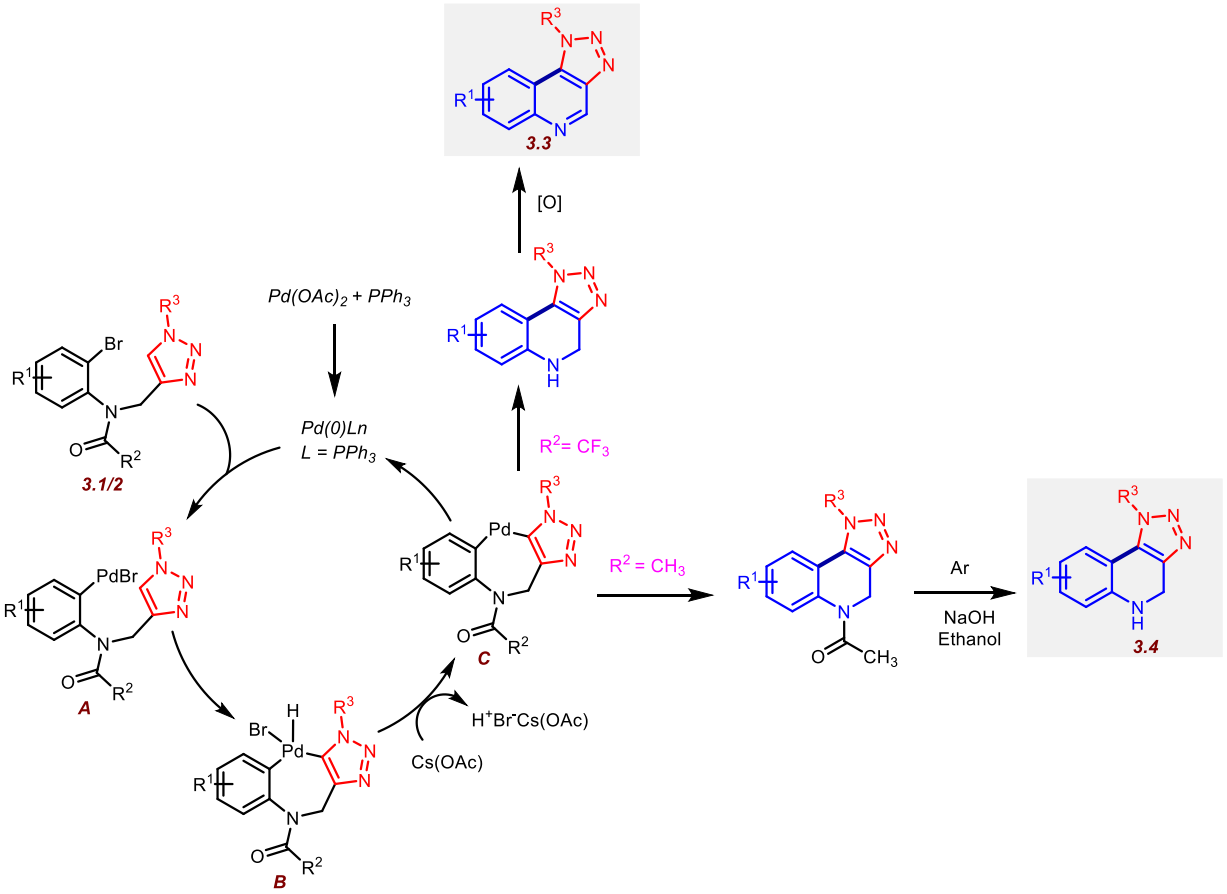

Scheme 3.5. Proposed mechanism

3.3 Conclusion

In summary, we have designed a controlled approach to perform intramolecular ring closure *via* Pd-catalyzed C–H annulation. This transformation gave direct access to the quinoline and/or dihydroquinoline fused-1,2,3-triazole. Utilizing these pathways, a wide variety of quinoline and dihydroquinoline fused-1,2,3-triazole can be quickly and easily obtained in good to excellent yields. The scope and functional-group tolerance of the reaction are also effectively illustrated with a diverse array of substrates. Further post-synthetic modifications of the synthesized compounds have been investigated.

Chapter 4. Pd-catalyzed intramolecular C–H activation for the synthesis of functionalized polyfused N-heterocyclic 1,2,3-triazole derivatives

4.1 Introduction

The indole and quinoline nuclei hold a prominent and pivotal role within the realms of organic and medicinal chemistry due to the significance of the structural motif found in a plethora of both natural and synthetic biological active compounds.[127] Polyfused N-heterocycles, especially polyfused indoles and quinolines, represent highly significant structures found in a wide range of natural and synthetic compounds, exhibiting diverse biological functions and extensive medicinal applications.[128] The pyrrolo[3,2,1-ij]quinoline skeleton plays a crucial role in medicinal chemistry and material sciences and their frequent presence in various natural products, such as **Lycoranine A** (Figure 4.1, I).[129] Additionally, these compounds have attracted considerable interest due to their remarkable bioactivities, such as **anticonvulsant** (Figure 4.1, II),[130] **anti-epileptic** (Figure 4.1, III),[131] anti-inflammatory,[132] and anticancer effects.[133] Furthermore, these compounds have also demonstrated potential as red-emitting dopants (DCQTB) for organic **light-emitting diodes** (Figure 4.1, IV) (Figure 4.1).[134]

Fully and extensively functionalized 1,2,3-triazoles, characterized by their comprehensive and diverse functionalization patterns, serve as pivotal structural motifs with extensive multidisciplinary applications.[110c, 110d, 135] Heterocyclic systems fused with a 1,2,3-triazole ring, particularly among fully substituted 1,2,3-triazoles, have gained prominence due to their increasing importance in drug discovery and chemical biology.[57, 136] Biologically active 1,2,3-triazole polycyclic compounds, such as [1,2,3]-triazole-fused piperidine have been designed as **Hsp90 inhibitors** (Figure 4.1, V),[137] and compound (Figure 4.1, VI) has been identified as an **antitumor agent** (Figure 1).[133]

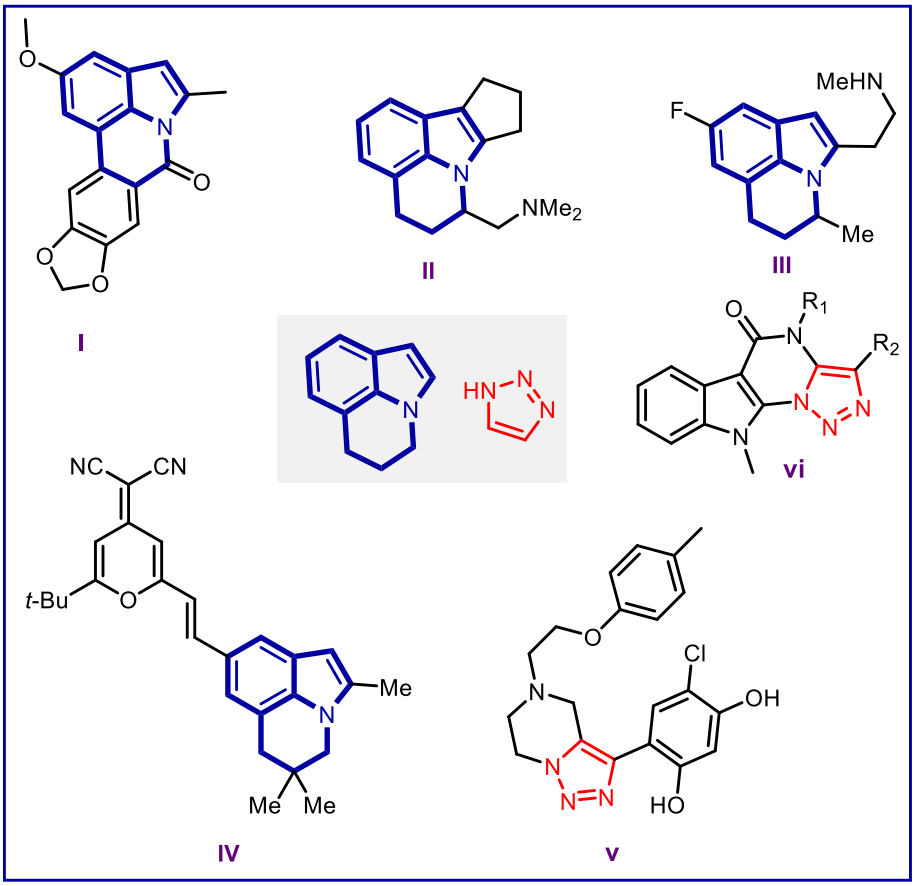

Figure 4.1. Biologically important heterocycles

Presently, the deliberate integration of diverse pharmacophores, such as heterocycles, into a single molecular entity is a commonly employed strategy in the search for novel therapeutic agents. This approach often leads to the development of hybrid compounds that display amplified biological activity.[138] Within this contest, C–H activation emerges as a highly powerful tool for combining two distinct biologically significant moieties, thereby expanding the structural diversity and potential pharmacological properties of the resulting compounds.[120, 139] Particularly, palladium (Pd)-catalyzed C–H activation has gained widespread recognition and finds extensive application in organic synthesis, enabling the rapid and efficient assembly of diverse molecular architectures.[121a, 121c, 121d] In this context, our research group has made significant contributions to the field of Pd-catalysed C–H functionalization, encompassing variety of transformative reactions such as Heck coupling, Suzuki-Miyaura coupling, Tsuji-Trost allylation, and Buchwald-Hartwig amination.[122a, 122b, 122d, 127a, 140] Through our work, we have advanced these synthetic methodologies, enabling the efficient construction of diverse and complex organic molecules.

Throughout our investigations in the field of heterocyclic compound synthesis, we have placed significant emphasis on the development and functionalization of both indole and quinoline, as

well as their fused polycyclic structures *via* palladium-catalysed reactions. In our endeavour to pioneer innovative scaffolds involving 1,2,3-triazole-fused heterocycles, we hypothesized the synthesis of the novel compounds pyrrolo[3,2,1-*ij*][1,2,3]triazolo[4,5-*c*]quinoline *via* intramolecular C–H activation. We believe that these novel compounds could have significant implications in both pharmaceutical and material science. To validate the viability of this proposed pathway, as illustrated in Scheme 4.1b, we initiated investigations into the practicability of this transformation.

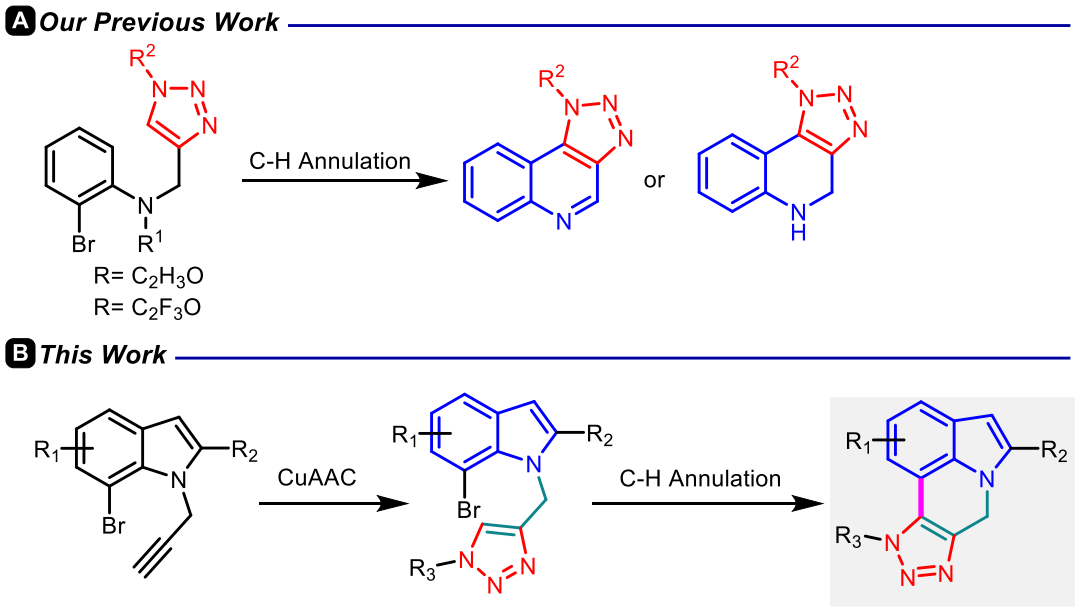

Scheme 4.1. Previous and this work

The strategy followed for the synthesis of pyrrolo[3,2,1-*ij*][1,2,3]triazolo[4,5-*c*]quinoline derivatives is depicted in Scheme 4.2.

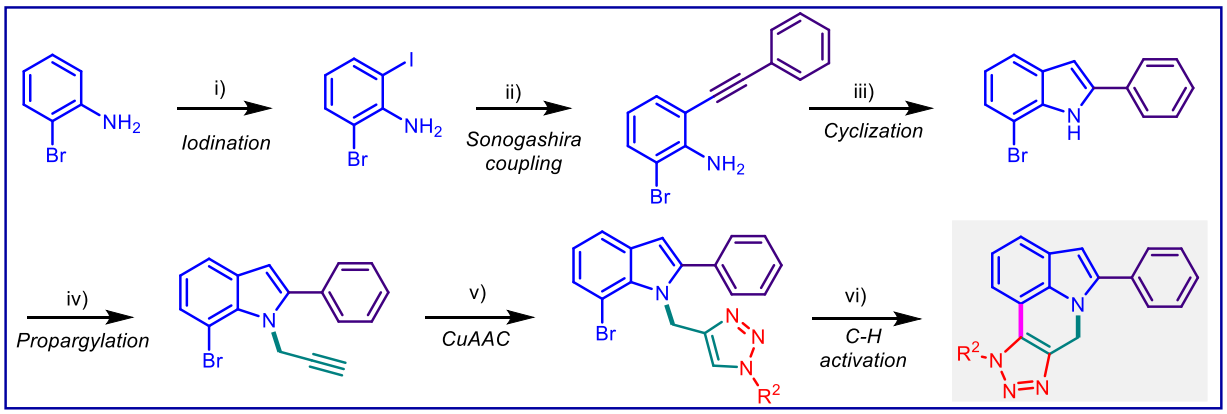

Scheme 4.2. Synthetic pathway

4.2 Results and Discussion

We initiated our study by employing (4.1a) as a model substrate to synthesize a novel derivative of 10-benzyl-5-phenyl-7,10-dihydropyrrolo[3,2,1-ij][1,2,3]triazolo[4,5-c]quinoline (4.2a).

Different reaction conditions were screened by varying the nature of transition metal catalysts, ligands, solvents, and different reaction temperatures. Initially, we attempted the reaction using various Cu catalysts, solvents, and bases (Table 4.1, entries 1-5); however, the reaction did not proceed. The utilization of copper in intramolecular C–H activation processes is motivated to facilitate one-pot transformations. Consequently, we decided to switch to a Pd catalyst for the intramolecular C–H activation. The intramolecular C–H activation failed to occur for substrate 4.1a using $Pd_2(dba)_3$, base (K_2CO_3), and xphose as a ligand in dry dioxane at 120°C (Table 4.1, entry 6), and gave only the reduced product. Gratifyingly, the reaction proceeds to give the desired product 4.2a in 68% yield by using $Pd(OAc)_2$, PPh_3, and CsOAc in dry DMF (Table 4.1, entry 7). Encouraged by this promising result, we thoroughly investigated various reaction parameters to further improve the reaction (Table 4.1, entries 8-13). To our delight, $Pd(OAc)_2$, PPh_3 and CsOAc in dry DMSO were demonstrated to be the most efficient optimized conditions to afford the 4.2a compound with an excellent yield of 82% (Table 4.1, entry 8).

Table 4.1: Optimization of reaction conditions

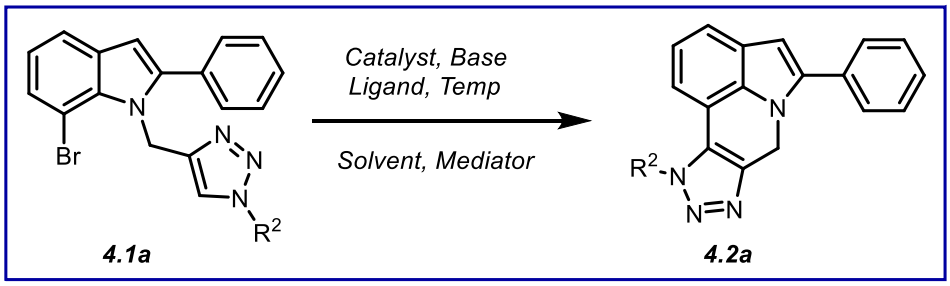

S.No	Catalyst	Ligand	Base	Solvents	Temp °C	Time (h)	Yield[c] (%)
1	CuI	1,10-Phen	K_2CO_3	DMF	120	48	-
2	CuI	1,10-Phen	K_2CO_3	DMSO	120	48	-
3	CuI	DMEDA	Cs_2CO_3	DMF	120	48	-
4	CuOAc	1,10-Phen	K_2CO_3	DMF	120	48	-
5	CuBr	1,10-Phen	K_2CO_3	DMF	120	48	-
6	Pd_2dba_3	Xphose	K_2CO_3	DMF	120	2	-
7	$Pd(OAc)_2$	PPh_3	Cs(OAc)	DMF	120	1	68%
8	**$Pd(OAc)_2$**	**PPh_3**	**Cs(OAc)**	**DMSO**	**120**	**1**	**82%**
9	$Pd(OAc)_2$	PPh_3	Cs(OAc)	DMSO	100	2	69%
10	$Pd(OAc)_2$	PPh_3	Cs(OAc)	DMSO	80	4	58%
11	$Pd(OAc)_2$	PPh_3	Cs(OAc)	Dioxane	100	24	-

12	$Pd(OAc)_2$	PPh_3	Cs(OAc)	MeCN	100	2	25%
13[d]	$Pd(OAc)_2$	PPh_3	Cs(OAc)	DMSO	120	1	60%

[a]*Reaction Conditions: 4.1a (0.25 mmol), catalyst (5 mol%), base (2 equiv.,) Ligand (20 mol %), solvent (2 ml);* [b]*Reactions performed under argon atmosphere;* [c]*Isolated yield;* [d]*catalyst (2 mol%), Ligand (8 mol %).*

We next investigated the substrate scope of the reaction under the optimized reaction conditions, an array of substrates bearing distinct R_1, R_2, and R_3 substituents, as summarized in Table 4.2. The intramolecular C–H activation demonstrated remarkable versatility, showing broad applicability across a variety of functional groups attached to R_1, R_2, and R_3. According to the screening, various R_1, R_2, and R_3, including benzyl, electron-rich (CF_3, halogens), diverse aromatic (including heterocyclic) moieties, and an electron-donating group (Me and OMe), participated in intramolecular C–H activation. These substrates exhibited consistent reactivity, yielding products with a range of good to excellent yields.

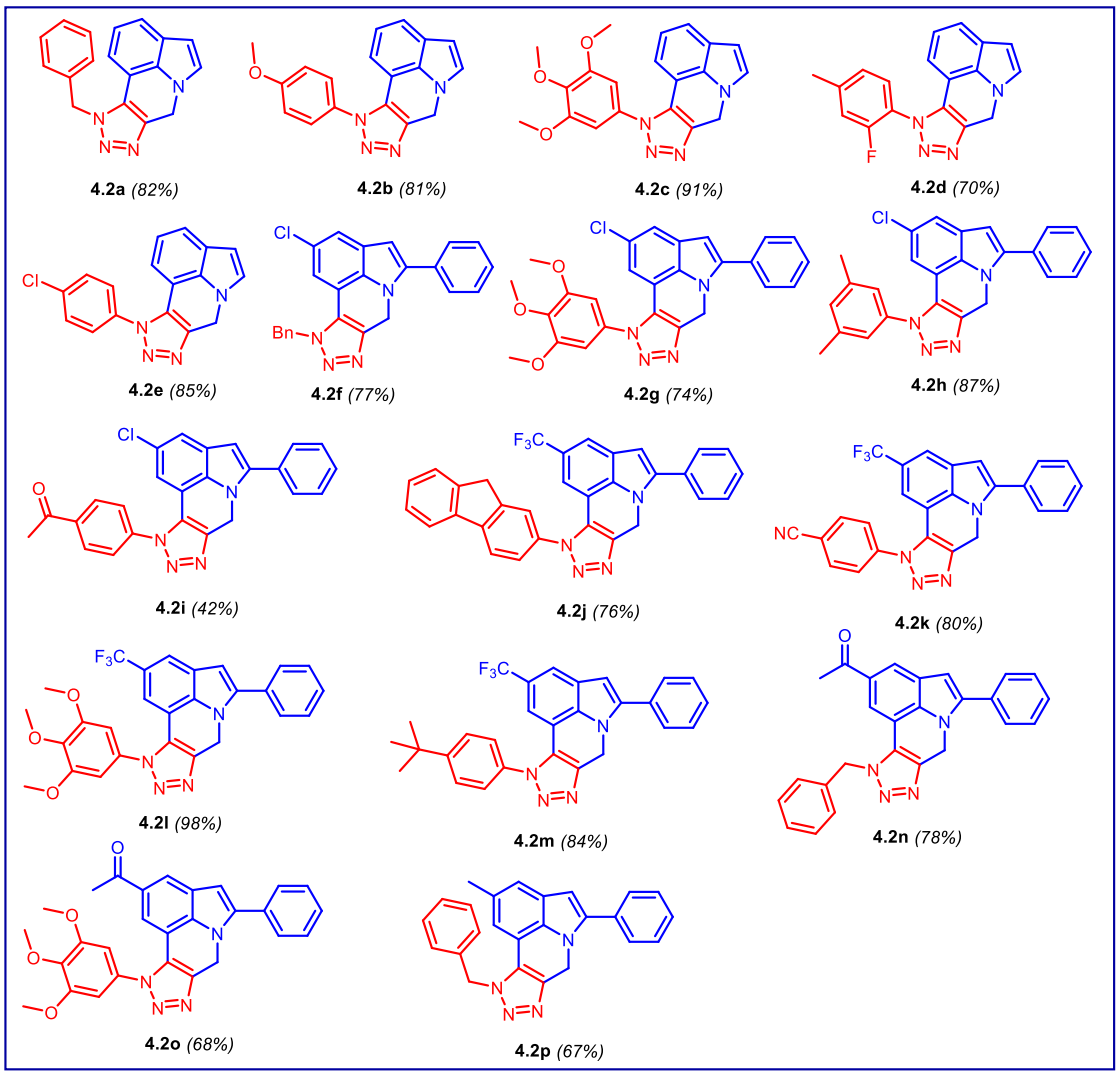

Table 4.2: *[a]Reaction Conditions: 4.1a (0.25 mmol), catalyst (5 mol%), base (2 equiv.,) Ligand (20 mol %), solvent (2 ml); [b]Isolated yield;*

Subsequently, the newly developed pathway was applied to the gram scale to further strengthen this reaction and make it more attractive in terms of synthetic applicability. Next, we performed post-synthetic modification by employing various palladium-catalyzed reactions, including the Suzuki reaction, Buchwald-Hartwig amination, and reduction with formate anion. As shown in Scheme 4.3, the compound 4.2e was treated with diverse boronic acid derivatives using $Pd(OAc)_2$, XPhose in dioxane at 100 °C. Gratifyingly, we obtained the desired products 4.3a and 4.3b in excellent yields of 95% and 90% respectively. The Buchwald coupling proceeded smoothly, resulting in the desired product 4.4 with a yield of 51% yield. Furthermore, compound 4.2e participated in a Pd-catalyzed selective reduction of the C–Cl bond, leading to the desired product 4.5 in a yield of 72%.

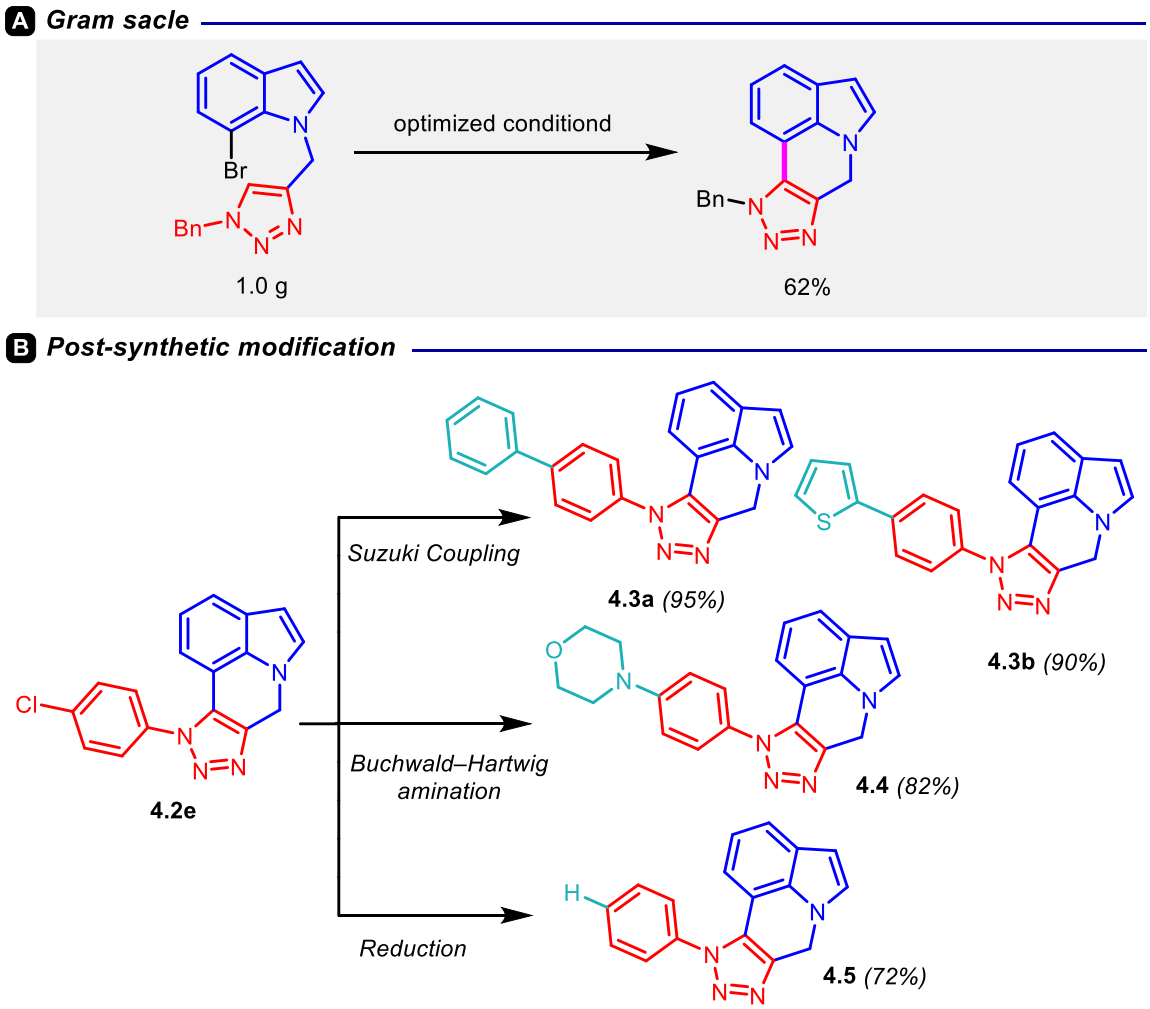

Scheme 4.3. Gram scale and post-synthetic modification

The plausible mechanism for the synthesis of desired products 4.2 can be rationalized in Scheme 4.4. First, the active Pd (0) is presumably generated *in situ* during the reaction from $Pd(OAc)_2$.

The first step involves the oxidative addition of compound 1 to active Pd (0), resulting in the formation of aryl palladium species (A), followed by the dissociation of Br with acetate ion (B). In intermediate (C), a hydrogen bond forms between the electron-rich C-5 proton of triazole and the oxygen of acetate, leading to the elimination of acetic acid and the formation of the seven-member palladacycle intermediate (D). Finally, Pd (0) is regenerated to continue the catalytic cycle after the reductive elimination of intermediate (D) from Pd (II) to synthesize the desired product.

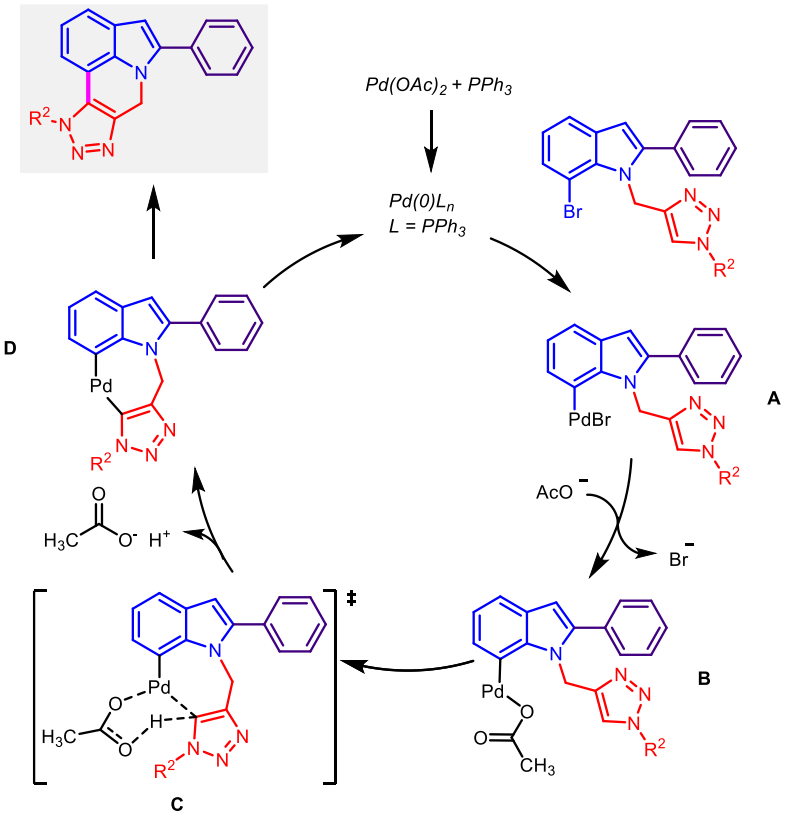

Scheme 4.4. Proposed mechanism

In the final phase of our investigation, we assessed the photophysical properties of 16 distinct compounds. As depicted in Figure 4.2, these pyrrolo-triazole derivatives exhibited emission in both the blue and greenish regions when excited at 365 nm. To further investigate their optical characteristics, UV-VIS spectroscopy was performed in acetonitrile. Compound 4.3a was selected as the reference model, against which compounds with various electron-donating (–Me, –OMe) and electron-withdrawing substituents (–F, –Cl, $–CF_3$) on the phenyl ring were compared, along with different heterocyclic moieties attached to the 1,2,3-triazole core. The absorption spectra for each compound are provided in Figure 4.3.

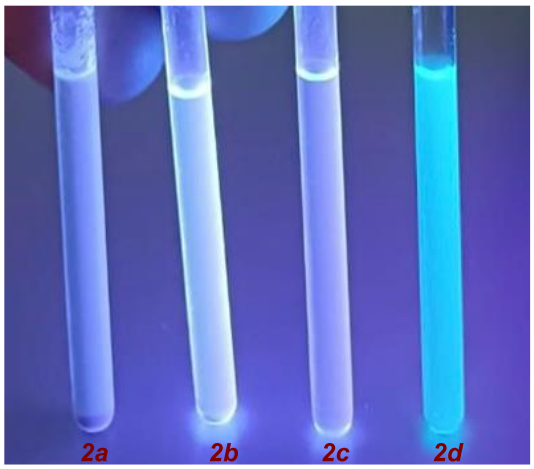

Figure 4.2. Fluorescence of pyrrolo quinoline triazole (1 mg/mL in MeCN) under a 365 nm UV lamp.

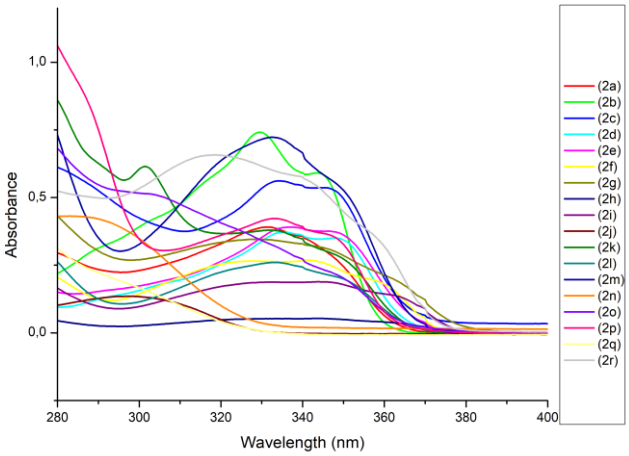

Figure 4.3. Absorption spectra of various pyrrolo quinoline triazole recorded in MeCN under room temperature

4.3 Conclusion

In conclusion, we have successfully developed an efficient strategy for the synthesis of diverse and functionalized novel pyrrolo[3,2,1-*ij*][1,2,3]triazolo[4,5-*c*]quinoline derivatives. In this strategy, Cu-catalyzed intermolecular [3+2] cycloaddition occurs between alkynes and azides to synthesize the 1,2,3-triazole precursor, followed by the intramolecular Pd-catalyzed C–H activation. A diverse array of substrates displayed compatibility within the reaction, affording the respective products in yields ranging from good to high. Furthermore, we validated the practicality of this methodology by conducting scale-up synthesis and extended the scope of functionalization through the incorporation of diverse post-synthetic modification reactions. We also explored the photophysical characteristics of the newly synthesized compounds. We believe that this research study will serve as a foundation, paving the way for a multitude of valuable improvements in the fields of medicinal chemistry and organic synthesis in the forthcoming years.

Chapter 5. Synthesis of functionalized azepino[1,2-a]indole [1,2,3]triazole derivative through Pd-catalyzed intramolecular C–H activation

5.1 Introduction

The indole ring system serves as a prominent and privileged structural motif widely encountered in organic chemistry.[141] Indole derivatives, owing to indole diverse structural characteristics, manifest significant biological activities, including anticancer, anti-inflammatory, antimicrobial, analgesic, antihypertensive, and antiatherogenic effects. This multifaceted nature highlights the importance of indole-based molecules within the field of organic chemistry, particularly in the context of pharmaceutical research and drug development.[142]

Heterocyclic compounds fused with the indole ring system are commonly encountered in natural products and pharmaceutical drugs.[143] Among these, the azepino indole class of compounds stands out as a significant scaffold, demonstrating a wide array of bioactive properties. For instance, derivatives of benzo[3,4]azepino[1,2-*a*]indole function as effective inhibitors of HCV **NS5B RNA polymerase** (Scheme 5.1, A),[144] potent antagonists of the **MT_2 receptor** (Scheme 5.1, A),[145] and modulators of neurotransmitter receptors in the central nervous system. Azepino[2,1-*a*]indole has demonstrated antagonistic efficacy against MT_1 and MT_2 melatonin receptors, rendering it a viable candidate for the treatment of insomnia.[145] An azepino indole compounds serve as a **prostaglandin D2 receptor antagonist** (Scheme 5.1, A),[146] making it valuable for treating niacin-induced vasodilatation.

The 1,2,3-triazole nucleus is a privileged structural motif with extensive applications in materials science,[62a, 147] biology,[110a, 110b, 148] and chemical sciences.[149] Among these, triazole-fused polycyclic heterocycles are particularly attractive due to their significant pharmaceutical and biological activities. The advent of C–H activation has further enhanced the development and application of these triazole-containing compounds, paving the way for profound advancements in medicinal and biological fields.[120b, 150] Notably, palladium (Pd)-catalyzed C–H activation is renowned in organic synthesis for rapidly and efficiently constructing diverse molecular frameworks [11].[121c, 121d] Within this framework, our research group has significantly contributed to the field of Pd-catalyzed C–H functionalization, developing a variety of transformative reactions.[121d, 122e]

In our quest to pioneer novel molecular scaffolds featuring 1,2,3-triazole-fused heterocycles, we hypothesized the synthesis of azepino[1,2-a]indole [1,2,3]triazole compounds using intramolecular C–H activation (Scheme 5.1, B). We envision that these newly devised

compounds may have significant implications in both pharmaceutical and materials science. To validate the feasibility of this proposed route, as outlined in (Scheme 5.1, B), we initiated a detailed mechanistic investigation and optimization studies to establish the practicality and efficiency of this transformation. In this work, 2-bromo-substituted alkyne compound, which undergoes a CuAAC reaction with an azide to form a 1,2,3-triazole moiety. Following this, a C–H activation step is employed to fuse the triazole-containing intermediate with the indole core, resulting in the indole-fused azepine product (Scheme 5.1, C).

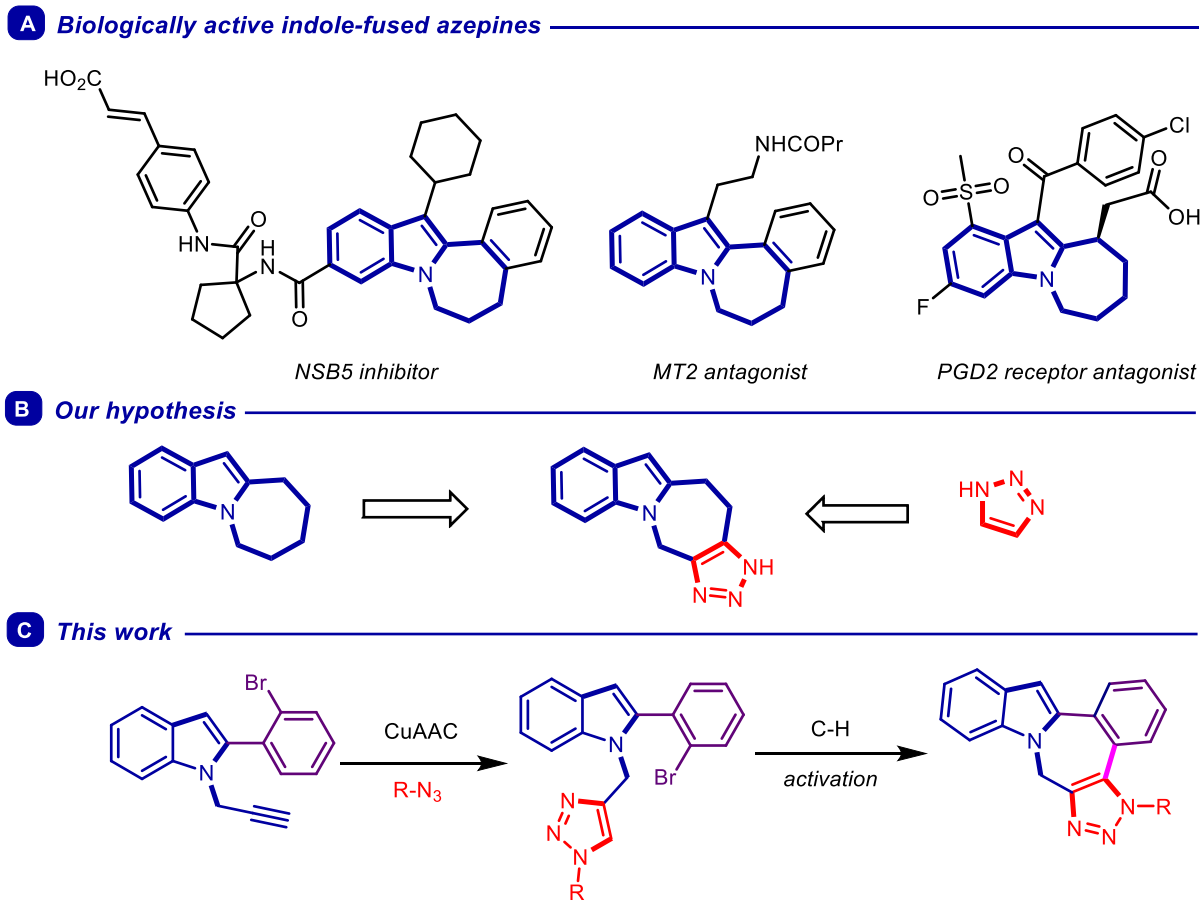

Scheme 5.1. Biologically important related heterocycles, our hypothesis and this work

The retrosynthesis of azepino[1,2-a]indole [1,2,3]triazole derivatives is outlined in Scheme 5.2 and further elaborated in the *supporting information*.

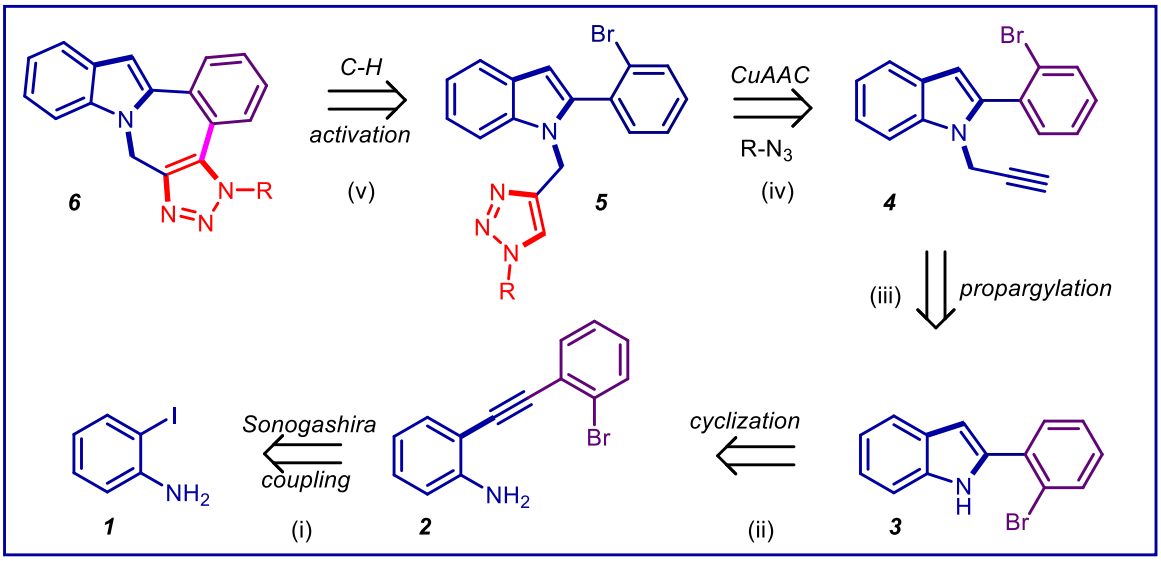

Scheme 5.2. Retrosynthetic pathway

5.2 Results and Discussion

In our quest to develop innovative molecular scaffolds with potential medical relevance, we recently established a versatile approach that combines the CuAAC reaction with intramolecular C–H annulation. Building on our previous procedure, we selected 2-(2-bromophenyl)-1-((1-(4-chlorophenyl)-1H-1,2,3-triazol-4-yl)methyl)-1H-indole (5.1a) as a model substrate for intramolecular C–H activation.

In our experimental setup, we reacted model substrate 1a with $Pd(OAc)_2$ (2 mol %), PPh_3 (4 mol %), and CsOAc (2 equiv.) in DMSO at 120 ^oC. The reaction proceeded smoothly, demonstrating the efficiency of our method. We successfully isolated the final product, 5-(4-chlorophenyl)-5,8-dihydrobenzo[3,4][1,2,3]triazolo[4',5':5,6]azepino[1,2-a]indole (3a), with 83% yield (scheme 5.3).

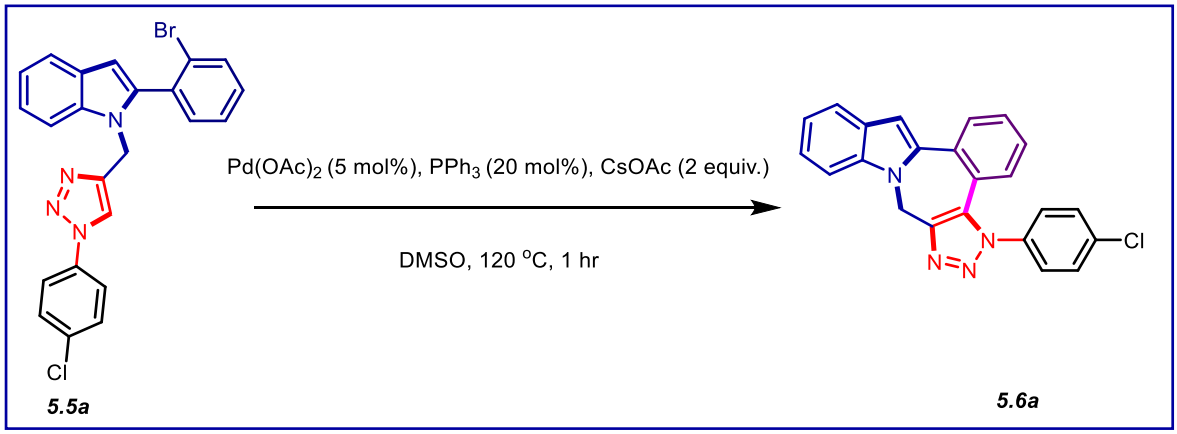

Scheme 5.3. Optimized reaction condition

Under the optimized reaction conditions in hand, we further investigate the substrate scope to demonstrate the versatility of this intramolecular C–H annulation under the optimized reaction

condition. A variety of substrates with different R^1, R^2, R^3, substituents were subjected to the optimized reaction conditions, as summarized in Table 5.1. The intramolecular C–H annulation was versatile and showed broad scope, wherein diverse functional groups on R^1, R^2, R^3, were tolerated. According to the screening, various R^1, R^2, R^3, including benzyl, electron-rich (halogens, CF_3, $COOCH_3$) and an electron-donating group (Me and OMe) participated in C–H annulation, and displayed similar reaction activity, and offered good to excellent yields from 83 to 96 % (5.3a-5.3q).

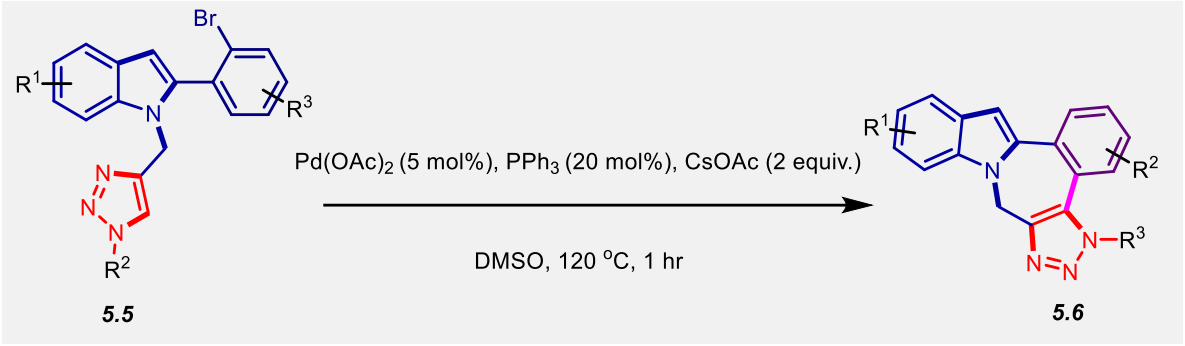

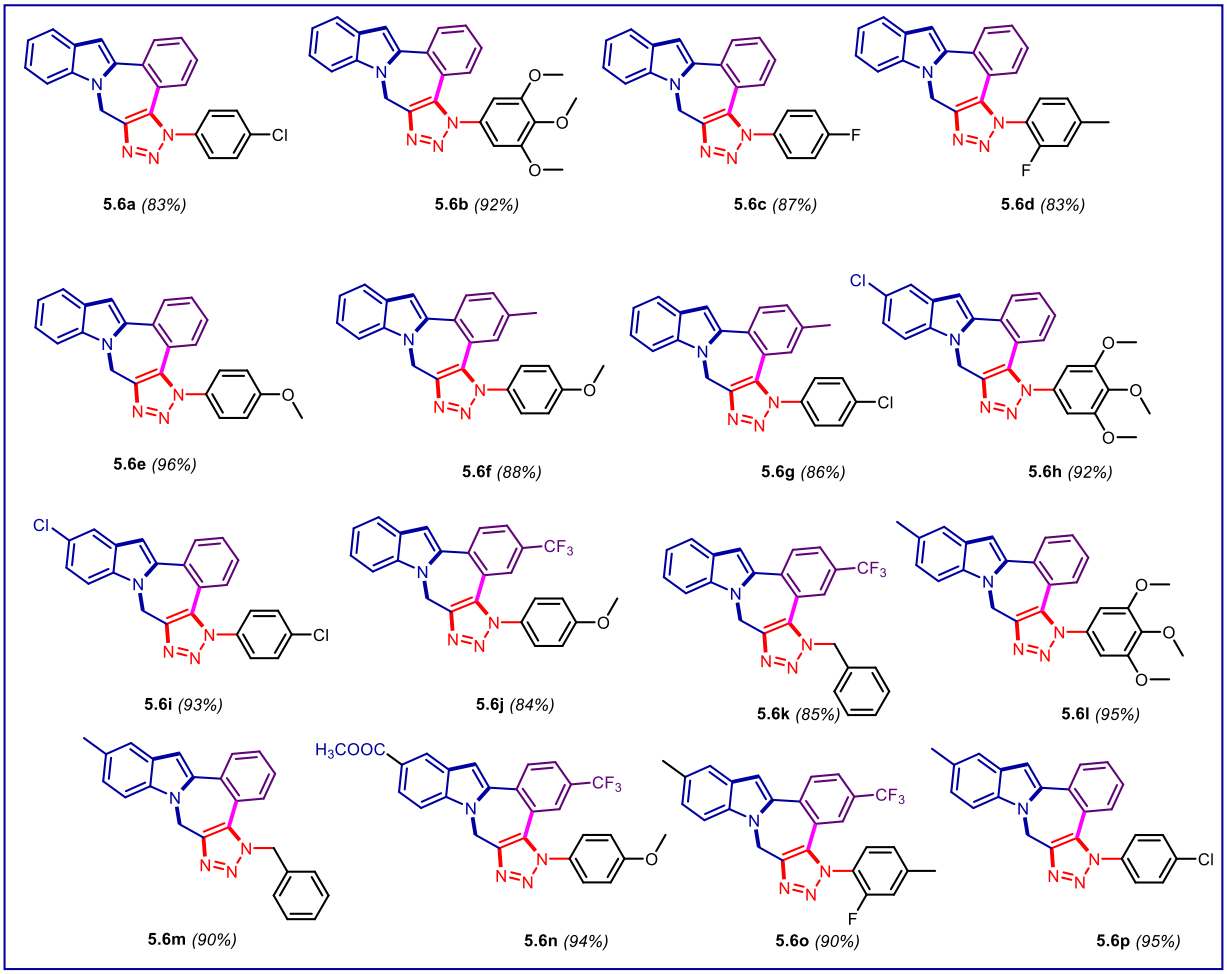

Table 5.2: [a]*Reaction Conditions: 5.1a (0.25 mmol), catalyst (5 mol%), base (2 equiv.,) Ligand (20 mol %), solvent (2 ml);* [b]*Isolated yield;*

Subsequently, we applied the newly developed pathway on a gram scale to further validate its robustness and enhance its synthetic applicability. We then performed post-synthetic modifications using various palladium-catalyzed reactions, including the Suzuki reaction, Buchwald-Hartwig amination, and chlorine reduction. As shown in Scheme 5.4, compound 5.2a was treated with different boronic acid derivatives using $Pd(OAc)_2$ and XPhos in dioxane at 100°C. We were pleased to obtain the desired products 5.7a, 5.7b and 5.7c in excellent yields of 96%, 98% and 71%, respectively. The Buchwald-Hartwig amination proceeded smoothly, resulting in the desired product 5.8 with a yield of 92%.

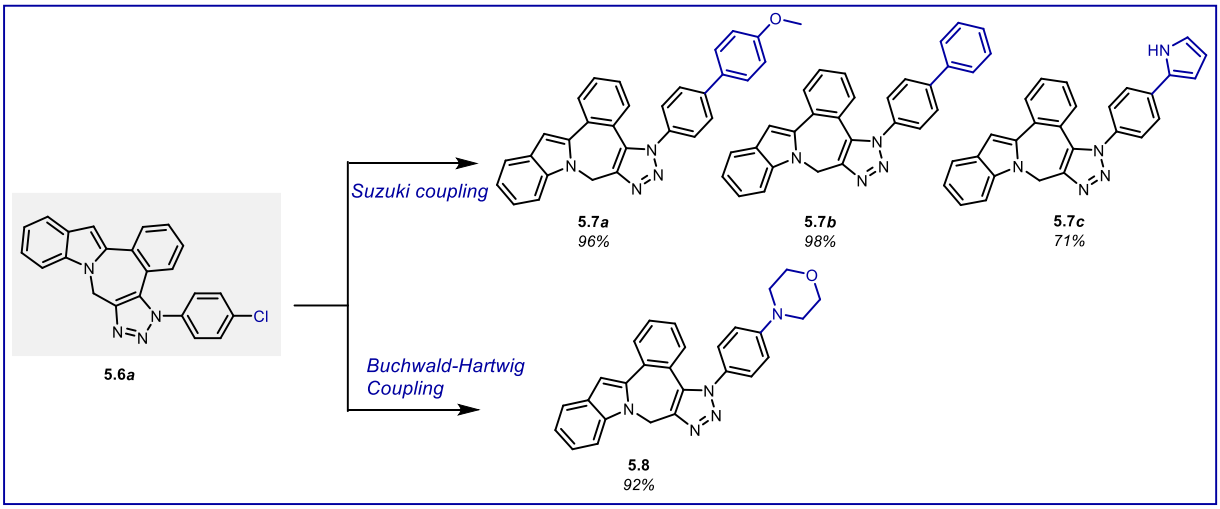

Scheme 5.4: Post-synthetic modification or downstream derivatives

5.3 Conclusion

In summary, we successfully synthesized a series of novel azepino[1,2-a]indole [1,2,3]triazole compounds through a Pd-catalyzed C–H annulation strategy. This methodology enabled the efficient formation of these fused heterocycles with various functional groups. We introduced strong electron-withdrawing, moderate electron-withdrawing, and electron-donating groups to the final compounds. The reactions proceeded smoothly, yielding the desired products in good to excellent yields. Our subsequent focus will be to investigate the anticancer properties of all the synthesized compounds, aiming to uncover potential therapeutic applications.

Chapter 6. Sequential CuAAC and Pd-Catalyzed C–H Annulation for the Synthesis of Diverse Azepine-Fused 1,2,3-Triazoles

6.1 Introduction

The advent of click chemistry, particularly copper(I)-catalyzed azide-alkyne cycloaddition (CuAAC), have revolutionized the landscape of synthetic organic chemistry, enabling the rapid assembly of complex molecular architectures with remarkable efficiency and selectivity.[110a, 111, 148a, 151] The 1,2,3-triazole moiety serves not only as a connecting linker but also as a privileged scaffold employed as important pharmacophores in medicinal chemistry.[110b, 152] A number of triazole derivatives exhibit inducing therapeutic activities and have emerged as promising drug candidates for conditions such as cancer, HIV, among others.[110b, 152] Furthermore, 1,2,3-triazole-fused polycycles, a distinct subclass of triazoles, demonstrate a broad spectrum of biological activities. For instance, 1,2,3-triazole-fused polycycles, shown in (Figure 6.1, I and II) have demonstrated considerable cancer activity.[115, 117, 153] Additionally, fused triazoles derived from sugar compounds, such as (Figure 6.1, III) have exhibited notable inhibitory effects against glycosidase, galactosidase, and SGLT2 enzymes, showcasing their potential as therapeutic agents in various metabolic disorders.[154]

Azepines[155] and oxepines[156] are fascinating classes of heterocycles found in numerous bioactive natural products and have extensive applications in medicinal chemistry. These compounds are known for their unique structural features, which contribute to their versatility and effectiveness in drug design. Their biological activities are often enhanced when these structures are fused with other molecular scaffolds.[157] Among the alkaloids which have been isolated from Cephalotaxus harringtonia plant material are cephalotaxine and a number of its esters and these compounds are active against lymphocytic leukemia (Figure 6.1, IV).[158] Alprazolam (Figure 6.1, V), a widely used commercially available drug, is primarily prescribed for the management of anxiety disorders, panic disorders, and nausea related to chemotherapy.[157c] Oxepine derivative, (−)-janoxepin (Figure 6.1, VI) was isolated from *Aspergillus janus* in 2005 and showed interesting antimalarial properties.[159]

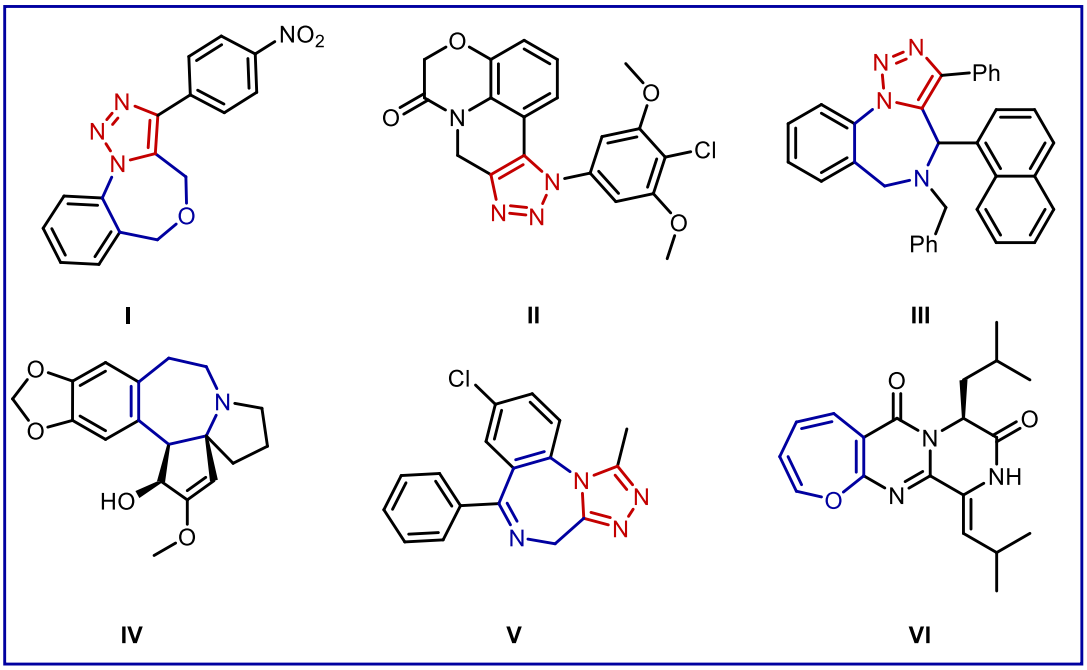

Figure 6.1. Representative bioactive triazole, azepine/oxepine-fused heterocycles

Following our previous syntheses of quinoline-fused and indole-fused 1,2,3-triazoles in (Scheme 6.1A), we aimed to explore the synthesis of azepines and oxepines fused with 1,2,3-triazole (Scheme 6.1B). This extension is motivated by the recognition of the structural and pharmacological potential of azepines and oxepines, and the underexplored possibilities of incorporating them into the 1,2,3-triazole framework.

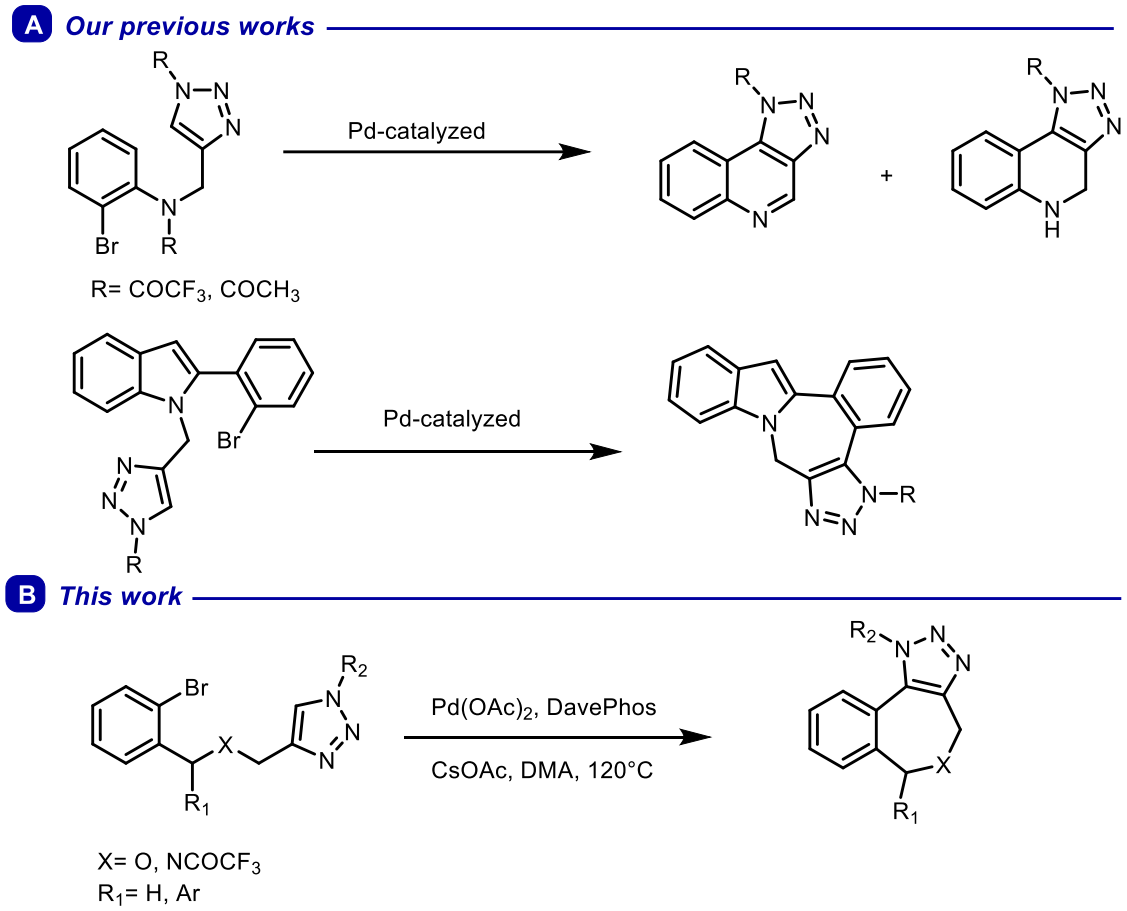

Scheme 6.1. A) Previous work B) This work

Employing the well-established CuAAC reaction for 1,2,3-triazole precursor synthesis, followed by palladium-catalyzed intramolecular annulation, we sought to generate azepine- and oxepine-fused 1,2,3-triazoles. The synthetic pathway depicted in Scheme 6.2 illustrates our proposed approach towards achieving this objective.

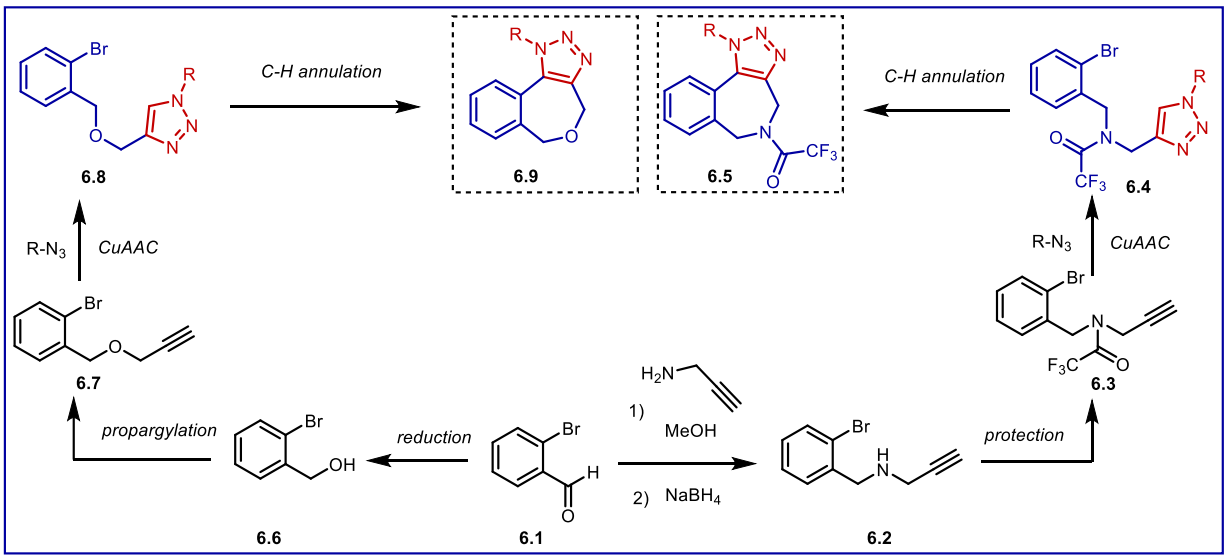

Scheme 6.2. Synthetic pathways

6.2 Results and Discussion

We commenced our study by optimizing the intramolecular C–H annulation using N-(2-bromobenzyl)-N-((1-(3,4,5-trimethoxyphenyl)-1H-1,2,3-triazol-4-yl)methyl)acetamide as the starting material. Employing $Pd(OAc)_2$ (5 mol%) as a catalyst, PPh_3 (20 mol%) as a ligand, and CsOAc (2 equiv.) as a base in DMSO at 120°C, we obtained the desired product with a 60% yield in 3 hours (entry 1). Modifying the protecting group to Ts and substituting the halogen with iodine increased the yield to 78% (entry 2). Substituting the protecting group to $COCF_3$ and retaining bromine as the halogen resulted in a 69% yield (entry 3). Using NH without protecting group, no product was obtained (entry 4). Changing the solvent to DMF and DMA with the $COCF_3$ protecting group resulted in yields of 83% and 89%, respectively (entries 5 and 6). Using DavePhos (10 mol%) as a ligand in DMF, we achieved a 95% yield (entry 7). Further, switching the solvent from DMF to DMA increased the yield to 98% (entry 8). However, extending the reaction time from 1 hour to 5 hours decreased the yield to 65% (entry 9). Finally, exploring Cu as a catalyst for C–H activation did not yield the desired product (entries 10 and 11).

Table 6.1. C-H annulation optimization of reaction conditions [a]

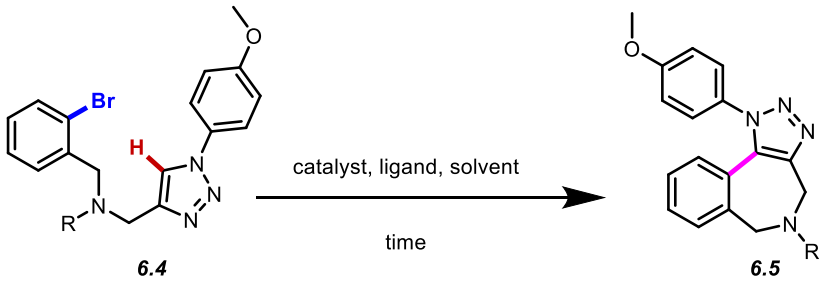

6.4 *6.5*

entry	Catalyst	Ligand(mol%)	Solvent	Base	R	X	Time	Yield(%)[b]
1	$Pd(OAc)_2$	PPh_3 (20)	DMSO	CsOAc	$COCH_3$	Br	3h	60
2	$Pd(OAc)_2$	PPh_3 (20)	DMSO	CsOAc	Ts	I	1h	78
3	$Pd(OAc)_2$	PPh_3 (20)	DMSO	CsOAc	$COCF_3$	Br	1h	69
4	$Pd(OAc)_2$	PPh_3 (20)	DMSO	CsOAc	H	Br	1h	-
5	$Pd(OAc)_2$	PPh_3 (20)	DMF	CsOAc	$COCF_3$	Br	1h	83

6	$Pd(OAc)_2$	PPh_3 (20)	DMA	CsOAc	$COCF_3$	Br	1h	89
7	$Pd(OAc)_2$	DavePhos (10)	DMF	CsOAc	$COCF_3$	Br	1h	95
8	$Pd(OAc)_2$	DavePhos (10)	DMA	CsOAc	$COCF_3$	Br	1h	98
9	$Pd(OAc)_2$	DavePhos (10)	DMA	CsOAc	$COCF_3$	Br	6h	65
10	CuI	1,10-Phen (10)	DMA	K_3PO_4	$COCF_3$	Br	24 h	-
11	CuI	1,10-Phen (10)	DMA	^{t}BuOK	$COCF_3$	Br	24 h	-

[a] Reaction conditions: All the reactions were carried out using compound 6.4 (0.25 mmol), catalyst (5 mol%), ligand (20 mol%), base (2 equiv.) at 120 °C; [b] Isolated yield;

Next, we attempted a one-pot synthesis of the desired compound (6.5a) starting from N-(2-bromobenzyl)-2,2,2-trifluoro-N-(prop-2-yn-1-yl)acetamide (6.3). Following the C–H annulation in DMA, we used DMA as the solvent for the CuAAC reaction. The change in solvent did not affect the yield of the CuAAC reaction. We then combined both reactions in the same reactor without isolating the triazole precursor. The CuAAC reaction was run overnight in DMA. After the starting material was fully consumed, $Pd(OAc)_2$, DavePhos, and CsOAc were added to the reactor, and the reaction mixture was stirred for 12 hours, yielding the desired product in 71% yield (entry 1). In the next experiment, we added both Cu and Pd catalysts along with the ligand and base simultaneously, stirring the reaction for 4 hours. This approach yielded compound 5a in 60% and the 1,2,3-triazole precursor 6.4a in 35% yield (entry 2). Adjusting the ligand loading increased the yield of compound 6.5a and decreased the yield of compound 6.4a (entry 3). Further increasing the Pd loading resulted in a yield of 77% for compound 5a, with no traces of compound 6.4a (entry 4).

Table 6.2. One-pot optimization of reaction conditions [a]

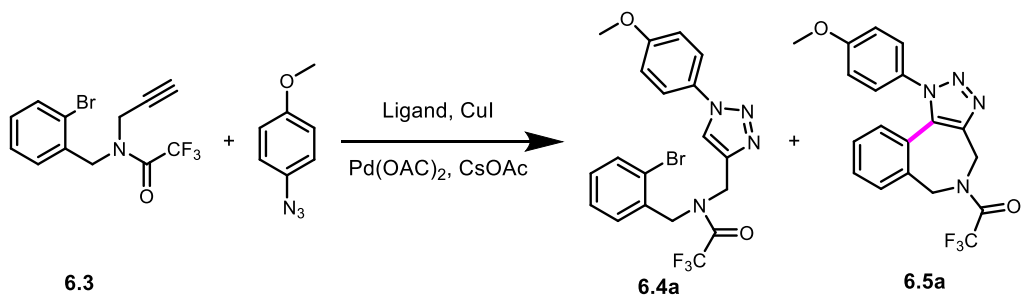

6.3 **6.4a** **6.5a**

Entry	Ligand (mol%)	$Pd(OAc)_2$ (mol%)	Time	Yield 6.4a (%)[b]	Yield 6.5a (%)[b]
1	DavePhos (10)	5	25 h	-	71
3	DavePhos (10)	5	4 h	35	60
4	DavePhos (20)	5	4 h	10	67
5	DavePhos (20)	10	4 h	-	77

[a] *Reaction conditions: All the reactions were carried out using compound 5.4 (0.25 mmol), catalyst (5 mol%), ligand (20 mol%), base (2 equiv.) at 120 °C;* [b] *Isolated yield;*

With the optimized conditions in hand, we explored the substrate scope to demonstrate the practicality and versatility of both methods. The C–H annulation proceeded smoothly, yielding the final products in good to excellent yields. Substrates bearing either electron-donating or electron-withdrawing groups at the *ortho*, *meta*, and *para* positions on R_1 and R_2 were successfully transformed into the final products (6.5a-5i) as shown in Scheme 2. The reaction conditions tolerated a variety of functional groups, including methoxy, benzyl, cyano, ketone, and sulfonyl groups on the aromatic core of R_1 and R_2, yielding products 6.5a–5k. Furthermore, variations in R_2 and X were successfully converted to the final products 6.5l–5p. Notably, pyridine derivative was transformed into the desired product successfully 6.5r.

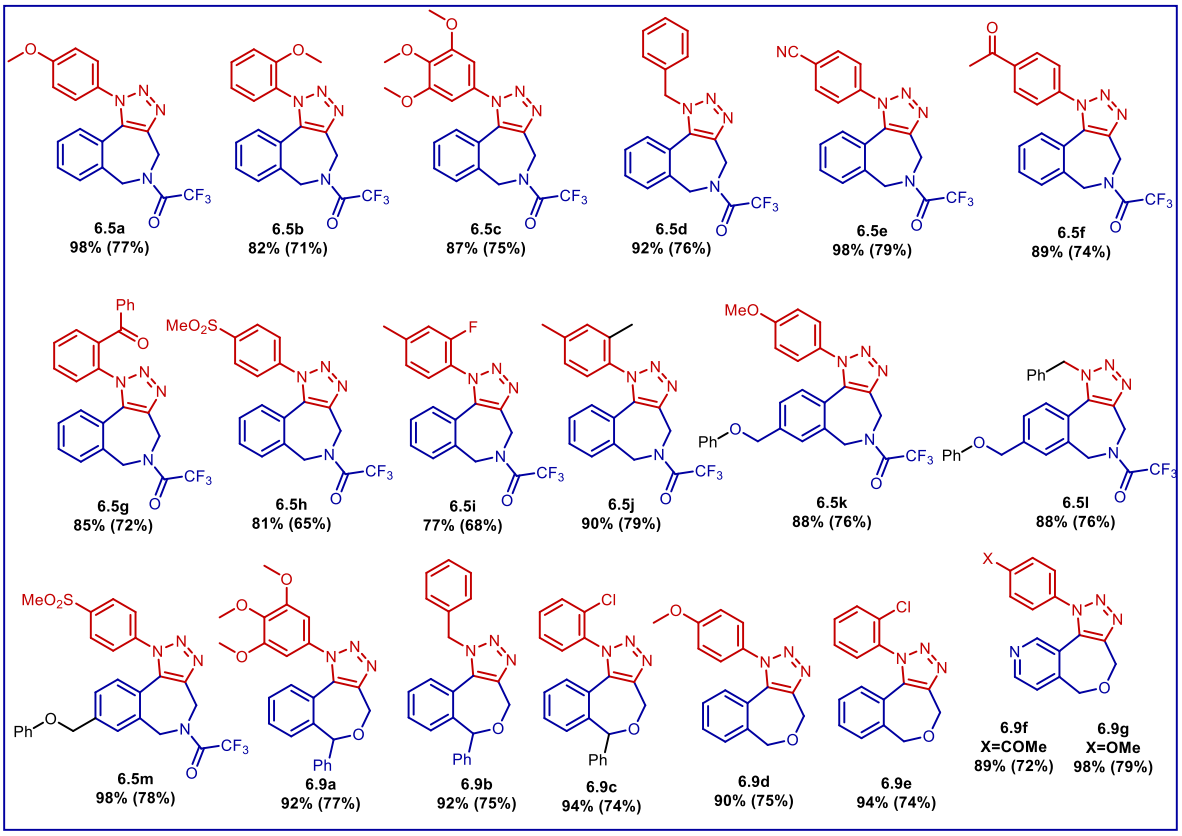

Scheme 6.3: [a] Reaction conditions: All the reactions were carried out using compound 4 (0.25 mmol), catalyst (5 mol%), ligand (20 mol%), base (2 equiv.) at 120 °C, parenthesis yield is fpr one-pot reaction; [b] Isolated yield;

The structures of the obtained compounds were elucidated using one-dimensional and two-dimensional NMR studies. As an example, the structural assignment of the derivative 2,2,2-trifluoro-1-(1-(2-methoxyphenyl)-4,6-dihydrobenzo[c][1,2,3]triazolo[4,5-e]azepin-5(1H)-yl)ethan-1-one, depicted in (6.5e, Figure 6.2).

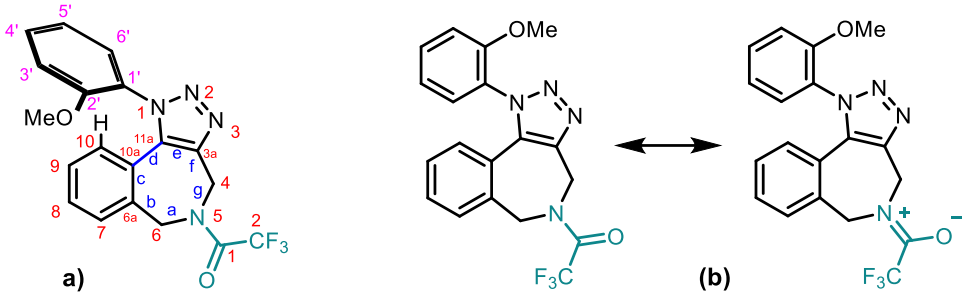

*Figure 6.2: For the compound **(6.5e)** (a) Numbering; (b) Double Bond Character of N5-C1*

The compound **5e** exhibits unique stereochemical properties due to several structural factors. Firstly, the rotation around the N1-C1' bond is restricted due to the presence of the OMe group on C2', which creates a chirality axis parallel to this bond. This restricted rotation significantly influences the molecule's stereochemical attributes. Additionally, the inversion of the seven-membered azepine ring is slow in relation to NMR timescales, introducing a second axis of chirality parallel to the bond between C(6b) and C(6c). This slow ring inversion stabilizes the molecule's chiral features. Furthermore, the bond order between C1 and N5 in the trifluoroacetamidic function is intermediate between a single and double bond, resulting in compound 5e existing as a mixture of *E/Z* diastereomers at room temperature (Figure 6.3). These aspects collectively contribute to the complex chiral nature of 5e, impacting both its physical properties and its spectroscopic behavior, particularly in NMR studies where these features are critical for understanding molecular interactions and reactivity.

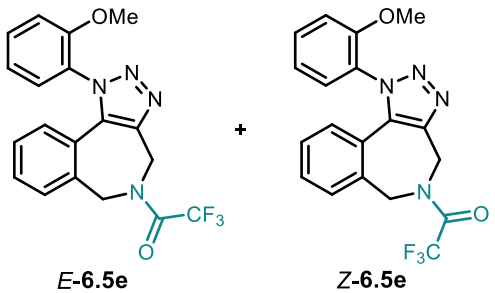

*Figure 6.3: E/Z isomers of compound **(6.5e)***

The ^{1}H NMR spectrum of compound 6.5e, as shown in figure 6.4 a, reveals the presence of *E/Z* diastereomers with distinct methoxy (CH_3O) signals at 3.31 and 3.35 ppm, indicates the diastereomeric mixture in a ratio of approximately 65/35. This differentiation in the proton environment is a characteristic feature in diastereomers where subtle changes in molecular geometry around the methoxy groups affect their chemical shift. The ^{13}C NMR spectrum in (figure 6.4 b) offers further insights with a broader spectral window allowing for a clearer resolution of carbon signals. Notably, the spectral expansion from 44 to 50 ppm focuses on the methylene (CH_2) groups at C4 and C6, where the signals distinctly display the two diastereomers in a ratio of about 2 to 1. These observations from both ^{1}H and ^{13}C NMR spectra are crucial for understanding the stereochemical nature of 5e, helping in the precise identification and quantification of its diastereomeric forms, which is essential for both synthetic optimization and detailed structural analysis in chemical research.

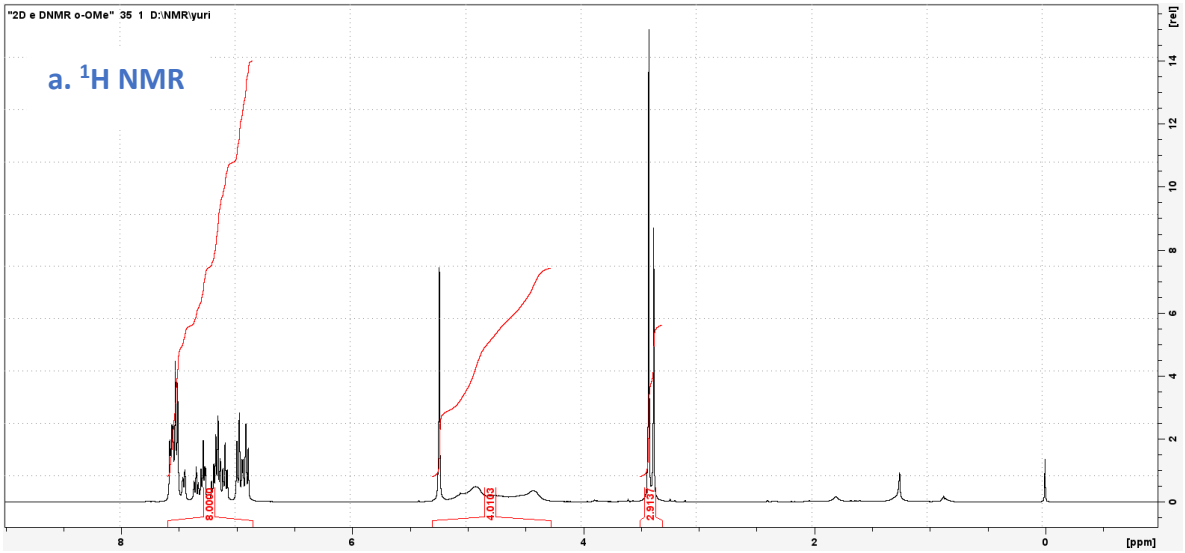

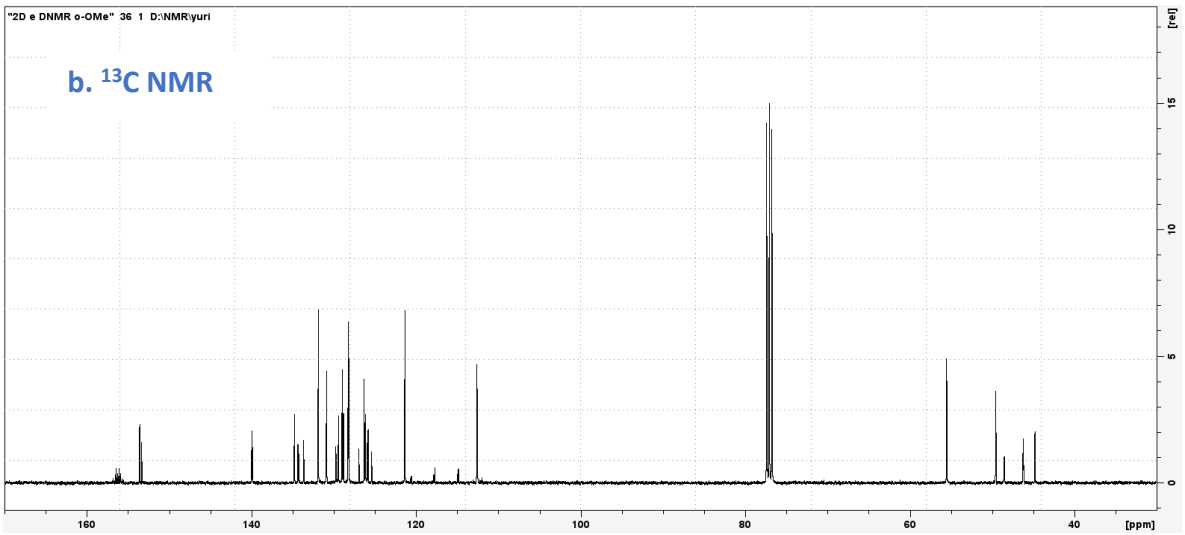

Figure 6.4: a) The ^{1}H NMR spectrum of compound 6.5e in $CDCl_3$ at 298 K (25°C); b) The ^{13}C NMR spectrum of compound 6.5e in $CDCl_3$ at 298 K (25°C)

In the analysis of compound 6.5e using ^{13}C NMR spectroscopy, the major diastereomer, representing approximately 65% of the mixture, shows methylene group resonances at 49.6 ppm as a singlet and 46.2 ppm as a quartet with a coupling constant J = 4.3 Hz, while the minor diastereomer, about 35% of the mixture, displays peaks at 48.5 ppm as a quartet with J = 4.4 Hz and 44.8 ppm as a singlet (figure 6.5). The distinct chemical shifts and coupling constants reflect the different electronic environments influenced by the *E* and *Z* configurations of the diastereomers. The assignment of *E* and *Z* configurations in compound 5e was determined through extensive one-dimensional and two-dimensional NMR experiments. These sophisticated NMR techniques are fundamental for accurately establishing the spatial arrangement of atoms and their interconnectivity within the molecule. This level of detailed analysis is essential for unveiling the structural subtleties that influence the compound's physical and chemical properties, providing a deeper understanding of how structural variations impact molecular behavior and functionality.

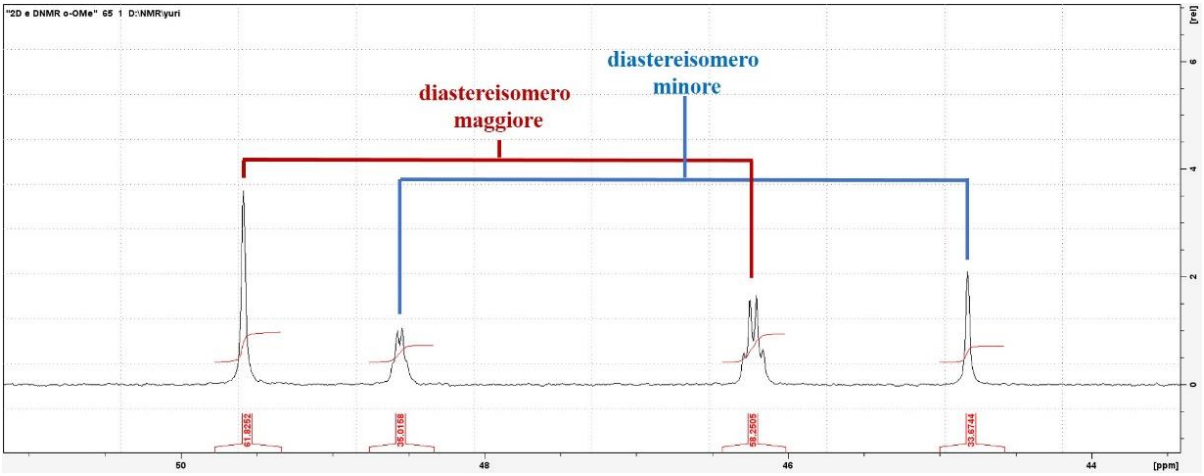

Figure 6.5: ^{13}C NMR spectrum of compound 5e, recorded in $CDCl_3$ at 298 K

The analysis of the HSQC experiment confirms that the described signals are indeed the carbon atoms C4 and C6: in fact, as illustrated in figure 6.6, the four signals show H, C correlation through a σ bond with the hydrogen atoms present in the ^{1}H NMR spectrum between 4.2 and 5.2

ppm.

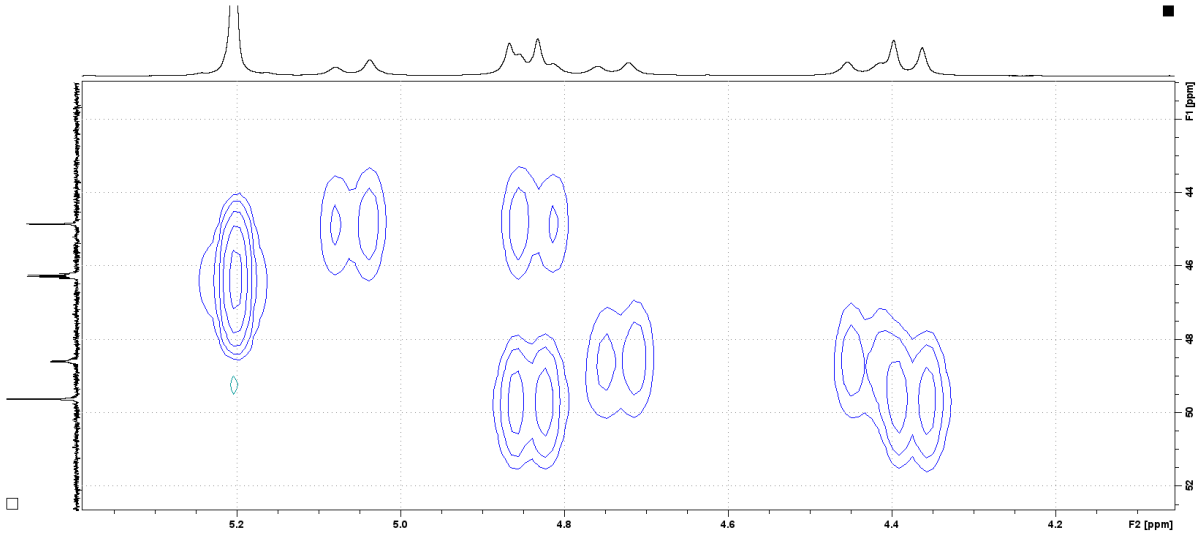

Figure 6.6: Two-dimensional HSQC spectrum of compound 5e, recorded in CDCl3 at 288 K

An interesting feature of the ^{13}C spectrum is that only one of the two methylene carbon atoms shows multiplicity: for example, considering the *E* diastereoisomer, the signal at 49.6 ppm is a singlet while the one at 46.2 ppm is a quartet, with a coupling constant J = 4.3 Hz.

The trifluoroacetamide of compound 5e allows for the existence of resonance structures I and II (shown in Figure 6.7). These resonance structures highlight the flexibility and electronic distribution within the molecule, affecting its chemical reactivity and physical properties. In such molecules, the distribution of electron density across different atomic sites can lead to various interaction phenomena, including those affecting NMR spectral characteristics like chemical shifts and spin-spin coupling, which are crucial for detailed molecular characterization.

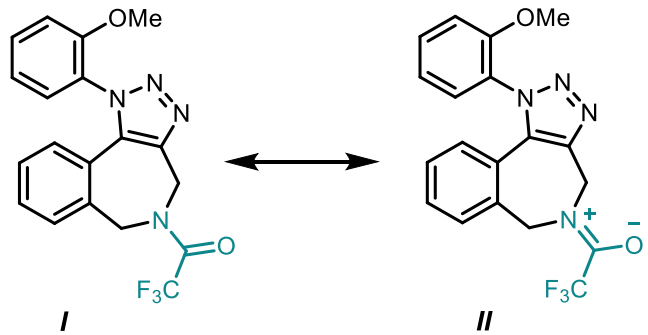

Figure 6.7: Resonance structures of compound ***(6.5e)***

As a result, the N5-C1 bond exhibits slow rotation at 298 K due to its partial double bond character. This characteristic leads to the formation of two diastereomers, *E*-5e and Z-5e, and

causes the trifluoromethyl group (CF3) to adopt specific spatial orientations. In both stereoisomers, the CF_3 group aligns *syn*-coplanar and *syn*-periplanar relative to the two methylene groups, C4 and C6, as illustrated in Figure 6.8. Consequently, the CF_3 group is positioned in close proximity to one of the methylene groups while being significantly distant from the other, on the scale of molecular interatomic distances. Therefore, it is reasonable to expect the through-space (TS) coupling only for the one that is closer, which will be diagnostic for assigning the partial double bond as either *E* or *Z*.

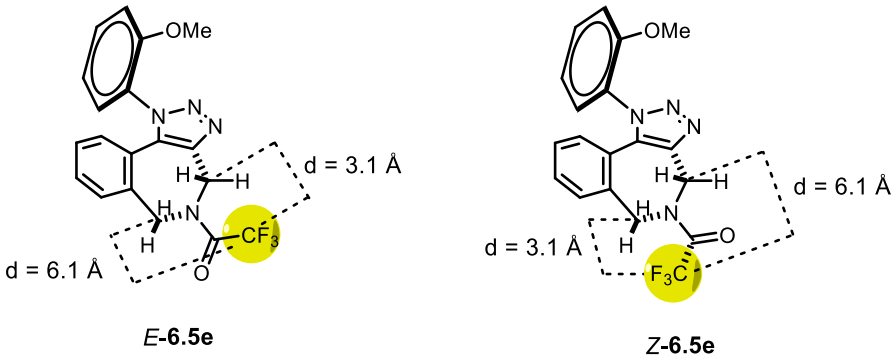

Figure 6.8: Spatial Arrangement of the CF_3 Group Relative to C4 and C6 in the Diastereoisomers E-6.5e and Z-6.5e:

As previously illustrated in figure 6.5.5, the *E* isomer is identified by the signal at 46.2 ppm appearing as a quartet with a coupling constant J = 4.3 Hz, and the signal at 49.6 ppm appearing as a singlet. Therefore, the identification of the stereoisomer *E* as either *E*-6.5e or *Z*-6.5e requires the assignment of these signals to either C4 or C6 of the compound. Specifically, the major stereoisomer will be identified as *E*-6.5e if the singlet at 49.6 ppm is attributed to C6, and the quartet at 46.2 ppm to C4, as it is coupled to the CF3 group through through-space (TS) coupling. Given that empirical simulations, based on existing databases, and the examination of the two-dimensional HMBC spectrum (Figure 6.9) indicate that the signal at 46.2 ppm corresponds to C4 and the signal at 49.6 ppm to C6, the *E* isomer is confirmed to have the *E* configuration.

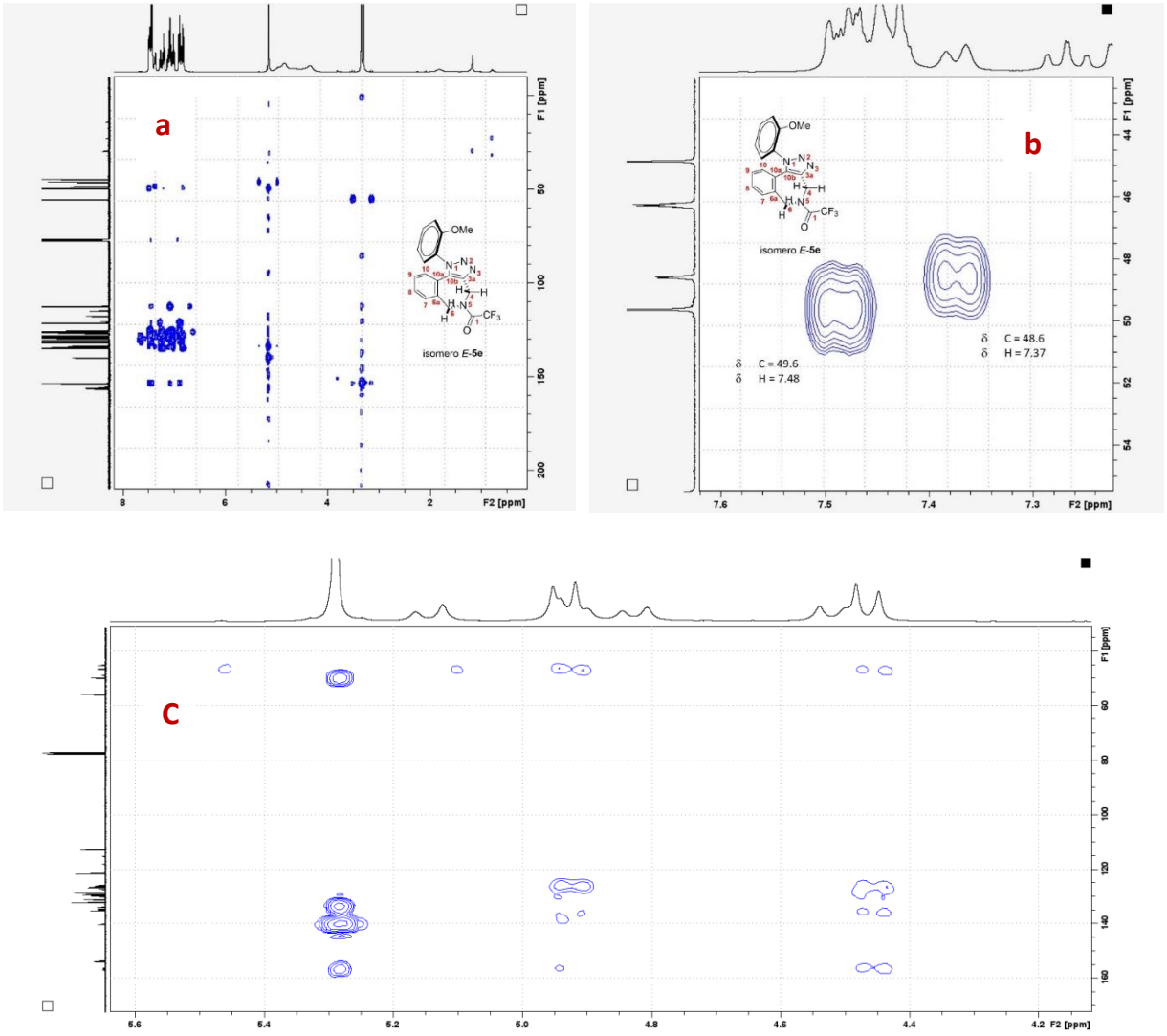

Figure 6.9: a) Two-dimensional HMBC spectrum of 6.5: b) Expansion of the methylene group area showing long-range correlations between the aromatic protons and the benzylic carbons C4 and C6: c) Long-range correlations between the methylene protons and adjacent carbons

The NMR study of the stereodynamic properties of compound 6.5e was conducted on 0.1M solutions in $CDCl_3$ and DMSO-d_6 for experiments at low temperatures (range 263 – 298 K) and high temperatures (range 298 – 400 K), respectively. Figure 6.10 shows the overlay of the spectra obtained at temperatures from 298 to 263 K.

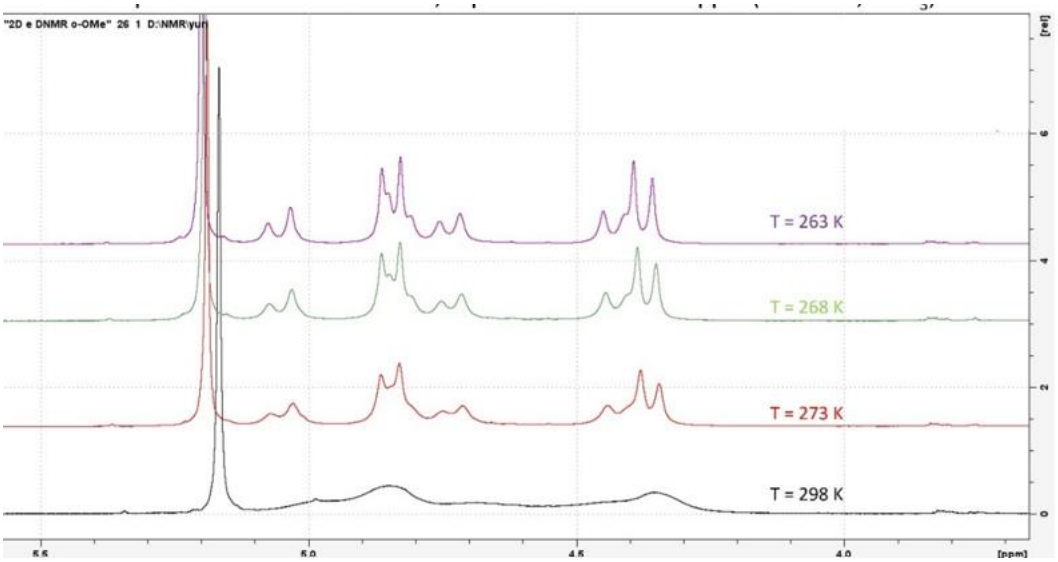

Figure 6.10. ^{1}H Spectrum of 6.5e (c = 0.1M, in CDCl3). Expansion 3.85–5.50 ppm

The low-temperature spectra show the progressive slowing of the ring inversion phenomenon of the seven-membered azepine ring, as depicted in Figure 6.11.

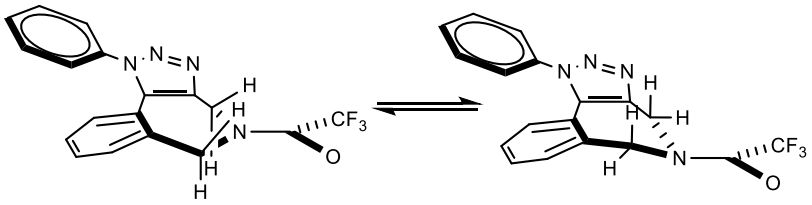

Figure 6.11. Inversion of the seven-membered azepine ring in 6.5e

The experiments conducted at increasing temperatures confirm the previously reported interpretation, namely that the diastereoisomers are stereo-labile and that providing the appropriate amount of energy allows for their rapid interconversion on the NMR time scale. This phenomenon involves both the flipping of the seven-membered ring and the rotation of the N5-C1 bond of the trifluoroacetamide group. However, the two phenomena require different coalescence temperatures, confirming the different energy barriers needed to reach equilibrium: specifically, while the azepine ring is in rapid equilibrium at about 320 K (figure 6.12 a), it is necessary to heat up to 380 K for the coalescence of the trifluoroacetamide bond (figure 6.12 b).

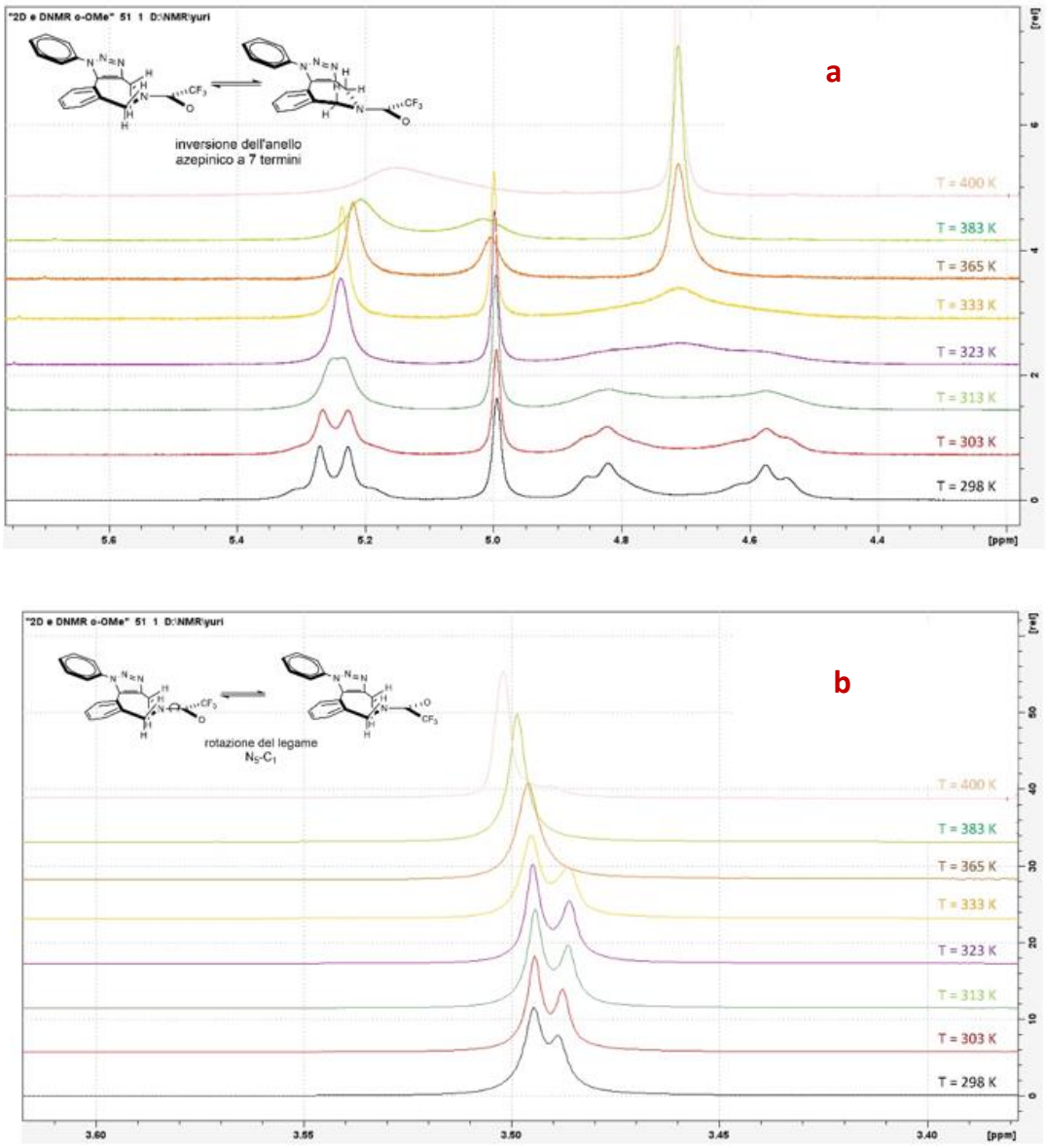

Figure 6.12. ^{1}H NMR of compound 6.5e in different temperature

6.3 Conclusion

In conclusion, we have developed two efficient and versatile approaches for the synthesis of azepine-fused 1,2,3-triazoles via sequential CuAAC and Pd-catalyzed C–H annulation. The first method involves the formation of a 1,2,3-triazole precursor through CuAAC, followed by Pd-catalyzed ring closure. The second method employs a one-pot synthesis where both CuAAC and Pd-catalyzed C–H annulation occur sequentially in the same reactor. Both approaches exhibit high yields and excellent functional group tolerance, accommodating a broad spectrum of substituents. These methods provide a robust platform for the synthesis of diverse azepine-fused triazole frameworks, demonstrating their practicality and versatility in organic synthesis. The synthesis work was complemented by a detailed analysis of the stereodynamic properties of the

products obtained, studied through variable-temperature NMR experiments. The compound 6.5e was further characterized to understand the energy barriers of various interconversions, facilitated by both low and high-temperature NMR experiments which illustrated the progressive slowing of the ring inversion phenomenon and the practical implications of substituent effects on the molecule's behavior.

Chapter 7. Synthesis of Polysubstituted 1,2-Dihydro-3*H*-pyrrolo[1,2-*a*]indol-3-ones through Domino Palladium-Catalyzed Reactions of Indol-2-ylmethyl Acetates with 1,3-Dicarbonyl Derivatives

7.1 Introduction

The tricyclic 2,3-dihydro-1*H*-pyrrolo[1,2-*a*]-indole core and its oxidized derivatives represent an important structural motif found in many biologically active natural products and drug candidates.[160] For example, flinderole C exhibits excellent antimalarial activity against the Plasmodium falciparum parasite[161] and mitomycin C is an effective antitumor agent.[162] Moreover, the antiviral[163] as well as antinociceptive[164] and psychotropic[165] properties of these derivatives boosted the development of effective strategies for their rapid construction. In 1983, Danishefsky described the formation of the 2-methyl-1,2-dihydro-3*H*-pyrrolo[1,2-*a*]indol-3-one through the palladium-catalyzed cyclization of the *N*-(2-allylphenyl)acrylamide;[166] subsequently, various cascade reactions have been used as powerful tools to construct the 2,3-dihydro-1*H*-pyrrolo[1,2-*a*]-indoles in a pot fashion, achieving also remarkable progress in the rapid construction of enantioenriched pyrroloindolones.[167]

Indeed, because of the problems of chemical sustainability of resources, the application of efficient methods for the concise synthesis of valuable scaffolds by avoiding a step-by-step approach, which involves tedious isolation processes, has attracted a great deal of attention from the synthetic community.[168]

During our studies in the field of the synthesis of heterocyclic compounds, great interest has been devoted to the formation/functionalization of indole/benzofuran rings and the construction of indole-fused polycyclic systems through simple domino processes.[122c, 169] Nevertheless, the diversity-oriented synthesis of polysubstituted 1,2-dihydro-3*H*-pyrrolo[1,2-*a*]indol-3-ones through straightforward one-pot approaches from easily available building blocks would be particularly significant considering the structural variety of the biologically active derivatives. From all possible retrosynthetic schemes of 1,2-dihydro-3*H*-pyrrolo[1,2-*a*]indol-3-ones, a simple one requires one C–C bond and one C–N disconnection. It was plausible to suppose that the reaction of 2-indolylmethyl acetates 7.1 with various common active methylene compounds **7.2** should achieve a general entry into the title target through the *in situ* generation of 2-methide-2*H*-indole intermediate 7.I/nucleophile Michael addition/cyclization/ decarboxylation cascade reaction (Scheme 7.1).

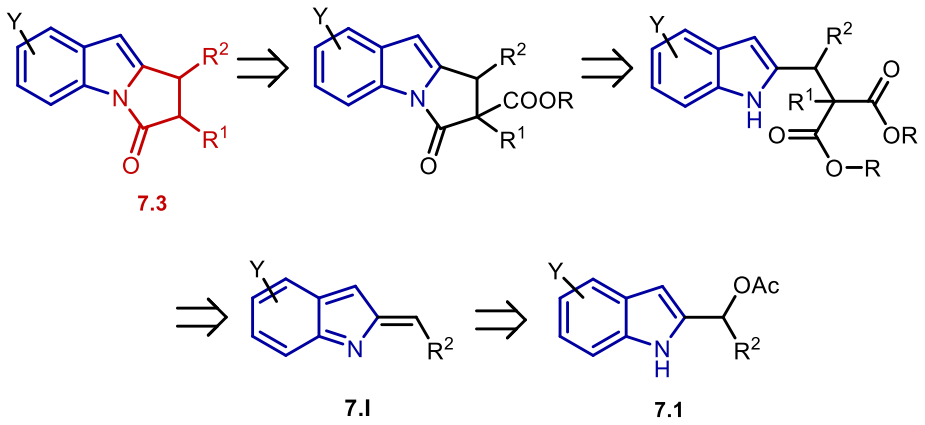

Scheme 7.*1***.** *Retrosynthetic approach to the 1,2-dihydro-3H-pyrrolo[1,2-a]indol-3-one scaffold.*

The sequential addition/annulation reaction of Meldrum's acid, malononitrile, and 1,3-dicarbonyls with *ortho*-quinone methides generated *in situ* under basic conditions was previously reported to achieve the one-pot synthesis of 3,4-dihydrocoumarins, 4H-chromenes, and xanthenones.[170] Moreover, the *in situ* generated aza-ortho-quinone methydes from *o*-aminobenzyl alcohol derivatives were reacted with Meldrum's acid to afford dihydroquinolinones.[171]

In literature, methodologies are also reported to easily obtain indolo[1,2-*a*]indoles derivatives from 1*H*-indol-2-yl carbinols via the *in situ* generation of 2-methide-2*H*-indoles intermediates. Particularly, the enantioselective Brønsted acid catalyzed [3 + 2]-cycloaddition of cyclic enamides and organocatalyzed asymmetric (4 + 3) cycloaddition with dienolsilanes to bicyclo[3.2.2]cyclohepta[*b*]indoles have been described.[172] In addition, recently, we observed the formation of reactive indole-methides under basic conditions, starting from indolylmethyl acetates.[173]

In the following, we describe the scope and limitations of this approach to the synthesis of the 1,2-dihydro-3*H*-pyrrolo[1,2-*a*]indol-3-ones 7.3.

7.2 Results and Discussion

We started our investigation by examining the reaction of (1H-indol-2-yl)methyl acetate 7.1a with (1H-indol-2-yl)methyl ethyl carbonate 1b with the 2,2,5-trimethyl-1,3-dioxane-4,6-dione 7.2a under basic conditions as the model system. Pleasingly, the desired 2-methyl-1,2-dihydro-3H-pyrrolo[1,2-a]indol-3-one 7.3a was isolated in 55% yield by

reacting 7.1a with 7.2a in DMSO at 100 °C in the presence of K_2CO_3 as the base (Table 7.1, entry 1).

Table 7.1. Optimization studies for the reaction of 7.1 with methyl Meldrum's acid 7.3a. [a]

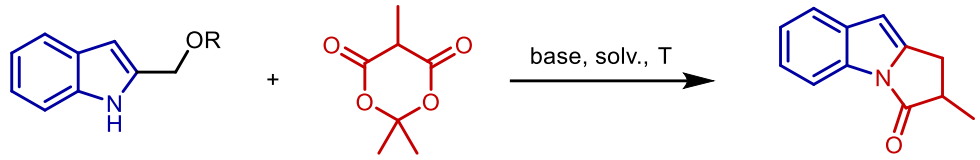

7.1 **7.2a** **7.3a**

Entry	**1**	**Catalyst**	**Base**	**Solvent**	**T (°C)**	**t (h)**	**yield 7.3a (%)** [b]
1	**1a**	/	K_2CO_3	DMSO	100	7	55
2	**1b**	/	NaH	DMSO	100	72	42(17)[c]
3	**1b**	$Pd_2(dba)_3/PPh_3$	K_2CO_3	MeCN	70	5.5	68
4	**1b**	$Pd_2(dba)_3/PPh_3$	K_2CO_3	MeCN	80	7	68
5	**1b**	$Pd_2(dba)_3/PPh_3$	K_2CO_3	DMSO	80	1.5	75
6	**1b**	$Pd_2(dba)_3/P(2\text{-furyl})_3$	K_2CO_3	DMSO	80	1	78
7	**1b**	$Pd_2(dba)_3$/dppf	K_2CO_3	DMSO	80	1.5	85
8	**1b**	$Pd_2(dba)_3$/dppf	/	DMSO	80	24	(30)[c]
9	**1a**	$Pd_2(dba)_3/PPh_3$	K_2CO_3	MeCN	100	40	67
10	**1a**	$Pd_2(dba)_3/PPh_3$	K_2CO_3	DMSO	100	5.5	75
11	**1a**	$Pd_2(dba)_3$/dppf	K_2CO_3	DMSO	100	2	88

[a] Unless otherwise stated, reactions were carried out on a 0.35 mmol scale under an argon atmosphere using 0.02 equiv. of $Pd_2(dba)_3$, 0.04 equiv. of dppf or 0.08 mmol of PPh_3 or P(2-furyl)$_3$, 1.5 equiv. of 2a, 1.5 equiv. of K_2CO_3 in 1.5 mL of DMSO. [b] Yields are given for isolated products. [c] Numbers in brackets refer to the percentage of the recovered 1. [d] The reaction was carried out without 2a.

A poorer result was observed by reacting 7.1b under the same reaction conditions in the presence of the stronger base NaH (Table 7.1, entry 2).

The advantages of the palladium catalysis in the reaction of benzofuran-2-ylmethyl acetates with nucleophiles[122a] prompted us to explore the palladium-catalyzed version of the same reaction using different ligands and solvents, as shown in Table 7.1. The palladium-catalyzed reaction of indolemethyl acetates **1** with boronic acid to afford the corresponding indole-containing diarhylmethanes has been previously investigated.[174] The formation of the target 7.3a occurred in good-to-high yields in DMSO or MeCN, both in the presence of a palladium complex containing a monodentate phosphine ligand (Table 7.1, entries 3–6 and 9–10) or bidentate phosphine one (Table 7.1, entries 7–8, 11–12). The best result was obtained by carrying out the reaction in DMSO at 100 °C in the presence of $Pd_2(dba)_3$/dppf as the catalyst (Table 7.1, entry 11). In previous studies on palladium-catalyzed benzylic substitution reactions, it was shown that the yields of the benzylation products were strongly affected by the bite angle of the bidentate bisphosphine ligand on the palladium catalyst.[175] The ligands dppf and DPEPhos were preferred for the benzylation of stabilized carbanions and amines, respectively. A complex mixture was observed when the reaction was performed without 7.2a and the starting material 7.1a was not recovered.

The exploration of the substrate scope of the procedure under the optimized condition reaction (Table 7.2) showed that 1,2-dihydro-3H-pyrrolo[1,2-a]indol-3-ones 7.3 bearing a variety of useful functional groups can be prepared in moderate-to-good yields.

Table 7.2. Synthesis of 2-substituted 1,2-dihydro-3*H*-pyrrolo[1,2-*a*]indol-3-one 3 from indol-2-ylmethyl acetates 7.1 and Meldrum's acid derivatives 7.2.[a]

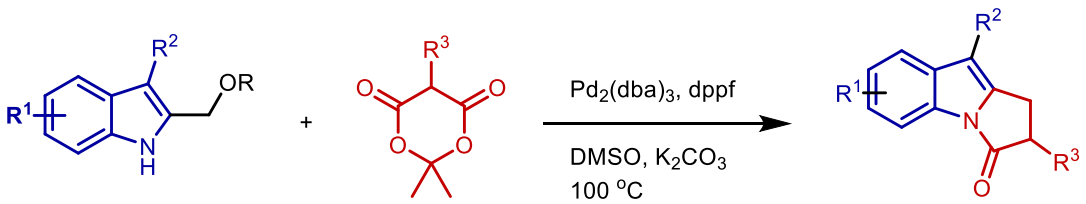

7.1 **7.2** **7.3**

Entry	**7.1**	**R^1**	**R^2**	**7.2**	**R^3**	**t (h)**	**Yield 7.3 (%) [b]**

1	**7.1a**	H	H	**7.2b**	-CH_2(4-OMe-C_6H_4)	1	**3b** (78)
2	**7.1a**	H	H	**7.2c**	-CH_2(furyl)	4	**3c** (63)
3	**7.1a**	H	H	**7.2d**	-Ph	24	(/)
4	**7.1a**	H	H	**7.2e**	-$CH_2CH_2CO_2Me$	3	**3d** (74)
5	**7.1c**	5-Me	H	**7.2a**	-Me	3	**3e** (70)
6	**7.1d**	5-Br	H	**7.2a**	-Me	5	**3f** (50)
7	**7.1e**	5-(4-Me-C_6H_4)	H	**7.2a**	-Me	4.5	**3g** (70)
8	**7.1f**	5-(4-F,3-Me-C_6H_3)	H	**7.2a**	-Me	5	**3h** (70)
9	**7.1g**	H	Ph	**7.2a**	-Me	3	**3i** (58)
10	**7.1g**	H	-Ph	**7.2b**	-CH_2(4-OMe-C_6H_4)	2	**3j** (64)
11	**7.1g**	H	-Ph	**7.2c**	-CH_2(2-furyl)	2	**3k**(54)
12	**7.1g**	H	-Ph	**7.2e**	-$CH_2CH_2CO_2Me$	2.5	**3l** (66)
13	**7.1h**	H	4-CF_3-C_6H_4	**7.2a**	-Me	1	**3m** (71)

*[a] Unless otherwise stated, reactions were carried out on a 0.35 mmol scale under an argon atmosphere using 0.02 equiv. of $Pd_2(dba)_3$, 0.04 equiv. of dppf, 1.5 equiv. of **2**, 1.5 equiv. of K_2CO_3 in 1.5 mL of DMSO at 100 °C. [b] Yields are given for isolated products. [c] The reaction was carried out on a 5.28 mmol scale.*

Several substituents, including methyl, nitro, fluoro, bromo, and tolyl, on the indole moiety of 7.3 were tolerated. A gram-scale experiment was also performed and showed the practicability

of this methodology (Table 7.2, entry 14) Moreover, we tested the reactivity of the (1H-indol-2-yl)(phenyl)methyl acetate **7.4a** and the 1-(1H-indol-2-yl)ethyl acetate 7.4b with some 5-substituted Meldrum's acid derivatives (Table 7.3).

Table 7.3. Synthesis of 1,2-disubstituted 1,2-dihydro-3*H*-pyrrolo[1,2-*a*]indol-3-one 5/5′ from indol-2-ylmethyl acetates 7.4 and Meldrum's acid derivatives 7.2.[a]

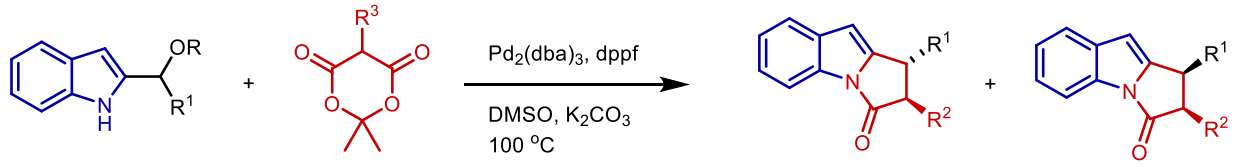

7.4 **7.2** **7.5** **7.5'**

Entry	**7.4**	R^1	**7.2**	R^2	t (h)	Ratio **7.5/5'** [b]	Yield **7.5+5'** (%) [c]
1	**7.4a**	-Ph	**7.2a**	-Me	2	84/16	**5a**+**5'a** (74)
2	**7.4a**	-Ph	**7.2b**	-CH_2(4-OMe-C_6H_4)	3	94/6	**5b**+**5'b** (50)
3	**7.4a**	-Ph	**7.2c**	-CH_2(furyl)	2	74/26	**5c**+**5'c** (52)
4	**7.4b**	-Me	**7.2a**	-Me	24	84/16	**5d**+**5'd** (76)

[a] *Unless otherwise stated, reactions were carried out on a 0.35 mmol scale under an argon atmosphere at 100 °C using 0.02 equiv. of $Pd_2(dba)_3$, 0.04 equiv. of dppf, 1.5 equiv. of **7.2**, 1.5 equiv. of K_2CO_3 in 1.5 mL of DMSO.* [b] *Diastereomeric ratios were calculated from the ^1H NMR analyses.* [c] *Yields are given for isolated products.*

In all the tested cases, the reaction led to the formation of the corresponding 1,2-dihydro-3*H*-pyrrolo[1,2-*a*]indol-3-one with good-to-excellent diastereoselectivity. Control experiments have shown that the observed diastereoselectivity depends on the relative stability of the *trans* 7.5 compared to the *cis*- diastereomer 7.5′. In fact, by heating the pure diastereomer 7.5a or 7.5a′ (R^1 = Ph, R^2 = Me) at 100 °C in DMSO for 1h in the presence of K_2CO_3, a rapid equilibrium occurred, leading to the formation of the mixture of the two diastereomers in equal ratio to that observed in the synthetic run (Table 7.3, entry 1). These data match with ΔG°calculated with Gaussian (HF, 3–21G*) (the *trans* stereoisomer is more stable than *cis* by 1.23 Kcal/mol, corresponding to the 88/12 7.5a/5a′ ratio).

Regarding the reaction mechanism for the one-pot synthesis of 1,2-dihydro-3*H*-pyrrolo[1,2-*a*]indol-3-one 7.3 from indol-2-ylmethyl acetates and Meldrum's acid derivatives, we believe that the *in situ* generation of the indolyl methide intermediate 7.I could be a common intermediate both for the base promoted and the palladium-catalyzed process (Scheme 7.2). Experiments to detect the key intermediate 7.I under basic conditions have been previously described.[172c] Regarding the palladium-catalyzed procedure, it is well known that the oxidative addition of the Pd(0) to the indol-2-ylmethyl acetate generates the η^3 palladium complex 7.III in equilibrium with the η^1 palladium complex 7.II. It may be supposed that an unusual 1,4-elimination from this later intermediate, involving cleavage of the N-H bond,[176] may afford the indolyl methide 7.I with the regeneration of the Pd(0) catalyst. Although the formation of the intermediate derivative 7.6 via the palladium-catalyzed Tsuji–Trost-type reaction could not be ruled out, we failed to isolate any C_3 functionalized indole derivative.

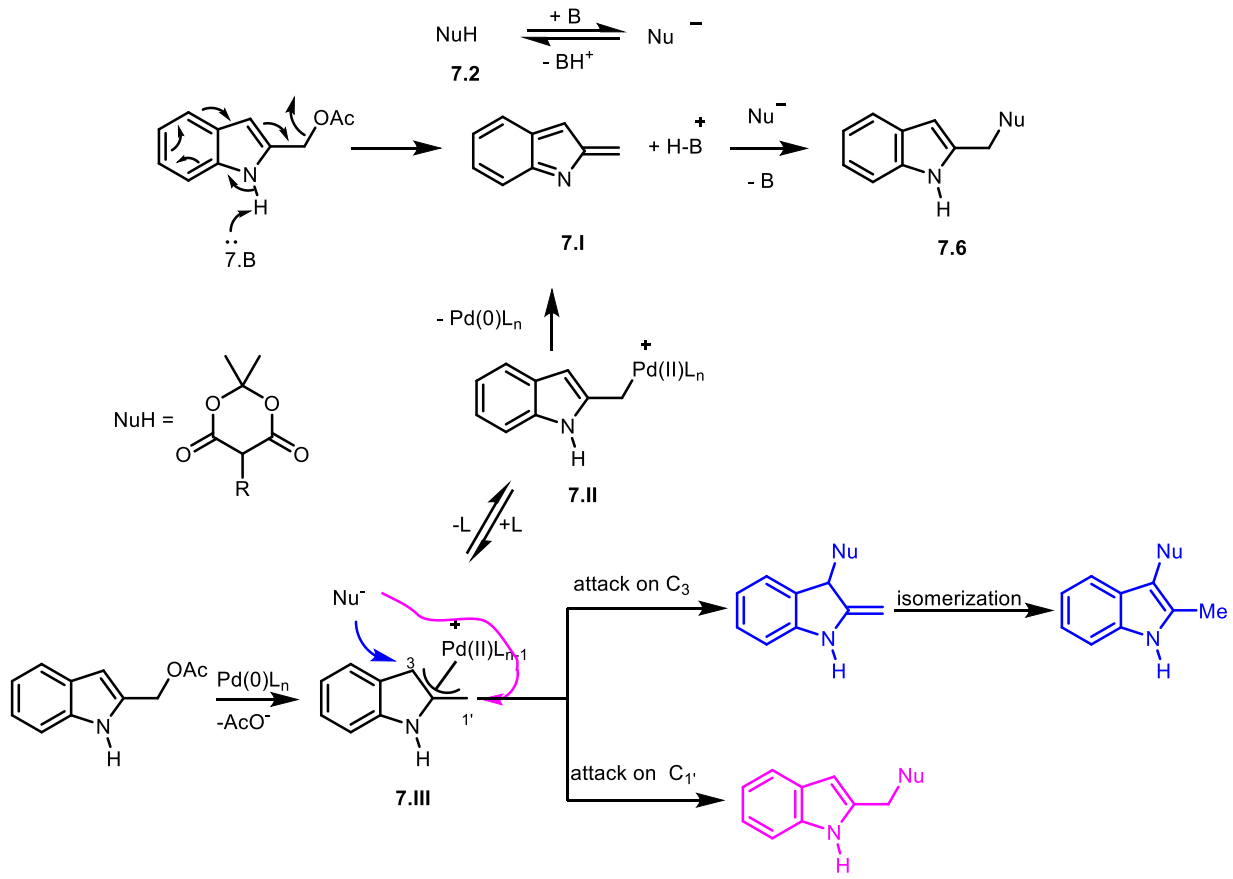

Scheme 7.2. The reaction of 7.1a with Meldrum's acid 7.2.

The subsequent sequential cyclization of 7.6, followed by the elimination of acetone and CO_2, affords the target products (Scheme 7.3).

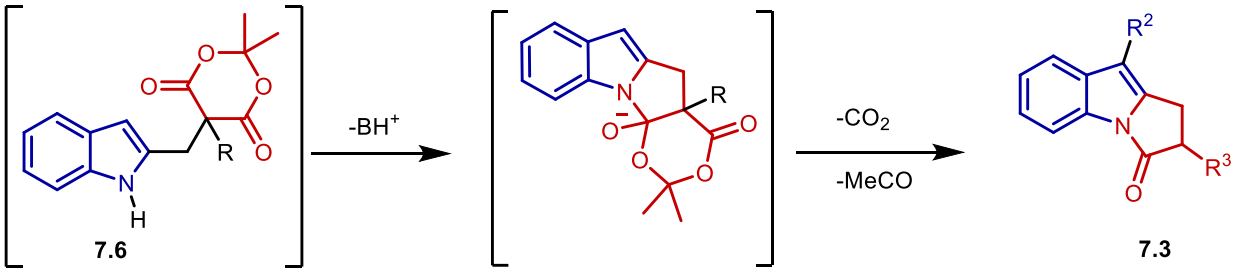

Scheme 7.3. Cyclization of 7.6.

Accordingly, we continued our studies to address product selectivity control. For this purpose, we analyzed the reaction outcome when the indol-2-ylmethyl acetate 7.1a was reacted with unsubstituted Meldrum's acid 7.7 in different stoichiometric ratios. Our result suggested that the competitive deprotonation of the Michael adduct 7.6a under the basic reaction conditions generates a new enolate species which is prone to undergo a second Michael addition over the indolyl methide intermediate to afford the 2-((1*H*-indol-2-yl)methyl)-1,2-dihydro-3*H*-pyrrolo[1,2-a]indol-3-one 7.9 after cyclization. Conversely, the prevalence of the cyclization of 7.6a allowed the isolation of the 1,2-dihydro-3*H*-pyrrolo[1,2-a]indol-3-one 7.8 when the reaction was carried out in the presence of a large excess of Meldrum's acid (Scheme 7.4).

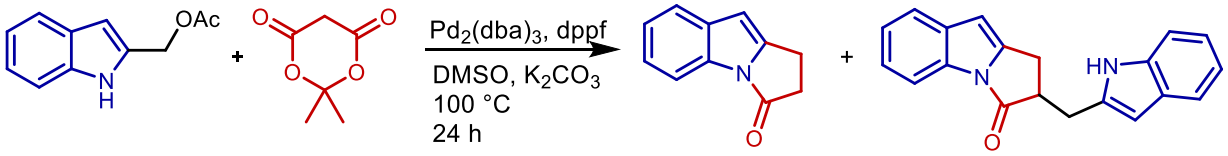

7.1a *[1.0 equiv]*	***7.7*** *[1.5 equiv.]*	***7.8*** *(/)*	***7.9*** *(54 %)*
7.1a *[2.5 equiv]*	***7.7*** *[1.0 equiv.]*	***7.8*** *(/)*	***7.9*** *(42 %)*
7.1a *[1.0 equiv]*	***7.7*** *[5.0 equiv.]*	***7.8*** *(52%)*	***7.9*** *(/)*

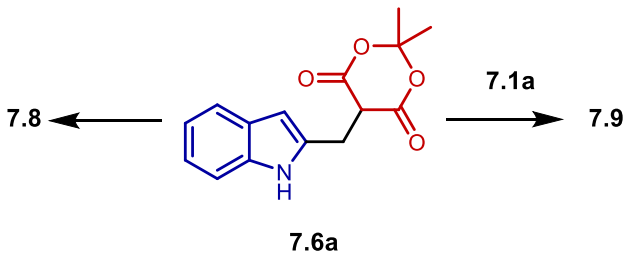

Scheme 7.4. The reaction of 7.1a with Meldrum's acid 7.7.

Next, we explored the reactivity of building block 7.1a with other methylene active compounds. Both the ethyl malonate 7.10 and the ethyl-3-oxobutanoate 7.12 were compatible with the procedure, allowing to obtain, respectively, the title products 7.11 and 7.13 in moderate yields in the presence of 5 equiv. excess of the starting dicarbonyl (Scheme 7.5).

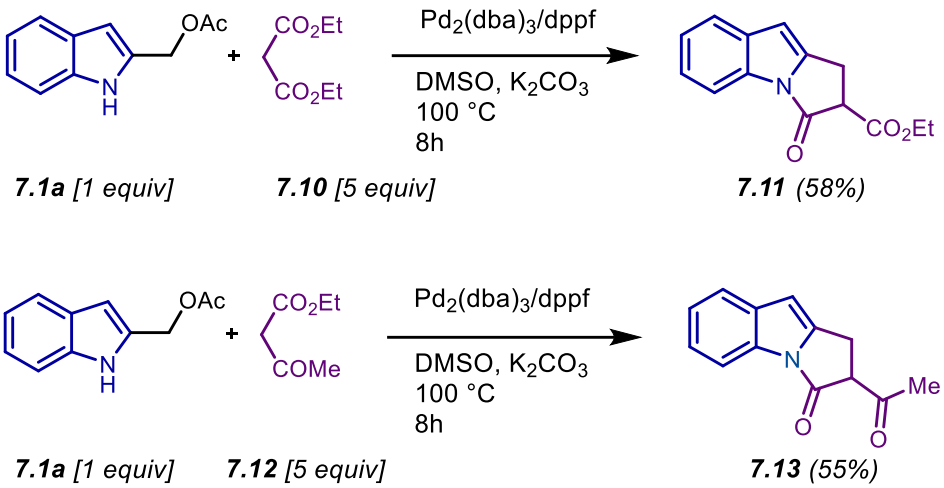

Scheme 7.5. Reaction of 7.1a with ethyl malonate 7.10 and the ethyl-3-oxobutanoate 7.12.

More intriguing results were observed when 7.1a was reacted with the ethyl 2-methyl-3-oxobutanoate 7.14a or the diethyl 2-methylmalonate 7.14b (Scheme 7.6). Surprisingly, both the palladium reaction of the ethyl 2-methyl-3-oxobutanoate 7.14a and its base-promoted one occurred with poor results, while a good yield of the corresponding product 3 was observed in the reaction of 1a with the ethyl 2-acetylpent-4-enoate 7.14c (Table 7.4, entries 3). Moreover, we isolated in satisfactory yield the ethyl 2-methyl-3-oxo-2,3-dihydro-1*H*-pirrolo[1,2-a]indole-2-carboxylate 7.15 in the palladium-catalyzed reaction of 7.1a with 7.14b.

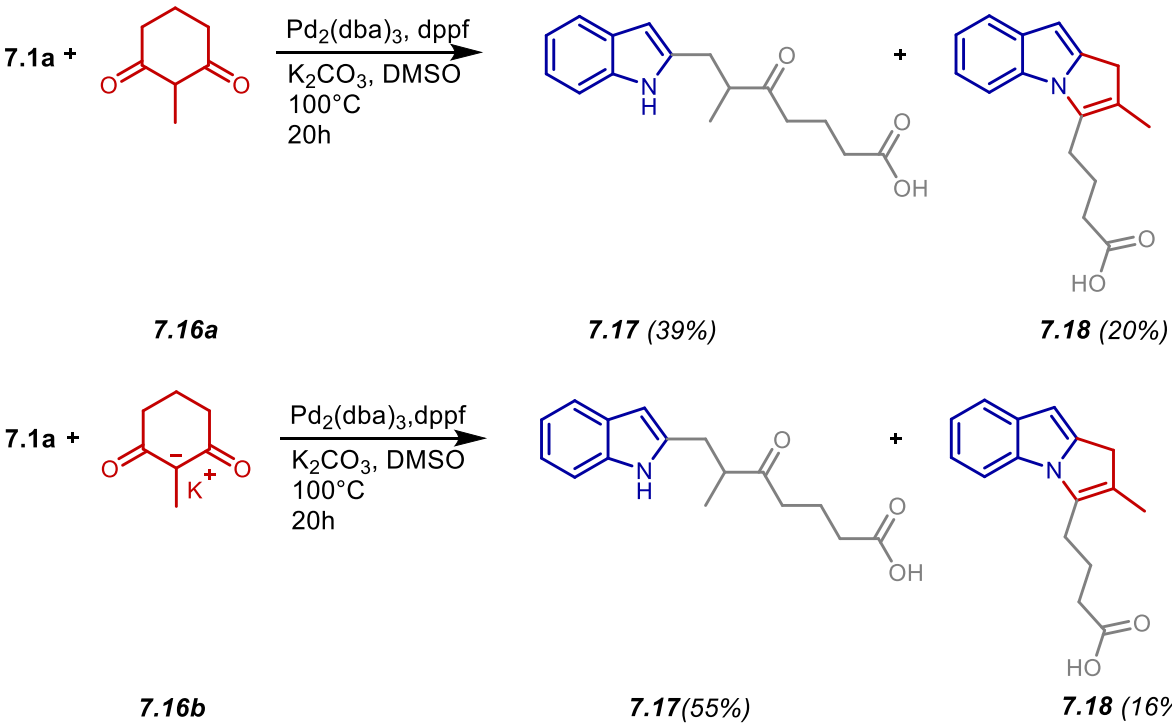

Scheme 7.6. Reaction of indol-2-ylmethyl acetate 7.1a with 2-methylciclohexan-1,3-dione 7.16a and its potassium salt 7.16b.

Table 7.4. Synthesis of 2-substituted 1,2-dihydro-3*H*-pyrrolo[1,2-*a*]indol-3-one 7.3/15 from indol-2-ylmethyl acetates 7.1a and substituted methylene active compound 7.14.[a]

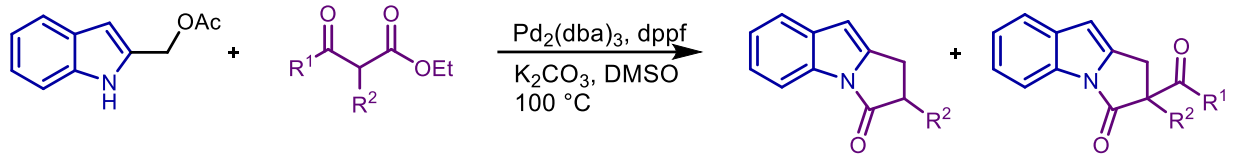

7.1a **7.14** **7.3** **7.15**

a: R^1 = Me
b: R^1 = OEt

Entry	**7.14**	R^1	R^2	t (h)	Yield **7.3** (%)	Yield **7.15** (%) [b]
1	**7.14a**	-Me	-Me	1	**7.3a** (45)	**7.15a** (18) [c]
2	**7.14a**	-Me	-Me	3	**7.3a** (46)	traces
3	**7.14a**	-Me	$-CH_2CH=CH$	4	**7.3n** (71)	/
4	**7.14b**	-OEt	-Me	24	/	**7.15b** (60)

[a] *Unless otherwise stated, reactions were carried out on a 0.35 mmol scale under an argon atmosphere at 100 °C using 0.02 equiv. of $Pd_2(dba)_3$, 0.04 equiv. of dppf, 1.5 equiv. of **7.14**, 1.5 equiv. of K_2CO_3 in 1.5 mL of DMSO.* [b] *Yields are given for isolated products.* [c] *The reaction was carried out without a catalyst.*

Finally, we examined the reaction of 7.1a with the 2-methylcyclohexan-1,3-dione 7.16a or its potassium salt 7.16b. In both cases, the product of sequential Michael addition/retro Dieckmann reaction 7-(1*H*-indol-2-yl)-6-methyl-5-oxoheptanoic acid 7.17, together with its cyclized derivative 4-(2-methyl-1*H*-pyrrolo[1,2-*a*]indol-3-yl)butanoic acid 7.18 (16% yield), was isolated (Scheme 7.6).

7.3 Conclusion

In summary, a viable approach to polysubstituted 1,2-dihydro-3*H*-pyrrolo[1,2-*a*]indol-3-ones through a domino palladium-catalyzed reaction of the readily available indol-2-ylmethyl acetates with 1,3-dicarbonyl derivatives has been developed. The employment of 5-substituted Meldrum's as the dicarbonyl source in the palladium-catalyzed reaction with indol-2-ylmethyl acetates method allowed the synthesis of the 2-substituted-1,2-dihydro-3*H*-pyrrolo[1,2-*a*]indol-3-one derivatives in moderate-to-high yields and tolerates a variety of useful functional groups both in the indole and in Meldrum's acids, including bromo, fluoro, nitro, aryl, heteroaryl ether,

and ester groups. The extension of the procedure to the highly diastereoselective synthesis of the *trans*- 1,2-disubstituted-1,2-dihydro-3*H*-pyrrolo[1,2-*a*]indol-3-ones from the (1*H*-indol-2-yl)phenyl acetate under the same reaction conditions has been explored. The product selectivity control of the outcome of the reaction of indol-2-ylmethyl acetate with various alicyclic 1,3-dicarbonyls was addressed by a suitable choice of the reagent ratio. A different cascade reaction of the indol-2-ylmethyl acetate with 2-methylcyclohexan-1,3-dione and the corresponding potassium salt involving Michael addition/retro Dieckmann or/and Michael addition/retro Dieckmann/cyclization sequences provides promise for further challenging the elaboration of the indole nucleus and is under investigation in our laboratories

Chapter 8. Synthesis of functionalized 3H-pyrrolo-[1,2,3-de] quinoxalines via gold-catalyzed intramolecular hydroamination of alkynes

8.1 Introduction

Nitrogen-containing heterocycles are a class of compounds of great importance to life science since they are present as scaffolds in several biologically active natural products and synthetic drugs.[107a] For this reason, a great deal of attention has been devoted to the development of methods for their preparation and, in particular, to those catalytic protocols that overcome the limits of traditional C-N bond-forming reactions. In this regard, the transition metal-catalyzed hydroamination assumed great significance,[177] with a lot of expedient routes based on gold catalysis.[178]

In this regard, we previously described a domino approach to 4-substituted 1,5-benzodiazepines based on the reactive sequence gold-catalyzed hydroamination/cyclization (scheme 8.1A),[179] as well as a stereo and regioselective approach to Z-enamine products via an intermolecular gold-catalyzed reaction of the 2-(arylethynyl)pyridines with anilines (scheme 8.1B).[180] Continuing our investigations in this research field, we focused on the construction of 3H-pyrrolo-[1,2,3-de] quinoxalines 8.2 starting from suitable substituted N-alkynyl indoles 8.1. (Scheme 8.1, C).

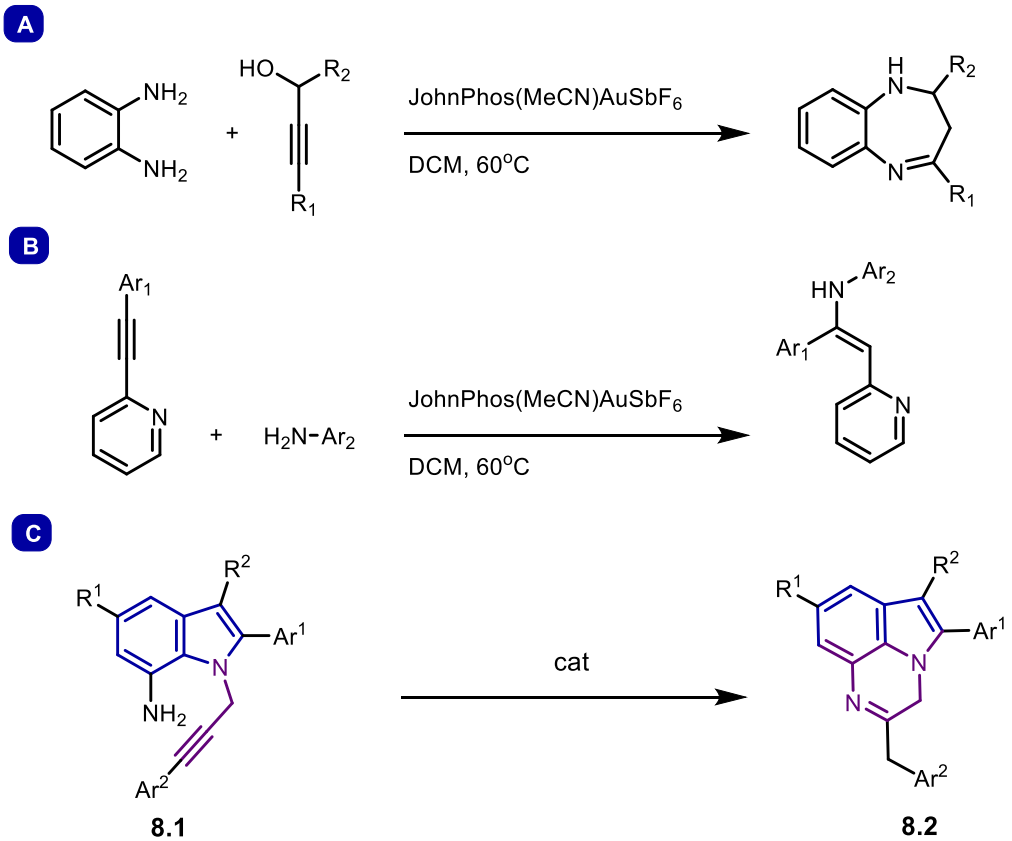

8.1 **8.2**

Scheme 8.1. Work hypothesis gold-catalyzed synthesis of functionalized 3H-pyrrolo-[1,2,3-de] quinoxalines from substituted N-alkynyl-indoles.

To the best of our knowledge, the derivatives of which the synthesis was pursued are unknown compounds with a rather infrequently reported heterocyclic core.[181] Extensive state-of-the-art studies revealed a lack of methods to achieve their construction, even though their synthesis might be of interest in medicinal chemistry. Indeed, the tricyclic quinoxaline-containing compounds are widespread in a variety of therapeutic agents such as anti-HIV,[182] antiparasitic,[183] and antitumoral[183d] (Figure 8.1), and make our new condensed cyclic systems promising candidates for diverse uses.

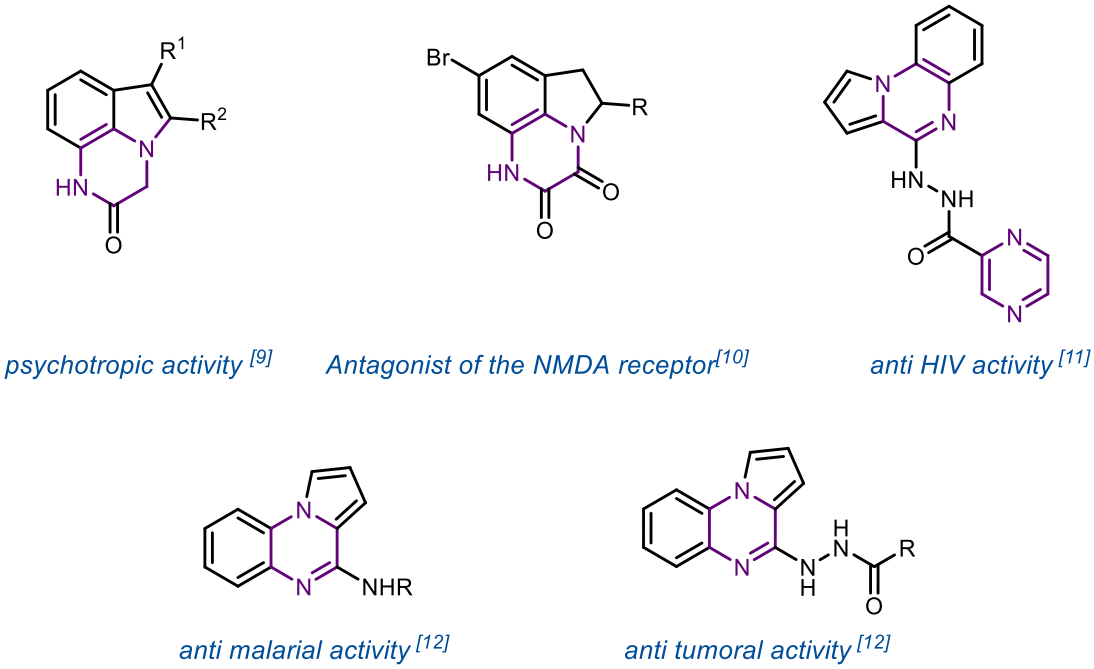

Figure 8.1. Bioactive synthetic products containing tricyclic quinoxaline-containing scaffold.

7.2 Results and Discussion

Substrates for our studies have been synthesized according to slightly modified known procedures detailed in the Supplementary Materials and depicted in the following scheme 8.2.

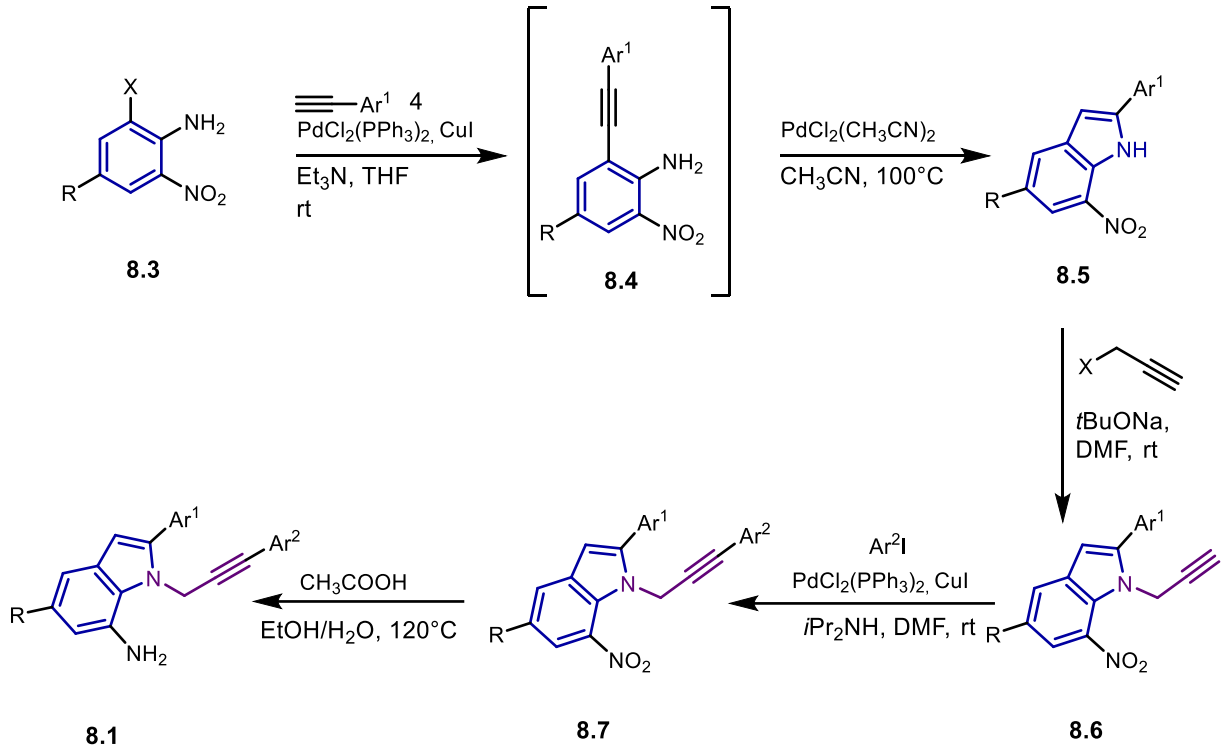

Scheme 8.2. Synthesis of substrates 8.1

Based on the working hypothesis (Scheme 8.2), the reaction of substrate 8.1a was selected as the model system for a series of preliminary experiments aimed at identifying the best reaction conditions. For our first attempt, we decided to perform the reaction under the same condition previously used for the synthesis of 1,5 benzodiazepines.[179] Pleasingly, a smooth gold-catalyzed intramolecular hydroamination of 8.1a took place and the 6-*exo*-dig cyclization product 8.2a was isolated in almost quantitative yield after 1 hour (Table 8.1, entry 1).

Table 8.1. Synthesis of 2-benzyl-7-chloro-5-phenyl-3*H*-pyrrolo[1,2,3-*de*]quinoxaline 8.2a from 4-chloro-2-phenyl-1-(3-phenylprop-2-yn-1-yl)-1*H*-indol-7-amine 8.1a.

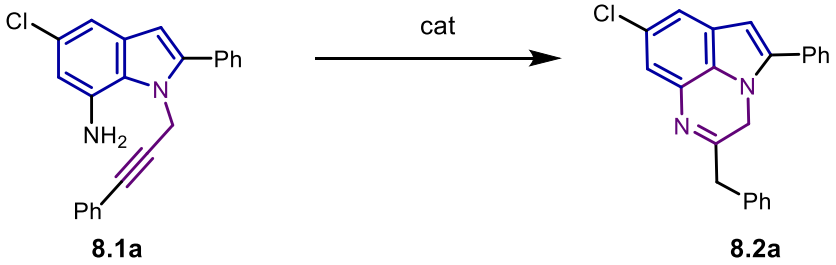

Entry[a]	Catalysts (mmol%)	Solvent	T (°C)	Time (h)	Yield 8.2a[b] (%)
1	JP(MeCN)AuSb$_6$ [c] (2)	CH_2Cl_2	60	1	98
2	JP(MeCN)AuSb$_6$ [c] (2)	CH_2Cl_2	rt	7	98
3	$PPh_3AuCl/AgSbF_6$ (2/2)	CH_2Cl_2	rt	24	42[d]

4	$PtCl_2$ (4)	EtOH	80	24	83[e]
5	$PdCl_2(CH_3CN)_2$ (5)	CH_3CN	80	2	36

[a] *Reactions were carried out on 0.25 mmol of* ***8.2a*** *in 1.0 mL of solvent and in the presence of catalyst in the reported mmol percentage.* [b] *Yields are given for isolated products.* [c] *JP = JohnPhos.* [d] *55% of starting material* ***8.2a*** *recovered.* [e] *14% of starting material* ***8.2a*** *recovered.*

Given the high reaction rate, we decided to carry out the reaction at room temperature obtaining similar results in terms of yield even though with a longer reaction time (Table 8.1, entry 2). A lower yield was obtained by switching to the $PPh_3AuCl/AgSbF_6$ combination (Table 8.1, entry 3), while the reaction carried out in the presence of palladium or platinum catalysts resulted in a slower and less efficient cyclization (Table 8.1, entries 4 and 5).

Once established the best reaction conditions, we investigated this method's scope. Variously substituted quinoxaline derivatives were obtained in good to excellent yield both in the presence of electron-donating groups and electron-withdrawing groups (Table 8.2).

Table 8.2. Synthesis of functionalized 3*H*-pyrrolo-[1,2,3-*de*] quinoxalines **8.2** from substituted *N*-propargyl indoles **8.1** through a gold-catalyzed intramolecular hydroamination**.**

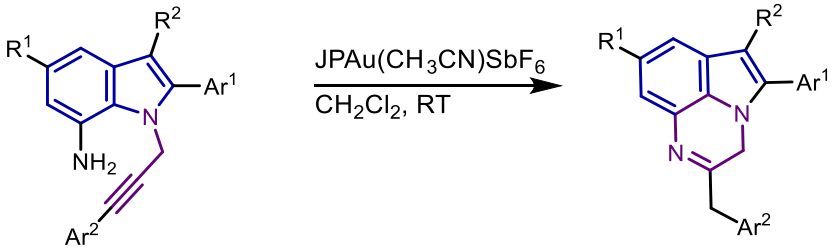

8.1 **8.2**

Entry[1]	8.1	R^1	R^2	Ar^1	Ar^2	8.2	Time (h)	Yield (%)[2]
1	**8.1a**	C	H	Ph	Ph	**8.2a**	7	98
2	**8.1b**	Cl	H	Ph	4-Cl-C_6H_4	**8.2b**	1	86
3	**8.1c**	Cl	H	Ph	4-OMe-C_6H_4	**8.2c**	1.5	80
4	**8.1d**	Cl	H	Ph	4-COMe-C_6H_4	**8.2d**	1.5	85
5	**8.1e**	Cl	H	4-OMe	3-CF_3-C_6H_4	**8.2e**	4	80
6	**8.1f**	Cl	H	4-OMe	4-OMe-C_6H_4	**8.2f**	18	80
7	**8.1g**	Me	H	Ph	4-COMe-C_6H_4	**8.2g**	24	90

8	**8.1h**	Me	H	4-CO_2Me	4-Cl-C_6H_4	**8.2h**	3	80
9	**8.1i**	Me	H	Ph	4-Cl-C_6H_4	**8.2i**	5	79
10	**8.1j**	Me	H	Ph	-	**8.2j**	1	-[3]
11	**8.1k**[4]	Me	4-OMe-C_6H_4	4-COMe-C_6H_4	Ph	**95k**	3	84

[1] *Reactions were carried out on 0.25 mmol of* ***8.2*** *in 1.0 mL of* CH_2Cl_2*, in the presence of 0.02 equiv of* $JPAu(CH_3CN)SbF_6$. [2] *Yields are given for isolated products.* [3] *Degradation compounds.* [4] *Starting material* ***8.2l*** *has been prepared according to the procedure detailed in Supplementary Materials.*

Notably, in all experiments, compound **8.2** was the only observed product, with no traces of any 7-*endo*-dig cyclization product (compounds **8.8** and **8.8'**, Figure 8.2).

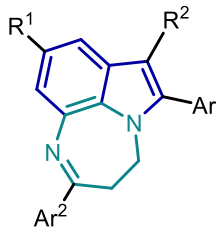

8.8

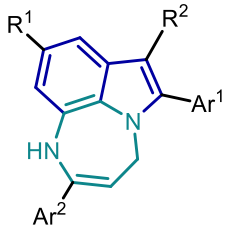

8.8'

Figure 8.2. Structures of two possible isomeric 7-endo-dig cyclization products. The formation of these compounds was never observed.

The formation of 95 may be rationalized based on the general mechanism of the gold-catalyzed hydroamination,[184] by admitting the initial formation of the intermediate II, deriving from the Au(I)-catalyzed 6-*exo-dig* cyclization of the starting compound 8.1 (Scheme 8.3).

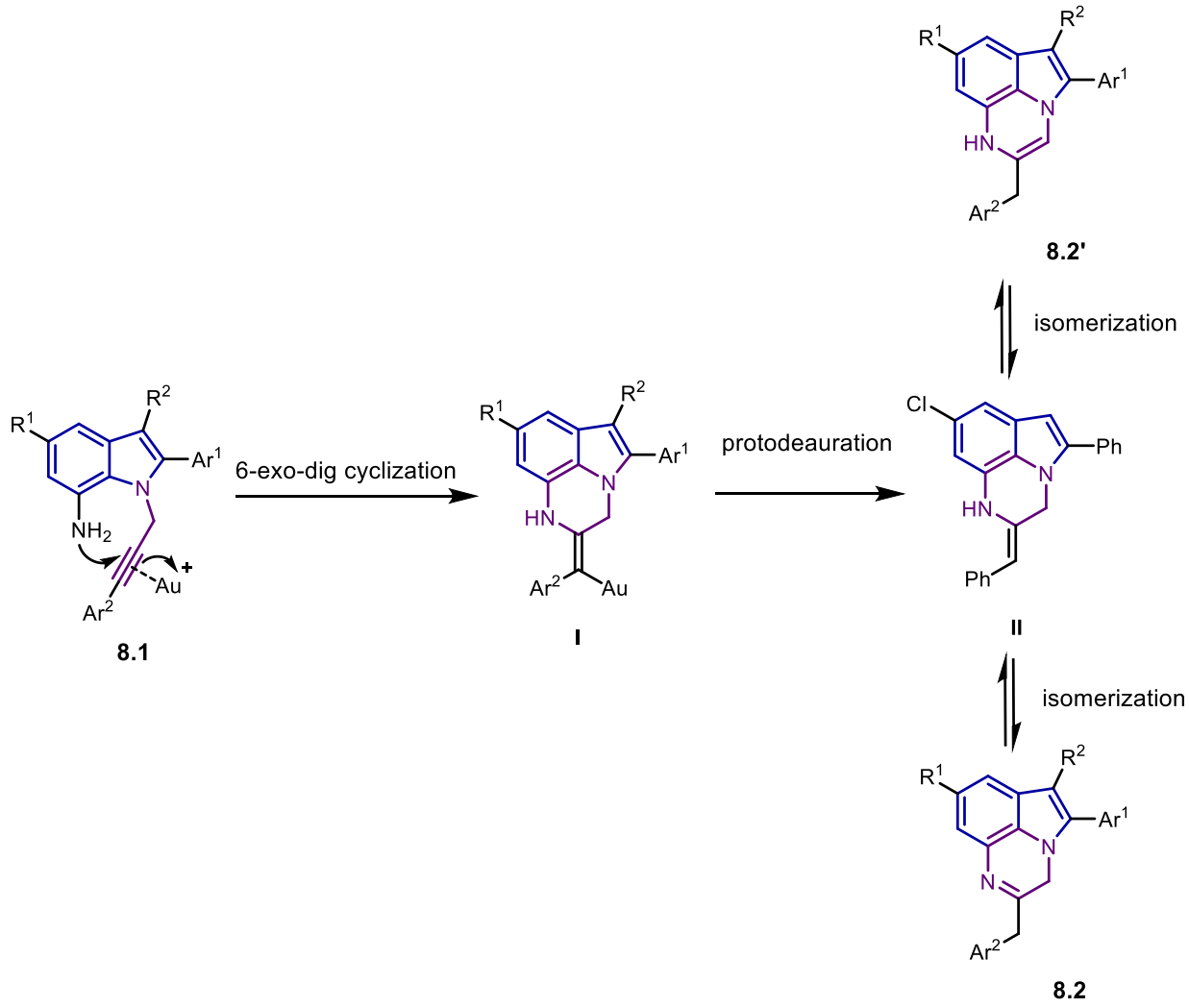

Scheme 8.3. Hypothesized mechanism for the formation of 8.2.

Then, the isomerization of II could take place giving the imine-derivative 8.2 or the enamine-derivative 8.2', with the first more stable than the second.

In this regard, HF (6-31G**) calculations performed on the two isomeric compounds 8.2a and 8.2'a revealed a higher stability of 8.2a than 8.2'a by 5.2 kcal/mol (Figure 8.3)[185] and justified the exclusive formation of imine-derivative 8.2 in the reaction conditions. In addition, similar isomerization modes are described in the literature.

8.2a **8.2'a**

*Figure 8.3. HF (6-31G**) calculations on 8.2a and 8.2'a*

The 5-aryl-3*H*-pyrrole[1,2,3-*de*]quinoxaline derivatives synthesized according to the proposed method are synthetic intermediates useful for the preparation of other polycyclic compounds through easy reactive steps. For instance, by treating 8.2d with $LiAlH_4$, compound 8.9d is obtained in almost quantitative yield (Scheme 8.4).

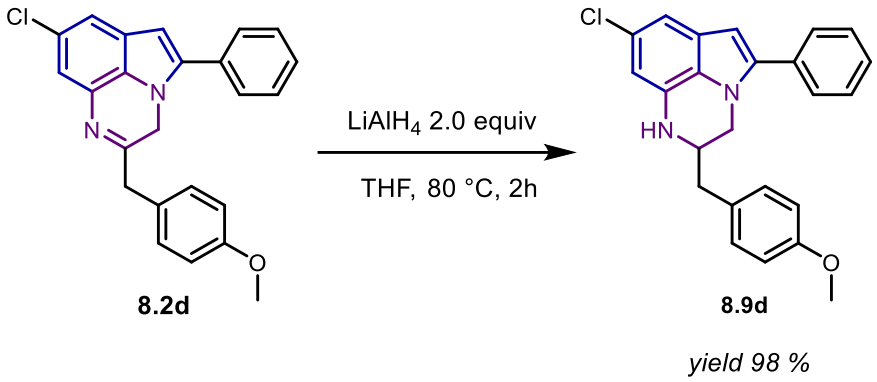

Scheme 8.4. Reduction of compound 8.2d to obtain 8.9d

This compound is similar in structure to a class of potent Mcl-1 inhibitors (Figure 8.4),[186] and may be poised for further manipulations on the NH position.

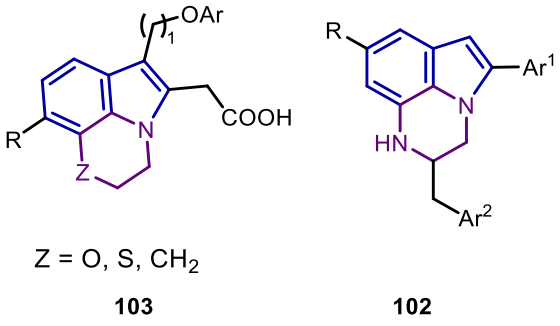

Figure 8.4. Structure of known Mcl-1 inhibitors 103 and of synthesized compounds 102.

8.3 Conclusion

A protocol for the synthesis of functionalized 3*H*-pyrrolo-[1,2,3-*de*] quinoxalines from substituted *N*-alkynyl-indoles has been developed. The mild reaction conditions in which the reaction takes place make the method compatible with useful functional groups including halogen, alkoxyl, cyano, ketone, and ester, with yields from good to high in all the cases. A rationale for the formation of the title compound has been provided supporting the hypothesis with theoretical calculations.

Chapter 9. Perfluorooxosulfate Salts as SOF_4-Gas-Free Precursors to Multidimensional SuFEx Electrophiles

9.1 Introduction

The role of S^{VI}–F bonds as connective hubs has significantly heightened interest in high-valent sulfur species..[187] Sulfur(VI)−Fluoride Exchange (SuFEx) chemistry encompasses a series of reactions in which fluoride is replaced at the electrophilic sulfur center.[79a, 188] These sulfur-based linkages are instrumental in enabling the synthesis of covalently linked structures through S(VI) hubs (Scheme 1A). In 2014, Sharpless introduced this area of click chemistry by exploring the unique reactivity of sulfonyl fluorides ($R-SO_2F$) and fluorosulfates ($R-OSO_2F$).[72] This was later extended to include sulfurimidoyl fluoride ($RN=SOF_2$)[189] and thiazyl fluoride (NSF_3)[190] compounds, which represented a significant advancement due to their multiple-bonded azasulfur(VI) moieties and readily interchangeable S-F bonds that facilitate consecutive nucleophilic exchanges (Scheme 9.1B). A growing form of research has since delved into the chemistry of [RN=S=O]-based SuFExable compounds, uncovering intriguing reactivity across a spectrum of applications, from small molecules[81, 191] to bioconjugation[189a, 192] and polymers.[193]

Sulfurimidoyl fluorides, which are tetravalent azasulfur(VI) compounds, are produced through the reaction of a primary amine with thionyl tetrafluoride (SOF_4), a fluorosulfane gas that boils at -49°C. This reaction, first described by Cramer and Coffman,[194] yields difluorides that are notably stable and resistant to hydrolysis, attribute shared by many S^{VI} fluorides. Following 1970, these compounds were rarely discussed in the literature,[195] until Sharpless and others significantly expanded the understanding of SOF_4 as a SuFEx hub, leading to the synthesis of sulfurimidoyl fluorides[189c] and their subsequent reactions with phenols,[193c] amines,[189a] organosilanes[196] or organolithiums.[189b] (Scheme 9.1C).

Although the downstream potential of iminosulfur oxydifluorides is significant, their preparation remains a critical bottleneck. While synthesis from SOF_4 gas and primary amines is highly efficient, the limited availability and high cost of SOF_4 pose challenges.[197] This scarcity has prompted some laboratories to produce SOF_4 in-house, typically through the NO_2-catalyzed oxygenation of SF_4 gas (Scheme 9.1D).[189c, 198] However, for laboratories without specialized expertise, the complexities of gas-phase synthesis and the lack of appropriate equipment for condensing and storing the product hinder the adoption of this promising area of SuFEx

chemistry (Scheme 9.1A). To fully unlock the potential of these three-dimensional click hubs, a more accessible method for preparing iminosulfur oxydifluorides is urgently needed.

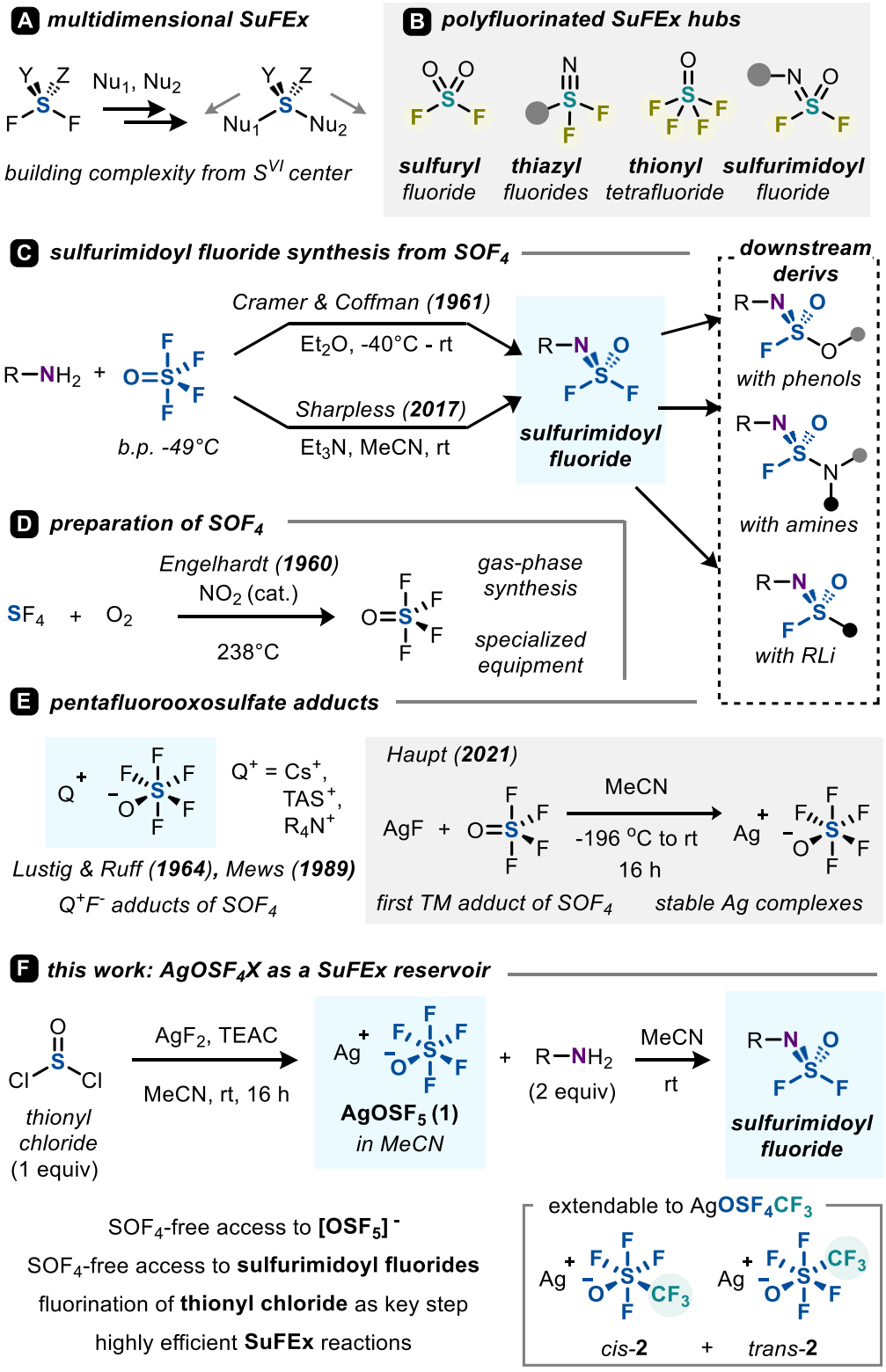

Scheme. 9.1 *A) Multidimensional SuFEx; B) Polyfluorinated SuFEx hubs; C) Sulfurimidoyl fluoride synthesis from SOF_4; D) Preparation of SOF_4; E) Pentafluorooxosulfate adducts F) This work: $AgOSF_4X$ as a SuFEx reservoir.*

We identified pentafluorooxosulfate ($Q^+OSF_5^-$) salts as promising non-gaseous reservoirs for SOF_4. Although pentafluorooxochalcogenate salts [O(S, Se, Te)F_5] have been documented in the literature for some time, their stability and accessibility vary significantly.[199] Broad research has focused on compounds containing the $[OSeF_5]^-$ anion, with particular emphasis on $[OTeF_5]^-$ and M($OTeF_5$)n derivatives.[200] However, the investigation of $HOSF_5$ remains limited due to its its instability, as it decomposition at -60 °C.[201] Since the 1960s, researchers have synthesized Q^+F^- adducts of SOF_4, such as the partially stable $CsOSF_5$ (Scheme 9.1E).[202] Later work by Mews and others introduced organic salts of $[OSF_5]^-$, which have even been employed to incorporate this functional group into organic compounds.[203] A notable advancement occurred in 2021 when Haupt, Röschenthaler, and their team developed the first transition metal complexes containing $[OSF_5^-]$ anions, specifically silver pentafluorooxosulfate ($Ag^+OSF_5^-$).[204] They synthesized $AgOSF_5$ by reacting AgF with OSF_4 in MeCN at -196°C over 20 hours. Despite these important developments, the synthesis of valuable $[OSF_5^-]$ structures still rely on the use of SOF_4 gas.

In this study, we seek to address the persistent reliance on SOF_4 by developing a novel synthesis method for $AgOSF_5$ and exploring its potential as an alternative SuFEx hub. Our goal was to establish a broadly applicable protocol for producing $AgOSF_5$ efficiently from commercially available starting materials. Building on Nozaki's work, we proposed that $AgOSF_5$ could be synthesized through the oxidative fluorination of thionyl chloride ($SOCl_2$) using an excess of AgF_2 and a tetralkylammonium halide catalyst.[205] Our experiments confirmed that this combination of reagents reliably produced MeCN stock solutions of $AgOSF_5$ with nearly quantitative yields (Scheme 9.1F). Moreover, by combining a primary amine directly with this hexacoordinate Ag complex in a one-pot reaction, we could regenerate the reactivity of SOF_4 without the need for a separate gas evolution step. As a result, both aromatic and aliphatic amines were successfully converted into sulfurimidoyl fluorides ($RNSOF_2$), compounds that are typically difficult to obtain, with high efficiency. Additionally, we applied this methodology to synthesize $AgOSF_4CF_3$, a previously unreported trifluoromethyl analogue of $AgOSF_5$, and used it to produce a range of triflimidoyl fluorides ($CF_3SO(NR)F$). This work highlights the broad applicability and effectiveness of $AgOSF_4X$ salts as novel SuFEx hubs.

9.2 Results and Discussion

Building on the established stability of $AgOSF_5$ demonstrated in Haupt's work (Scheme 9.1E), we hypothesized that generating $AgOSF_5$ under mild and safe conditions could provide a practical approach for its use as a novel SuFEx hub. Our study began by employing $SOCl_2$, tetraethylammonium chloride (TEAC), and AgF_2 as an oxidizing agent in anhydrous MeCN to

synthesize $AgSOF_5$, as detailed in Table 9.1. We achieved an excellent yield using 2 equivalents of TEAC and 16 equivalents of AgF_2 after an overnight reaction (Table 9.1, entry 1). We then explored other conditions to reduce the amount of AgF_2 (Table 9.1, entries 2-3) and shorten the reaction time (Table 9.1, entries 4-6). However, these adjustments resulted in lower yields, leading us to retain the conditions in entry 1 as our final protocol. Nonetheless, commendable yields of 79% and 86% were obtained after only 3 and 6 hours, respectively (Table 9.1, entries 4 and 5).

Table 9.1. Investigation of the reaction parameters for the synthesis of $AgOSF_5$[a]

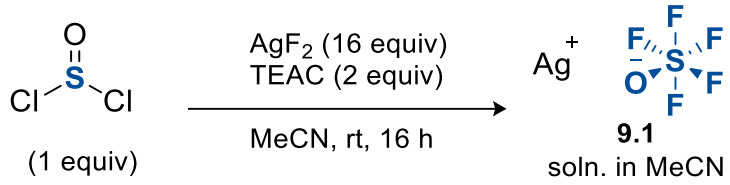

entry	variation from the standard conditions	yield (%) of **9.1**[b]
1	none	98
2	AgF_2 (12 equiv.)	71
3	AgF_2 (8 equiv.)	38
4	3 hours reaction time	79
5	6 hours reaction time	86
6	AgF_2 (12 equiv.), 3 hours reaction time	68

With optimized condition in hand, we proceeded to utilize $AgOSF_5$ as a versatile SuFEx hub by examining its reactivity with a wide array of aromatic and aliphatic primary amines. The amine nucleophiles were simply added to the prepared $AgOSF_5$ solution in MeCN. To our satisfaction, these reactions proceeded exceptionally well, typically achieving quantitative conversions to sulfurimidoyl difluorides within just 1 hour (Scheme 9.2). Anilines with either electron-withdrawing or electron-donating groups at the *ortho-*, *para-*, or *meta-* positions were successfully converted into iminosulfur oxydifluorides (9.3a-9.3l), as illustrated in Scheme 9.2. The mild reaction conditions proved compatible with various functional groups, including halogens, ethers, cyano groups, as well as alkenes and alkynes on the aromatic core (9.3a-i). Notably, an N-heterocyclic ring such as aminopyridine was efficiently converted to the desired

product (9.3j). Furthermore, aromatic amines containing functional groups like aldehyde (9.3k) and ester (9.3l) at the ortho position were smoothly transformed into the corresponding products.

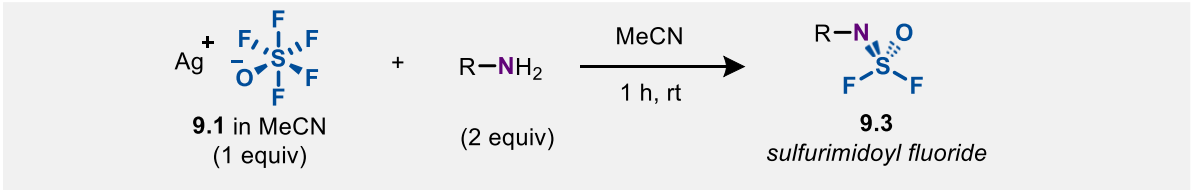

aromatic amines

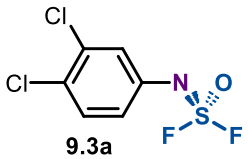
9.3a
92% (100%)

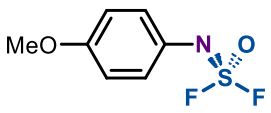
9.3b
93% (100%)

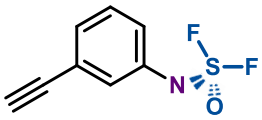
9.3c
91% (100%)

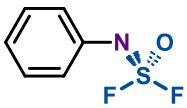
9.3d
86% (100%)

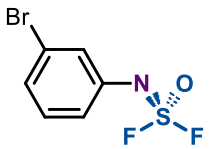
9.3e
92% (100%)

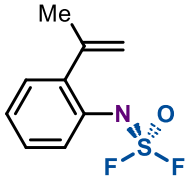
9.3f
95% (100%)

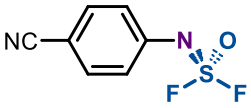
9.3g
98% (100%)

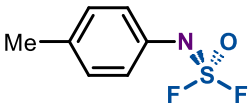
9.3h
81% (100%)

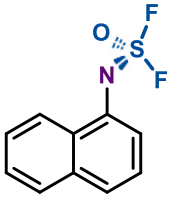
9.3i
89% (100%)

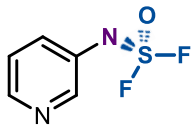
9.3j
72% (100%)

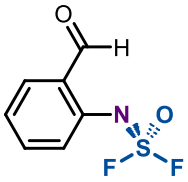
9.3k
73% (100%)

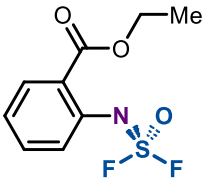
9.3l
72% (100%)

aliphatic amines

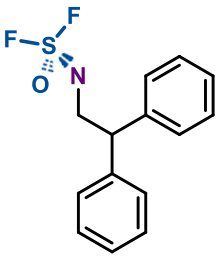
9.3m
73% (100%)

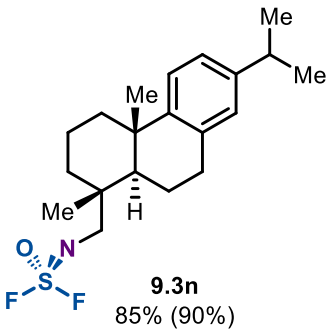
9.3n
85% (90%)

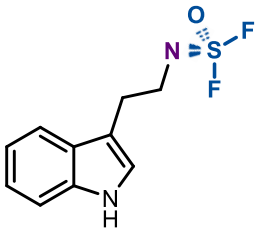
9.3o
(100%)

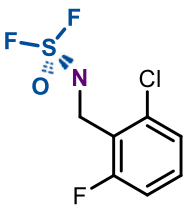
9.3p
84% (100%)

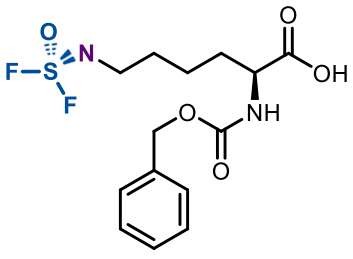
9.3q
(100%)

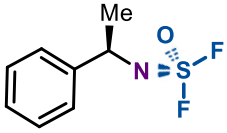
9.3r
90% (100%)

Scheme 9.2. Synthesis of sulfurimidoyl fluorides using $AgOSF_5$ stock solution in MeCN (1 equiv) with amines (2 equiv). Isolated yields shown, ^{19}F NMR yield based on internal standard ($PhCF_3$) shown in parentheses. (a) Using Z-Lys-OH as amine starting material but isolated as the methyl ester.

Aliphatic amines also yielded N-alkyl sulfurimidoyl fluorides in good to high yields. The reaction was effective for various linear amines, including 9.3m, natural product-derived 9.3n, indole-containing 9.3o, and benzylamine 9.3p. Additionally, the Lys derivative 9.3q and the secondary amine 9.3r successfully participated in the SuFEx assembly (Scheme 9.2)

After thoroughly investigating the synthesis and 'SuFExability' of the $AgOSF_5$ complex, we turned our attention to the related $AgOSF_4CF_3$ compound. Our goal was to determine whether the method used to prepare the silver salt from $SOCl_2$ could be adapted to produce a CF_3SOX derivative. We selected triflinyl fluoride (CF_3SOF) as the precursor, hypothesizing that it could be generated in a two-chamber reactor due to its gaseous nature.[206] Indeed, the careful addition of DAST as a deoxofluorinating agent to sodium triflinate (CF_3SO_2Na) in chamber A efficiently evolved CF_3SOF. This gas was then captured in a MeCN solution for subsequent oxidative fluorination (Scheme 9.3A). However, the most effective protocol involved the direct one-step preparation of $AgOSF_4CF_3$ by introducing the AgF_2/TEAC combination in chamber B (Scheme 9.3B). This approach yielded 64% of the desired complex using 4 equivalents of AgF_2 over 3.5 hours. Interestingly, both the *cis* and *trans* isomers of the complex were isolated in a 1:2.3 ratio.

We next explored trifluoromethanesulfonyl (triflimidoyl) fluorides as products derived from the newly synthesized $AgOSF_4CF_3$. Triflimidoyl fluorides are mentioned in only a few prior studies and are typically produced by oxidative halogenation of an S(IV) species that already possesses an S–N bond,[207] with Oehlrich's two-step synthesis via the sulfinamide intermediate being particularly notable.[207d] The precursor $AgOSF_4CF_3$, as a trifluoromethyl analogue of $AgOSF_5$, presents an appealing alternative by enabling direct synthesis from a primary amine. We were pleased to find that the simple addition of a primary amine to the MeCN solution of the oxosulfate salt efficiently produced the triflimidoyl fluorides (Scheme 3C), mirroring the results obtained with sulfurimidoyl fluorides described earlier. A variety of amines, including anilines (9.4a-d)

and aliphatic amines (9.4e-f), were tested, yielding excellent results ranging from 82% to 92%.

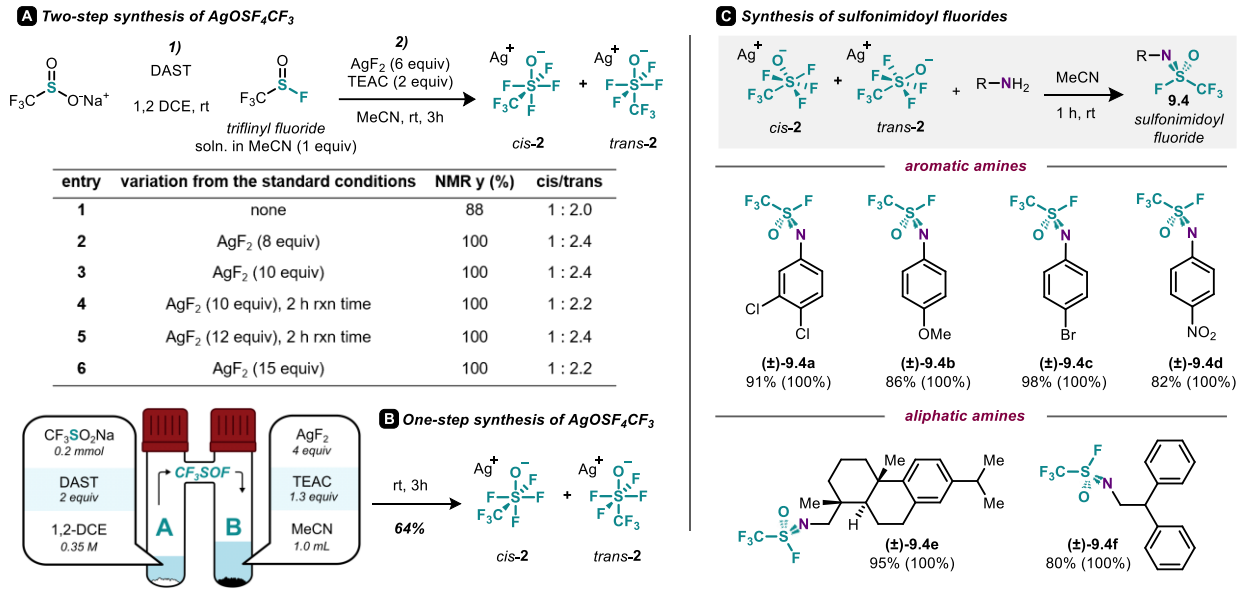

entry	variation from the standard conditions	NMR y (%)	cis/trans
1	none	88	1 : 2.0
2	AgF_2 (8 equiv)	100	1 : 2.4
3	AgF_2 (10 equiv)	100	1 : 2.4
4	AgF_2 (10 equiv), 2 h rxn time	100	1 : 2.2
5	AgF_2 (12 equiv), 2 h rxn time	100	1 : 2.4
6	AgF_2 (15 equiv)	100	1 : 2.2

Scheme 9.3. A) Synthesis of $AgOSF_4CF_3$ solution in two-step procedure, with intermediate isolation of CF_3SOF; B) Synthesis of $AgOSF_4CF_3$ solution in one-step procedure; C) Synthesis of sulfonimidoyl fluorides using $AgOSF_4CF_3$ stock solution in MeCN (1 equiv) with amines (2 equiv). Isolated yields shown, ^{19}F NMR yield based on internal standard ($PhCF_3$) shown in parentheses. TEAC = tetraethylammonium chloride.

To assess the scalability of the method, we conducted selected reactions on a larger scale. Using 3,4-dichloroaniline as a starting substrate, we reacted it with both $AgOSF_4X$ (X=F, CF_3) salts (Scheme 9.4A). Remarkably, the desired products, 9.3a and 9.4a, were obtained with yields nearly identical to those achieved in smaller scale reactions. Additionally, we explored a few post-transformations for the triflimidoyl fluorides obtained in the previous section. Given that these fluorides can be synthesized efficiently in a single step from the amine, they can serve as valuable starting materials for other CF_3-containing sulfur(VI) compounds. We concentrated on two transformations previously reported for sulfurimidoyl fluorides, aiming to adapt them to the CF_3 counterparts. First, the reaction with silylated O-nucleophiles, using TBS-protected phenol and catalytic DBU,[189c] produced the triflimidate ester 9.5 in good yield (Scheme 9.4B).[207e, 207f] Next, we employed phenyllithium as a C-nucleophile to efficiently synthesize trifluoromethyl sulfoximine 9.6,[189b] representing a novel disconnection approach for perfluoroalkyl sulfoximines (Scheme 9.4C).

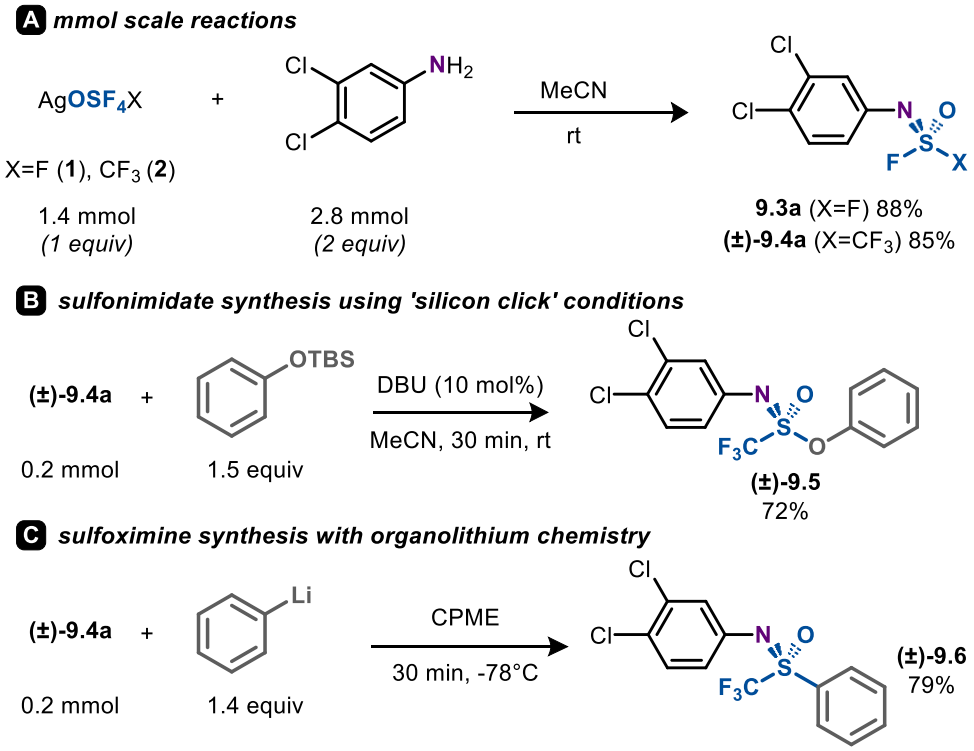

Scheme 9.4. A) Scale-up synthesis of sulfurimidoyl fluoride and sulfonimidoyl fluoride derivative; B) Sulfonimidate synthesis; C) Sulfoximine synthesis. Isolated yields shown.

$AgOSF_4CF_3$ is produced as a mixture of *cis-trans* stereoisomers in a 69:31 ratio, as confirmed by ^{19}F NMR analysis. With the high field strengths of current NMR spectrometers (e.g., 9.4 Tesla, 377 MHz for ^{19}F), both isomers yield spectra that can be analyzed within the weak coupling limit. The more symmetrical trans-isomer appears as an A_4X_3 spin system with a $^3J_{FF}$ coupling constant of 30.6 Hz, while the *cis-isomer* is characterized by an AMP_2X_3 spin system (Figure 9.1). The peak assignment for the ^{19}F nuclei in the *cis-isomer* was straightforward for the P_2X_3 portion of the spectrum, based on the integration values of the signals. For the AM portion, a tentative assignment was made using DFT-calculated chemical shifts (Figure 1 and SI). By combining these chemical shift assignments with the coupling constants extracted from the

experimental spectrum, we successfully simulated the ^{19}F spectra of cis-$[OSF_4CF_3]^-$, achieving an excellent match (Figure 9.1).

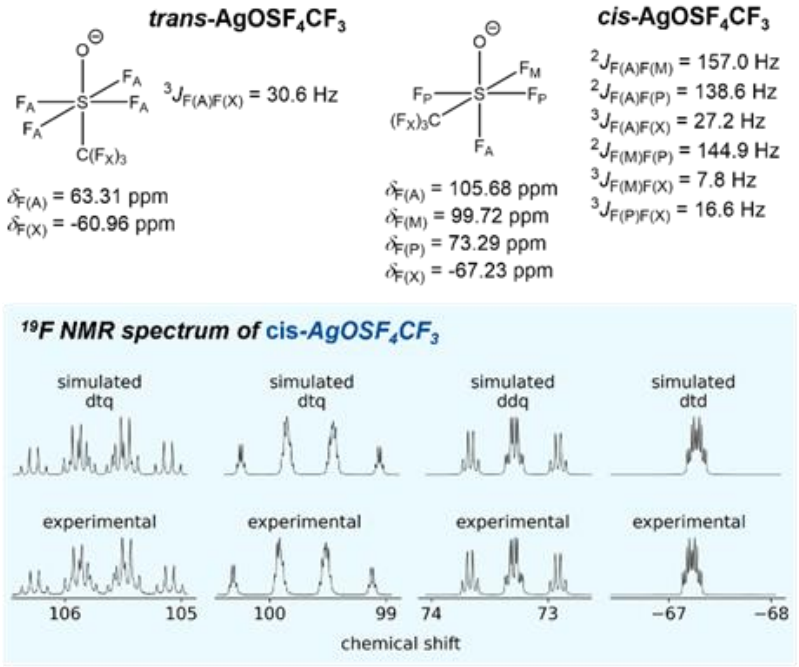

Figure 9.1. Summary of chemical shifts and coupling constants for the trans- and cis-isomers respectively giving rise to A_4X_3 and AMP_2X_3 spectra. The labels for the fluorine atoms refer to the Pople spin-system notation and simulated (top) stacked over experimental (bottom) AMP_2X_3 spectrum of cis-$AgOSF_4CF_3$.

9.3 Conclusion

In conclusion, we have successfully developed a novel method for synthesizing $AgOSF_5$, marking the first preparation of pentafluorooxosulfate salts without the reliance on SOF_4 gas. This method employs thionyl chloride and AgF_2 as starting materials under mild reaction conditions. The subsequent reactions with primary amines demonstrated that the $[OSF_5]^-$ salt can effectively function as a SuFEx hub, comparable in reactivity to its gaseous counterpart, SOF_4. Both aromatic and aliphatic amines were converted into sulfurimidoyl fluorides with excellent yields. Furthermore, our findings with $AgOSF_5$ were also applicable to the carbon-bound analogue $AgOSF_4CF_3$, which was obtained as a mixture of cis and trans isomers, exhibiting intriguing ^{19}F NMR spectra that we sought to elucidate. This mixture of isomeric complexes similarly yielded sulfonimidoyl fluorides in high yields. By eliminating the need for SOF_4 gas, these novel SuFEx hubs open up the potential for laboratories worldwide to explore this area of multidimensional SuFEx chemistry, paving the way for new applications of sulfurimidoyl fluorides and advancing the field.

Chapter 10. Ex-situ ChloGen: A Facile and Straightforward Entry to Aryl-IF_4 Compounds

10.1 Introduction

The increasing number of applications of organofluorides in various fields impacting modern society [208] underscore the significance of the fluorine atom in organic synthesis. Fluorine's unique features—small atomic radii, large electronegativity, high reduction potential—impact overall scaffold properties once embedded, thus imparting unusual stability, and modulating among others major physico-chemical properties including lipophilicity, conformation, and pKa of adjacent functional groups.[209] Additionally, the pursuit for next-generation motifs with enhanced properties boosted the interest towards polyfluorinated groups such as $–CF_3$,[210] and -SF_5,[211].

Hypervalent fluoroiodanes—previously seen as mere laboratory curiosities—are currently receiving an upsurge of attention in organofluorine chemistry as alternatives to fluoraza reagents in electrophilic fluorination reactions (Scheme 10.1, A).[212] For instance, both difluoro(aryl)-λ^3-iodanes (10.1)[213] as well as fluorinated benziodoxole (10.2)[214] are efficient fluorinating sources (Scheme 10.1, B).[212b] Their inherent reactivity is strictly related to their bonding features, better explained via a 3-center-4-electron model given the presence of 10 valence electrons surrounding the iodine atom present in both fluoro-λ^3- and fluoro-λ^5-iodane motifs. While for the synthesis of fluoro-λ^3-iodane arenes several methodologies have been described to date,[215] the tetrafluoro(aryl)-λ^5-iodane core relies on the use of the hazardous IF_5[216] or the highly toxic and corrosive SF_4 gas[217] (Scheme 10.1, C). More recently, Togni and colleagues reported the sole viable methodology to access fluoro-λ^5-iodanes (10.4) by using the TCICA/KF method (Scheme 10.1, C).[218] While this method overcomes past challenges in synthesizing IF_4-compounds, it relies heavily on organic precursors, reducing the efficiency of the reaction due to the waste production. Consequently, there is a notable demand for innovative techniques that enhance overall efficiency. In this context, we present a method for producing IF_4-containing molecules with greater efficiency in atom usage. Additionally, this approach eliminates the need for expensive specialized equipment such as glove boxes. Importantly, the reactions reach completion much faster and do not require external heating (Scheme 10.1, D).

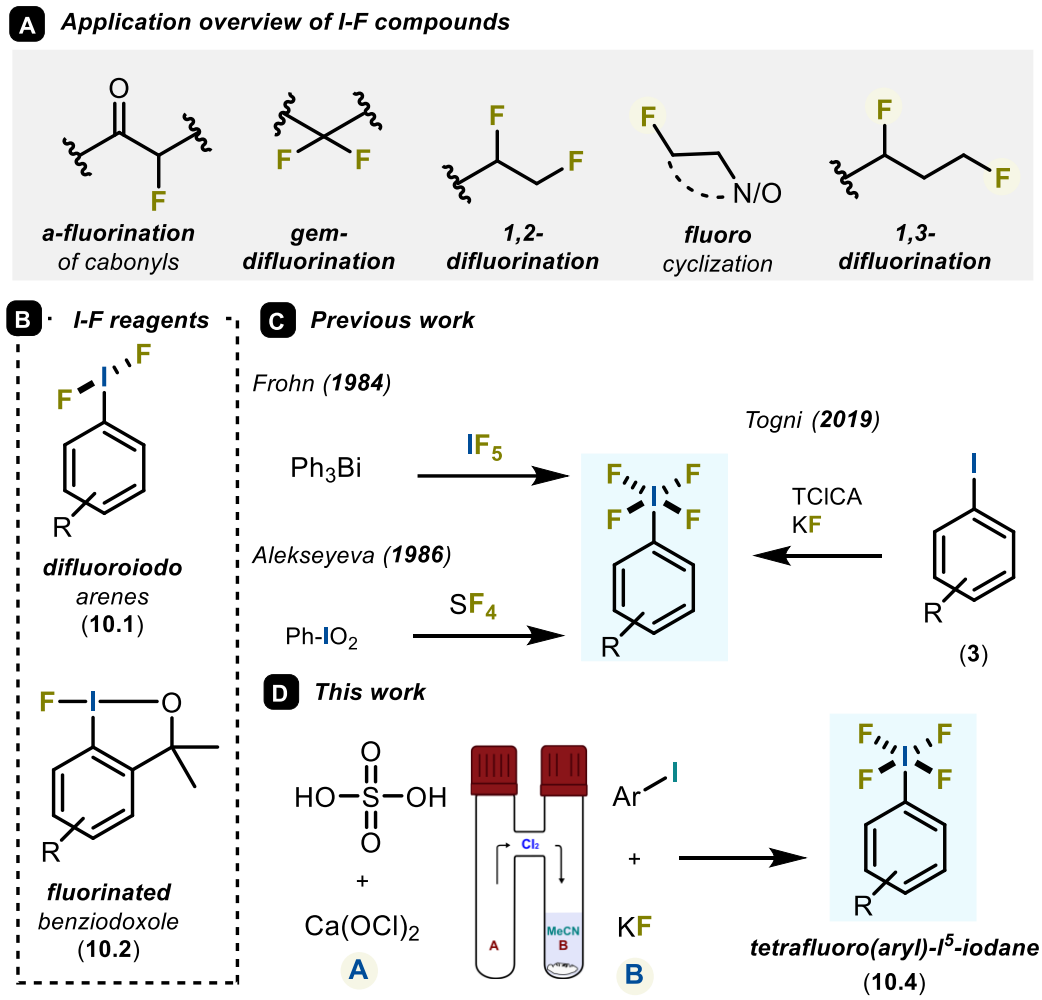

Scheme 10.1. Background and hypothesis

10.2 Results and Discussion

In continuation to our previous studies on the use of ex-situ gas generation setups,[219] we envisaged on leveraging the on-demand ChloGen (chlorine generation) in a two-chamber reactor to create a more straightforward entry to the preparation of aryl-IF_4 compounds. Indeed, we expected that chlorine-mediated oxidation of iodoarenes in presence of a fluoride salt would lead to the formation of tetrafluoro(aryl)-λ^5-iodane (10.4). To test the proposed hypothesis, a model substrate was placed in chamber B in the presence of KF in CH_3CN, and a mixture of $Ca(OCl)_2$ and H_2SO_4 in chamber A for chlorine generation. Subsequently, in the gas-consumption chamber (B), iodobenzene (10.3a) would react with the chlorine gas generated in the presence of potassium fluoride. This initiated an optimization campaign that led to the final conditions, affording phenyl-IF_4 (10.4a) in 90% ^{19}F NMR yield (Table 10.1, entry 5). More to the satisfying results is the fact that replacing TCICA with chlorine gas creates smaller leftover chemical waste, thus substantially improving the atom-economy of the transformation. Firstly, the number of

equivalents of reagents were evaluated. The best results in this case were obtained by employing 6 equiv. of KF, 8 equiv. of $Ca(OCl)_2$ and 1 ml of concentrated H_2SO_4. (Supplementary materials, Table S1, entries 1-16). As expected, initially we observed the formation of phenyl-IF_2—assumably the *en route* product—which slowly converted to phenyl-IF_4 (10.4a) when the reaction was left overnight. While longer reaction times did not benefit the yield as much (Supplementary materials, Table S1, entries 17 and 19-23), the addition of TFA resulted in a 14% increase in yield (Supplementary materials, Table S1, entries 24). On the other hand, increasing the temperature to 40 °C did not result in a higher yield (Supplementary materials, Table S1, entries 25). Control experiments were conducted to test the necessity of inert and dry conditions (Supplementary materials, Table S1, entries 26 and 27). It was found that the use of inert atmosphere as well as anhydrous media and moisture-free starting materials significantly enhances the yield. This is possibly due to the fact that aryl-IF_4 compounds (10.4) are moisture-sensitive.[218] To carry out the reactions, however, simple Schlenk techniques give satisfying results, obviating the need for a glove box. Additionally, it is worth mentioning that the surplus of sulfuric acid serves an additional purpose. Its dessicating power prevents moisture (produced in chamber A) from escaping to the gas-consumption chamber (B). While a selection of results of the optimization process have been mentioned in Table 1, comprehensive optimization results can be found in the supplementary materials for a more thorough comparison.

Table 10.1. Summary of the optimization process

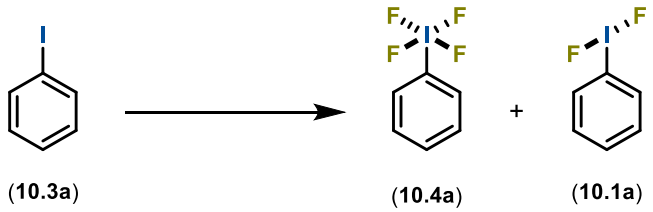

(**10.3a**) (**10.4a**) (**10.1a**)

Entry	$Ca(OCl)_2$ (equiv.)	KF (equiv.)	MeCN (mL)	Time (h)	Temp. Chamber B (°C)	Catalyst (equiv.)	**10.4a** yield (%)[a]	**10.1a** yield (%)[a]
1	2	6	2	16	25	-	0	34
2	8	2	2	16	25	-	17	9
3	8	6	1	4	25	-	9	8
4	8	6	1	16	25	-	76	2
5	**8**	**6**	**1**	**16**	**25**	**TFA (0.1)**	**90**	**0**
6	8	6	1	16	40	TFA (0.1)	86	0

[a] ^{19}F NMR yields are reported.

With the optimized results at hand, we turned to examine the scope. For that purpose, we exposed an array of aryl iodides (10.3) to the ex-situ ChloGen setup (Scheme 10.2). Aryl iodides with an electron-rich group such as an alkyl subtituent on the *meta* or *para* position gave good to excellent product yields (10.4b-10.4e). In addition, *meta*- and *para*-chlorine and bromine containing precursors reacted smoothly affording very high yields (10.4f-10.4h). The yield decreases when the electron-withdrawing cyano group is present on the core, being in *meta* or *para* position (10. 4i and 10.4j). As expected, *ortho*-subtituted aryl iodides (10.3k and 10.3l) gave almost exclusively the corresponding IF_2-containing products (10.1k and 10.1l) in line with the reported literature.[218] This clearly indicates that the IF_4 group is quite bulky. Thus, the steric hindrance from the ortho group creates a significant barrier for the formation of the IF_4 group from IF_2. A limitation of the method is the presenece of protic moieties such as OH, NH_2, or CO_2H. In these cases, no product could be detected. Product 10.4m with both alkyl and bromine subtituents on the aromatic ring was obtained with a moderate 42% yield. A phenoxy substituent in *meta*-position was also well tolerated (product 10.4n). Moreover, the biphenyl derivative 10.3o afforded product 10.4o in a moderate yield (56%).

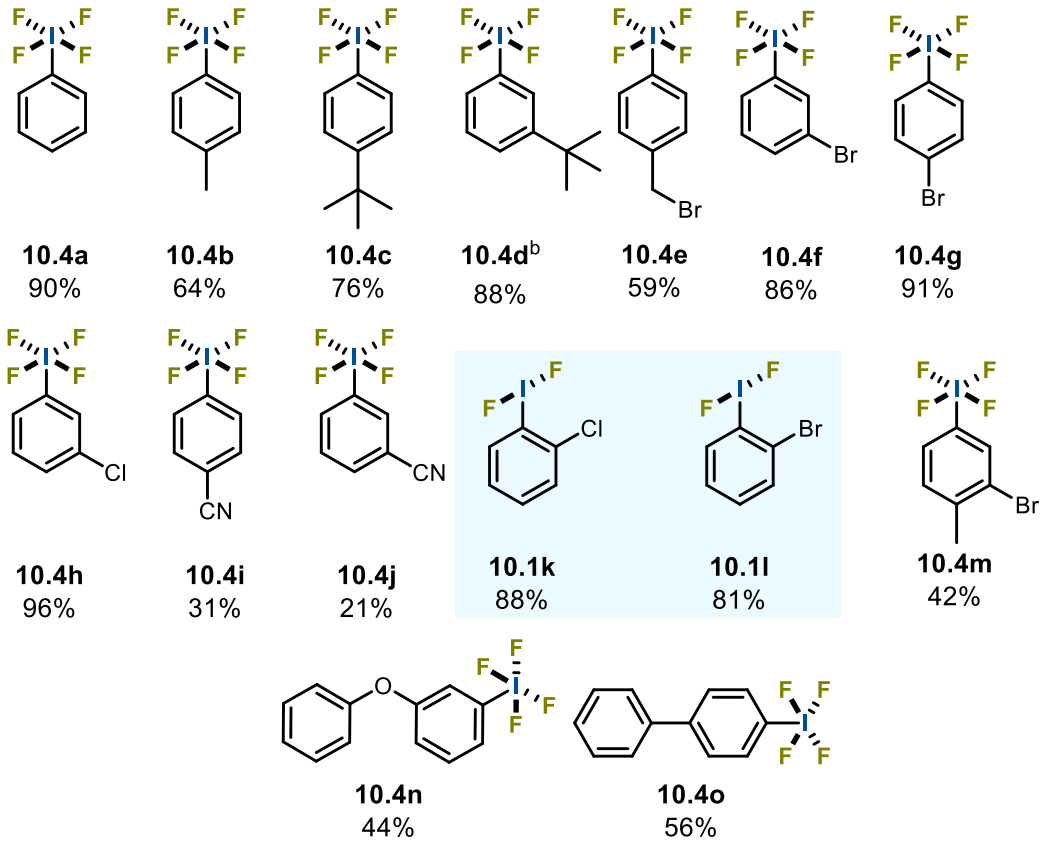

*Scheme 10.2. Scope of aryl-IF_4 (**10.4**) formation via the ex-situ ChloGen steup. a) Reaction conditions; Chamber A: calcium hypochlorite (0.404 g, 2.8 mmol, 8 equiv.), concentrated sulfuric acid (1 mL, 18 mmol, 51.4 equiv.), 0 °C→rt; Chamber B: aryl iodide (0.35 mmol, 1 equiv.), potassium fluoride (0.123 g, 2.1 mmol, 6 equiv.), TFA (3 µL, 0.035 mmol, 0.1 equiv.), acetonitrile (1 mL), rt, 16 h b) The reaction was run on a slightly higher scale; Chamber A: calcium hypochlorite (0.577 g, 4 mmol, 8 equiv.), concentrated sulfuric acid (1.4 mL, 25.7 mmol, 51.4 equiv.); Chamber B: 3-(t-butyl)phenyl iodide (**3d**) (0.5 mmol, 1 equiv.), potassium fluoride (0.176 g, 3 mmol, 6 equiv.), TFA (4 µL, 0.05 mmol, 0.1 equiv.), acetonitrile (1.4 mL).*

It is logical to assume that the chlorine gas generated plays role of oxidant in the reaction. In the first step, the aryl iodide is oxidized via chlorine to produce the corresponding dichloro(aryl)-λ^3-iodane as a stable intermediate, oxidising iodine(I) to iodine(III).[220] As it is reported in the literature, dichloro(aryl)-λ^3-iodanes can be readily turned into difluoro(aryl)-λ^3-iodanes by using a source of fluoride.[221] In our case, KF is the source of fluorine in the process. Assumably, the next two steps, first oxidation and then Cl–F exchange, occur in a similar manner as the previous steps (Scheme 10.3). Dichloro, difluoro(aryl)-λ^5-iodane is generated from the reaction of difluoro(aryl)-λ^3-iodanes with chlorine. Then, dichloro, difluoro(aryl)-λ^5-iodane goes through a Cl–F exchange with KF to give the final product (Scheme 10.3). In-depth mechanistics studies, however, are a further opportunity for future works.

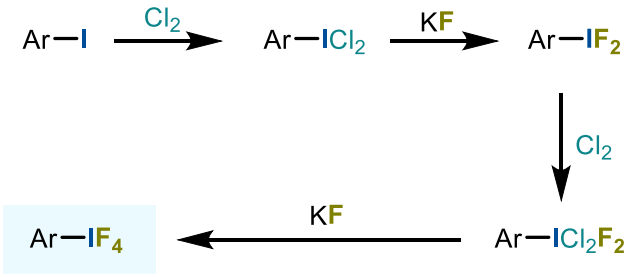

Scheme 10.3. Steps of oxidative halogenation on aryl iodines

10.3 Conclusion

In summary, we introduce a methodology that takes advantage of our ChloGen setup to pave the way to aryl-IF_4 compounds (**4**). Through an ex-situ (two-chamber reactor) approach, we produce chlorine gas which in turn reacts with aryl iodides in the presence of potassium fluoride to afford aryl-IF_4 compounds. The facile and easy-to-handle setup renders the chemistry feasible for most laboratories without specialized and expensive equipment. Furthermore, the choice of the oxidant reduces chemical waste. Additionaly, utilization of the two-chamber reactors for this transformation renders the gas handling safer and more user-friendly, lifting the restrictions on the lab-scale synthesis. The method is applicable to a significant range of substrates as well. We

hope that our methodology assists researchers in the field to sidestep the synthetic challenges in making hypervalent I–F compounds. The easier availability will in turn result in higher chances of valuable discoveries in their applications.

11. Experimental Section

Reagents and Methods

All the commercially available reagents, catalysts, bases and solvents were used as purchased, without further purification. Starting materials and reaction products were purified by flash chromatography using SiO_2 as stationary phase, eluting with *n*-hexane/ethyl acetate (EtOAc) mixtures. ^{1}H NMR (400.13 MHz), ^{13}C NMR (100.6 MHz), and ^{19}F spectra (376.5 MHz) were recorded with a Bruker Avance 400 spectrometer. Splitting patterns are designed as s (singlet), d (doublet), t (triplet), dt (doublets of triplets), td (triplet of doublets), triplets of triplets (tt), q (quartet), m (multiplet), or br s (broad singlet). IR spectra were recorded with a Jasco FT/IR-430 spectrometer or Jasco FT/IR 6800 (ATR) HRMS samples were recorded on Orbitrap Exactive (Thermo Fisher). Source ESI positive as well negative. Parameters: Capillary temperature: 270 °C (in positive), 230°C (in negative), Spray Voltage (|kV|): 4.5 (in positive), 3.0 (in negative). Resolution input 100000, scans n. 20-25. Data were collected on Xcalibur (Thermo Scientific, Bremen, Germany). Melting points were determined with a Büchi B-545 apparatus and are uncorrected.

11.1 General procedures and Characterization of Chapter 3

GENERAL INFORMATION

Reagents and methods

All of the commercially available reagents, catalysts, bases and solvents were used as purchased, without further purification. Starting materials and reaction products were purified by flash chromatography using SiO_2 as stationary phase, eluting with *n*-hexane/ethyl acetate (EtOAc) mixtures. ^{1}H NMR (400.13 MHz), ^{13}C NMR (100.6 MHz), and ^{19}F spectra (376.5 MHz) were recorded with a Bruker Avance 400 spectrometer. Splitting patterns are designed as s (singlet), d (doublet), t (triplet), dt (doublets of triplets), td (triplet of doublets), triplets of triplets (tt), q (quartet), m (multiplet), or bs (broad singlet). IR spectra were recorded with a PerkinElmer SpectrumOne FT-ATR spectrophotometer. Melting points were determined with a Büchi B-545 apparatus and are uncorrected.

Synthetic procedures

Typical procedure for the preparation of [1,2,3]triazolo[4,5-c]quinoline 3.3a-3.3n

1-benzyl-1H-[1,2,3]triazolo[4,5-c]quinoline 3.3**a**-3.3n were prepared according to the sequence outlined in Scheme 1.

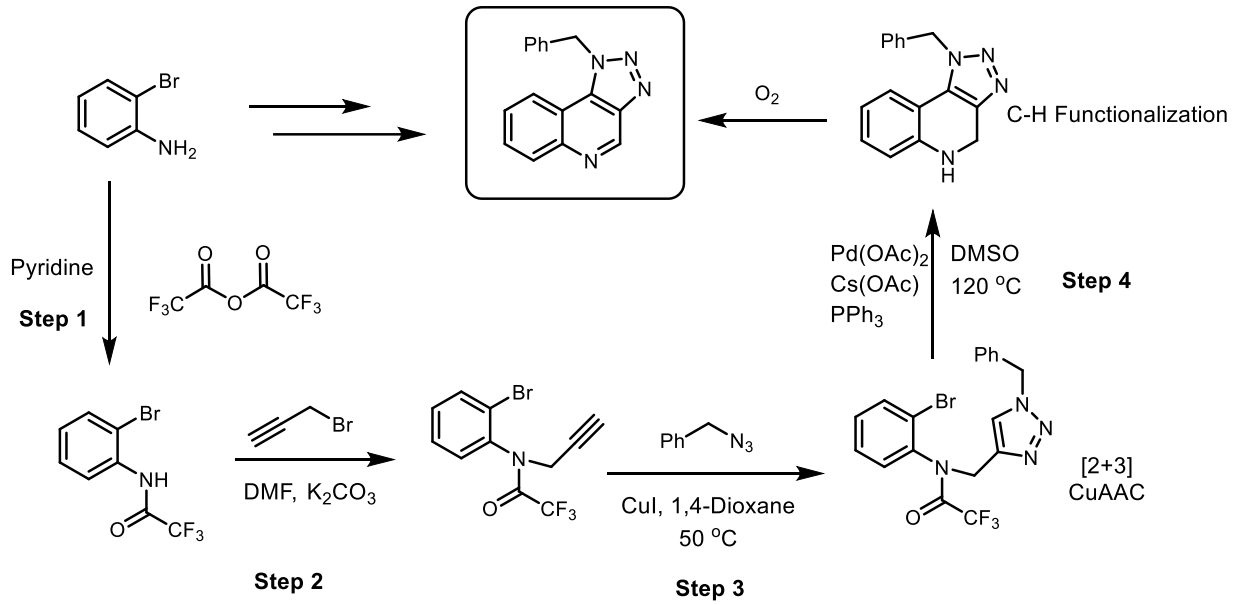

Scheme 1

STEP 1*: *synthesis of N-(2-bromophenyl)-2,2,2-trifluoroacetamide

To a stirred solution of 2-bromoaniline (1 equiv.) in pyridine (5 mL) 2,2,2-trifluoroacetic anhydride was added drop wise at 0°C. The reaction mixture was warmed to room temperature and stirred for 1 hour. The progress of reaction was monitored by TLC (*n*-hexane-AcOEt, 80:20), the reaction was diluted with Et_2O, washed with a solution of HCl (2N), a saturated solution of $NaHCO_3$, water and brine. The organic layer was dried over Na_2SO_4, filtered, and concentrated under vacuum. The residue was obtained (97% yield) of N-(2-bromophenyl)-2,2,2-trifluoroacetamide.

STEP 2*: *synthesis of N-(2-bromophenyl)-2,2,2-trifluoro-N-(prop-2-yn-1-yl)acetamide

Following a slight modification of the literature procedure.[222]

To a solution of N-(2-bromophenyl)-2,2,2-trifluoroacetamide product (1.00 equiv.) in DMF, K_2CO_3 (3 equiv.) propargyl bromide (1.1 equiv.) was added. The mixture was stirred at RT for 6 hours. After the reaction was complete, the mixture was extracted with diethyl ether and dried over anhydrous Na_2SO_4, concentrated under vacuum and purified by flash column

chromatography to give the N-(2-bromophenyl)-2,2,2-trifluoro-N-(prop-2-yn-1-yl)acetamide (90% yield).

STEP 3*: *synthesis of N-((1-benzyl-1H-1,2,3-triazol-4-yl)methyl)-N-(2-bromophenyl)-2,2,2-trifluoroacetamide

To a vial containing N-(2-bromophenyl)-2,2,2-trifluoro-N-(prop-2-yn-1-yl)acetamide (306 mg, 1 mg, 1 mmol, 1 equiv) in dioxane (2 mL) was added CuI (38 mg, 20 mol%) and benzyl azide (146 mg, 1.1 equiv,). The vial was closed, and the mixture was stirred at 50 ^{o}C for overnight, concentrated under vacuum. The mixture was purified with flash column chromatography 70/30 *n*-hexane/EtOAc (R_f = 0.22) to give the pure product 413 mg (94% yield) as a yellow solid.

STEP 3*: *synthesis of 1-benzyl-1H-[1,2,3]triazolo[4,5-c]quinoline

To a vial containing $Pd(OAc)_2$ (2.8 mg, 5 mol%), PPh_3 (13.1 mg, 20 mol%) in DMSO (2 ml) was added N-((1-benzyl-1H-1,2,3-triazol-4-yl)methyl)-N-(2-bromophenyl)-2,2,2-trifluoro acetamide (110 mg, 1 equiv., 0.25 mmol), and Cs(OAc) (96 mg, 2 equiv.). The mixture was stirred at 120 ^{o}C for 0.5 hour. After the reaction was completed (monitored by TLC), oxygen balloon was then applied. The reaction was monitored by TLC, extracted with diethyl ether and dried over anhydrous Na_2SO_4. The residue was purified by flash column chromatography 50/50 *n*-hexane and EtOAc (R_f = 0.19) to give the pure product (61 mg, 95%) as white solid.

Typical procedure for the preparation of 4,5-dihydro-1H-[1,2,3]triazolo[4,5-c]quinoline 3.4a-3.4h

1-benzyl-1H-[1,2,3]triazolo[4,5-c]quinoline 3.4a-3.4h were prepared according to the sequence outlined in Scheme 2.

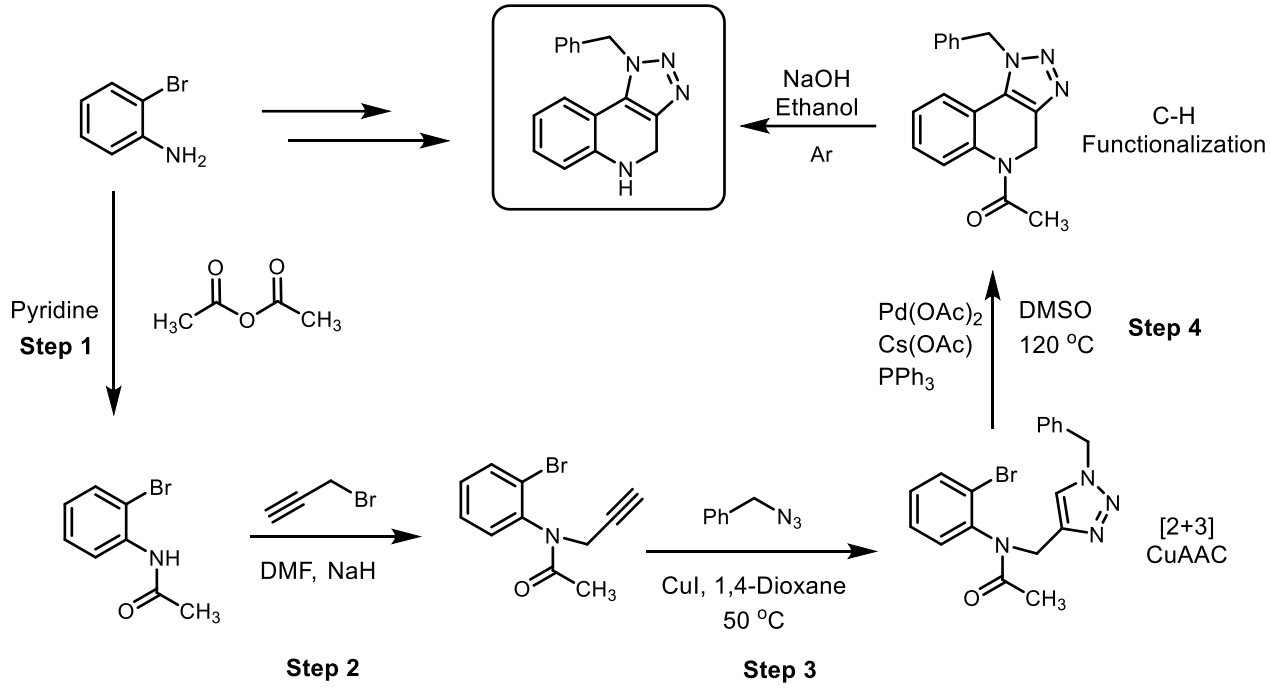

Scheme 2

STEP 1*: *N-(2-bromophenyl)acetamide

To a stirred solution of 2-bromoaniline (1 equiv.) in pyridine (5 mL) acetic anhydride was added drop wise at 0°C. The reaction mixture was warmed to room temperature, stirred for 3 hours. The progress of reaction was monitored by TLC (*n*-hexane-AcOEt, 80:20), the reaction was diluted with Et_2O, washed with a solution of HCl (2N), a saturated solution of $NaHCO_3$, water and brine. The organic layer was dried over Na_2SO_4, filtered, and concentrated under vacuum. The residue was obtained (95% yield) of N-(2-bromophenyl)-2,2,2-trifluoroacetamide.

***STEP 2: synthesis of N-(2-bromophenyl)-N-(prop-2-yn-1-yl)acetamide*[222]**

To a solution of N-(2-bromophenyl)-2,2,2-trifluoroacetamide product (1.00 equiv.) in DMF, K_2CO_3 (3 equiv.) propargyl bromide (1.1 equiv.) was added. The mixture was stirred at RT for 6 hours. After the reaction was complete, the mixture was extracted with diethyl ether and dried over anhydrous Na2SO4, concentrated under vacuum and purified by flash column chromatography to give the N-(2-bromophenyl)-2,2,2-trifluoro-N-(prop-2-yn-1-yl)acetamide (90% yield).

STEP 3: synthesis of N-((1-benzyl-1H-1,2,3-triazol-4-yl)methyl)-N-(2-bromophenyl) acetamide

To a vial containing N-(2-bromophenyl)-2,2,2-trifluoroacetamide (268 mg, 1 mmol, 1 equiv) in dioxane (2 mL) was added CuI (38 mg, 20 mol%) and benzyl azide (146 mg, 1.1 equiv.). The vial was closed and the mixture was stirred at 50 ^{o}C for overnight, concentrated under vacuum. The mixture was purified with flash column chromatography 70/30 n-hexane/EtOAc (R_f = 0.20) to give the pure product 366 mg (95% yield) as a yellow solid.

STEP 4*: *1-benzyl-4,5-dihydro-1H-[1,2,3]triazolo[4,5-c]quinoline

To a vial containing $Pd(OAc)_2$ (2.8 mg, 5 mol%), PPh_3 (52mg, 20 mol%) in DMSO (2 ml) was added N-((1-benzyl-1H-1,2,3-triazol-4-yl)methyl)-N-(2-bromophenyl)acetamide (96 mg, 1 equiv., 0.25 mmol), Cs(OAc) (96 mg, 2 equiv.). The mixture was stirred at 120 ^{o}C for 0.5 hour. After the reaction completed (monitored by TLC), NaOH (2N, 1 ml) and EtOH (1 ml) was added. The reaction was monitored by TLC, extracted with diethyl ether and dried over anhydrous Na_2SO_4. The residue was purified by flash column chromatography 50/50 hexane and EtOAc (R_f = 0.21) to give the pure product (50 mg, 77%) as yellow solid.

Typical procedure for the preparation of azides

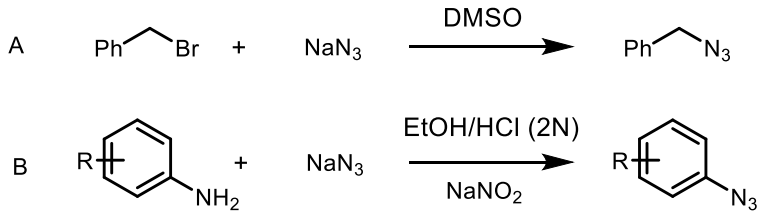

Scheme 3

***Procedure for A*[110d]**

To a stirred solution of NaN_3 (1.1 mmol) in DMSO (2 mL) was added benzyl bromide (1 mmol). The reaction mixture was stirred at RT overnight. Then the reaction mixture was diluted with water (5 mL) and extracted with ether (3×5 mL) and washed by brine, dried over Na_2SO_4 and concentrated under vacuum to give the products in quantitative yields. It was used directly without further purification.

***Procedure for B*[223]**

The aniline derivative (1 mmol) was suspended in hydrochloric acid (17%) at room temperature and then ethanol was added until a clear solution was obtained. The solution was cooled to 0 °C

and $NaNO_2$ (1.5 eq.) was added in small portions. After stirring at 0 °C for 15-30 min. NaN_3 (1.5 eq.) was slowly added and the mixture was stirred for an additional 2 h at room temperature. The reaction mixture was extracted with diethyl ether and the combined organic fractions were washed with saturated $NaHCO_3$-solution and with brine, dried over Na_2SO_4 and concentrated under pressure and the desired azides were obtained without further purification.

Procedure for the synthesis of compounds (3.6a, 3.6b, 3.6c)

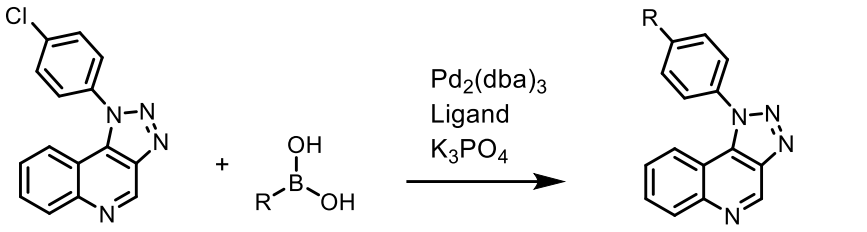

3.3k 3.6a, 3.6b, 3.6c

To a mixture of $Pd_2(dba)_3$ (2 mol%) and Xphos ligand (4 mol%) in dry dioxane (2.0 mL), compound 3.3k (70 mg, 0.25 mmol), boronic acid derivatives (1.5 equiv, 0.37 mmol) and K_3PO_4 (3.0 equiv, 0.75 mmol) were added. Then, the reaction mixture was stirred under argon at 100 ^oC. The reaction was monitored by TLC, concentrated under pressure. The mixture was purified with flash column chromatography (90:10 hexane and EtOAc) to give the pure products.

Procedure for the synthesis of compound 3.7

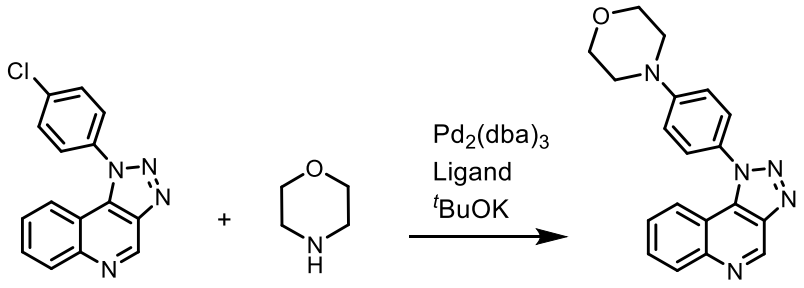

3.3k 3.7

To a mixture of $Pd(OAc)_2$ (2.5 mol%) and Xphos ligand (5 mol%) in dry toluene (2.0 mL), compound 3.3k (70 mg, 0.25 mmol), morpholine (1.5 equiv, 0.37 mmol)and ^tBuOK (2.0 equiv, 0.5 mmol) were added. Then, the reaction mixture was stirred under argon at 100 ^oC. The reaction was monitored by TLC, concentrated under pressure. The mixture was purified with flash column chromatography (50:50 hexane and EtOAc) to give the pure products.

Procedure for the synthesis of compound 3.8

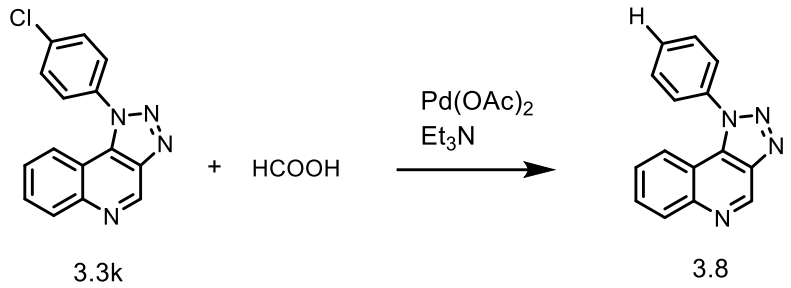

3.3k 3.8

To a mixture of $Pd(OAc)_2$ (2.5 mol%) and Et_3N (3.0 equiv) in dry DMSO (2.0 mL), compound 3.3l (70 mg, 0.25 mmol), formic acid (2 equiv, 0.5 mmol) were added. Then, the reaction mixture was stirred under argon at 120 ^oC. The reaction was monitored by TLC, extracted with diethyl ether and washed with water and brine, dried over Na_2SO_4 and concentrated under pressure. The mixture was purified with flash column chromatography (60:40 hexane and EtOAc) to give the pure products.

Procedure for the synthesis compound 3.9

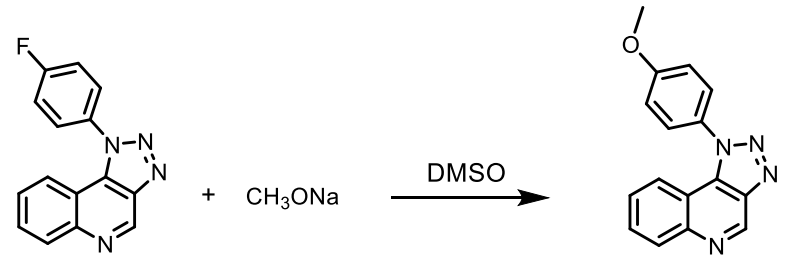

3.3l 3.9

Compound 3.3l (66 mg, 0.25 mmol), sodium methoxide (1.5 equiv, 0.37 mmol) added to DMSO. Then, the reaction mixture was stirred at 140 ^oC for 10 hrs. The reaction was monitored by TLC, extracted with diethyl ether and washed with water and brine, dried over Na_2SO_4 and concentrated under pressure to obtain the final product without further purification.

CHARACTERIZATION DATA

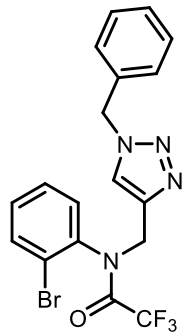

N-((1-benzyl-1H-1,2,3-triazol-4-yl)methyl)-N-(2-bromophenyl)-2,2,2-trifluoroacetamide, 3.1a:

90% yield; white solid; mp: 120-122 °C; R_f = 0.23 (n-hexane-EtOAc, 70:30); IR (neat): 3121, 3073, 1694, 1478, 1149, 719 cm^{-1};

^{1}H NMR (400.13 MHz) ($CDCl_3$): δ 7.59 – 7.56 (m, 1H), 7.50 (s, 1H), 7.31 - 7.28 (m, 3H), 7.20 – 7.14 (m, 4H), 7.00 - 6.96 (m, 1H), 5.49 (*d*, *J* = 14.6 Hz, 1H), 5.39 – 5.28 (m, 2H), 4.36 (d, *J* = 14.6 Hz, 1H);

^{13}C NMR (100.6 MHz) ($CDCl_3$): δ 156.9 (q, J_{C-F} = 36.7 Hz) (C), 142.0 (C), 137.6 (C), 134.4 (C), 133.5 (CH), 131.6 (CH), 130.9 (CH), 129.2 (CH), 128.9 (CH), 128.2 (CH), 128.0 (CH), 124.0 (CH), 123.4 (C), 155.8 (q, J_{C-F} = 288.9 Hz) (C), 54.2 (CH_2), 45.7 (CH_2);

^{19}F NMR (400.13 MHz) ($CDCl_3$): δ -68.9.

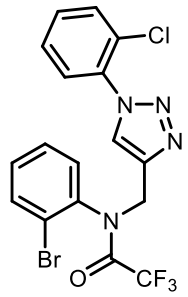

N-(2-bromophenyl)-N-((1-(2-chlorophenyl)-1H-1,2,3-triazol-4-yl)methyl)-2,2,2-trifluoroacetamide, 3.1b:

93% yield; white solid; mp: 121-123 °C; R_f = 0.19 (n-hexane-EtOAc, 70:30); IR (neat): 3144, 3071, 1698, 1481, 1153, 762 cm^{-1};

^{1}H NMR (400.13 MHz) ($CDCl_3$): δ 8.14 (s, 1H), 7.75 – 7.70 (m, 3H), 7.55 – 7.50 (m, 2H), 7.37 – 7.25 (m, 2H), 7.16 (dd, J_1 = 6.8 Hz, J_2 = 2.4 Hz, 1H), 5.48 (d, *J* = 14.7 Hz, 1H), 4.48 (d, *J* = 14.7 Hz, 1H);

^{13}C NMR (100.6 MHz) ($CDCl_3$): δ 157 (q, J_{C-F} = 36.6 Hz) (C), 142.7 (C), 137.8 (C), 135.3 (C), 134.8 (C), 133.7 (CH), 131.5 (CH), 131.1 (CH), 130.0 (CH), 128.4 (CH), 123.3 (C), 122.2 (CH), 121.6 (CH), 115.9 (q, J_{C-F} = 287.9 Hz) (C), 46.0 (CH_2);

^{19}F NMR (400.13 MHz) ($CDCl_3$): δ -68.9.

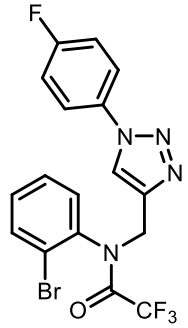

N-(2-bromophenyl)-2,2,2-trifluoro-N-((1-(4-fluorophenyl)-1H-1,2,3-triazol-4-yl)methyl)acetamide, 3.1c:

85% yield; brown solid; mp: 115-117 °C; R_f = 0.25 (n-hexane-EtOAc, 70:30); IR (neat): 3145, 3100, 1685, 1519, 1149, 833 cm^{-1};

^{1}H NMR (400.13 MHz) ($CDCl_3$): δ 8.05 (s, 1H), 7.68 – 7.61 (m, 3H), 7.27 – 7.19 (m, 2H), 7.18 – 7.12 (m, 2H), 7.11 – 7.07 (m, 1H), 5.41 (d, *J* = 14.8 Hz, 1H), 4.40 (d, *J* = 14.8 Hz, 1H);

^{13}C NMR (100.6 MHz) ($CDCl_3$): δ 162.5 (d, J_{C-F} = 249.5 Hz) (C), 157.0 (d, J_{C-F} = 36.7 Hz) (C), 142.5 (C), 137.8 (C), 133.6 (CH), 131.51 (C), 131.48 (C), 129.8 (d, J_{C-F} = 279 Hz), 127.3 (*d*, J_{C-F} = 8.7 Hz) (C), 123.3 (C), 123.3 (C), 122.47 (d, J_{C-F} = 8.5 Hz) (CH), 122.5 (CH), 122.42 (CH), 116.9 (CH), 116.7 (CH), 15.8 (q, J_{C-F} = 288.4 Hz) (C), 46.9 (CH_2);

^{19}F NMR (400.13 MHz) ($CDCl_3$): δ -68.9, -111.78, -111.79, -111.80, -111.81.

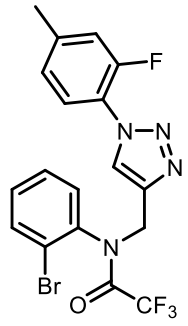

N-(2-bromophenyl)-2,2,2-trifluoro-N-((1-(2-fluoro-4-methylphenyl)-1H-1,2,3-triazol-4-yl)methyl)acetamide, 3.1d:

86% yield; pale pink solid; mp: 83-85 °C; R_f = 0.17 (n-hexane-EtOAc, 70:30); IR (neat): 3178, 3076, 1694, 1477, 1143 cm^{-1};

^{1}H NMR (400.13 MHz) ($CDCl_3$): δ 8.16 (d, *J* = 2.7 Hz, 1H), 7.83 – 7.77 (m, 1H), 7.75 – 7.71 (m, 1H), 7.37 – 7.29 (m, 2H), 7.21 – 7.10 (m, 1H), 7.14 – 7.07 (m, 2H), 5.54 (d, *J* = 14.8 Hz, 1H), 4.51 (d, *J* = 14.8 Hz, 1H), 2.43 (s, 3H);

^{13}C NMR (100.6 MHz) ($CDCl_3$): δ 162.5 (q, $J_{C\text{-}F}$ = 249.2 Hz) (C), 157.2 (d, $J_{C\text{-}F}$ = 37.6 Hz) (C), 142.6 (C), 141.8 (C), 135.1 (C), 134.0 (CH), 133.2 (C), 131.0 (CH), 129.0 (CH), 122.8 (C), 122.5 (CH), 122.4 (CH), 122.4 (CH), 116.9 (CH), 116.7 (CH), 115.9 (q, $J_{C\text{-}F}$ = 288.5 Hz) (C), 46.0 (CH_2), 20.9 (CH_3);

^{19}F NMR (400.13 MHz) ($CDCl_3$): δ -68.9, -124.39.

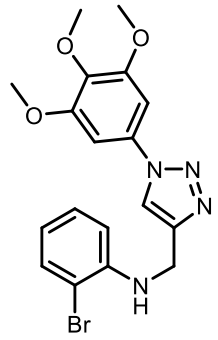

2-bromo-N-((1-(3,4,5-trimethoxyphenyl)-1H-1,2,3-triazol-4-yl)methyl)aniline, 3.1e:

81% yield; pale yellow solid; mp: 138-141 °C; R_f = 0.20 (n-hexane-EtOAc, 70:30); IR (neat): 3346, 2938, 1595, 1508, 1126 cm^{-1};

^{1}H NMR (400.13 MHz) ($CDCl_3$): δ 7.86 (s, 1H), 7.46 (dd, J_1 = 7.7 Hz, J_2 = 1.2 Hz, 1H), 7.19 (m, 1H), 6.93 (s, 2H), 6.75 (dd, J_1 = 8.3 Hz, J_2 = 1.2 Hz, 1H), 6.63 (td, J_1 = 7.7 Hz, J_2 = 1.2 Hz, 1H), 4.92 (s, 1H), 4.61 (d, *J* = 4.2 Hz, 2H), 3.93 (s, 6H), 3.89 (s, 3H);

^{13}C NMR (100.6 MHz) ($CDCl_3$): δ 153.9 (C), 146.7 (C), 144.3 (C), 138.4 (C), 132.9 (C), 132.6 (CH), 128.6 (CH), 120.1 (CH), 118.6 (CH), 111.7 (CH), 110.0 (C), 98.5 (CH), 61.1 (CH_3), 56.5 (CH_2), 40.0 (CH_3).

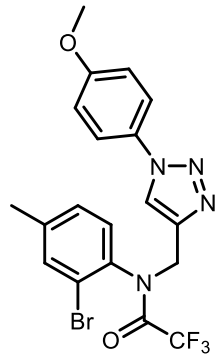

N-(2-bromo-4-methylphenyl)-2,2,2-trifluoro-N-((1-(4-methoxyphenyl)-1H-1,2,3-triazol-4-yl)methyl)acetamide, 3.1f:

98% yield; pale yellow solid; mp: 124-126 °C; Rf = 0.24 (n-hexane-EtOAc, 60:40); IR (neat): 3153, 2962, 1677, 1151, 600 cm-1;

^{1}H NMR (400.13 MHz) ($CDCl_3$): δ 8.06 (*S*, 1H), 7.65 – 7.60 (m, 2H), 7.50 (d, *J* = 1.5 Hz, 1H), 7.07 (dd, J_1 = 8.1 Hz, J_2 = 1.2 Hz, 1H), 7.05 – 6.94 (m, 3H), 5.47 (d, *J* = 14.7 Hz, 1H), 4.45 (d, *J* = 14.7 Hz, 1H), 3.85 (s, 3H), 2.34 (s, 3H);

^{13}C NMR (100.6 MHz) ($CDCl_3$): δ 159.9 (C), 157, (q, $J_{C\text{-}F}$ = 36.5 Hz) (C), 142.2 (C), 141.7 (C), 135.0 (C), 133.9 (CH), 131.1 (CH), 130.3 (C), 128.9 (CH), 122.8 (C), 122.2 (CH), 122.0 (CH), 115.7 (q, $J_{C\text{-}F}$ = 285.2 Hz) (C), 114.8 (CH), 55.6 (CH_3), 46.0 (CH_2), 20.9 (CH_3);

^{19}F NMR (400.13 MHz) ($CDCl_3$): δ -68.9.

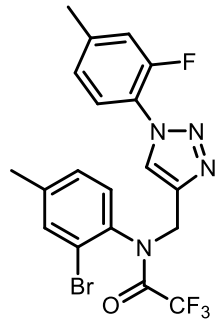

N-(2-bromo-4-methylphenyl)-2,2,2-trifluoro-N-((1-(2-fluoro-4-methylphenyl)-1H-1,2,3-triazol-4-yl)methyl)acetamide, 3.1g:

91% yield; yellow solid; mp: 82-84 °C; R_f = 0.23 (n-hexane-EtOAc, 70:30); IR (neat): 3155, 1695, 1497, 1148, 823 cm^{-1};

^{1}H NMR (400.13 MHz) ($CDCl_3$): δ 8.14 (d, *J* = 2.5 Hz, 1H), 7.79 (t, *J* = 8.0 Hz, 1H), 7.53 (*s*, 1H), 7.12 (t, *J* = 7.0 Hz 3H), 7.00 (d, *J* = 8.0 Hz, 1H), 5.53 (d, *J* = 14.7 Hz, 1H), 4.50 (d, *J* = 14.7 Hz, 1H), 2.44 (*s*, 3H), 2.38 (*s*, 3H);

^{13}C NMR (100.6 MHz) ($CDCl_3$): δ 157.1 (q, $J_{C\text{-}F}$ = 36.6 Hz) (C), 153 (d, $J_{C\text{-}F}$ = 250.5 Hz) (C), 141.97 (C), 141.46 (d, $J_{C\text{-}F}$ = 7.8 Hz) (C), 141.43 (C), 135.0 (C), 134.0 (CH), 131.1 (CH), 129.0 (CH), 125.82 (d, $J_{C\text{-}F}$ = 3.3 Hz) (C), 125.21 (d, $J_{C\text{-}F}$ = 7.6 Hz) (C), 124.5 (CH), 122.9 (C), 117.5 (CH), 117.3 (CH), 45.8 (CH_2), 21.2 (CH_3), 20.9 (CH_3);

^{1}F NMR (400.13 MHz) ($CDCl_3$): δ -68.9, -124.39.

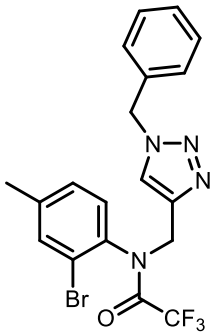

N-((1-benzyl-1H-1,2,3-triazol-4-yl)methyl)-N-(2-bromo-4-methylphenyl)-2,2,2-trifluoroacetamide, 3.1h:

97% yield; white solid; mp: 112-114 °C; R_f = 0.26 (n-hexane-EtOAc, 70:30); IR (neat): 3061, 1692, 1496, 1151, 727 cm^{-1};

^{1}H NMR (400.13 MHz) ($CDCl_3$): δ 7.58 (s, 1H), 7.47 (d, J_1 = 1.2 Hz, 1H), 7.43 – 7.36 (m, 3H), 7.29 – 7.24 (m, 2H), 7.09 - 7.04 (dd, J_1 = 8.0 Hz, J_2 = 1.2 Hz, 1H), 6.91 (d, *J* = 8.0 Hz, 1H), 5.58 (d, *J* = 14.8 Hz, 1H), 5.43 (d, *J* = 14.8 Hz, 1H), 5.37 (d, *J* = 14.6 Hz, 1H), 4.39 (d, *J* = 14.6 Hz, 1H), 2.34 (s, 3H);

^{13}C NMR (100.6 MHz) ($CDCl_3$): δ 157.1 (q, $J_{C\text{-}F}$) (C), 142.1 (C), 141.6 (C), 134.9 (C), 134.5 (C), 133.9 (CH), 131.0 (CH), 129.2 (CH), 128.9 (CH), 128.0 (CH), 124.0 (CH), 122.9 (C), 115.8 (q, $J_{C\text{-}F}$ = 287.5 Hz) (C), 54.2 (CH_2), 45.8 (CH_2), 20.9 (CH_3);

^{19}F NMR (400.13 MHz) ($CDCl_3$): δ -68.9.

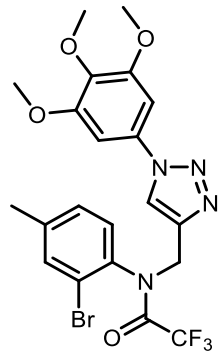

N-(2-bromo-4-methylphenyl)-2,2,2-trifluoro-N-((1-(3,4,5-trimethoxyphenyl)-1H-1,2,3-triazol-4-yl)methyl)acetamide, 3.1i:

92% yield; white solid; mp: 108-110 °C; R_f = 0.22 (n-hexane-EtOAc, 70:30); IR (neat): 3008, 1695, 1508, 1151, 774 cm^{-1};

^{1}H NMR (400.13 MHz) ($CDCl_3$): δ 8.05 (s, 1H), 7.46 (d, *J* = 1.22 Hz, 1H), 7.04 (dd, J_1 = 8.05 Hz, J_2 = 1.24 Hz, 1H), 6.93 (d, *J* = 8.05 Hz, 1H), 6.89 (s, 2H), 5.39 (d, *J* = 14.7 Hz, 1H), 4.44 (d, *J* = 14.7 Hz, 1H), 3.86 (*s*, 6H), 3.81 (*s*, 3H), 2.30 (*s*, 3H);

^{13}C NMR (100.6 MHz) ($CDCl_3$): δ 157.2 (q, J_{C-F} = 36.7 Hz) (C), 142.4 (C), 141.8 (C), 138.4 (C), 135.1 (C), 134.0 (CH), 132.7 (C), 131.0 (CH), 129.0 (CH), 122.8 (q), 122.3 (CH), 115.8 (q, J_{C-F} = 287.5 Hz) (C),98.2 (CH), 61.1 (CH_3), 56.5 (CH_3), 46.1 (CH_2), 20.9 (CH_3);

^{19}F NMR (400.13 MHz) ($CDCl_3$): δ -68.9.

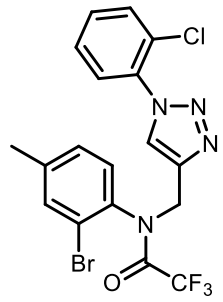

N-(2-bromophenyl)-N-((1-(2-chlorophenyl)-1H-1,2,3-triazol-4-yl)methyl)-2,2,2-trifluoroacetamide, 3.1j:

89% yield; pale brown solid; mp: 125-127 °C; R_f = 0.24 (n-hexane-EtOAc, 70:30); IR (neat): 3142, 1694, 1518, 1148, 840 cm^{-1};

^{1}H NMR (400.13 MHz) ($CDCl_3$): δ 8.08 (*s*, 1H), 7.67 – 7.56 (m, 2H), 7.53 (d, *J* = 1.2 Hz, 1H), 7.50 – 7.45 (m, 2H), 7.11 (dd, J_1 = 8.1 Hz, J_2 = 1.2 Hz, 1H), 7.01 (d, *J* = 8.1 Hz, 1H), 5.55 (d, *J* = 14.7 Hz, 1H), 4.55 (d, *J* = 14.7 Hz, 1H), 2.38 (s, 3H);

^{13}C NMR (100.6 MHz) ($CDCl_3$): δ 157.1 (q, J_{C-F} = 107.8 Hz) (C), 141.7 (C), 141.4 (C), 134.8 (C), 134 (CH), 131.1 (CH), 130.9 (CH), 130.7 (CH), 128.9 (CH), 128.6 (C), 127.9 (CH), 127.7 (CH), 126.1 (CH), 123 (CH), 116.1 (q, J_{C-F} = 866.2 Hz) (C), 45.6 (CH_2), 20.9 (CH_3);

^{1}F NMR (400.13 MHz) ($CDCl_3$): δ -68.91

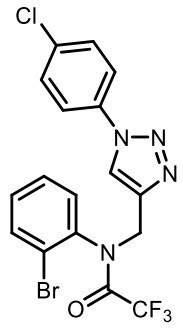

N-(2-bromophenyl)-N-((1-(4-chlorophenyl)-1H-1,2,3-triazol-4-yl)methyl)-2,2,2-trifluoroacetamide, 3.1k:

93.5% yield; pale yellow solid; mp: 127-129 °C; R_f = 0.21 (n-hexane-EtOAc, 70:30); IR (neat): 3146, 1698, 1473, 1155, 727 cm^{-1};

^{1}H NMR (400.13 MHz) ($CDCl_3$): δ 8.16 (s, 1H), 7.76 – 7.68 (m, 3H), 7.55 – 7.50 (m, 2H), 7.38 – 7.30 (m, 2H), 7.23 – 7.14 (m, 1H), 5.51 (d, *J* = 14.7 Hz, 1H), 4.50 (d, *J* = 14.7 Hz, 1H);

^{13}C NMR (100.6 MHz) ($CDCl_3$): δ 157 (q, J_{C-F} = 36.7 Hz) (C), 142.7 (C), 137.3 (C), 135.3 (C), 134.8 (C), 133.7 (CH), 131.5 (CH), 131.1 (CH), 130.0 (CH), 128.4 (CH), 123.3 (C), 122.2 (CH), 121.6 (CH), 115.9 (q, J_{C-F} = 285.8 Hz) (C), 46.0 (CH_2);

^{19}F NMR (400.13 MHz) ($CDCl_3$): δ -68.9.

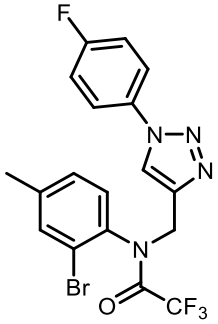

N-(2-bromo-4-methylphenyl)-2,2,2-trifluoro-N-((1-(4-fluorophenyl)-1H-1,2,3-triazol-4-yl)methyl)acetamide, 3.1l:

94% yield; yellow solid; mp: 128-130 °C; R_f = 0.19 (n-hexane-EtOAc, 70:30); IR (neat): 3138, 1695, 1518, 1144, 840 cm^{-1};

^{1}H NMR (400.13 MHz) ($CDCl_3$): δ 8.13 (s, 1H), 7.78 – 7.71 (m, 2H), 7.54 (d, *J* =1.2 Hz, 1H), 7.29 – 7.21 (m, 2H), 7.13 (dd, J_1 = 8.0 Hz, J_2 = 1.2 Hz, 1H), 7.03 (d, J_1 = 8.0 Hz, 1H), 5.49 (d, *J* = 14.6 Hz, 1H), 4.48 (d, *J* = 14.6 Hz, 1H), 2.39 (s, 3H);

^{13}C NMR (100.6 MHz) ($CDCl_3$): δ 162.5 (q, $J_{C\text{-}F}$ = 248.5 Hz) (C), 157.2 (d, $J_{C\text{-}F}$ = 37.2 Hz) (C), 142.6 (C), 141.8 (C), 135.1 (C), 134.0 (CH), 133.2 (C), 131.0 (CH), 129.0 (CH), 122.8 (C), 122.5 (CH), 122.4 (d, $J_{C\text{-}F}$ = 3.7 Hz) (CH), 116.9 (CH), 116.7 (CH), 115.8 (q, $J_{C\text{-}F}$ = 288.2 Hz) (C), 46.1 (CH_2), 20.9 (CH_3);

^{19}F NMR (400.13 MHz) ($CDCl_3$): δ -68.9, -111.83.

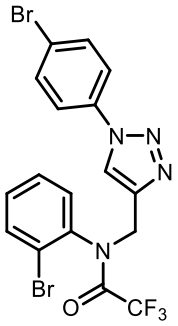

N-(2-bromophenyl)-N-((1-(4-bromophenyl)-1H-1,2,3-triazol-4-yl)methyl)-2,2,2-trifluoroacetamide, 3.1m:

81% yield; pale yellow solid; mp: 135-137 °C; R_f = 0.22 (n-hexane-EtOAc, 85:15); IR (neat): 3149, 1698, 1483, 1159, 731 cm^{-1};

^{1}H NMR (400.13 MHz) ($CDCl_3$): δ 8.16 (*s*, 1H), 7.75 – 7.71 (m, 1H), 7.71 – 7.63 (m, 4H), 7.38 – 7.29 (m, 2H), 7.21 – 7.14 (m, 1H), 5.50 (d, *J* = 14.7 Hz, 1H), 4.50 (d, J_1 = 14.7 Hz, 1H);

^{13}C NMR (100.6 MHz) ($CDCl_3$): δ 156.9 (q, J_{C-F}), 142.7 (C), 137.8 (C), 135.8 (C), 133.7 (CH), 133.0 (CH), 131.5 (CH), 131.1 (CH), 128.4 (CH), 123.3 (C), 122.6 (C), 122.1 (CH), 121.9 (CH), 117.3 (q, J_{C-F}), 46.0 (CH_2);

^{19}F NMR (400.13 MHz) ($CDCl_3$): δ -68.9.

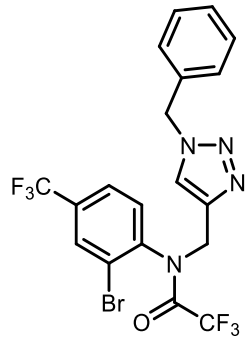

N-((1-benzyl-1H-1,2,3-triazol-4-yl)methyl)-N-(2-bromo-4-(trifluoromethyl)phenyl)-2,2,2-trifluoroacetamide, 3.1n:

70% yield; yellow solid; mp: 118-120 °C; R_f = 0.16 (n-hexane-EtOAc, 75:25); IR (neat): 3378, 3068, 1610, 1324, 1109 cm^{-1};

^{1}H NMR (400.13 MHz) ($CDCl_3$): δ 7.67 (d, *J* = 1.2 Hz, 1H), 7.45 – 7.32 (m, 5H), 7.31 – 7.21 (m, 2H), 6.70 (d, *J* = 8.6 Hz, 1H), 5.51 (s, 2H), 4.54 (d, *J* = 5.7 Hz, 2H);

^{13}C NMR (100.6 MHz) ($CDCl_3$): δ 171.2 (C), 146.8 (C), 145.3 (C), 134.5 (C), 129.6 (q, J_{C-F} = 12.2 Hz) (C), 129.15 (C), 128.8 (CH), 128.9 (CH), 128.3 (CH), 125.8 (*q*, J_{C-F} = 12.4 Hz) (C), 123.8 (d, J_{C-F} = 271.8 Hz) (C), 121.6 (C), 119.9 (q, J_{C-F} = 99.8 Hz) 110.6 (CH), 108.9 (C), 54.3 (CH_2), 39.6 (CH_2);

^{19}F NMR (400.13 MHz) ($CDCl_3$): δ -61.2, 62.2.

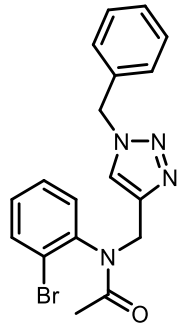

N-((1-benzyl-1H-1,2,3-triazol-4-yl)methyl)-N-(2-bromophenyl)acetamide, 3.2a:

92% yield; pale yellow solid; mp: 112-114 °C; R_f = 0.20 (n-hexane-EtOAc, 60:40); IR (neat): 3139, 2955, 1655, 1369, 1044, 709 cm^{-1};

^{1}H NMR (400.13 MHz, $CDCl_3$) δ 7.65 (dd, J_1 = 8.0 Hz, J_2 = 1.3 Hz, 1H), 7.60 (s, 1H), 7.41 – 7.35 (m, 3H), 7.32 – 7.19 (m, 4H), 7.11 (dd, J_1 = 8.0 Hz, J_2 = 1.3 Hz, 1H), 5.56 (d, J = 14.8 Hz, 1H), 5.44 (d, J = 14.8 Hz, 1H), 5.26 (d, J = 14.8 Hz, 1H), 4.45 (d, J = 14.8 Hz, 1H), 1.81 (s, 3H);

^{13}C NMR (100.6 MHz, $CDCl_3$) δ 170.4 (C), 144.1 (C), 141.5 (C), 134.7 (C), 133.8 (CH), 131.0 (CH), 130.0 (CH), 129.1 (CH), 128.8 (CH), 128.7 (CH), 128.0 (CH), 123.7 (CH), 123.7 (C), 54.1 (CH_2), 43.6 (CH_2), 22.3 (CH_3).

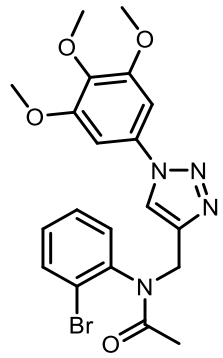

N-(2-bromophenyl)-N-((1-(3,4,5-trimethoxyphenyl)-1H-1,2,3-triazol-4-yl)methyl)acetamide, 3.2b:

96% yield; pale yellow solid; mp: 156-158 °C; R_f = 0.24 (n-hexane-EtOAc, 60:40); IR (neat): 3117, 2983, 1663, 1473, 763 cm^{-1};

^{1}H NMR (400.13 MHz, $CDCl_3$) δ 8.14 (s, 1H), 7.67 (dd, J_1 = 8.0 Hz, J_2 = 1.0 Hz, 1H), 7.34 (dt, J_1 = 7.7 Hz, J_2 = 1.3 Hz, 1H), 7.25 (dt, J_1 = 7.7 Hz, J_2 = 1.3 Hz, 1H), 7.19 (dd, J_1 = 7.8 Hz, J_2 =

1.5 Hz, 1H), 6.97 (s, 2H), 5.35 (d, *J* = 14.8 Hz, 1H), 4.45 (d, *J* = 14.8 Hz, 1H), 3.93 (s, 6H), 3.88 (s, 3H), 1.84 (s, 3H);

^{13}C NMR (100.6 MHz, $CDCl_3$) δ 170.6 (C), 153.9 (C), 144.5 (C), 141.7 (C), 138.2 (C), 133.8 (CH), 132.9 (C), 131.0 (CH), 130.1 (CH), 129.0 (CH), 123.7 (C), 122.1 (CH), 98.1 (CH), 61.1 (CH_3), 56.5 (CH_3), 43.8 (CH_2), 22.3 (CH_3).

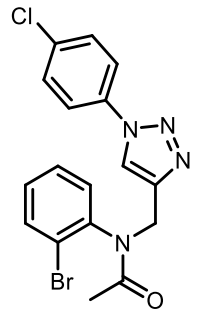

N-(2-bromophenyl)-N-((1-(2-chlorophenyl)-1H-1,2,3-triazol-4-yl)methyl)acetamide, 3.2c:

85% yield; yellow liquid; R_f = 0.18 (n-hexane-EtOAc, 60:40); IR (neat): 3068, 1665, 1476, 1038, 759 cm^{-1};

^{1}H NMR (400.13 MHz, $CDCl_3$) δ 8.09 (s, 1H), 7.70 (dd, J_1 = 8.0 Hz, J_2 = 1.2 Hz, 1H), 7.65 – 7.55 (m, 2H), 7.49 – 7.40 (m, 2H), 7.35 (td, J_1 = 7.6 Hz, J_2 = 1.2 Hz, 1H), 7.29 – 7.16 (m, 2H), 5.40 (d, *J* = 14.8 Hz, 1H), 4.57 (d, *J* = 14.8 Hz, 1H), 1.86 (s, 3H);

^{13}C NMR (100.6 MHz, $CDCl_3$) δ 170.5 (C), 143.5 (C), 141.5 (C), 134.9 (C), 133.8 (CH), 131.1 (CH), 130.7 (CH), 130.1 (CH), 128.9 (CH), 128.7 (C), 127.9 (CH), 127.8 (CH), 125.9 (CH), 123.7 (C), 43.5 (CH_2), 22.3 (CH_3).

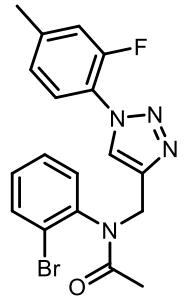

N-(2-bromophenyl)-N-((1-(2-fluoro-4-methylphenyl)-1H-1,2,3-triazol-4-yl)methyl)acetamide, 3.2d:

85% yield; white oil; R_f = 0.25 (n-hexane-EtOAc, 50:50); IR (neat): 3178, 1657, 1046, 766, 562 cm^{-1};

^{1}H NMR (400.13 MHz, $CDCl_3$) δ 8.14 (d, *J* = 2.8 Hz, 1H), 7.75 (m, 1H), 7.69 (m, 1H), 7.35 (dt, J_1 = 7.7 Hz, J_2 = 1.3 Hz, 1H), 7.25 (dt, J_1 = 7.8 Hz, J_2 = 1.6 Hz, 1H), 7.20 (dd, J_1 = 7.8 Hz, J_2 = 1.6 Hz, 1H) 7.14 – 7.06 (m, 2H), 5.41 (d, *J* = 14.8 Hz, 1H), 4.49 (d, *J* = 14.8 Hz, 1H), 2.43 (s, 3H), 1.85 (*s*, 3H);

^{13}C NMR (100.6 MHz) ($CDCl_3$): δ 170.6 (C), 153.2 (d, J_{C-F} = 250.9 Hz) (C), 144.0 (C), 141.6 (C), 141.2 (d, J_{C-F} = 7.9 Hz) (C),133.9 (CH), 131.2 (CH), 130.2 (CH), 129.0 (CH), 125.73 (d, J_{C-F} = 3.1 Hz) (C), 124.98 (d, J_{C-F} = 7.3 Hz) (C), 124.5 (CH), 123.7 (C), 117.3 (d, J_{C-F} = 19.7 Hz) (CH), 43.6 (CH_2), 22.4 (CH_3), 21.3 (CH_3);

^{19}F NMR (400.13 MHz) ($CDCl_3$): δ -124.29, -124.30, -124.31.

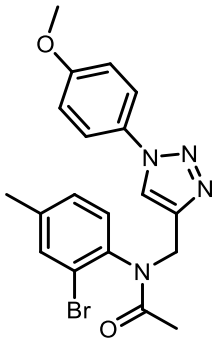

N-(2-bromo-4-methylphenyl)-N-((1-(4-methoxyphenyl)-1H-1,2,3-triazol-4-yl)methyl)acetamide, 3.2e:

98% yield; white solid; mp: 120-122 °C; R_f = 0.24 (n-hexane-EtOAc, 60:40); IR (neat): 3144, 1649, 1431, 1042, 567 cm^{-1};

^{1}H NMR (400.13 MHz, $CDCl_3$) δ 8.07 (*s*, 1H), 7.62 (dd, J_1 = 9.0 Hz, J_2 = 2.30, 2H), 7.50 (d, *J* = 1.07 Hz, 1H), 7.12 (dd, J_1 = 8.10 Hz, J_2 = 1.25 Hz, 1H), 7.07-6.98 (*m*, 3H), 5.33 (*d*, J_1 = 14.8 Hz, 1H), 4.41 (*d*, J_1 = 14.8 Hz, 1H), 3.86 (*s*, 3H), 2.35 (*s*, 3H), 1.82 (*s*, 3H);

^{13}C NMR (100.6 MHz) ($CDCl_3$): δ 170.7 (C), 159.7 (C), 144.3 (CH), 140.5 (C), 139.0 (C), 134.1 (CH), 130.56 (C), 130.47 (CH), 129.6 (CH), 123.1 (C), 122.0 (CH), 122.0 (CH), 114.7 (CH), 55.6 (CH_3), 43.8 (CH_2), 22.3 (CH_3), 20.8 (CH_3).

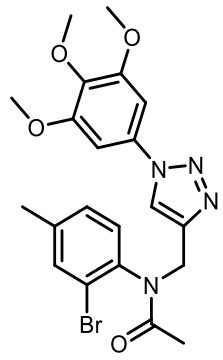

N-(2-bromo-4-methylphenyl)-N-((1-(3,4,5-trimethoxyphenyl)-1H-1,2,3-triazol-4-yl)methyl)acetamide, 3.2f:

83% yield; white oil; mp: 138-140 °C; lit.9 mp: 138-140 °C; R_f = 0.22 (n-hexane-EtOAc, 60:40); IR (neat): 3415, 2967, 1656, 1127, 572 cm^{-1};

^{1}H NMR (400.13 MHz) ($CDCl_3$): δ 8.14 (s, 1H), 7.50 (d, J_1 = 1.2 Hz, J_2 = 0.9 Hz, 1H), 7.11 (ddd, J_1 = 8.0 Hz, J_2 = 1.2, J_3 = 0.5 Hz, 1H), 7.05 (*d*, *J* = 8.0 Hz, 1H), 6.98 (*s*, 2H), 5.32 (*d*, *J* = 14.8 Hz, 1H), 4.42 (d, *J* = 14.8 Hz, 1H), 3.95 (s, 6H), 3.90 (s, 3H), 2.37 (s, 3H), 1.85 (s, 3H);

^{13}C NMR (100.6 MHz) ($CDCl_3$): δ 170.8 (C), 153.9 (C), 144.5 (C), 140.6 (C), 139.0 (C), 138.2 (C), 134.2 (CH), 132.9 (C), 130.4 (CH), 129.6 (CH), 123.1 (C), 122.1 (CH), 98.2 (CH), 61.1 (CH_3), 56.5 (CH_3), 43.9 (CH_2), 22.3 (CH_3), 20.8 (CH_3).

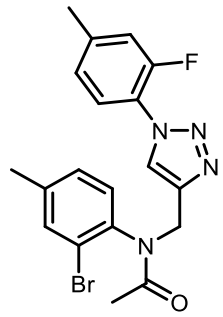

N-(2-bromo-4-methylphenyl)-N-((1-(2-fluoro-4-methylphenyl)-1H-1,2,3-triazol-4-yl)methyl)acetamide, 3.2g:

99% yield; yellow solid; mp: 119-121 °C; R_f = 0.21 (n-hexane-EtOAc, 50:50); IR (neat): 3074, 2922, 1665, 1042, 824 cm^{-1};

^{1}H NMR (400.13 MHz, $CDCl_3$) δ 8.16 – 8.11 (m, 1H), 7.80 – 7.73 (m, 1H), 7.53 – 7.48 (m, 1H), 7.16 – 7.04 (m, 4H), 5.39 (d, *J* = 14.8 Hz, 1H), 4.48 (d, *J* = 14.8 Hz, 1H), 2.43 (s, 3H), 2.36 (s, 3H), 1.82 (s, 3H);

^{13}C NMR (100.6 MHz, $CDCl_3$) δ 170.7 (C), 153.2 (d, $J_{C\text{-}F}$ = 250.6 Hz) (C), 144.0 (C), 141.15 (d, $J_{C\text{-}F}$ = 7.3 Hz) (C), 140.5 (C), 138.9 (C), 134.1 (CH), 130.5 (CH), 129.6 (CH), 125.72 (*d*, $J_{C\text{-}F}$ = 3.1 Hz) (CH), 124.93 (d, $J_{C\text{-}F}$ = 7.3 Hz) (C), 124.6 (C), 123.2 (C), 117.30 (d, $J_{C\text{-}F}$ = 19.9 Hz) (CH), 98.2 (CH), 43.5 (CH_2), 22.3 (CH_3), 21.2 (CH_3), 20.8 (CH_3);

^{19}F NMR (400.13 MHz) ($CDCl_3$): δ -124.29, -124.30, -124.31.

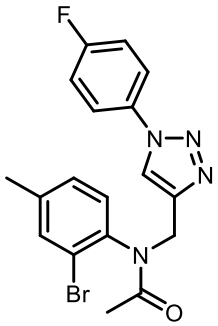

N-(2-bromo-4-methylphenyl)-N-((1-(4-fluorophenyl)-1H-1,2,3-triazol-4-yl)methyl)acetamide, 3.2h:

93% yield; white solid; mp: 155-157 °C; R_f = 0.23 (n-hexane-EtOAc, 60:40); IR (neat): 3140, 1653, 1515, 1042, 839 cm^{-1};

^{1}H NMR (400.13 MHz, $CDCl_3$) δ 8.12 (s, 1H), 7.76 – 7.67 (m, 2H), 7.50 (d, *J* = 1.5 Hz, 1H), 7.25 – 7.14 (m, 2H), 7.13 (dd, J_1 = 8.2 Hz, J_2 = 1.5 Hz, 1H), 7.05 (d, *J* = 8.2 Hz, 1H), 5.33 (d, *J* = 14.8 Hz, 1H), 4.45 (d, *J* = 14.8 Hz, 1H), 2.36 (*s*, 3H), 1.83 (*s*, 3H);

^{13}C NMR (100.6 MHz, $CDCl_3$) δ 170.8 (C), 162.3 (d, $J_{C\text{-}F}$ = 250.1 Hz) (C), 144.7 (C), 140.6 (C), 139.0 (C), 134.2 (CH), 133.35 (d, $J_{C\text{-}F}$ = 3.0 Hz) (C), 130.4 (CH), 129.7 (CH), 123.1 (C), 122.37 (d, $J_{C\text{-}F}$ = 8.7 Hz) (CH), 122.1 (CH), 116.6 (d, $J_{C\text{-}F}$ = 23.2 Hz) (CH), 43.8 (CH_2), 22.3 (CH_3), 20.8 (CH_3);

^{19}F NMR (400.13 MHz) ($CDCl_3$): δ -68.9, -111.83.

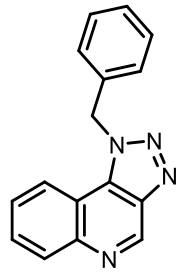

1-benzyl-1H-[1,2,3]triazolo[4,5-c]quinoline, 3.3a:

95% yield; yellow solid; mp: 140-142 °C; R_f = 0.22 (n-hexane-EtOAc, 50:50); IR (neat): 3386, 2961, 1688, 1453, 722 cm^{-1};

^{1}H NMR (400.13 MHz) ($CDCl_3$): δ 9.47 (s, 1H), 8.19 (*d*, *J* = 8.3 Hz, 1H), 7.97 (dd, J_1 = 8.3 Hz, J_2 = 0.80 Hz, 1H), 7.69 – 7.64 (m, 1H), 7.52 – 7.46 (m, 1H), 7.29 – 7.15 (m, 3H), 7.08 (d, *J* = 7.50, 2H), 6.16 (s, 2H);

^{13}C NMR (100.6 MHz) ($CDCl_3$): δ 145.7 (C), 145.0 (CH), 141.2 (C), 134.2 (C), 133.2 (C), 130.8 (CH), 129.6 (CH), 129.3 (CH), 128.6 (CH), 127.7 (CH), 126.4 (CH), 122.1 (CH), 115.2 (C), 53.9 (CH_2);

MS (EI, 70 eV): *m/z* (%)= 231 (100), 260 (M^+, 100), 91 (100), 128 (90).

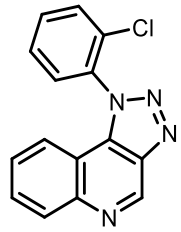

1-(2-chlorophenyl)-1H-[1,2,3]triazolo[4,5-c]quinoline, 3.3b:

72% yield; yellow solid; mp: 130-132 °C; R_f = 0.21 (n-hexane-EtOAc, 60:40); IR (neat): 3142, 1699, 1203, 1167, 767 cm^{-1};

^{1}H NMR (400.13 MHz) ($CDCl_3$): δ 9.56 (*s*, 1H), 8.27 (d, *J* = 8.10 Hz, 1H), 7.84 – 7.71 (m, 2H), 7.68 – 7.61 (m, 4H), 7.52 (t, *J* = 7.50 Hz, 1H);

^{13}C NMR (100.6 MHz) ($CDCl_3$): δ 146.0 (C), 144.7 (CH), 140.4 (C), 136.9 (C), 135.5 (C), 133.6 (C), 132.5 (CH), 131 (CH), 130.7 (CH), 130 (CH), 129.5 (CH), 128.4 (CH), 127.7 (CH), 121.3 (CH), 115.1 (C);

MS (EI, 70 eV): *m/z* (%)= 217 (100), 252 (80), 280 (M^+, 20), 128(65).

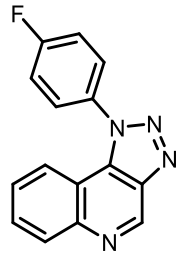

1-(4-fluorophenyl)-1H-[1,2,3]triazolo[4,5-c]quinoline, 3.3c:

80% yield; yellow solid; mp: 145-147 °C; R_f = 0.22 (n-hexane-EtOAc, 70:30); IR (neat): 3145, 3102, 1685, 1519, 1164, 722 cm^{-1};

^{1}H NMR (400.13 MHz) ($CDCl_3$): δ 9.57 (s, 1H), 8.27 (d, *J* = 8.4 Hz, 1H), 7.78 (t, *J* = 7.80 Hz, 1H), 7.71 – 7.62 (m, 3H), 7.49 (t, *J* = 7.8 Hz, 1H), 7.43 – 7.33 (m, 2H);

^{13}C NMR (100.6 MHz) ($CDCl_3$): δ 163.8 (d, J_{C-F} = 252.0 Hz) (C), 145.9 (C), 144.9 (CH), 140.4 (C), 133.8 (C), 133.07 (d, J_{C-F} = 3.2 Hz) (C), 130.8 (C), 130.0 (C), 128.57 (d, J_{C-F} = 8.6 Hz) (CH), 127.5 (CH), 121.5 (CH), 117.21 (d, J_{C-F} = 23.1 Hz) (CH), 115.0 (C);

^{19}F NMR (400.13 MHz) ($CDCl_3$): δ -108.54, -108.55, -108.56, -108.59;

MS (EI, 70 eV): *m/z* (%)= 236 (100), 264 (M^+, 12), 208 (37), 75(27).

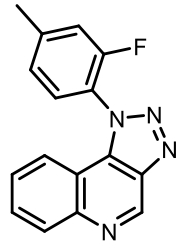

1-(2-fluoro-4-methylphenyl)-1H-[1,2,3]triazolo[4,5-c]quinoline, 3.3d:

90% yield; yellow liquid; R_f = 0.19 (n-hexane-EtOAc, 70:30); IR (neat): 3151, 3067, 1703, 1467, 1206, 1159 cm^{-1};

^{1}H NMR (400.13 MHz) ($CDCl_3$): δ 9.57 (s, 1H), 8.27 (d, *J* = 8.4 Hz, 1H), 7.81 – 7.73 (m, 1H), 7.63 (d, *J* = 8.3 Hz, 1H), 7.56 (t, *J* = 8.0 Hz, 1H), 7.53 – 7.47 (m, 1H), 7.30 – 7.20 (m, 2H), 2.55 (*s*, 3H);

^{13}C NMR (100.6 MHz) ($CDCl_3$): δ 156.6 (d, J_{C-F} = 253.6 Hz) (C), 145.9 (C), 144.8 (CH), 144.28 (*d*, J_{C-F} = 7.5 Hz) (C),140.2 (C), 134.6 (C), 130.6 (CH), 130.0 (CH), 128.5 (CH), 127.6 (CH), 126.13 (d, J_{C-F} = 3.2 Hz) (CH), 122.4 (C), 122.38 (d, J_{C-F} = 13.2 Hz) (C), 117.7 (d, J_{C-F} = 18.4 Hz) (CH), 115.2 (C), 21.62 (CH_3);

^{19}F NMR (400.13 MHz) ($CDCl_3$): δ -108.54;

MS (EI, 70 eV): *m/z* (%)= 162 (100), 83 (24), 109 (21), 279 (M+1, 2).

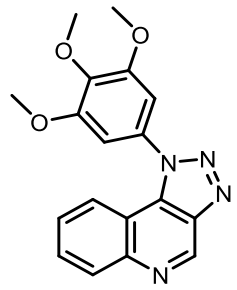

1-(3,4,5-trimethoxyphenyl)-1H-[1,2,3]triazolo[4,5-c]quinoline, 3.3e:

82% yield; white solid; mp: 238-241 °C; R_f = 0.20 (n-hexane-EtOAc, 70:30); IR (neat): 3081,1599, 1246, 1120, 770 cm^{-1};

^{1}H NMR (400.13 MHz) ($CDCl_3$): δ 9.59 (s, 1H), 8.30 (d, J_1 = 8.40 Hz, 1H), 7.86 – 7.76 (m, 2H), 7.60 – 7.52 (m, 1H), 6.90 (s, 2H), 4.02 (s, 3H), 3.91 (s, 6H);

^{13}C NMR (100.6 MHz) ($CDCl_3$): δ 154.1 (C), 153.9 (C), 146.0 (C), 144.9 (CH), 140.3 (C), 139.8 (C), 133.7 (C), 132.3 (C), 130.8 (CH), 130.0 (CH), 129.3 (CH), 127.5 (CH), 121.9 (CH), 115.2 (C), 113.2 (CH), 104.0 (CH), 98.5 (CH), 61.2 (CH_3), 56.5 (CH_3););

MS (EI, 70 eV): *m/z* (%)= 307 (100), 249 (90), 264 (86), 338 (1), 336 (M^+, 1).

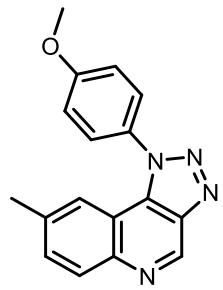

1-(4-methoxyphenyl)-8-methyl-1H-[1,2,3]triazolo[4,5-c]quinoline, 3.3f:

80% yield; pale yellow solid; mp: 170-172 °C; R_f = 0.22 (n-hexane-EtOAc, 70:30); IR (neat): 3050, 1586, 1522, 1250, 834 cm^{-1};

^{1}H NMR (400.13 MHz) ($CDCl_3$): δ 9.40 (s, 1H), 8.06 (d, *J* = 8.52 Hz, 1H), 7.51 – 7.44 (m, 3H), 7.39 (s, 1H), 7.09 (dd, J_1 = 2.25 Hz, J_2 = 8.90 Hz, 2H), 3.83 (s, 3H), 2.31 (s, 3H);

^{13}C NMR (100.6 MHz) ($CDCl_3$): δ 161.2 (C), 144.2 (C), 143.9 (CH), 140.4 (C), 137.5 (C), 133.5 (C), 131.6 (CH), 130.4 (CH), 129.7 (C), 127.8 (CH), 121.2 (CH), 115.2 (C), 115.0 (CH), 55.8 (CH_3), 21.9 (CH_3);

MS (EI, 70 eV): *m/z* (%)= 219 (100), 247 (86), 262 (21), 290 (M^+, 15).

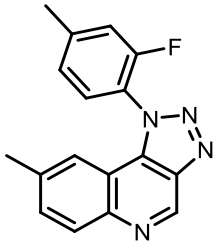

1-(2-fluoro-4-methylphenyl)-8-methyl-1H-[1,2,3]triazolo[4,5-c]quinoline, 3.3g:

90% yield; brown solid; mp: 190-192 °C; Rf = 0.22 (n-hexane-EtOAc, 70:30); IR (neat): 3043, 2948, 1628, 1525, 1267, 827 cm-1;

^{1}H NMR (400.13 MHz) ($CDCl_3$): δ 9.45 (s, 1H), 8.06 (d, *J* = 8.5 Hz, 1H), 7.54 – 7.44 (m, 2H), 7.29 (s, 1H), 7.22 - 7.14 (m, 2H), 2.49 (s, 3H), 2.33 (s, 3H);

^{13}C NMR (100.6 MHz) ($CDCl_3$): δ 156.7 (d, J_{C-F} = 253.9 Hz) (C), 144.3 (C), 144.19 (d, J_{C-F} = 7.2 Hz) (C), 143.8 (CH), 140.3 (C), 137.8 (C), 134.3 (C), 131.9 (CH), 130.3 (CH), 128.6 (CH), 126.04 (d, J_{C-F} = 3.6 Hz) (CH), 122.51 (d, J_{C-F} = 13.1 Hz) (C), 120.6 (CH), 117.60 (*d*, J_{C-F} = 19.1 Hz) (CH), 115.1 (C), 21.9 (CH_3), 21.66 (CH_3), 21.65 (CH_3);

^{1}F NMR (400.13 MHz) ($CDCl_3$): δ -120.62, -120.84, -120.89;

MS (EI, 70 eV): *m/z* (%)= 263 (100), 249 (20), 292 (M^+, 14), 83 (12).

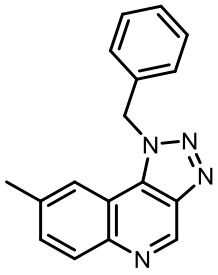

1-benzyl-8-methyl-1H-[1,2,3]triazolo[4,5-c]quinoline, 3.3h:

83% yield; pale yellow solid; mp: 155-157 °C; lit.9 mp: 138-140 °C; R_f = 0.22 (n-hexane-EtOAc, 70:30); IR (neat): 3032, 2948, 1525, 1254, 827 cm^{-1};

^{1}H NMR (400.13 MHz) ($CDCl_3$): δ 9.51 (s, 1H), 8.15 (d, *J* = 8.5 Hz, 1H), 7.83 (s, 1H), 7.56 (dd, J_1 = 8.5 Hz, J_2 = 1.8 Hz, 1H), 7.40 – 7.30 (m, 3H), 7.22 – 7.16 (m, 2H), 6.24 (s, 2H), 2.49 (s, 3H);

^{13}C NMR (100.6 MHz) ($CDCl_3$): δ 144.08 (CH), 144.05 (C), 141.3 (C), 137.8 (C), 134.5 (C), 132.9 (C), 131.4 (CH), 130.4 (CH), 129.3 (CH), 128.6 (CH), 126.6 (CH), 121.7 (CH), 115.1 (C), 53.9 (CH_2), 21.8 (CH_3);

MS (EI, 70 eV): *m/z* (%)= 91 (100), 245 (30), 274 (M^+, 29), 65 (18).

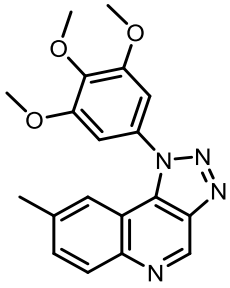

8-methyl-1-(3,4,5-trimethoxyphenyl)-1H-[1,2,3]triazolo[4,5-c]quinoline, 3.3i:

71% yield; brown solid; mp: 221-223 °C; R_f = 0.19 (n-hexane-EtOAc, 50:50); IR (neat): 3047, 2930, 1599, 1416, 1229, 1127 cm^{-1};

^{1}H NMR (400.13 MHz) ($CDCl_3$): δ 9.45 (s, 1H), 8.12 (d, *J* = 8.4 Hz, 1H), 7.58 – 7.51 (m, 2H), 6.83 (s, 2H), 3.93 (s, 3H), 3.83 (s, 6H), 2.37 (s, 3H);

^{13}C NMR (100.6 MHz) ($CDCl_3$): δ 154.0 (C), 144.4 (C), 144.0 (CH), 140.5 (C), 139.7 (C), 137.7 (C), 133.3 (C), 132.4 (C), 131.8 (CH), 130.5 (CH), 121.2 (CH), 115.1 (C), 104.0 (CH), 61.2 (CH_3), 56.5 (CH_3), 21.9 (CH_3);

MS (EI, 70 eV): *m/z* (%)= 307 (100), 264 (99), 249 (91), 350 (M^+, 36).

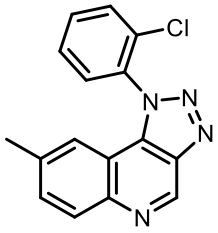

1-(2-chlorophenyl)-8-methyl-1H-[1,2,3]triazolo[4,5-c]quinoline, 3.3j:

85% yield; white solid; mp: 187-189°C; lit.9 mp: 138-140 °C; Rf = 0.23 (n-hexane-EtOAc, 70:30); IR (neat): 3045, 1511, 1225, 815, 560 cm-1;

^{1}H NMR (400.13 MHz) ($CDCl_3$): δ 9.46 (s, 1H), 8.12 (d, *J* = 8.5 Hz, 1H), 7.65 – 7.58 (m, 3H), 7.53 (dd, J_1 = 8.5 Hz, J_2 = 1.8 Hz, 1H), 7.39 – 7.30 (m, 3H), 2.35 (s, 3H);

^{13}C NMR (100.6 MHz) ($CDCl_3$): δ 144.3 (C), 143.8 (CH), 140.2 (C), 137.9 (CH), 134.9 (C), 134.3 (C), 132.55 (C), 132.46 (CH), 131.9 (CH), 130.9 (CH), 130.3 (CH), 129.6 (CH), 128.3 (CH), 120.6 (CH), 115.1 (CH), 21.9 (CH_3).

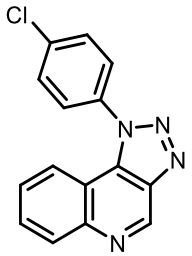

1-(4-chlorophenyl)-1H-[1,2,3]triazolo[4,5-c]quinoline, 3.3k:

82% yield; yellow solid; mp: 157-159 °C; R_f = 0.21 (n-hexane-EtOAc, 60:40); IR (neat): 3070, 1699, 1203, 1167, 767 cm^{-1};

^{1}H NMR (400.13 MHz) ($CDCl_3$): δ 9.56 (s, 1H), 8.29 (d, *j* = 8.5, 1H), 7.84 – 7.72 (m, 2H), 7.72 – 7.64 (*m*, 4H), 7.52 (t, *J* = 7.8 Hz, 1H), 7.47 (ddd, J_1 = 8.2 Hz, J_2 = 7.0 Hz, J_3 = 1.2 Hz, 1H), 7.40 (dd, J_1 = 8.2 Hz, J_2 = 1.6 Hz, 1H);

^{13}C NMR (100.6 MHz) ($CDCl_3$): δ 145.9 (C), 144.9 (CH), 140.1 (C), 134.8 (C), 134.5 (C), 132.51 (CH), 132.47 (C), 131.0 (CH), 130.6 (CH), 130.1 (CH), 129.6 (CH), 128.4 (CH), 127.7 (CH), 121.4 (CH), 115.2 (C);

MS (EI, 70 eV): *m/z* (%)= 252 (100), 217 (92), 190 (73), 280 (M^+, 14).

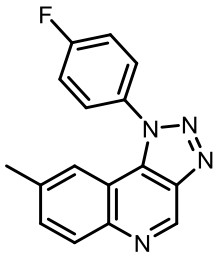

1-(4-fluorophenyl)-8-methyl-1H-[1,2,3]triazolo[4,5-c]quinoline, 3.3l:

83% yield; pale yellow solid; mp: 187-189 °C; Rf = 0.24 (n-hexane-EtOAc, 70:30); IR (neat): 3055, 1515, 1225, 816, 564 cm-1;

^{1}H NMR (400.13 MHz) ($CDCl_3$): δ 9.52 (s, 1H), 8.19 (*d*, *J* = 8.5 Hz, 1H), 7.71 – 7.64 (m, 2H), 7.61 (dd, J_1 = 8.5 Hz, J_2 = 1.9 Hz, 1H), 7.43 (m, 1H), 7.49 – 7.36 (m, 2H), 2.43 (s, 3H);

^{13}C NMR (100.6 MHz) ($CDCl_3$): δ 163.7 (d, $J_{C\text{-}F}$ = 252.9 Hz) (C), 144.4 (C), 143.9 (CH), 140.5 (C), 137.8 (C), 133.5 (C), 133.18 (d, $J_{C\text{-}F}$ = 3.4 Hz) (C), 131.9 (CH), 130.6 (CH), 128.56 (d, $J_{C\text{-}F}$ = 8.9 Hz) (CH), 120.9 (CH), 117.08 (d, $J_{C\text{-}F}$ = 22.8 Hz) (CH), 115.0 (C), 21.9 (CH_3);

^{1}F NMR (400.13 MHz) ($CDCl_3$): δ -108.54, -108.55, -108.56, -108.59; MS (EI, 70 eV): *m/z* (%)= 250 (100), 75 (30), 278 (M^+, 16), 222 (9).

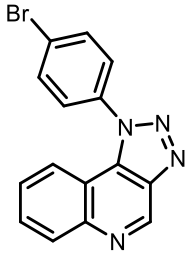

1-(4-bromophenyl)-1H-[1,2,3]triazolo[4,5-c]quinoline, 3.3m: 0% yield.

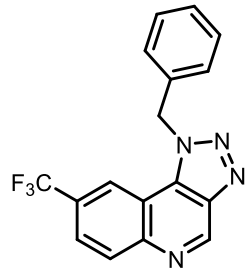

1-benzyl-8-(trifluoromethyl)-1H-[1,2,3]triazolo[4,5-c]quinoline, 3.3n:

61% yield; brown solid; mp: 133-135°C; mp: 138-140 °C; Rf = 0.18 (n-hexane-EtOAc, 70:30); IR (neat): 2922, 1294, 1114, 847, 721 cm-1;

^{1}H NMR (400.13 MHz) ($CDCl_3$): δ 9.59 (s, 1H), 8.31 (*d*, *J* = 8.4 Hz, 1H), 8.27 (s, 1H), 7.86 (dd, J_1 = 8.7 Hz, J_2 = 1.9 Hz, 1H), 7.34 – 7.21 (m, 3H), 7.17 – 7.12 (m, 2H), 6.19 (s, 2H);

^{13}C NMR (100.6 MHz) ($CDCl_3$): δ 147.2 (CH), 146.9 (C), 141.7 (C), 133.5 (C), 133.2 (C), 131.8 (CH), 129.5 (CH), 129.4 (C), 129.1 (C), 129.0 (CH), 126.7 (CH), 125.56 (t, $J_{C\text{-}F}$ = 2.8 Hz, $J_{C\text{-}F}$ =5.8 Hz) (CH), 120.38 (d, $J_{C\text{-}F}$ = 4.0 Hz) (CH), 114.7 (C), 54.3 (CH_2), 30.3 (CH_3);

^{19}F NMR (400.13 MHz) ($CDCl_3$): δ -68.9;

MS (EI, 70 eV): *m/z* (%)= 250 (100), 75 (30), 278 (M^+, 16), 222 (9).

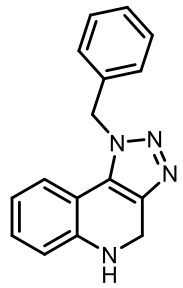

1-benzyl-4,5-dihydro-1H-[1,2,3]triazolo[4,5-c]quinoline, 3.4a:

77% yield; pale yellow solid; mp: 182-184 °C; R_f = 0.21 (*n*-hexane-EtOAc, 50:50); IR (neat): 3367, 3063, 1622, 1122, 713 cm^{-1};

^{1}H NMR (400.13 MHz, $CDCl_3$) δ 7.29 – 7.15 (m, 3H), 7.07 (*d*, *J* = 7.7 Hz, 2H), 7.01 (d, *J* = 7.7 Hz, 1H), 6.95 – 6.88 (m, 1H), 6.55 – 6.40 (m, 2H), 5.69 (s, 2H), 4.72 (s, 2H), 4.09 (s, 1H);

^{13}C NMR (100.6 MHz, $CDCl_3$) δ 144.8 (C), 140.0 (C), 135.0 (C), 130.0 (CH), 129.4 (C), 129.3 (C), 129.1 (CH), 128.2 (CH), 126.5 (C), 126.4 (CH), 122.9 (CH), 118.1 (CH), 114.6 (CH), 110.5 (C), 53.1 (CH_2), 41.4 (CH_2);

MS (EI, 70 eV): *m/z* (%)= 207 (100), 73 (76), 281 (47), 260 (30), 262 (M^+, 6).

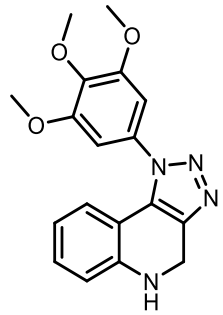

1-(3,4,5-trimethoxyphenyl)-4,5-dihydro-1H-[1,2,3]triazolo[4,5-c]quinoline, 3.4b:

96% yield; yellow solid; mp: 230-232 °C; R_f = 0.25 (*n*-hexane-EtOAc, 50:50); IR (neat): 3365, 2837, 1603, 1229, 1122 cm^{-1};

^{1}H NMR (400.13 MHz) ($CDCl_3$): δ 7.04 – 6.92 (m, 1H), 6.75 (dd, J_1 = 7.9 Hz, J_2 = 1.2 Hz, 1H), 6.68 (s, 2H), 6.56 (d, *J* = 7.9 Hz 1H), 6.45 (t, *J* = 7.6 Hz 1H), 4.80 (s, 2H), 4.06 (s, 1H), 3.87 (*s*, 3H), 3.78 (*s*, 6H);

^{13}C NMR (100.6 MHz) ($CDCl_3$): δ 153.7 (C), 144.4 (C), 139.1 (C), 132.6 (CH), 130.2 (CH), 129.9 (C), 123 (CH), 118 (CH), 114.7 (CH), 110.5 (CH), 103.5 (CH), 61.1 (CH_3), 56.4 (CH_3), 41.2 (CH2);

MS (EI, 70 eV): *m/z* (%)= 293 (100), 250 (94), 336 (27), 338 (M^+, 1).

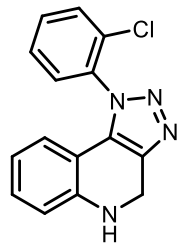

1-(2-chlorophenyl)-4,5-dihydro-1H-[1,2,3]triazolo[4,5-c]quinoline, 3.4c:

80% yield; yellow solid; mp: 137-139 °C; R_f = 0.21 (*n*-hexane-EtOAc, 60:40); IR (neat): 3292, 2916, 1630, 1095, 511 cm^{-1};

^{1}H NMR (400.13 MHz, $CDCl_3$) δ 7.65 (dd, J_1 = 7.9 Hz, J_2 = 1.1 Hz, 1H), 7.61 – 7.47 (m, 4H), 7.08 – 6.94 (m, 1H), 6.60 (*d*, *J* = 7.9 Hz, 1H), 6.50 – 6.37 (m, 1H), 4.94 (*t*, *J* = 13.8 Hz, *2H*), 4.28 (*s*, 1H);

^{13}C NMR (100.6 MHz, $CDCl_3$) δ 144.8 (C), 138.6 (C), 132.2 (C), 131.9 (CH), 130.8 (CH), 130.5 (CH), 129.7 (C), 129.3 (CH), 128.1 (CH), 126.1 (C), 122.8 (CH), 122.1 (CH), 117.9 (CH), 114.5 (CH), 110.1 (C), 41.4 (CH_2);

MS (EI, 70 eV): *m/z* (%)= 252 (100), 217 (96), 280 (15), 282 (M^+, 6).

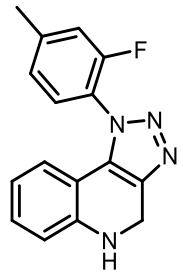

1-(2-fluoro-4-methylphenyl)-4,5-dihydro-1H-[1,2,3]triazolo[4,5-c]quinoline, 3.4d:

84% yield; yellow solid; mp: 126-128 °C; R_f = 0.18 (*n*-hexane-EtOAc, 75:25); IR (neat): 3319, 2979, 1523, 1034, 744 cm^{-1};

^{1}H NMR (400.13 MHz, $CDCl_3$) δ 7.43 (t, *J* = 8.0 Hz, 1H), 7.19 – 7.11 (m, 2H), 7.07 – 7.00 (m, 1H), 6.66 – 6.55 (m, 2H), 6.46 (td, J_1 = 8.0 Hz, J_2 = 1.2 Hz, 1H), 4.91 (d, *J* = 1.5 Hz, 2H), 4.14 (s, 1H); 2.49 (s, 3H);

^{13}C NMR (100.6 MHz, $CDCl_3$) δ 156.5 (d, $J_{C\text{-}F}$ = 253.2 Hz) (C), 144.7 (C), 143.42 (d, $J_{C\text{-}F}$ = 6.9 Hz) (C), 138.8 (C), 131.0 (C), 130.3 (CH), 128.4 (CH), 125.72 (d, $J_{C\text{-}F}$ = 3.1 Hz) (CH), 122.75 (d, $J_{C\text{-}F}$ = 13.1 Hz) (C), 122.1 (CH), 117.9 (CH), 117.51 (d, $J_{C\text{-}F}$ = 18.9 Hz) (CH), 114.5 (CH), 110.3 (C), 41.5 (CH_2), 21.6 (CH_3);

^{19}F NMR (400.13 MHz) ($CDCl_3$): δ -121.27, -121.28, -121.30;

MS (EI, 70 eV): *m/z* (%)= 251 (100), 207 (86), 278 (5), 280 (M^+, 30).

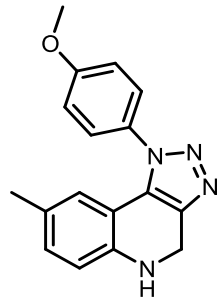

1-(4-methoxyphenyl)-8-methyl-4,5-dihydro-1H-[1,2,3]triazolo[4,5-c]quinoline, 3.4e:

86% yield; pale yellow solid; mp: 162-164 °C; R_f = 0.20 (*n*-hexane-EtOAc, 60:40); IR (neat): 3678, 2960, 1515, 1252, 820 cm^{-1};

^{1}H NMR (400.13 MHz, $CDCl_3$) δ 7.46 – 7.39 (m, 2H), 7.08 – 7.01 (m, 2H), 6.82 (ddd, J_1 = 8.2 Hz, J_2 = 2.0 Hz, J_3 = 0.8 Hz, 1H), 6.52 (m, 2H), 4.78 (*s*, 2H), 3.98 (s, 1H), 3.89 (s, 3H), 2.00 (s, 3H);

^{13}C NMR (100.6 MHz, $CDCl_3$) δ 160.7 (C), 142.6 (C), 139.8 (C), 130.8 (CH), 130.2 (C), 127.4 (CH), 127.2 (C), 123.2 (CH), 114.8 (CH), 114.7 (CH), 110.9 (C), 55.7 (CH_3), 41.4 (CH_2), 20.6 (CH_3);

MS (EI, 70 eV): *m/z* (%)= 219 (100), 247 (72), 290 (12), 292 (M^+, 1).

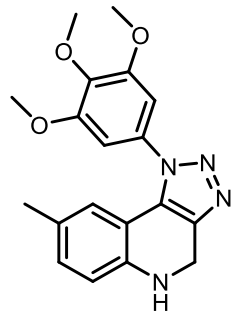

8-methyl-1-(3,4,5-trimethoxyphenyl)-4,5-dihydro-1H-[1,2,3]triazolo[4,5-c]quinoline, 3.4f:

85% yield; yellow solid; mp: 158-160 °C; R_f = 0.17 (*n*-hexane-EtOAc, 60:40); IR (neat): 3690, 3281, 2948, 1225, 1053 cm^{-1};

^{1}H NMR (400.13 MHz, $CDCl_3$) δ 6.86 (dd, J_1 = 8.2 Hz, J_2 = 2.0 Hz, 1H), 6.77 (s, 2H), 6.68 (d, *J* = 2.0 Hz, 1H), 6.56 (d, *J* = 8.2 Hz, 1H), 4.80 (s, 2H), 4.04 (s, 1H), 3.93 (s, 3H), 3.85 (s, 6H), 2.04 (s, 3H);

^{13}C NMR (100.6 MHz, $CDCl_3$) δ 153.8 (C), 142.7 (C), 140.1 (C), 139.2 (C), 132.8 (C), 131.0 (CH), 130.0 (C), 127.4 (C), 123.5 (CH), 114.9 (CH), 110.8 (C), 103.6 (CH), 61.2 (CH_3), 56.5 (CH_3), 41.5 (CH_2), 20.6 (CH_3);

MS (EI, 70 eV): *m/z* (%)= 249 (100), 207 (80), 350 (34), 352 (M^+, 7).

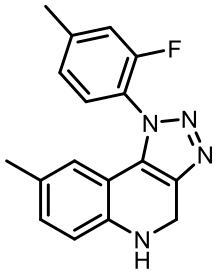

1-(2-fluoro-4-methylphenyl)-8-methyl-4,5-dihydro-1H-[1,2,3]triazolo[4,5-c]quinoline, 3.4g:

81% yield; pale yellow solid; mp: 147-149 °C; R_f = 0.19 (*n*-hexane-EtOAc, 60:40); IR (neat): 3343, 2914, 1535, 1106, 816 cm^{-1};

^{1}H NMR (400.13 MHz, $CDCl_3$) δ 7.41 (t, *J* = 8.2 Hz, 1H), 7.20 – 7.11 (m, 2H), 6.84 (dd, J_1 = 8.2 Hz, J_2 = 2.0 Hz, 1H), 6.52 (d, *J* = 8.2 Hz, 1H), 6.43 (d, *J*= 2.0 Hz, 1H), 4.85 (s, 2H), 4.01 (s, 1H), 2.50 (s, 3H), 2.01 (s, 3H);

^{13}C NMR (100.6 MHz, $CDCl_3$) δ 156.5 (d, $J_{C\text{-}F}$ = 252.1 Hz) (C), 143.35 (d, $J_{C\text{-}F}$ = 7.4 Hz) (C), 142.5 (C), 139.3 (C), 131.2 (C), 131.1 (CH), 128.5 (CH), 127.2 (C), 125.64 (d, $J_{C\text{-}F}$ = 3.5 Hz) (CH), 122.79 (d, $J_{C\text{-}F}$ = 12.9 Hz) (C), 122.5 (CH), 117.36 (d, $J_{C\text{-}F}$ = 18.6 Hz) (CH), 114.7 (CH), 110.7 (C), 41.5 (CH_2), 21.6 (CH_3), 20.6 (CH_3);

^{1}F NMR (400.13 MHz) ($CDCl_3$): δ -121.27, -121.28, -121.30;

MS (EI, 70 eV): *m/z* (%) = 265 (100), 207 (70), 292 (9), 294 (M^+, 39).

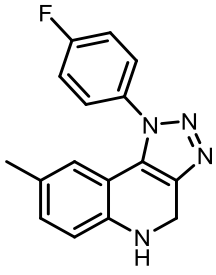

1-(4-fluorophenyl)-8-methyl-4,5-dihydro-1H-[1,2,3]triazolo[4,5-c]quinoline, 3.4h:

92% yield; pale green solid; mp: 194-196 °C; R_f = 0.17 (*n*-hexane-EtOAc, 70:30); IR (neat): 3388, 3074, 1523, 1213, 808 cm^{-1};

^{1}H NMR (400.13 MHz, $CDCl_3$) δ 7.50 – 7.37 (m, 2H), 7.25 – 7.13 (m, 2H), 6.77 (dd, J_1 = 8.2 Hz, J_2 = 1.9 Hz, 1H), 6.48 (d, J = 8.2 Hz, 1H), 6.41 (d, J_1 = 1.9 Hz, 1H), 4.72 (d, J = 1.9 Hz, 2H), 4.01 (*s*, 1H); 1.94 (s, 3H);

^{13}C NMR (100.6 MHz, $CDCl_3$) δ 163.2 (d, J_{C-F} = 253.3 Hz) (C), 142.7 (C), 140.1 (C), 133.37 (d, J_{C-F} = 3.45 Hz) (C), 131.0 (CH), 130.3 (C), 127.99 (d, J_{C-F} = 8.9 Hz) (CH), 127.3 (C), 123.1 (CH), 116.62 (d, J_{C-F} = 22.9 Hz) (CH), 115.0 (CH), 110.6 (C), 41.4 (CH_2), 20.6 (CH_3);

^{19}F NMR (400.13 MHz) ($CDCl_3$): δ -108.54;

MS (EI, 70 eV): *m/z* (%)= 250 (100), 222 (20), 278 (15), 280 (M^+, 2).

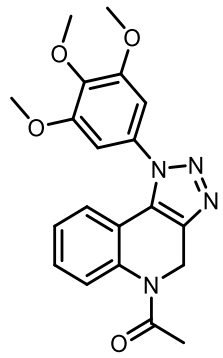

1-(1-(3,4,5-trimethoxyphenyl)-1,4-dihydro-5H-[1,2,3]triazolo[4,5-c]quinolin-5-yl)ethan-1-one, 3.5:

89% yield; pale yellow solid; mp: 202-204 °C; R_f = 0.17 (*n*-hexane-EtOAc, 50:50); IR (neat): 3074, 1653, 1233, 1130, 540 cm^{-1};

^{1}H NMR (400.13 MHz, $CDCl_3$) δ 7.64 (dd, J_1 = 8.1 Hz, J_2 = 1.2 Hz, 1H), 7.43 – 7.36 (m, 1H), 7.23 (dd, J_1 = 7.6 Hz, J_2 = 1.2 Hz, 1H), 7.05 (dd, J_1 = 7.8 Hz, J_2 = 1.5 Hz, 1H), 7.02 (s, 2H), 5.09 (s, 2H), 3.81 (s, 6H), 3.68 (s, 3H), 2.20 (s, 3H);

^{13}C NMR (100.6 MHz, $CDCl_3$) δ 169.8 (C), 153.9 (C), 139.3 (C), 143.9 (C), 139.3 (C), 136.8 (C), 132 (C), 129.4 (CH), 128.9 (CH), 126.2 (CH), 123.3 (CH), 119 (C), 102.8 (CH), 61.1 (CH_3), 56.5 (CH_3), 40.0 (CH_2), 22.8 (CH_3);

MS (EI, 70 eV): *m/z* (%)= 277 (100), 199 (37), 378 (38), 77 (33), 230 (M^+, 0.5).

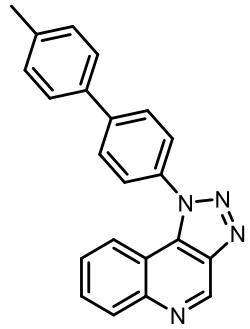

1-(4'-methyl-[1,1'-biphenyl]-4-yl)-1H-[1,2,3]triazolo[4,5-c]quinoline, 3.6a:

86% yield; pale yellow solid; mp: 197-199 °C; R_f = 0.24 (n-hexane-EtOAc, 75:25); IR (neat): 3055, 1504, 992, 801, 767 cm^{-1};

^{1}H NMR (400.13 MHz) ($CDCl_3$): δ 9.51 (s, 1H), 8.23 (d, *J* = 8.3 Hz, 1H), 7.83 – 7.73 (m, 3H), 7.72 – 7.66 (m, 1H), 7.65 – 7.61 (m, 2H), 7.53 (*d*, *J* = 8.3 Hz, 2H), 7.42 (m, 1H), 7.24 (d, *J* = 8.3 Hz, 2H), 2.35 (s, 3H);

^{13}C NMR (100.6 MHz) ($CDCl_3$): δ 145.9 (C), 145.0 (CH), 143.7 (C), 140.5 (C), 138.4 (C), 136.4 (C), 135.7 (C), 133.7 (C), 130.8 (CH), 130.06 (CH), 129.96 (CH), 129.87 (CH), 128.3 (CH), 127.4 (CH), 127.1 (CH), 126.7 (CH), 126.5 (C), 121.9 (CH), 115.3 (C), 21.2 (CH_3);

MS (EI, 70 eV): *m/z* (%)= 207 (100), 73 (82), 281 (49), 336 (M^+, 4).

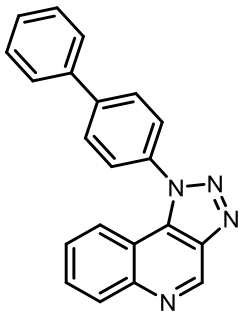

1-([1,1'-biphenyl]-4-yl)-1H-[1,2,3]triazolo[4,5-c]quinoline, 3.6b:

95% yield; grey solid; mp: 178-180 °C; R_f = 0.22 (n-hexane-EtOAc, 75:25); IR (neat): 3063, 1527, 1087, 984, 758 cm^{-1};

^{1}H NMR (400.13 MHz) ($CDCl_3$): δ 9.49 (s, 1H), 8.21 (d, *J* = 8.2, 1H), 7.80 (d, *J* = 8.2 Hz, 2H), 7.85 (d, *J* = 8.3, 1H), 7.80 – 7.70 (m, 5H), 7.57 – 7.48 (m, 3H), 7.48 – 7.39 (m, 1H);

^{13}C NMR (100.6 MHz) ($CDCl_3$): δ 145.9 (C), 144.9 (CH), 143.8 (C), 140.5 (C), 139.3 (C), 136.0 (C), 133.7 (C), 130.8 (CH), 130.06 (CH), 129.98 (CH), 129.1 (CH), 128.6 (CH), 128.4 (CH), 127.4 (CH), 127.3 (CH), 126.8 (CH), 121.8 (CH), 115.2 (C);

MS (EI, 70 eV): *m/z* (%)= 207 (100), 73 (73), 281 (55), 322 (M^+, 1).

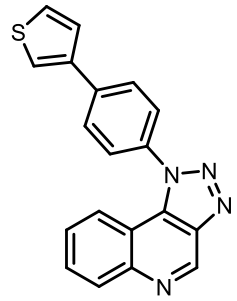

1-(4-(thiophen-3-yl)phenyl)-1H-[1,2,3]triazolo[4,5-c]quinoline 3.6c:

85% yield; pale yellow solid; mp: 230-232 °C; R_f = 0.18 (n-hexane-EtOAc, 70:30); IR (neat): 2967, 1535, 1267, 762, 567 cm^{-1};

^{1}H NMR (400.13 MHz) ($CDCl_3$): δ 9.58 (s, 1H), 8.29 (d, J_1 = 8.3 Hz, 1H), 7.95 – 7.88 (m, 2H), 7.82 (dd, J_1 = 8.4 Hz, J_2 = 1.4 Hz, 1H), 7.82 – 7.75 (m, 1H), 7.73 – 7.68 (m, 2H), 7.64 (q, J_1 = 1.4 Hz, 1H), 7.51 – 7.46 (m, 3H);

^{13}C NMR (100.6 MHz) ($CDCl_3$): δ 145.9 (C), 144.9 (CH), 140.50 (C), 140.47 (C), 138.3 (C), 135.6 (C), 133.7 (C), 130.8 (CH), 129.9 (CH), 127.7 (CH), 127.4 (CH), 127.1 (CH), 126.9 (CH), 126.1 (CH), 122.0 (CH), 121.8 (CH), 115.2 (C);

MS (EI, 70 eV): *m/z* (%)= 207 (100), 73 (83), 281 (34), 328 (M^+, 2).

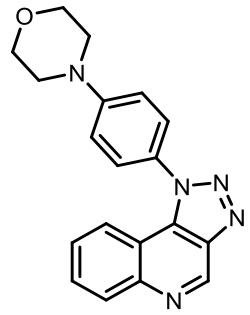

4-(4-(1H-[1,2,3]triazolo[4,5-c]quinolin-1-yl)phenyl)morpholine, 3.7:

52% yield; grey solid; mp: 245-247 °C; R_f = 0.21 (n-hexane-EtOAc, 50:50); IR (neat): 2841, 1527, 1110, 754, 560 cm^{-1};

^{1}H NMR (400.13 MHz) ($CDCl_3$): δ 9.58 (s, 1H), 8.29 (d, *J* = 8.2 Hz, 1H), 7.75 – 7.66 (m, 2H), 7.49 – 7.38 (m, 3H), 7.09 – 7.02 (m, 2H), 3.86 (t, *J* = 4.8 Hz, 4H), 3.28 (t, *J* = 4.9 Hz, 4H);

^{13}C NMR (100.6 MHz) ($CDCl_3$): δ 152.6 (C), 145.9 (C), 145.0 (CH), 140.3 (C), 133.9 (C), 130.7 (CH), 129.7 (CH), 128.1 (C), 127.4 (CH), 127.3 (CH), 121.8 (CH), 115.5 (CH), 66.7 (CH_2), 48.4 (CH_2);

MS (EI, 70 eV): *m/z* (%)= 300 (100), 115 (55), 207 (36), 331 (M^+, 4).

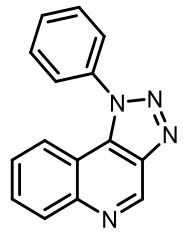

1-phenyl-1H-[1,2,3]triazolo[4,5-c]quinoline, 3.8:

71% yield; pale yellow solid; mp: 153-155 °C; R_f = 0.16 (n-hexane-EtOAc, 60:40); IR (neat): 3073, 1504, 992, 767, 696 cm^{-1};

^{1}H NMR (400.13 MHz) ($CDCl_3$): δ 9.60 (s, 1H), 8.32 (d, *J* = 8.1 Hz, 1H), 7.77 (ddd, J_1 = 7.7 Hz, J_2 = 1.4 Hz, 1H), 7.74 – 7.66 (m, 6H), 7.48 (ddd, J_1 = 7.7 Hz, J_2 = 1.4 Hz, 1H);

^{13}C NMR (100.6 MHz) ($CDCl_3$): δ 146.0 (C), 144.9 (CH), 140.5 (C), 137.1 (C), 133.7 (C), 130.8 (CH), 130.1 (CH), 129.9 (CH), 127.4 (CH), 126.5 (CH), 121.7 (CH), 115.2 (C);

MS (EI, 70 eV): *m/z* (%)= 218 (100), 190 (37), 77 (40), 246 (M^+, 15).

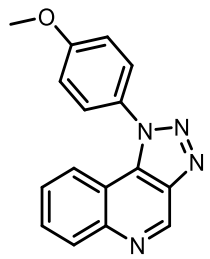

1-(4-methoxyphenyl)-1H-[1,2,3]triazolo[4,5-c]quinoline, 3.9:

78% yield; brown solid; mp: 174-176 °C; R_f = 0.22 (n-hexane-EtOAc, 70:30); IR (neat): 2922, 1522, 1253, 843, 760 cm^{-1};

^{1}H NMR (400.13 MHz) ($CDCl_3$): δ 9.58 (s, 1H), 8.29 (d, *J* = 8.8 Hz, 1H), 7.73 – 7.63 (m, 2H), 7.53 – 7.46 (m, 2H), 7.44 – 7.38 (m, 1H), 7.14 – 7.08 (m, 2H), 3.96 (*s*, 3H);

^{13}C NMR (100.6 MHz) ($CDCl_3$): δ 161.3 (C), 145.9 (C), 145.0 (CH), 140.3 (C), 134.0 (C), 130.7 (CH), 129.8 (CH), 129.7 (C), 127.9 (CH), 127.4 (CH), 121.7 (CH), 115.4 (C), 115.1 (CH), 55.8 (CH_3);

MS (EI, 70 eV): *m/z* (%)= 205 (100), 233 (75), 151 (16), 276 (M^+, 10).

11.2 General procedures and Characterization of Chapter 4

GENERAL INFORMATION

Reagents and methods

All of the commercially available reagents, catalysts, bases and solvents were used as purchased, without further purification. Starting materials and reaction products were purified by flash chromatography using SiO_2 as stationary phase, eluting with *n*-hexane/ethyl acetate (EtOAc) mixtures. ^{1}H NMR (400.13 MHz), ^{13}C NMR (100.6 MHz), and ^{19}F spectra (376.5 MHz) were recorded with a Bruker Avance 400 spectrometer. Splitting patterns are designed as s (singlet), d (doublet), t (triplet), dt (doublets of triplets), td (triplet of doublets), triplets of triplets (tt), q (quartet), m (multiplet), or bs (broad singlet). IR spectra were recorded with a PerkinElmer SpectrumOne FT-ATR spectrophotometer. Melting points were determined with a Büchi B-545 apparatus and are uncorrected.

Synthetic procedures

Typical procedure for the preparation of 7,10-dihydropyrrolo[3,2,1-ij][1,2,3]triazolo[4,5-c]quinoline 4.2a-4.2n

1-benzyl-1H-[1,2,3]triazolo[4,5-c]quinoline 3.3**a**-3.3n were prepared according to the sequence outlined in Scheme 1.

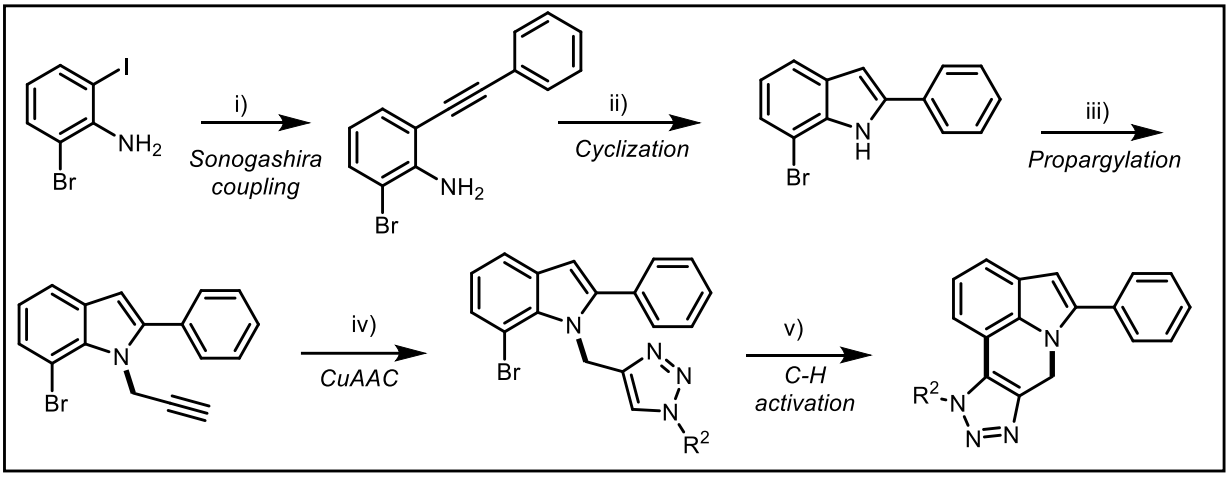

Scheme 1

STEP 1*: *Synthesis of 2-bromo-6-(phenylethynyl)aniline

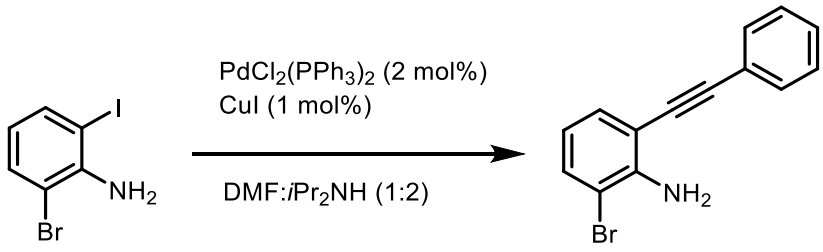

Step 1

An oven-dried 50 mL two-necked round-bottom flask, equipped with a magnetic stirrer, was added DMF and *i*Pr_2NH in a 1:2 ratio (24 mL) under an argon atmosphere. Subsequently, $PdCl_2(PPh_3)_2$ (2 mol%, 60 mg,) and CuI (1 mol%, 32 mg) were added and stirred for 10 minutes. To the solution, 1-bromo-2-iodoaniline (1 equiv., 10.20 mmol) was added, followed by 2-ethynylbenzene (1.1 equiv., 11.22 mmol). The reaction mixture was stirred at room temperature for 6 hours, with progress monitored by TLC using *n*-hexane/EtOAc (80/20) as the eluent. Upon completion of the reaction, the mixture was diluted with Et_2O (50 mL) and sequentially washed with saturated solutions of NH_4Cl, $NaHCO_3$, and brine. The organic phase was then dried over

Na_2SO_4, filtered, and concentrated under reduced pressure. The crude product was purified by flash column chromatography on silica gel using n-hexane/EtOAc (90/10) as the eluent (R_f = 0.20). This yielded 2.32 g of 2-bromo-6-(phenylethynyl)aniline with an 86% yield.

STEP 2*: *Synthesis of 7-bromo-2-phenyl-1H-indole

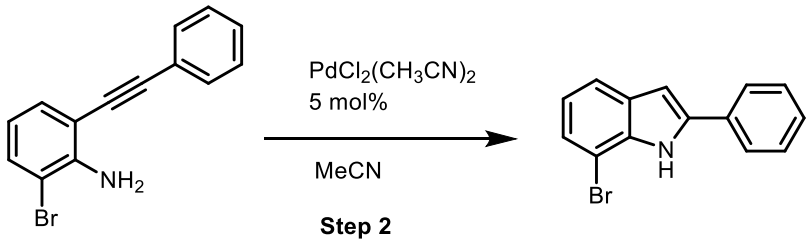

Step 2

An oven-dried 50 mL two-necked round-bottom flask, equipped with a magnetic stirrer, was added $PdCl_2(CH_3CN)_2$ 5 mol% to anhydrous MeCN under argon and stirred until complete dissolution. Subsequently, 2-bromo-6-(phenylethynyl)aniline (2.0 g, 7.35 mmol) was added and The reaction mixture was heated to reflux at 80 °C for 12 hours until the disappearance of the starting material, monitoring the progress of the reaction by HPLC (chromatographic conditions: RP18 5µm column, mobile phase MeCN/H_2O 70/30). After the completion of the reaction, the mixture was cooled to room temperature and the MeCN was removed under reduced pressure. The crude mixture was then purified by flash column chromatography on silica gel (n-hexane/EtOAc, 95/5, R_f=0.22), obtained 1.69 g of 7-bromo-2-phenyl-1H-indole with 82% yield.

STEP 3*: *Synthesis of 7-bromo-2-phenyl-1-(prop-2-yn-1-yl)-1H-indole

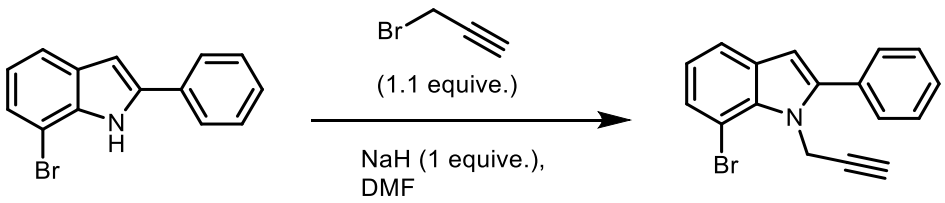

Step 3

In a 50 mL two-necked flask equipped with a magnetic stirrer, 5 mL of *n*-hexane and NaH (60% in mineral oil, 1 equive., 5.53 mmol) were added under an inert argon atmosphere and stirred for 10 minutes. Subsequently, stirring was stopped to allow the removal of the hexane containing the dissolved mineral oil using a Pasteur pipette. After the activation of sodium hydride, anhydrous DMF (10 mL) was added at 0°C, followed by dropwise addition of 7-bromo-2-phenyl-1H-indole (1 equive., 5.53 mmol), previously dissolved in 2 mL of anhydrous DMF. Propargyl

bromide (80% in toluene, 1.2 equive., 6.63 mmol) was added dropwise to the solution at 0 ^{o}C. After the addition of propargyl bromide, the reaction was brought to room temperature and stirred for 3 hours until the complete consumption of the starting material 2-(2-bromophenyl)-1H-indole (3), monitored the reaction progress using TLC (*n*-hexane/EtOAc, 80/20) as the eluent. Quench the reaction reaction with 15 mL of water under 0 ^{o}C. Subsequently, the reaction mixture was diluted with Et_2O, and the combined organic phase was washed with a 5% $KHSO_4$ solution and brine, dried over Na_2SO_4, and concentrated under reduced pressure. The residue was then purified by flash column chromatography on silica gel using *n*-hexane and EtOAc (95/5, R_f=0.21) as the eluent, obtained 1.45 g of 7-bromo-2-phenyl-1-(prop-2-yn-1-yl)-1H-indole with 87% yield.

STEP 4*: *Synthesis of 7-bromo-1-((1-(4-chlorophenyl)-1H-1,2,3-triazol-4-yl)methyl)-2-phenyl-1H-indole (4.1)

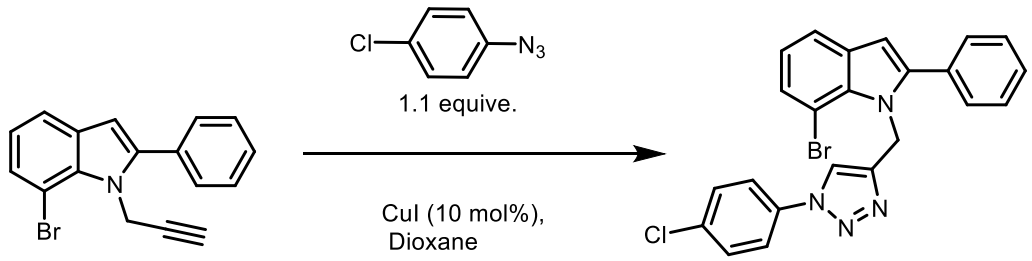

Step 4

In a 50 mL Carousel reactor equipped with a magnetic stirrer, 7-bromo-2-phenyl-1-(prop-2-yn-1-yl)-1H-indole (1 mmol, 1 equive.) was dissolved in 1,4-dioxane (2 mL). To the solution CuI (0.2 mmol, 20 mol% were added and 4-chlorophenylazide (1.1 mmol, 1.1 equive.). The reaction mixture was stirred at 50 °C for 12 hours. The progress of the reaction was monitored by TLC (n-hexane/EtOAc 70/30), the mixture was concentrated under reduced pressure and the crude product was purified by flash chromatography (silica gel, n-hexane/EtOAc 70/30, R_f = 0.22), Obtained of 7-bromo-1-((1-(4-chlorophenyl)-1H-1,2,3-triazol-4-yl)methyl)-2-phenyl-1H-indole (4.1) with 92% yield.

STEP 5*: *Synthesis of 5-(4-chlorophenyl)-5,8-dihydrobenzo[3,4][1,2,3]triazolo[4',5':5,6] azepino[1,2-a]indole (4.2)

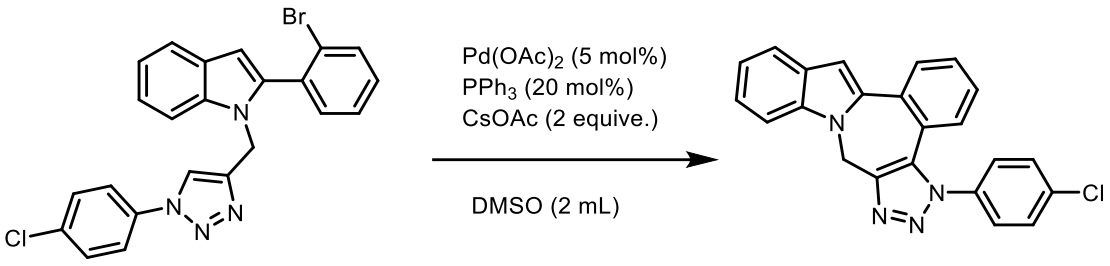

Step 5

In a 50 mL Carousel reactor equipped with a magnetic stirrer, $Pd(OAc)_2$ (5 mol%, 0.05 mmol) and PPh_3 (20 mol%, 0.2 mmol) were dissolved in anhydrous DMSO (2 mL) under argon atmosphere at room temperature. 7-bromo-1-((1-(4-chlorophenyl)-1H-1,2,3-triazol-4-yl)methyl)-2-phenyl-1H-indole (4.1) (1.00 mmol, 1 equive.) and CsOAc (2.00 mmol, 2 equiv.) was added to the solution. The reaction mixture was stirred at 120 °C under an inert atmosphere, the reaction progress was monitored by TLC (n-hexane/EtOAc, 80/20). The reaction mixture was then diluted with Et_2O (50 mL) and washed with brine, then dried over Na_2SO_4, filtered, and concentrated under reduced pressure. The residue obtained was then purified by flash chromatography using n-hexane and EtOAc 70/30, R_f = 0.19, as the eluent, obtained 5-(4-chlorophenyl)-5,8-dihydrobenzo[3,4][1,2,3]triazolo[4',5':5,6] azepino[1,2-a]indole (4.2) with 92% yield.

Typical procedure for the preparation of azides

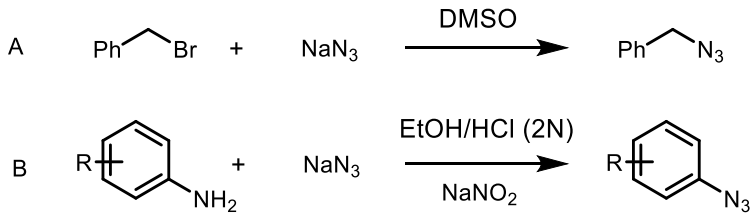

Scheme 3

Procedure for A

To a stirred solution of NaN_3 (1.1 mmol) in DMSO (2 mL) was added benzyl bromide (1 mmol). The reaction mixture was stirred at RT overnight. Then the reaction mixture was diluted with water (5 mL) and extracted with ether (3×5 mL) and washed by brine, dried over Na_2SO_4 and concentrated under vacuum to give the products in quantitative yields. It was used directly without further purification.

Procedure for B

The aniline derivative (1 mmol) was suspended in hydrochloric acid (17%) at room temperature and then ethanol was added until a clear solution was obtained. The solution was cooled to 0 °C and $NaNO_2$ (1.5 eq.) was added in small portions. After stirring at 0 °C for 15-30 min. NaN_3 (1.5 eq.) was slowly added and the mixture was stirred for additional 2 h at room temperature. The reaction mixture was extracted with diethyl ether and the combined organic fractions were washed with saturated $NaHCO_3$-solution and with brine, dried over Na_2SO_4 and concentrated under pressure and the desired azides were obtained without further purification.

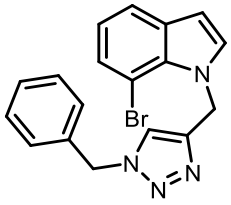

1-((1-benzyl-1H-1,2,3-triazol-4-yl)methyl)-7-bromo-1H-indole 4.1a:

89% yield; white solid; mp: 120-122 °C; Rf = 0.21 (n-hexane/EtOAc 85/15);

^{1}H NMR (400.13 MHz) ($CDCl_3$): δ 7.65 (s, 1H), 7.59 (d, *J* = 7.7 Hz, 1H), 7.53 (d, *J* = 8.8 Hz, 2H), 7.39 (d, *J* = 7.7 Hz, 1H), 7.32 (d, *J* = 3.2 Hz, 1H), 7.02 – 6.91 (m, 4H), 6.57 (d, *J* = 3.2 Hz, 1H), 6.01 (s, 2H), 4.25 (s, 2H);

^{13}C NMR (100.6 MHz) ($CDCl_3$): δ 159.8 (C), 146.2 (C), 132.1 (C), 132.1 (C), 131.1 (CH), 130.3 (C), 127.2 (CH), 122.2 (CH), 121.0 (CH), 120.7 (CH), 120.4 (CH), 114.7 (CH), 103.4 (C), 103.0 (CH), 43.6 (CH_2), 40.1 (CH_2);

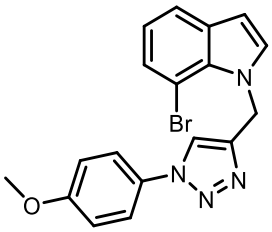

7-bromo-1-((1-(4-methoxyphenyl)-1H-1,2,3-triazol-4-yl)methyl)-1H-indole 4.1b:

82% yield; white solid; mp: 120-122 °C; Rf = 0.19 (n-hexane/EtOAc 85/15);

^{1}H NMR (400.13 MHz) ($CDCl_3$): δ 7.65 (s, 1H), 7.59 (d, *J* = 7.7 Hz, 1H), 7.53 (d, *J* = 8.8 Hz, 2H), 7.39 (d, *J* = 7.7 Hz, 1H), 7.32 (d, *J* = 3.2 Hz, 1H), 7.02 – 6.91 (m, 3H), 6.57 (d, *J* = 3.2 Hz, 1H), 6.01 (s, 2H), 3.84 (s, 3H);

^{13}C NMR (100.6 MHz) ($CDCl_3$): δ 159.8 (C), 146.2 (C), 132.1 (C), 132.1 (C), 131.1 (CH), 130.3 (C), 127.2 (CH), 122.2 (CH), 121.0 (CH), 120.7 (CH), 120.4 (CH), 114.7 (CH), 103.4 (C), 103.0 (CH), 55.6 (CH_3), 43.6 (CH_2);

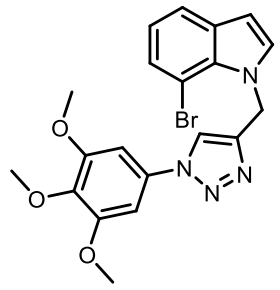

7-bromo-1-((1-(3,4,5-trimethoxyphenyl)-1H-1,2,3-triazol-4-yl)methyl)-1H-indole 4.1c:

94% yield; white solid; mp: 120-122 °C; Rf = 0.20 (n-hexane/EtOAc 60/40);

^{1}H NMR (400.13 MHz) ($CDCl_3$): δ 7.59 (s, 1H), 7.50 (d, *J* = 7.8 Hz, 1H), 7.30 (d, *J* = 7.8 Hz, 1H), 7.22 (d, *J* = 3.3 Hz, 1H), 6.88 (t, *J* = 7.7 Hz, 1H), 6.76 (s, 2H), 6.49 (d, *J* = 3.3 Hz, 1H), 5.93 (s, 2H), 3.80 (s, 6H), 3.78 (s, 3H);

^{13}C NMR (100.6 MHz) ($CDCl_3$): δ 153.9 (C), 146.4 (C), 138.4 (C), 132.8 (C), 132.09 (C), 132.06 (C), 131.0 (CH), 127.3 (CH), 121.0 (CH), 120.7 (CH), 120.6 (CH), 103.5 (C), 103.0 (CH), 98.7 (CH), 61.0 (CH_3), 56.5 (CH_3), 43.5 (CH_2);

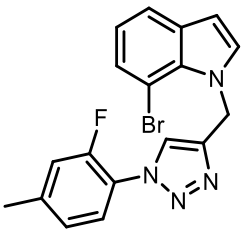

7-bromo-1-((1-(2-fluoro-4-methylphenyl)-1H-1,2,3-triazol-4-yl)methyl)-1H-indole 4.1d:

82% yield; white solid; mp: 120-122 °C; Rf = 0.22 (n-hexane/EtOAc 70/30);

^{1}H NMR (400.13 MHz) ($CDCl_3$): δ 7.71 (d, *J* = 2.6 Hz, 1H), 7.62 (t, *J* = 15.9, 7.9 Hz, 1H), 7.47 (dd, *J* = 7.8, 0.6 Hz, 1H), 7.28 (d, *J* = 7.6 Hz, 1H), 7.23 (d, *J* = 3.3 Hz, 1H), 6.96 (t, *J* = 21.8 Hz, 2H), 6.86 (t, *J* = 15.6 Hz, 1H), 6.47 (d, *J* = 3.3 Hz, 1H), 5.92 (s, 2H), 2.30 (s, 3H);

^{13}C NMR (100.6 MHz) ($CDCl_3$): δ 154.4 (C), 151.9 (C), 145.8 (C), 141.35 (C), 141.27 (C), 132.14 (C), 132.09 (C), 131.1 (CH), 127.2 (CH), 125.8 (CH), 125.7 (CH), 124.6 (CH), 123.34 (CH), 123.27 (CH), 122.7 (C), 122.6 (C), 121.0 (CH), 120.7 (CH), 117.3 (CH), 117.1 (CH), 103.5 (C), 103.0 (CH), 43.4 (CH_2), 21.18 (CH_3), 21.17 (CH_3); ^{19}F NMR (376 MHz, $CDCl_3$) δ -124.39;

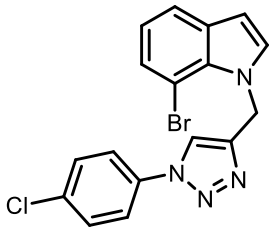

7-bromo-1-((1-(4-chlorophenyl)-1H-1,2,3-triazol-4-yl)methyl)-1H-indole 4.1e:

84% yield; white solid; mp: 120-122 °C; Rf = 0.20 (n-hexane/EtOAc 95/5);

^{1}H NMR (400.13 MHz) ($CDCl_3$): δ 7.58 (s, 1H), 7.51 – 7.47 (m, 3H), 7.35 – 7.32 (m, 2H), 7.28 (dd, *J* = 7.6, 1.1 Hz, 1H), 7.20 (d, *J* = 3.4 Hz, 1H), 6.87 (t, *J* = 7.6 Hz, 1H), 6.47 (d, *J* = 3.4 Hz, 1H), 5.91 (s, 2H);

^{13}C NMR (100.6 MHz) ($CDCl_3$): δ 146.8 (C), 134.6 (C), 132.1 (C), 132.0 (C), 131.0 (CH), 129.9 (CH), 127.3 (CH), 121.7 (CH), 121.1 (CH), 120.8 (CH), 120.1 (CH), 103.4 (C), 103.1 (CH), 43.5 (CH_2);

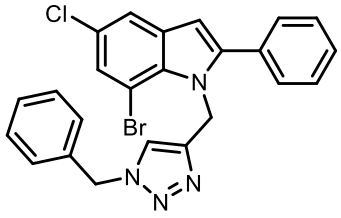

1-((1-benzyl-1H-1,2,3-triazol-4-yl)methyl)-7-bromo-5-chloro-2-phenyl-1H-indole 4.1f:

88% yield; white solid; mp: 120-122 °C; Rf = 0.23 (n-hexane/EtOAc 90/10);

^{1}H NMR (400.13 MHz) ($CDCl_3$): δ 7.54 (d, *J* = 2.0 Hz, 1H), 7.48 – 7.30 (m, 9H), 7.16 – 7.07 (m, 2H), 6.86 (s, 1H), 6.51 (s, 1H), 5.43 (s, 2H);

^{13}C NMR (100.6 MHz) ($CDCl_3$): δ 146.9 (C), 145.5 (C), 134.8 (C), 132.7 (C), 132.3 (C), 131.5 (C), 129.6 (CH), 129.0 (CH), 128.9 (CH), 128.7 (CH), 128.6 (CH), 127.5 (CH), 127.0 (CH), 126.2 (C), 121.5 (CH), 119.4 (CH), 104.3 (C), 103.8 (CH), 54.0 (CH_2), 41.7 (CH_2);

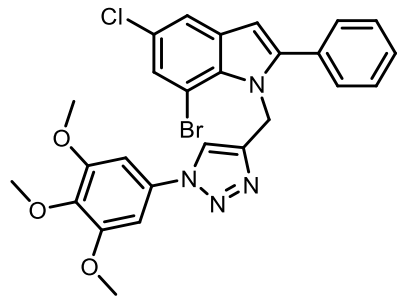

7-bromo-5-chloro-2-phenyl-1-((1-(3,4,5-trimethoxyphenyl)-1H-1,2,3-triazol-4-yl)methyl)-1H-indole 4.1g:

79% yield; white solid; mp: 120-122 °C; Rf = 0.18 (n-hexane/EtOAc 70/30);

^{1}H NMR (400.13 MHz) ($CDCl_3$): δ 7.65 (d, *J* = 8.3 Hz, 1H), 7.54 (d, *J* = 2.0 Hz, 1H), 7.38 – 7.19 (m, 4H), 7.10 (dd, *J* = 8.7, 2.1 Hz, 1H), 6.70 (s, 2H), 6.47 (s, 1H), 5.28 (s, 2H), 3.78 (s, 6H), 3.77 (s, 3H);

^{13}C NMR (100.6 MHz) ($CDCl_3$): δ 153.8 (C), 145.0 (C), 139.9 (C), 138.4 (C), 134.9 (C), 133.3 (CH), 133.1 (C), 132.7 (CH), 132.6 (C), 130.8 (CH), 129.0 (C), 127.5 (CH), 126.1 (C), 124.9 (C), 122.6 (CH), 120.3 (CH), 120.2 (CH), 111.4 (CH), 103.6 (CH), 98.5 (CH), 61.0 (CH_3), 56.5 (CH_3), 40.1 (CH_2);

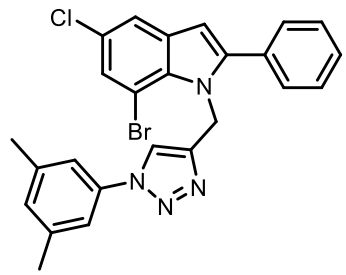

7-bromo-5-chloro-1-((1-(3,5-dimethylphenyl)-1H-1,2,3-triazol-4-yl)methyl)-2-phenyl-1H-indole 4.1h:

90% yield; white solid; mp: 120-122 °C; Rf = 0.21 (n-hexane/EtOAc 85/15);

^{1}H NMR (400.13 MHz) ($CDCl_3$): δ 7.48 (d, *J* = 2.0 Hz, 1H), 7.36 (s, 5H), 7.30 (d, *J* = 2.0 Hz, 1H), 7.24 (s, 1H), 7.13 (s, 2H), 6.93 (s, 1H), 6.48 (s, 1H), 5.83 (s, 2H), 2.27 (s, 6H);

^{13}C NMR (100.6 MHz) ($CDCl_3$): δ 147.0 (C), 145.4 (C), 139.7 (C), 136.7 (C), 132.7 (C), 132.3 (C), 131.5 (C), 130.4 (CH), 129.7 (CH), 129.0 (CH), 128.8 (CH), 127.1 (CH), 126.3 (C), 119.6 (CH), 119.5 (CH), 118.2 (CH), 104.3 (C), 103.9 (CH), 41.7 (CH_2), 21.3 (CH_3);

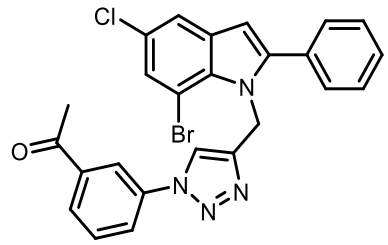

1-(3-(4-((7-bromo-5-chloro-2-phenyl-1H-indol-1-yl)methyl)-1H-1,2,3-triazol-1-yl)phenyl)ethan-1-one 4.1i:

83% yield; white solid; mp: 120-122 °C; Rf = 0.23 (n-hexane/EtOAc 60/40);

^{1}H NMR (400.13 MHz) ($CDCl_3$): δ 8.16 (s, 1H), 7.98 (d, *J* = 7.8 Hz, 1H), 7.90 (d, *J* = 7.8 Hz, 1H), 7.71 – 7.18 (m, 9H), 6.60 (s, 1H), 5.96 (s, 2H), 2.66 (s, 3H);

^{13}C NMR (100.6 MHz) ($CDCl_3$): δ 196.7 (C), 147.4 (C), 145.4 (C), 138.4 (C), 137.3 (C), 132.7 (C), 132.4 (C), 131.5 (C), 130.2 (CH), 129.7 (CH), 129.1 (CH), 128.8 (CH), 128.4 (CH), 127.2 (CH), 126.4 (C), 124.7 (CH), 119.6 (CH), 119.5 (CH), 119.4 (CH), 104.3 (C), 104.1 (CH), 41.5 (CH3), 26.8 (CH2);

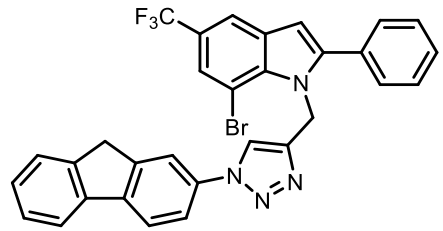

1-((1-(9H-fluoren-2-yl)-1H-1,2,3-triazol-4-yl)methyl)-7-bromo-2-phenyl-5-(trifluoromethyl)-1H-indole 4.1j:

71% yield; white solid; mp: 120-122 °C; Rf = 0.23 (n-hexane/EtOAc 80/20);

^{1}H NMR (400.13 MHz) ($CDCl_3$): δ 7.81 (s, 1H), 7.71 (t, *J* = 16.8 Hz, 3H), 7.56 (s, 1H), 7.49 (t, *J* = 18.3 Hz, 2H), 7.39 (s, 5H), 7.36 (s, 1H), 7.29 (m, 2H), 6.64 (s, 1H), 5.91 (s, 2H), 3.86 (s, 2H);

^{13}C NMR (100.6 MHz) ($CDCl_3$): δ 145.7 (C), 144.7 (C), 143.5 (C), 140.3 (C), 131.1 (C), 129.8 (CH), 129.2 (CH), 128.9 (CH), 127.5 (CH), 127.1 (CH), 125.2 (CH), 120.6 (CH), 120.3 (CH), 119.7 (CH), 119.4 (CH), 117.5 (CH), 105.0 (CH), 104.2 (C), 41.7 (CH_2), 37.0 (CH_2); ^{19}F NMR (376 MHz, $CDCl_3$) δ -60.77;

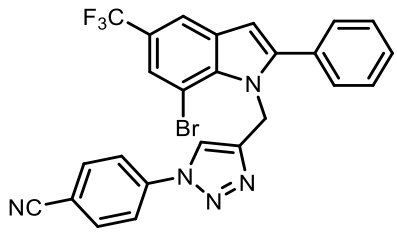

4-(4-((7-bromo-2-phenyl-5-(trifluoromethyl)-1H-indol-1-yl)methyl)-1H-1,2,3-triazol-1-yl)benzonitrile 4.1k:

74% yield; white solid; mp: 120-122 °C; Rf = 0.21 (n-hexane/EtOAc 70/30);

^{1}H NMR (400.13 MHz) ($CDCl_3$): δ 7.68 (s, 1H), 7.42 (s, 1H), 7.36 (d, *J* = 8.6 Hz, 2H), 7.30 – 7.19 (m, 7H), 7.16 (s, 1H), 6.51 (s, 1H), 5.79 (s, 2H);

^{13}C NMR (100.6 MHz) ($CDCl_3$): δ 147.2 (C), 145.6 (C), 135.3 (C), 134.6 (C), 131.2 (C), 131.1 (C), 129.88 (CH), 129.76 (CH), 129.2 (CH), 128.9 (CH), 124.2 (CH), 121.6 (CH), 119.4 (CH), 117.8 (CH), 105.1 (CH), 41.6 (CH_2);

^{19}F NMR (376 MHz, $CDCl_3$) δ -60.71;

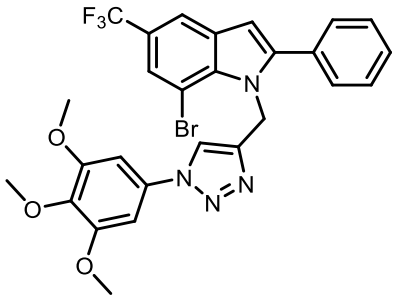

7-bromo-2-phenyl-5-(trifluoromethyl)-1-((1-(3,4,5-trimethoxyphenyl)-1H-1,2,3-triazol-4-yl)methyl)-1H-indole 4.1l:

93% yield; white solid; mp: 120-122 °C; Rf = 0.23 (n-hexane/EtOAc 70/30);

^{1}H NMR (400.13 MHz) ($CDCl_3$): δ 7.91 (s, 1H), 7.65 (s, 1H), 7.49 (s, 5H), 7.40 (s, 1H), 6.83 (s, 2H), 6.74 (s, 1H), 5.99 (s, 2H), 3.91 (s, 6H), 3.87 (s, 3H);

^{13}C NMR (100.6 MHz) ($CDCl_3$): δ 153.9 (C), 142.6 (C), 140.1 (C), 139.7 (C), 136.0 (C), 131.9 (C), 131.1 (C), 129.1 (CH), 128.6 (CH), 128.4 (C), 125.8 (C), 123.0 (C), 122.7 (C), 119.7 (CH), 111.0 (CH), 109.9 (C), 104.2 (CH), 103.2 (CH), 61.2 (CH_3), 56.4 (CH3), 44.2 (CH_2);

^{19}F NMR (376 MHz, $CDCl_3$) δ -60.79

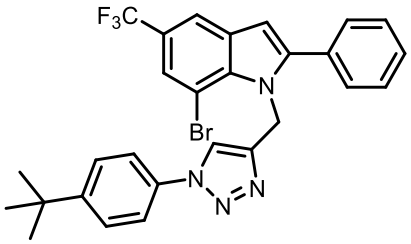

7-bromo-1-((1-(4-(tert-butyl)phenyl)-1H-1,2,3-triazol-4-yl)methyl)-2-phenyl-5-(trifluoromethyl)-1H-indole 4.1m:

89% yield; white solid; mp: 120-122 °C; Rf = 0.20 (n-hexane/EtOAc 90/10);

^{1}H NMR (400.13 MHz) ($CDCl_3$): δ 7.91 (s, 1H), 7.65 (s, 1H), 7.65 (s, 1H), 7.54 (s, 1H), 7.50 – 7.46 (m, 7H), 7.37 (s, 1H), 6.73 (s, 1H), 6.00 (s, 2H), 1.35 (s, 9H);

^{13}C NMR (100.6 MHz) ($CDCl_3$): δ 152.2 (C), 146.7 (C), 145.7 (C), 134.4 (C), 131.3 (C), 131.1 (C), 129.8 (CH), 129.2 (CH), 128.8 (CH), 128.3 (C), 126.6 (CH), 124.1 (CH), 120.1 (CH), 119.5 (CH), 117.7 (CH), 105.0 (CH), 104.2 (C), 41.6 (CH_2), 34.8 (C), 31.2 (CH_3);

^{19}F NMR (376 MHz, $CDCl_3$) δ -60.81;

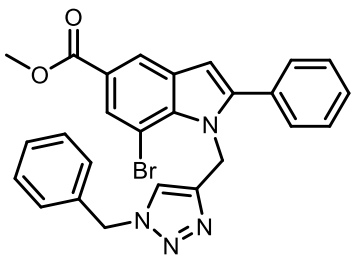

methyl1-((1-benzyl-1H-1,2,3-triazol-4-yl)methyl)-7-bromo-2-phenyl-1H-indole-5 carboxylate 4.1n:

90% yield; white solid; mp: 120-122 °C; Rf = 0.22 (n-hexane/EtOAc 70/30);

^{1}H NMR (400.13 MHz) ($CDCl_3$): δ 8.20 (s, 1H), 7.98 (s, 1H), 7.47 – 7.21 (m, 8H), 7.02 – 7.01 (m, 2H), 6.80 (s, 1H), 6.57 (s, 1H), 5.80 (s, 2H), 5.33 (s, 2H), 3.86 (s, 3H);

^{13}C NMR (100.6 MHz) ($CDCl_3$): δ 166.8 (C), 146.8 (C), 145.2 (C), 136.2 (C), 134.7 (C), 131.4 (C), 131.1 (C), 129.7 (CH), 129.0 (CH), 128.7 (CH), 128.6 (CH), 128.5 (CH), 127.5 (CH), 123.7 (C), 122.6 (CH), 121.6 (CH), 105.3 (CH), 103.7 (C), 54.0 (CH_2), 52.1 (CH_3), 41.7 (CH_2);

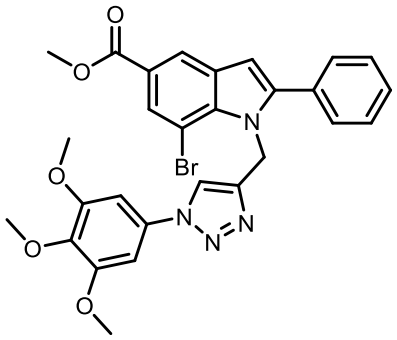

methyl 7-bromo-2-phenyl-1-((1-(3,4,5-trimethoxyphenyl)-1H-1,2,3-triazol-4-yl)methyl)-1H-indole-5-carboxylate 4.1o:

84% yield; white solid; mp: 120-122 °C; Rf = 0.24 (n-hexane/EtOAc 50/50);

^{1}H NMR (400.13 MHz) (DMSO): δ 8.52 (s, 1H), 8.31 (s, 1H), 7.90 (s, 1H), 7.61 – 7.47 (m, 5H), 7.11 (s, 2H), 6.91 (s, 1H), 5.87 (s, 2H), 3.86 (s, 3H), 3.83 (s, 6H), 3.68 (s, 3H);

^{13}C NMR (100.6 MHz) (DMSO): δ 166.2 (C), 154.2 (C), 145.7 (C), 137.9 (C), 136.2 (C), 132.7 (C), 131.6 (C), 131.4 (C), 130.0 (CH), 129.5 (CH), 129.2 (CH), 127.7 (CH), 123.4 (C), 122.7 (CH), 121.4 (CH), 105.7 (CH), 103.8 (C), 98.5 (CH), 60.7 (CH_3), 56.8 (CH_3), 52.6 (CH_3) 41.7 (CH_2);

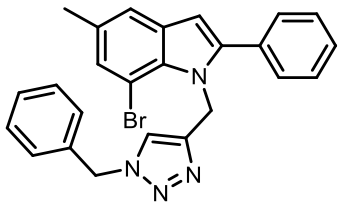

1-((1-benzyl-1H-1,2,3-triazol-4-yl)methyl)-7-bromo-5-methyl-2-phenyl-1H-indole 4.1p:

74% yield; white solid; mp: 120-122 °C; Rf = 0.18 (n-hexane/EtOAc 90/10);

^{1}H NMR (400.13 MHz) ($CDCl_3$): δ 7.32 – 7.15 (m, 9H), 7.11 (s, 1H), 7.05 – 6.94 (m, 2H), 6.76 (s, 1H), 6.38 (d, *J* = 1.5 Hz, 1H), 5.75 (s, 2H), 5.31 (s, 2H), 2.31 (s, 3H)

^{13}C NMR (100.6 MHz) ($CDCl_3$): δ 147.2 (C), 145.6 (C), 135.3 (C), 134.6 (C), 131.2 (C), 131.1 (C), 129.88 (CH), 129.76 (CH), 129.2 (CH), 128.9 (CH), 124.2 (CH), 121.6 (CH), 119.4 (CH), 117.8 (CH), 105.1 (CH), 41.6 (CH_2);

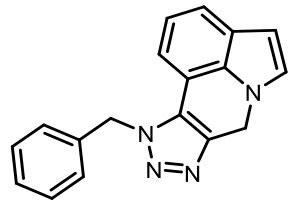

10-benzyl-7,10-dihydropyrrolo[3,2,1-ij][1,2,3]triazolo[4,5-c]quinoline 4.2a:

80% yield; white solid; mp: 120-122 °C; Rf = 0.20 (n-hexane/EtOAc 80/20);

^{1}H NMR (400.13 MHz) ($CDCl_3$): δ 7.37 (dd, *J* = 8.0, 1.0 Hz, 1H), 7.29 – 7.09 (m, 5H), 7.03 (d, *J* = 3.1 Hz, 1H), 6.94 – 6.87 (m, 1H), 6.83 (t, *J* = 7.6 Hz, 1H), 6.43 (d, *J* = 3.2 Hz, 1H), 5.73 (s, 2H), 5.57 (s, 2H);

^{13}C NMR (100.6 MHz) ($CDCl_3$): δ 139.9 (C), 134.6 (C), 133.4 (C), 129.1 (CH), 128.3 (CH), 126.8 (CH), 126.6 (CH), 125.9 (C), 122.4 (CH), 120.1 (CH), 114.5 (CH), 109.1 (C), 103.6 (CH), 53.3 (CH_2), 44.6 (CH_2);

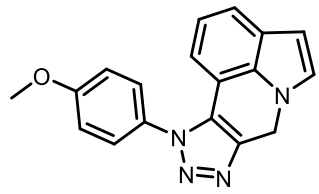

10-(4-methoxyphenyl)-7,10-dihydropyrrolo[3,2,1-ij][1,2,3]triazolo[4,5-c]quinoline 4.2b:

81% yield; white solid; mp: 120-122 °C; Rf = 0.18 (n-hexane/EtOAc 70/30);

^{1}H NMR (400.13 MHz) ($CDCl_3$):δ 7.45 (d, *J* = 8.8 Hz, 2H), 7.40 (d, *J* = 8.3 Hz, 1H), 7.11 (d, *J* = 3.1 Hz, 1H), 7.03 (d, *J* = 8.8 Hz, 2H), 6.76 (t, *J* = 15.6, 7.7 Hz, 1H), 6.59 (d, *J* = 7.3 Hz, 1H), 6.48 (d, *J* = 3.1 Hz, 1H), 5.69 (s, 2H), 3.85 (s, 3H);

^{13}C NMR (100.6 MHz) ($CDCl_3$): δ 161.0 (C), 139.1 (C), 133.6 (C), 129.9 (C), 129.8 (C), 127.4 (CH), 126.8 (CH), 125.9 (C), 122.5 (CH), 119.9 (CH), 114.8 (CH), 114.2 (CH), 109.3 (C), 103.7 (CH), 55.7 (CH_3), 44.6 (CH_2);

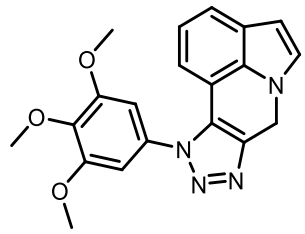

10-(3,4,5-trimethoxyphenyl)-7,10-dihydropyrrolo[3,2,1-ij][1,2,3]triazolo[4,5-c]quinoline 4.2c:

91% yield; white solid; mp: 120-122 °C; Rf = 0.22 (n-hexane/EtOAc 50/50);

^{1}H NMR (400.13 MHz) ($CDCl_3$): δ 7.40 (d, *J* = 7.9 Hz, 1H), 7.08 (d, *J* = 2.9 Hz, 1H), 6.84 – 6.72 (m, 4H), 6.46 (d, *J* = 2.9 Hz, 1H), 5.63 (s, 2H), 3.88 (s, 3H), 3.77 (s, 6H);

^{13}C NMR (100.6 MHz) ($CDCl_3$): δ 153.8 (C), 139.4 (C), 139.2 (C), 133.6 (C), 132.3 (C), 129.8 (C), 126.9 (CH), 126.0 (C), 122.7 (CH), 120.0 (CH), 114.4 (CH), 109.1 (C), 103.7 (CH), 103.6 (CH), 61.2 (CH_3), 56.5 (CH_3), 44.5 (CH_2);

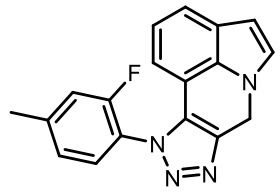

10-(2-fluoro-4-methylphenyl)-7,10-dihydropyrrolo[3,2,1-ij][1,2,3]triazolo[4,5-c]quinoline 4.2d:

70% yield; white solid; mp: 120-122 °C; Rf = 0.18 (n-hexane/EtOAc 60/40);

^{1}H NMR (400.13 MHz) ($CDCl_3$): δ 7.46 – 7.36 (m, 2H), 7.21 – 7.10 (m, 3H), 6.77 (t, *J* = 7.7 Hz, 1H), 6.52 – 6.45 (m, 2H), 5.73 (s, 2H), 2.46 (s, 3H);

^{13}C NMR (100.6 MHz) ($CDCl_3$): δ 157.8 (C), 155.3 (C), 143.8 (C), 143.7 (C), 138.9 (C), 133.6 (C), 131.0 (C), 128.3 (CH), 126.8 (CH), 125.89 (C), 125.81 (CH), 125.77 (CH), 122.7 (CH), 122.5 (C), 122.3 (C), 120.1 (CH), 117.7 (CH), 117.5 (CH), 113.7 (CH), 109.0 (C), 103.7 (CH), 44.6 (CH_2), 21.6 (CH_3);

^{19}F NMR (376 MHz, $CDCl_3$) δ -121.3;

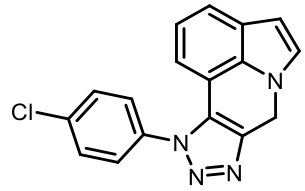

10-(4-chlorophenyl)-7,10-dihydropyrrolo[3,2,1-ij][1,2,3]triazolo[4,5-c]quinoline 4.2e:

85% yield; white solid; mp: 120-122 °C; Rf = 0.24 (n-hexane/EtOAc 60/40);

^{1}H NMR (400.13 MHz) ($CDCl_3$): δ 7.59 – 7.47 (m, 4H), 7.41 (d, *J* = 8.1 Hz, 1H), 7.11 (d, *J* = 3.2 Hz, 1H), 6.77 (t, *J* = 7.7 Hz, 2H), 6.61 (d, *J* = 7.3 Hz, 1H), 6.49 (d, *J* = 3.2 Hz, 1H), 5.68 (s, 2H);

^{13}C NMR (100.6 MHz) ($CDCl_3$): δ 139.4 (C), 136.5 (C), 135.5 (C), 133.6 (C), 130.0 (C), 129.8 (CH), 127.3 (CH), 126.9 (CH), 126.1 (C), 122.9 (CH), 120.0 (CH), 114.2 (CH), 108.9 (C), 103.8 (CH), 44.5 (CH_2);

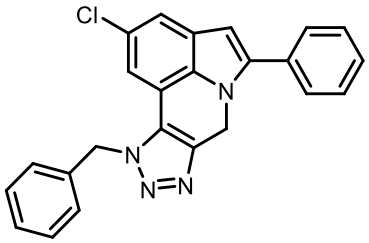

10-benzyl-2-chloro-5-phenyl-7,10-dihydropyrrolo[3,2,1-ij][1,2,3]triazolo[4,5-c]quinoline 4.2f:

77% yield; white solid; mp: 120-122 °C; Rf = 0.20 (n-hexane/EtOAc 80/20);

^{1}H NMR (400.13 MHz) ($CDCl_3$): δ 7.63 – 7.21 (m, 9H), 7.17 (d, *J* = 7.3 Hz, 2H), 6.91 (s, 1H), 6.43 (s, 1H), 5.77 (s, 2H), 5.54 (s, 2H);

^{13}C NMR (100.6 MHz) ($CDCl_3$): δ 142.0 (C), 140.8 (C), 134.2 (C), 132.9 (C), 131.4 (C), 129.2 (CH), 129.0 (CH), 128.8 (CH), 128.6 (CH), 128.5 (CH), 128.0 (C), 127.1 (C), 126.8 (CH), 126.0 (C), 121.0 (CH), 114.7 (CH), 110.3 (C), 102.9 (CH), 53.5 (CH_2), 44.2 (CH_2);

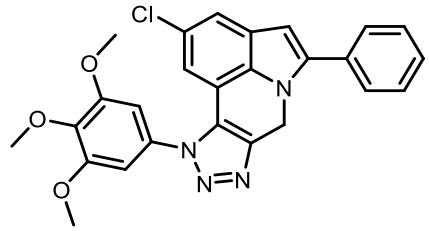

2-chloro-5-phenyl-10-(3,4,5-trimethoxyphenyl)-7,10-dihydropyrrolo[3,2,1-ij][1,2,3] triazolo[4,5-c]quinoline 4.2g:

74% yield; white solid; mp: 120-122 °C; Rf = 0.18 (n-hexane/EtOAc 75/25);

^{1}H NMR (400.13 MHz) ($CDCl_3$): δ 7.53 – 7.48 (m, 2H), 7.46 (t, *J* = 14.8, 7.5 Hz, 2H), 7.42 – 7.39 (m, 2H), 6.83 (s, 1H), 6.80 (s, 2H), 6.49 (s, 1H), 5.62 (s, 2H), 3.91 (s, 3H), 3.85 (s, 6H);

^{13}C NMR (100.6 MHz) ($CDCl_3$): δ 161.4 (C), 153.9 (C), 142.1 (C), 139.6 (C), 133.3 (C), 131.9 (C), 131.4 (C), 129.0 (CH), 128.9 (CH), 128.6 (CH), 127.3 (C), 125.9 (C), 121.3 (CH), 114.7 (CH), 110.4 (C), 103.3 (C), 103.0 (CH), 61.2 (CH_3), 56.5 (CH3), 44.1 (CH_2);

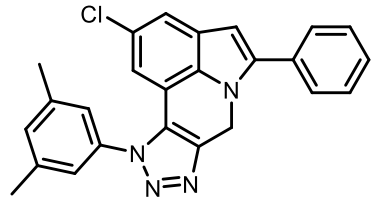

2-chloro-10-(3,5-dimethylphenyl)-5-phenyl-7,10-dihydropyrrolo[3,2,1-ij][1,2,3]triazolo [4,5-c]quinoline 4.2h:

87% yield; white solid; mp: 120-122 °C; Rf = 0.21 (n-hexane/EtOAc 95/5);

^{1}H NMR (400.13 MHz) ($CDCl_3$): δ 7.53 – 7.47 (m, 2H), 7.47 – 7.41 (m, 2H), 7.41 – 7.38 (m, 1H), 7.37 (d, *J* = 1.8 Hz, 1H), 7.19 (s, 1H), 7.15 (s, 2H), 6.65 (d, *J* = 1.8 Hz, 1H), 6.46 (s, 1H), 5.60 (s, 2H), 2.38 (s, 6H);

^{13}C NMR (100.6 MHz) ($CDCl_3$): δ 142.0 (C), 140.0 (C), 139.8 (C), 136.4 (C), 133.2 (C), 132.2 (CH), 131.4 (C), 129.0 (CH), 128.9 (C), 128.8 (CH), 128.6 (CH), 128.4 (C), 127.2 (C), 125.8 (C), 123.4 (CH), 121.1 (CH), 114.6 (CH), 110.5 (C), 103.0 (CH), 44.1 (CH_2), 21.3 (CH_3);

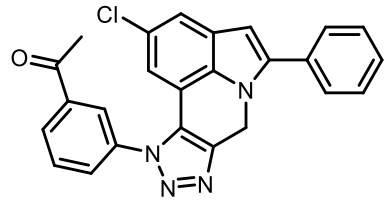

1-(3-(4-((7-bromo-5-chloro-2-phenyl-1H-indol-1-yl)methyl)-1H-1,2,3-triazol-1-yl)phenyl) ethan-1-one 4.2i:

52% yield; white solid; mp: 120-122 °C; Rf = 0.22 (n-hexane/EtOAc 70/30);

^{1}H NMR (400.13 MHz) ($CDCl_3$): δ 8.24 – 8.14 (m, 2H), 7.89 – 7.62 (m, 2H), 7.58 – 7.34 (m, 5H), 6.56 (s, 1H), 6.48 (s, 1H), 5.62 (s, 2H), 5.21 (s, 1H), 2.61 (s, 3H);

^{13}C NMR (100.6 MHz) ($CDCl_3$): δ 196.2 (C), 142.2 (C), 140.4 (C), 138.6 (C), 137.0 (C), 133.2 (C), 131.3 (C), 130.3 (CH), 130.2 (CH), 129.9 (CH), 129.0 (CH), 128.9 (CH), 128.7 (C), 128.59 (C), 128.56 (CH), 127.4 (C), 125.8 (C), 125.7 (CH), 121.6 (CH), 114.3 (CH), 110.1 (C), 103.1 (CH), 44.1 (CH_2), 26.8 (CH_3);

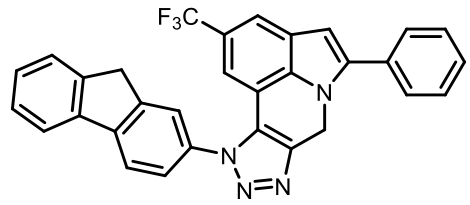

10-(9H-fluoren-2-yl)-5-phenyl-2-(trifluoromethyl)-7,10-dihydropyrrolo[3,2,1-ij][1,2,3] triazolo[4,5-c]quinoline 4.2j:

76% yield; white solid; mp: 120-122 °C; Rf = 0.18 (n-hexane/EtOAc 80/20);

^{1}H NMR (400.13 MHz) ($CDCl_3$): δ 7.94 (d, J = 8.1 Hz, 1H), 7.84 (d, *J* = 7.5 Hz, 1H), 7.77 – 7.70 (m, 2H), 7.61 – 7.30 (m, 9H), 7.00 (d, *J* = 1.5 Hz, 1H), 6.62 (s, 1H), 5.67 (s, 2H), 3.97 (s, 2H);

^{13}C NMR (100.6 MHz) ($CDCl_3$): δ 144.8 (C), 144.1 (C), 143.8 (C), 142.6 (C), 140.2 (C), 140.1 (C), 134.7 (C), 131.2 (C), 129.1 (CH), 128.65 (CH), 128.56 (C), 127.9 (CH), 127.2 (CH), 125.7 (C), 125.3 (CH), 124.4 (CH), 122.5 (CH), 120.72 (CH), 120.69 (CH), 119.71 (CH), 119.66 (CH), 110.84 (CH), 110.81 (CH), 110.0 (C), 104.2 (CH), 44.2 (CH_2), 37.0 (C);

^{19}F NMR (376 MHz, $CDCl_3$) δ -60.92;

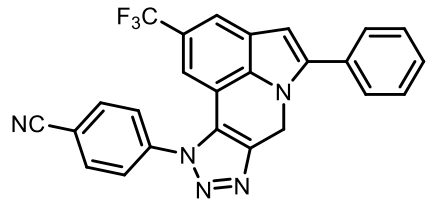

4-(5-phenyl-2-(trifluoromethyl)pyrrolo[3,2,1-ij][1,2,3]triazolo[4,5-c]quinolin-10(7H)-yl)benzonitrile 4.2k:

80% yield; white solid; mp: 120-122 °C; Rf = 0.19 (n-hexane/EtOAc 85/15);

^{1}H NMR (400.13 MHz) ($CDCl_3$): δ 7.84 (s, 1H), 7.67 – 7.52 (m, 9H), 7.00 (s, 1H), 6.73 (s, 1H), 5.75 (s, 2H);

^{13}C NMR (100.6 MHz) ($CDCl_3$): δ 161.4 (C), 142.7 (C), 140.3 (C), 136.9 (C), 135.9 (C), 135.0 (C), 131.1 (C), 130.1 (CH), 129.14 (CH), 129.10 (CH), 128.63 (CH), 128.60 (C), 127.0 (CH), 125.8 (C), 122.8 (C), 119.9 (CH), 110.5 (CH), 109.6 (C), 104.3 (CH), 44.2 (CH2), 38.1 (CF3);

^{19}F NMR (376 MHz, $CDCl_3$) δ -60.93;

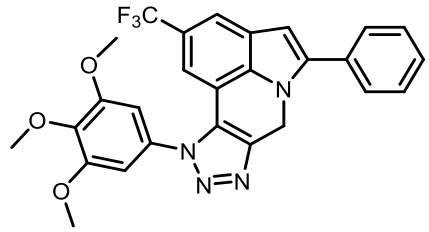

5-phenyl-2-(trifluoromethyl)-10-(3,4,5-trimethoxyphenyl)-7,10-dihydropyrrolo[3,2,1ij][1,2,3]triazolo[4,5-c]quinoline 4.2l:

99% yield; white solid; mp: 120-122 °C; Rf = 0.20 (n-hexane/EtOAc 70/30);

^{1}H NMR (400.13 MHz) ($CDCl_3$): δ 7.91 (s, 1H), 7.65 (s, 1H), 7.49 (s, 4H), 7.40 (s, 1H), 6.83 (s, 2H), 6.74 (s, 1H), 5.99 (s, 2H), 3.91 (s, 6H), 3.87 (s, 3H);

^{13}C NMR (100.6 MHz) ($CDCl_3$): δ 161.4 (C), 153.9 (C), 146.8 (C), 145.7 (C), 138.5 (C), 135.2 (C), 132.7 (C), 131.3 (C), 131.1 (C), 129.8 (CH), 129.2 (CH), 128.8 (CH), 124.1 (CH), 119.8 (CH), 117.7 (CH), 105.0 (CH), 104.2 (C), 98.5 (CH), 61.1 (CH3), 56.5 (CH_3), 41.6 (CH_2), 38.6 (C);

^{19}F NMR (376 MHz, $CDCl_3$) δ -60.78;

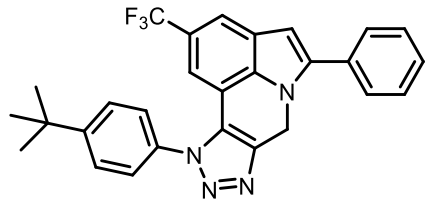

10-(4-(tert-butyl)phenyl)-5-phenyl-2-(trifluoromethyl)-7,10-dihydropyrrolo[3,2,1-ij][1,2,3]triazolo[4,5-c]quinoline 4.2m:

84% yield; white solid; mp: 120-122 °C; Rf = 0.19 (n-hexane/EtOAc 95/5);

^{1}H NMR (400.13 MHz) ($CDCl_3$): δ 7.91 (s, 1H), 7.65 (s, 1H), 7.61 – 7.44 (m, 8H), 7.37 (s, 1H), 6.73 (s, 1H), 6.00 (s, 2H), 1.35 (s, 9H);

^{13}C NMR (100.6 MHz) ($CDCl_3$): δ 154.4 (C), 142.5 (C), 139.9 (C), 136.0 (C), 133.8 (C), 131.2 (C), 129.07 (CH), 129.05 (C), 128.7 (CH), 128.6 (C), 126.8 (C), 125.7 (C), 125.5 (CH), 123.0 (C), 122.7 (C), 120.5 (C), 119.64 (CH), 119.59 (CH), 110.6 (CH), 109.8 (C), 104.1 (CH), 44.2 (CH_2), 35.1 (C), 31.3 (CH_3);

^{19}F NMR (376 MHz, $CDCl_3$) δ -60.93;

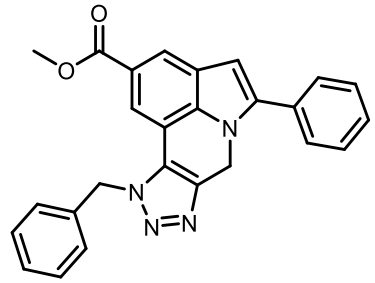

methyl 10-benzyl-5-phenyl-7,10-dihydropyrrolo[3,2,1-ij][1,2,3]triazolo[4,5-c]quinoline-2-carboxylate 4.2n:

78% yield; white solid; mp: 120-122 °C; Rf = 0.20 (n-hexane/EtOAc 70/30);

^{1}H NMR (400.13 MHz) ($CDCl_3$): δ 8.15 (s, 1H), 7.74 (s, 1H), 7.50 – 7.34 (m, 5H), 7.33 – 7.16 (m, 5H), 6.56 (s, 1H), 5.83 (s, 2H), 5.56 (s, 2H), 3.85 (s, 3H);

^{13}C NMR (100.6 MHz) ($CDCl_3$): δ 167.4 (C), 142.1 (C), 140.4 (C), 136.8 (C), 134.3 (C), 131.3 (C), 129.1 (CH), 129.0 (CH), 128.9 (CH), 128.6 (CH), 128.5 (CH), 128.2 (C), 127.1 (CH), 125.7 (C), 124.8 (C), 122.6 (C), 115.5 (C), 109.1 (C), 104.6 (CH), 53.6 (CH_2), 52.1 (CH_3), 44.3 (CH_2);

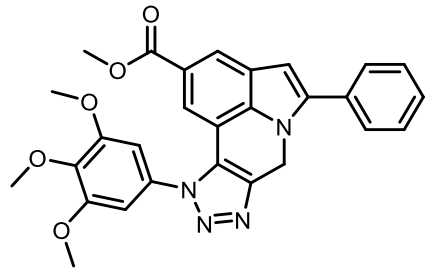

methyl 5-phenyl-10-(3,4,5-trimethoxyphenyl)-7,10-dihydropyrrolo[3,2,1-ij][1,2,3]triazolo [4,5-c]quinoline-2-carboxylate 4.2o:

68% yield; white solid; mp: 120-122 °C; Rf = 0.24 (n-hexane/EtOAc 50/50);

^{1}H NMR (400.13 MHz) ($CDCl_3$): δ 8.34 (d, *J* = 1.6 Hz, 1H), 8.12 (d, J = 1.6 Hz, 1H), 7.48 (s, 4H), 7.42 (s, 1H), 6.83 (s, 2H), 6.74 (s, 1H), 5.99 (s, 2H), 3.96 (s, 3H), 3.90 (s, 6H), 3.87 (s, 3H);

^{13}C NMR (100.6 MHz) ($CDCl_3$): δ 166.7 (C), 153.9 (C), 147.0 (C), 145.2 (C), 138.4 (C), 136.2 (C), 132.7 (C), 131.4 (C), 131.2 (C), 129.8 (CH), 129.1 (CH), 128.9 (C), 128.8 (CH), 128.6 (CH), 123.8 (C), 122.7 (CH), 119.9 (CH), 105.5 (CH), 103.7 (C), 98.5 (CH), 61.1 (CH_3), 56.5 (CH_3), 52.2 (CH_3), 41.6 (CH_2);

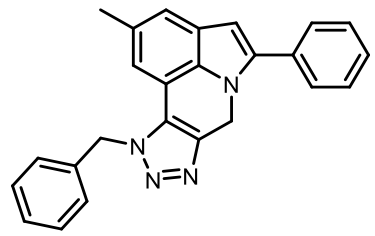

10-benzyl-2-methyl-5-phenyl-7,10-dihydropyrrolo[3,2,1-ij][1,2,3]triazolo[4,5-c]quinoline 4.2p:

67% yield; white solid; mp: 120-122 °C; Rf = 0.19 (n-hexane/EtOAc 60/40);

^{1}H NMR (400.13 MHz) ($CDCl_3$): δ 7.65 – 7.42 (m, 5H), 7.42 – 7.22 (m, 6H), 6.91 (s, 1H), 6.53 (s, 1H), 5.91 (s, 2H), 5.67 (s, 2H), 2.37 (s, 3H);

^{13}C NMR (100.6 MHz) ($CDCl_3$): δ 159.8 (C), 146.2 (C), 132.1 (C), 132.1 (C), 131.1 (CH), 130.3 (C), 127.2 (CH), 122.2 (CH), 121.0 (CH), 120.7 (CH), 120.4 (CH), 114.7 (CH), 103.4 (C), 103.0 (CH), 55.6 (CH_3), 43.6 (CH_2);

11.3 General procedures and Characterization of Chapter 5

SYNTHETIC PROCEDURES

Typical procedure for the preparation of [1,2,3]triazolo[4',5':5,6]azepino[1,2-a]indole 5.6a-5.6p

1-benzyl-1H-[1,2,3]triazolo[4,5-c]quinoline 3**a**-3n were prepared according to the sequence outlined in Scheme 1.

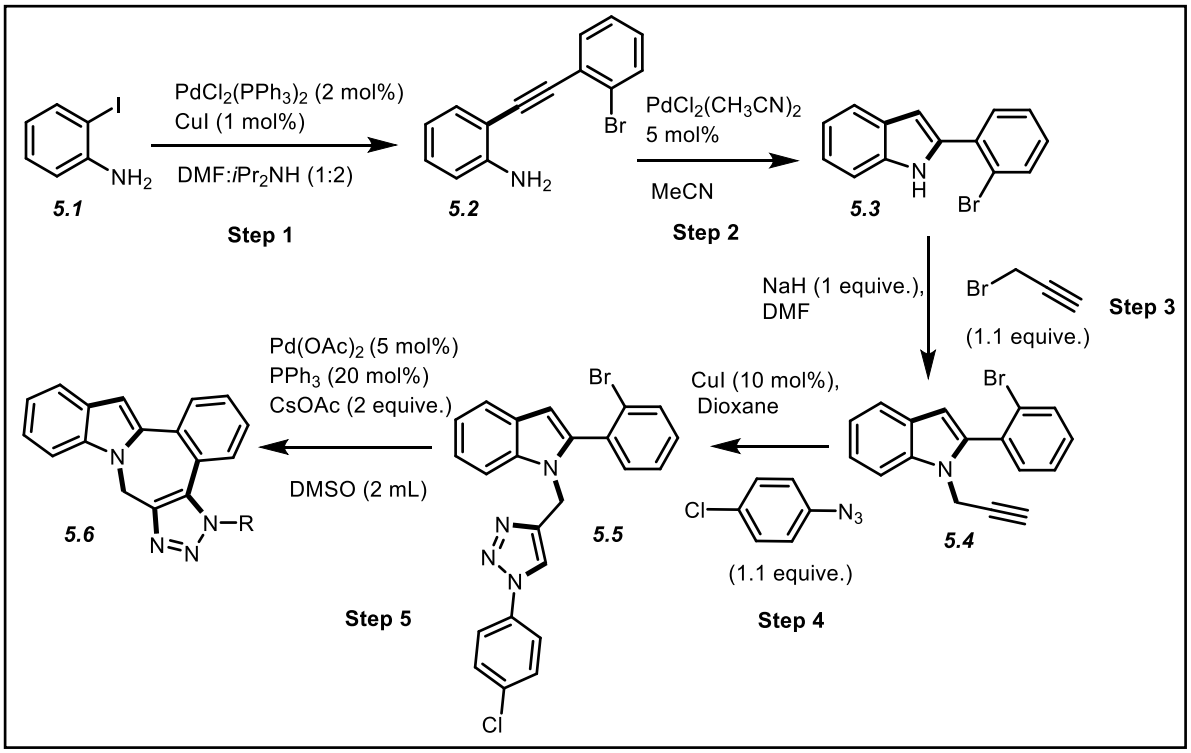

Scheme 1

STEP 1*: *Synthesis of 2-((2-bromophenyl)ethynyl)aniline (5.2)

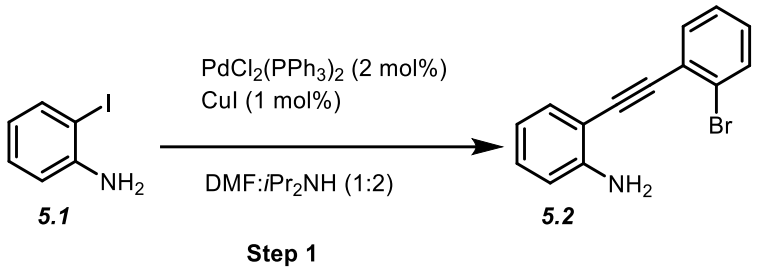

An oven-dried 50 mL two-necked round-bottom flask, equipped with a magnetic stirrer, was added DMF and *i*Pr_2NH in a 1:2 ratio (24 mL) under an argon atmosphere. Subsequently, $PdCl_2(PPh_3)_2$ (2 mol%, 60 mg,) and CuI (1 mol%, 32 mg) were added and stirred for 10 minutes. To the solution, 1-bromo-2-iodobenzene (1 equiv., 10.20 mmol) was added, followed by 1-bromo-2-ethynylbenzene (1.1 equiv., 11.22 mmol). The reaction mixture was stirred at room temperature for 6 hours, with progress monitored by TLC using *n*-hexane/EtOAc (80/20) as the eluent. Upon completion of the reaction, the mixture was diluted with Et_2O (50 mL) and sequentially washed with saturated solutions of NH_4Cl, $NaHCO_3$, and brine. The organic phase was then dried over Na_2SO_4, filtered, and concentrated under reduced pressure. The crude product was purified by flash column chromatography on silica gel using n-hexane/EtOAc (90/10) as the eluent (R_f = 0.20). This yielded 2.32 g of 2-((2-bromophenyl)ethynyl)aniline (2) with an 83% yield.

STEP 2*: *Synthesis of 2-(2-bromophenyl)-1H-indole (5.3)

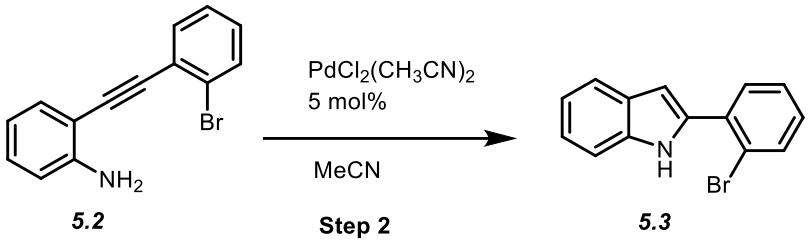

An oven-dried 50 mL two-necked round-bottom flask, equipped with a magnetic stirrer, was added $PdCl_2(CH_3CN)_2$ 5 mol% to anhydrous MeCN under argon and stirred until complete dissolution. Subsequently, 2-((2-bromophenyl)ethynyl)aniline (2) (2.0 g, 7.35 mmol) was added and The reaction mixture was heated to reflux at 80 °C for 12 hours until the disappearance of the starting material [2-((2-bromophenyl)ethynyl)aniline (2), monitoring the progress of the

reaction by HPLC (chromatographic conditions: RP18 5µm column, mobile phase MeCN/H_2O 70/30). After the completion of the reaction, the mixture was cooled to room temperature and the MeCN was removed under reduced pressure. The crude mixture was then purified by flash column chromatography on silica gel (n-hexane/EtOAc, 95/5, R_f=0.22), obtained 1.69 g of 2-(2-bromophenyl)-1H-indole (3) with 84% yield.

STEP 3*: *Synthesis of 2-(2-bromophenyl)-1-(prop-2-yn-1-yl)-1H-indole (5.4)

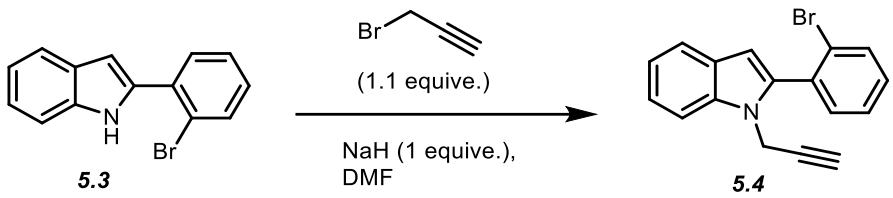

Step 3

In a 50 mL two-necked flask equipped with a magnetic stirrer, 5 mL of *n*-hexane and NaH (60% in mineral oil, 1 equive., 5.53 mmol) were added under an inert argon atmosphere and stirred for 10 minutes. Subsequently, stirring was stopped to allow the removal of the hexane containing the dissolved mineral oil using a Pasteur pipette. After the activation of sodium hydride, anhydrous DMF (10 mL) was added at 0°C, followed by dropwise addition of 2-(2-bromophenyl)-1H-indole (3) (1 equive., 5.53 mmol), previously dissolved in 2 mL of anhydrous DMF. Propargyl bromide (80% in toluene, 1.2 equive., 6.63 mmol) was added dropwise to the solution at 0 °C. After the addition of propargyl bromide, the reaction was brought to room temperature and stirred for 3 hours until the complete consumption of the starting material 2-(2-bromophenyl)-1H-indole (3), monitored the reaction progress using TLC (*n*-hexane/EtOAc, 80/20) as the eluent. Quench the reaction reaction with 15 mL of water under 0 °C. Subsequently, the reaction mixture was diluted with Et_2O, and the combined organic phase was washed with a 5% $KHSO_4$ solution and brine, dried over Na_2SO_4, and concentrated under reduced pressure. The residue was then purified by flash column chromatography on silica gel using *n*-hexane and EtOAc (95/5, R_f=0.21) as the eluent, obtained 1.45 g of 2-(2-bromophenyl)-1-(prop-2-yn-1-yl)-1H-indole (4) with 85% yield.

STEP 4*: *Synthesis of 2-(2-bromophenyl)-1-((1-(4-chlorophenyl)-1H-1,2,3-triazol-4-yl)methyl)-1H-indole (5.5a)

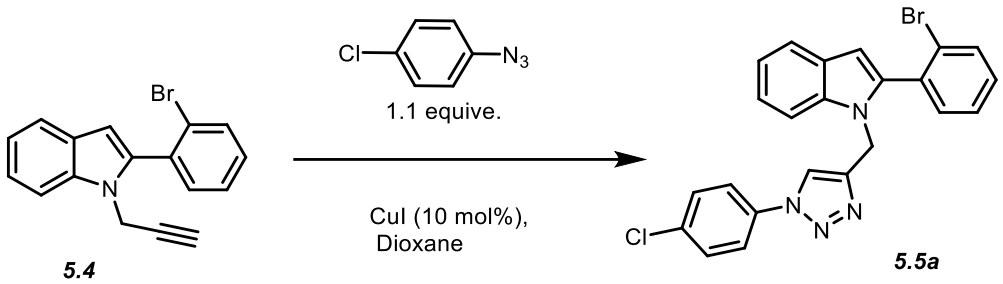

Step 4

In a 50 mL Carousel reactor equipped with a magnetic stirrer, 2-(2-bromophenyl)-1-(prop-2-yn-1-yl)-1H-indole 4 (1 mmol, 1 equive.) was dissolved in 1,4-dioxane (2 mL). To the solution were added CuI (0.2 mmol, 20 mol% and 4-chlorophenylazide (1.1 mmol, 1.1 equive.). The reaction mixture was stirred at 50 °C for 12 hours. The progress of the reaction was monitored by TLC (n-hexane/EtOAc 70/30), the mixture was concentrated under reduced pressure and the crude product was purified by flash chromatography (silica gel, n-hexane/EtOAc 70/30, R_f = 0.22), Obtained of 2-(2-bromophenyl)-1-((1-(4-chlorophenyl)-1H-1,2,3-triazol-4-yl)methyl)-1H-indole 5a with 86% yield.

STEP 4*: *Synthesis of 5-(4-chlorophenyl)-5,8-dihydrobenzo[3,4][1,2,3]triazolo[4',5':5,6] azepino[1,2-a]indole (5.6a)

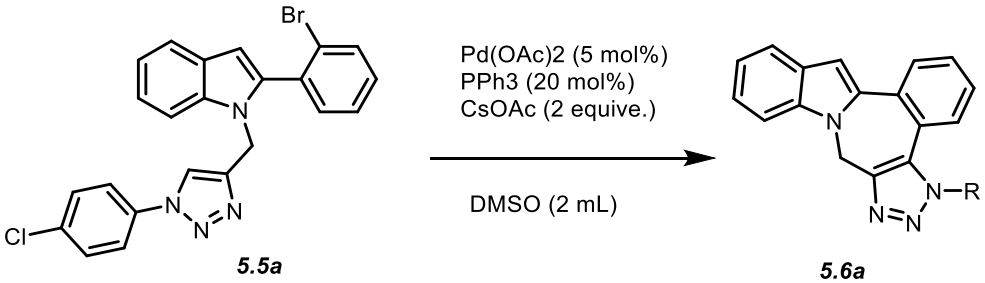

Step 5

In a 50 mL Carousel reactor equipped with a magnetic stirrer, Pd(OAc)2 (5 mol%, 0.05 mmol) and PPh3 (20 mol%, 0.2 mmol) were dissolved in anhydrous DMSO (2 mL) under argon atmosphere at room temperature. 2-(2-bromophenyl)-1-((1-(4-chlorophenyl)-1H-1,2,3-triazol-4-yl)methyl)-1H-indole (6a) (1.00 mmol, 1 equive.) and CsOAc (2.00 mmol, 2 equiv.) was added to the solution. The reaction mixture was stirred at 120 °C under an inert atmosphere, the reaction progress was monitored by TLC (n-hexane/EtOAc, 80/20). The reaction mixture was then diluted with Et2O (50 mL) and washed with brine, then dried over Na2SO4, filtered, and concentrated under reduced pressure. The residue obtained was then purified by flash chromatography using

n-hexane and EtOAc 70/30, R_f = 0.19, as the eluent, obtained 5-(4-chlorophenyl)-5,8-dihydrobenzo[3,4][1,2,3]triazolo[4',5':5,6] azepino[1,2-a]indole (6a) with 96 % yield.

with diethyl ether and dried over anhydrous Na2SO4, concentrated under vacuum and purified by flash column chromatography to give the N-(2-bromophenyl)-2,2,2-trifluoro-N-(prop-2-yn-1-yl)acetamide (90% yield).

Typical procedure for the preparation of azides

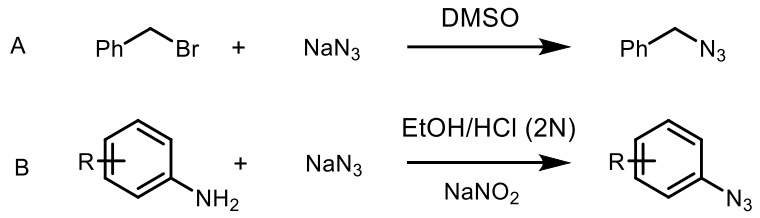

Scheme 3

Procedure for A

To a stirred solution of NaN_3 (1.1 mmol) in DMSO (2 mL) was added benzyl bromide (1 mmol). The reaction mixture was stirred at RT overnight. Then the reaction mixture was diluted with water (5 mL) and extracted with ether (3×5 mL) and washed by brine, dried over Na_2SO_4 and concentrated under vacuum to give the products in quantitative yields. It was used directly without further purification.

Procedure for B

The aniline derivative (1 mmol) was suspended in hydrochloric acid (17%) at room temperature and then ethanol was added until a clear solution was obtained. The solution was cooled to 0 °C and $NaNO_2$ (1.5 eq.) was added in small portions. After stirring at 0 °C for 15-30 min. NaN_3 (1.5 eq.) was slowly added and the mixture was stirred for additional 2 h at room temperature. The reaction mixture was extracted with diethyl ether and the combined organic fractions were washed with saturated $NaHCO_3$-solution and with brine, dried over Na_2SO_4 and concentrated under pressure and the desired azides were obtained without further purification.

Procedure for the synthesis of compounds (5.7a, 5.7b, 5.7c)

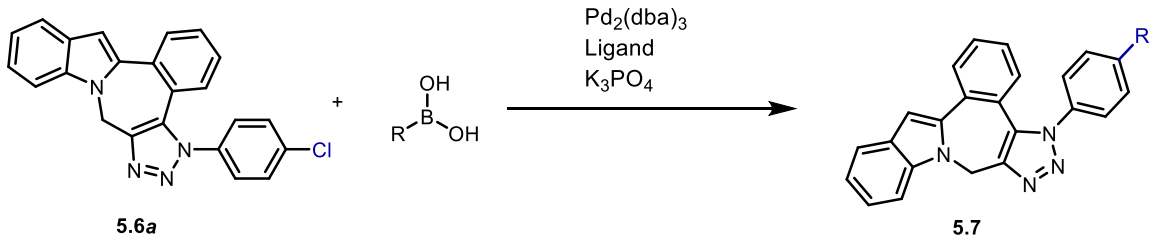

To a mixture of $Pd_2(dba)_3$ (2 mol%) and Xphos ligand (4 mol%) in dry dioxane (2.0 mL), compound 5.6a (70 mg, 0.25 mmol), boronic acid derivatives (1.5 equiv, 0.37 mmol) and K_3PO_4 (3.0 equiv, 0.75 mmol) were added. Then, the reaction mixture was stirred under argon at 100 ^oC. The reaction was monitored by TLC, concentrated under pressure. The mixture was purified with flash column chromatography (90:10 hexane and EtOAc) to give the pure products.

Procedure for the synthesis of compound 5.8

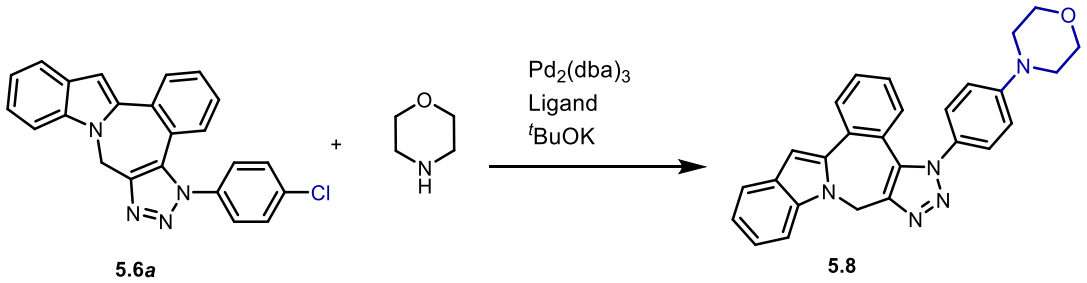

To a mixture of $Pd(OAc)_2$ (2.5 mol%) and Xphos ligand (5 mol%) in dry toluene (2.0 mL), compound 5.6a (70 mg, 0.25 mmol), morpholine (1.5 equiv, 0.37 mmol)and ^tBuOK (2.0 equiv, 0.5 mmol) were added. Then, the reaction mixture was stirred under argon at 100 ^oC. The reaction was monitored by TLC, concentrated under pressure. The mixture was purified with flash column chromatography (50:50 hexane and EtOAc) to give the pure products.

Characterization of starting material (5)

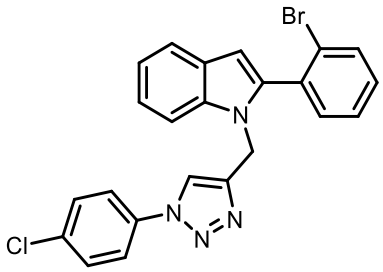

(5.5a) 2-(2-bromophenyl)-1-((1-(4-chlorophenyl)-1H-1,2,3-triazol-4-yl)methyl)-1H-indole:

Yellow solid; **Yield**: 86%; **M.P**: 78°C;

^{1}H NMR (400.13 MHz) ($CDCl_3$): δ 7.61 (dd, J_1= 14.80 Hz, J_2= 7.93 Hz, 2H), 7.44-7.40 (m, 2H), 7.37-7.31 (m, 5H), 7.28 (s, 1H), 7.25-7.21 (m, 1H), 7.18-7.14 (m, 1H), 7.11-7.07 (m, 1H), 6.53 (s,1H), 5.31 (s, 2H);

^{13}C NMR (100.6 MHz) ($CDCl_3$): δ 145.94 (C), 138.78 (C), 136.59 (C), 135.40 (C), 134.61 (C), 133.58 (C), 133.30 (CH), 132.90 (CH), 130.63 (CH), 129.94 (CH), 128.19 (C), 127.53 (CH), 125.16 (C), 122.50 (CH), 121.66 (CH), 121.11 (CH), 120.54 (CH), 119.89 (CH), 110.36 (CH), 104.15 (CH), 40.06 (CH_2).

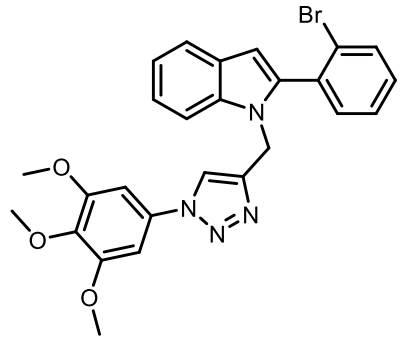

(**5.5b**) **2-(2-bromophenyl)-1-((1-(3,4,5-trimethoxyphenyl)-1H-1,2,3-triazol-4-yl)methyl)-1H-indole:**

Yellow solid; **Yield**: 98%; **M.P**: 147°C;

^{1}H NMR (400.13 MHz) ($CDCl_3$): δ 7.73 (dd, J_1= 14.25 Hz, J_2= 7.80 Hz, 2H), 7.49 (d, J=8.12 Hz, 1H), 7.46-7.41 (m, 3H), 7.37-7.32 (m, 1H), 7.30-7.26 (m, 1H), 7.20 (t, J=7.40 Hz, 1H), 6.81 (s, 2H), 6.66 (s, 1H), 5.43 (s, 2H), 3.89 (s, 6H), 3.87 (s, 3H);

^{13}C NMR (100.6 MHz) ($CDCl_3$): δ 153.90 (C), 145.55 (C), 138.72 (C), 138.39 (C), 136.64 (C), 133.57 (C), 133.32 (CH), 132.90 (CH) , 132.79 (C), 130.59 (CH), 128.13 (C), 127.54 (CH), 125.11 (C), 122.48 (CH), 121.03 (CH), 120.51 (CH), 120.28 (CH), 110.41 (CH), 104.18 (CH), 98.56 (CH), 61.12 (CH_3), 56.56 (CH_3), 40.07 (CH_2).

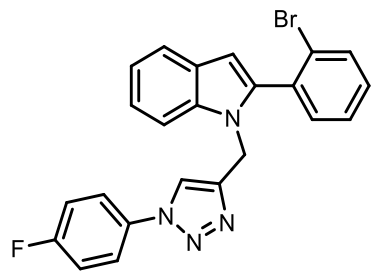

(5.5c) 2-(2-bromophenyl)-1-((1-(4-fluorophenyl)-1H-1,2,3-triazol-4-yl)methyl)-1H-indole:

Orange solid; **Yield**: 96%; **M.P**: 136°C;

^{1}H NMR (400.13 MHz) ($CDCl_3$): δ 7.73 (dd, J_1= 15.60 Hz, J_2= 7.80 Hz, 2H), 7.59-7.54 (m, 2H), 7.48 (d, *J*=8.27 Hz, 1H), 7.45-7.41 (m, 2H), 7.37-7.32 (m, 2H), 7.29-7.27 (m, 1H), 7.22-7.14 (m, 3H), 6.64 (s, 1H), 5.43 (s, 2H);

^{13}C NMR (100.6 MHz) ($CDCl_3$): δ 162.49 (*d*, J_{C-F}= 250 Hz) (C), 145.84 (C), 138.81 (C), 136.61 (C), 133.61 (C), 133.31 (CH), 133.23 (*d*, J_{C-F}= 2,70 Hz) (C), 132.92 (CH), 130.63 (CH), 128.20 (C), 127.54 (CH), 125.18 (C), 122.58 (CH), 122.50 (CH), 121.11 (CH), 120.53 (CH), 120.17 (CH), 116.75 (d, J_{C-F}= 21.87 Hz) (CH), 110.40 (CH), 104.13 (CH), 40.08 (CH_2).

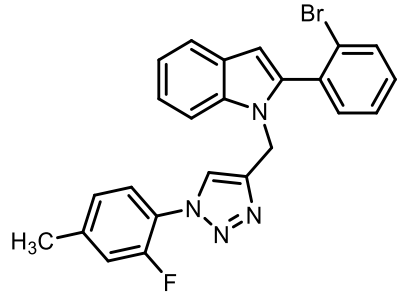

(**5.5d) 2-(2-bromophenyl)-1-((1-(2-fluoro-4-methylphenyl)-1H-1,2,3-triazol-4-yl)methyl)-1H-indole**:

Yellowish Solid; **Yield:** 95% **M.P:** 65°C

^{1}H NMR (400.13 MHz) ($CDCl_3$): δ 7.75 (d, *J*= 7.90 Hz, 1H), 7.72-7.68 (m, 2H), 7.53 (d, *J*= 8.30 Hz, 1H), 7.47-7.40 (m, 3H), 7.37-7.32 (m, 1H), 7.30-7.26 (m, 1H), 7.19 (t, *J*= 7.50 Hz, 1H), 7.07 (d, *J*= 8.50 Hz, 1H), 7.04 (d, *J*= 12.25 Hz, 1H), 6.62 (s, 1H), 5.43 (s, 2H), 2.41 (s, 3H);

^{13}C NMR (100.6 MHz) ($CDCl_3$): δ 154.40-151.91 (*d*, J_{C-F}= 250 Hz) (C), 145.12 (C), 141.35 (*d*, J_{C-F}= 7.66 Hz) (C), 138.95 (C), 136.64 (C), 133.76 (C), 133.16 (CH),133.09 (CH), 130.58 (CH), 128.19 (C), 127.45 (CH), 125.86-125.83 (*d*, J_{C-F}= 2.94 Hz) (CH), 125.22 (C), 124.57 (CH), 123.11 (*d*, J_{C-F}= 7.45 Hz) (CH), 122.67 (*d*, J_{C-F}= 10.87 Hz) (C), 122.37 (CH), 121.01 (CH), 120.40 (CH), 117.31 (*d*, J_{C-F}= 19.38 Hz) (CH), 110.45 (CH), 103.82 (CH), 40.01 (CH_2), 21.27 (CH_3).

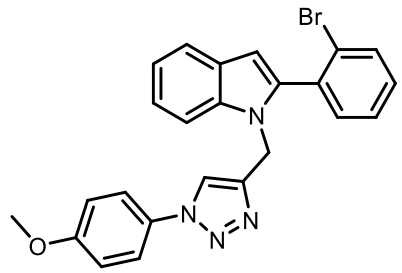

(5.5e) 2-(2-bromophenyl)-1-((1-(4-methoxyphenyl)-1H-1,2,3-triazol-4-yl)methyl)-1H-indole:

Yellowish Solid; **Yield:** 90%; **M.P:** 76°C;

^{1}H NMR (400.13 MHz) ($CDCl_3$): δ 7.74 (d, *J*= 7.80 Hz, 1H), 7.70 (d, *J*= 7.80 Hz, 1H), 7.50-7.46 (m, 3H), 7.43-7.42 (m, 2H), 7.36-7.31 (m, 2H), 7.28-7.25 (m, 1H), 7.20 (td, J_1= 14.80 Hz, J_2= 7.80 Hz, J_3= 0.80 Hz, 1H), 6.98-6.94 (m, 2H), 6.63 (s, 1H), 5.42 (s, 2H), 3.85 (s, 3H);

^{13}C NMR (100.6 MHz) ($CDCl_3$): δ 159.89 (C), 145.47 (C), 138.86 (C), 136.64 (C), 133.68 (C), 133.28 (CH), 132.95 (CH), 130.59 (CH), 130.43 (C), 128.18 (C), 127.51 (CH), 125.20 (C), 122.44 (CH), 122.20 (CH), 121.04 (CH), 120.46 (CH) , 120.16 (CH), 114.77 (CH), 110.48 (CH), 104.00 (CH), 55.72 (CH_3), 40.17 (CH_2).

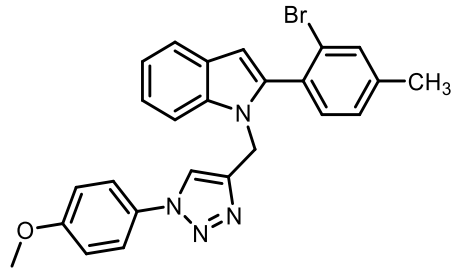

(5.5f) 2-(2-bromo-4-methylphenyl)-1-((1-(4-methoxyphenyl)-1H-1,2,3-triazol-4-yl)methyl)-1H-indole:

Pink Solid; **Yield:** 70%; **M.P**: 71°C;

^{1}H NMR (400.13 MHz) ($CDCl_3$): δ 7.59 (d, *J*= 7.70 Hz, 1H), 7.49 (d, *J*= 8.24 Hz, 1H), 7.40-7.36 (m, 3H), 7.23 (s, 1H), 7.17-7.13 (m, 2H), 7.08 (t, *J*= 7.45 Hz, 1H), 7.04 (dd, J_1= 8.50 Hz, J_2= 1.80 Hz, 1H), 6.87-6.83 (m, 2H), 6.51 (s, 1H), 5.32 (s, 2H), 3.74 (s, 3H), 2.25 (s, 3H);

^{13}C NMR (100.6 MHz) ($CDCl_3$): δ 159.88 (C), 145.53 (C), 139.02 (C), 137.50 (C), 136.63 (C), 133.56 (CH), 133.30 (C), 132.95 (CH), 131.44 (C), 130.44 (CH), 128.19 (C), 122.34 (CH),

122.16 (CH), 121.71 (CH), 121.01 (CH), 120.40 (CH), 120.23 (C), 114.67 (CH), 110.35 (CH), 103.78 (CH), 55.61 (CH_3), 40.08 (CH_2), 20.90 (CH_3).

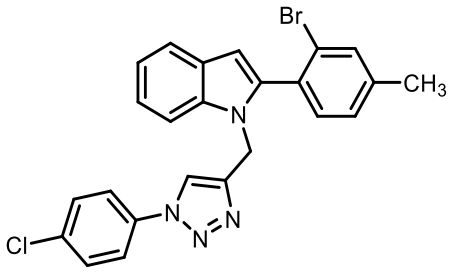

(**5.5g**) **2-(2-bromo-4-methylphenyl)-1-((1-(4-chlorophenyl)-1H-1,2,3-triazol-4-yl)methyl)-1H-indole:**

Yellow Solid; **Yield:** 91%; **M.P**: 86°C;

^{1}H NMR (400.13 MHz) ($CDCl_3$): δ 7.70 (d, *J*= 7.76 Hz, 1H), 7.60 (d, *J*= 8.20 Hz, 1H), 7.55-7.52 (m, 2H), 7.47-7.43 (m, 3H), 7.40 (s, 1H), 7.26-7.24 (m, 2H), 7.19 (dt, J_1= 14.87 Hz, J_2= 7.85 Hz, J_3= 0.80 Hz, 1H), 7.15 (dd, J_1=8.15 Hz, J_2=1.95 Hz, 1H), 6.62 (s, 1H), 5.43 (s, 2H), 2.36 (s, 3H);

^{13}C NMR (100.6 MHz) ($CDCl_3$): δ 146.02 (C), 138.95 (C), 137.57 (C), 136.59 (C), 135.43 (C), 134.60 (C), 133.53 (CH), 133.21 (C), 133.01 (CH), 131.49 (CH), 129.95 (CH), 128.22 (C), 122.42 (CH), 121.68 (CH), 121.65 (C), 121.08 (CH), 120.49 (CH), 119.97 (CH), 110.35 (CH), 104.07 (CH), 40.09 (CH_2), 21.00 (CH_3).

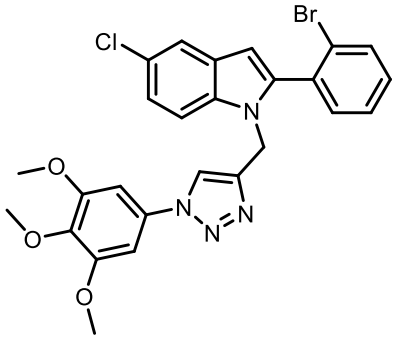

(**5.5h**) **2-(2-bromophenyl)-5-chloro-1-((1-(3,4,5-trimethoxyphenyl)-1H-1,2,3-triazol-4-yl)methyl) -1H-indole**:

Yellowish Solid; **Yield:** 86%; **M.P**: 152°C;

^{1}H NMR (400.13 MHz) ($CDCl_3$): δ 7.65 (d, *J*= 7.90 Hz, 1H), 7.55 (d, *J*= 1.90 Hz, 1H), 7.35-7.30 (m, 3H), 7.29 (s, 1H), 7.28-7.23 (m, 1H), 7.10 (dd, J_1= 8.80 Hz, J_2= 2.05 Hz, 1H), 6.70 (s, 2H), 6.47 (s, 1H), 5.28 (s, 2H), 3.78 (s, 6H), 3.77 (s, 3H);

^{13}C NMR (100.6 MHz) ($CDCl_3$): δ 153.93 (C), 145.04 (C), 140.02 (C), 138.49 (C), 135.01 (C), 133.35 (CH), 133.14 (C), 132.83 (CH), 132.71 (C), 130.85 (CH), 129.08 (C), 127.63 (CH), 126.19 (C), 125.01 (C), 122.73 (CH), 120.39 (CH), 120.27 (CH), 111.51 (CH), 103.70 (CH), 98.59 (CH), 61.13 (CH_3), 56.56 (CH_3), 40.14 (CH_2).

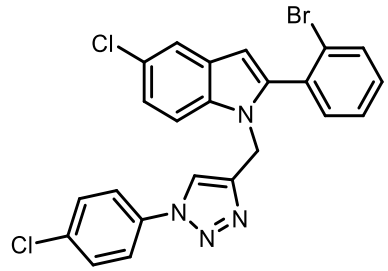

(**5.5i**) **2-(2-bromophenyl)-5-chloro-1-((1-(4-chlorophenyl)-1H-1,2,3-triazol-4-yl)methyl)-1H-indole:**

Yellow Solid; **Yield:** 92%; **M.P**: 188°C;

^{1}H NMR (400.13 MHz) ($CDCl_3$): δ 7.65 (d, *J*= 80 Hz, 1H), 7.55 (d, *J*= 1.90 Hz, 1H), 7.44 (m, 2H), 7.36-7.35 (m, 1H), 7.34-7.31 (m, 3H), 7.29-7.27 (m, 2H), 7.11 (dd, J_1= 8.60 Hz, J_2= 2.00 Hz, 1H), 6.47 (s, 1H), 5.28 (s, 2H);

^{13}C NMR (100.6 MHz) ($CDCl_3$): δ 145.46 (C), 140.11 (C), 135.35 (C), 134.98 (C), 134.77 (C), 133.37 (CH), 133.15 (C), 132.83 (CH), 130.90 (CH), 130.01 (CH), 129.16 (C), 127.64 (CH), 126.26 (C), 125.07 (C), 122.80 (CH), 121.70 (CH), 120.49 (CH), 119.86 (CH), 111.47 (CH), 103.68 (CH), 40.16 (CH_2).

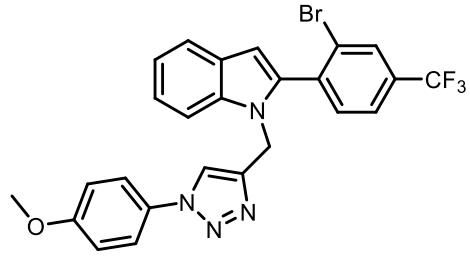

(**5.5j**) **2-(2-bromo-4-(trifluoromethyl)phenyl)-1-((1-(4-methoxyphenyl)-1H-1,2,3-triazol-4-yl)methyl)-1H-indole**:

Orange Solid; **Yield:** 92%; **M.P**: 76°C;

^{1}H NMR (400.13 MHz) ($CDCl_3$): δ 8.01 (s, 1H), 7.72 (d, *J*= 7.98 Hz, 1H), 7.69 (dd, J_1= 7.81 Hz, J_2= 1.02 Hz, 1H), 7.58 (d, *J*= 7.81 Hz, 1H), 7.51-7.47 (m, 3H), 7.36 (s, 1H), 7.32-7.28 (m, 1H), 7.22 (td, J_1= 15.00 Hz, J_2= 7.87 Hz, J_3= 0.90 Hz, 1H), 6.98-6.94 (m, 2H), 6.67 (s, 1H), 5.41 (s, 2H), 3.85 (s, 3H);

^{13}C NMR (100.6 MHz) ($CDCl_3$): δ 159.98 (C), 145.07 (C), 137.49 (C), 137.40 (C), 136.90 (C), 133.35 (CH), 133.51 (q, J_{1C-F} = 67.65 Hz, J_{2C-F} = 32.99 Hz) (C), 130.27 (q, J_{1C-F} = 7.30 Hz, J_{2C-F} = 3.65 Hz) (CH), 128.10 (C), 125.49 (C), 124.39 (q, J_{1C-F} = 6.55 Hz, J_{2C-F} = 3.40 Hz) (CH), 122.95 (CH), 122.22 (CH), 121.73 (C), 121.30 (CH), 120.76 (CH), 120.03 (CH), 114.83 (CH), 110.51 (CH), 104.79 (CH), 55.74 (CH_3), 40.59 (CH_2).

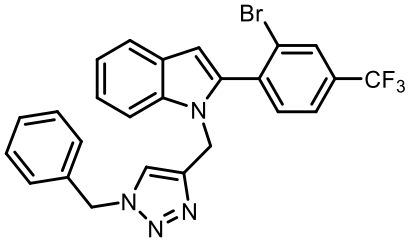

(**5.5k**) **1-((1-benzyl-1H-1,2,3-triazol-4-yl)methyl)-2-(2-bromo-4-(trifluoromethyl)phenyl)-1H-indole:**

Orange Solid; **Yield:** 94%; **M.P**: 102°;

^{1}H NMR (400.13 MHz) ($CDCl_3$): δ 7.83 (s, 1H), 7.58 (d, *J*= 7.71 Hz, 1H), 7.45 (d, *J*= 7.90 Hz, 1H), 7.32 (q J_1= 7.74 Hz, J_2= 5.57 Hz, 2H), 7.26-7.24 (m, 3H), 7.18-7.14 (m, 1H), 7.09 (t, *J*= 7.48 Hz, 1H), 7.05-7.03 (m, 2H), 6.79 (s, 1H), 6.48 (s, 1H), 5.28 (s, 2H), 5.20 (s, 2H);

^{13}C NMR (100.6 MHz) ($CDCl_3$): 145.00 (C), 137.52 (C), 137.38 (C), 136.89 (C), 134.56 (C), 133.32 (CH), 132.48 (d, J_{1C-F} = 30.85 Hz) (C), 130.14 (q, J_{1C-F} = 8.00 Hz, J_{2C-F} = 3.80 Hz) (CH), 129.19 (CH), 128.90 (CH), 128.04 (CH), 128.02 (C), 125.44 (C), 124.43 (C), 124.21 (q, J_{1C-F} = 6.85 Hz, J_{2C-F} = 3.62 Hz) (CH), 122.82 (CH), 121.72 (CH), 121.20 (CH), 120.65 (CH), 110.45 (CH), 104.56 (CH), 54.22 (CH_2), 40.24 (CH_2).

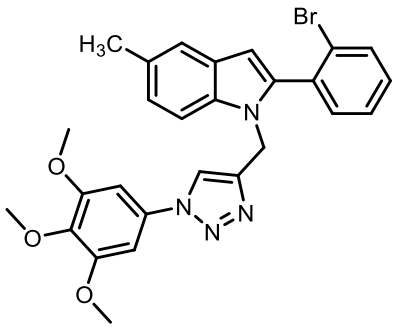

(5.5l) 2-(2-bromophenyl)-5-methyl-1-((1-(3,4,5-trimethoxyphenyl)-1H-1,2,3-triazol-4-yl)methyl)-1H-indole:

Yellowish Solid; **Yield:** 97%; **M.P**: 74°C;

^{1}H NMR (400.13 MHz) ($CDCl_3$): δ 7.64 (d, *J*= 8.07 Hz, 1H), 7.40 (s, 1H), 7.34-7.31 (m, 3H), 7.28-7.21 (m, 2H), 7.00 (dd, J_1= 8.50 Hz, J_2= 1.20 Hz, 1H), 6.71 (s, 2H), 6.47 (s, 1H), 5.30 (s, 2H), 3.79 (s, 6H), 3.77 (s, 3H), 2.39 (s, 3H);

^{13}C NMR (100.6 MHz) ($CDCl_3$): δ 153.91 (C), 145.71 (C), 138.79 (C), 138.40 (C), 135.05 (C), 133.68 (C), 133.32 (CH), 132.85 (CH), 132.83 (C), 130.50 (CH), 129.87 (C), 128.39 (C), 127.53 (CH), 125.12 (C), 124.08 (CH), 120.67 (CH), 120.25 (CH), 110.13 (CH), 103.76 (CH), 98.58 (CH), 61.14 (CH_3), 56.57 (CH_3), 40.13 (CH_2), 21.52 (CH_3).

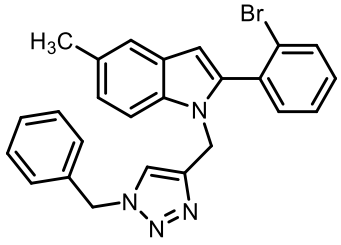

(**5.5m**) **1-((1-benzyl-1H-1,2,3-triazol-4-yl)methyl)-2-(2-bromophenyl)-5-methyl-1H-indole:**

Orange Solid; **Yield:** 97%; **M.P:** 85°C;

^{1}H NMR (400.13 MHz) ($CDCl_3$): δ 7.53-7.51 (m, 1H), 7.31 (s, 1H), 7.21-7.10 (m, 7H), 7.00-6.97 (m, 2H), 6.93 (dd, J_1= 8.40 Hz, J_2=1.08 Hz, 1H), 6.76 (s, 1H), 6.33 (s, 1H), 5.19 (s, 2H), 5.15 (s, 2H), 2.34 (s, 3H);

^{13}C NMR (100.6 MHz) ($CDCl_3$): δ 145.38 (C), 138.85 (C), 134.95 (C), 134.59 (C), 133.69 (C), 133.00 (CH), 132.80 (CH), 130.31 (CH), 129.52 (C), 129.00 (CH), 128.66 (CH), 128.26 (C),

127.88 (CH), 127.21 (CH), 125.05 (C), 123.82 (CH), 121.75 (CH), 120.52 (CH), 110.05 (CH), 103.20 (CH), 53.99 (CH_2), 40.10 (CH_2), 51.45 (CH_3).

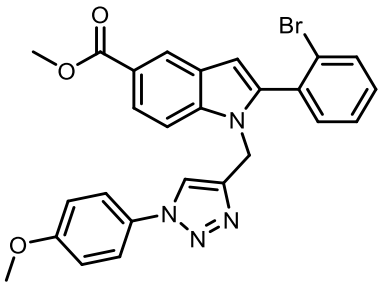

(5.5n) methyl 2-(2-bromophenyl)-1-((1-(4-methoxyphenyl)-1H-1,2,3-triazol-4-yl)methyl)-1H-indole-5-carboxylate:

Yellowish Solid; **Yiled:** 96%; **M.P**: 200°C;

^{1}H NMR (400.13 MHz) ($CDCl_3$): δ 8.36 (d, *J*= 1.36 Hz, 1H), 7.87 (dd, J_1= 8.70 Hz, J_2= 1.57 Hz, 1H), 7.65 (d, *J*= 7.78 Hz, 1H), 7.42 (d, *J*= 8.90 Hz, 1H), 7.40-7.36 (m, 2H), 7.34 (d, *J*= 0.69 Hz, 1H), 7.33 (s, 1H), 7.28-7.24 (m, 1H), 7.22 (s, 1H), 6.88-6.84 (m, 2H), 6.60 (s, 1H), 5.32 (s, 2H), 3.86 (s, 3H), 3.74 (s, 3H);

^{13}C NMR (100.6 MHz) ($CDCl_3$): δ 168.14 (C) ,159.98 (C), 144.82 (C) ,140.29 (C), 139.11 (C), 133.31 (CH), 133.11 (C), 132.92 (CH), 130.32 (CH), 127.71 (CH), 127.60 (C), 125.14 (C), 124.02 (CH), 123.78 (CH), 122.56 (C), 122.21 (CH), 120.15 (CH), 114.82 (CH), 110.16 (CH), 105.20 (CH), 55.72 (CH_3), 52.03 (CH_3), 40.28 (CH_2).

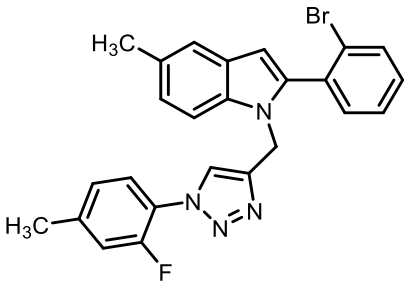

(**5.5o**) **2-(2-bromophenyl)-1-((1-(2-fluoro-4-methylphenyl)-1H-1,2,3-triazol-4-yl)methyl)-5-methyl-1H-indole**:

Brown Solid; **Yield:** 91%; **M.P**: 62°C;

^{1}H NMR (400.13 MHz) ($CDCl_3$): δ 7.62 (dd, J_1= 7.80 Hz, J_2= 0.79 Hz, 1H), 7.58 (t, J= 8.02 Hz, 1H), 7.37-7.28 (m, 5H), 7.24-7.21 (m, 1H), 6.98 (td, J_1= 17.33 Hz, J_2= 8.45 Hz, J_3= 1.20 Hz, 2H), 6.93 (d, J= 11.45 Hz, 1H), 6.42 (d, J= 0.60 Hz, 1H), 5.28 (s, 2H), 2.38 (s, 3H), 2.30 (s, 3H);

^{13}C NMR (100.6 MHz) ($CDCl_3$): δ 153.18 (d, J_{C-F} = 254 Hz) (C), 145.29 (C), 141.33 (d, J_{C-F} =8.15 Hz (C), 139.04 (C), 135.04 (C), 133.89 (C), 133.17 (CH), 133.05 (CH), 130.51 (CH), 129.71 (C), 128.45 (C), 127.44 (CH), 125.86 (d, J_{C-F} = 2.97 Hz) (CH), 125.26 (C), 124.61 (CH), 123.97 (CH), 123.09 (d, J_{C-F} = 7.35 Hz) (CH), 122.75 (d, J_{C-F} = 11.12 Hz) (C), 120.67 (CH), 117.32 (d, J_{C-F} =20.51 Hz) (CH), 110.15 (CH), 103.37 (CH), 40.08 (CH_2), 21.54 (CH_3), 21.28 (CH_3).

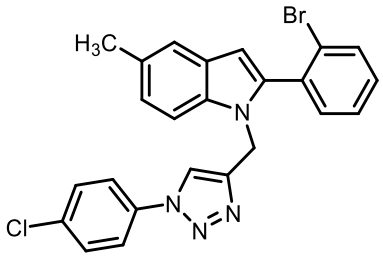

(5.5p) 2-(2-bromophenyl)-1-((1-(4-chlorophenyl)-1H-1,2,3-triazol-4-yl)methyl)-5-methyl-1H-indole:

Yellowish Solid; **Yield:** 99%; **M.P**: 197°;

^{1}H NMR (400.13 MHz) ($CDCl_3$): δ 7.68 (d, J= 7.80 Hz, 1H), 7.50-7.46 (m, 2H), 7.44 (s, 1H), 7.40-7.36 (m, 4H), 7.33 (s, 1H), 7.31 (m, 2H), 7.04 (dd, J_1= 8.46 Hz, J_2= 1.20 Hz, 1H), 6.50 (d, J= 0.64 Hz, 1H), 5.34 (s, 2H), 2.43 (s, 3H);

^{13}C NMR (100.6 MHz) ($CDCl_3$): δ 146.09 (C), 138.85 (C), 135.4 (C), 135.00 (C), 134.60 (C), 133.68 (C), 133.31 (CH), 132.86 (CH), 130.54 (CH), 129.94 (CH), 129.88 (C), 128.45 (C), 127.52 (CH), 125.17 (C), 124.10 (CH), 121.68 (CH), 120.75 (CH), 119.86 (CH), 110.07 (CH), 103.72 (CH), 40.11 (CH_2), 21.53 (CH_3).

Characterization of Final Products (6)

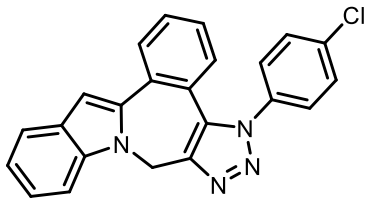

(5.6a) 5-(4-chlorophenyl)-5,8-dihydrobenzo[3,4][1,2,3]triazolo[4',5':5,6]azepino[1,2-a]indole:

Yellow Solid; **Yield:** 83%; **M.P**: 232°C;

^{1}H NMR (400.13 MHz) ($CDCl_3$): δ 7.91 (d, *J*= 8.09 Hz, 1H), 7.67 (d, *J*= 7.81 Hz, 1H), 7.59 (d, *J*= 8.30 Hz, 1H), 7.50-7.44 (m, 3H), 7.39-7.37 (m, 2H), 7.31 (td, J_1= 15.51 Hz, J_2= 7.95 Hz, J_3= 0.80 Hz, 1H), 7.25 (td, J_1= 15.21 Hz, J_2= 6.81 Hz, J_3= 1.09 Hz, 1H), 7.15 (t, *J*= 7.50 Hz, 1H), 6.97 (d, *J*= 7.91 Hz, 1H), 6.86 (s, 1H), 5.44 (s, 2H);

^{13}C NMR (100.6 MHz) ($CDCl_3$): δ 145.06 (C),138.45 (C), 137.01 (C), 135.68 (C), 135.20 (C), 133.84 (C), 132.48 (C), 131.88 (CH), 129.99 (CH), 129.81 (CH), 128.57 (CH), 127.86 (C), 127.81 (CH), 126.33 (CH), 122.72 (CH), 122.67 (C), 121.04 (CH), 120.25 (CH), 109.32 (CH), 104.03 (CH), 39.47 (CH_2).

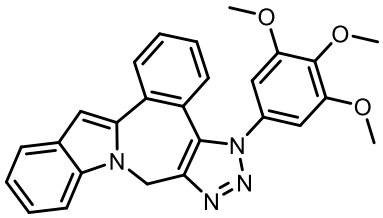

(5.6b) 5-(3,4,5-trimethoxyphenyl)-5,8-dihydrobenzo[3,4][1,2,3]triazolo[4',5':5,6]azepino [1,2-a]indole:

Yellow Solid; **Yield:** 92%; **M.P**: 192°C;

^{1}H NMR (400.13 MHz) ($CDCl_3$): δ 7.81 (d, *J*=7.88 Hz, 1H), 7.56 (d, *J*=7.88 Hz, 1H), 7.49 (d, *J*=8.41 Hz, 1H), 7.36 (t, *J*=7.66 Hz, 1H), 7.22-7.15 (m, 2H), 7.05-6.99 (m, 2H), 6.77 (s, 1H), 6.53 (s, 2H), 5.33 (s, 2H), 3.80 (s, 3H), 3.65 (s, 6H);

^{13}C NMR (100.6 MHz) ($CDCl_3$): δ 153.77 (C), 144.58 (C), 138.91 (C), 138.55 (C), 136.89 (C), 133.77 (C), 132.21 (C), 132.17 (C), 131.60 (CH), 129.62 (CH), 128.62 (CH), 127.75 (CH), 127.59 (C), 122.71 (C), 122.62 (CH), 120.87 (CH), 120.18 (CH), 109.29 (CH), 103.90 (CH), 102.82 (CH), 61.10 (CH_3), 56.40 (CH_3), 39.44 (CH_2).

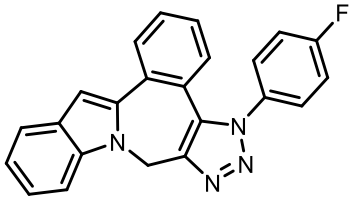

(5.6c) 5-(4-fluorophenyl)-5,8-dihydrobenzo[3,4][1,2,3]triazolo[4',5':5,6]azepino [1,2-a]indole:

White Solid; **Yield:** 87%; **M.P:** 243°C;

^{1}H NMR (400.13 MHz) ($CDCl_3$): δ 7.81 (d, *J*=7.88 Hz, 1H), 7.56 (d, *J*=7.88 Hz, 1H), 7.49 (d, *J*=7.34 Hz, 1H), 7.38-7.30 (m, 3H), 7.21 (t, *J*=7,55 Hz, 1H), 7.14 (t, *J*= 7.15 Hz, 1H), 7.10-7.03 (m, 3H), 6.87 (d, *J*=7.85 Hz, 1H), 6.76 (s, 1H), 5.34 (s, 2H);

^{13}C NMR (100.6 MHz) ($CDCl_3$): δ 162.98 (d, J_{C-F} = 254 Hz) (C), 144.87, 138.50, 137.01, 133.92, 132.85 (d, J_{C-F} = 3.15 Hz) (C), 132.51, 131.85 (CH), 129.75 (CH), 128.49 (CH), 127.86, 127.77 (CH), 127.16-10 (d, J_{C-F} = 8.72 Hz) (CH), 122.73, 122.70 (CH), 121.03 (CH), 120.24 (CH), 116.85 (d, J_{C-F} = 22.67 Hz) (CH), 109.34 (CH), 104.02 (CH), 39.48 (CH_2).

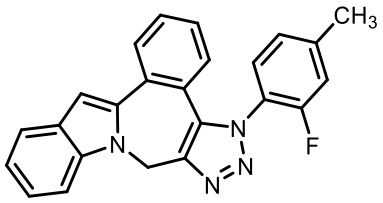

(5.6d) 5-(2-fluoro-4-methylphenyl)-5,8-dihydrobenzo[3,4][1,2,3]triazolo[4',5':5,6]azepino [1,2-a]indole:

Orange Solid; **Yield:** 83%; **M.P**: 255°C;

^{1}H NMR (400.13 MHz) ($CDCl_3$): δ 7.78 (d, *J*=7.85 Hz, 1H), 7.56 (d, *J*=7.85 Hz, 1H), 7.49 (d, *J*=8.31 Hz, 1H), 7.34-7.26 (m, 2H), 7.20 (t, *J*=7.40 Hz, 1H), 7.10 (td, J_1= 15.29 Hz, J_2= 7.71 Hz, J_3= 0.85 Hz; 1H), 7.03 (t, *J*=7.48 Hz, 1H), 6.99 (d, *J*=8.02 Hz, 1H), 6.92-6.89 (m, 2H), 6.74 (s, 1H), 5.34 (s, 2H), 2.32 (s, 3H);

^{13}C NMR (100.6 MHz) ($CDCl_3$): δ 155.66 (d, J_{C-F} = 254 Hz) (C), 143.84, 143.15(d, J_{C-F} = 7.41 Hz) (C), 138.61, 137.00, 135.30, 132.19, 131.71 (CH), 129.68 (CH), 127.90, 127.83 (d, J_{C-F} = 8.12 Hz) (CH), 126.91 (CH), 125.91 (d, J_{C-F} = 3.54 Hz) (CH), 122.96, 122.52 (CH), 122.26 (d, J_{C-F} = 12.56 Hz), 120.98 (CH), 120.11 (CH), 117.63 (d, J_{C-F} = 18.30Hz) (CH), 109.30 (CH), 104.03 (CH), 39.43 (CH_2), 21.48 (CH_3).

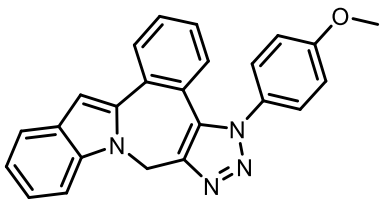

(5.6e) 5-(4-methoxyphenyl)-5,8-dihydrobenzo[3,4][1,2,3]triazolo[4',5':5,6]azepino[1,2-a]indole:

White Solid; **Yield:** 96%; **M.P**: 211°C;

^{1}H NMR (400.13 MHz) ($CDCl_3$): δ 7.81 (dd, J_1=7.88 Hz, J_2=0.6 Hz 1H), 7.59 (d, J=7.87 Hz, 1H), 7.51 (d, J=8.35 Hz, 1H), 7.36 (td, J_1= 15.39 Hz, J_2= 7.70 Hz, J_3= 1.14 Hz, 1H), 7.27-7.20 (m, 3H), 7.13 (td, J_1= 15.34 Hz, J_2= 7.88 Hz, J_3= 1.09 Hz, 1H), 7.06 (t, J= 7.50 Hz, 1H), 6.93-6.87 (m, 3H), 6.76 (s, 1H), 5.36 (s, 2H), 3.78 (s, 3H);

^{13}C NMR (100.6 MHz) ($CDCl_3$): 160.45 (C), 144.61 (C), 138.70 (C), 137.00 (C), 133.78 (C), 132.43 (C), 131.74 (CH), 129.74 (C), 129.50 (CH), 128.53 (CH), 127.89 (C), 127.72 (CH), 126.58 (CH), 123.14 (C), 122.62 (CH), 120.98 (CH), 120.19 (CH), 114.86 (CH), 109.38 (CH), 103.90 (CH), 55.72 (CH_3), 39.48 (CH_2).

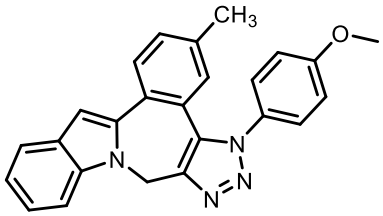

(5.6f) 5-(4-methoxyphenyl)-3-methyl-5,8-dihydrobenzo[3,4][1,2,3]triazolo[4',5':5,6] azepino[1,2-a]indole:

Yellow Solid; **Yield:** 88%; **M.P**: 237°;

^{1}H NMR (400.13 MHz) ($CDCl_3$): δ 7.63 (s, 1H), 7.58 (d, J=7.81 Hz, 1H), 7.51 (d, J=8.28 Hz, 1H), 7.26-7.20 (m, 3H), 7.05 (t, J=7.46, 1H), 6.95 (dd, J_1=7.93 Hz, J_2=1.07 Hz, 1H), 6.91-6.87 (m, 2H), 6.80 (d, J= 8.05 Hz, 1H), 6.76 (s, 1H), 5.33 (s, 2H), 3.78 (s, 3H), 2.35 (s, 3H);

^{13}C NMR (100.6 MHz) ($CDCl_3$): δ 160.40 (C), 144.24 (C), 139.68 (C), 138.87 (C), 136.94 (C), 133.92 (C), 132.30 (C), 132.16 (CH), 129.82 (C), 128.72 (CH), 128.43 (CH), 127.87 (C), 126.58

(CH), 122.52 (CH), 120.93 (CH), 120.37 (C), 120.12 (CH), 114.81 (CH), 109.37 (CH), 103.70 (CH), 55.71 (CH_3), 39.57 (CH_2), 21.50 (CH_3).

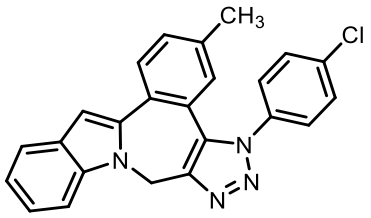

(5.6g) 5-(4-chlorophenyl)-3-methyl-5,8-dihydrobenzo[3,4][1,2,3]triazolo[4',5':5,6]azepino [1,2-a]indole:

Yellow Solid; **Yield:** 86%; **M.P**: 281°C;

^{1}H NMR (400.13 MHz) ($CDCl_3$): δ 7.63 (s, 1H), 7.57 (d, *J*=7.88 Hz, 1H), 7.49 (d, *J*=8.34 Hz, 1H), 7.37-7.35 (m, 2H), 7.29-7.27 (m, 2H), 7.23-7.19 (m, 1H), 7.05 (t, *J*=7.43 Hz, 1H), 6.97 (dd, J_1=7.95 Hz, J_2=0.65 Hz, 1H), 6.76 (d, *J*= 7.85 Hz, 2H), 5.33 (s, 2H), 2.36 (s, 3H);

^{13}C NMR (100.6 MHz) ($CDCl_3$): δ 144.68 (C), 140.07 (C), 138.63 (C), 136.95 (C), 135.58 (C), 135.29 (C), 133.98 (C), 132.36 (C), 132.29 (CH), 129.94 (CH), 128.82 (CH), 128.49 (CH), 127.84 (C), 126.33 (CH), 122.62 (CH), 120.98 (CH), 120.19 (CH), 119.90 (C), 109.32 (CH), 103.83 (CH), 39.47 (CH_2), 21.51 (CH_3).

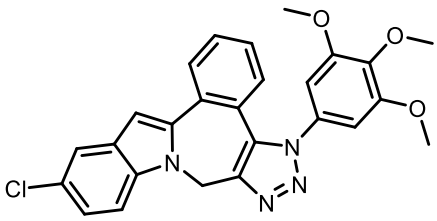

(7h) 12-chloro-5-(3,4,5-trimethoxyphenyl)-5,8-dihydrobenzo[3,4][1,2,3]triazolo[4',5':5,6] azepino[1,2-a]indole:

Yellow Solid; **Yield:** 92%; **M.P:** 232°C;

^{1}H NMR (400.13 MHz) ($CDCl_3$): δ 7.81 (dd, J_1= 7.93 Hz, J_2= 0.78Hz, 1H), 7.54 (d, *J*= 1.96 Hz, 1H), 7.43-7.38 (m, 2H); 7.21 (td, J_1= 15.32 Hz, J_2= 7.75 Hz, J_3= 1.25 Hz, 1H), 7.17 (dd, J_1= 8.82 Hz, J_2= 1.87 Hz, 1H), 7.02 (dd, J_1= 7.94 Hz, J_2= 0.71 Hz; 1H), 6.72 (s, 1H), 6.56 (s, 2H), 5.33 (s, 2H), 3.83 (s, 3H), 3.68 (s, 6H);

^{13}C NMR (100.6 MHz) ($CDCl_3$): δ 153.89 (C), 144.39 (C), 139.89 (C), 139.08 (C), 135.37 (C), 133.75 (C), 132.15 (C), 131.81 (C), 131.75 (CH), 129.79 (CH), 128.74 (CH), 128.74 (C), 128.04 (CH), 125.87 (C), 122.96 (CH), 122.86 (C), 120.21 (CH), 110.47 (CH), 103.41 (CH), 102.90 (CH), 61.21 (CH_3), 56.50 (CH_3), 39.82 (CH_2).

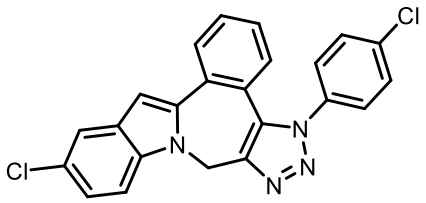

(5.6i) 12-chloro-5-(4-chlorophenyl)-5,8-dihydrobenzo[3,4][1,2,3]triazolo[4',5':5,6]azepino [1,2-a]indole:

Yellow Solid; **Yield:** 93%; **M.P:** 273°C;

^{1}H NMR (400.13 MHz) ($CDCl_3$): δ 7.81 (d, J_1= 7.93 Hz, J_2=0.52 Hz, 1H), 7.55 (d, J= 1.77 Hz, 1H), 7.43-7.38 (m, 4H), 7.31 (d, J= 8.73 Hz, 2H), 7.20-7.16 (m, 2H), 6.91 (dd, J_1=7.90 Hz, J_2= 0.46 Hz, 1H), 6.71 (s, 1H), 5.33 (s, 2H);

^{13}C NMR (100.6 MHz) ($CDCl_3$): δ 144.81 (C), 139.73 (C), 135.84 (C), 135.43 (C), 135.15 (C), 133.79 (C), 132.02 (C), 131.97 (CH), 130.07 (CH), 129.95 (CH), 128.76 (C), 128.64 (CH), 128.21 (CH), 126.36 (CH), 125.90 (C), 123.02 (CH), 122.76 (C), 120.32 (CH), 110.45 (CH), 103.48 (CH), 39.78 (CH_3).

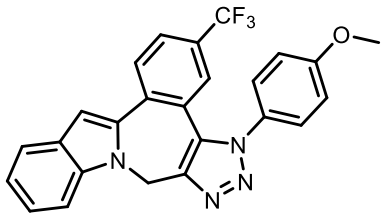

(5.6j) 5-(4-methoxyphenyl)-3-(trifluoromethyl)-5,8-dihydrobenzo[3,4][1,2,3]triazolo [4',5':5,6]azepino[1,2-a]indole: Yellow Solid; **Yield:** 84%; **M.P:** 260°C;

^{1}H NMR (400.13 MHz) ($CDCl_3$): δ 7.93 (d, J=8.27 Hz, 1H), 7.62-7.57 (m, 2H), 7.53 (d, J=8.43 Hz, 1H), 7.29-7.22 (m, 3H), 7.14-7.07 (m, 2H), 6.95-6.1 (m, 2H), 6.85 (s, 1H), 5.40 (s, 2H), 3.79 (s, 3H);

^{13}C NMR (100.6 MHz) ($CDCl_3$): δ 160.88 (C), 144.83 (C), 137.44 (C), 137.22 (C), 135.53 (C), 132.76 (C), 132.07 (CH), 129.63 (d, J_{C-F} = 33.013 Hz) (C), 129.09 (C), 127.79 (C), 126.62 (CH), 125.85 (*q*, J_{1C-F} = 6.80 Hz, J_{2C-F} = 3.59 Hz) (CH), 125.57(*q*, J_{1C-F} = 7.67 Hz, J_{2C-F} = 3.78 Hz) (CH) , 124.83 (C), 123.46 (C), 123.41 (CH), 122.12 (C), 121.33 (CH), 120.58 (CH), 115.09 (CH), 109.53 (CH), 105.41 (CH), 55.84 (CH3), 39.67 (CH_2).

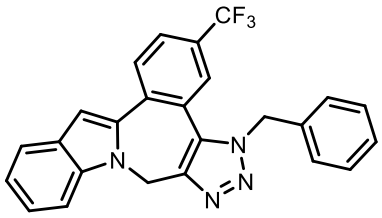

(5.6k) 5-benzyl-3-(trifluoromethyl)-5,8-dihydrobenzo[3,4][1,2,3]triazolo[4',5':5,6]azepino [1,2-a]indole:

Grey Solid; **Yield:** 85%; **M.P**: 227°C;

^{1}H NMR (400.13 MHz) ($CDCl_3$): δ 7.90 (d, *J*=8.22 Hz, 1H), 7.62 (dd, J_1=8.34 Hz, J_2= 1.20 Hz, 1H), 7.57 (d, *J*=8.06 Hz, 1H), 7.51 (d, *J*=8.45 Hz, 2H), 7.33-7.23 (m, 4H), 7.21 (m, 2H), 7.09-7.05 (m, 1H), 6.67 (s, 1H), 5.58 (s, 2H), 5.33 (s, 2H);

^{13}C NMR (100.6 MHz) ($CDCl_3$): δ 144.65 (C), 137.38-137.00 (d, J_{C-F} = 37.77 Hz) (C), 135.64-135.63 (*d*, J_{C-F} = 1.46 Hz) (C), 134.79 (C), 133.37 (C), 132.31 (CH), 131.18 (C), 130.18-129.86 (*d*, J_{C-F} = 33.45 Hz) (C), 129.36 (CH), 128.78 (CH), 127.71 (C), 127.08 (CH), 126.25-126.15 (*q*, J_{1C-F} = 6.58 Hz, J_{2C-F} = 3.64 Hz) (CH), 125.16-125.05 (*q*, J_{1C-F} = 7.33 Hz, J_{2C-F} = 3.69 Hz) (CH), 125.01-122.30 (d, J_{C-F} = 275 Hz) (C), 123.40 (C), 123.34 (CH), 121.30 (CH), 120.50 (CH), 109.52 (CH), 105.23 (CH), 53.06 (CH_2), 39.54 (CH_2).

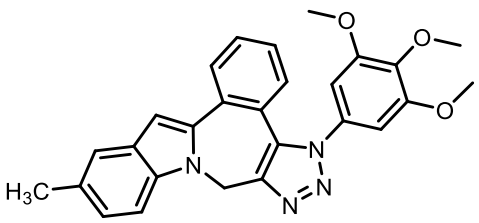

(5.6l) 12-methyl-5-(3,4,5-trimethoxyphenyl)-5,8-dihydrobenzo[3,4][1,2,3]triazolo[4',5':5,6] azepino[1,2-a]indole:

White Solid; **Yield**: 95%; **M.P:** 234°C;

^{1}H NMR (400.13 MHz) ($CDCl_3$): δ (dd, J_1=7.98 Hz, J_2=0.78 Hz, 1H), 7.51-7.46 (m, 3H), 7.29-7.25 (m, 1H), 7.16 (dd, J_1=8.50 Hz, J_2=1.23 Hz, 1H), 7.10 (dd, J_1=7.96 Hz, J_2=0.79 Hz, 1H), 6.81 (s, 1H), 6.65 (s, 2H), 5.44 (s, 2H), 3.93 (s, 3H), 3.78 (s, 6H), 2.49 (s, 3H);

^{13}C NMR (100.6 MHz) ($CDCl_3$): δ153.86 (C), 144.74 (C), 138.99 (C), 138.60 (C), 135.51 (C), 133.57 (C), 1332.44 (C), 132.29 (C), 131.60 (CH), 129.63 (C), 129.54 (CH), 128.69 (CH), 128.07 (C), 127.52 (CH), 124.46 (CH), 122.72 (C), 120.42 (CH), 109.07 (CH), 103.41 (CH), 102.92 (CH), 61.19 (CH_3), 56.49 (CH_3), 39.62 (CH_2), 21.51 (CH_3).

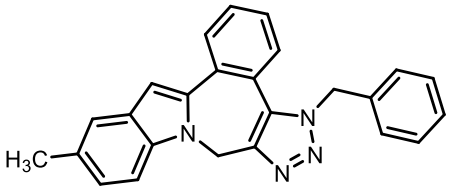

(5.6m) 5-benzyl-12-methyl-5,8-dihydrobenzo[3,4][1,2,3]triazolo[4',5':5,6]azepino[1,2-a] indole:

White Solid; **Yield:** 90%; **M.P:** 163°C;

^{1}H NMR (400.13 MHz) ($CDCl_3$): δ 7.80 (d, J=7.87 Hz, 1H), 7.43-7.37 (m, 2H), 7.33 (s, 1H), 7.31-7.24 (m, 5H), 7.14-7.12 (m, 2H), 7.05-7.03 (m, 1H), 6.6 (s, 1H), 5.59 (s, 2H), 5.29 (s, 2H), 2.37 (s, 3H);

^{13}C NMR (100.6 MHz) ($CDCl_3$): δ 144.30 (C), 138.43 (C), 135.52 (C), 134.57 (C), 132.76 (C), 131.97 (CH), 129.77 (CH), 129.36 (C), 129.21 (CH), 128.39 (CH), 128.05 (C), 128.00 (CH), 127.67 (CH), 126.82 (CH), 124.31 (CH), 122.96 (C), 120.45 (CH), 109.08 (CH), 103.27 (CH), 52.52 (CH_2), 39.56 (CH_2), 21.50 (CH_3).

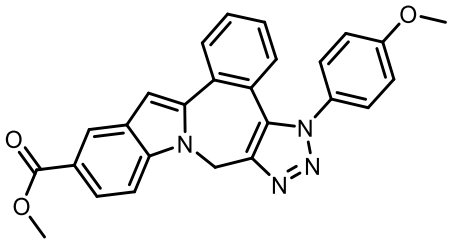

(5.6n) methyl 5-(4-methoxyphenyl)-5,8-dihydrobenzo[3,4][1,2,3]triazolo[4',5':5,6] azepino[1,2-a]indole-12-carboxylate:

White Solid; **Yield:** 94%; **M.P**: 200°C;

^{1}H NMR (400.13 MHz) ($CDCl_3$): δ 8.34 (d, *J*=1,10 Hz, 1H), 7.90 (dd, J_1=8.80 Hz, J_2=1.45 Hz, 1H), 7.79 (d, *J*=7.92 Hz, 1H), 7.49 (d, *J*= 8.80 Hz, 1H), 7.35 (dt, J_1= 15.17 Hz, J_2=7.97 Hz J_3=1.03 Hz, 1H), 7.24- 7.22 (m, 2H), 7.17-7.13 (m, 1H), 6.93-6.87 (m, 3H), 6.82 (s, 1H), 5.35 (s, 2H), 3.84 (s, 3H), 3.76 (s, 3H);

^{13}C NMR (100.6 MHz) ($CDCl_3$): δ 168.03 (C), 160.48 (C), 144.09 (C), 140.18 (C), 139.20 (C), 133.67 (C), 131.79 (CH), 131.75 (C), 129.62 (CH), 129.54 (C), 128.54 (CH), 128.15 (CH), 127.36 (C), 126.51 (CH), 124.07 (CH), 123.73 (CH), 123.15 (C), 122.13 (C), 114.84 (CH), 109.03 (CH), 105.15 (CH), 55.68 (CH_3), 51.97 (CH_3), 39.88 (CH_2).

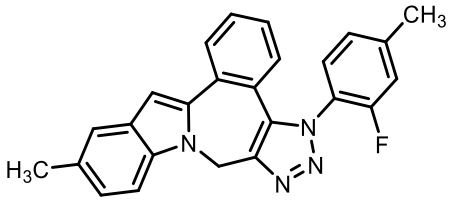

(5.6o)5-(2-fluoro-4-methylphenyl)-12-methyl-5,8-dihydrobenzo[3,4][1,2,3]triazolo [4',5':5,6]azepino[1,2-a]indole:

Whit Solid; **Yield:** 90%; **M.P**: 231°C;

^{1}H NMR (400.13 MHz) ($CDCl_3$): δ 7.78 (dd, J_1= 8.01 Hz, J_2= 0.83 Hz, 1H), 7.39-7.27 (m, 4H), 7.12-7.08 (m, 1H), 7.05-6.99 (m, 2H), 6.94-6.89 (m, 2H), 6.66 (s, 1H), 5.33 (s, 2H), 2.36 (s, 3H), 2.34 (s, 3H);

^{13}C NMR (100.6 MHz) ($CDCl_3$): δ 155.73 (d, J_{C-F} = 253 Hz) (C), 143.93(C), 143.14 (d, J_{C-F} = 7.49 Hz) (C), 138.61(C), 135.55(C), 135.33(C), 132.37(C), 131.67 (CH), 129.64 (CH), 129.38(C), 128.16(C), 127.78 (d, J_{C-F} = 10.24 Hz) (CH), 126.93 (CH), 125.92 (d, J_{C-F} = 3.16 Hz) (CH), 124.29 (CH), 122.91(C), 122.34 (*d*, J_{C-F} = 12.45 Hz) (C), 120.48 (CH), 117.66 (*d*, J_{C-F} = 18.81 Hz) (CH), 109.02 (CH), 103.50 (CH_3), 39.53 (CH_2), 21.49 (CH_3).

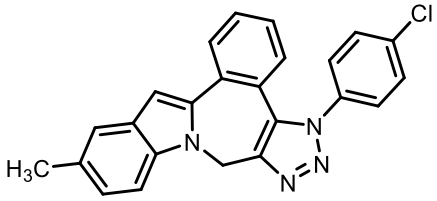

(5.6p)5-(4-chlorophenyl)-12-methyl-5,8-dihydrobenzo[3,4][1,2,3]triazolo[4',5':5,6] azepino [1,2-a]indole:

White Solid; **Yield**: 89%; **M.P**: 215°C;

^{1}H NMR (400.13 MHz) ($CDCl_3$): δ (dd, J_1= 7.89 Hz, J_2= 0.76 Hz, 1H), 7.39-.7.36 (*m*, 5H), 7.30-7.28 (*m*, 2H), 7.17-7.13 (m, 1H), 7.05 (dd, J_1= 8.50 Hz, J_2= 1.16 Hz, 1H); 6.88 (dd, J_1=7.86 Hz, J_2= 0.80 Hz, 1H), 6.68 (*s*, 1H), 5.32 (*s*, 2H), 2.37 (*s*, 3H);

^{13}C NMR (100.6 MHz) ($CDCl_3$): δ 145.14 (C), 138.44 (C), 135.69 (C), 135.57 (C), 135.27 (C), 133.88 (C), 132.65 (C), 131.82 (CH), 130.01 (CH), 129.78 (CH), 129.53 (C), 128.59 (CH), 128.12 (C), 127.68 (CH), 126.37 (CH), 124.48 (CH), 122.60 (C), 120.53 (CH), 109.04 (CH), 103.50 (CH), 39.56 (CH_2), 21.52 (CH_3).

Characterization of Post-Synthetic Modification 5.7a, 5.7b, 5.7c, 5.8

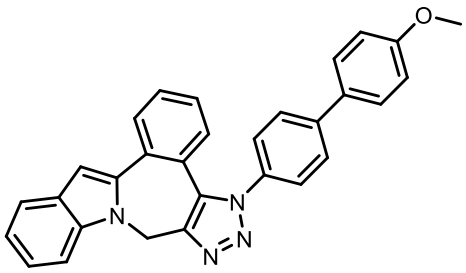

(5.7a) 5-(4'-methoxy-[1,1'-biphenyl]-4-yl)-5,8-dihydrobenzo[3,4][1,2,3]triazolo[4',5':5,6] azepino[1,2-a]indole:

Yellow Solid; **Yield:** 96%;

^{1}H NMR (400.13 MHz) ($CDCl_3$): δ 7.84 (d, *J*= 7.72 Hz, 1H), 7.61-7.57 (m, 3H), 7.53 (d, *J*=8.59 Hz, 1H), 7.49 (d, *J*=8.46 Hz, 2H), 7.40-7.38 (m, 3H), 7.24 (td, J_1=18.58 Hz, J_2=8.20 Hz, J_3=0.80 Hz, 1H), 7.18-7.16 (m, 1H), 7.07 (t, *J*=7.45 Hz, 1H), 7.00 (dd, J_1=7.90 Hz, J_2=0.90 Hz, 1H), 6.94-6.92 (m, 2H), 6.79 (s, 1H), 5.39 (s, 2H), 3.79 (s, 3H);

^{13}C NMR (100.6 MHz) ($CDCl_3$): δ 159.89 (C), 144.92 (C), 142.24 (C), 138.68 (C), 137.04 (C), 136.27 (CH), 135.22 (C), 133.80 (C), 131.45 (C), 132.07 (C), 131.80 (CH), 129.63 (CH), 128.76 (CH), 128.36 (CH), 127.91 (C), 127.78 (CH), 125.42 (CH), 123.11 (C), 122.68 (CH), 121.02 (CH), 120.23 (CH), 114.57 (CH), 109.39 (CH), 103.95 (CH), 55.52 (CH_3), 39.59 (CH_2).

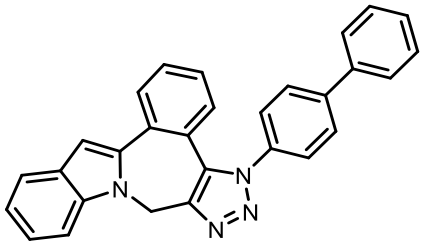

(5.7b)-5-([1,1'-biphenyl]-4-yl)-5,8-dihydrobenzo[3,4][1,2,3]triazolo[4',5':5,6]azepino[1,2-a]indole:

White Solid; **Yield:** 98%;

^{1}H NMR (400.13 MHz) ($CDCl_3$): δ 7.84 (d, *J*= 7.95 Hz, 1H), 7.63-7.59 (m, 3H), 7.55-7.51 (m, 3H), 7.43-7.37 (m, 5H), 7.33 (d, *J*= 7.48 Hz, 1H), 7.23 (td, J_1= 15.19 Hz, J_2= 7.75 Hz, J_3= 0.88 Hz, 1H), 7.18-7.14 (m, 1H), 7.07 (t, *J*= 7.54 Hz, 1H), 7.00 (dd, J_1= 7.89 Hz, J_2= 0.63 Hz, 1H), 6.80 (s, 1H), 5.38 (s, 2H);

^{13}C NMR (100.6 MHz) ($CDCl_3$): δ 144.87 (C), 142.54 (C), 139.53 (C), 138.56 (C), 136.94 (C), 135.70 (C), 133.74 (C), 132.36 (C), 131.72 (CH), 129.56 (CH), 129.04 (CH), 128.67 (CH), 128.24 (CH), 128.13 (CH), 127.82 (C), 127.70 (CH), 127.18 (CH), 125.34 (CH), 122.96 (C), 122.59 (CH), 120.94 (CH), 120.14 (CH), 109.29 (CH), 103.87 (CH), 39.49 (CH_2).

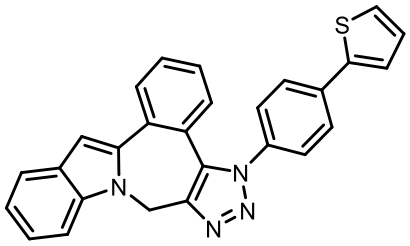

(5.7c) 5-(4-(thiophen-2-yl)phenyl)-5,8-dihydrobenzo[3,4][1,2,3]triazolo[4',5':5,6]azepino [1,2-a]indole:

Grey Solid; **Yield:** 71%;

^{1}H NMR (400.13 MHz) ($CDCl_3$): δ 7.83 (d, *J*=8.06 Hz, 1H), 7.62-7.59 (m, 3H), 7.52 (d, *J*= 8.35, 1H), 7.46-7.44 (m, 1H), 7.39-7.32 (m, 5H), 7.23 (dt, *J*= 15.23 Hz, J= 6.98 Hz, *J*=0.88 Hz, 1H), 7.17-7.12 (m, 1H), 7.07 (t, *J*= 7.30 Hz, 1H), 6.97 (d, *J*= 7.86 Hz, 1H), 6.79 (s, 1H), 5.33 (s, 2H);

^{13}C NMR (100.6 MHz) ($CDCl_3$): δ 144.93 (C), 140.77 (C), 138.65 (C), 137.18 (C), 137.03 (C), 135.42 (C), 133.80 (C), 132.44 (C), 131.80 (CH), 129.65 (CH), 128.73 (CH), 127.90 (C), 127.79

(CH)**,** 127.52 (CH), 127.01 (CH), 126.19 (CH), 126.04 (C),125.53 (CH), 122.68 (CH), 121.66 (CH), 121.02 (CH), 120.24 (CH), 109.38 (CH), 103.96 (CH), 39.57 (CH_2).

11.4 General procedures and Characterization of Chapter 6

Synthetic procedures

Procedure for 1,4,5,6-Tetrahydrobenzo[c][1,2,3]triazolo[4,5-e]azepine 5 and 4,6-Dihydro-1H-benzo[5,6]oxepino[3,4-d][1,2,3]triazoles

Step 1. Synthesis of N-(2-bromobenzyl)prop-2-yn-1-amine

2-Bromobenzaldehyde (4 g, 21.62 mmol, 1.00 eq.) was added to the oven dried 50 mL flask, methanol was added and stirred for 10 minutes. Prop-2-yn-1-amine (1.42 g, 25.95 mmol, 1.2 eq.) was added to the reaction and stirred at room temperature for 24 hours, until the disappearance of 2-bromobenzaldehyde on TLC (alugram ALOX N/UV254), using n-hexane/EtOAc 80/20 as the eluent. Subsequently, at 0°C, $NaBH_4$ (3.21 g, 86.48 mmol, 4 eq.) was added and stirred for 2 hours. To the resulting mixture, water (H_2O, 15 mL) was added dropwise at 0°C. The reaction mixture was diluted with diethyl ether (50 mL) and washed with brine, dried over Na_2SO_4, filtered, and the solvent was removed under reduced pressure, and the residue was purified by flash chromatography on a silica gel column (60 g, n-hexane/EtOAc 90/10, Rf = 0.22), giving 4.355 g of N-(2-bromobenzyl)prop-2-yn-1-amine with a 90% yield.

Step 2. Synthesis of N-(2-bromobenzyl)-2,2,2-trifluoro-N-(prop-2-yn-1-yl)acetamide.

In over dried 50 mL flask equipped with a magnetic stirrer, N-(2-bromobenzyl)prop-2-yn-1-amine (3.24 g, 14.50 mmol, 1.00 equiv.) was dissolved in pyridine (10 mL). The solution was cooled using an ice bath, and trifluoroacetic anhydride (4.56 g, 21.75 mmol, 1.50 equiv.) was added gradually. The reaction mixture was then allowed to warm to room temperature and monitored by TLC (n-hexane/EtOAc, 80/20). After the completion of reaction, the reaction mixture was diluted with diethyl ether (Et_2O) and extracted sequentially with 2N HCl solution, saturated $NaHCO_3$ solution, water, and brine. The organic phase was dried over anhydrous Na_2SO_4, filtered, and concentrated under reduced pressure. Isolated 4.57 g of N-(2-bromobenzyl)-2,2,2-trifluoro-N-(prop-2-yn-1-yl)acetamide with a 98% yield.

Step 3. Synthesis of N-(2-bromobenzyl)-2,2,2-trifluoro-N-((1-(4-methoxyphenyl)-1H-1,2,3-triazol-4-yl)methyl)acetamide

In a 50 mL Carousel reactor (Radley Discovery Technology) equipped with a magnetic stirrer, N-(2-bromobenzyl)-2,2,2-trifluoro-N-(prop-2-yn-1-yl)acetamide (0.320 g, 1 mmol, 1.00 equiv.) was dissolved in 1,4-dioxane (2 mL). To the solution were added CuI (0.038 g, 0.2 mmol, 0.20 equiv.) and 4-methoxyphenyl azide 11b (0.168 g, 1.1 mmol, 1.10 equiv.). The reaction mixture was stirred at 50 °C for 12 hours. The progress of the reaction was monitored by TLC (n-hexane/EtOAc 70/30). After completion, the reaction mixture was concentrated under reduced pressure, and the crude product was purified by flash chromatography (30 g SiO_2, n-hexane/EtOAc 70/30, Rf = 0.22). Isolated 0.463 g of N-(2-bromobenzyl)-2,2,2-trifluoro-N-((1-(4-methoxyphenyl)-1H-1,2,3-triazol-4-yl)methyl)acetamide with a yield of 98%.

Step 4. Synthesis of 2,2,2-Trifluoro-1-(1-(4-methoxyphenyl)-4,6-dihydrobenzo[c][1,2,3]triazolo [4,5-e]azepin-5(1H)-yl)ethan-1-one (**7a**).

In a 50 mL Carousel reactor (Radley Discovery Technology) equipped with a magnetic stirrer, $Pd(OAc)_2$ (0.011 g, 0.05 mmol, 0.05 equiv.) and DavePhos (0.053 g, 0.2 mmol, 0.1 equiv.) were dissolved in anhydrous DMA (3 mL) under an argon atmosphere at room temperature. To the solution N-(2-bromobenzyl)-2,2,2-trifluoro-N-((1-(4-methoxyphenyl)-1H-1,2,3-triazol-4-yl)methyl)acetamide (0.469 g, 1.00 mmol, 1.00 equiv.) and CsOAc (0.382 g, 2.00 mmol, 2.00 equiv.) was added. The reaction mixture was stirred at 120 °C under an inert atmosphere, with the progress monitored by TLC (n-hexane/EtOAc, 80/20). After completion, the reaction mixture was diluted with diethyl ether (Et_2O, 50 mL) and washed sequentially with a saturated solution of $NaHSO_4$ and brine. The organic phase was dried over Na_2SO_4, filtered, and concentrated under reduced pressure. The residue was purified by flash chromatography using n-hexane and EtOAc (70/30, Rf = 0.19) as the eluent. Isolated 0.380 g of 2,2,2-trifluoro-1-(1-(4-methoxyphenyl)-4,6-dihydrobenzo[c][1,2,3]triazolo[4,5-e]azepin-5(1H)-yl)ethan-1-one with a yield of 98%.

Step 5. Synthesis of (2-Bromophenyl)methanol

In a 50 mL flask equipped with a magnetic stirrer, 2-bromobenzaldehyde (1.22 g, 6.63 mmol, 1.00 equiv.) was dissolved in methanol (MeOH, 10 mL). The solution was cooled using an ice bath, and sodium borohydride ($NaBH_4$, 0.98 g, 26.53 mmol, 4.00 equiv.) was added gradually. The reaction mixture was then allowed to warm to room temperature and monitored by TLC (n-hexane/EtOAc, 80/20). After the completion of reaction quenched the reaction by the dropwise addition of water (15 mL) under 0°C. The reaction mixture was then diluted with diethyl ether (50 mL) and washed brine. The organic phase was dried over anhydrous Na_2SO_4, filtered, and

evaporated under reduced pressure. Isolated 1.14 g of (2-bromophenyl)methanol with a yield of 94%.

Step 6. Synthesis of 1-Bromo-2-((prop-2-ynyloxy)methyl)benzene

In a 50 mL two-neck flask equipped with a magnetic stirrer, 5 mL of *n*-hexane and sodium hydride (NaH, 60% in mineral oil, 0.76 g, 19.04 mmol, 1.2 equiv.) were added under an inert argon atmosphere and stirred for 10 minutes. The stirring was then stopped to allow the removal of hexane containing dissolved mineral oil using a Pasteur pipette. After activation of NaH, anhydrous DMF (10 mL) was added at 0 °C, followed by the dropwise addition of (2-bromophenyl)methanol (2.97 g, 15.87 mmol, 1.0 equiv.) previously dissolved in 2 mL of anhydrous DMF. Propargyl bromide (80% in toluene, 2052 µL, 19.04 mmol, 1.2 equiv.) was added dropwise using a dropping funnel while maintaining temperature control with an ice bath. After the addition of propargyl bromide was complete, the reaction mixture was allowed to warm to room temperature and stirred for 1 hour until the complete consumption of the starting material, (2-bromophenyl) methanol, as monitored by TLC using n-hexane/EtOAc (80/20) as the eluent. The resulting mixture was quenched with water under 0^{o}C. The reaction mixture was then diluted with diethyl ether, and the organic phase was washed with 5% $KHSO_4$ solution, brine, dried over Na_2SO_4, filtered, and concentrated under reduced pressure. The residue was purified by flash column chromatography using silica gel and n-hexane/EtOAc (90/10, Rf = 0.21) as the eluent. Isolated 3.51 g of 1-bromo-2-((prop-2-ynyloxy)methyl)benzene with a yield of 98.31%.

One-Pot Synthesis Procedure

In a 50 mL Carousel reactor (Radley Discovery Technology) equipped with a magnetic stirrer and maintained under an inert argon atmosphere, N-(2-bromobenzyl)-2,2,2-trifluoro-N-(prop-2-yn-1-yl)acetamide (0.167 g, 0.5 mmol, 1 equiv.) was dissolved in anhydrous DMA (3 mL). Subsequently, copper(I) iodide (CuI, 0.019 g, 0.1 mmol, 0.20 equiv.), 1-azido-4-methoxybenzene (0.73 g, 0.5 mmol, 1 equiv.), ($Pd(OAc)_2$, 0.011 g, 0.05 mmol, 0.010 equiv.), DavePhos (0.040 g, 0.1 mmol, 0.2 equiv.), and cesium acetate (Cs(OAc), 0.198 g, 1.00 mmol, 2.00 equiv.) were added. The reaction mixture was stirred at 120 °C under an inert atmosphere for 1 hour until complete consumption of the starting material, N-(2-bromobenzyl)-2,2,2-trifluoro-N-(prop-2-yn-1-yl) acetamide, as monitored by thin-layer chromatography (TLC) using *n*-hexane/ethyl acetate (80/20) as the eluent. After the reaction, the mixture was diluted with diethyl ether and washed with brine The organic phase was dried over anhydrous Na_2SO_4, filtered, and concentrated under reduced pressure. The crude product was purified by flash

chromatography using n-hexane/EtOAc (70/30, Rf = 0.19), isolated the final product with a 54% yield.

Characterization

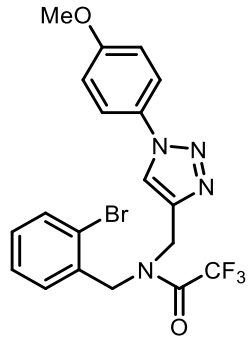

(6.4a)N-(2-bromobenzyl)-2,2,2-trifluoro-N-((1-(4-methoxyphenyl)-1H-1,2,3-triazol-4-yl) methyl)acetamide: Brown liquid; **Yield:** 99%

^{1}H NMR ($CDCl_3$): δ 7.91 (isomer E, s, 1H), 7.73 (isomer Z, s, 1H), 7.57-7.45 (m, 3H), 7.53 (m, 1H), 7.33-7.06 (m, 3H), 6.97-6.90 (m, 2H), 4.80 (isomer E, s, 2H), 4.79 (isomer Z, s, 2H), 4.66 (isomer Z, s, 2H), 3.81-7.75 (m, 3H).

^{13}C NMR ($CDCl_3$): δ 160.3 (isomer Z, C), 160.2 (isomer E, C), 158.2 (isomer E, q, *J* = 36.3 Hz, C), 157.3 (isomer Z, q, *J* = 36.3 Hz, C), 142.9 (C), 142.6 (C), 134.1 (C), 134.1 (C), 133.6 (CH), 133.5 (CH), 130.5 (C) 130.4 (C), 129.86 (CH), 129.81 (CH), 129.7 (CH), 128.19 (CH), 128.13 (CH), 127.6 (CH), 124.0 (C), 123.1 (C), 121.2 (CH), 116.9 (isomer Z, q *J* = 288.1 Hz, C), 116.4 (isomer Z, q *J* = 288.1 Hz, C) 115.1 (C), 115.0 (C), 55.95 (isomer Z, CH), 55.91 (isomer E, CH), 51.5 (isomer E, q, *J* = 3.1 Hz, CH_2), 49.7 (isomer Z, CH_2), 42.48 (isomer E, CH_2), 42.41 (isomer Z, q, *J* = 3.6 Hz, CH_2).

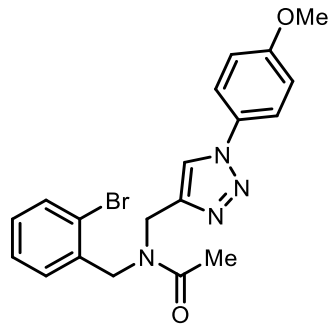

(6.4b) N-(2-bromobenzyl)-N-((1-(4-methoxyphenyl)-1H-1,2,3-triazol-4-yl)methyl) acetamide brownish liquid; **Yield:** 95%

^{1}H NMR ($CDCl_3$): δ 7.94-7.43 (m, 4H) 7.31-7.01 (m, 3H), 6.97-6.90 (m, 2H), 4.74 (isomer Z, s, 2H), 4.65 (isomer E, s, 2H), 4.63 (isomer E, s, 3H) 3.89 (isomer Z, s, 3H), 3.78 (s, 3H), 2.33 (isomer Z, s, 3H) 2.02 (isomer E, s, 3H).

^{13}C NMR ($CDCl_3$): δ 171.8 (isomer E, C), 171.6 (isomer Z, C), 160.2 (C), 160.1 (C), 144.8 (C), 144.6 (C), 136.6 (C), 135.6 (C), 133.6 (CH) 133.1 (CH), 130.1 (C), 130.5 (C), 130.1 (CH), 129.5 (CH), 129.3 (CH), 128.2 (CH), 128.1 (CH), 127.5 (CH), 124.0 (C), 123.1 (C), 122.4 (CH), 122.4 (CH), 121.9 (CH), 120.3 (CH), 55.9 (isomer Z, CH), 55.9 (isomer E, CH_2), 53.0 (isomer E, CH_2), 48.7 (isomer Z, CH_2), 44.0 (isomer Z, CH_2), 41.4 (isomer E, CH_2), 22.2 (isomer Z, CH), 21.8 (isomer E, CH).

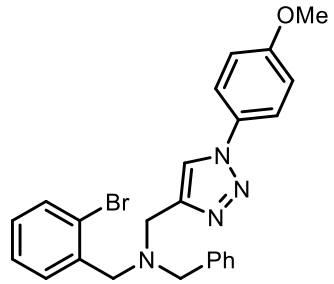

(6.4c) N-benzyl-N-(2-bromobenzyl)-1-(1-(4-methoxyphenyl)-1H-1,2,3-triazol-4-yl)methanamine: Yellow liquid; **Yield:** 94%

^{1}H NMR ($CDCl_3$): δ 7.78 (s, 1H), 7.71 (d, J = 7.75 Hz, 1H), 7.67-7.59 (m, 2H), 7.55 (d, J = 8.07 Hz, 1H), 7.49-7.41 (m, 2H), 7.38-7.23 (m, 4H), 7.12 (t, J_1 = 14.95 Hz, J_2 = 7.20 Hz, 1H), 7.06-7.01 (m, 2H), 3.89 (s, 5H), 3.81 (s, 2H), 3.76 (s, 2H).

^{13}C NMR ($CDCl_3$): δ 160.0 (C), 145.9 (C), 139.3 (C), 138.7 (C), 133.0 (CH), 130.9 (CH), 129.1 (CH), 128.7 (CH), 128.6 (CH), 127.6 (CH), 127.4 (CH), 124.7 (C), 122.4 (CH), 121.2 (CH), 115.0 (CH), 58.4 (CH_2), 57.7 (CH_2), 55.9 (CH), 48.5 (CH_2).

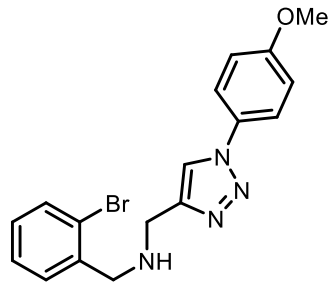

(6.4d) N-(2-bromobenzyl)-1-(1-(4-methoxyphenyl)-1H-1,2,3-triazol-4-yl)methanamine: Yellow solid; **Yield:** 91%

^{1}H NMR (DMSO): δ 8.58 (s, 1H), 7.86-7-74 (m, 2H), 7.67-7.59 (m, 2H), 7.64-7.55 (m, 2H), 7.38 (td, J_1 = 14.96 Hz, J_2 = 7.82 Hz, J_3 = 1.63 Hz, 1H), 7.16-7.08 (m, 1H), 7.38-7.23 (m, 4H), 3.86 (s, 2H), 3.83 (s, 5H), 2.71 (bs, 1H).

^{13}C NMR (DMSO): δ 158.9 (C), 147.0 (C), 139.1 (C), 132.1 (CH), 130.1 (C), 129.8 (CH), 128.5 (CH), 127.4 (CH), 123.1 (C), 121.4 (CH), 120.8 (CH), 114.7 (CH), 55.4 (CH), 51.8 (CH_2), 43.4 (CH_2).

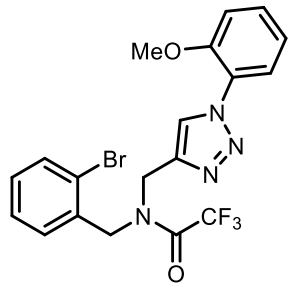

(6.4e) N-(2-bromobenzyl)-2,2,2-trifluoro-N-((1-(2-methoxyphenyl)-1H-1,2,3-triazol-4-yl)methyl)acetamide: Yellow liquid; **Yield:** 87%

^{1}H NMR ($CDCl_3$): δ 8.19 (isomer E, s, 1H), 8.04 (isomer Z, s, 1H) 7.82-7.74 (m, 1H), 7.61 (isomer E, d, J = 7.82, 1H), 7.58 (isomer Z, d, J = 7.82, 1H), 7.47-7.05 (m, 6H), 4.89 (s, 2H), 4.79 (isomer Z, s, 2H), 4.72 (isomer E, s, 2H), 3.90 (isomer Z, s, 3H) 3.89 (isomer E, s, 3H).

^{13}C NMR ($CDCl_3$): δ 158.2 (isomer E, q, J = 37.2 Hz, C), 157.3 (isomer Z, q, J = 37.2 Hz, C), 151.3 (C), 151.3 (C), 141.8 (C), 141.6 (C), 134.3 (C), 134.2 (C), 133.6 (CH) 133.5 (CH), 130.7 (CH), 130.5 (CH), 129.8 (CH), 129.8 (CH), 129.7 (CH), 128.1 (CH), 128.1 (CH), 127.5 (CH), 126.4 (C), 126.3 (C), 126.1 (CH), 125.7 (CH), 125.0 (CH), 125.0 (CH), 124.1 (C), 123.1 (C), 121.6 (CH), 121.5 (CH), 116.9 (isomer Z, q, J = 287.7 Hz, C), 116.6 (isomer E, q, J = 287.7 Hz, C), 112.6 (CH), 112.5 (CH), 56.3 (isomer Z, CH) 56.2 (isomer E, CH), 51.4 (isomer E, q, J = 3.4 Hz, CH_2), 49.7 (isomer Z, CH_2), 42.4 (isomer E, CH_2), 42.3 (isomer Z, q, J = 3.74 Hz, CH_2).

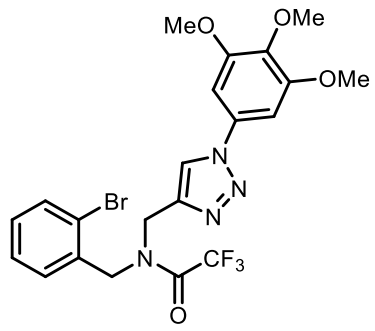

(6.4f) N-(2-bromobenzyl)-2,2,2-trifluoro-N-((1-(3,4,5-trimethoxyphenyl)-1H-1,2,3-triazol-4-yl)methyl)acetamide: Yellow solid; **Yield:** 98%; **b.p**: 136-138;

^{1}H NMR ($CDCl_3$): δ 7.48 (isomer E, d, *J* = 7.32 Hz, 1H), 7.37 (isomer Z, d, *J* = 7.32 Hz, 1H), 7.33-7.05 (m, 2H), 6.94 (isomer Z, d, *J* = 7.78 Hz, 1H), 6.89 (isomer E, d, *J* = 7.78 Hz, 1H), 6.46 (s, 2H), 5.12 (isomer E, s, 2H), 4.89 (isomer Z, s, 2H), 4.59 (isomer E, s, 2H), 4.57 (isomer Z, s, 2H), 3.80 (isomer E, s, 3H), 3.80 (isomer Z, s, 3H), 3.65 (isomer E, s, 6H), 3.64 (isomer Z, s, 6H).

^{13}C NMR ($CDCl_3$): δ 156.5 (isomer E, q, *J* = 36.6 Hz, C), 154.4 (isomer Z, q, *J* = 36.6 Hz, C), 154.1 (C), 154.0 (C), 141.1 (C), 141.0 (C), 139.4 (C), 139.4 (C), 135.5 (C) 135.1 (C), 132.6 (C), 132.4 (C), 132.3 (C), 132.3 (C), 132.0 (C), 131.5 (CH), 130.5 (CH), 130.5 (CH), 130.1 (CH), 129.7 (CH), 129.1 (CH), 128.7 (CH), 128.5 (CH), 126.0 (C), 124.8 (C), 116.6 (isomer Z, q, *J* = 287.7 Hz, C), 116.5 (isomer E, q, *J* = 287.7 Hz, C), 103.7 (CH), 103.3 (CH), 61.4 (CH), 56.6 (CH), 50.0 (isomer E, CH_2), 49.0 (isomer Z, CH_2).

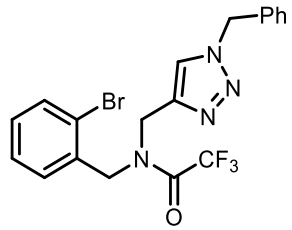

(6.4g) N-((1-benzyl-1H-1,2,3-triazol-4-yl)methyl)-N-(2-bromobenzyl)-2,2,2-trifluoro acetamide: Yellowish solid; **Yield:** 86%; **m.p**: 96-98;

^{1}H NMR ($CDCl_3$): δ 7.54-7.44 (m, 1H), 7.37-7.28 (m, 3H), 7.28-7.16 (m, 4H), 7.15-7.09 (m, 1H), 7.08-7.02 (m, 1H), 5.44 (isomer Z, s, 2H), 5.43 (isomer E, s, 2H), 4.76 (isomer E, s, 2H), 4.72 (isomer Z, s, 2H), 4.57 (isomer Z, s, 2H), 4.51 (isomer E, s, 2H).

^{13}C NMR ($CDCl_3$): δ 158.2 (isomer E, q, *J* = 36.36 Hz, C), 157.3 (isomer Z, q, *J* = 36.3 Hz, C), 142.9 (C), 142.6 (C), 134.6 (C), 134.5 (C), 134.2 (C), 134.1 (C), 133.6 (CH) 133.5 (CH), 129.8 (CH), 129.7 (CH), 129.6 (CH), 129.5 (CH), 129.5 (CH), 129.3 (CH), 129.2 (CH), 128.5 (CH), 128.4 (CH), 128.1 (CH), 128.1 (CH), 127.5 (CH), 124.0 (C), 123.8 (CH), 123.1 (C), 122.5 (CH), 122.5 (CH), 116.8 (isomer Z, q, *J* = 288.2 Hz, C), 116.8 (isomer E, q, *J* = 288.2 Hz, C), 54.6 (isomer Z, CH_2), 54.6 (isomer E, CH_2), 51.5 (isomer E, q, *J* = 3.3 Hz, CH_2), 49.6 (isomer Z, CH_2), 42.5 (isomer E, CH_2), 42.4 (isomer E, q, *J* = 3.6 Hz, CH_2).

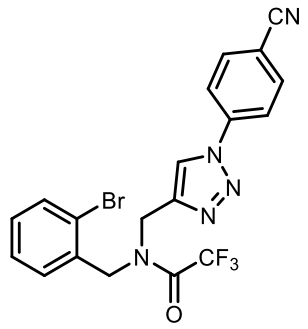

(6.4h) N-(2-bromobenzyl)-N-((1-(4-cyanophenyl)-1H-1,2,3-triazol-4-yl)methyl)-2,2,2-trifluoroacetamide: Yellowish solid; **Yield:** 93%; **m.p**: 181-183°;

^{1}H NMR ($CDCl_3$): δ 8.06 (s, 1H), 7.85-7.72 (m, 4H), 7.53 (isomer E, dd, J_1 = 7.8 Hz, J_2 = 0.9 Hz, 1H), 7.43 (isomer Z, dd, J_1 = 7.89 J_2=0.9, 1H), 7.48-7.04 (m, 6H), 4.89 (s, 2H), 4.76 (isomer Z, s, 2H), 4.72 (isomer E, s, 2H), 3.90 (isomer Z, s, 3H) 3.89 (isomer E, s, 3H).

^{13}C NMR ($CDCl_3$): δ 158.4 (isomer E, q, *J* = 36.9, C), 157.3 (isomer Z, q, *J* = 36.9, C), 144.1 (C), 143.7 (C), 139.9 (C), 139.7 (C), 134.3 (CH), 134.3 (CH), 134.0 (C) 133.9 (C), 133.7 (CH), 133.6 (CH), 130.0 (CH), 130.0 (CH), 129.9 (CH), 128.3 (CH), 128.2 (CH), 127.8 (CH), 124.2 (C), 123.3 (C), 122.0 (CH), 121.0 (CH), 120.9 (CH), 120.6 (CH), 120.6 (CH), 117.9 (C), 117.8 (C), 116.9 (isomer Z, q, *J* = 288.1 Hz, C), 116.5 (isomer E, q, *J* = 288.1 Hz, C), 113.2 (C), 113.0 (C), 51.7 (isomer E, q, *J* = 3.7 Hz, CH_2), 49.8 (isomer Z, CH_2), 42.4 (isomer E, CH_2), 42.3 (isomer Z, q, *J* = 3.6 Hz, CH_2).

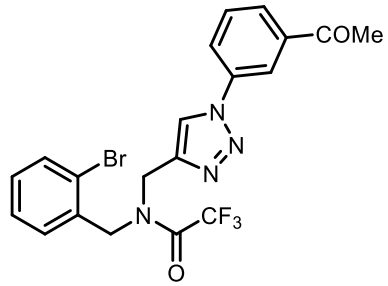

(6.4i) N-((1-(3-acetylphenyl)-1H-1,2,3-triazol-4-yl)methyl)-N-(2-bromobenzyl)-2,2,2-trifluoroacetamide: Yellowish solid; **Yield:** 88%; **m.p**: 116-118;

^{1}H NMR ($CDCl_3$): δ 8.19 (isomer E, t, *J* = 1.84 Hz, 1H) , 8.14 (isomer Z, t, J = 1.84 Hz, 1H), 7.44 (m, 1H), 8.07-7.82 (m, 3H), 7.60-7.45 (m, 2H), 7.32-7.06 (m, 3H), 4.79 (s, 2H), 4.68 (isomer Z, s, 2H), 4.59 (isomer E, s, 2H), 2.58 (isomer Z, s, 3H) 2.58 (isomer E, s, 3H).

^{13}C NMR ($CDCl_3$): δ 196.8 (isomer E, C), 196.8 (isomer Z, C), 158.3 (isomer E, q, *J* = 36.0 Hz, C), 157.4 (isomer Z, q, *J* = 36.08 Hz, C), 143.7 (C), 143.2 (C), 138.8 (C), 137.5 (C), 137.4 (C), 134.1 (C), 134.1 (C) 133.7 (C), 133.6 (CH), 130.7 (CH), 130.6 (CH), 130.0 (CH), 129.9 (CH), 129.8 (CH), 129.1 (CH), 128.9 (CH), 128.2 (CH), 128.2 (CH), 127.7 (CH), 125.1 (CH), 125.0 (C), 124.2 (CH), 123.2 (C), 122.2 (CH), 120.9 (CH), 120.2 (CH), 120.0 (CH), 116.9 (isomer Z, q, *J* = 288.6 Hz, C), 116.5 (isomer E, q, *J* = 288.6 Hz, C), 51.6 (isomer E, q, *J* = 3.6 Hz, CH_2), 49.8 (isomer Z, CH_2), 42.4 (isomer E, CH_2), 42.4 (isomer Z, CH_2), 27.1 (CH)

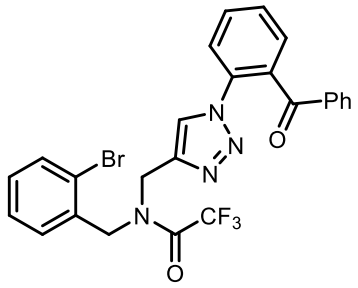

(6.4j) N-((1-(2-benzoylphenyl)-1H-1,2,3-triazol-4-yl)methyl)-N-(2-bromobenzyl)-2,2,2-trifluoroacetamide: Yellow solid; **Yield:** 96%

^{1}H NMR ($CDCl_3$): δ 7.75-7.43 (m, 8H), 7.43-7.34 (m, 1H), 7.27-7.17 (m, 1H), 7.12-6.92 (m, 2H), 4.51 (isomer E, s, 2H), 4.49 (isomer E, s, 2H), 4.41 (isomer Z, s, 2H), 4.37 (isomer E, s, 2H)

^{13}C NMR ($CDCl_3$): δ 194.8 (C), 194.7 (C), 158.1 (isomer E, q, *J* = 36.6 Hz, C), 157.0 (isomer Z, q, *J* = 36.6 Hz, C), 142.8 (C), 142.6 (C), 136.6 (C), 136.3 (C), 135.1 (C), 135.0 (C), 135.0 (C) 134.9 (C), 134.1 (CH), 134.0 (C), 134.0 (C), 133.6 (CH), 133.6 (CH), 133.5 (CH), 132.0 (CH), 132.0 (CH), 130.5 (CH), 130.4 (CH), 130.2 (CH), 130.0 (CH), 130.0 (CH), 129.9 (CH), 129.8 (CH), 129.6 (CH), 129.5 (CH), 128.8 (CH), 128.6 (CH), 128.2 (CH), 128.1 (CH), 127.5 (CH), 125.1 (CH), 124.7 (CH), 124.3 (CH), 124.3 (CH), 124.1 (C), 116.6 (isomer Z, q, *J* = 287.6 Hz, C), 116.5 (isomer E, q, *J* = 287.6 Hz, C), 51.3 (isomer Z, q, *J* = 3.4 Hz, CH_2), 49.3 (isomer E, CH_2), 42.1 (isomer E, CH_2), 42.5 (isomer Z, q, *J* = 3.4 Hz, CH_2).

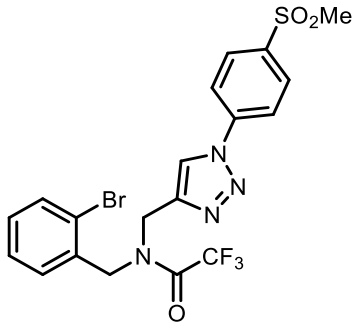

(6.4k) N-(2-bromobenzyl)-2,2,2-trifluoro-N-((1-(4-(methylsulfonyl)phenyl)-1H-1,2,3-triazol-4-yl) methyl)acetamide: Brown solid; **Yield:** 87%; **m.p**: 192-194;

^{1}H NMR ($CDCl_3$): δ 8.13 -7.98 (m, 3H), 7.92-7.94 (m, 2H), 7.52 (isomer E, d, *J* = 7.96 Hz, 1H), 7.46 (isomer Z, d, *J* = 7.96 Hz, 1H), 7.32-7.06 (m, 3H), 4.79 (isomer E, s, 2H), 4.78 (isomer E, s, 2H), 4.67 (isomer Z, s, 2H), 4.58 (isomer E, s, 2H), 3.01 (s, 3H).

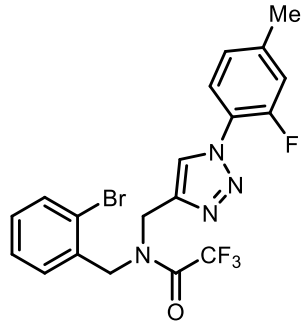

(6.4l) N-(2-bromobenzyl)-2,2,2-trifluoro-N-((1-(2-fluoro-4-methylphenyl)-1H-1,2,3-triazol-4-yl)methyl)acetamide: brownish liquid; **Yield:** 95%

^{1}H NMR ($CDCl_3$): δ 8.02 (isomer E, d, *J* = 2.54 Hz, 1H), 7.86 (isomer Z, d, *J* = 1.96 Hz, 1H), 7.76-7.65 (m, 1H), 7.54 (isomer E, d, *J* = 7.87 Hz, 1H), 7.50 (isomer Z, d, *J* = 7.87 Hz, 1H), 7.37-7.22 (m, 1H), 7.22-6.99 (m, 4H), 4.82 (bs, 2H), 4.68 (isomer Z, s, 2H), 4.63 (isomer E, s, 2H), 2.36 (isomer Z, s, 3H), 2.36 (isomer E, s, 3H).

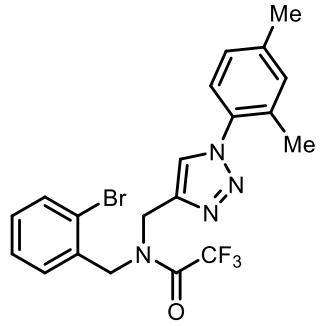

(6.4m) N-(2-bromobenzyl)-N-((1-(2,4-dimethylphenyl)-1H-1,2,3-triazol-4-yl)methyl)-2,2,2-trifluoroacetamide: brownish liquid; **Yield:** 93%**.**

^{1}H NMR ($CDCl_3$): δ 7.72-7.47 (m, 2H), 7.32-7.21 (m, 1H), 7.21-7.02 (m, 5H), 4.83 (s, 2H), 4.69 (isomer Z, s, 2H), 4.63 (isomer E, s, 2H), 2.31 (s, 2H), 2.07 (isomer, E s, 3H), 2.04 (isomer Z, s, 3H)

^{13}C NMR ($CDCl_3$): δ 158.2 (isomer E, q, *J* = 36.1 Hz, C), 157.3 (isomer Z, q, *J*,= 36.1 Hz, C), 142.1 (C), 141.8 (C), 140.6 (C), 140.3 (C), 134.2 (C), 134.1 (C), 134.1 (C) 134.0 (C), 133.6 (CH), 133.5 (CH), 133.5 (C), 133.4 (C), 132.4 (CH), 132.3 (CH), 129.8 (CH), 129.8 (CH), 129.7 (CH), 128.1 (CH), 128.14 (CH), 127.7 (CH), 127.7 (CH), 127.6 (CH), 125.9 (CH), 125.5 (CH), 124.3 (CH), 124.3 (CH), 124.0 (C), 123.1 (C), 116.9 (isomer Z, q, *J* = 287.47 Hz, C), 116.5 (isomer E, q, *J* = 287.4 Hz, C), 51.63 (isomer E, q, *J* = 3.8 Hz, CH_2), 49.8 (isomer Z, CH_2), 42.5 (isomer E, CH_2), 42.4 (isomer Z, q, *J* = 3.7 Hz, CH_2), 21.4 (CH), 18.0 (CH), 17.9 (CH)

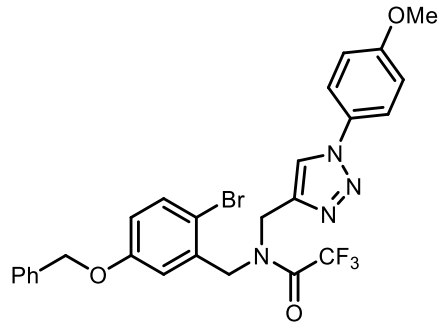

(6.4n) N-(5-(benzyloxy)-2-bromobenzyl)-2,2,2-trifluoro-N-((1-(4-methoxyphenyl)-1H-1,2,3-triazol-4-yl)methyl)acetamide: Yellow solid; **Yield:** 88%; **m.p**: 100-102° ;

^{1}H NMR ($CDCl_3$): δ 7.86 (isomer E, s, 1H), 7.62 (isomer Z, s, 1H), 7.53-7.45 (m, 2H), 7.38 (isomer E, d, *J* = 8.75 Hz, 1H), 7.33 (isomer Z, d, *J* = 8.75 Hz, 1H), 7.31-7.18 (m, 5H), 6.94-6.86 (m, 2H), 6.79-6.61 (m, 2H), 4.93 (s, 2H), 4.71 (isomer Z, s, 2H), 4.70 (isomer E, s, 2H), 4.60 (isomer Z, s, 2H), 4.49 (isomer E, s, 2H), 3.76 (isomer Z, s, 3H), 3.76 (isomer E s, 3H).

^{13}C NMR ($CDCl_3$): δ 160.3 (C), 160.2 (C), 158.7 (C), 158.6 (C), 158.3 (isomer E, q, *J*= 36.6 Hz, C), 157.3 (isomer Z, q, *J* = 36.6 Hz, C), 150.3 (C), 142.9 (C), 142.6 (C), 136.6 (C), 136.5 (C), 136.5 (CH), 135.2 (C) 135.2 (C), 134.2 (CH), 134.1 (CH), 130.5 (C), 130.4 (C), 129.0 (CH), 128.9 (CH), 128.5 (CH), 128.4 (CH), 127.8 (CH), 127.7 (CH), 122.6 (CH), 122.4 (CH), 122.3 (CH), 127.7 (CH), 123.8 (CH), 122.5 (CH), 116.9 (isomer Z, q *J* = 288.0 Hz, C), 116.5 (isomer E, q, *J* = 288.0 Hz, C), 116.6 (CH), 116.1 (CH), 115.9 (CH), 115.1 (CH), 115.1 (CH), 114.9 (CH), 114.5 (C), 113.4 (C), 70.7 (isomer E, CH_2), 70.5 (isomer Z, CH_2), 55.9 (isomer Z, CH_2), 55.9 (isomer E, CH_2), 51.6 (isomer E, q, *J* = 3.6 Hz, CH_2), 49.8 (isomer Z, CH_2), 42.6 (isomer E, CH_2), 42.5 (isomer Z, q, *J* = 3.20 Hz, CH_2).

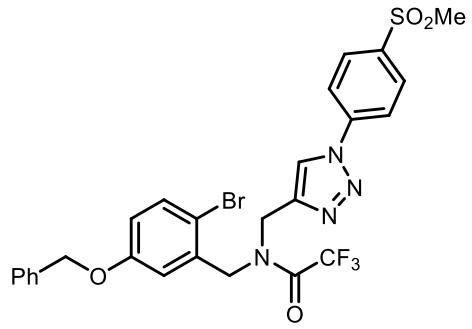

(6.4o) N-(5-(benzyloxy)-2-bromobenzyl)-2,2,2-trifluoro-N-((1-(4-(methylsulfonyl)phenyl)-1H-1,2,3-triazol-4-yl)methyl)acetamide: brownish liquid; **Yield:** 86%;

^{1}H NMR ($CDCl_3$): δ 8.12-8.00 (m, 2H), 7.95-7.79 (m, 2H), 7.46-7.16 (m, 7H), 6.85-6.65 (m, 2H), 4.97 (s, 2H), 4.78-4.72 (m, 2H), 4.66 (isomer Z, s, 2H), 4.53 (isomer E, s, 2H), 3.04 (s, 3H).

^{13}C NMR ($CDCl_3$): δ 158.5 (C), 153.3 (C), 158.0 (q, *J*= 36.6, C), 143.7 (C), 143.3 (C), 140.8 (C), 140.6 (C), 140.4 (C), 140.3 (C), 136.2 (C) 136.1 (C), 134.8 (C), 134.6 (C), 134.0 (CH), 133.8 (CH), 129.5 (CH), 129.5 (C), 128.7 (CH), 128.7 (CH), 128.3 (CH), 128.3 (CH), 128.2 (CH), 127.5 (CH), 127.4 (CH), 121.9 (CH), 120.9 (CH), 120.8 (CH), 116.5 (isomer Z, q, *J* = 288.3 Hz, C), 116.1 (isomer E, q, *J* = 288.3 Hz, C), 116.4 (CH), 116.0 (CH), 115.7 (CH), 113.2 (C), 70.4 (isomer E, CH_2), 51.4 (isomer E, q, *J* = 3.5 Hz, CH_2), 49.6 (isomer Z, CH_2), 44.5 (CH), 42.1 (isomer E, CH_2), 42.0 (isomer Z, q, *J* = 3.53 Hz, CH_2).

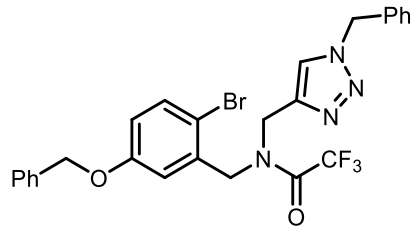

(6.4p) N-((1-benzyl-1H-1,2,3-triazol-4-yl)methyl)-N-(5-(benzyloxy)-2-bromobenzyl)-2,2,2-trifluoroacetamide: Yellow solid; **Yield:** 87%; **m.p**: 97-99;

^{1}H NMR ($CDCl_3$): δ 7.53 (isomer E, s, 1H), 7.49 (isomer Z, s, 1H), 7.48-7.37 (m, 7H), 7.46-7.16 (m, 7H), 7.36-7.24 (m, 4H), 6.89-6.70 (m, 2H), 5.52 (isomer Z, s, 2H), 5.51 (isomer E, s, 2H), 5.06 (m, 2H), 4.76 (bs, 2H), 4.61 (isomer Z, s, 2H), 4.52 (isomer E, s, 2H)

^{13}C NMR ($CDCl_3$): δ 158.7 (C), 158.6 (C), 158.1 (isomer E, q, *J*= 36.7 Hz, C), 157.34 (isomer Z, q, *J* = 36.7 Hz, C), 142.8 (C), 142.5 (C), 136.6 (C), 136.5 (C), 135.3 (C), 135.1 (C), 134.5 (C) 134.5 (C), 134.2 (CH), 134.1 (CH), 129.5 (CH), 129.5 (CH), 129.2 (CH), 129.2 (CH), 129.0

(CH), 128.9 (CH), 128.5 (CH), 128.5 (CH), 128.4 (CH), 128.3 (CH), 127.8 (CH), 127.7 (CH), 123.8 (CH), 122.59 (CH), 116.8 (isomer Z, q, *J* = 288.2 Hz, C), 116.5 (isomer E, q, *J* = 288.3 Hz, C), 116.6 (CH), 116.0 (CH), 115.9 (CH), 114.8 (CH), 114.4 (C), 113.4 (C), 70.7 (isomer E, CH_2), 70.5 (isomer Z, CH_2), 54.6 (isomer Z, CH_2), 54.6 (isomer E, CH_2), 51.4 (isomer E, q, *J* = 3.6 Hz, CH_2), 49.6 (isomer Z, CH_2), 42.4 (isomer E, CH_2), 42.3 (isomer Z, q, *J* = 3.8 Hz, CH_2)

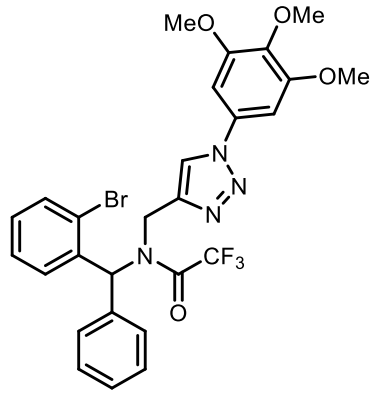

(6.4q) N-((2-bromophenyl)(phenyl)methyl)-2,2,2-trifluoro-N-((1-(3,4,5-trimethoxyphenyl)-1H-1,2,3-triazol-4-yl)methyl)acetamide: Brownish liquid; **Yield:** 99%;

^{1}H NMR ($CDCl_3$): δ 7.82 (s, 1H) 7.52-7.42 (m, 2H), 7.38-7.30 (m, 2H), 7.27-7.21 (m, 3H), 7.20-7.16 (m, 1H), 7.05 (td, J_1 = 15.28 Hz, J_2 = 7.73 Hz, J_3 = 1.56 Hz, 1H), 6.82 (s, 2H), 5.87 (s, 1H), 4.72-4.63 (m, 2H), 3.82 (s, 6H), 3.78 (s, 3H)

^{13}C NMR ($CDCl_3$): δ 154.2 (C), 146.0 (C), 140.8 (C), 140.3 (C), 138.6 (C), 133.2 (C), 133.2 (C) 129.5 (CH), 129.1 (CH), 128.7 (CH), 128.2 (CH), 128.1 (CH), 127.8 (CH), 123.9 (C), 121.5 (CH), 98.8 (CH), 82.0 (CH), 63.2 (CH_2), 61.3 (CH), 56.7 (CH)

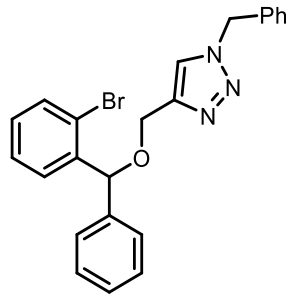

(6.8a) 1-benzyl-4-(((2-bromophenyl)(phenyl)methoxy)methyl)-1H-1,2,3-triazole: yellow solid; **Yield:** 99%;

^{1}H NMR ($CDCl_3$): δ 7.60-7.50 (m, 2H), 7.47 (s,1H), 7.44-7.36 (m, 5H), 7.36 (m, 6H), 7.13 (td, J_1 = 15.58 Hz, J_2 = 7.62 Hz, J_3 = 1.72 Hz, 1H), 5.91 (s, 1H), 5.53 (s, 2H), 4.71 (d, J = 12.25 Hz, 1H), 4.67 (d, J = 12.25 Hz, 1H).

^{13}C NMR ($CDCl_3$): δ 145.7 (C), 140.9 (C), 140.4 (C), 134.9 (C), 133.1 (CH), 129.4 (CH), 129.4 (CH) 129.1 (CH), 129.0 (CH), 128.6 (CH), 128.44 (CH), 128.0 (CH), 127.7 (CH), 123.8 (C), 122.8 (CH), 81.6 (CH), 62.1 (CH_2), 54.4 (CH_2).

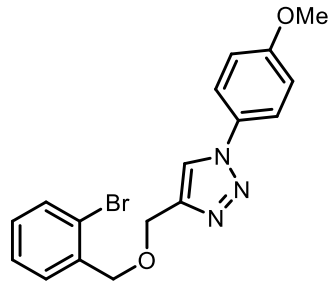

(6.8b) 4-(((2-bromobenzyl)oxy)methyl)-1-(4-methoxyphenyl)-1H-1,2,3-triazole: Yellow solid; **Yield:** 82%; **m.p**: 131-133°;

^{1}H NMR ($CDCl_3$): δ 7.83 (s, 1H) 7.56-7.48 (m, 2H), 7.44 (dd, J_1 = 8.03 Hz, J_2 = 0.85 Hz, 1H), 7.41 (m, 1H), 7.21 (td, J_1 = 14.79 Hz, J_2 = 7.39 Hz, J_3 = 1.13 Hz, 1H), 7.15 (s, 1H), 7.05 (td, J_1 = 15.46 Hz, J_2 = 7.99 Hz, J_3 = 1.86 Hz, 1H), 6.94-6.87 (m, 2H), 4.73 (s, 2H), 4.61 (s, 2H), 3.76 (s, 3H).

^{13}C NMR ($CDCl_3$): δ 160.1 (C), 145.8 (C), 132.9 (CH), 130.8 (C), 129.8 (CH), 129.5 (CH), 127.7 (CH) 123.3 (C), 122.5 (CH), 121.3 (CH), 115.1 (CH), 72.2 (CH_2), 64.5 (CH_2), 55.9 (CH).

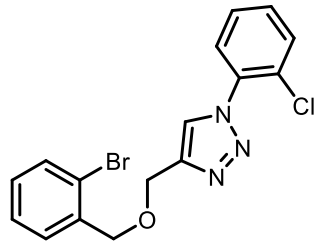

(6.8c) 4-(((2-bromobenzyl)oxy)methyl)-1-(2-chlorophenyl)-1H-1,2,3-triazole: Brown solid; **Yield:** 82%;

^{1}H NMR ($CDCl_3$): δ 7.93 (s, 1H) 7.54-7.49 (m, 1H), 7.49-7-40 (m, 3H), 7.38-7.32 (m, 2H), 7.22 (td, J_1 = 15.01 Hz, J_2 = 7.59 Hz, J_3 = 0.91 Hz, 1H), 7.15 (s, 1H), 7.05 (td, J_1 = 15.50 Hz, J_2 = 7.93 Hz, J_3 = 1.71 Hz, 1H), 4.77 (s, 2H), 4.63 (s, 2H)

^{13}C NMR ($CDCl_3$): δ 145.1 (C), 137.4 (C), 135.2 (CH), 132.9 (CH), 131.1 (CH), 129.8 (CH), 129.5 (CH) 128.9 (C), 128.2 (CH), 128.1 (CH), 127.80 (CH), 125.1 (CH), 125.1 (CH), 123.3 (C), 71.9 (CH_2), 64.4 (CH_2)

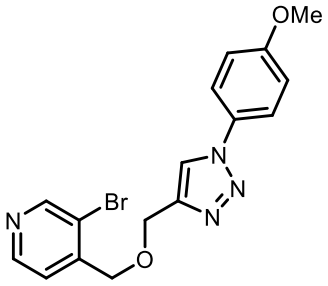

(6.8d) 3-bromo-4-(((1-(4-methoxyphenyl)-1H-1,2,3-triazol-4-yl)methoxy)methyl)pyridine: Yellow solid; **Yield:** 91%; **m.p**: 122-124° ;

^{1}H NMR ($CDCl_3$): δ 8.49 (s, 1H) 8.35 (d, *J* = 4.72 Hz, 1H), 7.81 (s, 1H), 7.52-7.43 (m, 2H), 7.35 (d, *J* = 4.72 Hz, 1H), 6.91-6.83 (m, 2H), 4.71 (s, 2H), 4.53 (s, 2H), 3.71 (s, 3H).

^{13}C NMR ($CDCl_3$): δ 160.2 (C), 151.5 (CH), 148.6 (CH), 146.8 (CH), 145.1 (C), 130.6 (C), 123.1 (CH) 122.5 (CH), 121.4 (C), 120.3 (C), 115.1 (CH), 70.7 (CH_2), 64.8 (CH_2), 55.9 (CH).

Characterization of final product

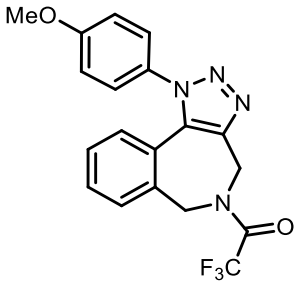

(6.5a) 2,2,2-trifluoro-1-(1-(4-methoxyphenyl)-4,6-dihydrobenzo[c][1,2,3]triazolo[4,5-e]azepin-5 (1H)-yl)ethan-1-one: Yellow solid; **Yield:** 98%, **m.p**: 171-174°;

^{1}H NMR ($CDCl_3$): δ 7.49 (isomer E, d, *J* = 7.56 Hz, 1H), 7.39 (isomer Z, d, *J* = 7.56 Hz, 1H), 7.33-7.03 (m, 4H), 6.95-6.79 (m, 3H), 5.13 (isomer Z, s, 2H), 4.88 (isomer Z, s, 2H), 4.60 (isomer E, s, 2H), 4.58 (isomer Z, s, 2H), 3.79 (isomer E, s, 3H), 3.78 (isomer Z, s, 3H).

^{13}C NMR ($CDCl_3$): δ 160.8 (C), 156.4 (isomer E, q, *J* = 36.8 Hz, C), 156.2 (isomer Z, q, *J* = 36.8 Hz, C), 140.8 (C), 135.4 (C), 135.0 (C), 132.7 (C), 132.3 (C), 131.4 (CH), 130.4 (CH), 130.4

(CH), 129.9 (CH), 129.8 (C), 129.4 (CH), 129.3 (C). 129.1 (CH), 128.5 (CH), 128.5 (CH), 128.2 (CH), 127.3 (CH), 126.9 (CH), 126.2 (C), 125.0 (C), 116.6 (isomer Z, q, *J* = 287.9 Hz, C), 123.7 (isomer E, q, *J* = 287.9 Hz, C), 55.8 (CH), 49.9 (isomer E, CH), 48.8 (isomer Z, q, *J* = 3.6 Hz, CH), 46.43 (isomer E, q, *J* = 4.5 Hz, CH), 44.9 (isomer Z, CH).

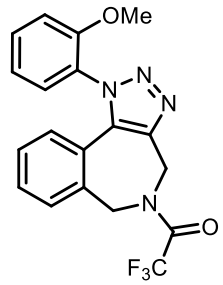

(6.5b) 2,2,2-trifluoro-1-(1-(2-methoxyphenyl)-4,6-dihydrobenzo[c][1,2,3]triazolo[4,5-e]azepin-5 (1H)-yl)ethan-1-one: Brown Solid; **Yield:** 82%%; **m.p**:173-175 °;

^{1}H NMR ($CDCl_3$): δ 7.63-7.40 (m, 3H), 7.38-7.25 (m, 1H), 7.23-7.05 (m, 2H), 7.02-6.86 (m, 2H), 5.31-4.28 (bm, 4H), 3.42 (isomer E, s, 3H), 3,38 (isomer Z, s, 3H).

^{13}C NMR ($CDCl_3$): δ 156.5 (isomer E, q, *J* = 36.5 Hz, C), 156.3 (isomer Z, q, *J* = 36.5 Hz, C), 153.85 (C), 153.63 (C), 140.2 (C), 140.1 (C), 135.0 (C), 134.62 (C), 134.5 (C), 133.94 (C), 132.1 (CH), 131.1 (CH), 130.0 (CH), 130.01 (CH), 129.7 (CH), 129.25 (CH), 129.09 (CH), 128.5 (CH), 128.4 (CH), 127.22 (C), 126.5 (CH), 126.41 (CH), 126.1 (C), 126.0 (C), 125.6 (C), 121.6 (CH), 116.6 (isomer Z, q, *J* = 287.6 Hz, C), 116.5 (isomer E, q, *J* = 287.6 Hz, C), 112.8 (CH), 112.8 (CH), 55.8 (CH), 55.7 (CH), 49.8 (isomer E, CH_2), 48.8 (isomer Z, q, *J* = 3.0 Hz, CH_2), 46.5 (isomer E, q, *J* = 4.3 Hz, CH_2), 45.0 (isomer Z, CH_2).

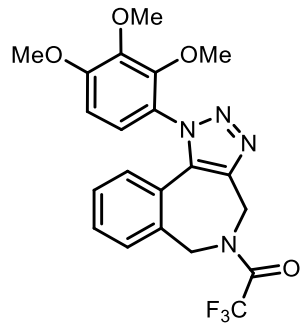

(6.5c) 2,2,2-trifluoro-1-(1-(2,3,4-trimethoxyphenyl)-4,6-dihydrobenzo[c][1,2,3]triazolo[4,5-e]azepin-5(1H)-yl)ethan-1-one: Yellow solid; **Yield:** 87%; **m.p**: 201-203°;

^{1}H NMR ($CDCl_3$): δ 7.48 (isomer E, d, *J* = 7.63 Hz, 2H), 7.37 (isomer Z, d, *J* = 7.47 Hz, 1H), 7.32-7.05 (m, 2H), 6.94 (isomer Z, d, *J* = 7.66 Hz, 2H), 6.89 (isomer E, d, *J* = 7.66 Hz, 1H), 6.46 (s, 2H), 5.12 (isomer E, s, 2H), 4.89 (isomer E, s, 2H), 4.59 (isomer E, s, 2H), 4.57 (isomer Z, s, 2H), 3.81 (isomer E, s, 3H), 3.80 (isomer Z, s, 3H), 3.65 (isomer E, s, 6H), 3.64 (isomer Z, s, 6H).

^{13}C NMR ($CDCl_3$): δ 156.5 (isomer E, q, *J* = 36.5 Hz, C), 156.4 (isomer Z, q, *J* = 36.3 Hz, C), 154.1 (C), 154.0 (C), 141.1 (C), 141.0 (C), 139.4 (C), 139.4 (C), 135.5 (C), 135.1 (C), 132.6 (C), 132.4 (C), 132.3 (C), 132.0 (C), 131.5 (CH), 130.5 (CH), 130.5 (CH), 130.1 (CH), 129.6 (CH), 129.1 (CH), 128.7 (CH), 128.5 (CH), 126.01 (C), 124.8 (C), 116.6 (isomer Z, q, *J* = 287.0 Hz, C), 116.5 (isomer E, q, *J* = 287.0 Hz, C), 103.7 (CH), 103.3 (CH), 61.4 (CH), 56.6 (CH), 50.0 (isomer E, CH_2), 49.0 (isomer Z, q, *J* = 3.2 Hz, CH_2), 46.5 (isomer E, q, *J* = 4.0, CH_2), 45.0 (isomer Z, CH_2).

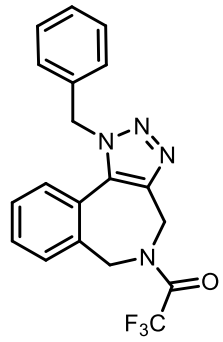

(6.5d) 1-(1-benzyl-4,6-dihydrobenzo[c][1,2,3]triazolo[4,5-e]azepin-5(1H)-yl)-2,2,2-trifluoroethan-1-one: Yellow solid; **Yield:** 92%; **m.p**: 165-167°;

^{1}H NMR ($CDCl_3$): δ 7.55-7.33 (m, 2H), 7.32-7.20 (m, 5H), 7.15-7.02 (m, 2H), 5.65 (isomer E, s, 2H), 5.63 (isomer Z, s, 2H), 5.07 (isomer E, s, 2H), 4.80 (isomer Z, s, 2H), 5.23 (isomer Z, s, 2H), 4.45 (isomer E, s, 2H), 4.37 (isomer Z, s, 2H).

^{13}C NMR ($CDCl_3$): δ 156.5 (isomer E, q, *J* = 36.3 Hz, C), 156.1 (isomer Z, q, *J* = 36.3 Hz, C), 141.0 (C), 135.7 (C), 135.5 (C), 135.4 (C), 135.2 (C), 133.4 (C), 133.1 (C), 131.7 (CH), 130.6 (CH), 130.6 (CH), 130.2 (CH), 129.8 (CH), 129.6 (CH), 129.4 (CH), 129.4 (CH), 129.1 (CH), 128.7 (CH), 128.6 (CH), 127.5 (CH), 127.3 (CH), 126.9 (CH), 126.8 (CH), 126.3 (C), 125.4 (C), 116.6 (isomer Z, q, *J* = 287.1 Hz, C), 116.5 (isomer E, q, *J* = 287.1 Hz, C), 52.9 (CH_2), 52.6 (CH_2), 49.3 (isomer E, CH_2), 48.6 (isomer Z, q, *J* = 3.0 Hz, CH_2), 46.1 (isomer E, q, *J* = 4.2 Hz, CH_2), 44.8 (isomer Z, CH_2).

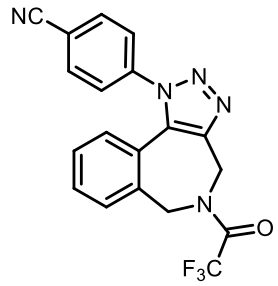

(6.5e) 4-(5-(2,2,2-trifluoroacetyl)-5,6-dihydrobenzo[c][1,2,3]triazolo[4,5-e]azepin-1(4H)-yl)benzonitrile: Yellow solid; **Yield:** 98%; **m.p**: 220-222°;

^{1}H NMR ($CDCl_3$): δ 7.77-7.67 (m, 2H), 7.56-7.40 (m, 3H), 7.35 (isomer Z, td, J_1 = 15.12 Hz, J_2 = 7.50 Hz, J_3 = 0.78 Hz, 1H), 7.28 (isomer E, td, J_1 = 15.12 Hz, J_2 = 7.80 Hz, J_3 = 0.78 Hz, 1H), 7.21 (isomer Z, td, J_1 = 15.36 Hz, J_2 = 7.84 Hz, J_3 = 0.90 Hz, 1H), 7.09 (isomer E, td, J_1 = 15.36 Hz, J_2 = 7.84 Hz, J_3 = 0.90 Hz, 1H), 6.82 (isomer Z, d, J = 7.64 Hz, 1H), 6.75 (isomer E, d, J = 7.64, 1H), 5.13 (isomer E, s, 2H), 4.88 (isomer Z, s, 1H), 4.61 (isomer Z, s, 2H), 4.59 (isomer Z, s, 2H).

^{13}C NMR ($CDCl_3$): δ 156.5 (isomer E, *q*, J = 36.8 Hz, C), 156.3 (isomer Z, *q*, J = 36.8 Hz, C), 141.8 (C), 141.6 (C), 140.3 (C), 139.8 (C), 135.7 (C), 135.2 (C), 133.9 (CH), 132.8 (C), 132.5 (C), 131.9 (CH), 130.8 (CH), 130.87 (CH), 130.7 (CH), 130.21 (CH), 129.5 (CH), 128.8 (CH), 128.4 (CH), 126.52 (CH), 125.9 (CH), 125.4 (C), 124.2 (C), 117.7 (C), 116.6 (isomer Z, *q*, J = 287.4 Hz, C), 116.4 (isomer E, *q*, J = 287.4 Hz, C), 114.1 (C), 114.0 (C), 49.8 (isomer E, CH_2), 48.8 (isomer Z, q, J = 3.0 Hz, CH_2), 46.3 (isomer E, q, J = 4.23 Hz, CH_2), 44.8 (isomer Z, CH_2).

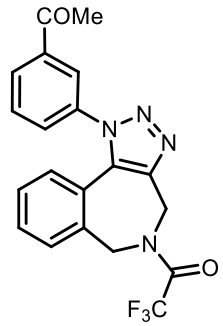

(6.5f) 1-(1-(3-acetylphenyl)-4,6-dihydrobenzo[c][1,2,3]triazolo[4,5-e]azepin-5(1H)-yl)-2,2,2-trifluoroethan-1-one: Yellow solid; **Yield:** 89%; **m.p**: 184-186 °;

^{1}H NMR ($CDCl_3$): δ 8.14-8.05 (m, 1H), 8.01-7.93 (m, 1H), 7.67 -7.46 (m, 3H), 7.39 (isomer Z, td, J_1 = 15.32 Hz, J_2 = 7.48 Hz, J_3 = 1.00 Hz, 1H), 7.32 (isomer E, td, J_1 = 15.32 Hz, J_2 = 7.48 Hz,

J_3 = 1.00 Hz, 1H), 7.23 (isomer Z, td, J_1 = 15.33 Hz, J_2 = 7.72 Hz, J_3 = 1.06 Hz, 1H), 7.11 (isomer E, td, J_1 = 15.33 Hz, J_2 = 7.72 Hz, J_3 = 1.06 Hz, 1H), 6.89 (isomer Z, d, J = 7.74 Hz, 1H), 6.83 (isomer E, d, J = 7.74 Hz, 1H), 5.23 (isomer E, s, 2H), 4.98 (isomer Z, s, 2H), 4.71 (isomer E, s, 2H), 4.69 (isomer Z, s, 2H), 2.58 (s, 3H).

^{13}C NMR ($CDCl_3$): δ 196.5 (C), 156.5 (isomer E, q, J = 36.6 Hz, C), 156.3 (isomer Z, q, J = 36.6 Hz, C), 141.3 (C), 141.3 (C), 138.8 (C), 138.7 (C), 137.5 (C), 137.0 (C), 135.6 (C), 135.2 (C), 132.8 (C), 132.5 (C), 131.8 (CH), 130.75 (CH), 130.7 (CH), 130.4 (CH), 130.3 (CH), 130.2 (CH), 129.8 (CH), 129.8 (CH), 129.7 (CH), 129.7 (CH), 129.2 (CH), 128.6 (CH), 128.5 (CH), 128.2 (CH), 125.7 (C), 125.7 (CH), 125.2 (CH), 124.5 (C), 116.6 (isomer Z, q, J = 287.2 Hz, C), 116.5 (isomer E, q, J = 287.2 Hz, C), 49.9 (isomer E, CH_2), 46.47 (isomer Z, q, J = 3.8 Hz, CH_2), 46.2 (isomer E, q, J = 4.3 Hz, CH_2), 44.9 (isomer Z, CH_2), 26.9 (CH).

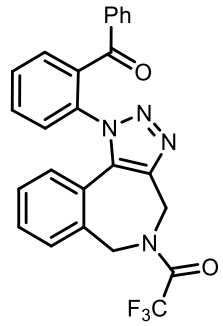

(6.5i) 1-(1-(2-benzoylphenyl)-4,6-dihydrobenzo[c][1,2,3]triazolo[4,5-e]azepin-5(1H)-yl)-2,2,2-trifluoroethan-1-one: Yellow solid; **Yield:** 85%; **m.p**: 184-186°;

^{1}H NMR ($CDCl_3$): δ 7.74-7.55 (m, 3H), 7.55-7.37 (m, 2H), 7.36-7.03 (m, 7H), 7.25-7.10 (m, 2H), 6.88 (isomer Z, d, J = 7.42, 1H), 6.83 (isomer E, d, J = 7.42 Hz, 1H), 4.98 (isomer E, s, 2H), 4.79 (isomer Z, s, 2H), 4.24 (isomer Z, s, 2H), 4.21 (isomer E, s, 2H).

^{13}C NMR ($CDCl_3$): δ 193.3 (isomer E, C), 193.2 (isomer Z, C), 156.6 (isomer E, q, J = 36.8 Hz, C), 156.3 (isomer Z, q, J = 36.8 Hz, C), 140.6 (C), 140.6 (C), 135.7 (C), 135.7 (C), 135.6 (C), 135.4 (C), 135.3 (C), 135.2 (C), 134.3 (C), 133.8 (C), 133.8 (CH), 133.7 (CH), 132.7 (CH), 132.6 (CH), 131.2 (CH), 131.1 (CH), 131.0 (CH), 130.2 (CH), 130.2 (CH), 130.2 (CH), 130.1 (CH), 129.8 (CH), 129.7 (CH), 129.2 (CH), 128.6 (CH), 128.5 (CH), 128.4 (CH), 128.3 (CH), 128.2 (CH), 128.0 (CH), 125.7 (C), 124.5 (C), 116.5 (isomer Z, q, J = 287.3 Hz, C), 116.4 (isomer E, q, J = 287.33 Hz, C), 49.4 (isomer E, CH), 48.4 (isomer Z, q, J = 3.2 Hz, CH), 46.2 (isomer E, q, J = 4.2 Hz, CH), 44.9 (isomer Z, CH).

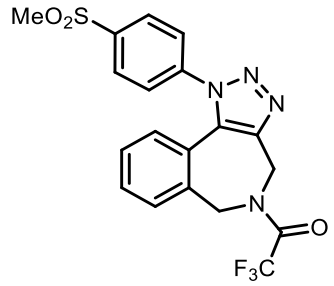

(6.5j)2,2,2-trifluoro-1-(1-(4-(methylsulfonyl)phenyl)-4,6-dihydrobenzo[c][1,2,3] triazolo[4,5-e]azepin-5(1H)-yl)ethan-1-one: Yellow solid; **Yield:** 81%; **m.p**: 212-214°;

^{1}H NMR (CDCl$_3$): δ 8.04-7.91 (m, 2H), 7.58-7.39 (m, 3H), 7.34 (isomer Z, td, J_1 = 15.13 Hz, J_2 = 7.66 Hz, J_3 = 1.08 Hz, 1H), 7.27 (isomer E, td, J_1 = 15.13 Hz, J_2 = 7.66 Hz, J_3 = 1.08 Hz, 1H), 7.20 (isomer Z, td, J_1 = 15.41 Hz, J_2 = 7.66 Hz, J_3 = 1.14 Hz, 1H), 7.09 (isomer E, td, J_1 = 15.41 Hz, J_2 = 7.66 Hz, J_3 = 1.14 Hz, 1H), 6.82 (isomer Z, d, J = 8.00, 1H), 6.75 (isomer E, d, J = 8.00, 1H) 5.13 (isomer Z, s, 2H), 5.12 (isomer E, s, 2H), 4.85 (isomer Z, s, 2H), 4.61 (isomer E, s, 2H), 4.59 (isomer E, s, 3H), 3.02 (s, 3H).

^{13}C NMR (CDCl$_3$): δ 156.4 (isomer E, q, J = 36.8 Hz, C), 156.3 (isomer Z, q, J = 36.8 Hz, C), 141.9 (C), 141.9 (C), 141.7 (C), 141.6 (C), 141.2 (C), 141.7 (C), 135.6 (C), 135.2 (C), 132.9 (C), 132.65 (C), 131.9 (CH), 130.8 (CH). 130.8 (CH), 130.6 (CH), 130.1 (CH), 129.5 (CH), 129.4 (CH), 128.8 (CH), 128.82 (CH), 128.4 (CH), 126.6 (CH), 126.11 (CH), 125.4 (C), 124.2 (C), 116.6 (isomer Z, q, J = 287.5 Hz, C), 116.4 (isomer E, q, J = 287.5 Hz, C), 49.8 (isomer E, CH), 48.8 (isomer Z, q, J = 3.3 Hz, CH), 46.3 (isomer E, q, J = 4.4 Hz, CH), 44.7 (isomer Z, CH), 44.7 (CH).

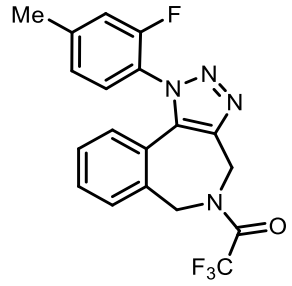

(6.5k) 2,2,2-trifluoro-1-(1-(2-fluoro-4-methylphenyl)-4,6-dihydrobenzo[c][1,2,3]triazolo [4,5-e]azepin-5(1H)-yl)ethan-1-one: Yellow solid; **Yield:** 77%; **m.p**: 168-170°;

^{1}H NMR (CDCl$_3$): δ 7.60-7.42 (m, 2H), 7.37 (isomer Z, td, J_1 = 15.32 Hz, J_2 = 7.52 Hz, J_3 = 1.12 Hz, 1H), 7.32 (isomer E, td, J_1 = 15.32 Hz, J_2 = 7.52 Hz, J_3 = 1.12 Hz, 1H), 7.25-7.10 (m, 2H),

7.02 -6.89 (m, 2H), 5.21 (isomer E, s, 2H), 5.00 (isomer Z, s, 2H), 4.64 (isomer Z, s, 2H), 4.63 (isomer E, s, 2H), 2.46 (isomer E, s, 3H), 2.45 (isomer Z, s, 3H).

^{13}C NMR ($CDCl_3$): δ 157.2 (C), 157.0 (C), 156.5 (isomer E, q, *J* = 36.7 Hz, C), 156.4 (isomer Z, q, *J* = 36.8 Hz, C), 154.7 (C), 154.5 (C), 143.8 (C), 143.7 (C), 140.5 (C), 140.5 (C), 135.4 (C), 135.0 (C), 134.3 (C), 133.8 (C), 131.5 (CH), 130.4 (CH). 130.4 (CH), 130.1 (CH), 129.6 (CH), 129.3 (CH), 128.7 (CH), 128.3 (CH), 128.2 (CH), 126.8 (CH), 126.6 (CH), 126.3 (C), 126.3 (d, *J* = 3.7 Hz), 125.1 (C), 125.1 (C), 122.6 (d, *J* = 12.54 Hz, C), 122.2 (d, *J* = 12.5 Hz, C), 116.64 (isomer Z, q, *J* = 287.6 Hz, C), 116.6 (isomer E, q, *J* = 287.6 Hz, C), 50.0 (isomer E, CH), 48.9 (isomer Z, q, *J* = 3.5 Hz, CH), 46.5 (isomer E, q, *J* = 4.4 Hz, CH), 45.0 (isomer Z, CH), 21.7 (CH).

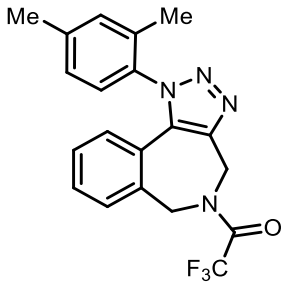

(6.5l) 1-(1-(2,4-dimethylphenyl)-4,6-dihydrobenzo[c][1,2,3]triazolo[4,5-e]azepin-5(1H)-yl)-2,2,2-trifluoroethan-1-one: Yellow solid; **Yield:** 90%; **m.p**: 162-164°;

^{1}H NMR ($CDCl_3$): δ 7.48 (isomer E, d, *J* = 7.68 Hz, 2H), 7.36 (isomer Z, d, *J* = 7.68 Hz, 2H), 7.29-7.18 (m, 1H), 7.14-6.94 (m, 4H), 6.79-6.70 (m, 1H), 5.17 (isomer E, s, 2H), 4.96 (isomer Z, s, 2H), 4.55 (bm, 2H), 2.33 (bs, 3H), 1.77 (isomer E, s, 3H), 1.74 (isomer Z, s, 3H)

^{13}C NMR ($CDCl_3$): δ 156.5 (isomer E, q, *J* = 37.0 Hz, C), 156.4 (isomer Z, q, *J* = 37.0 Hz, C), 141.0 (C), 141.0 (C), 140.5 (C), 140.4 (C), 135.2 (C), 134.8 (C), 134.7 (C), 134.7 (C), 133.7 (C), 133.5 (C), 133.3 (C), 133.0 (C). 132.4 (CH), 132.4 (CH), 131.4 (CH), 130.3 (CH), 130.3 (CH), 129.8 (CH), 129.4 (CH), 129.3 (CH), 128.7 (CH), 128.2 (CH), 128.1 (C), 127.5 (C),127.4 (C), 127.3 (C), 127.23 (C), 126.3 (C), 125.2 (C), 116.6 (isomer Z, q, *J* = 287.5 Hz, C), 116.5 (isomer E, q, *J* = 287.5 Hz, C), 50.0 (isomer E, CH_2), 49.0 (isomer Z, q, *J* = 2.9 Hz, CH_2), 46.6 (isomer E, q, *J* = 4.4 Hz, CH_2), 45.2 (isomer Z, CH_2), 21.54 (CH), 17.5 (CH), 17.4 (CH).

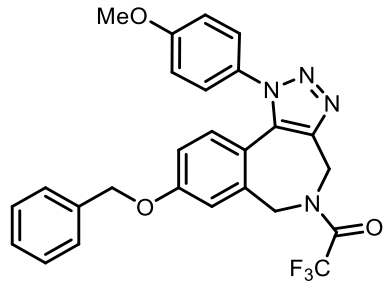

(6.5m) 1-(8-(benzyloxy)-1-(4-methoxyphenyl)-4,6-dihydrobenzo[c][1,2,3]triazolo[4,5-e]azepin-5(1H)-yl)-2,2,2-trifluoroethan-1-one: Yellow solid; **Yield:** 88%; **m.p**: 189-191°

^{1}H NMR ($CDCl_3$): δ 7.35-6.97 (m, 8H), 6.95-6.88 (m, 2H), 6.81-6.63 (m, 2H), 5.13 (isomer E, s, 2H), 4.99 (isomer Z, s, 2H), 4.97 (isomer E, s, 2H), 4.88 (isomer Z, s, 2H), 4.57 (isomer E, s, 2H), 4.51 (isomer Z, s, 2H), 3.80 (isomer E, s, 3H), 3.79 (isomer Z, s, 3H).

^{13}C NMR ($CDCl_3$): δ 160.7 (C), 160.7 (C), 159.7 (C), 159.3 (C), 156.6 (isomer E, q, *J* = 36.5 Hz, C), 156.3 (isomer Z, q, *J* = 36.5 Hz, C), 140.0 (C), 139.9 (C), 137.3 (C), 136.8 (C), 136.4 (C), 136.2 (C), 132.8 (C), 132.4 (C), 130.0 (C), 129.9 (CH), 129.7 (CH), 129.5 (C), 129.0 (CH), 128.9 (CH), 128.6 (CH), 128.5 (CH), 127.9 (CH), 127.8 (CH), 127.4 (CH), 127.0 (CH), 118.6 (C), 117.5 (C), 127.4 (CH), 116.7 (C), 116.7 (isomer Z, q, *J* = 287.6 Hz, C), 116.5 (isomer E, q, *J* = 287.5 Hz, C) 115.7 (C), 115.1 (CH), 115.1 (CH), 115.0 (CH), 70.6 (isomer Z, CH), 70.4 (isomer E, CH), 55.9 (CH), 50.1 (isomer E, CH), 48.8 (isomer Z, q, *J* = 3.0, CH), 46.5 (isomer E, q, J = 4.3 Hz, CH), 45.1 (isomer Z, CH).

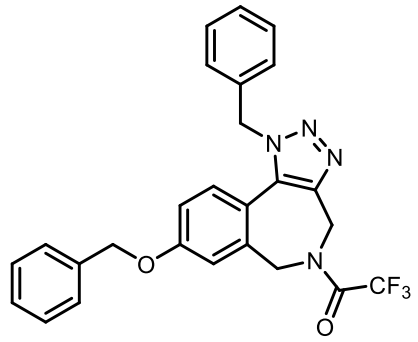

(6.5n) 1-(1-benzyl-8-(benzyloxy)-4,6-dihydrobenzo[c][1,2,3]triazolo[4,5-e]azepin-5(1H)-yl)-2,2,2-trifluoroethan-1-one: Brown Solid; **Yield:** 90%; **m.p**: 134-136°;

^{1}H NMR ($CDCl_3$): δ 7.34-7.16 (m, 9H), 7.14 -6.95 (m, 3H), 6.92 (isomer Z, dd, J_1 = 8.41 J_2 = 2.59, 2H), 5.61 (isomer E, s, 2H), 5.59 (isomer Z, s, 2H), 5.06 (isomer E, s, 2H), 5.01 (isomer

Z, s, 2H), 5.00 (isomer E, s, 2H), 4.79 (isomer Z, s, 2H), 4.42 (isomer E, s, 2H), 4.31 (isomer Z, s, 2H).

^{13}C NMR ($CDCl_3$): δ 159.9 (C), 159.6 (C), 156.6 (isomer E, q, *J* = 36.2 Hz, C), 156.1 (isomer Z, q, *J* = 36.2 Hz, C), 140.3 (C), 140.2 (C), 137.5 (C), 136.9 (C), 136.3 (C), 136.2 (C), 135.6 (C), 135.5 (C), 133.4 (C), 133.1 (C), 129.4 (CH), 129.4 (CH), 129.0 (CH), 128.9 (CH), 128.8 (CH), 128.8 (CH), 128.6 (CH), 128.6 (CH), 128.5 (CH), 127.8 (CH), 127.7 (CH), 126.8 (CH), 126.8 (CH), 118.6 (C), 118.0 (CH), 117.8 (CH), 117.3 (CH), 117.2 (CH), 116.6 (isomer Z, q, *J* = 287.3 Hz, C), 116.5 (isomer E, q, *J* = 287.3 Hz, C) 115.68 (CH), 115.4 (CH), 70.6 (isomer Z, CH_2), 70.4 (isomer E, CH_2), 52.7 (isomer E, CH_2), 52.5 (isomer Z, CH_2), 49.5 (isomer E, CH_2), 48.7 (isomer Z, q, *J* = 2.9 Hz, CH_2), 46.1 (isomer E, q, *J* = 4.3 Hz, CH_2), 44.9 (isomer Z, CH_2).

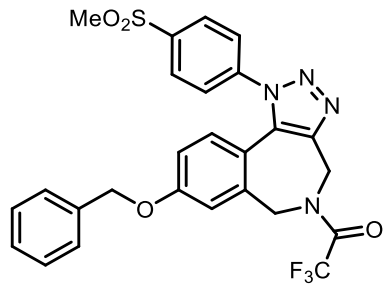

(6.5o) 1-(8-(benzyloxy)-1-(4-(methylsulfonyl)phenyl)-4,6-dihydrobenzo[c][1,2,3]triazolo [4,5-e]azepin-5(1H)-yl)-2,2,2-trifluoroethan-1-one: Yellow liquid; **Yield:** 98%,

^{1}H NMR ($CDCl_3$): δ 8.03-7.96 (m, 2H), 7.57-7.49 (m, 2H), 7.34-6.96 (m, 6H), 6.83-6.63 (m, 2H) 5.12 (isomer E, s, 2H), 4.99 (isomer Z s, 2H), 4.97 (isomer E, s, 2H), 4.86 (isomer Z, s, 2H), 4.58 (isomer E, s, 2H), 4.53 (isomer Z, s, 2H), 3.03 (s, 3H).

^{13}C NMR ($CDCl_3$): δ 159.9 (C), 159.6 (C), 156.3 (isomer E, q, *J* = 36.2 Hz, C), 156.0 (isomer Z, q, *J* = 36.4 Hz, C), 141.5 (C), 141.5 (C), 141.0 (C), 140.6 (C), 140.5 (C), 140.3 (C), 137.1 (C), 136.6 (C), 135.9 (C), 135.7 (C), 132.73 (C), 132.4 (C), 129.9 (CH), 129.6 (CH), 129.4 (CH), 129.1 (CH), 128.8 (CH), 128.7 (CH), 128.4 (CH), 128.3 (CH), 127.6 (CH), 127.5 (CH), 127.4 (CH), 126.3 (CH), 125.8 (CH), 117.7 (CH), 117.2 (C), 117.0 (CH), 116.1 (C), 116.0 (isomer Z, q, *J* = 288.1 Hz, C), 116.2 (isomer E, q, J = 288.1 Hz, C), 115.4 (CH), 115.0 (CH), 70.44 (isomer Z, CH_2), 70.3 (isomer E, CH_2), 49.7 (isomer E, CH_2), 48.6 (isomer Z, q, *J* = 2.7 Hz, CH_2), 46.1 (isomer E, q, *J* = 4.4 Hz, CH_2), 44.6 (isomer Z, CH_2), 44.4 (isomer Z, CH_2).

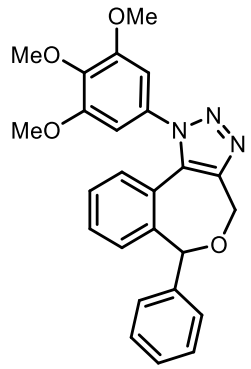

(6.9a) 6-phenyl-1-(3,4,5-trimethoxyphenyl)-4,6-dihydro-1H-benzo[5,6]oxepino[3,4-d][1,2,3]triazole: Yellow solid; **Yield:** 92%; **m.p**: 162-164°;

^{1}H NMR ($CDCl_3$): δ 7.33-7.22 (m, 5H), 7.10-7.01 (m, 2H), 6.97-6.93 (m, 1H), 6.73-6.67 (m, 1H), 6.48 (s, 2H), 5.67 (s, 1H), 5.27-5.17 (m, 2H), 3.81 (s, 3H), 3.67 (s, 6H)

^{13}C NMR ($CDCl_3$): δ 154.0 (C), 145.4 (C), 142.7 (C), 139.5 (C), 139.2 (C), 132.8 (C), 132.3 (C), 128.9 (CH), 128.8 (CH), 128.6 (CH), 128.6 (CH), 128.13 (CH), 127.8 (CH), 127.6 (CH), 125.7 (C), 103.7 (CH), 80.4 (CH), 67.3 (isomer Z, CH_2), 66.8 (isomer E, CH_2), 61.4 (CH), 56.7 (CH).

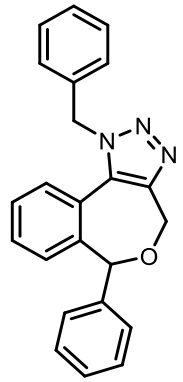

(6.9b) 1-benzyl-6-phenyl-4,6-dihydro-1H-benzo[5,6]oxepino[3,4-d][1,2,3]triazole: Yellow solid; **Yield:** 92%; **m.p**: 117-119°;

^{1}H NMR ($CDCl_3$): δ 7.35-7.19 (m, 9H), 7.17-7.16 (dd, J_1 = 7.66 Hz, J_2 = 1.12 Hz, 2H), 7.14-7.05 (m, 3H), 6.63 (d, *J* = 7.72 Hz, 1H), 5.82 (d, J = 16.02 Hz, 1H), 5.51 (d, J = 16.02 Hz, 1H), 5.44 (s, 1H), 5.25 (d, J = 14.59 Hz, 1H), 5.12 (d, J = 1 4.59 Hz, 1H).

^{13}C NMR ($CDCl_3$): δ 145.3 (C), 143.0 (C), 138.9 (C), 135.8 (C), 132.8 (C), 129.3 (2CH), 128.8 (CH), 128.5 (2CH), 128.5 (CH), 128.4 (CH), 128.2 (CH), 128.0 (CH), 127.6 (2CH), 127.5 (CH), 126.8 (2CH), 126.2 (C), 79.5 (CH), 66.93 (CH_2), 52.7 (CH_2)

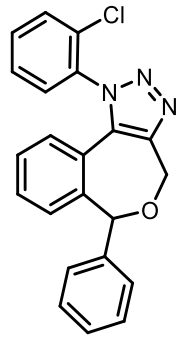

(6.9c) 1-(2-chlorophenyl)-6-phenyl-4,6-dihydro-1H-benzo[5,6]oxepino[3,4-d][1,2,3]triazole : Brownish liquid; **Yield:** 94%

^{1}H NMR ($CDCl_3$): δ 7.56-7.21 (m, 9H), 7.04 (t, J_1 = 15.37 Hz, J_2 = 7.18 Hz, 1H), 6.96 (t, J_1 = 15.15 Hz, J_2 = 7.50 Hz, 1H), 6.80 (d, J = 7.44 Hz, 3H), 6.63 (d, J = 7.62 Hz, 1H), 5.62 (s, 1H) MANCANO I CH E CH2 DIASTEROTOPICI

^{13}C NMR ($CDCl_3$): δ 145.3 (C), 143.0 (C), 138.9 (C), 135.8 (C), 132.8 (C), 129.3 (2CH), 128.8 (CH), 128.5 (CH), 128.5 (CH), 128.4 (CH), 128.2 (CH), 128.0 (CH), 127.6 (2CH), 127.5 (CH), 126.8 (2CH), 126.2 (C), 79.5 (CH), 66.9 (CH_2), 52.7 (CH_2)

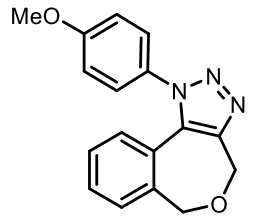

(6.9d) 1-(4-methoxyphenyl)-4,6-dihydro-1H-benzo[5,6]oxepino[3,4-d][1,2,3]triazole: Yellow solid; Y**ield:** 90%; **m.p**: 177-179°;

^{1}H NMR ($CDCl_3$): δ 7.36-7.24 (m, 4H), 7.13 (td, J_1 = 15.41 Hz, J_2 = 7.59 Hz, J_3 = 1.30 Hz, 1H), 7.05-6.98 (m, 2H), 6.95 (d, J = 7.84 Hz, 1H), 5.26 (s, 1H), 4.71 (s, 2H), 3.89 (s, 3H)

^{13}C NMR ($CDCl_3$): δ 160.6 (C), 144.9 (C), 139.5 (C), 131.9 (C), 130.4 (C), 129.7 (CH), 128.3 (CH), 128.3 (CH), 128.2 (CH), 127.5 (CH), 125.8 (C), 115.0 (CH), 71.7 (CH_2), 68.0 (CH_2), 55.9 (CH)

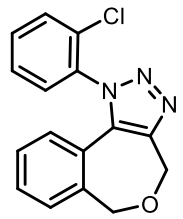

(6.9e) 1-(2-chlorophenyl)-4,6-dihydro-1H-benzo[5,6]oxepino[3,4-d][1,2,3]triazole: Yellw solid; **Yield:** 90%; **m.p**: 209-211°;

^{1}H NMR ($CDCl_3$): δ 7.51-7.39 (m, 4H), 7.23 (dd, J_1= 7.67 Hz, J_2 = 1.07 Hz, 1H), 7.18 (td, J_1 = 14.77 Hz, J_2 = 7.42 Hz, J_3 = 1.01 Hz 1H), 6.99 (td, J_1 = 15.15 Hz, J_2 = 7.76 Hz, J_3 = 1.26 Hz, 1H), 6.73 (d, J = 7.95 Hz, 1H) 5.24-5.17 (m, 2H), 4.66-4.57 (m, 2H)

^{13}C NMR ($CDCl_3$): δ 144.7 (C), 139.3 (C), 135.5 (C), 133.4 (C), 131.9 (C), 131.9 (CH), 131.1 (CH), 129.6 (CH), 129.0 (CH), 128.4 (CH), 128.4 (CH), 126.5 (CH), 125.9 (C), 71.8 (CH_2), 68.2 (CH_2)

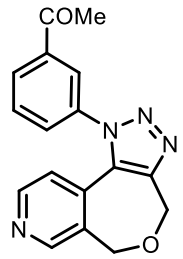

(6.9f) 1-(3-(4,6-dihydro-1H-[1,2,3]triazolo[4',5':5,6]oxepino[3,4-c]pyridin-1-yl)phenyl) ethan-1-one: Yellow solid; **Yield:** 89%; **m.p**: 104-106°;

^{1}H NMR ($CDCl_3$): δ 8.28 (d, *J* = 4.70 Hz, 1H), 8.00-7.87 (m, 2H), 7.76 (t, *J* = 1.76 Hz, 1H), 7.53-7.41 (m, 2H), 7.08 (d, *J* = 4.70 Hz, 1H) 5.12 (s, 2H), 4.56 (s, 2H), 2.42 (s, 3H).

^{13}C NMR ($CDCl_3$): δ 196.3 (C), 149.8 (CH), 148.2 (CH), 147.2 (C), 138.9 (C), 137.7 (C), 130.7 (CH), 130.3 (CH), 130.1 (CH), 129.3 (C), 125.7 (CH), 123.8 (CH), 121.7 (C), 71.3 (CH_2), 68.7 (CH_2), 26.9 (CH).

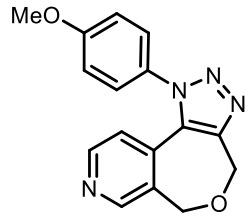

(6.9g) 1-(4-methoxyphenyl)-4,6-dihydro-1H-[1,2,3]triazolo[4',5':5,6]oxepino[3,4-c]pyridine: Yellow solid; **Yield:** 98%; **m.p**: 184-186°;

^{1}H NMR ($CDCl_3$): δ 8.30 (d, *J* = 4.87 Hz, 1H), 8.02 (s, 1H), 7.17-7.12 (m, 2H), 7.07 (d, *J* = 4.43 Hz, 1H), 6.89-6.83 (m, 2H), 5.13 (s, 2H), 4.55 (s, 2H), 3.71 (s, 3H).

^{13}C NMR ($CDCl_3$): δ 160.8 (C), 149.3 (CH), 148.1 (CH), 146.8 (C), 145.7 (C), 129.6 (C), 129.1 (C), 127.2 (CH), 123.3 (C), 121.8 (CH), 115.2 (CH), 71.1 (CH_2), 68.6 (CH_2), 55.6 (CH).

11.5 General procedures and Characterization of Chapter 7

General Procedure for the Preparation of (1H-indol-2-yl)methyl Acetates

Characterization Data of (1H-indol-2-yl)methyl Acetates (**7.1a**, **7.c-h**; **7.4a-b**)

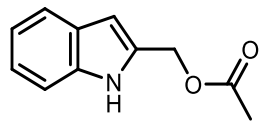

(1H-indol-2-yl)methyl acetate (**7.1a**): known compound; 95% yield (7.47 mmol scale, 1.34 g); yellow solid; mp: 111–112 °C;. mp: 111–112 °C; R_f = 0.27 (*n*-hexane-EtOAc, 80:20); IR (neat): 3303, 1726, 1045, 1454, 1274, 805 cm^{-1};

^{1}H NMR (400.13 MHz) ($CDCl_3$): δ = 8.51 (br s, 1 H), 7.52 (d, *J* = 8.0 Hz, 1H), 7.27 (d, *J* = 8.0 Hz, 1H), 7.13 (t, *J* = 7.6 Hz, 1H), 7.00 (t, J_1 = 7.6 Hz, 1H), 6.46 (s, 1H), 5.15 (s, 2H), 2.03 (s, 3H);

^{13}C NMR (100.6 MHz) ($CDCl_3$): δ 172.3 (C), 136.6 (C), 133.0 (C), 127.5 (C), 122.8 (CH), 120.9 (CH), 120.1 (CH), 111.1 (CH), 103.9 (CH), 59.8 (CH_2), 21.0 (CH_3);

HRMS: *m/z* $[M + H]^+$ calcd. for $C_{11}H_{12}NO_2$: 188.0717; found: 188.0705.

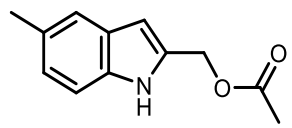

(5-methyl-1H-indol-2-yl)methyl acetate (**7.1c**): known compound; 98% yield (7.47 mmol scale, 1.49 g); brown solid; mp: 84–86 °C; mp: 84–86 °C; R_f = 0.24 (*n*-hexane-EtOAc, 75:25); IR (neat): 3427, 1718, 1361, 806 cm^{-1};

^{1}H NMR (400.13 MHz) ($CDCl_3$): δ 8.42 (br s, 1H), 7.31 (q, *J* = 0.80 Hz, 1H), 7.16 (d, *J* = 8.2 Hz, 1H), 6.96 (dd, J_1 = 8.2 Hz, J_2 = 1.6 Hz, 1H), 6.38 (d, *J* = 1.6 Hz, 1H), 5.14 (s, 2 H), 2.36 (s, 3H), 2.03 (s, 3H);

^{13}C NMR (100.6 MHz) ($CDCl_3$): δ 172.3 (C), 134.9 (C), 133.1 (C), 129.2 (C), 127.8 (C), 124.5 (CH), 120.5 (CH), 110.8 (CH), 103.4 (CH), 59.8 (CH_2), 21.5 (CH_3), 21.0 (CH_3);

HRMS: *m/z* $[M + Na]^+$ calcd. for $C_{12}H_{15}NO_2Na$: 226.0838; found: 226.0838.

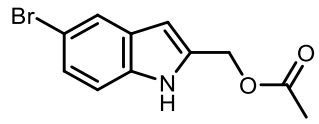

(5-bromo-1H-indol-2-yl)methyl acetate (7.1d): 98% yield (7.47 mmol scale, 1.96 g); brown solid; mp: 69–71 °C; R_f = 0.21 (*n*-hexane-EtOAc, 87:13); IR (neat): 3323, 2916, 1714, 1383, 1211, 1133 cm^{-1};

^{1}H NMR (400.13 MHz) ($CDCl_3$): δ 8.87 (br s, 1H), 7.71 (d, *J* = 1.2 Hz, 1H), 7.28 (dd, J_1 = 8.5 Hz, J_2 = 1.7 Hz, 1H), 7.21 (d, *J* = 8.5 Hz, 1H), 6.47 (d, *J* = 1.2 Hz, 1H), 5.20 (s, 2 H), 2.11 (s, 3H);

^{13}C NMR (100.6 MHz) ($CDCl_3$): δ 172.5 (C), 135.2 (C), 134.4 (C), 129.4 (C), 125.8 (CH), 123.5 (CH), 113.2 (C), 112.7 (CH), 103.5(CH), 59.6 (CH_2), 21.1 (CH_3);

HRMS: *m/z* $[M - H]^-$ calcd. for $C_{11}H_9BrNO_2$: 265.9822; found: 265.9818.

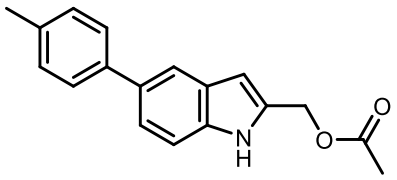

(5-(p-tolyl)-1H-indol-2-yl)methyl acetate (**7.1e**): 98% yield (4.35 mmol scale, 1.19 g); yellow solid; mp: 178–180 °C; R_f = 0.23 (*n*-hexane-EtOAc, 75:25); IR (KBr): 3399, 2919, 1728, 1385, 1235;

^{1}H NMR (400.13 MHz) ($CDCl_3$): δ = 8.62 (br s, 1H), 7.79 (s, 1 H), 7.55–7.53 (m, 2H), 7.45 (dd, J_1 = 8.50 Hz, J_2 = 1.62, 1H), 7.39 (d, *J* = 8.50 Hz, 1H), 7.25 (m, 2H), 6.58 (d, *J* = 1.17 Hz, 1H), 5.24 (s, 2H), 2.40 (s, 3H), 2.11 (s, 3H);

^{13}C NMR (100.6 MHz) ($CDCl_3$): δ = 172.5 (C), 139.6 (C), 136.1 (C), 136.0 (C), 133.8 (C), 133.7 (C), 129.5 (CH), 128.2 (C), 127.3 (CH), 122.8 (CH), 119.2 (CH), 111.4 (CH), 104.3 (CH), 59.9 (CH_2), 21.2 (CH_3), 21.1 (CH_3); HRMS: *m/z* $[M + Na]^+$ calcd. for $C_{18}H_{17}NO_2Na$: 302.1152; found: 302.1153.

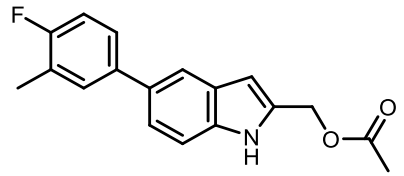

(5-(4-fluoro-3-methylphenyl)-1H-indol-2-yl)methyl acetate (**7.1f**): 97% yield (3.14 mmol scale, 0.90 g); yellow solid; mp: 98–100 °C; R_f = 0.26 (*n*-hexane-EtOAc, 80:20); IR (KBr): 3366, 2919, 1712, 1472, 1385, 1265;

^{1}H NMR (400.13 MHz) ($CDCl_3$): δ = 8.55 (s, 1H), 7.73 (s, 1H), 7.543–7.37 (m, 4H), 7.51–7.34 (m, 3H), 7.05 (t, *J* = 8.9 Hz, 1H), 6.57 (d, *J* = 1.4 Hz, 1H), 5.24 (s, 2H), 2.34 (s, 3H), 2.11 (s, 3H);

^{13}C NMR (100.6 MHz) ($CDCl_3$): δ = 172.5 (C), 161.0 (d, *J* = 241.5 Hz) (C), 138.3 (d, *J* = 3.2 Hz) (C), 136.1 (C), 134.0 (C), 133.0 (C), 130.3 (d, *J* = 5.0 Hz), 128.2 (C), 126.2 (d, *J* = 7.0 Hz) (CH), 125.0 (d, *J* = 15.5 Hz) (C), 122.7 (CH), 119.3 (CH), 121.4, 118.6, 115.16 (d, *J* = 15.5 Hz) (C), 111.5 (CH), 104.3 (CH), 59.86 (CH_2), 21.2 (CH_3), 14.9 (d, *J* = 3.5 Hz); ^{1}H-coupled ^{19}F (376.5 MHz) ($CDCl_3$): δ −121.6 (hept, *J* = 3.0 Hz);

HRMS: *m/z* $[M + Na]^+$ calcd. for $C_{18}H_{16}FNO_2Na$: 320.1057; found: 320.1051.

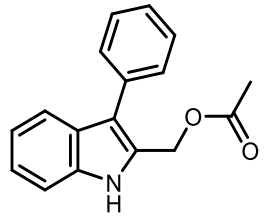

(3-phenyl-1H-indol-2-yl)methyl acetate (**7.1g**): yield quantitative (5.15 mmol scale, 1.37 g); yellow solid; mp: 133–135 °C; R_f = 0.25 (*n*-hexane-EtOAc, 80:20); IR (neat): 3391, 2917, 1730, 1456, 1384, 1231 cm^{-1};

^{1}H NMR (400.13 MHz) ($CDCl_3$): δ 8.71 (br s, 1H), 7.65 (d, *J* = 8.0 Hz, 1H), 7.47 (d, *J* = 7.5 Hz, 2H), 7.41 (t, *J* = 7.5 Hz, 2H), 7.30 (t, *J* = 8.3 Hz, 2H), 7.17 (d, *J* = 7.0 Hz, 1H), 7.06 (t, *J* = 7.5 Hz, 1H), 5.19 (s, 2H), 2.06 (s, 3H);

^{13}C NMR (100.6 MHz) ($CDCl_3$): δ 172.8 (C), 135.8 (C), 134.2 (C), 129.8 (CH), 129.4 (C), 128.8 (CH), 126.8 (CH), 126.7 (C) 123.5 (CH), 120.4 (CH), 120.2(CH), 118.8 (C), 111.4(CH), 58.5 (CH_2), 21.2 (CH_3);

HRMS: *m/z* $[M + Na]^+$ calcd. for $C_{17}H_{15}NO_2Na$: 288.0995; found: 288.0997.

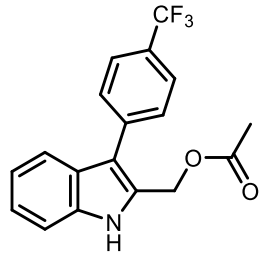

(3-(4-(trifluoromethyl)phenyl)-1H-indol-2-yl)methyl acetate (**7.1h**): 95% yield (5.39 mmol scale, 1.71 g); red solid; mp: 120–122 °C; R_f = 0.30 (*n*-hexane-EtOAc, 75:25); IR (neat): 3388, 3287, 2941, 1730, 1616, 1384, 1326 cm^{-1}; ^{1}H NMR (400.13 MHz) ($CDCl_3$): δ 8.81 (br s, 1H), 7.67 (d, *J* = 8.2 Hz, 2H), 7.62–7.57 (m, 3H), 7.33 (d, *J* = 8.1 Hz, 1H), 7.21 (t, *J* = 7.4 Hz, 1H), 7.09 (t, *J* = 7.4 Hz, 1H), 5.17 (s, 2H), 2.07 (s, 3H);

^{13}C NMR (100.6 MHz) ($CDCl_3$): δ 172.6 (C), 138.0 (C), 135.7 (C), 129.9 (C), 129.8 (CH), 128.7 (q, J_{CF} = 33.2 Hz, C), 126.2 (C), 125.7 (q, J_{CF} = 3.6 Hz, CH), 124.3 (q, J_{CF} = 273.4 Hz, C), 123.7 (CH), 120.7 (CH), 119.6 (CH), 117.3 (C), 111.5 (CH), 58.1 (CH_2), 21.0 (CH_3); ^{19}F NMR (376.5 MHz) ($CDCl_3$): δ = −62.3;

HRMS: *m/z* $[M - H]^-$ calcd. for $C_{18}H_{13}F_3NO_2$: 332.0904; found: 332.0894.

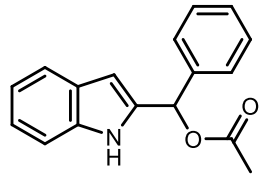

(1H-indol-2-yl)(phenyl)methyl acetate (7.4a): 95% yield (6.20 mmol scale, 1.56 g); yellow solid; mp: 93–95 °C; R_f = 0.25 (*n*-hexane-EtOAc, 85:15); IR (neat): 3362, 2919, 1445, 1383, 1238 cm^{-1};

^{1}H NMR (400.13 MHz) ($CDCl_3$): δ 8.45 (br s, 1H), 7.53 (d, J = 8.3 Hz, 1H), 7.50–7.48 (m, 2H), 7.45–7.39 (m, 3H), 7.34–7.32 (m, 1H), 7.19 (td, J_1 = 7.7 Hz, J_2 = 1.1 Hz, 1H), 7.01 (td, J_1 = 7.7 Hz, J_2 = 1.1 Hz, 1H), 7.05 (s, 1H), 6.22–6.21 (m, 1H), 2.18 (s, 3H);

^{13}C NMR (100.6 MHz) ($CDCl_3$): δ = 171.2 (C), 137.6 (C), 136.9 (C), 136.4 (C), 128.6 (CH), 128.5 (CH), 127.5 (C), 127.2 (CH), 122.7 (CH), 120.9 (CH), 120.0 (CH), 111.1 (CH), 103.4 (CH), 71.8 (CH), 21.3 (CH_3);

HRMS: *m/z* $[M + Na]^+$ calcd. for $C_{17}H_{15}NO_2Na$: 288.0995; found: 288.0989.

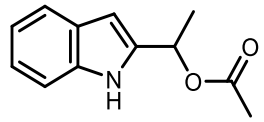

1-(1H-indol-2-yl)ethyl acetate (**7.4b**): 96% yield (6.20 mmol scale, 1.18 g); brown solid; mp: 209–211 °C; R_f = 0.23 (*n*-hexane-EtOAc, 80:20); IR (neat): 3330, 2918, 1713, 1455, 1384 cm^{-1};

^{1}H NMR (400.13 MHz) ($CDCl_3$): δ 8.60 (br s, 1H), 7.60 (d, J = 8.0 Hz, 1H), 7.35 (dd, J_1 = 8.2 Hz, J_2 = 0.7 Hz, 1H), 7.19 (td, J_1 = 7.2 Hz, J_2 = 1.1 Hz, 1H), 7.10 (td, J_1 = 7.2 Hz, J_2 = 1.1 Hz, 1H), 6.53–6.53 (m, 1H), 6.07 (q, J = 6.4 Hz, 1H), 2.09 (s, 3H), 1.74 (d, J = 6.4 Hz, 3H);

^{13}C NMR (100.6 MHz) ($CDCl_3$): δ 172.1 (C), 138.0 (C), 136.1 (C), 127.5 (CH), 122.7 (CH), 121.0 (CH), 120.1, 111.2 (CH), 100.7, 66.5 (CH), 21.4 (CH_3), 18.7 (CH_3);

HRMS: *m/z* $[M + Na]^+$ calcd. for $C_{12}H_{13}NO_2Na$: 266.0838; found: 266.0838.

General Procedure for the Preparation of 5-(aryl-2-ylmethyl)-2,2-dimethyl-1,3-dioxane-4,6-diones (7.2)

Characterization Data of 5-(aryl-2-ylmethyl)-2,2-dimethyl-1,3-dioxane-4,6-diones (**7.2**)

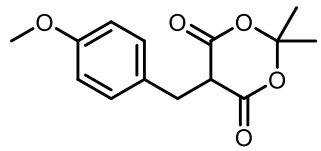

5-(4-Methoxybenzyl)-2,2-dimethyl-1,3-dioxane-4,6-dione (**7.2b**): known compound; 98% yield (4.50 mmol scale, 1.17 g); yellow solid; mp: 82–85 °C; mp: 83–85 °C; R_f 0.24 (*n*-hexane-EtOAc, 75:25); IR (neat): 3036, 2920, 1784, 1743, 1514, 1243 cm^{-1};

^{1}H NMR (400.13 MHz, $CDCl_3$): δ 7.25 (d, *J* = 8.8 Hz, 2H), 6.82 (d, *J* = 8.8 Hz, 2H), 3.77 (s, 3 H), 3.72 (t, *J* = 4.9 Hz, 1H), 3.44 (d, *J* = 4.9 Hz, 2H), 1.72 (s, 3H), 1.48 (d, 3H);

^{13}C NMR (100.6 MHz, $CDCl_3$): δ 165.6 (C), 158.9 (C), 131.1 (CH), 129.2 (C), 114.1 (CH), 105.3 (C), 55.4 (CH_3), 48.5 (CH), 31.7 (CH_2), 28.6 (CH_3), 27.5 (CH_3);

HRMS: *m/z* $[M + H]^+$ calcd. for $C_{14}H_{15}O_5$: 263.0925; found: 263.0922.

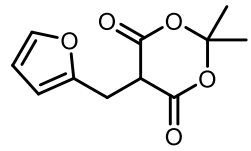

5-(Furan-2-ylmethyl)-2,2-dimethyl-1,3-dioxane-4,6-dione (**7.2c**): known compound; 98% yield (4.50 mmol scale, 988.8 mg); grey solid; mp: 92–93 °C; mp: 92–93 °C; R_f 0.30 (R_f = 0.24 (*n*-hexane-EtOAc, 85:15); IR (neat): 3123, 2896, 1783, 1740, 1067, 907 cm^{-1};

^{1}H NMR (400.13 MHz, $CDCl_3$): δ 7.30 (dd, J_1 = 1.8 Hz, J_2 = 0.7 Hz, 1H), 6.29 (dd, J_1 = 3.2 Hz, J_2 = 1.8 Hz, 1H), 6.18 (dd, J_1 = 3.2 Hz, J_2 = 0.7 Hz, 1H), 3.83 (t, *J* = 5.0 Hz, 1H), 3.51 (d, *J* = 5.0 Hz, 2H), 1.79 (s, 3H), 1.67 (s, 3H);

^{13}C NMR (100.6 MHz, $CDCl_3$): δ 164.9 (C), 150.7 (C), 141.7 (CH), 110.8 (CH), 107.9 (CH), 105.4 (C), 45.6 (CH), 28.5 (CH_3), 27.2 (CH_3), 25.1 (CH_2);

HRMS: *m/z* $[M + Na]^+$ calcd. for $C_{11}H_{12}O_5Na$: 247.0577; found: 247.0581.

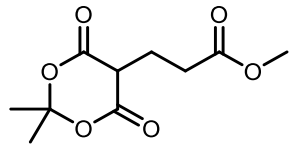

Methyl 3-(2,2-dimethyl-4,6-dioxo-1,3-dioxan-5-yl)propanoate (**7.2e**): known compound; 78% yield (4.50 mmol scale, 1.10 g); white solid; mp: 75–76 °C; mp: 78–80 °C; R_f 0.21 (R_f = 0.24 (*n*-hexane-EtOAc, 75:25); IR (KBr): 2995, 2952, 2893, 1749 cm^{-1};

^{1}H NMR (400.13 MHz) ($CDCl_3$): δ = 3.92 (t, *J* = 5.5 Hz, 1H), 3.67 (s, 3H), 2.64 (t, *J* = 7.2 Hz, 2H), 2.40–2.35 (m, 2H), 1.82 (s, 3H), 1.77 (s, 3H),

^{13}C NMR (100.6 MHz) ($CDCl_3$): δ = 173.4 (C), 165.2 (C), 105.2 (C), 51.8 (CH_3), 44.8 (CH), 30.1 (CH_2), 28.6 (CH_3), 26.5 (CH_3), 21.2 (CH_2);

HRMS: *m/z* $[M + H]^+$ calcd. for $C_{19}H_{18}NO_2$: 292.1332; found: 292.1321.

Typical Procedure for the Preparation of 1,2-dihydro-3H-pyrrolo[1,2-a]indol-3-ones (**7.3a-m**; **7.5a-d**): Synthesis of 2-methyl-1,2-dihydro-3H-pyrrolo[1,2-a]indol-3-one (**7.3a**)

In a 50 mL Carousel Tube Reactor (Radely Discovery Technology) containing a magnetic stirring bar, Pd_2dba_3 (6.4 mg, 0.007 mmol, 0.025 equiv.) and dppf (7.8 mg, 0.014 mmol, 0.04 equiv.) were dissolved with 1.5 mL of anhydrous DMSO, at room temperature under Ar. Then, (1*H*-indol-2-il)methyl acetate (**7.1a**) (66.15 mg, 0.35 mmol, 1.0 equiv.), 2,2,5-trimethyl-1,3-dioxane-4,6-dione (**7.5a**) (138.6, 0.525 mmol, 1.5 equiv.) and K_2CO_3 (72.5 mg, 0.525 mmol, 1.5 equiv.) were added and the mixture reaction was stirred for 1h at 100 °C. After this time, the reaction mixture was cooled to room temperature, diluted with Et_2O, and washed with a solution of $KHSO_4$ (10% w/w) and with brine. The organic extract was dried over Na_2SO_4, filtered, and concentrated under reduced pressure. The residue was purified by chromatography on SiO_2 (25–40 μm), eluting with a 80/20 (v/v) *n*-hexane/EtOAc mixture (R_f = 0.22) to obtain 102.4 mg (85% yield) of **2-methyl-1,2-dihydro-3*H*-pyrrolo[1,2-*a*]indol-3-one** (**7.3a**): known compound; 85% yield (0.35 mmol scale, 102.4 mg); yellow solid; mp: 73–76 °C; R_f = 0.22 (*n*-hexane-EtOAc, 80:20); IR (KBr): 3052, 2969, 1729, 1589, 1384 cm^{-1}; **^{1}H NMR** (400.13 MHz) ($CDCl_3$): δ = 8.00–7.97 (m, 1H), 7.42–7.40 (m, 1H), 7.20–7.15 (m, 2H), 6.17 (s, 1H), 3.31 (m, 1H), 3.19–3.10 (m, 1H), 2.68 (m, 1H), 1.37 (d, *J* = 7.5 Hz, 3H); **^{13}C NMR** (100.6 MHz) ($CDCl_3$): δ = 174.7 (C), 142.0 (C), 135.3 (C), 130.5 (C), 124.0 (C), 123.2 (CH), 120.5 (CH), 113.6 (CH), 100.3 (CH), 41.6 (CH), 28.4 (CH_2), 17.0 (CH_3); **HRMS**: *m/z* $[M + H]^+$ calcd. for $C_{12}H_{12}NO$: 186.0913; found: 186.0902.

3.2.6. Characterization Data of of 1,2-dihydro-3H-pyrrolo[1,2-a]indol-3-ones (**7.3b-3m**; **7.5a-d**)

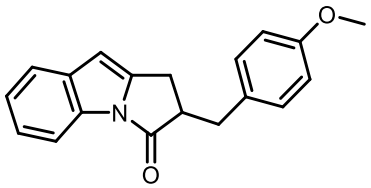

2-(4-methoxybenzyl)-1,2-dihydro-3H-pyrrolo[1,2-a]indol-3-one (**7.3b**): known compound; 78% yield (0.35 mmol scale, 79mg); yellow solid; mp: 109–110 °C; R_f = 0.23 (*n*-hexane-EtOAc, 85:15); IR (KBr): 3098, 2924, 1744, 1384 cm^{-1};

^{1}H NMR (400.13 MHz) ($CDCl_3$): δ = 8.09–8.07 (m, 1H), 7.48–7.45 (m, 1H), 7.27–7.25 (m, 2H), 7.16 (d, J = 8.6 Hz, 2H), 6.83 (d, J = 8.6 Hz, 2H), 6.20 (br s, 1H), 3.77 (s, 3H), 3.48–3.41 (m, 1H), 3.32 (dd, J_1 = 14.1 Hz, J_2 = 4.5 Hz, 1H), 3.17–3.10 (m, 1H), 2.91–2.84 (m, 2H);

^{13}C NMR (100.6 MHz) ($CDCl_3$): δ 173.4 (C), 158.6 (C), 142.2 (C), 135.4 (C), 130.5 (C), 130.2 (C), 130.1 (CH), 124.2 (CH), 123.4 (CH), 120.6 (CH), 114.2 (CH), 113.8 (CH), 100.5 (CH), 55.4 (CH_3), 48.5 (CH), 36.3 (CH_2), 25.4 (CH_2);

HRMS: *m/z* $[M + H]^+$ calcd. for $C_{19}H_{18}NO_2$: 292.1332; found: 292.1321.

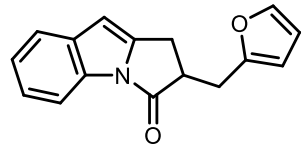

2-(furan-2-ylmethyl)-1,2-dihydro-3H-pyrrolo[1,2-a]indol-3-one (**7.3c**): 63% yield (0.35 mmol scale, 55 mg); brown solid; mp: 95–97 °C; R_f = 0.25 (*n*-hexane-EtOAc, 85:15); IR (KBr): 3092, 2917, 1737, 1454, 1384 cm^{-1};

^{1}H NMR (400.13 MHz) ($CDCl_3$): δ 8.03–7.97 (m, 2H), 7.42–7.38 (m, 2H), 7.22–7.15 (m, 3H), 6.19 (dd, J_1 = 3.3 Hz, J_2 = 1.9 Hz, 1H), 6.15 (br s, 1H), 6.02 (dd, J_1 = 3.14 Hz, J_2 = 0.6 Hz, 1H), 3.46–3.39 (m, 1H), 3.27 (dd, J_1 = 15.3 Hz, J_2 = 4.4 Hz 1H), 3.23–3.17 (m, 1H), 2.95 (dd, J_1 = 15.3 Hz, J_2 = 9.2 Hz 1H), 2.90–2.85 (m, 1H);

^{13}C NMR (100.6 MHz) ($CDCl_3$): δ 172.3 (C), 152.2 (C), 142.0 (C), 141.9 (CH), 135.3 (C), 130.5 (C), 124.1 (CH), 123.3 (CH), 120.6 (CH), 113.7 (CH), 110.3 (CH), 107.0 (CH), 100.5 (CH), 46.0 (CH), 29.6 (CH_2), 25.8 (CH_2);

HRMS: *m/z* $[M + H]^+$ calcd. for $C_{16}H_{14}NO_2$: 252.1019; found: 252.1009.

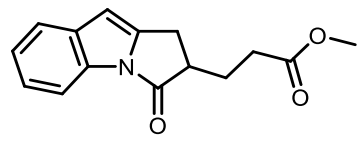

methyl 3-(3-oxo-2,3-dihydro-1H-pyrrolo[1,2-a]indol-2-yl)propanoate (**7.3d**): 74% yield (0.35 mmol scale, 67 mg); brown solid; mp: 41–43 °C; R_f = 0.25 (*n*-hexane-EtOAc, 80:20); IR (KBr): 3007, 2916, 1754, 1455, 1385 cm^{-1};

^{1}H NMR (400.13 MHz) ($CDCl_3$): δ = 8.06–8.03 (m, 1H), 7.50–7.48 (m, 1H), 7.27–7.25 (m, 2H), 6.27 (br s, 1H), 3.70 (s, 3H), 3.39–3.32 (m, 1H), 3.26–3.19 (m, 1H), 2.82 (dd, J_1 = 15.3 Hz, J_2 = 4.4 Hz, 1H), 2.58 (m, 1H), 2.34–2.26 (m, 1H), 2.08–2.00 (m, 1H);

^{13}C NMR (100.6 MHz) ($CDCl_3$): δ = 173.3 (C), 173.2 (C), 141.7 (C), 135.4 (C), 130.5 (C), 124.2 (CH), 123.4 (CH), 120.7 (CH), 113.8 (CH), 100.6 (CH), 52.0 (CH_3), 45.8 (CH), 31.4 (CH_2), 27.1 (CH_2), 26.4 (CH_2);

HRMS: *m/z* $[M + H]^+$ calcd. for $C_{15}H_{16}NO_3$: 258.1114; found: 258.1124.

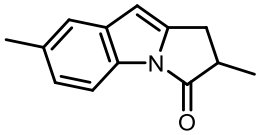

2,7-dimethyl-1,2-dihydro-3H-pyrrolo[1,2-a]indol-3-one (7.3e): 70% yield (0.35 mmol scale, 49 mg); brown wax; R_f = 0.20 (*n*-hexane-EtOAc, 90:10); IR (KBr): 3004, 2918, 1717, 1475, 1352 cm^{-1};

^{1}H NMR (400.13 MHz) ($CDCl_3$): δ = 7.93 (d, J = 8.2 Hz, 1H), 7.29 (br s, 1H), 7.09 (dd, J_1 = 1.1 Hz, J_2 = 8.2 Hz, 1H), 6.19–6.18 (m, 1H), 3.42–3.34 (m, 1H), 3.26–3.20 (m, 1H), 2.78–2.72 (m, 1H), 2.44 (br s, 3H), 1.45 (d, J = 7.4 Hz, 3H);

^{13}C NMR (100.6 MHz) ($CDCl_3$): δ = 174.7 (C), 142.2 (C), 135.8 (C), 133.8 (C), 128.8 (CH), 124.6 (CH),120.6 (CH), 113.3 (CH), 100.2 (CH), 41.7 (CH_3), 28.5 (CH_3), 21.8 (CH_2), 17.7 (CH);

HRMS: *m/z* $[M + H]^+$ calcd. for $C_{13}H_{14}NO$: 200.1070; found: 200.1062.

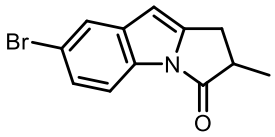

7-bromo-2-methyl-1,2-dihydro-3H-pyrrolo[1,2-a]indol-3-one (**7.3f**): 50% yield (0.35 mmol scale, 46 mg); yellow solid; mp: 96–99 °C; R_f = 0.21 (*n*-hexane-EtOAc, 90:10; IR (KBr): 3091.0, 2918.7, 1731.8, 1590.0, 1447.5, 1384.6 cm^{-1};

^{1}H NMR (400.13 MHz) (DMSO-d_6): δ = 7.85 (d, J = 8.3 Hz, 1H), 7.79 (d, J = 1.6 Hz, 1H), 7.40 (dd, J_1 = 8.5 Hz, J_2 = 1.9 Hz, 1H), 6.39 (s, 1H), 3.45–3.30 (m, 2H), 2.82–2.77 (m, 1H), 1.34 (d, J = 7.3 Hz, 3H);

^{13}C NMR (100.6 MHz) (DMSO-*d*$_6$): δ 175.3 (C), 145.3 (C), 137.5 (C), 128.9 (C), 125.9 (CH) (CH), 123.6 (CH), 116.6 (C), 114.8 (CH), 99.5 (CH), 41.4 (CH), 28.4 (CH_2), 16.9 (CH_3);

HRMS: *m/z* $[M + H]^+$ calcd. for $C_{12}H_{11}BrNO$: 264.0019; found: 264.0008.

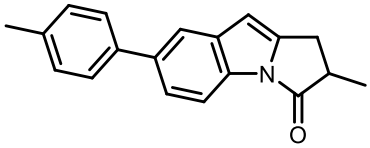

2-methyl-7-(p-tolyl)-1,2-dihydro-3H-pyrrolo[1,2-a]indol-3-one (**7.3g**): 70% yield (0.35 mmol scale, 67 mg); yellow solid; mp: 140–143 °C; R_f = 0.18 R_f = 0.24 (*n*-hexane-EtOAc, 75:25); IR (KBr): 3071, 2917, 1728, 1585, 1470, 1384 cm^{-1};

^{1}H NMR (400.13 MHz) ($CDCl_3$): δ 8.09 (d, *J* = 8.5 Hz, 1H), 7.68 (d, *J* = 1.3 Hz, 1H), 7.55–7.52 (m, 3H), 7.50 (dd, J_1 = 8.4 Hz; J_2 = 1.7Hz, 1H), 7.26 (d, *J* = 7.8 Hz, 2H), 6.31 (s, 1H), 3.46–3.39 (m, 1H), 3.30–3.21 (m, 1H), 2.82–2.77 (m, 1H), 3.10 (s, 3H); 1.48 (d, *J* = 7.4 Hz, 3H);

^{13}C NMR (100.6 MHz) ($CDCl_3$): δ 174.7 (C), 142.7 (C), 139.0 (C), 137.5 (C), 136.8 (C), 136.0 (C), 129.8 (CH), 129.6 (CH), 127.4 (CH), 122.8 (CH), 118.9 (CH), 113.8 (CH), 100.7 (CH), 41.7 (CH), 28.5 (CH_2), 21.1 (CH_3), 17.1 (CH_3);

HRMS: *m/z* $[M + H]^+$ calcd. for $C_{19}H_{18}NO$: 276.1383; found: 276.1372.

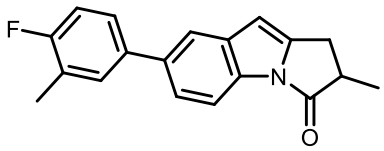

7-(4-fluoro-3-methylphenyl)-2-methyl-1,2-dihydro-3H-pyrrolo[1,2-a]indol-3-one (**7.3h**): 70% yield (0.35 mmol scale, 72 mg); pink solid; mp: 136–139 °C; R_f = 0.23 (*n*-hexane-EtOAc, 85:15); IR (KBr): 3102, 2972, 1743, 1586, 1467, 1384 cm^{-1};

^{1}H NMR (400.13 MHz) ($CDCl_3$): δ 8.09 (d, *J* = 8.5 Hz, 1H), 7.68 (d, *J* = 1.3 Hz, 1H), 7.46–7.37 (m, 3H), 7.07 (t, J_1 = 8.4 Hz, 1H), 6.31 (s, 1H), 3.46–3.39 (m, 1H), 3.30–3.21 (m, 1H), 2.82–2.77 (m, 1H), 2.34 (s, 3H); 1.48 (d, *J* = 7.4 Hz, 3H);

^{13}C NMR (100.6 MHz) ($CDCl_3$): δ 174.7 (C), 161.0 (d, *J* = 249.3 Hz) (C), 142.8 (C), 137.8 (d, *J* = 3.5 Hz) (C), 136.8 (C), 136.0 (C), 130.6 (d, *J* = 5.12 Hz) (CH), 129.8 (C), 126.3 (d, *J* = 7.9

Hz) (CH), 125.2 (C)., 125.0 (C), 120.9 (d, J = 380.8 Hz) (CH), 115.4 (CH), 115.2 (CH), 107.2 (d, J = 1337.1 Hz), 41.8 (CH), 28.6 (CH_2), 17.2 (CH_3), 14.8 (d, J = 3.4 Hz) (CH_3); ^{1}H-coupled ^{19}F (376.5 MHz) ($CDCl_3$): δ −120.6 (hept, J = 2.9 Hz);

HRMS: *m/z* $[M + H]^+$ calcd. for $C_{19}H_{17}FNO$: 294.1289; found: 294.1275.

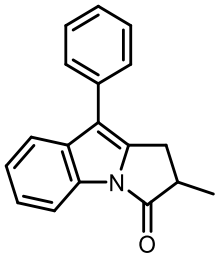

2-methyl-9-phenyl-1,2-dihydro-3H-pyrrolo[1,2-a]indol-3-one (7.3i): 58% yield (0.35 mmol scale, 53 mg); white solid; mp: 148–149 °C; R_f = 0.24(*n*-hexane-EtOAc, 85:15); IR (neat): 2973, 2924, 1720, 1603, 1079 cm^{-1};

^{1}H NMR (400.13 MHz) ($CDCl_3$): δ 8.16–8.13 (m, 1H), 7.80–7.77(m, 1H), 7.61 (d, J = 7.9 Hz 2H), 7.49 (d, J = 7.9 Hz 2H), 7.36–7.33 (m, 3H), 3.60–3.54 (m, 1H), 3.34–3.25 (m, 1H), 2.97–2.92 (m, 1H), 1.50 (d, J = 7.5 Hz, 3H);

^{13}C NMR (100.6 MHz) ($CDCl_3$): δ 174.7 (C), 138.4 (C), 133.8 (C), 133.7 (C), 130.9 (C), 129.0 (CH), 128.5 (CH), 127.9 (CH), 126.8(CH), 124.4 (CH), 123.8 (CH), 119.8 (CH), 114.8 (C), 114.0 (CH), 41.5 (CH), 28.8 (CH_2), 17.2 (CH_3);

HRMS: *m/z* $[M + Na]^+$ calcd. for $C_{18}H_{15}NONa$: 284.1046; found: 284.1046.

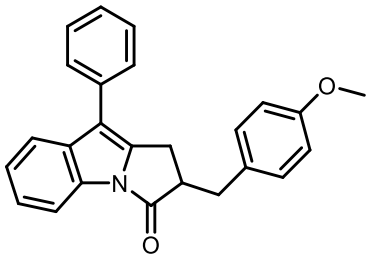

2-(4-methoxybenzyl)-9-phenyl-1,2-dihydro-3H-pyrrolo[1,2-a]indol-3-one (**7.3j**): 64% yield (0.35 mmol scale, 82 mg); white solid; mp: 156–159 °C; R_f = 0.21 (*n*-hexane-EtOAc, 85:15); IR (KBr): 3093, 2917, 1742, 1582 cm^{-1};

^{1}H NMR (400.13 MHz) ($CDCl_3$): δ 8.09–8.04 (m, 1H), 7.68–7.63 (m, 1H), 7.46–7.43 (m, 2H), 7.37–7.33 (m, 2H), 7.27–7.20 (m, 3H), 7.09–7.06 (m, 2H), 6.77–6.73 (m, 2H), 3.68 (s, 3H), 3.44–3.37 (m, 1H), 3.28 (dd, J_1 = 14.2 Hz, J_2 = 4.6 Hz, 1H), 3.20 (dd, J_1 = 17.8 Hz, J_2 = 8.7 Hz, 1H), 2.90 (dd, J_1 = 17.5 Hz, J_2 = 5.0 Hz, 1H), 2.81 (dd, J_1 = 14.2 Hz, J_2 = 9.8 Hz, 1H);

^{13}C NMR (100.6 MHz) ($CDCl_3$): δ 173.2 (C), 158.6 (C), 138.4 (C), 133.9 (C), 133.6 (C), 130.9 (C), 130.2 (C), 130.0 (CH), 129.0 (CH), 127.9 (CH), 126.9 (CH), 124.5 (CH), 123.9 (CH), 119.8 (CH), 114.9 (C), 114.3 (CH), 114.0 (CH), 55.4 (CH_3), 48.3 (CH), 36.3 (CH_2), 25.7 (CH_2).);

HRMS: *m/z* $[M + H]^+$ calcd. for $C_{25}H_{22}NO_2$: 368.1645; found: 368.1629.

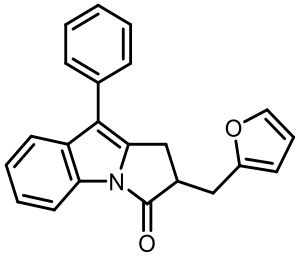

2-(furan-2-ylmethyl)-9-phenyl-1,2-dihydro-3H-pyrrolo[1,2-a]indol-3-one (**7.3k**): 54% yield (0.35 mmol scale, 62 mg); white solid; mp: 162–165 °C; R_f = 0.23 (*n*-hexane-EtOAc, 85:15); IR (KBr): 3002, 2917, 1733, 1576, 1455 cm^{-1};

^{1}H NMR (400.13 MHz) ($CDCl_3$): δ 8.18–8.12 (m, 1H), 7.79–7.76 (m, 1H), 7.58–7.56 (m, 2H), 7.49–7.45 (m, 2H), 7.35–7.33 (m, 2H), 7.31–7.30 (m, 1H), 6.29 (dd, J_1 = 3.3 Hz, J_2 = 1.9 Hz, 1H), 6.13 (dd, J_1 = 3.3 Hz, J_2 = 0.5 Hz, 1H), 3.61–3.55 (m, 1H), 3.49–3.38 (m, 2H), 3.15–3.13 (m, 2H);

^{13}C NMR (100.6 MHz) ($CDCl_3$): δ 172.7 (C), 152.2 (C), 142.0 (CH), 138.2 (C), 133.9 (C), 133.5 (C), 130.9 (C), 129.0 (CH), 128.0(CH), 126.9 (CH), 124.5 (CH), 123.9 (CH), 119.9 (CH), 115.0 (C), 114.1 (CH), 110.5 (CH), 107.2 (CH), 46.0 (CH), 29.8 (CH_2), 26.2 (CH_2);

HRMS: *m/z* $[M + H]^+$ calcd. for $C_{22}H_{18}NO_2$: 328.1332; found: 328.1317.

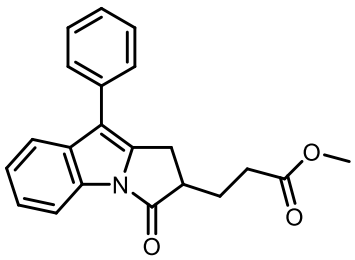

methyl 3-(3-oxo-9-phenyl-2,3-dihydro-1H-pyrrolo[1,2-a]indol-2-yl)propanoate (**7.3l**): 66% yield (0.35 mmol scale, 77 mg); brown solid; mp: 126–129 °C; R_f = 0.19 (*n*-hexane-EtOAc, 85:15); IR (KBr): 3004, 2918, 1737, 1454, 1383 cm^{-1};

^{1}H NMR (400.13 MHz) ($CDCl_3$): δ 8.15–8.10 (m, 1H), 7.80–7.76 (m, 1H), 7.61–7.59 (m, 2H), 7.51–7.47 (m, 2H), 7.37–7.32 (m, 3H), 3.70 (s, 3H), 3.53 (dd, J_1 = 17.3 Hz, J_2 = 8.8 Hz, 1H), 3.33–3.26 (m, 1H), 2.99 (dd, J_1 = 17.3 Hz, J_2 = 4.9 Hz, 1H), 2.67–2.54 (m, 2H), 2.40–2.31 (m, 1H), 2.11–2.02 (m, 1H);

^{13}C NMR (100.6 MHz) ($CDCl_3$): δ 173.2 (C), 173.1 (C), 138.0 (C), 133.9 (C), 133.5 (C), 130.8 (C), 129.1 (CH), 127.9 (CH), 127.0 (CH), 124.5 (CH), 124.0 (CH), 119.9 (CH), 115.0 (C), 114.1 (CH), 51.9 (CH_3), 45.6 (CH), 31.4 (CH_2), 27.2 (CH_2), 26.8 (CH_2);

HRMS: *m/z* $[M + H]^+$ calcd. for $C_{21}H_{20}NO_3$: 334.1438; found: 334.1421.

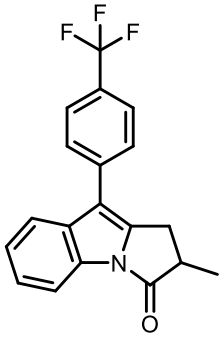

2-methyl-9-(4-(trifluoromethyl)phenyl)-1,2-dihydro-3H-pyrrolo[1,2-a]indol-3-one (**7.3m**): 71% yield (0.35 mmol scale, 82 mg); white solid; mp: 128–130 °C; R_f = 0.19 (*n*-hexane-EtOAc, 85:15); IR (KBr): 3103, 2972, 1753, 1323, 1132 cm^{-1};

^{1}H NMR (400.13 MHz) ($CDCl_3$): δ 8.17–8.14 (m, 1H), 7.76–7.69 (m, 5H), 7.38–7.33 (m, 2H), 3.56 (dd, J_1 = 8.8 Hz, J_2 = 8.7 Hz, 1H), 3.35–3.27 (m, 1H), 2.95 (dd, J_1 = 17.4 Hz, J_2 = 4.7 Hz, 1H), 1.51 (d, J = 7.5 Hz, 3H);

^{13}C NMR (100.6 MHz) ($CDCl_3$): δ 174.5 (C), 139.5 (C), 137.5 (C), 133.3 (C), 130.9 (C), 128.9 (q, J = 32.4 Hz) (CH), 128.0 (CH), 126.0 (q, J = 3.7 Hz) (CH), 124.8 (CH), 124.5 (q, J = 272.1 Hz) (CH), 124.2 (CH), 119.5 (CH), 114.2 (CH), 113.6 (C), 41.6 (CH), 29.09 (CH_2), 17.0 (CH_3); ^{19}F (376.5 MHz) ($CDCl_3$): δ −62.4;

HRMS: *m/z* $[M + H]^+$ calcd. for $C_{19}H_{15}F_3NO$: 330.1100; found: 330.1084.

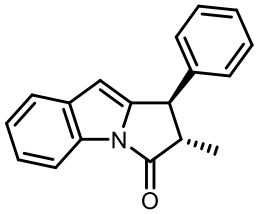

(trans)- 2-methyl-1-phenyl-1,2-dihydro-3H-pyrrolo[1,2-a]indol-3-one (**7.5a**): 62% yield (0.35 mmol scale, 57 mg); yellow wax; R_f = 0.24 (*n*-hexane-EtOAc, 85:15); IR (KBr): 3021, 2919, 1736, 1587, 1452, 1385 cm^{-1};

^{1}H NMR (400.13 MHz) (DMSO-*d*$_6$): δ = 7.98 (d, *J* = 7.42 Hz, 1H), 7.58–7.56 (m, 1H), 7.43–7.37 (m, 4H), 7.35–7.26 (m, 3H), 6.27 (s, 1H), 4.37 (d, *J* = 6.5 Hz, 1H), 3.28–3.21 (m, 1H), 3.15 (d, *J* = 7.2, 3H);

^{13}C NMR (100.6 MHz) (DMSO-*d*$_6$): δ 173.4, 146.4, 140.6, 135.3, 130.3, 129.3 (CH), 128.3 (CH), 127.8 (CH), 124.3 (CH), 123.8 (CH), 121.5 (CH), 113.4 (CH), 100.5 (CH), 51.5 (CH), 47.3 (CH), 14.5 (CH_3);

HRMS: *m/z* $[M + H]^+$ calcd. for $C_{18}H_{16}NO$: 262.1226; found: 262.1215.

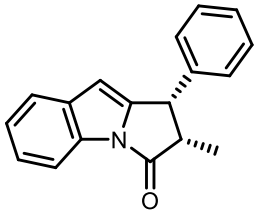

(cis)- 2-methyl-1-phenyl-1,2-dihydro-3H-pyrrolo[1,2-a]indol-3-one (**7.5′a**): 12% yield (0.35 mmol scale, 11 mg); yellow wax; R_f = 0.24 (*n*-hexane-EtOAc, 85:15); IR (KBr): 3060, 2919, 1736, 1452, 1386 cm^{-1};

^{1}H NMR (400.13 MHz) (DMSO-d_6): δ 8.01–7.97 (m, 1H), 7.61–7.56 (m, 1H), 7.36–7.26 (m, 5H), 7.13–7.10 (m, 2H), 6.41 (m, 1H), 4.94 (dd, J_1 = 8.7 Hz, J_2 = 0.83 Hz, 1H), 3.78–3.70 (m, 1H), 0.80 (d, *J* = 7.7, 3H).

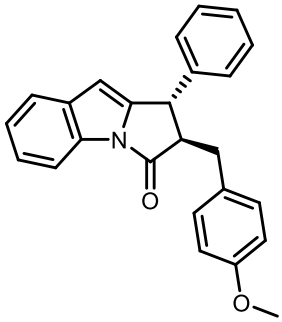

(trans)-2-(4-methoxybenzyl)-1-phenyl-1,2-dihydro-3H-pyrrolo[1,2-a]indol-3-one (**7.5b**): 48% yield (0.35 mmol scale, 62 mg); orange solid; mp: 111–113 °C; R_f = 0.19 (*n*-hexane-EtOAc, 85:15); IR (KBr): 3074, 2918, 1738, 1451, 1384 cm^{-1};

^{1}H NMR (400.13 MHz) ($CDCl_3$): δ 8.14 (d, *J* = 7.9 Hz, 1H), 7.48 (d, *J* = 7.3 Hz, 1H), 7.34–7.21 (m, 5H), 7.19 (d, *J* = 8.6 Hz, 2H), 7.02–6.99 (m, 2H), 6.84–6.80 (m, 2H), 6.13 (d, *J* = 0.9 Hz, 1H), 4.30 (dd, J_1 = 5.2 Hz, J_2 = 1.1 Hz, 1H), 3.78 (s, 3H), 3.42–3.37 (m, 1H), 3.25–3.15 (m, 2H);

^{13}C NMR (100.6 MHz) ($CDCl_3$): δ 172.2 (C), 158.7 (C), 145.6 (C), 141.1 (C), 135.3 (C), 130.7 (CH), 130.5 (C), 129.5 (C), 128.9 (CH), 127.7 (CH), 127.4 (CH), 124.3 (CH), 123.8 (CH), 121.0 (CH), 114.3 (CH), 114.1 (CH), 101.5 (CH), 58.8 (CH_3), 55.4 (CH), 43.6 (CH), 34.9 (CH_2);

HRMS: *m/z* $[M + H]^+$ calcd. for $C_{25}H_{22}NO_2$: 368.1645; found: 368.1627.

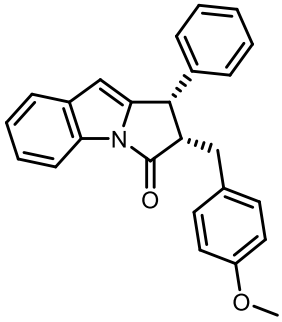

(cis)-2-(4-methoxybenzyl)-1-phenyl-1,2-dihydro-3H-pyrrolo[1,2-a]indol-3-one (**7.5′b**): 2% yield (0.35 mmol scale, 3 mg); yellow solid; mp: 135–138 °C; R_f = 0.19 (*n*-hexane-EtOAc, 85:15); IR (KBr): 3074, 2919, 1737, 1512, 1452, 1385 cm^{-1};

^{1}H NMR (400.13 MHz) ($CDCl_3$): δ 8.15 (d, *J* = 7.9 Hz, 1H), 7.51 (d, *J* = 7.2 Hz, 1H), 7.36–7.22 (m, 5H), 6.91–6.89 (m, 2H), 6.75–6.71 (m, 4H), 6.24 (s, 1H), 4.70 (d, *J* = 8.4 Hz, 1H), 3.88–

3.82 (m, 1H), 3.78 (s, 3H), 3.17 (dd, J_1 = 15.0 Hz, J_2 = 4.9 Hz, 1H), 2.43 (dd, J_1 = 15.0 Hz, J_2 = 10.1 Hz, 1H).

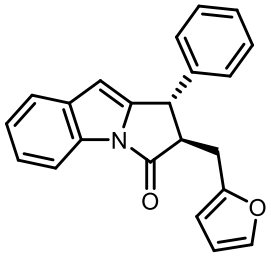

(trans)-2-(furan-2-ylmethyl)-1-phenyl-1,2-dihydro-3H-pyrrolo[1,2-a]indol-3-one (**7.5c**): 39% yield (0.35 mmol scale, 44.2 mg); red solid; mp: 101–103 °C; R_f = 0.19 (*n*-hexane-EtOAc, 90:10); IR (KBr): 3053, 2197, 1739, 1586, 1453 cm^{-1};

^{1}H NMR (400.13 MHz) ($CDCl_3$): δ 8.14 (d, *J* = 7.8 Hz, 1H), 7.49 (d, *J* = 7.2 Hz, 1H), 7.35–7.24 (m, 6H), 7.12–7.10 (m, 2H), 6.28–6.27 (m, 1H), 6.18 (d, *J* = 0.9 Hz, 1H), 6.16 (d, *J* = 2.8 Hz, 1H), 4.35 (dd, J_1 = 5.4 Hz, J_2 = 1.3 Hz, 1H), 3.43–3.39 (m, 1H), 3.33–3.22 (m, 2H);

^{13}C NMR (100.6 MHz) ($CDCl_3$): δ 171.6 (C), 151.7 (C), 145.3 (C), 142.0 (CH), 140.8 (C), 135.3 (C), 130.6 (C), 129.0 (CH), 127.7 (CH), 127.6 (CH), 124.4 (CH), 123.8 (CH), 121.0 (CH), 114.1 (CH), 110.5 (CH), 108.0 (CH), 101.6 (CH), 56.7 (CH), 44.3 (CH), 28.3 (CH_2);

HRMS: *m/z* $[M + H]^+$ calcd. for $C_{22}H_{18}NO_2$: 328.1332; found: 328.1316.

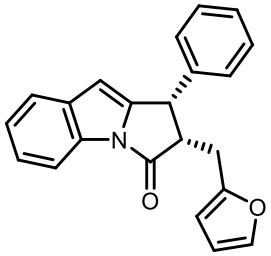

(cis)-2-(furan-2-ylmethyl)-1-phenyl-1,2-dihydro-3H-pyrrolo[1,2-a]indol-3-one (**7.5′c**): 13% yield (0.35 mmol scale, 15.5 mg); a suitable characterization is not available.

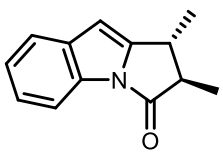

(trans)- 1,2-dimethyl-1,2-dihydro-3H-pyrrolo[1,2-a]indol-3-one (**7.5d**): 64% yield (0.35 mmol scale, 45 mg); yellow solid; mp: 46–49 °C; R_f = 0.23 (*n*-hexane-EtOAc, 85:15); IR (KBr): 3058, 2918, 1741, 1453, 1384 cm^{-1};

^{1}H NMR (400.13 MHz) ($CDCl_3$): δ 8.05–8.03 (m, 1H), 7.51–7.49 (m, 1H), 7.29–7.23 (m, 2H), 6.27 (d, *J* = 0.9 Hz, 1H), 3.08–3.04 (m, 1H), 2.78–2.71 (m, 1H), 1.47 (d, *J* = 7.1 Hz, 3H), 1.45 (d, *J* = 7.5 Hz, 3H);

^{13}C NMR (100.6 MHz) ($CDCl_3$): δ 174.0 (C), 147.6 (C), 135.3 (C), 130.5 (C), 124.1 (CH), 123.5 (CH), 120.7 (CH), 113.9 (CH), 99.4 (CH), 50.4 (CH), 36.6 (CH), 18.7 (CH_3), 15.2 (CH_3);

HRMS: *m/z* $[M + H]^+$ calcd. for $C_{13}H_{14}NO$: 200.1070; found: 200.1061.

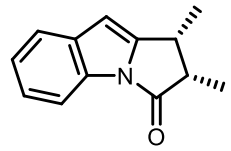

(cis)-1,2-dmethyl-1,2-dihydro-3H-pyrrolo[1,2-a]indol-3-one (**7.5′d**): 12% yield (0.35 mmol scale, 8 mg); yellow solid; mp: 58–61 °C; R_f = 0.23 (*n*-hexane-EtOAc, 85:15); IR (KBr): 3060, 2917, 1735, 1584, 1453 cm^{-1};

^{1}H NMR (400.13 MHz) ($CDCl_3$): δ 8.06–8.04 (m, 1H), 7.52–7.50(m, 1H), 7.30–7.24 (m, 2H), 6.29 (s, 1H), 3.63–3.55 (m, 1H), 3.31 (quint, *J* = 7.8 Hz, 1H), 1.34 (d, *J* = 5.7 Hz, 3H), 1.32 (d, *J* = 5.4 Hz, 3H).

Typical Procedure for the Preparation of 1,2-dihydro-3H-pyrrolo[1,2-a]indol-3-one (**7.8**), ethyl 3-oxo-2,3-dihydro-1H-pyrrolo[1,2-a]indole-2-carboxylate (**7.11**) and 2-acetyl-1,2-dihydro-3H-pyrrolo[1,2-a]indol-3-one (**7.13**)

The products 10 and 12 were synthesized according to the typical procedure described for the preparation of 1,2-dihydro-3H-pyrrolo[1,2-a]indol-3-ones using 5 equiv. of 7.9 and 7.11, respectively, as a nucleophile instead of 7.5.

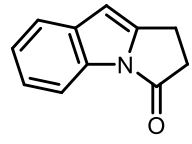

1,2-dihydro-3H-pyrrolo[1,2-a]indol-3-one (**7.8**): known compound of 52% yield (0.35 mmol scale, 31 mg); grey solid; mp: 150–151 °C, mp: 153–154; R_f = 0.20 (*n*-hexane-EtOAc, 85:15); IR (neat): 2973, 2937, 1722, 1387, 1168 cm^{-1};

^{1}H NMR (400.13 MHz) ($CDCl_3$): δ = 8.11–8.08 (m, 1H), 7.53–7.51 (m, 1H), 7.30–7.28 (m, 2H), 6.32 (s, 1H), 3.20–3.17 (m, 2H), 3.13–3.09 (m, 2H);

^{13}C NMR (100.6 MHz) ($CDCl_3$): δ = 171.8 (C), 143.7 (C), 135.4 (C), 124.2 (CH), 123.4 (CH), 120.6 (CH), 113.7 (CH), 100.5 (CH), 35.0 (CH_2), 19.7 (CH_2);

HRMS: *m/z* $[M + Na]^+$ calcd. for $C_{11}H_9NONa$: 194.0576; found: 194.0578.

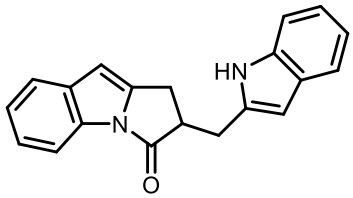

2-((1H-indol-2-yl)methyl)-1,2-dihydro-3H-pyrrolo[1,2-a]indol-3-one (**7.9**): 54% yield (0.35 mmol scale, 57 mg); purple solid; mp: 164–165 R_f = 0.24 (*n*-hexane-EtOAc, 85:15); IR (neat): 3404, 1715, 1593, 1544, 1173, 667 cm^{-1};

^{1}H NMR (400.13 MHz) ($CDCl_3$): δ 8.64 (br s, 1H), 8.02–8.00 (m, 1H), 7.45 (d, J = 7.8 Hz, 1H), 7.41–7.39 (m, 1H), 7.25 (d, J = 7.8 Hz, 2H), 7.22–7.17 (m, 2H), 7.05 (dd, J_1 = 7.3 Hz, J_2 = 1.1 Hz, 1H), 6.99 (dd, J_1 = 7.3 Hz, J_2 = 1.1 Hz, 1H), 6.24 (s, 1H), 6.17 (s, 1H), 3.52–3.48 (m, 1H), 3.32–3.28 (m, 1H), 3.25–3.22 (m, 2H), 2.92 (dd, J_1 = 16.9 Hz, J_2 = 1.3 Hz, 1H);

^{13}C NMR (100.6 MHz) ($CDCl_3$): δ 174.1, 141.7, 136.6, 135.5, 135.3, 130.5, 128.4, 124.5, 123.6, 121.7, 120.8, 120.1, 119.9, 113.8, 110.9, 101.8, 101.2, 47.1, 29.6, 26.1;

HRMS: *m/z* $[M + Na]^+$ calcd. for $C_{20}H_{16}N_2ONa$: 323.1155; found: 323.1154.

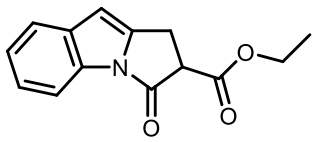

ethyl 3-oxo-2,3-dihydro-1H-pyrrolo[1,2-a]indole-2-carboxylate (**7.11**): 58% yield (0.35 mmol scale, 49 mg); white solid; mp: 99–100; R_f = 0.23 (*n*-hexane-EtOAc, 80:20); IR (neat): 2991, 2919, 1726, 1596, 1187, 743 cm^{-1};

^{1}H NMR (400.13 MHz) ($CDCl_3$): δ 8.10–8.08 (m, 1H), 7.55–7.53 (m, 1H), 7.33–7.31 (m, 2H), 6.34 (s, 1H), 4.25 (dd, J_1 = 7.3 Hz, J_2 = 0.8 Hz, 1H), 4.22 (dd, J_1 = 7.3 Hz, J_2 = 0.8 Hz, 1H), 3.68 (dd, J_1 = 17.4 Hz, J_2 = 1.5 Hz, 1H), 3.07 (dd, J_1 = 17.4 Hz, J_2 = 1.5 Hz, 1H), 1.72 (s, 3H), 1.26 (t, J = 7.3 Hz, 3H);

^{13}C NMR (100.6 MHz) ($CDCl_3$): δ 168.2 (C), 166.1 (C), 141.1 (C), 135.6 (C), 130.6 (C), 124.6 (CH), 123.7 (CH), 120.8 (CH), 113.8 (CH), 101.2 (CH), 62.4 (CH_2), 52.7 (CH), 24.3 (CH_2), 14.2 (CH_3);

HRMS: *m/z* $[M + H]^+$ calcd. for $C_{14}H_{14}NO_3$: 244.0868; found: 244.0857.

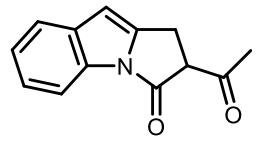

2-acetyl-1,2-dihydro-3H-pyrrolo[1,2-a]indol-3-one (**7.13**): 55% yield (0.35 mmol scale, 40 mg); brown solid; mp: 96–97; R_f = 0.21 (*n*-hexane-EtOAc, 85:15); IR (neat): 2916, 2849, 1641, 1454, 1190, 772 cm^{-1}. In a chloroform solution, this compound has as an equilibrium mixture of ketone and enol forms; both tautomers were observed by ^{1}H NMR, and the peaks of enol form were reported as marked with an asterisk*;

^{1}H NMR (400.13 MHz) ($CDCl_3$) (ketone: enol = 75/25): δ 11.41* (br s, 1H) 8.04–7.98 (m, 2H, aromatic protons of both tautomers), 7.53–7.47 (m, 2H, aromatic protons of both tautomers), 7.29–7.25 (m,4 H aromatic protons of both tautomers), 6.32* (br s, 1H), 6.30 (br s, 1H), 4.26 (dd, J_1 = 8.7 Hz, J_2 = 4.3 Hz, 1H), 3.76* (m, 1H), 3.64* (s, 2H), 3.17–3.10 (m, 1H), 2.56 (s, 3H), 2.06* (s, 3H);

^{13}C NMR (100.6 MHz) ($CDCl_3$) (unselected signals): δ 200.2 (C), 169.5 (C), 167.7 (C), 166.5 (C), 141.4 (C), 139.7 (C), 135.6 (C), 134.6 (C), 130.6 (C), 124.7 (CH), 123.8 (CH), 123.7 (CH), 123.2 (CH), 120.9 (CH), 120.8 (CH), 113.7 (CH), 113.5 (CH), 102.7 (C), 101.3 (CH), 100.2 (CH), 60.5 (CH), 29.8 (CH_2), 29.7 (CH_3), 23.6 (CH_2), 21.5 (CH_2), 19.1 (CH_3);

HRMS: *m/z* $[M + H]^+$ calcd. for $C_{13}H_{12}NO_2$: 214.0862; found: 214.0887.

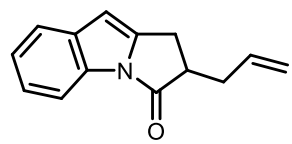

2-allyl-1,2-dihydro-3H-pyrrolo[1,2-a]indol-3-one (**7.3n**): 71% yield (0.35 mmol scale, 52 mg); brown oil; R_f = 0.25 (*n*-hexane-EtOAc, 85:15); IR (KBr): 3081, 2918, 1714, 1454, 1385 cm^{-1};

^{1}H NMR (400.13 MHz) ($CDCl_3$): δ 8.11–8.09 (m, 1H), 7.53–7.50 (m, 1H), 7.32–7.27 (m, 2H), 6.29 (s, 1H), 5.89–5.78 (m, 1H), 5.23–5.11 (m, 2H), 3.34–3.26 (m, 2H), 2.96–2.88 (m, 1H), 2.81–2.75 (m, 1H), 2.53–2.46 (m, 1H);

^{13}C NMR (100.6 MHz) ($CDCl_3$): δ 173.5 (C), 142.3 (C), 135.5 (C), 134.2 (CH), 130.5 (C), 124.2 (CH), 123.4 (CH), 120.6 (CH), 118.2 (CH_2), 113.8 (CH), 100.5 (CH), 46.2 (CH), 35.8 (CH_2), 25.5 (CH_2);

HRMS: *m/z* $[M + H]^+$ calcd. for $C_{14}H_{14}NO$: 212.1070; found: 212.1057.

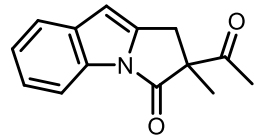

2-acetyl-2-methyl-1,2-dihydro-3H-pyrrolo[1,2-a]indol-3-one (**7.15a**): 18% yield (0.35 mmol scale, 14 mg); brown oil; R_f = 0.23 (*n*-hexane-EtOAc, 85:15); IR (KBr): 3073, 2919, 1736, 1714, 1455, 1386 cm^{-1};

^{1}H NMR (400.13 MHz) ($CDCl_3$): δ 8.05–8.02 (m, 1H), 7.52–7.50 (m, 1H), 7.30–7.28 (m, 2H), 6.32 (s, 1H), 3.84 (dd, J_1 = 17.6 Hz, J_2 = 1.3 Hz, 1H), 2.88 (dd, J_1 = 17.6 Hz, J_2 = 1.5 Hz, 1H), 2.37 (s, 3H), 1.70 (s, 3H);

^{13}C NMR (100.6 MHz) ($CDCl_3$): δ 203.5 (C), 170.8 (C), 140.0 (C), 135.5 (C), 130.6 (C), 124.6 (CH), 123.7 (CH), 120.8 (CH), 113.8 (CH), 101.4 (CH), 63.9 (C), 30.9 (CH_2), 25.8 (CH_3), 21.9 (CH_3);

HRMS: *m/z* $[M + H]^+$ calcd. for $C_{13}H_{11}NO_2$: 214.0862; found: 214.0887.

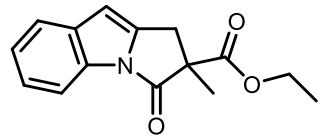

ethyl 2-methyl-3-oxo-2,3-dihydro-1H-pyrrolo[1,2-a]indole-2-carboxylate (**7.15b**): 60% yield (0.35 mmol scale, 54 mg); yellow oil; R_f = 0.23 (*n*-hexane-EtOAc, 80:20); IR (KBr): 2984, 2934, 1710, 1602, 1127 cm^{-1};

^{1}H NMR (400.13 MHz) ($CDCl_3$): δ 8.10–8.08 (m, 1H), 7.55–7.53 (m, 1H), 7.33–7.31 (m, 2H), 6.34 (s, 1H), 4.25 (dd, J_1 = 7.3 Hz, J_2 = 0.8 Hz, 1H), 4.22 (dd, J_1 = 7.3 Hz, J_2 = 0.8 Hz, 1H), 3.68 (dd, J_1 = 17.4 Hz, J_2 = 1.5 Hz, 1H), 3.07 (dd, J_1 = 17.4 Hz, J_2 = 1.5 Hz, 1H), 1.72 (s, 3H), 1.26 (t, J = 7.3 Hz, 3H);

^{13}C NMR (100.6 MHz) ($CDCl_3$): δ 168.2 (C), 166.1 (C), 141.1 (C), 135.6 (C), 130.6 (C), 124.6 (CH), 123.7 (CH), 120.8 (CH), 113.8 (CH), 101.2 (CH), 62.4 (CH_2), 52.7 (CH), 24.3 (CH_2), 14.2 (CH_3);

HRMS: *m/z* $[M + Na]^+$ calcd. for $C_{15}H_{15}NO_3Na$: 280.0944; found: 280.0943.

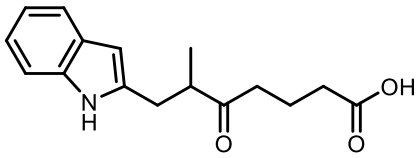

7-(1H-indol-2-yl)-6-methyl-5-oxoheptanoic acid (**7.17**): 47% yield (0.35 mmol scale, 45 mg); red solid; mp: 112–115 °C; R_f = 0.18 (*n*-hexane-EtOAc, 70:30, 10% $MeCO_2H$); IR (neat): 3055, 2951, 1735, 1713, 1456 cm^{-1};

^{1}H NMR (400.13 MHz) (DMSO-*d*$_6$): δ 12.08 (br s, 1H), 10.90 (s, 1H), 7.40 (d, J = 7.8 Hz, 1H), 7.28 (d, J = 7.9 Hz, 1H), 7.00 (td, J_1 = 7.1 Hz, J_2 = 1.1 Hz, 1H), 6.92 (td, J_1 = 7.1 Hz, J_2 = 1.0 Hz, 1H), 6.11 (d, J = 1.1 Hz, 1H), 3.04–2.98 (m, 2H), 2.68–2.56 (m, 2H), 2.49–2.45 (m, 1H), 2.17 (t, J = 7.3 Hz, 2H), 1.66 (quint, J = 7.3 Hz, 2H), 1.03 (d, J = 6.6 Hz, 3H);

^{13}C NMR (100.6 MHz) (DMSO-*d*$_6$): δ 213.2 (C), 174.7 (C), 138.2 (C), 136.4 (C), 128.7 (C), 120.6 (CH), 119.6 (CH), 119.1 (CH), 111.1 (CH), 99.7 (CH), 45.8 (CH), 39.9 (CH_2), 33.2 (CH_2), 31.2 (CH_2), 19.1 (CH_2), 16.6. (CH_3);

HRMS: *m/z* $[M + H]^+$ calcd. for $C_{16}H_{20}NO_3$: 274.1438; found: 274.1425.

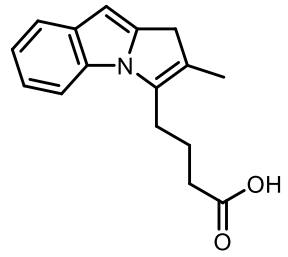

4-(2-methyl-1H-pyrrolo[1,2-a]indol-3-yl)butanoic acid (**7.18**): 22% yield (0.35 mmol scale, 20 mg); red solid; mp: 130–133 °C; R_f = 0.25 (*n*-hexane-EtOAc, 70:30, 10% $MeCO_2H$); IR (KBr): 3102, 2918, 1699, 1485, 1452, 1384 cm^{-1};

^{1}H NMR (400.13 MHz) (DMSO-*d*$_6$): δ 12.18 (br s, 1H), 7.48 (d, *J* = 7.5 Hz, 1H), 7.43 (d, *J* = 7.5 Hz, 1H), 7.30 (t, *J* = 7.5 Hz, 1H), 7.06 (t, *J* = 7.5 Hz, 1H), 5.83 (s, 1H), 3.77 (s, 2H), 2.85 (t, *J* = 7.5 Hz, 2H), 2.30 (t, *J* = 6.9 Hz, 2H), 2.02 (s, 3H), 1.76 (quint., *J* = 7.5 Hz, 2H);

^{13}C NMR (100.6 MHz) (DMSO-*d*$_6$): δ 179.1 (C), 142.0 (C), 135.2 (C), 134.0 (C), 127.5 (CH), 125.9 (CH), 122.3 (CH), 122.2 (C), 120.8 (C), 110.3 (CH), 102.8 (CH), 32.8 (CH_2), 28.7 (CH_2), 24.9 (CH_2), 23.9 (CH_2), 11.6 (CH3);

HRMS: *m/z* $[M - H]^-$ calcd. for $C_{16}H_{16}NO_2$: 254.1187; found: 254.1179.

11.6 General procedures and Characterization of Chapter 8

General procedure for the preparation of substituted 1-(3-arylprop-2-yn-1-yl)-2-aryl-1*H*-indol-7-amine 8.1

Starting materials **8.1** were prepared according to literature procedures through the four-step sequence of reactions depicted in scheme 8.1.

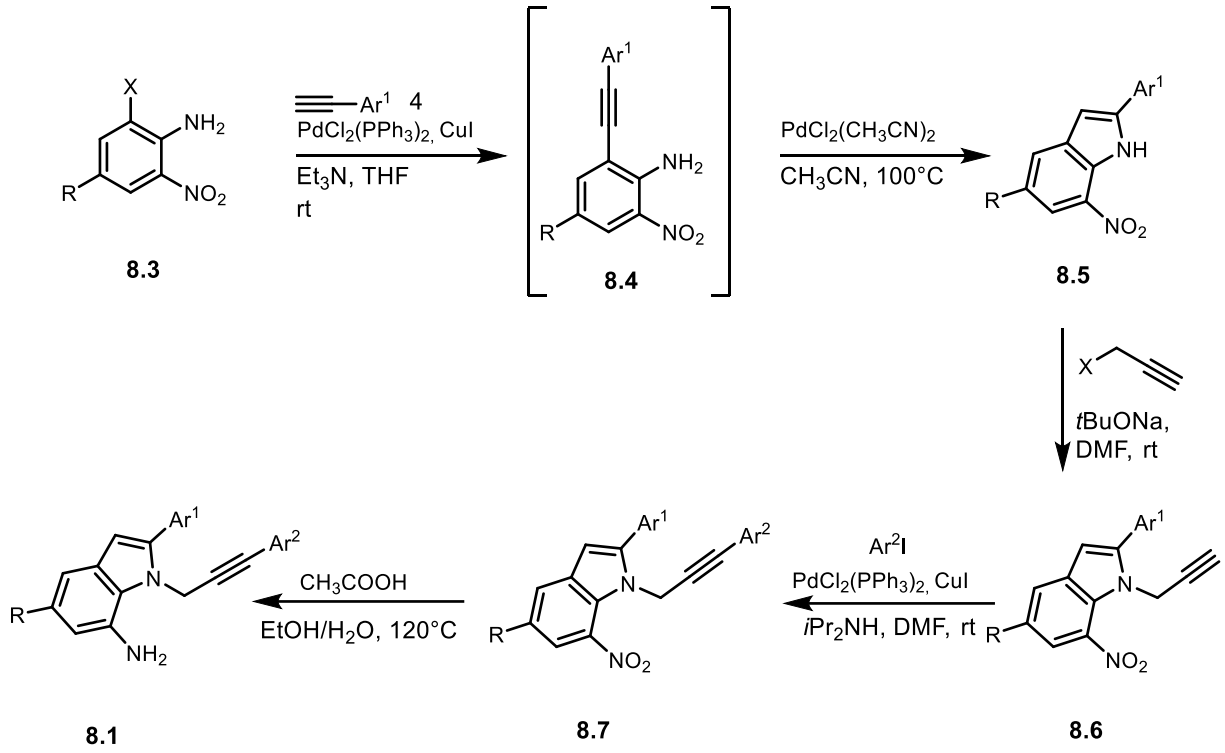

Scheme 1. Preparation of starting materials **94**

1.1.a. Typical procedure for the preparation of 5- substituted-7-nitro-2-phenyl-1H-indole **8.5**

STEP 1: synthesis of 5-chloro-7-nitro-2-phenyl-1H-indole **8.5a**

In a 100 ml two-necked round bottom flask, equipped with a magnetic stirring bar, $PdCl_2(PPh_3)_2$ (0.329 g, 0.469 mmol, 0.04 equiv.) and CuI (0.045 g, 0.234 mmol, 0.02 equiv.) were dissolved in 36.0 mL of THF and 1.56 mL of Et_3N at room temperature and under a nitrogen atmosphere. Then, 2-iodo-4-chloro-6-nitroaniline (3.5 g, 11.74 mmol, 1.0 equiv.) was added and, dropwise, phenylacetylene (1.93 mL, 17.61 mmol, 1.5 equiv.). The solution was stirred for 2h. After this time, the reaction mixture was diluted with Et_2O, and washed with a saturated solution of NH_4Cl, $NaHCO_3$, and brine. The organic layer was separated, dried over Na_2SO_4, filtered, and concentrated under reduced pressure. The residue, containing 4-chloro-2-nitro-6-(phenylethynyl)aniline **8.4a**, was transferred with 60 mL of MeCN in a two-necked 100-mL round bottom flask equipped with a condenser, and a magnetic stirring bar, then $PdCl_2(CH_3CN)_2$ was added. The solution was stirred for 2.5 h at 100 °C. After this time, the mixture was cooled to room temperature, concentrated under reduced pressure, purified by chromatography on SiO_2 (25-40 μm), eluting with an 92/8 (v/v) *n*-hexane-AcOEt mixture (R_f = 0.26) to obtain 5-chloro-7-nitro-2-phenyl-1*H*-indole **8.5a** (2,57 g, 80 % yield).

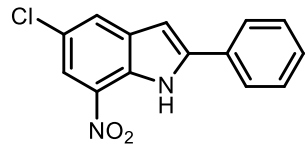

5-chloro-7-nitro-2-phenyl-1H-indole 8.5a: yield: 80%; orange solid; mp: 83 - 84 °C;

^{1}H NMR (400.13 MHz) ($CDCl_3$): δ 10.07 (bs, 1H), 8.11 (d, *J* = 1.5 Hz, 1H), 7.93 - 7.88 (m, 1H), 7.74 (d, *J* = 7.8 Hz, 1H), 7.53 (t, *J* = 7.3 Hz, 2H), 7.45 (t, *J* = 7.3 Hz, 2H), 6.90 (d, *J* = 2.4 Hz, 1H), 5.05 (d, *J* = 2.4 Hz, 2H), 2.20 (t, *J* = 2.4 Hz, 1H);

^{13}C NMR (100.6 MHz) ($CDCl_3$): δ 142.0 (C), 133.7 (C), 133.5 (C), 130.4 (C), 129.34 (CH), 129.27 (CH), 128.8 (C), 127.6 (CH), 125.7 (CH), 125.1 (C), 118.7 (CH), 100.1 (CH).

1.1.b. Typical procedure for the preparation of substituted 7-nitro-2-phenyl-1-(prop-2-yn-1-yl)-1H-indoles **8.6**

STEP 2: synthesis of 5-chloro-7-nitro-2-phenyl-1-(prop-2-yn-1-yl)-1H-indole **8.6a**

A 250 mL round bottom flask, equipped with a magnetic stirring bar, was charged with ^{t}BuONa (1.35 g, 14.02 mmol, 1.5 equiv) and 90 mL of anhydrous DMF. The reaction mixture was cooled at 0°C and 5-chloro-7-nitro-2-phenyl-1*H*-indole **8.5a** (2.4 g, 9.35 mmol, 1.0 equiv) was added dropwise. Then, propargyl bromide (1.21 mL, 14.02 mmol, 1.5 equiv) was added and the solution was warmed to room temperature and stirred for 6 h. After this time, the reaction mixture was diluted with Et_2O and washed with saturated solution of $NaHCO_3$ and brine. The organic layer was dried over Na_2SO_4, filtered, and concentrated under reduced pressure. The residue was purified by chromatography on SiO_2 (25-40 μm), eluting with an 96/4 (v/v) *n*-hexane-AcOEt mixture (R_f = 0.25) to obtain 5-chloro-7-nitro-2-phenyl-1-(prop-2-yn-1-yl)-1*H*-indole **8.6a** (2.324 g, 80 % yield).

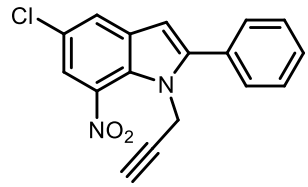

5-chloro-7-nitro-2-phenyl-1-(prop-2-yn-1-yl)-1H-indole 8.6a: 80 % yield; brown solid; mp 103 - 104 °C;

^{1}H NMR (400.13 MHz) ($CDCl_3$): δ 7.92 (d, *J* = 1.9 Hz, 1H), 7.87 (d, *J* = 1.9 Hz, 1H), 7.58-7.50 (m, 5H), 6.70 (s, 1H), 5.05 (d, *J* = 2.4 Hz, 2H), 2.20 (t, *J* = 2.4 Hz, 1H);

^{13}C NMR (100.6 MHz) ($CDCl_3$): δ 146.8 (C), 137.3 (C), 134.3 (C), 130.6 (C), 129.6 (CH), 129.4 (CH), 129.1 (CH), 127.1 (C), 126.0 (CH), 125.2 (C), 119.8 (CH), 104.1 (CH), 77.1 (C), 74.4 (CH), 37.1 (CH_2).

1.1.c. Typical procedure for the preparation of substituted 1-(3-arylprop-2-yn-1-yl)-7-nitro-2-phenyl-1H-indoles **8.7**

STEP 3: synthesis of 5-chloro-1-(3-(4-methoxyphenyl)prop-2-yn-1-yl)-7-nitro-2-phenyl-1H-indole **8.7c**

In a two-necked 50-mL round bottom flask, equipped with a magnetic stirring bar, $PdCl_2(PPh_3)_2$ (0.084 g, 0.119 mmol, 0.04 equiv.) and CuI (0.011 g, 0.0597 mmol, 0.02 equiv.) were dissolved in 12.3 mL of *i*Pr_2NH and 6.1 mL of DMF at room temperature and under nitrogen; then, 4-iodoanisole (0.839 g, 3.584 mmol, 1.2 equiv.) and 5-chloro-7-nitro-2-phenyl-1-(prop-2-yn-1-yl)-1*H*-indole **8.6c** (0.928 g, 2.98 mmol, 1.0 equiv.) were added and the resulting mixture was stirred for 24 h. After this time, the mixture was diluted with Et_2O and washed with a saturated solution of NH_4Cl, a saturated solution of $NaHCO_3$, and with brine. The organic layer was dried over Na_2SO_4, filtered, and concentrated under reduced pressure. The residue was purified by chromatography on SiO_2 (25-40 μm), eluting with a 93/7 (v/v) *n*-hexane/AcOEt mixture (R_f = 0.27) to obtain 5-chloro-1-(3-(4-methoxyphenyl)prop-2-yn-1-yl)-7-nitro-2-phenyl-1*H*-indole **8.7c** (0.860 g, 70% yield).

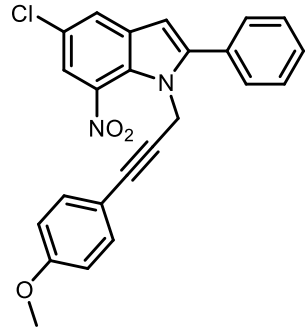

5-chloro-1-(3-(4-methoxyphenyl)prop-2-yn-1-yl)-7-nitro-2-phenyl-1H-indole 8.7c: 70 % yield; yellow solid; mp 133 - 134 °C;

^{1}H NMR (400.13 MHz) ($CDCl_3$): δ 7.91 (d, *J* = 1.9 Hz, 1H), 7.87 (d, *J* = 1.9 Hz, 1H), 7.60 - 7.50 (m, 5H), 7.21 (d, *J* = 8.8 Hz, 2H), 6.78 (d, *J* = 8.8 Hz, 2H), 6.70 (s, 1H), 5.23 (s, 2H), 3.78 (s, 3H);

^{13}C NMR (100.6 MHz) ($CDCl_3$): δ 159.9 (C), 146.7 (C), 138.2 (C), 137.5 (C), 134.2 (C), 133.2 (CH), 130.8 (C), 129.6 (CH), 129.3 (CH), 129.0 (CH), 127.1 (C), 125.8 (CH), 124.9 (C), 119.6 (CH), 113.8 (CH), 103.8 (CH), 86.1 (C), 80.9 (C), 55.2 (CH_3), 38.2 (CH_2).

1.1.d. Typical procedure for the synthesis of substutited 1-(3-arylprop-2-yn-1-yl)-2-aryl-1H-indol-7-amine ***8.1***

STEP 4: synthesis of 5-chloro-1-(3-(4-methoxyphenyl)prop-2-yn-1-yl)-2-phenyl-1H-indol-7-amine ***8.1c***

In a 50 mL Carousel Tube Reactor (Radely Discovery Technology), equipped with a magnetic stirring bar, 5-chloro-1-(3-(4-methoxyphenyl)prop-2-yn-1-yl)-7-nitro-2-phenyl-1*H*-indole **8.7c** (0.180 g, 0.431 mmol, 1.0 equiv.) was added to a solution of EtOH/H_2O (3:1) and stirred at 120°C for 10 minutes. Then, 51 µl of acetic acid and 72 mg of Fe (0) (0.431 mmol, 1.0 equiv.) were added in three portions every 15 minutes. The reaction mixture was then stirred for 2 hours before being cooled at room temperature and concentrated under reduced pressure. Subsequently, the mixture was diluted with Et_2O and washed with a saturated solution of $NaHCO_3$, and with brine. The organic layer was dried over Na_2SO_4, filtered, and concentrated under reduced pressure. The residue was purified by filtration on a pad of celite eluting with DCM to obtain 5-chloro-1-(3-(4-methoxyphenyl)prop-2-yn-1-yl)-2-phenyl-1*H*-indol-7-amine **8.1c** (0.140 g, 85% yield).

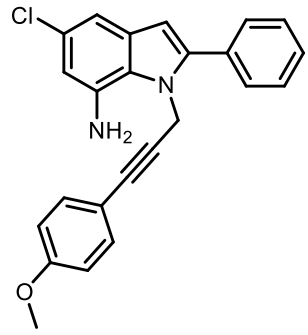

5-chloro-1-(3-(4-methoxyphenyl)prop-2-yn-1-yl)-2-phenyl-1H-indol-7-amine 8.1c: 85% yield; orange solid; mp 91 - 92 °C;

^{1}H NMR (400.13 MHz) ($CDCl_3$): δ 7.71 - 7.68 (m, 2H), 7.55 - 7.49 (m, 2H), 7.48 - 7.44 (m, 1H), 7.42 (d, , *J* = 8.8 Hz, 2H), 7.09 (d, *J* = 1.8 Hz, 1H), 6.89 (d, *J* = 8.8 Hz, 2H), 6.54 (d, *J* = 1.8 Hz, 1H), 6.47 (s, 1 H), 5.17 (s, 2H), 4.35 (bs, 2 H), 3.84 (s, 3H);

^{13}C NMR (100.6 MHz) ($CDCl_3$): δ 160.1 (C), 143.2 (C), 134.0 (C), 133.2 (CH), 131.9 (C), 130.8 (C), 129.3 (CH), 128.7 (CH), 128.3 (CH), 127.1 (C), 126.3 (C), 114.1 (CH), 113.8 (C), 111.3 (CH), 110.1 (CH), 102.4 (CH), 86.6 (C), 84.9 (C), 55.3 (CH_3), 36.5 (CH_2).

General procedure for the preparation of 1-(4-(3-(7-amino-5-methyl-2,3-diphenyl-1*H*-indol-1-yl)prop-1-yn-1-yl)phenyl)ethan-1-one 8.1l

Starting material 1l was prepared according to literature procedures from 5-methyl-7-nitro-2-phenyl-1*H*-indole through the sequence of reactions depicted in scheme 2.

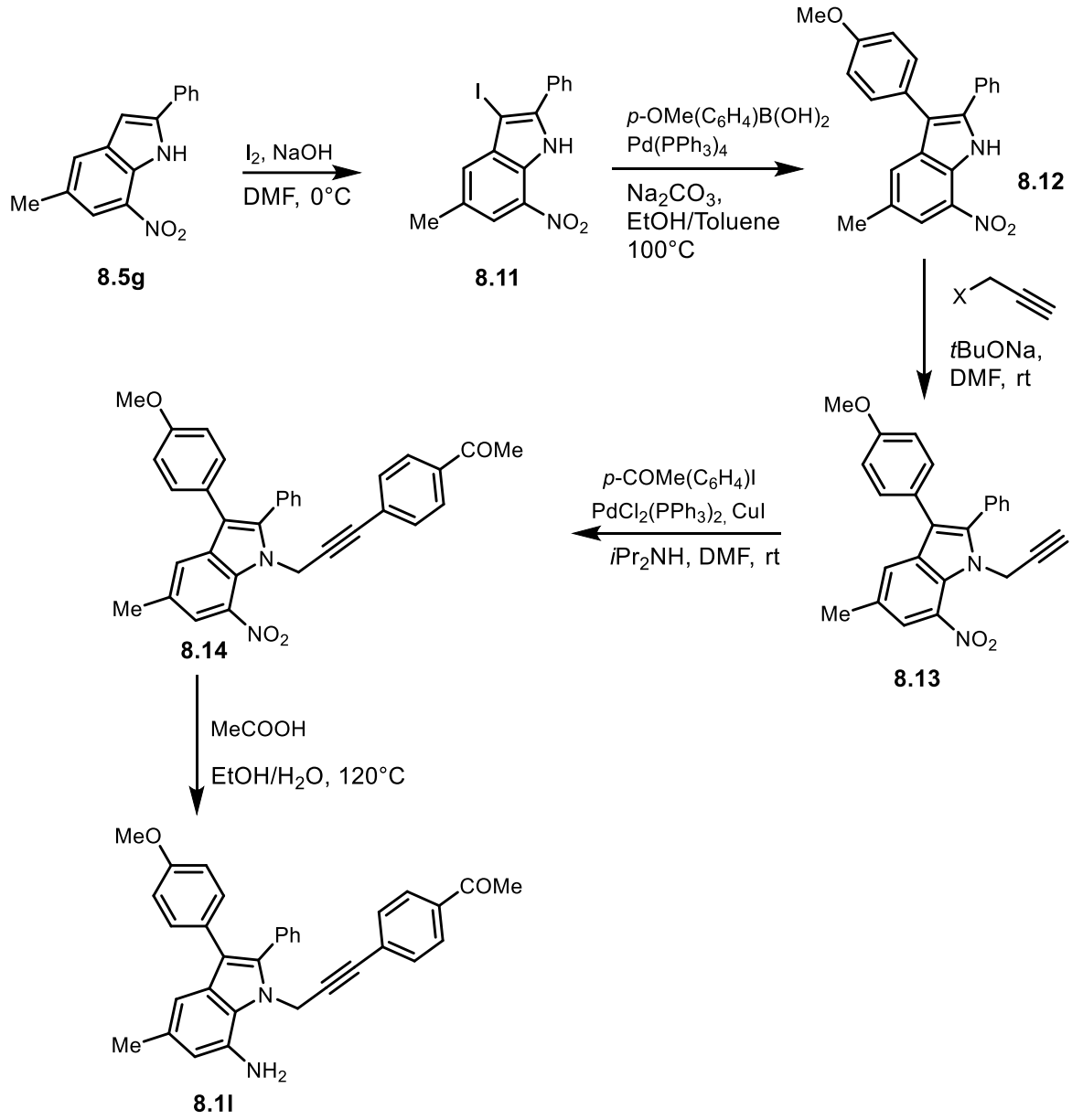

Scheme 2. Preparation of starting materials **8.1l**

STEP 1: synthesis of 3-iodo-5-methyl-7-nitro-2-phenyl-1H-indole

To a solution of 5-methyl-7-nitro-2-phenyl-1*H*-indole **8.5g** (1.0 g, 3.982 mmol, 1.0 equiv.) in DMF (8.0 mL) KOH (0.671 g, 11.94 mmol, 3.0 equiv.) was added at 0°C and the resulting mixture was stirred for 10 minutes before a solution of iodine (1.061 g, 4.181 mmol, 1.05 equiv.) in DMF (10.0 mL) was added dropwise over 5 minutes. After 1 h, the mixture was poured into a saturated solution of NH_4Cl and $Na_2S_2O_3$ to precipitate the product. The solid material was filtered off, solubilized in Et_2O, washed with water and dried over Na_2SO_4. After filtration, the mixture was concentrated under reduced pressure to give of 3-iodo-5-methyl-7-nitro-2-phenyl-1*H*-indole as an orange powder (0.97 g, 65% yield).

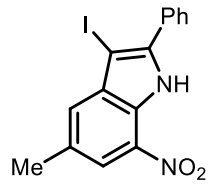

3-iodo-5-methyl-7-nitro-2-phenyl-1H-indole 8.11: 65% yield; orange solid; mp: 133-135 °C;

^{1}H NMR (400.13 MHz) ($CDCl_3$): δ10.06 (bs, 1H), 8.07 (s, 1H), 7.88-7.82 (m, 2H), 7.67 (s, 1H), 7.61-7.47 (m, 3H), 2.59 (s, 3H);

^{13}C NMR (100.6 MHz) ($CDCl_3$): δ 140.6 (C), 135.3 (C), 132.4 (C), 131.0 (C), 130.3 (C), 129.9 (CH), 129.4 (CH), 128.9 (CH), 128.6 (C), 128.5 (CH), 121.0 (CH), 58.4 (C), 21.2 (CH_3).

STEP 2: synthesis of 5-methyl-7-nitro-2,3-diphenyl-1H-indole **8.12**

In a three-necked round bottom flask, equipped with a condenser and magnetic stirring bar, [$Pd(PPh_3)_4$] (115.4 mg, 0.10 mmol, 0.05 equiv.) was dissolved at room temperature in 25 mL of EtOH/Toluene (2:1) under argon; then, 3-iodo-5-methyl-7-nitro-2-phenyl-1*H*-indole (0.756 g, 2.0 mmol, 1.0 equiv.), 4-methoxyphenylboronic acid (0.912 g, 6.0 mmol, 3.0 equiv.), and Na_2CO_3 (2.39 g, 22.6 mmol,3.0 equiv.) were added and the mixture was refluxed for 16 hours. After this time, the mixture was cooled to room temperature, diluted with CH_2Cl_2 and washed with brine. The organic layer was dried over Na_2SO_4, filtered, and concentrated under reduced pressure. The residue was purified by chromatography on SiO_2 (25-40 μm), eluting with an 80/20 (v/v) *n*-hexane-AcOEt mixture (R_f = 0.22) to obtain the desired product (0.609 g, 85% yield).

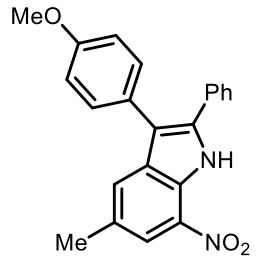

3-(4-methoxyphenyl)-5-methyl-7-nitro-2-phenyl-1H-indole *8.12*: 85% yield; yellow solid; mp: 133-135 °C;

^{1}H NMR (400.13 MHz) ($CDCl_3$): δ 9.89 (bs, 1H), 8.03 (s, 1H), 7.75 (s, 1H), 7.53-7.46 (m, 2H), 7.43-7.31 (m, 5H), 6.99 (d, *J* = 8.7 Hz, 1H), 3.89 (s, 3H), 2.52 (s, 3H);

^{13}C NMR (100.6 MHz) ($CDCl_3$): δ 158.7 (C), 136.1 (C), 133.1 (C), 132.3 (C), 131.5 (C), 131.3 (CH), 129.6 (C), 128.9 (CH), 128.7 (C), 128.4 (CH), 128.1 (CH), 127.9 (CH), 125.9 (C), 120.3 (CH), 115.0 (C), 114.3 (CH), 55.3 (CH_3), 21.1 (CH_3).

STEPS 3 – 5 were carried out with procedures described in paragraphs 8.2.1b-d

2. Procedure for the synthesis of compound 8.9d

A flame dried 50 mL Carousel Tube Reactor (Radely Discovery Technology), equipped with a magnetic stirring bar, was charged with 8-chloro-2-(4-methoxybenzyl)-5-phenyl-3*H*-pyrrolo[1,2,3-*de*]quinoxaline **8.2c** (50.0 mg, 0.13 mmol, 1.0 equiv) dissolved in anhydrous 2 mL of THF under argon. Then, a solution of $LiAlH_4$ 2 M in THF (108 µl, 0.26 mmol, 2.0 equiv.) was added at 0°C and the mixture was stirred for 15 minutes at 80°C. After this time, the mixture was diluted with Et_2O and washed with a saturated $NaHCO_3$ solution and brine. The organic layer was dried over Na_2SO_4, filtered, concentrated under reduced pressure. The resulting residue was purified by chromatography on SiO_2 (25-40 µm), eluting with a 93/7 (v/v) *n*-hexane/AcOEt mixture (R_f = 0.27) to obtain 8-chloro-2-(4-methoxybenzyl)-5-phenyl-2,3-dihydro-1*H*-pyrrolo[1,2,3-*de*]quinoxaline (49.5 mg, 98 % yield).

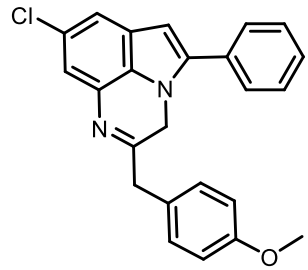

8-chloro-2-(4-methoxybenzyl)-5-phenyl-2,3-dihydro-1H-pyrrolo[1,2,3-de]quinoxaline 8.1l: 98 % yield; brown oil;

^{1}H NMR (400.13 MHz) ($CDCl_3$): δ 7.53-7.42 (m, 4H), 7.44-7.35 (m, 3H), 7.08 (d, *J* = 1.8 Hz, 1H), 6.93 (d, *J* = 8.8 Hz, 2H), 6.48 (s, 1H), 6.47 (d, *J* = 1.8 Hz, 1H), 4.76 (bs, 1H), 4.45 - 4.33 (m, 2H), 3.84 (s, 3H), 3.74-3.64 (m, 1H), 2.45-2.28 (m, 2H);

^{13}C NMR (100.6 MHz) ($CDCl_3$): δ 159.2 (C), 143.7 (C), 136.6 (C), 135.9 (C), 132.7 (C), 131.7 (C), 129.3 (CH), 128.6 (CH), 128.1 (CH), 127.7 (CH), 127.4 (C), 126.2 (C), 114.2 (CH), 110.4 (CH), 108.5 (CH), 103.4 (CH), 62.4 (CH), 55.4 (CH_3), 46.6 (CH_2), 38.6 (CH_2).

Characterization data of starting materials

Characterization data of 5-substituted 7-nitro-2-aryl-1*H*-indole 8.5

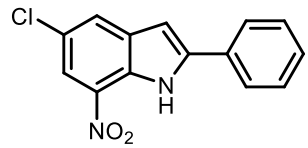

5-chloro-7-nitro-2-phenyl-1H-indole 8.5a 80 % yield; orange solid; mp 103 - 104 °C;

^{1}H NMR (400.13 MHz) ($CDCl_3$): δ10.07 (bs, 1H), 8.11 (d, *J* = 1.5 Hz, 1H), 7.93 - 7.88 (m, 1H), 7.74 (d, *J* = 7.8 Hz, 1H), 7.53 (t, *J* = 7.3 Hz, 2H), 7.45 (t, *J* = 7.3 Hz, 2H), 6.90 (d, *J* = 2.4 Hz, 1H), 5.05 (d, *J* = 2.4 Hz, 2H), 2.20 (t, *J* = 2.4 Hz, 1H);

^{13}C NMR (100.6 MHz) ($CDCl_3$): δ 142.0 (C), 133.7 (C), 133.5 (C), 130.4 (C), 129.34 (CH), 129.27 (CH), 128.8 (C), 127.6 (CH), 125.7 (CH), 125.1 (C), 118.7 (CH), 100.1 (CH).

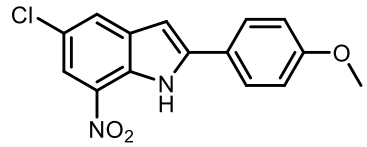

5-chloro-2-(4-methoxyphenyl)-7-nitro-1H-indole 8.5b: 72 % yield; yellow - orange solid; mp 103 - 104 °C;

^{1}H NMR (400.13 MHz) (DMSO-d_6): δ 11.78 (bs, 1H) 8.13 (d, *J* = 1.3 Hz, 1H), 8.05 (d, *J* = 1.3 Hz, 1H), 8.01 (d, *J* = 8.7 Hz, 2H), 7.12 (d, *J* = 8.7 Hz, 2H), 7.1 (s, 1H), 3.89 (s, 3H);

^{13}C NMR (100.6 MHz) (DMSO-d_6): δ 160.3 (C), 143.8 (C), 134.6 (C), 133.0 (C), 128.8 (CH), 128.7 (C), 127.0 (CH), 123.6 (C), 123.3 (C), 117.5 (CH), 114.7 (CH), 99.9 (CH), 55.8 (CH_3).

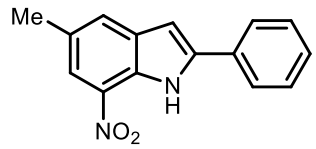

5-methyl-7-nitro-2-phenyl-1H-indole 8.5c*:* 97 % yield; yellow solid; mp 172 - 174 °C ;

^{1}H NMR (400.13 MHz) ($CDCl_3$): δ 9.87 (s, 1H), 7.88 (s, 1H), 7.73–7.57 (m, 3H), 7.56–7.24 (m, 3H), 6.78 (s, 1H), 2.47 (s, 3H);

^{13}C NMR (100.6 MHz, $CDCl_3$): δ 140.5 (C), 133.04 (C), 132.3 (C), 131.0 (C), 129.5 (C), 129.2 (CH), 128.8 (C), 128.8 (CH), 128.7(CH), 125.5 (CH), 119.9 (CH), 100.0 (CH), 21.1 (CH_3).

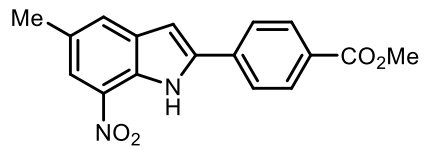

methyl 4-(5-methyl-7-nitro-1H-indol-2-yl)benzoate 8.5d*:* 98 % yield; yellow solid; mp 103 - 104 °C;

^{1}H NMR (400.13 MHz) ($CDCl_3$): δ 9.96 (s, 1H), 8.08 (d, *J* = 8.2 Hz, 2H), 7.93 (s, 1H), 7.72 (d, *J* = 8.7 Hz, 3H), 6.90 (d, *J* = 1.7 Hz, 1H), 3.89 (s, 3H), 2.46 (s, 3H).;

^{13}C NMR (100.6 MHz, $CDCl_3$): δ 166.5 (C), 139.1 (C), 135.1 (C), 132.8 (C), 132.5 (C), 130.5 (CH), 129.9 (C), 129.9 (C), 129.1 (CH), 125.2 (CH), 120.7 (CH), 101.7 (CH), 52.3 (CH_3), 21.1 (CH_3).

3.2 Characterization data of 7-nitro-2-aryl-1-(prop-2-yn-1-yl)-1*H*-indole 8.6

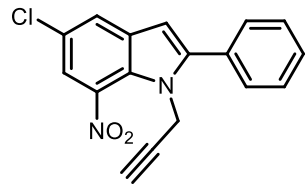

5-chloro-7-nitro-2-phenyl-1-(prop-2-yn-1-yl)-1H-indole 8.6a: 80 % yield; brown solid; mp 103 - 104 °C;

^{1}H NMR (400.13 MHz) ($CDCl_3$): δ 7.92 (d, *J* = 1.9 Hz, 1H), 7.87 (d, *J* = 1.9 Hz, 1H), 7.58-7.50 (m, 5 H), 6.70 (s, 1 H), 5.05 (d, *J* = 2.4 Hz, 2H), 2.20 (t, *J* = 2.4 Hz, 1H);

^{13}C NMR (100.6 MHz) ($CDCl_3$): δ 160.6 (C), 147.1 (C), 137.3 (C), 134.5 (C), 131.4 (CH), 126.7 (C), 126.3 (CH), 124.4 (C), 122.6 (C), 119.3 (CH), 115.1 (CH), 104.0 (CH), 78.0 (C), 77.5 (CH), 55.8 (CH_3), 37.2 (CH_2).

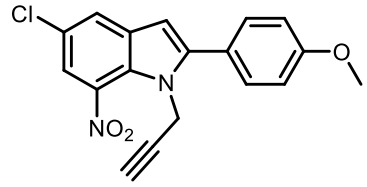

5-chloro-2-(4-methoxyphenyl)-7-nitro-1-(prop-2-yn-1-yl)-1H-indole 8.6b: 50 % yield; yellow solid; mp 103 - 104 °C;

^{1}H NMR (400.13 MHz) (DMSO d_6): δ8.12 (d, *J* = 1.7 Hz, 1H), 7.96 (d, *J* = 1.7 Hz, 1H), 7.56 (d, *J* = 8.6 Hz, 2H), 7.14 (d, *J* = 8.6 Hz, 2H), 6.80 (s, 1H), 4.97 (d, *J* = 2.4 Hz, 2H), 3.85 (s, 1H), 3.33 - 3.30 (m, 1H);

^{13}C NMR (100.6 MHz) (DMSO d_6): δ 160.5 (C), 146.8 (C), 137.2 (C), 134.4 (C), 130.9 (CH), 125.7 (CH), 125.1 (C), 122.8 (C), 119.5 (CH), 114.7 (C), 114.5 (CH), 103.5 (CH), 77.2 (C), 74.4 (CH), 55.45 (CH_3), 37.1 (CH_2).

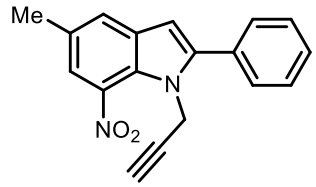

5-methyl-7-nitro-2-phenyl-1-(prop-2-yn-1-yl)-1H-indole 8.6c: 88 % yield; brown solid; mp 103 - 104 °C;

^{1}H NMR (400.13 MHz, $CDCl_3$): δ 7.63 (s, 1H), 7.53 (s, 1H), 7.49–7.10 (m, 5H), 6.50 (s, 1H), 4.90 (d, *J* = 2.3 Hz, 2H), 2.35 (s, 3H), 1.98 (t, *J* = 2.3 Hz, 1H).

^{13}C NMR (100.6 MHz) ($CDCl_3$): δ 145.6 (C), 137.1 (C), 133.7 (C), 131.3 (C), 129.9 (C), 129.6 (CH), 129.0 (CH), 129.0 (CH), 127.4 (C), 127.1 (CH), 121.2 (CH), 104.3 (CH), 77.68 (C), 73.93 (C), 36.94 (CH_2), 20.83 (CH_3).

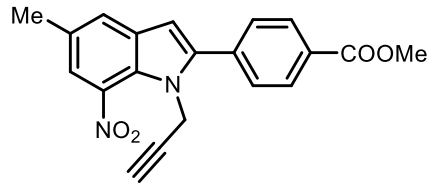

methyl 4-(5-methyl-7-nitro-1-(prop-2-yn-1-yl)-1H-indol-2-yl)benzoate 8.6d: 63 % yield; orange solid; mp 103 - 104 °C;

^{1}H NMR (400.13 MHz) ($CDCl_3$): δ 8.20 (d, *J* = 8.5 Hz, 2H), 7.82 (s, 1H), 7.74 (s, 1H), 8.20 (d, *J* = 8.5 Hz, 2H), 7.61 (d, *J* = 8.5 Hz, 2H), 6.75 (s, 1H), 5.05 (d, *J* = 2.4 Hz, 2H), 3.99 (s, 3H), 2.54 (s, 3H), 2.17 (t, *J* = 2.4 Hz, 2H);

^{13}C NMR (100.6 MHz) (400.13 MHz): δ 166.5 (C), 144.5 (C), 137.2 (C), 135.6 (C), 133.5 (C), 130.4 (C), 130.2 (C), 130.1 (CH), 129.3 (CH), 127.8 (C), 127.3 (CH), 121.8 (CH), 105.4 (CH), 77.3 (C), 74.0 (CH), 52.4 (CH_3), 37.1 (CH_2), 20.8 (CH_3).

3.3 Characterization data of 7-nitro-2-aryl-1-(3-phenylprop-2-yn-1-yl)-1*H*-indole 8.7

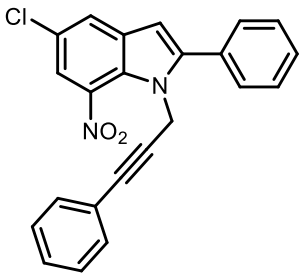

5-chloro-7-nitro-2-phenyl-1-(3-phenylprop-2-yn-1-yl)-1H-indole 8.7a: 73 % yield; yellow - orange solid; mp 152 - 153 °C;

^{1}H NMR (400.13 MHz) ($CDCl_3$): δ 7.92 (d, *J* = 1.9 Hz, 1H), 7.88 (d, *J* = 1.9 Hz, 1H), 7.61 - 7.52 (m, 5H), 7.32 - 7.22 (m, 5H), 6.72 (s, 1H), 5.26 (s, 2H);

^{13}C NMR (100.6 MHz) ($CDCl_3$): δ 146.8 (C), 137.5 (C), 134.2 (C), 131.7 (CH), 130.8 (C), 129.6 (CH), 129.3 (CH), 129.0 (CH), 128.7 (CH), 128.2 (CH), 127.1 (C), 125.9 (CH), 125.0 (C), 121.7 (C), 119.7 (CH), 103.9 (CH), 86.1 (C), 82.2 (C), 38.1 (CH_2).

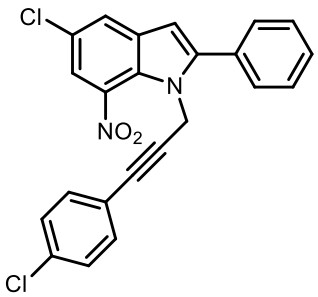

5-chloro-1-(3-(4-chlorophenyl)prop-2-yn-1-yl)-7-nitro-2-phenyl-1H-indole 8.7b: 73 % yield; orange solid; mp 109 - 110 °C;

^{1}H NMR (400.13 MHz) ($CDCl_3$): δ 7.91 (d, *J* = 1.7 Hz, 1H), 7.88 (d, *J* = 1.7 Hz, 1H), 7.62 - 7.50 (m, 5H), 7.26 - 7.17 (m, 4H), 6.72 (s, 1H), 5.24 (s, 2H);

^{13}C NMR (100.6 MHz) ($CDCl_3$): δ 146.8 (C), 137.4 (C), 134.9 (C), 134.2 (C), 133.0 (CH), 130.7 (C), 129.6 (CH), 129.4 (CH), 129.0 (CH), 128.6 (CH), 127.1 (C), 126.0 (CH), 125.1 (C), 120.2 (C), 119.7 (CH), 103.9 (CH), 85.1 (C), 83.3 (C), 38.0 (CH_2).

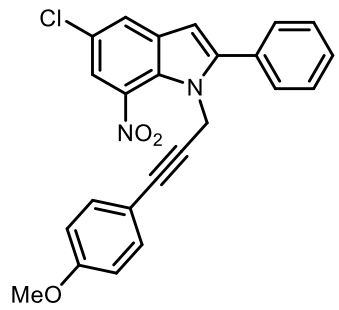

5-chloro-1-(3-(4-methoxyphenyl)prop-2-yn-1-yl)-7-nitro-2-phenyl-1H-indole 8.7c: 70 % yield; yellow solid; mp 133 - 134 °C;

^{1}H NMR (400.13 MHz) ($CDCl_3$): δ 7.91 (d, *J* = 1.9 Hz, 1H), 7.87 (d, *J* = 1.9 Hz, 1H), 7.60 - 7.50 (m, 5H), 7.21 (d, *J* = 8.8 Hz, 2H), 6.78 (d, *J* = 8.8 Hz, 2H), 6.70 (s, 1 H), 5.23 (s, 2H), 3.78 (s, 3H);

^{13}C NMR (100.6 MHz) ($CDCl_3$): δ 159.9 (C), 146.7 (C), 138.2 (C), 137.5 (C), 134.2 (C), 133.2 (CH), 130.8 (C), 129.6 (CH), 129.3 (CH), 129.0 (CH), 127.1 (C), 125.8 (CH), 124.9 (C), 119.6 (CH), 113.8 (CH), 103.8 (CH), 86.1 (C), 80.9 (C), 55.2 (CH_3), 38.2 (CH_2).

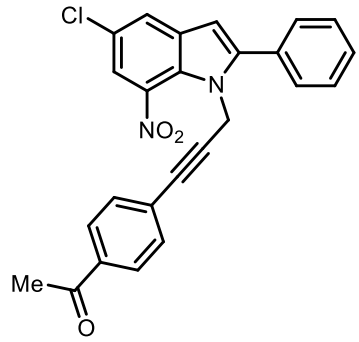

1-(4-(3-(5-chloro-7-nitro-2-phenyl-1H-indol-1-yl)prop-1-yn-1-yl)phenyl)ethan-1-one 8.7d: 52 % yield; brown solid; mp 133 - 134 °C;

^{1}H NMR (400.13 MHz) ($CDCl_3$): δ 7.92 (d, *J* = 1.9 Hz, 1H), 7.90 (d, *J* = 1.9 Hz, 1H), 7.84 (d, *J* = 8.5 Hz, 2H), 7.60 - 7.53 (m, 5H), 7.36 (d, *J* = 8.5 Hz, 2H), 6.73 (s, 1H), 5.27 (s, 2H), 2.58 (s, 3H);

^{13}C NMR (100.6 MHz) ($CDCl_3$): δ 197.2 (C), 146.8 (C), 137.4 (C), 136.6 (C), 134.2 (C), 131.9 (CH), 130.6 (C), 129.6 (CH), 129.4 (CH), 129.1 (CH), 128.1 (CH), 127.1 (C), 126.5 (C), 126.0 (CH), 125.2 (C), 119.7 (CH), 104.0 (CH), 85.4 (C), 85.3 (C), 38.0 (CH_2), 26.6 (CH_3).

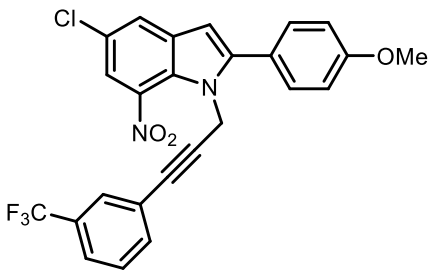

5-chloro-2-(4-methoxyphenyl)-7-nitro-1-(3-(3-(trifluoromethyl)phenyl)prop-2-yn-1-yl)-1H-indole 8.7e: 47 % yield; yellow - orange solid; mp 86 - 87 °C;

^{1}H NMR (400.13 MHz) ($CDCl_3$): δ 7.90 (d, *J* = 1.8 Hz, 1H), 7.87 (d, *J* = 1.8 Hz, 1H), 7.57 - 7.44 (m, 5H), 7.40 (t, *J* = 7.6 Hz,, 1H), 7.10 (d, *J* = 8.6 Hz, 2H), 6.67 (s, 1H), 5.24 (s, 2H), 3.92 (s, 3H);

^{13}C NMR (100.6 MHz) ($CDCl_3$): δ 160.5 (C), 146.7 (C), 137.3 (C), 135.0 (CH), 134.3 (C), 131.0 (CH), 130.8 (q, J_{CF} = 33 Hz, C), 128.8 (CH), 128.5 (q, J_{CF} = 4.0 Hz, CH), 126.9 (C), 125.7 (CH), 125.3 (q, J_{CF} = 4.0 Hz, CH), 125.1 (C), 123.5 (q, J_{CF} = 273 Hz, C), 122.9 (C), 122.7 (C), 119.4 (CH), 114.5 (CH), 103.4 (CH), 84.4 (C), 84.0 (C), 55.4 (CH_3), 37.8 (CH_2);

^{19}F NMR (376.5 MHz) ($CDCl_3$): δ 160.5.

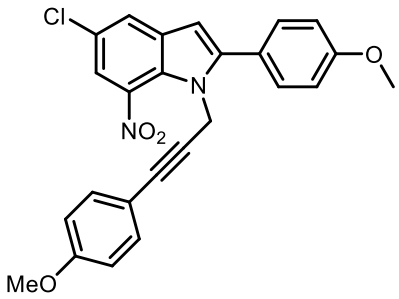

5-chloro-2-(4-methoxyphenyl)-1-(3-(4-methoxyphenyl)prop-2-yn-1-yl)-7-nitro-1H-indole 8.7f: 60 % yield; yellow - orange solid; mp 112 - 113 °C;

^{1}H NMR (400.13 MHz) ($CDCl_3$): δ 7.86 (d, *J* = 1.8 Hz, 1H), 7.85 (d, *J* = 1.8 Hz, 1H), 7.50 (d, *J* = 8.6 Hz, 2H), 7.22 (d, *J* = 8.6 Hz, 2H), 7.08 (d, *J* = 8.7 Hz, 2H), 6.78 (d, *J* = 8.7 Hz, 2H), 6.64 (s, 1H), 5.20 (s, 2H), 3.92 (s, 3H), 3.78 (s, 3H);

^{13}C NMR (100.6 MHz) ($CDCl_3$): δ 160.4 (C), 159.9 (C), 146.7 (C), 137.4 (C), 134.3 (C), 133.2 (CH), 131.0 (CH), 127.0 (C), 125.6 (CH), 124.9 (C), 123.1 (C), 119.3 (CH), 114.5 (CH), 113.9 (C), 113.8 (CH), 103.2 (CH), 86.0 (C), 81.1 (C), 55.5(CH_3), 55.2 (CH_3), 38.1 (CH_2).

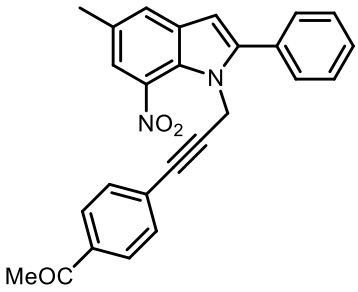

1-(4-(3-(5-methyl-7-nitro-2-phenyl-1H-indol-1-yl)prop-1-yn-1-yl)phenyl)ethan-1-one 8.7g: 73 % yield; yellow solid; mp 109 - 110 °C;

^{1}H NMR (400.13 MHz) ($CDCl_3$): δ 7.72 (d, *J* = 8.5 Hz, 2H), 7.69 (s, 1H), 7.63 (s, 1H), 7.52 - 7.38 (m, 5H), 7.22 (d, *J* = 8,. Hz, 2H), 6.60 (s, 1H), 5.18 (s, 2H), 2.47 (s, 3H), 2.44 (s, 3H);

^{13}C NMR (100.6 MHz) ($CDCl_3$): δ 197.3 (C), 145.5 (C), 137.2 (C), 136.5 (C), 133.6 (C), 131.9 (CH), 131.3 (C), 129.8 (C), 129.6 (CH), 129.0 (CH), 128.9 (CH), 128.0 (CH), 127.3 (C), 127.0 (CH), 126.9 (C), 121.1 (CH), 104.1 (CH), 86.1 (C), 84.8 (C), 38.4 (CH_2), 26.7 (CH_3), 20.9 (CH_3).

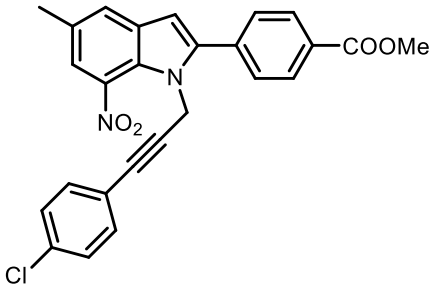

methyl 4-(1-(3-(4-chlorophenyl)prop-2-yn-1-yl)-5-methyl-7-nitro-1H-indol-2-yl)benzoate 8.7h: 58 % yield; yellow solid; mp 150 - 151 °C;

^{1}H NMR (400.13 MHz) ($CDCl_3$): δ 8.21 (d, *J* = 8.5 Hz, 2H), 7.80 (s, 1H), 7.73 (s, 1H), 7.66 (d, *J* = 8.5, 2H), 7.23 - 7.17 (m, 4H), 6.76 (s, 1H), 5.23 (s, 2H), 4.00 (s, 3H), 2.53 (s, 3H);

^{13}C NMR (100.6 MHz) ($CDCl_3$): δ 166.5 (C), 144.3 (C), 137.3 (C), 135.6 (C), 134.7 (C), 133.4 (C), 133.0 (CH), 130.2 (C), 130.16 (CH), 130.13 (C), 129.4 (CH), 128.5 (CH), 127.8 (C), 127.2 (CH), 121.6 (CH), 120.3 (C), 105.1 (CH), 84.8 (C), 83.4 (C), 52.4 (CH), 38.0 (CH_2), 20.8 (CH_3).

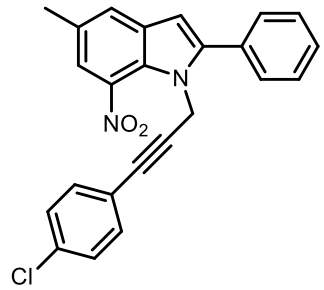

1-(3-(4-chlorophenyl)prop-2-yn-1-yl)-5-methyl-7-nitro-2-phenyl-1H-indole 8.7i: 63 % yield; yellow-orange solid; mp 122 - 123 °C;

^{1}H NMR (400.13 MHz) ($CDCl_3$): δ 7.78 (s, 1H), 7.72 (s, 1H), 7.62 - 7.42 (m, 5H), 7.24 - 7.17 (m, 4H), 6.69 (s, 1H), 5.24 (s, 2H), 2.53 (s, 3H);

^{13}C NMR (100.6 MHz) ($CDCl_3$): δ 145.5 (C), 137.2 (C), 134.6 (C), 133.5 (C), 133.0 (CH), 131.3 (C), 129.8 (C), 129.6 (CH), 128.96 (CH), 128.94 (CH), 128.5 (CH), 127.2 (C), 127.0 (CH), 121.1 (CH), 120.5 (C), 104.1 (CH), 84.6 (C), 83.8 (C), 37.8 (CH_2), 20.8 (CH_3).

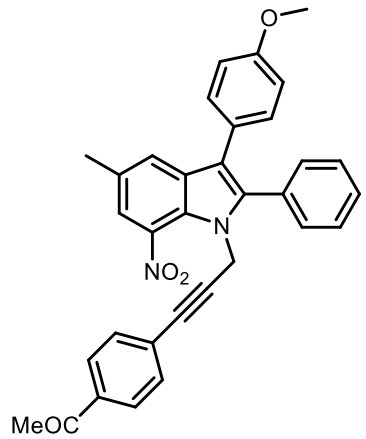

1-(4-(3-(3-(4-methoxyphenyl)-5-methyl-7-nitro-2-phenyl-1H-indol-1-yl)prop-1-yn-1-yl)phenyl)ethan-1-one 8.7l: 92 % yield; orange solid; mp 103 - 104 °C;

^{1}H NMR (400.13 MHz) ($CDCl_3$): δ 7.85 (d: *J* = 8.3 Hz, 2H), 7.81 (s, 1H), 7.76 (s, 1H), 7.49 - 7.35 (m, 7H), 7.19 (d, *J* = 8.7 Hz, 2H), 6.89 (d, *J* = 8.7 Hz, 2H), 5.20 (s, 2H), 3.83 (s, 3H), 2.58 (s, 3H), 2.52 (s, 3H);

^{13}C NMR (100.6 MHz) ($CDCl_3$): δ 197.3 (C), 158.3 (C), 140.9 (C), 137.1 (C), 136.5 (C), 133.3 (C), 131.9 (CH), 131.2 (CH), 131.1 (CH), 129.8 (CH), 128.9 (CH), 128.8 (CH), 128.1 (C), 127.0 (C), 126.2 (C), 126.0 (CH), 125.7 (C), 121.4 (CH), 116.9 (C), 114.0 (CH), 104.1 (C), 86.3 (C), 84.8 (CH), 55.2 (CH_3), 37.6 (CH_2), 26.6 (CH_3), 55.2 (CH_3),.20.9 (CH_3).

3.4 Characterization data of 2-aryl-1-(3-phenylprop-2-yn-1-yl)-1*H*-indol-7-amines 8.1

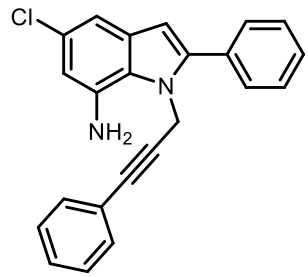

5-chloro-2-phenyl-1-(3-phenylprop-2-yn-1-yl)-1H-indol-7-amine 8.1a: 60% yield; brown oil;

^{1}H NMR (400.13 MHz) ($CDCl_3$): δ 7.68 (d, *J* = 8.8 Hz, 2H), 7.56 - 7.43 (m, 5H), 7.41 - 7.34 (m, 3H), 7.01 (d, *J* = 1.6 Hz, 1H), 6.47 (s, 1H), 6.50 (d, *J* = 1.6 Hz, 1H), 5.19 (s, 2H), 4.33 (bs, 2H);

^{13}C NMR (100.6 MHz) ($CDCl_3$): δ 143.2 (C), 134.0 (C), 131.8 (C), 131.7 (CH), 130.9 (C), 129.3 (CH), 129.0 (CH), 128.8 (CH), 128.49 (CH), 128.43 (CH), 127.2 (C), 126.4 (C), 121.8 (C), 111.4 (CH), 110.3 (CH), 102.5 (CH), 86.5 (C), 86.2 (C), 36.5 (CH_2).

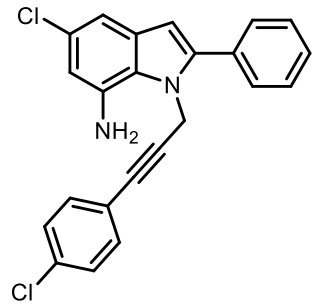

5-chloro-1-(3-(4-chlorophenyl)prop-2-yn-1-yl)-2-phenyl-1H-indol-7-amine 8.1b: 55% yield; yellow - orange solid; mp 109 - 110 °C;

^{1}H NMR (400.13 MHz) ($CDCl_3$): δ 7.60 - 7.64 (m, 2H), 7.56 - 7.45 (m, 3H), 7.41 (d, *J* = 8.6 Hz, 2H), 7.34 (d, *J* = 8.6 Hz, 2H), 7.11 (d, *J* = 1.9 Hz, 1H), 6.56 (d, *J* = 1.9 Hz, 1H), 6.48 (s, 1H), 5.19 (s, 2H), 4.27 (bs, 2H);

^{13}C NMR (100.6 MHz) ($CDCl_3$): δ 143.3 (C), 135.1 (C), 133.9 (C), 132.9 (CH), 131.8 (C), 130.9 (C), 129.3 (CH), 128.87 (CH), 128.83 (CH), 128.5 (CH), 127.2 (C), 126.5 (C), 120.3 (C), 111.6 (CH), 110.5 (CH), 102.7 (CH), 87.2 (C), 85.4 (C), 36.4 (CH_2).

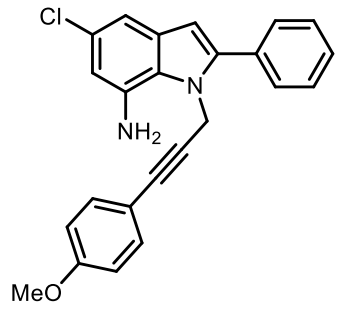

5-chloro-1-(3-(4-methoxyphenyl)prop-2-yn-1-yl)-2-phenyl-1H-indol-7-amine 8.1c: 85 % yield; yellow-orange solid; mp 91 - 92 °C;

^{1}H NMR (400.13 MHz) ($CDCl_3$): δ7.69 (d, *J*= 7.2 Hz, 2H), 7.52 (t, *J* = 7.5 Hz, 2H), 7.48 - 7.40 (m, 3H), 6.99 (d, *J* = 1.8 Hz, 1H), 7.00 (d, *J* = 1.9 Hz, 1H), 6.89 (d, *J* = 8.8 Hz, 2H), 6.55 (d, *J* = 1.9 Hz, 1H), 6.46 (s, 1H), 5.17 (s, 2H), 4.35 (bs, 2H), 3.8 (s, 3H);

^{13}C NMR (100.6 MHz) ($CDCl_3$): δ 160.1 (C), 143.2 (C), 134.0 (C), 133.2 (CH), 131.9 (C), 130.8 (C), 129.3 (CH), 128.7 (CH), 128.3 (CH), 127.1 (C), 126.3 (C), 114.1 (CH), 113.8 (C), 111.3 (CH), 110.1 (CH), 102.4 (CH), 86.6 (C), 84.9 (C), 55.3 (CH_3), 36.6 (CH_2).

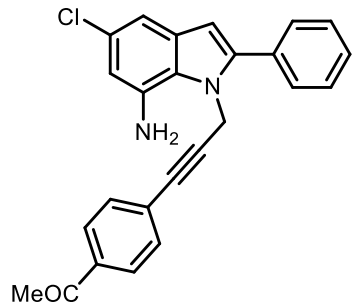

1-(4-(3-(7-amino-5-chloro-2-phenyl-1H-indol-1-yl)prop-1-yn-1-yl)phenyl)ethan-1-one 8.1d: 81 % yield; brown solid; mp 80 - 81 °C;

^{1}H NMR (400.13 MHz) (DMSO *d_6*): δ 7.90 (d, J_1 = 8.4 Hz, 2H), 7.60 (d, *J* = 7.4 Hz, 2H), 7.55 (t, *J* = 7.5 Hz, 2H), 7.48- 7.44 (m, 3H), 6.71 (s, 1H), 6.46 (s, 1H), 6.40 (d, *J* = 1.1 Hz, 1H), 5.31 (s, 2H), 4.89 (bs, 2H), 2.55 (s, 3H);

^{13}C NMR (100.6 MHz) (DMSO *d_6*): δ 197.7 (C), 142.7 (C), 136.8 (C), 134.9 (C), 132.6 (C), 132.1 (CH), 131.0 (C), 130.5 (C), 129.4 (CH), 129.2 (CH), 128.9 (CH), 128.8 (CH), 127.6 (C), 126.7 (C), 112.2 (CH), 110.8 (CH), 104.4 (CH), 90.2 (C), 84.0 (C), 36.3 (CH_2), 27.2 (CH_3).

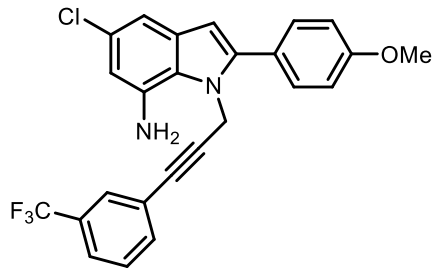

5-chloro-2-(4-methoxyphenyl)-1-(3-(3-(trifluoromethyl)phenyl)prop-2-yn-1-yl)-1H-indol-7-amine 8.1e: 93 % yield; brown solid; mp 101 - 102 °C;

^{1}H NMR (400.13 MHz) ($CDCl_3$): δ 7.73 (s, 1H), 7.67 - 7.61 (m, 2H), 7.58 (d, *J* = 8.6 Hz, 2H), 7.5 (t, *J* = 7.4 Hz, 1H), 7.09 (d, *J* = 1.5 Hz, 1H), 7.06 (d, *J* = 2 Hz, 2H), 6.55 (d, *J* = 1.5 Hz, 1H), 6.42 (s, 1H), 5.20 (s, 2H), 4.21 (bs, 2H), 3.90 (s, 3H);

^{13}C NMR (100.6 MHz) ($CDCl_3$): δ 159.9 (C), 143.2 (C), 134.9 (CH), 133.7 (C), 131.2 (q, J_{CF} = 32 Hz, C), 131.0 (C), 130.7 (CH), 129.1 (CH), 128.5 (q, J_{CF} = 4 Hz, CH), 127.0 (C), 126.4 (C), 125.8 (q, J_{CF} = 4 Hz, CH), 124.1 (C), 123.5 (q, J_{CF} = 273 Hz, C), 122.8 (CH), 114.3 (CH), 111.5 (CH), 110.4 (CH), 102.1 (CH), 87.9 (C), 84.7 (C), 55.4 (CH_3), 36.3 (CH_2);

^{19}F NMR (376.5 MHz) ($CDCl_3$): δ 159.4 (C).

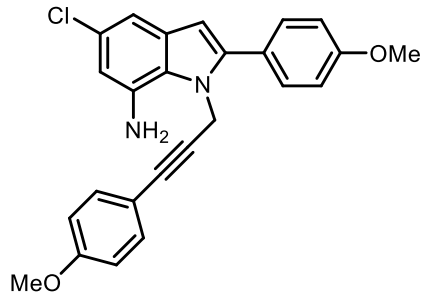

5-chloro-2-(4-methoxyphenyl)-1-(3-(4-methoxyphenyl)prop-2-yn-1-yl)-1H-indol-7-amine 8.1f: 95 % yield; brown solid; mp 105 - 106 °C;

^{1}H NMR (400.13 MHz) ($CDCl_3$): δ7.61 (d, *J* = 8.6 Hz, 2H), 7.42 (d, *J* = 8.4 Hz, 2H), 7.09 - 7.02 (m, 3H), 6.88 (d, *J* = 8.4 Hz, 2H), 6.52 (d, *J* = 1.4 Hz, 2H), 6.39 (s, 1H), 5.15 (s, 2H), 4.33 (bs, 2H), 3.89 (s, 3H), 3.85 (s, 3H);

^{13}C NMR (100.6 MHz) ($CDCl_3$): δ 160.1 (C), 159.8 (C), 143.1 (C), 134.0 (C), 133.2 (CH), 130.9 (C), 130.6 (CH), 126.9 (C), 126.2 (C), 124.3 (C), 120.4 (C), 114.2 (CH), 114.1 (CH), 111.2 (CH), 109.9 (CH), 101.7 (CH), 86.4 (C), 85.0 (C), 55.4 (CH_3), 55.3 (CH_2), 36.5 (CH_2).

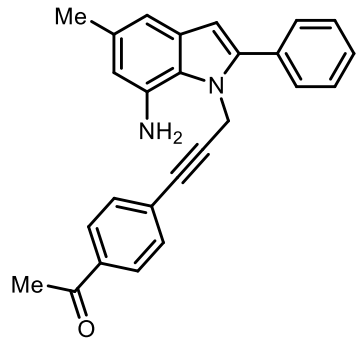

1-(4-(3-(7-amino-5-methyl-2-phenyl-1H-indol-1-yl)prop-1-yn-1-yl)phenyl)ethan-1-one
8.1g: 70 % yield; yellow - orange solid; mp 83 - 84 °C;

^{1}H NMR (400.13 MHz, $CDCl_3$): δ 7.84 (d, *J* = 8.2 Hz, 2H), 7.58 (d, *J* = 7.3 Hz, 2H), 7.50–7.30 (m, 5H), 6.85 (s, 1H), 6.38-6.35 (m, 2H), 5.15 (s, 2H), 4.04 (s, 2H), 2.53 (s, 3H), 2.29 (s, 3H);

^{13}C NMR (100.6 MHz) ($CDCl_3$): δ 197.2 (C), 142.4 (C), 136.7 (C), 132.5 (C), 132.4 (C), 131.9 (CH), 131.0 (C), 130.7 (C), 129.3 (CH), 128.7 (CH), 128.3 (CH), 128.1 (CH), 127.4 (C), 126.9 (C), 112.4 (CH), 112.3 (CH), 102.9 (CH), 90.0 (C), 85.2 (C), 36.5 (CH_2), 26.7 (CH_3), 21.3 (CH_3).

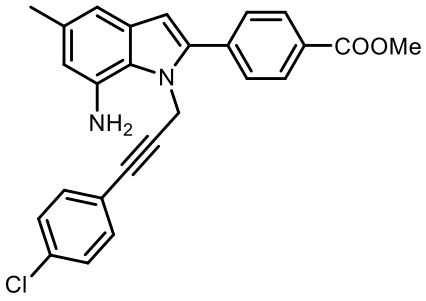

methyl 4-(7-amino-1-(3-(4-chlorophenyl)prop-2-yn-1-yl)-5-methyl-1H-indol-2-yl)benzoate
8.1h: 63 % yield; red wax;

^{1}H NMR (400.13 MHz) ($CDCl_3$): δ 8.08 (d, *J* = 8.5 Hz, 2H), 7.67 (d, *J* = 8.5 Hz, 2H), 7.28 (m, 4H), 6.85 (s, 1H), 6.46 (s, 1H), 6.36 (d, *J* = 1.0 Hz, 1H), 5.10 (s, 2H), 4.06 (s, 2H), 3.88 (s, 3H), 2.29 (s, 3H);

^{13}C NMR (100.6 MHz, $CDCl_3$): δ 166.8 (C), 141.3 (C), 136.8 (C), 135.1 (C), 133.0 (CH), 132.7 (C), 131.2 (C), 130.5 (C), 130.0 (CH), 129.4 (C), 128.9 (CH), 128.9 (CH), 128.1 (C), 120.4 (C), 112.8 (CH), 112.4 (CH), 104.0 (CH), 87.4 (C), 85.3 (C), 52.3 (CH3), 36.6 (CH_2), 21.3 (CH_3).

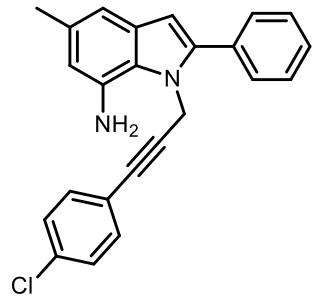

1-(3-(4-chlorophenyl)prop-2-yn-1-yl)-5-methyl-2-phenyl-1H-indol-7-amine 8.1i: 57 % yield; brown wax;

^{1}H NMR (400.13 MHz) ($CDCl_3$): δ 7.57 (d, *J* = 8.0 Hz, 2H), 7.40 (t, *J* = 8.0, 7.0 Hz, 2H), 7.37–7.27 (m, 3H), 7.23 (d, *J* = 8.5 Hz, 2H), 6.84 (s, 1H), 6.37–6.33 (m, 1H), 5.10 (s, 2H), 4.05 (s, 2H), 2.28 (s, 3H);

^{13}C NMR (100.6 MHz) ($CDCl_3$): δ 142.3 (C), 135.0 (C), 133.0 (CH), 132.6 (C), 132.5 (C), 130.9 (C), 130.6 (C), 129.3 (CH), 128.8 (CH), 128.7 (CH), 128.1 (CH), 127.4 (C), 120.6 (C), 112.3 (CH), 112.2 (CH), 102.7 (CH), 87.8 (C), 85.0 (C), 36.4 (CH_2), 21.3 (CH_3).

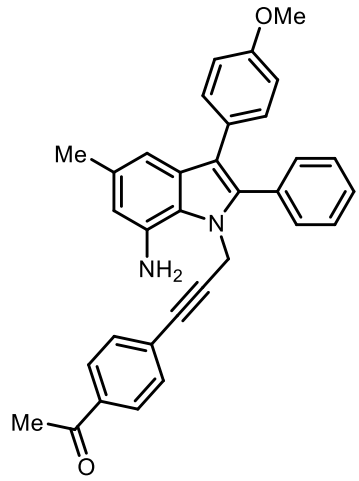

1-(4-(3-(7-amino-3-(4-methoxyphenyl)-5-methyl-2-phenyl-1H-indol-1-yl)prop-1-yn-1-yl)phenyl)ethan-1-one 8.1k: 57 % yield; brown wax;

^{1}H NMR (400.13 MHz) ($CDCl_3$): δ 7.84 (d, *J* = 8.4 Hz, 2H), 7.45 (d, *J* = 8.4 Hz, 2H), 7.38–7.29 (m, 5H), 7.12 (d, *J* = 8.7 Hz, 2H), 6.93 (s, 1H), 6.76 (d, *J* = 8.8 Hz, 2H), 6.40 (s, 1H), 5.10 (s, 2H), 4.05 (m, 2H), 3.72 (s, 3H), 2.53 (s, 3H), 2.28 (s, 3H);

^{13}C NMR (100.6 MHz) ($CDCl_3$): δ 197.2 (C), 157.7 (C), 138.1 (C), 136.7 (C), 132.5 (C), 131.9 (CH), 131.5 (C), 131.3 (CH), 131.1 (CH), 130.1 (C), 128.5 (CH), 128.3 (CH), 128.1 (CH), 127.5

(C), 127.0 (C), 126.3 (C), 115.8 (C), 113.7 (CH), 112.9 (CH), 111.3 (CH), 89.9 (C), 85.0 (C), 55.2 (CH_3), 36.3 (CH_2), 26.7 (CH_3), 21.4 (CH_3).

Typical procedure for the preparation of substituted 5-aryl-3*H*-pyrrolo[1,2,3-de] quinoxalines 8.2:

synthesis of 8-chloro-2-(4-methoxybenzyl)-5-phenyl-3*H*-pyrrolo[1,2,3-*de*]quinoxaline 8.2c.

A 50 mL Carousel Tube Reactor (Radely Discovery Technology), equipped with a magnetic stirring bar, was charged with 5-chloro-1-(3-(4-methoxyphenyl)prop-2-yn-1-yl)-2-phenyl-1*H*-indol-7-amine 1c (0.140 g, 0.361, 1.0 equiv.) and 2 mL di CH_2Cl_2 before adding 5.2 mg of (acetonitrile)-[(2-diphenyl)-di-*tert*-butylphosphine]Au(I) hexafluoroantimonate (0.0072 mmol, 0.02 equiv.). The solution was stirred for 1.5 h at room temperature, monitoring the disappearance of the starting material by TLC. Then, the mixture was concentered under reduced pressure and filtered on a pad of celite to obtain 8-chloro-2-(4-methoxybenzyl)-5-phenyl-3*H*-pyrrolo[1,2,3-*de*]quinoxaline **8.2c** (0.112 g, 80% yield).

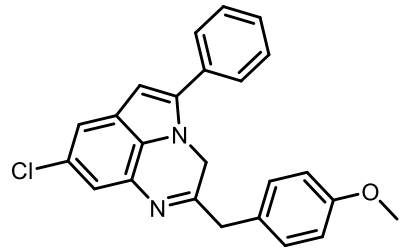

8-chloro-2-(4-methoxybenzyl)-5-phenyl-3H-pyrrolo[1,2,3-de]quinoxaline 8.2c: 80% yield; brown oil;

^{1}H NMR (400.13 MHz) ($CDCl_3$): δ 7.87 (d, *J* = 8.9 Hz, 2H), 7.41 - 7.30 (m, 6H), 7.29 (d, *J* = 1.9 Hz, 1H), 6.87 (d, *J* = 8.8 Hz, 2H), 6.46 (s, 1H), 4.32 - 4.27 (m, 2H), 3.76 (s, 3H), 3.13 - 3.08 (m, 2H);

^{13}C NMR (100.6 MHz) ($CDCl_3$): δ 167.1 (C), 161.7 (C), 161.4 (C), 142.8 (C), 134.3 (C), 132.1 (CH), 131.9 (C), 130.8 (C), 129.3 (CH), 129.0 (CH), 128.6 (CH), 128.4 (C), 128.3 (CH), 125.7 (C), 123.7 (CH), 117.9 (CH), 113.9 (CH), 101.9 (CH), 55.4 (CH_3), 48.5 (CH_2), 32.6 (CH_2).

HRMS: *m/z* $[M + H]^+$ calcd for $C_{24}H_{20}ClN_2O$: 387.1259; found: 387.1274.

Characterization data of synthesized compounds

3.3.1. Characterization data of final compounds **8.2a - i**, and **8.2k**

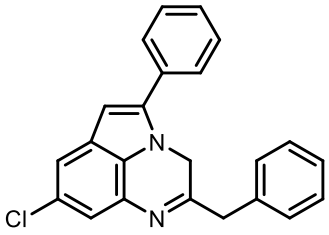

2-benzyl-8-chloro-5-phenyl-3H-pyrrolo[1,2,3-de]quinoxaline 8.1a: 98% yield; brown oil;

^{1}H NMR (400.13 MHz) ($CDCl_3$): δ 8.06 - 7.98 (m, 2H), 7.58 - 7.41 (m, 10 H), 6.60 (s, 1 H), 4.50-4.43 (m, 2H), 3.34-3.25 (m, 2H);

^{13}C NMR (100.6 MHz) ($CDCl_3$): δ 167.7 (C), 142.8 (C), 139.7 (C), 134.0 (C), 131.8 (C), 131.1(C), 130.8 (C), 130.4 (CH), 129.3 (CH), 128.67 (CH), 128.64 (CH), 128.3 (CH), 127.2 (CH), 125.7 (C), 124.1 (CH), 118.4 (CH), 102.0 (CH), 48.4 (CH_2), 33.08 (CH_2).

HRMS: *m/z* $[M + H]^+$ calcd for $C_{23}H_{18}ClN_2$: 357.1153; found: 357.1133.

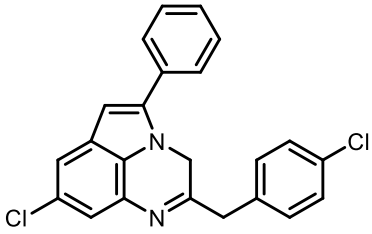

8-chloro-2-(4-chlorobenzyl)-5-phenyl-3H-pyrrolo[1,2,3-de]quinoxaline 98.2b: 86% yield; brown oil;

^{1}H NMR (400.13 MHz) ($CDCl_3$): δ 7.96 (d, *J* = 8.7 Hz, 2H), 7.56 - 7.42 (m, 10H), 6.59 (s, 1H), 4.46 - 4.48 (m, 2H), 3.26 - 3.20 (m, 2H);

^{13}C NMR (100.6 MHz) ($CDCl_3$): δ 166.2 (C), 142.8 (C), 138.0 (C), 136.7 (C), 133.7 (C), 131.7 (C), 130.9 (C), 129.3 (CH), 128.8 (CH), 128.7 (CH), 128.6 (CH), 128.4 (CH), 128.3 (CH), 125.7 (C), 124.2 (CH), 118.6 (CH), 102.1 (CH), 48.3 (CH_2), 32.8 (CH_2).

HRMS: *m/z* $[M + H]^+$ calcd for $C_{15}H_{22}N_3$: 391.0763; found: 391.0754.

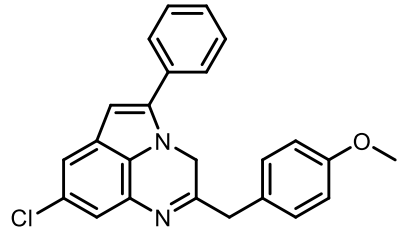

8-chloro-2-(4-methoxybenzyl)-5-phenyl-3H-pyrrolo[1,2,3-de]quinoxaline 8.2c: 80% yield; brown oil;

^{1}H NMR (400.13 MHz) ($CDCl_3$): δ 8.00 (d, *J* = 8.9 Hz, 2H), 7.59 - 7.39 (m, 7H), 7.00 (d, *J* = 8.9 Hz, 2H), 7.59 (s, 1H), 4.46 - 4.39 (m, 2H), 3.89 (s, 3H), 3.26-3.19 (m, 2H);

^{13}C NMR (100.6 MHz) ($CDCl_3$): δ 167.1 (C), 161.7 (C), 142.8 (C), 134.3 (C), 132.1 (C), 131.9 (C), 130.8 (C), 129.3 (CH), 129.0 (CH), 128.6 (CH), 128.4 (C), 128.3 (CH), 125.7 (C), 123.6 (CH), 117.9 (CH), 113.9 (CH), 101.9 (CH), 55.4 (CH_3), 48.5 (CH_2), 32.6 (CH_2).

HRMS: *m/z* $[M + H]^+$ calcd for $C_{24}H_{20}ClN_2O$: 387.1259; found: 387.1274.

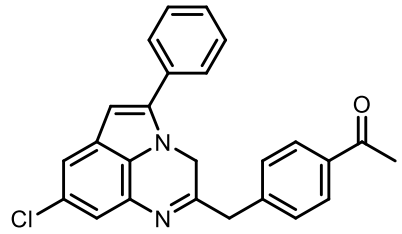

1-(4-((8-chloro-5-phenyl-3H-pyrrolo[1,2,3-de]quinoxalin-2-yl)methyl)phenyl)ethan-1-one 8.2d: 85% yield; brown solid; mp 77 - 78 °C;

^{1}H NMR (400.13 MHz) ($CDCl_3$): δ 8.12 - 8.0 (m, 4H), 7.57 - 7.41 (m, 7H), 6.60 (s, 1H), 4.50 - 4.42 (m, 2H), 3.33 - 3.25 (m, 2H), 2.67 (s, 3H);

^{13}C NMR (100.6 MHz) ($CDCl_3$): δ 197.6 (C), 166.3 (C), 143.6 (C), 142.9 (C), 138.1 (C), 133.6 (C), 131.7 (C), 130.9 (C), 129.3 (CH), 128.7 (CH), 128.6 (CH), 128.5 (CH), 128.4 (C), 128.3 (C), 127.4 (CH), 125.8 (C), 124.5 (CH), 119.0 (CH), 102.1 (CH), 48.2 (CH_2), 33.0 (CH_2).

HRMS: *m/z* $[M + H]^+$ calcd for $C_{25}H_{20}ClN_2O$: 399.1259; found: 399.1263.

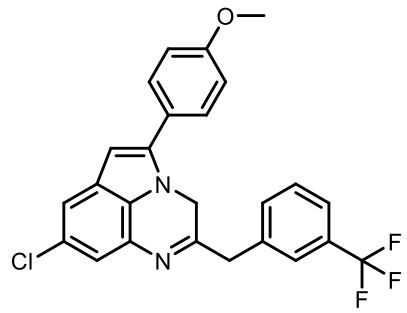

8-chloro-5-(4-methoxyphenyl)-2-(3-(trifluoromethyl)benzyl)-3H-pyrrolo[1,2,3-de]quinoxaline 8.2e: 80% yield; brown solid; mp 170 - 171 °C;

^{1}H NMR (400.13 MHz) ($CDCl_3$): δ 8.27 (s, 1H), 8.21 (d, *J* = 7.9 Hz, 1H), 7.76 (d, *J* = 7.9 Hz, 1H), 7.62 (t, *J* = 7.7 Hz, 1H), 7.53 - 7.49 (m, 1H), 7.48 - 7.40 (m, 3H), 7.00 (d, *J* = 8.6 Hz, 2H), 6.54 (s, 1H), 4.48 - 4.40 (m, 2H), 3.90 (s, 3H), 3.34 - 3.27 (m, 2H);

^{13}C NMR (100.6 MHz)($CDCl_3$): δ 165.6 (C), 159.9 (C), 142.8 (C), 140.4 (C), 133.4 (C), 131.1 (q, J_{CF} = 32.0 Hz, C), 131.0 (C), 130.6 (CH), 130.3 (CH), 129.2 (CH), 128.1 (C), 126.8 (q, J_{CF} = 3.6 Hz, CH), 125.7 (C), 124.0 (q, J_{CF} = 273.0 Hz, C), 124.1 (CH), 124.05 (C), 124.00 (q, J_{CF} = 3.6 Hz, CH), 118.8 (CH), 114.2 (CH), 101.4 (CH), 55.4 (CH_3), 48.1 (CH_2), 32.9 (CH_2);

^{19}F NMR (376.5 MHz)($CDCl_3$): δ 165.6.

HRMS: *m/z* $[M + H]^+$ calcd for $C_{25}H_{19}ClF_3N_2O$: 455.1133; found: 455.1147.

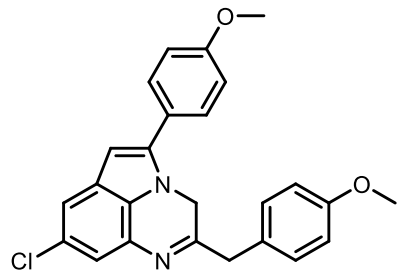

8-chloro-2-(4-methoxybenzyl)-5-(4-methoxyphenyl)-3H-pyrrolo[1,2,3-de]quinoxaline 8.2f: 80% yield; brown solid; mp 150 - 152 °C;

^{1}H NMR (400.13 MHz) ($CDCl_3$): δ 7.99 (d, *J* = 8.8 Hz, 2H), 7.46 - 7.37 (m, 4H), 7.05 - 7.35 (m, 4H), 6.51 (s, 1H), 4.44 - 4.35 (m, 2H), 3.89 (s, 6H), 3.28 - 3.16 (m, 2H);

^{13}C NMR (100.6 MHz) ($CDCl_3$): δ 167.0 (C), 161.7 (C), 159.7 (C), 142.7 (C), 134.2 (C), 132.1 (C), 130.8 (C), 130.6 (CH), 129.0 (CH), 128.2.0 (C), 125.6 (C), 124.0 (C), 123.3 (CH), 117.6 (CH), 114.1 (CH), 113.9 (CH), 101.2 (CH), 55.45 (CH_3), 55.41 (CH_3), 48.4 (CH_2), 32.6 (CH_2).

HRMS: *m/z* $[M + H]^+$ calcd for $C_{25}H_{22}ClN_2O_2$: 417.1364; found: 417.1351.

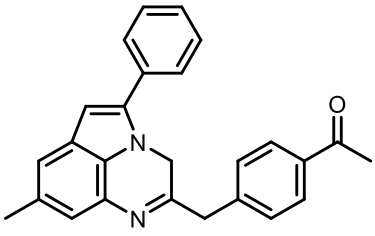

1-(4-((8-methyl-5-phenyl-3H-pyrrolo[1,2,3-de]quinoxalin-2-yl)methyl)phenyl)ethan-1-one 8.2g: 90% yield; brown solid; mp 141 - 142 °C;

^{1}H NMR (400.13 MHz) ($CDCl_3$): δ 8.10 (d, *J* = 8.51 Hz, 2H), 8.06 (d, *J* = 8.51 Hz, 2H), 7.55 - 7.46 (m, 4H), 7.45 - 7.40 (m, 1H), 7.39 (s, 1H), 7.35 (s, 1H), 6.60 (s, 1H), 4.51 - 4.46 (m, 2H), 3.32 - 3.27 (m, 2H), 2.67 (s, 3H), 2.54 (s, 3H);

^{13}C NMR (100.6 MHz) ($CDCl_3$): δ 197.7 (C), 164.9 (C), 144.3 (C), 141.7 (C), 137.7 (C), 132.7 (C), 132.3 (C), 130.4 (C), 130.0 (C), 129.3 (CH), 128.6 (CH), 128.5 (CH), 128.1 (C), 128.0 (CH), 127.3 (CH), 126.4 (CH), 120.0 (CH), 102.0 (CH), 48.4 (CH_2), 33.1 (CH_2), 26.8, (CH_3), 21.1 (CH_3);

HRMS: *m/z* $[M + H]^+$ calcd for $C_{26}H_{23}N_2O$: 379.1805; found: 379.1796.

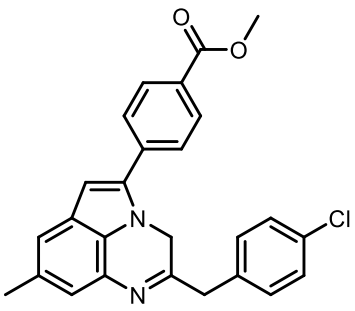

methyl 4-(2-(4-chlorobenzyl)-8-methyl-3H-pyrrolo[1,2,3-de]quinoxalin-5-yl)benzoate 8.2h: 80% yield; yellow solid; mp 215 - 216 °C;

^{1}H NMR (400.13 MHz) ($CDCl_3$): δ 8.14 (d, *J* = 8.0 Hz, 2H), 7.97 (d, J_1 = 8.3 Hz, 2H), 7.60 (d, *J* = 8.0 Hz, 2H), 7.46 (d, *J* = 8.3 Hz, 2H), 7.37 (s, 1H), 7.33 (s, 1H), 6.68 (s, 1H), 4.54 - 4.44 (m, 2H), 3.98 (s, 3H), 3.30 - 3.21 (m, 2H), 2.42 (s, 3H);

^{13}C NMR (100.6 MHz) ($CDCl_3$): δ 166.7 (C), 165.0 (C), 140.6 (C), 138.3 (C), 136.7 (C), 136.4 (C), 133.0 (C), 132.9 (C), 133.2 (C), 129.8 (CH), 129.3 (C), 128.9 (CH), 128.8 (CH), 128.5 (CH), 126.6 (CH), 119.8 (CH), 103.4 (CH), 52.3 (CH_3), 48.9 (CH_2), 32.7 (CH_2), 21.1 (CH_3).

HRMS: *m/z* $[M + H]^+$ calcd for $C_{26}H_{22}ClN_2O_2$: 429.1364; found: 429.1375.

2-(4-chlorobenzyl)-8-methyl-5-phenyl-3H-pyrrolo[1,2,3-de]quinoxaline 8.2i: 79% yield; brown solid; mp 128 - 129 °C;

^{1}H NMR (400.13 MHz) ($CDCl_3$): δ 7.96 (d, *J* = 8.6 Hz, 2H), 7.59 - 7.39 (m, 7H), 7.37 (s, 1H), 7.32 (s, 1H), 6.60 (s, 1H), 4.48 - 4.42 (m, 2H), 3.27 - 3.20 (m, 2H), 2.53 (s, 3H);

^{13}C NMR (100.6 MHz) ($CDCl_3$): δ 164.9 (C), 141.7 (C), 138.6 (C), 136.2 (C), 132.8 (C), 132.4 (C), 130.3 (C), 129.9 (C), 129.3 (CH), 128.9 (C), 128.7 (CH), 128.6 (CH), 128.5 (CH), 128.2 (C), 128.0 (CH), 126.1 (CH), 119.6 (CH), 102.0 (CH), 48.5 (CH_2), 32.8 (CH_2), 21.1 (CH_3).

HRMS: *m/z* $[M + H]^+$ calcd for $C_{24}H_{20}ClN_2$: 371.1310; found: 371.1321.

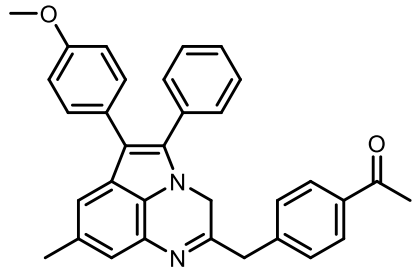

1-(4-((6-(4-methoxyphenyl)-8-methyl-5-phenyl-3H-pyrrolo[1,2,3-de]quinoxalin-2-yl)methyl)phenyl)ethan-1-one 8.2k: 84 % yield; orange solid; mp 128 - 129 °C;

^{1}H NMR (400.13 MHz) ($CDCl_3$): δ 8.10 (d, *J* = 8.4 Hz, 2H), 8.06 (d, *J* = 8.4 Hz, 2H), 7.46 (s, 1H), 7.42 - 7.31 (m, 6H), 7.24 (d, *J* = 8.4 Hz, 2H), 6.88 (d, *J* = 8.4 Hz, 2H), 7.37 (s, 1H), 7.32 (s, 1H), 6.60 (s, 1H), 4.41 - 4.34 (m, 2H), 3.83 (m, 3H), 3.38 - 3.31 (m, 2H), 2.68 (s, 3H);

^{13}C NMR (100.6 MHz) ($CDCl_3$): δ 197.7 (C), 164.8 (C), 157.8 (C), 144.4 (C), 137.7 (C), 137.3 (C), 132.6 (C), 131.5 (C), 131.1 (CH), 130.2 (C), 129.8 (C), 128.6 (CH), 128.4 (CH), 128.0 (CH),

127.29 (C), 127.27 (CH), 127.1 (C), 127.0 (CH), 119.2 (CH), 115.2 (C), 113.8 (CH) (overlapping), 55.2 (CH_3), 47.9 (CH_2), 32.2 (CH_2), 26.8 (CH_3), 21.1 (CH_3).

HRMS: *m/z* $[M + H]^+$ calcd for $C_{33}H_{29}N_2O_2$: 485.2224; found: 485.2239.

11.7 General procedures and Characterization of Chapter 9

General Information

All chemicals were purchased from commercially available sources and used without further purification. A vacuum manifold (Schlenk line) was employed to bring glassware under inert (N_2 or Ar) atmosphere. NMR spectra were recorded at room temperature on a Bruker Avance III HD 400 spectrometer (^{1}H NMR spectra at 400 MHz, ^{13}C NMR spectra at 101 MHz, ^{19}F NMR spectra at 377 MHz) and on a Magnitek Spinsolve (^{19}F NMR spectra at 80 MHz). $CDCl_3$ and CD_3CN were used as deuterated solvents for the NMR analyses. Chemical shifts (δ) are reported in ppm and coupling constant (J) in Hz. Data were acquired and analyzed using Bruker TopSpin 4.1.3 software. Mass spectrometry was acquired on a Radian ASAP equipped with a single quadrupole mass detector. Samples were infused at 3 μL/min and spectra were obtained in positive (or: negative) ionization mode with a resolution of 15000 (FWHM) using leucine enkephalin as lock mass. FT-IR spectra were measured on a Bruker Alpha-T FT-IR spectrometer (using a universal sampling module and Bruker OPUS 7.5.1.1 software for the acquisition and analysis of the data that are given in cm-1. Flash column chromatography was performed using silica gel (ACROS Silica gel for column chromatography, ultra-pure, 40–60 μM, the average pore diameter of 60 Å), while analytical thin-layer chromatography (TLC) was performed with aluminium-backed EMD Millipore Silica Gel 60 F254 pre-coated plates. Visualization was performed under ultraviolet (UV) light or using appropriate staining solutions. Flash column chromatography was performed using a Büchi Pure C815 flash apparatus with UV-vis and ELSD detectors. Büchi PP cartridges (12/150 mm) were filled with 8 g of Acros ultra-pure silica gel for column chromatography (particle size 40-60 μm, average pore diameter 60 Å) using a Büchi C-670 Cartridger.

Troubleshooting the experiments

- During the optimization process, we noticed that the synthesis of $AgOSF_4R$ (R=F, CF_3) was influenced by the purity of the AgF_2 batch. We observe that when the batch is exposed to the air, it loses its effectiveness in oxidizing the starting material. 'Fresh' AgF_2

should be an entirely black powder but specks of differently coloured material appear when a bottle is open for longer.

- It is recommended to store the tetraethylammonium chloride batch in extremely dry conditions due to its strong hygroscopic nature, as the reaction is ineffective in the presence of water.
- The equipment intended for reactions requiring anhydrous conditions, such as two-chamber reactors and vials were initially placed in the oven at a temperature of 150 °C for a duration of 3 hours. Subsequently, the reaction vessels were tightly sealed, and subjected to a minimum of three vacuum-inert gas cycles using a Schlenk line. Through the text, this is referred to as "oven- and Schlenk-dried" vessels.

General Procedures

General procedure for the synthesis of $AgOSF_5$

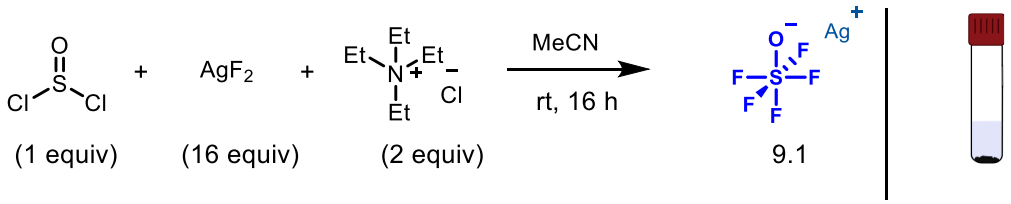

In an oven- and Schlenk-dried 10 mL vial, tetraethylammonium chloride (TEAC, 0.055 g, 0.32 mmol, 2 equiv) was added. Then, put in the Schlenk again, a heat gun was used for 10 seconds to remove possible residual moisture, and vacuum-N_2 cycles were performed. Separately, in a 10 mL tube AgF_2 (0.384 g, 2.58 mmol, 16 equiv) was added and put in the Schlenk under inert atmosphere and covered with aluminium foil. Following this, MeCN (2 mL) and thionyl chloride (12 µL, 0.16 mmol, 1 equiv) were added to the vial containing the TEAC, and the mixture was stirred at room temperature for a while. The solution from the vial was slowly transferred into the tube containing AgF_2 (covered with aluminium foil) and stirred overnight at room temperature. To filter the crude mixture easily, the tube was centrifuged, and then the supernatant was filtered through a PTFE syringe filter and transferred straight into 8 mL vial which was previously dried on the Schlenk line. An additional amount of MeCN (1 mL) was added to the solid residue and the procedure was repeated. Then α,α,α-trifluorotoluene (23 µL) was added to the vial, and the solution was homogenized. To measure the ^{19}F NMR yield, 0.1 mL of the solution was added in NMR tube followed by addition of 0.4 mL CD_3CN.

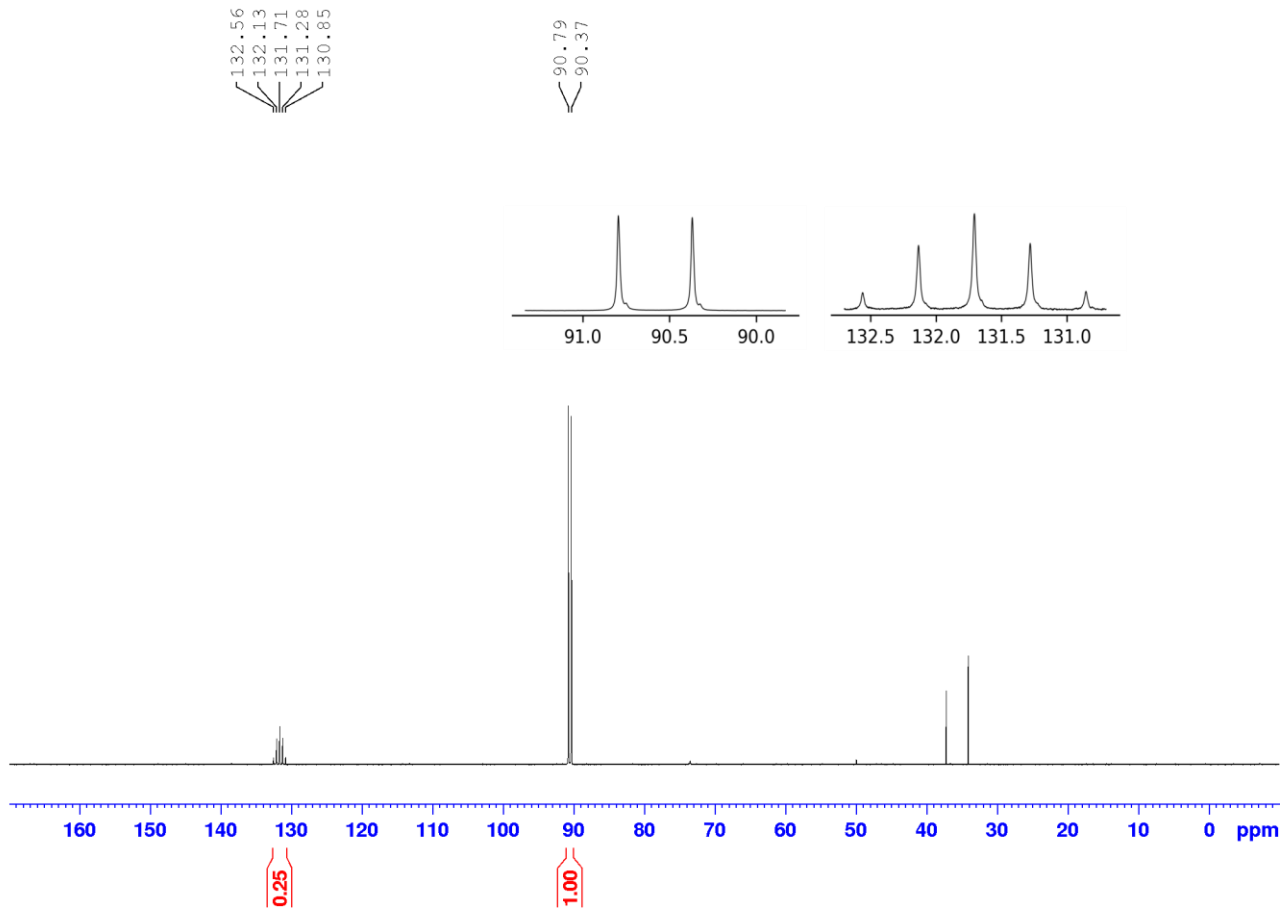

Figure 1. ^{19}F *NMR of* $AgOSF_5$

3.2. General procedure for the synthesis of $AgOSF_4CF_3$

3.2.1. Optimization

Table 1 details the optimization of $AgOSF_4CF_3$ using trifluoromethanesulfinyl fluoride (CF_3SOF) gas as a 0.15 M stock solution in MeCN. The two-step method is used here as described in Section 3.2.3, where CF_3SOF is generated and dissolved in MeCN, and subsequently oxidized using a AgF_2/TEAC combination in a separate step. The experimental procedure followed is described in Section 3.2.3.

When 1 equiv of CF_3SOF gas, 6 equiv of AgF_2 and 2 equiv of TEAC was utilized, we obtained an excellent yield of 88% of only *cis*-$AgOSF_4CF_3$ and *trans*-$AgOSF_4CF_3$ (Table 1, entry 1). When using >8 equiv of AgF_2, a 100% yield could be reached, but this resulted in a mixture of *cis*-$AgOSF_4CF_3$, *trans*-$AgOSF_4CF_3$ and traces of $AgOSF_5$ for unclear reasons (Table 1, entries 2-6).

Table 1. Investigation of the reaction parameters for the synthesis of $AgSOF_4CF_3$[a]

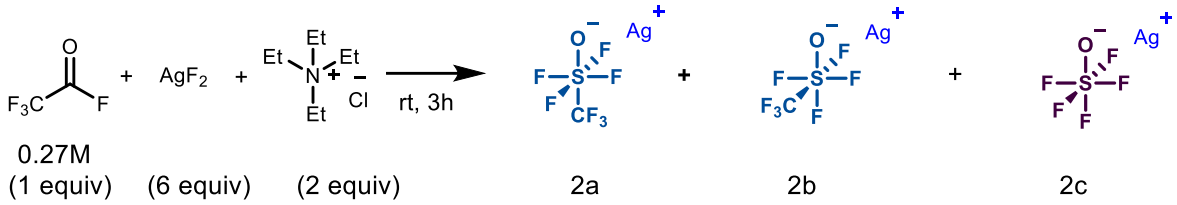

0.27M (1 equiv) | (6 equiv) | (2 equiv) | 2a | 2b | 2c

Entry	Variation from the standard conditions	Conversion (%) of 2a/2b/2c[b]
1	none	88 1/0.49/0
2	AgF_2 (8 equiv.)	100 1/0.42/0.25
3	AgF_2 (10 equiv.)	100 1/0.42/0.074
4	AgF_2 (10 equiv.), 2 hours reaction time	100 1/0.46/0.08
5	AgF_2 (12 equiv.), 2 hours reaction time	100 1/0.42/0.07
6	AgF_2 (15 equiv.)	100 1/0.46/0.04

[a] Reaction conditions. [b] ^{19}F NMR yield.

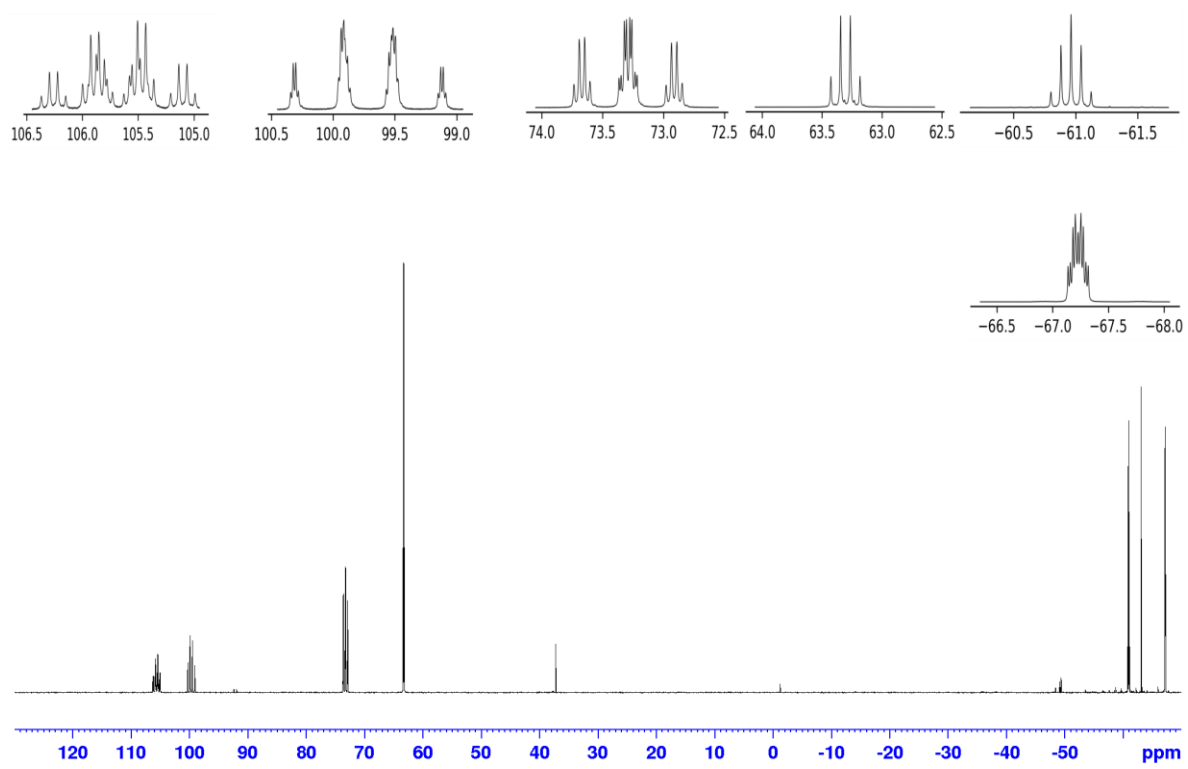

Figure 2. ^{19}F NMR of Cis and Trans isomers of $AgOSF_4CF_3$

DFT-assisted assignment of ^{19}F chemical shifts in *cis*-$[OSF_4CF_3]^-$

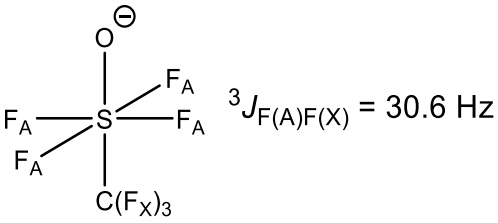

$^3J_{F(A)F(X)}$ = 30.6 Hz

$\delta_{F(A)}$ = 63.31 ppm
$\delta_{F(X)}$ = -60.96 ppm

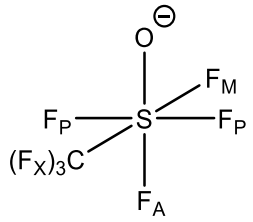

$\delta_{F(A)}$ = 105.68 ppm
$\delta_{F(M)}$ = 99.72 ppm
$\delta_{F(P)}$ = 73.29 ppm
$\delta_{F(X)}$ = -67.23 ppm

$^2J_{F(A)F(M)}$ = 157.0 Hz
$^2J_{F(A)F(P)}$ = 138.6 Hz
$^3J_{F(A)F(X)}$ = 27.2 Hz
$^2J_{F(M)F(P)}$ = 144.9 Hz
$^3J_{F(M)F(X)}$ = 7.8 Hz
$^3J_{F(P)F(X)}$ = 16.6 Hz

To help in the assignment of the two non-equivalent A and M ^{19}F nuclei in the AMP_2X_3 spin system, DFT calculations were used. For the scaling/calibration of the DFT calculated shifts, we used a small set of experimental chemical shifts of related compounds with known ^{19}F shifts recorded in CD_3CN (**Table2**, **Figure3**).[224]

DFT calculations consist of a geometry optimization followed by the calculation of the chemical shifts.

Initially, the geometries of compounds were optimized in Orca 5.0.4[225] via DFT calculations using the PBE0-D4[226] method with a def2-TZVP basis set[227] and def2/J auxiliary basis[228] and CPCM(acetonitrile) solvation.

Next, isotropic shieldings and coupling constants were calculated in Orca 5.0.4 at the DSD-PBEP86/PCSSEG-3[229] level of theory using the AUTOAUX[230] option with CPCM(acetonitrile) solvation.

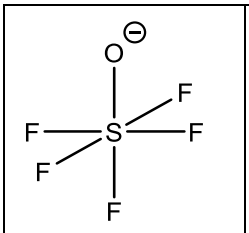		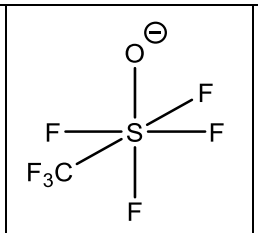		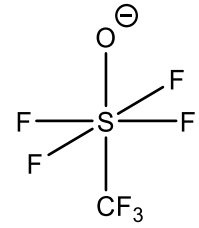		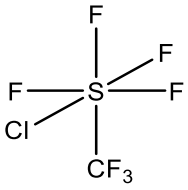		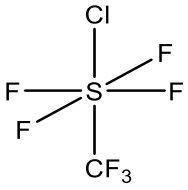	
Exp	Calc	Exp	Calc	Exp	Calc	Exp[224]	Calc	Exp[224]	Calc
134.17 91.61	43.82 91.58	73.29 -67.23	112.69 262.11	63.31 -60.96	123.04 253.11	83.55 40.83 134.48 -65.95	98.89 145.82 40.04 258.60	102.88 -65.39	73.23 257.76

Table 2. Chemical shifts used to calibrate the DFT shifts

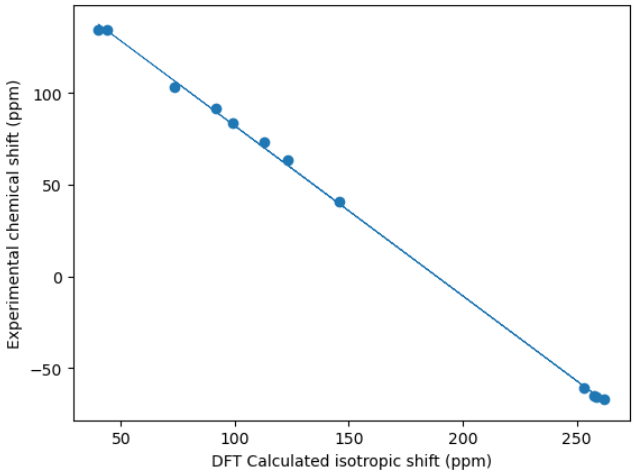

Figure 3. Regression curve: $\sigma_{calc,scaled} = -0.9258\,\sigma_{calc} + 174.5559$ *with* $\sigma_{calc,scaled}$ *being the scaled predicted chemical shift based on DFT calculations and* σ_{calc} *being the DFT calculated isotropic shift.*

The DFT calculated isotropic chemical shifts for F_A and F_M were respectively 76.592 and 80.053 ppm. After scaling these values, nuclei F_A and F_M are predicted to absorb at respectively 103.65 and 100.44 ppm. Based on this calculation, the experimental signal at 105.68 ppm is assigned as F_A and the experimental signal at 99.72 was assigned as F_M.

Procedure (A), stepwise reaction

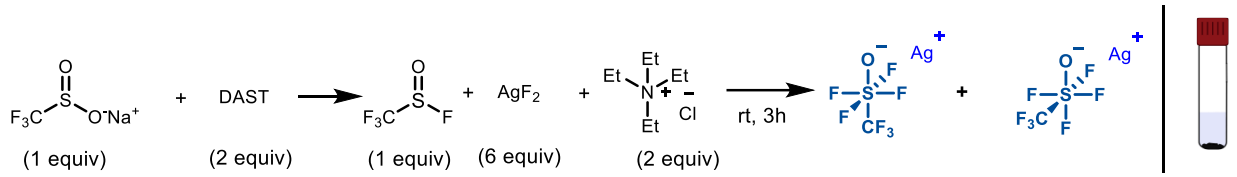

Step 1:

To chamber A of an oven- and Schlenk-dried 20 mL two-chamber reactor was added sodium triflinate (CF_3SO_2Na, 0.35 g, 2.2 mmol, 1 equiv) and dry 1,2-dichloroethane (6 mL) as a solvent. Dry MeCN (8 mL) was added to the chamber B to dissolve the generated gas from chamber A. The reactor was closed and diethylaminosulfur trifluoride (DAST, 0.59 mL, 4.4 mmol, 2 equiv) was added to the chamber A to generate CF_3SOF gas. The reaction was stirred for 3 hours. After 3 hours chamber B was cooled at 0 ^oC, and the solution was transferred to 20 mL vial which was previously dried in Schlenk. Then α,α,α-trifluorotoluene (23 μL) was added to the vial and the solution was homogenized. To measure the ^{19}F NMR yield, 0.1 mL of the solution was added in NMR tube followed by addition of 0.4 mL CD_3CN.

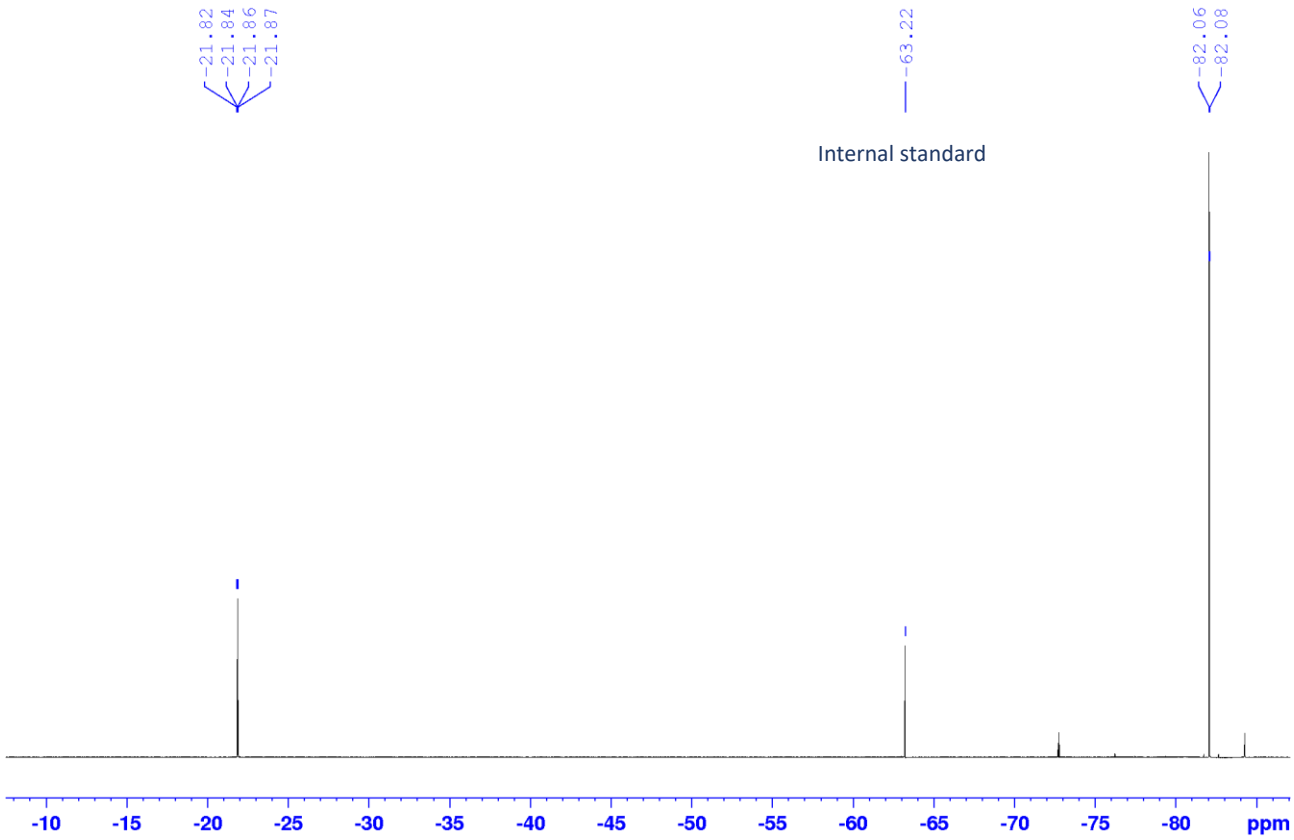

Figure 4. ^{19}F NMR of CF_3SOF gas in MeCN solution

Step 2:

Using a 10 mL vial, oven- and Schlenk-dried, tetraethylammonium chloride (TEAC, 0.068 g, 0.4 mmol, 2 equiv) was added. The vial was then reattached to the Schlenk line, a heat gun was used for 10 seconds to remove possible residual moisture, and vacuum-N_2 cycles were performed. Separately, another 10 mL tube was charged with AgF_2 (0.179 g, 1.2 mmol, 6 equiv) and attached to the Schlenk line under inert atmosphere and covered with aluminium foil. Subsequently, CF_3SOF (0.15 M) gas solution in MeCN was added to the vial containing TEAC and stirred for a while. The solution from the vial was slowly transferred into the tube containing AgF_2 (covered with aluminium foil) and was left to stir overnight at room temperature. To filter the crude mixture easily, the tube was centrifuged, and then the supernatant was filtered through a PTFE syringe filter and transferred straight into 8 mL vial which was previously dried on the Schlenk line. An additional amount of MeCN (1 mL) was added to the solid residue and the procedure was repeated. Then α,α,α-trifluorotoluene (23 µL) was added to the vial, and the solution was homogenized. To measure the ^{19}F NMR yield, 0.1 mL of the solution was added in NMR tube followed by addition of 0.4 mL CD_3CN.

Procedure (B), Reaction in two-chamber reactor

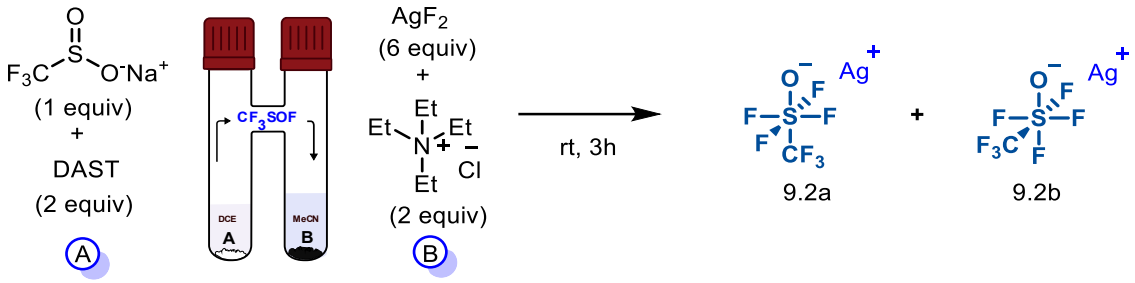

To chamber A of an oven- and Schlenk-dried 20 mL two-chamber reactor, was added sodium triflinate (CF_3SO_2Na, 0.032 g, 0.2 mmol, 1 equiv) in DCE (2 mL), while AgF_2 (0.12 g, 0.8 mmol, 4 equiv) was added in the MeCN (2 mL) to the chamber B. The reactor was closed and brought under high vacuum on the Schlenk line. Using a 10 mL vial that was dried in the Schlenk and was previously dried in the oven, tetraethylammonium chloride (TEAC, 0.045 g, 0.27, mmol, 1.3 equiv) was added. The vial was then reattached to the Schlenk line, a heat gun was used for 10 seconds to remove possible residual moisture, and vacuum-N_2 cycles were performed. The solution from the vial was transferred gradually to chamber B containing AgF_2, which was covered with aluminium foil at room temperature. DAST (0.054 mL, 0.4 mmol, 2 equiv) was then added to chamber A to generate CF_3SOF gas. The mixture was stirred for 3 hours. To filter the crude mixture easily, the tube was centrifuged, and then the supernatant was filtered through a PTFE syringe filter and transferred straight into 8 mL vial which was previously dried on the Schlenk line. An additional amount of MeCN (1 mL) was added to the solid residue and the procedure was repeated. Then α,α,α-trifluorotoluene (23 µL) was added to the vial, and the solution was homogenized. To measure the ^{19}F NMR yield, 0.1 mL of the solution was added in NMR tube followed by addition of 0.4 mL CD_3CN.

General procedure (C) for the synthesis of iminosulfur oxydifluorides

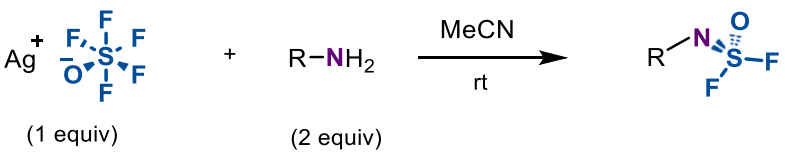

Using a 10 mL vial, oven- and Schlenk-dried, an aliphatic or aromatic amine (0.32 mmol, 2 equiv) was added. The vial was then reattached to the Schlenk line, and vacuum-N_2 cycles were performed. Subsequently, $AgOSF_5$ (0.14 – 0.40 mmol, 1 equiv, 0.05 – 0.1 M in MeCN) was added to the vial. The reaction mixture was stirred for 1 hour at room temperature, and the

progress of reaction was monitored by ^{19}F NMR, using a 80 MHz benchtop NMR. Upon completion of the reaction, MeCN was evaporated under vacuum at 25°C bath temperature. The crude residue was further purified with pentane as eluent using column chromatography on silica gel.

Note: The compounds are volatile; caution must be exercised during the rotavapor process to prevent the loss of compounds and ensure optimal final yield.

General procedure (D) for the synthesis of N-((5S)-5-(((benzyloxy)carbonyl)amino)-6-methoxy-6-oxohexyl)sulfurimidoyl difluoride

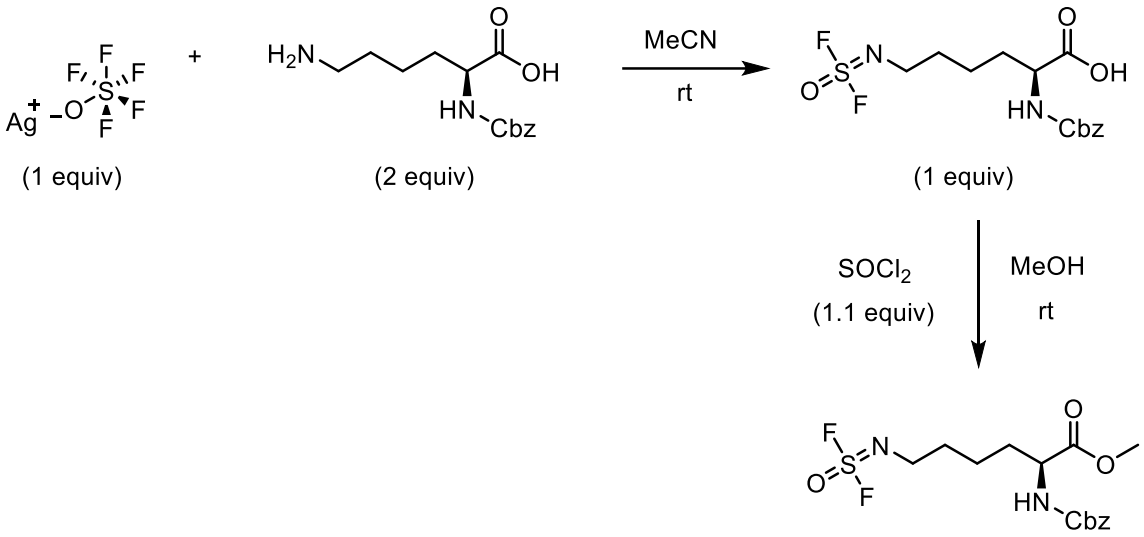

Following the general procedure **C,** upon completion of the reaction, MeCN was evaporated under vacuum at 25°C. Based on the literature procedure,[231] MeOH (2.5 mL) were used to dissolve the starting material. Subsequently, Thionyl chloride (0.22 mmol, 1.1 equiv) was added to the vial at 0°C. The reaction mixture was stirred overnigh at room temperature, and the progress of the reaction was monitored by ^{19}F NMR, using benchtop NMR. Upon completion of the reaction, solvent was evaporated under vacuum at 50 °C. The crude residue was further purified using column chromatography on silica gel.

General procedure (E) for the synthesis of sulfonimidoyl fluoride

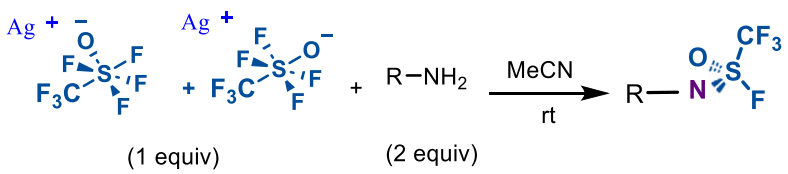

Using a 10 mL vial, oven and Schlenk-dried, an aliphatic or aromatic amine (0.26 mmol, 2 equiv) was added. The vial was then reattached to the Schlenk line, and vacuum-N_2 cycles were performed. Subsequently, $AgOSF_4CF_3$ (0.2 – 0.3 mmol, 1 equiv, 0.07 – 0.12 M in MeCN) was added to the vial. The reaction mixture was stirred for 1 hour at room temperature, and the progress of the reaction was monitored by ^{19}F NMR, using 80 MHz benchtop NMR. Upon completion of the reaction, MeCN was evaporated under vacuum at 25°C bath temperature. The crude residue was further purified using column chromatography on silica gel.

Note: The compounds are volatile; caution must be exercised during the rotavapor process to prevent the loss of compounds and ensure optimal final yield.

Scale up synthesis of iminosulfur oxydifluoride and sulfonimidoyl fluoride

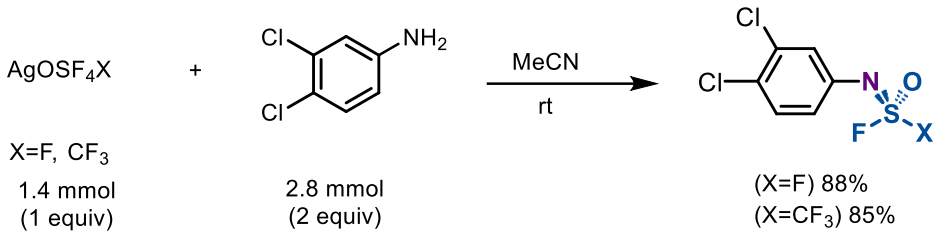

Using a 20 mL vial, oven and Schlenk-dried, an aliphatic or aromatic amine (2.8 mmol, 2 equiv) was added. The vial was then reattached to the Schlenk line, and vacuum-N_2 cycles were performed. Subsequently, $AgOSF_4CF_3$ or $AgOSF_5$ (1.4 mmol, 1 equiv) was added to the vial. The reaction mixture was stirred for 1 hour at room temperature, and the progress of the reaction was monitored by ^{19}F NMR, using 80 MHz benchtop NMR. Upon completion of the reaction, MeCN was evaporated under vacuum at 25°C bath temperature. The crude residue was further purified using column chromatography on silica gel. The title compound was obtained after column chromatography as colourless liquid.

General Procedure (F) for the synthesis of Triflimidates

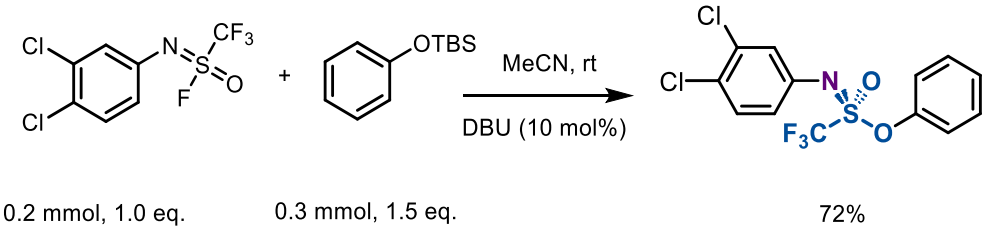

Based on the literature procedure.[232]

A 10 mL vial was filled with sulfonimidoyl fluoride (0.2 mmol, 1.0 eq.) and tert-butyldimethyl(phenoxy)silane (0.3 mmol, 1.5 eq.). Then MeCN (1 mL), α,α,α-trifluorotoluene (99 wt%, 25 μL, 1.0 mmol) as an internal standard and 1,8-Diazabicyclo[5.4.0]undec-7-ene (DBU, 2.94 μL, 10 mol%) were added. The reaction mixture was stirred for 0.5 hour at room temperature, and the progress of the reaction was monitored by ^{19}F NMR, using 80 MHz benchtop NMR. Upon completion of the reaction, MeCN was evaporated under vacuum. The crude residue was further purified using column chromatography on silica gel.

General Procedure (G) for the synthesis of Sulfoximines

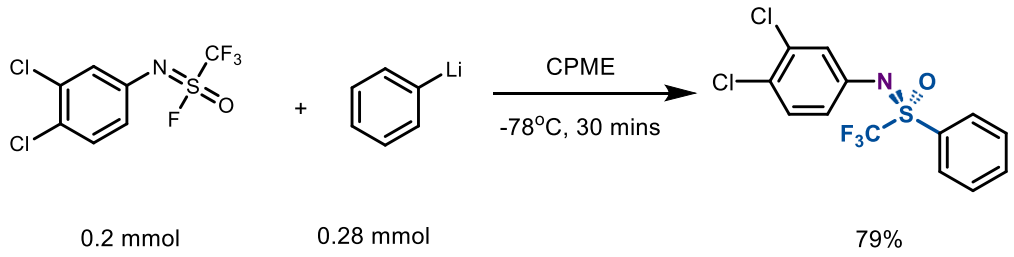

0.2 mmol 0.28 mmol 79%

Based on the literature procedure.[76]

Using a 10 mL vial, oven and Schlenk-dried, sulfonimidoyl fluoride (0.2 mmol, 1.0 eq.) and CPME (2.0 mL) were added. The mixture was cooled to –78 ^{o}C in a dry ice/acetone bath. Phenyllithium (0.27 mmol, 1.35 eq., 1.9M in dibutylther) was added dropwise under vigorous stirring. The reaction mixture was stirred for another 20 mins before being quenched by acetic acid (1.0 M in methanol, 1.0 mL). The mixture was warmed to room temperature, then transferred to a 5 mL round-bottomed flask. Solvent was removed on rotary evaporator. The crude residue was further purified using column chromatography on silica gel.

Characterization data

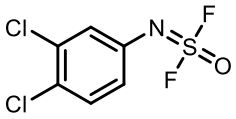

(3,4-Dichlorophenyl)sulfurimidoyl difluoride 9.3a;

Following the general procedure **C** (0.2 mmol scale), **9.3a** was obtained as a **colorless liquid** (45 mg, 92% yield); R_f = 0.71 (Pentane); **^{1}H NMR** (400 MHz, $CDCl_3$) δ 7.42 (d, J = 8.6 Hz, 1H), 7.24 (d, J = 2.5 Hz, 1H), 6.98 (dd, J_1 = 8.6 Hz, J_2 = 2.5 Hz, 1H); **^{13}C NMR** (150 MHz, $CDCl_3$)

δ 135.49 (t, *J* = 2.5 Hz), 133.69, 131.36, 130.53, 125.69 (t, *J* = 3.2 Hz), 123.07 (t, J = 2.9 Hz); **^{19}F NMR** (376 MHz, $CDCl_3$) δ 46.76 (s, 2F);

These data are in agreement with literature data.[233]

(4-methoxyphenyl)sulfurimidoyl difluoride, 9.3b;

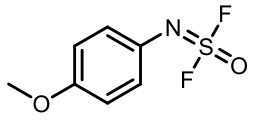

Following the general procedure **C** (0.18 mmol scale), **9.3b** was obtained as a **colorless liquid** (36 mg, 93% yield); R_f = 0.65 (Pentane, CH_2Cl_2, 90/10); **^{1}H NMR** (400 MHz, $CDCl_3$) δ 7.05 (d, *J* = 8.8 Hz, 2H), 6.87 (d, *J* = 8.8 Hz, 2H), 3.79 (s, 3H); **^{13}C NMR** (101 MHz, $CDCl_3$) δ 157.83, 129.12 (t, *J* = 3.2 Hz), 124.58 (t, *J* = 3.1 Hz), 114.99, 55.65; **^{19}F NMR** (377 MHz, $CDCl_3$) δ 46.15 (s, 2F);

These data are in agreement with literature data. [76]

(3-ethynylphenyl)sulfurimidoyl difluoride 9.3c;

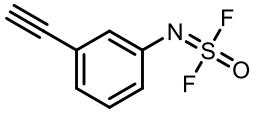

Following the general procedure **C** (0.17 mmol scale), **9.3c** was obtained as a **colorless liquid** (32 mg, 91% yield); R_f = 0.45. (Pentane, CH_2Cl_2, 95/5); **^{1}H NMR** (400 MHz, $CDCl_3$) δ 7.38 – 7.34 (m, 1H), 7.33 – 7.29 (m, 1H), 7.25 – 7.24 (m, 1H), 7.13 – 7.11 (m, 1H), 3.12 (s, 1H); **^{13}C NMR** (101 MHz, $CDCl_3$) δ 136.31 (t, *J* = 2.7 Hz), 130.02, 129.87, 127.16 (t, *J* = 3.0 Hz), 124.28 (t, *J* = 2.9 Hz), 123.94, 82.44, 78.54; **^{19}F NMR** (377 MHz, $CDCl_3$) δ 46.78 (s, 2F); ASAP-MS m/z: Calcd [M]+: 201.0, found: 200.9

Phenylsulfurimidoyl difluoride 9.3d;

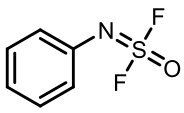

Following the general procedure **C** (0.21 mmol scale), **9.3d** was obtained as a **colorless liquid** (32 mg, 86% yield); R_f = 0.55 (Pentane); **^{1}H NMR** (400 MHz, $CDCl_3$) δ 7.36 (t, *J* = 7.9 Hz, 2H),

7.23 (t, *J* = 7.5 Hz, 1H), 7.13 (d, *J* = 7.5 Hz, 2H); **^{13}C NMR** (101 MHz, $CDCl_3$) δ 136.28 (t, *J* = 2.4 Hz); 129.84, 126.27, 123.68 (t, *J* = 2.7 Hz); **^{19}F NMR** (377 MHz, $CDCl_3$) δ 46.60 (s, 2F);

These data are in agreement with literature data. [76]

(3-bromophenyl)sulfurimidoyl difluoride 9.3e;

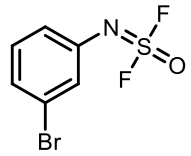

Following the general procedure **C** (0.2 mmol scale), **9.3e** was obtained as a **colorless liquid** (47 mg, 92% yield); R_f = 0.58 (Pentane); **^{1}H NMR** (400 MHz, $CDCl_3$) δ 7.38 (d, *J* = 8.0 Hz, 1H), 7.30 (t, *J* = 1.8 Hz, 1H), 7.23 (t, *J* = 8.0 Hz, 1H), 7.07 (dd, J_1 = 8.0 Hz, J_2 = 1.1 Hz, 1H), **^{13}C NMR** (101 MHz, $CDCl_3$) δ 137.34 (t, *J* = 2.7 Hz), 131.00, 129.51, 126.93 (t, *J* = 3.1 Hz), 123.15, 122.39 (t, *J* = 2.9 Hz); **^{19}F NMR** (377 MHz, $CDCl_3$) δ 46.78 (s, 2F); ASAP-MS m/z: Calcd [M]+: 254.9, found: 254.8

(2-(prop-1-en-2-yl)phenyl)sulfurimidoyl difluoride 9.3f;

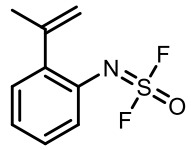

Following the general procedure **C** (0.14 mmol scale), **9.3f** was obtained as a **colorless liquid** (29 mg, 95% yield); R_f = 0.62 (Pentane); **^{1}H NMR** (400 MHz, $CDCl_3$) δ 7.28 – 7.24 (m, 2H), 7.22 – 7.18 (m, 1H), 7.12 – 7.10 (m, 1H), 5.24 - 5.22 (m, 1H), 5.03 – 5.02 (m, 1H), 2.11 – 2.10 (m, 3H), **^{13}C NMR** (101 MHz, $CDCl_3$) δ 143.42, 139.51 (t, *J* = 3.3 Hz), 133.06 (t, *J* = 3.0 Hz), 129.83, 128.30, 126.38, 123.65 (t, *J* = 3.0 Hz), 116.60, 23.29; **^{19}F NMR** (377 MHz, $CDCl_3$) δ 47.38 (s, 2F);

These data are in agreement with literature data. [76]

(4-cyanophenyl)sulfurimidoyl difluoride 9.3g;

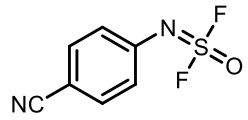

Following the general procedure **C** (0.17 mmol scale), **9.3g** was obtained as a **colorless liquid** (34 mg, 98% yield); 98% yield; colourless liquid; R_f = 0.33 (Pentane, CH_2Cl_2, 90/10); **^{1}H NMR** (400 MHz, $CDCl_3$) δ 7.67 (dt, J_1 = 8.6 Hz, J_2 = 2.0 Hz, 2H), 7.23 (dt, J_1 = 8.6 Hz, J_2 = 2.0 Hz, 2H); **^{13}C NMR** (101 MHz, $CDCl_3$) δ 140.33 (t, J = 2.6 Hz), 133.96, 124.56 (t, J = 3.0 Hz), 118.13, 110.23; **^{19}F NMR** (377 MHz, $CDCl_3$) δ 47.35 (s, 2F); ASAP-MS m/z: Calcd [M]+: 202.0, found: 202.0

***p*-tolylsulfurimidoyl difluoride 9.3h**;

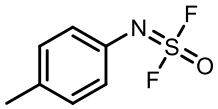

Following the general procedure **C** (0.15 mmol scale), **9.3h** was obtained as a **colorless liquid** (23 mg, 81% yield); R_f = 0.90 (Pentane); **^{1}H NMR** (400 MHz, $CDCl_3$) δ 7.15 (d, J = 8.2, 2H), 7.01 (d, J = 8.2, 2H), 2.34 (s, 3H); **^{13}C NMR** (101 MHz, $CDCl_3$) δ 136.06, 133.66 (t, J = 2.9 Hz), 130.37, 123.40 (t, J = 3.0 Hz), 21.00; **^{19}F NMR** (377 MHz, $CDCl_3$) δ 46.44 (s, 2F); ASAP-MS m/z: Calcd [M]+: 191.0, found: 191.0

Naphthalen-1-ylsulfurimidoyl difluoride 9.3i;

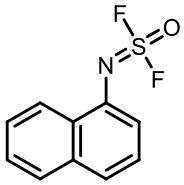

Following the general procedure **C** (0.21 mmol scale), **9.3i** was obtained as a **colorless liquid** (42 mg, 89% yield); R_f = 0.80 (Pentane); **^{1}H NMR** (400 MHz, $CDCl_3$) δ 8.18 (d, J = 7.7, 1H), 7.89 – 7.84 (m, 1H), 7.75 (d, J = 8.3, 1H), 7.62 – 7.52 (m, 2H), 7.43 (t, J = 7.8, 1H), 7.27 (d, J = 7.4, 1H); **^{13}C NMR** (101 MHz, $CDCl_3$) δ 134.57, 132.73 (t, J = 3.3 Hz), 128.88, 128.15, 127.02, 126.96, 126.456, 125.62, 123.26, 119.17 (t, J = 3.3 Hz); **^{19}F NMR** (377 MHz, $CDCl_3$) δ 47.15 (s, 2F); ASAP-MS m/z: Calcd [M]+: 227.0, found: 226.9

Pyridin-3-ylsulfurimidoyl difluoride 9.3j;

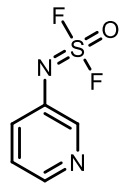

Following the general procedure **C** (0.2 mmol scale), **9.3j** was obtained as a **yellowish liquid** (26 mg, 72% yield); R_f = 0.32 (Pentane, CH_2Cl_2, 90/10); **^{1}H NMR** (400 MHz, $CDCl_3$) δ 8.49 (dd, J_1 = 4.8 Hz, J_2 = 1.1 Hz, 1H), 8.46 (d, J = 2.4 Hz, 1H), 7.47 – 7.44 (m, 1H), 7.34 – 7.29 (m, 1H); **^{13}C NMR** (101 MHz, $CDCl_3$) δ 147.39, 145.10 (t, J = 2.9 Hz), 133.43, 130.69 (t, J = 2.6 Hz), 124.28; **^{19}F NMR** (377 MHz, $CDCl_3$) δ 47.49 (s, 2F); ASAP-MS m/z: Calcd [M+H]+: 179.0, found: 178.9

(2-formylphenyl)sulfurimidoyl difluoride 9.3k;

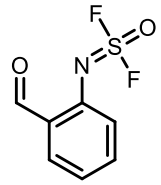

Following the general procedure **C** (0.2 mmol scale), **9.3k** was obtained as a **colorless liquid** (30 mg, 73% yield); R_f = 0.33 (Pentane, CH_2Cl_2, 70/30); **^{1}H NMR** (400 MHz, $CDCl_3$) δ 10.41 (s, 1H), 7.93 (dd, J_1 = 7.8 Hz, J_2 = 1.6 Hz, 1H), 7.61 (td, J_1 = 7.7 Hz, J_2 = 1.7 Hz, 1H), 7.37 (t, J = 7.6, 1H), 7.23 (dd, J_1 = 8.1 Hz, J_2 = 0.5 Hz, 1H); **^{13}C NMR** (101 MHz, $CDCl_3$) δ 189.61, 138.42, 135.50, 129.94, 129.57, 126.71, 123.89 (t, J = 2.4 Hz); **^{19}F NMR** (377 MHz, $CDCl_3$) δ 47.78 (s, 2F); ASAP-MS m/z: Calcd [M]+: 205.0, found: 205.1

Ethyl 2-((difluoro(oxo)-sulfaneylidene)amino)benzoate 9.3l;

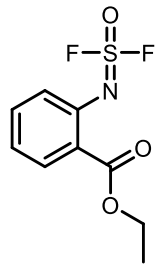

Following the general procedure **C** (0.4 mmol scale), **9.3l** was obtained as a **colorless liquid** (72 mg, 72% yield); R_f = 0.30 (Pentane, CH_2Cl_2, 80/20); **^{1}H NMR** (400 MHz, $CDCl_3$) δ 7.94 (dd, J_1 = 7.8 Hz, J_2 = 1.6 Hz, 1H), 7.49 (td, J_1 = 7.8 Hz, J_2 = 1.6 Hz, 1H), 7.29 (td, J_1 = 8.5 Hz, J_2 = 1.2

Hz, 1H), 7.17 (dd, J_1 = 8.1 Hz, J_2 = 1.0 Hz, 1H), 4.38 (q, J = 7.1, 2H), 1.39 (t, J = 7.1, 3H); **^{13}C NMR** (101 MHz, $CDCl_3$) δ 165.58, 135.53 (t, J = 2.3 Hz), 133.25, 131.79, 126.22, 126.07 (t, J = 3.1 Hz), 125.59 (t, J = 2.8 Hz), 61.56, 14.27; **^{19}F NMR** (377 MHz, $CDCl_3$) δ 47.12 (s, 2F); ASAP-MS m/z: Calcd [M]+: 249.0, found: 248.9

(2,2-diphenylethyl)sulfurimidoyl difluoride 9.3m;

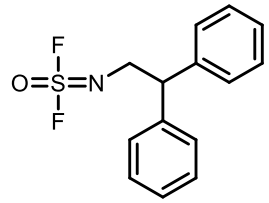

Following the general procedure **C** (0.23 mmol scale), **9.3m** was obtained as a **colorless liquid** (47 mg, 73% yield); R_f = 0.37 (Pentane); **^{1}H NMR** (400 MHz, $CDCl_3$) δ 7.39 – 7.33 (m, 4H), 7.31 – 7.25 (m, 6H), 4.28 (t, J = 7.6 Hz, 1H), 4.00 (dt, J_1 = 7.62 Hz, J_2 = 3.90 Hz, 2H); **^{13}C NMR** (101 MHz, $CDCl_3$) δ 141.21, 128.80, 128.16, 127.13, 52.01, 50.28; **^{19}F NMR** (377 MHz, $CDCl_3$) δ 47.54 (t, J = 4.0, 2F);

(((1R,4aS,10aR)-7-isopropyl-1,4a-dimethyl-1,2,3,4,4a,9,10,10a-octahydrophenanthren-1-yl)methyl)sulfurimidoyl difluoride 9.3n;

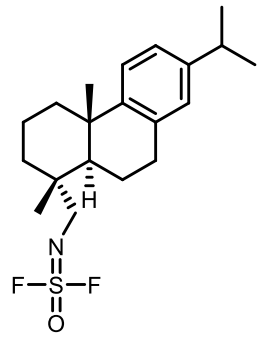

Following the general procedure **C** (0.15 mmol scale), **9.3n** was obtained as a **white solid** (47 mg, 85% yield); R_f = 0.80 (Pentane); **^{1}H NMR** (400 MHz, $CDCl_3$) δ 7.19 (d, J = 8.3 Hz, 1H), 7.01 (dd, J_1 = 6.6 Hz, J_2 = 1.6 Hz, 1H), 6.90 (d, , J = 1.7 Hz, 1H), 3.31 (dt, J_1 = 12.20 Hz, J_2 = 3.90 Hz, 1H), 3.03 (dt, J_1 = 12.20 Hz, J_2 = 4.0 Hz, 1H), 2.95 - 2.77 (m, 3H), 2.34 -2.23 (m, 1H), 1.84 - 1.65 (m, 5H), 1.58 - 1.37 (m, 3H), 1.25 (s, 3H), 1.23 (s, 6H), 0.95 (s, 3H); **^{13}C NMR** (101 MHz, $CDCl_3$) δ 147.15, 145.78, 134.71, 126.94, 124.42, 124.04, 56.84, 44.34, 38.34, 37.50, 37.47, 35.74, 33.59, 30.15, 25.32, 24.11, 18.92, 18.72, 18.46; **^{19}F NMR** (377 MHz, $CDCl_3$) δ 46.89 (t, J = 3.8 Hz, 2F);

These data are in agreement with literature data. [233]

(2-(1H-indol-3-yl)ethyl)sulfurimidoyl difluoride 9.3o;

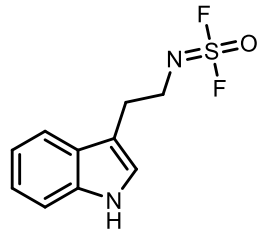

Following the general procedure **C** (0.21 mmol scale), **9.3o** was obtained as a **grey solid** (49 mg, 95% yield); R_f = 0.33 (Pentane:CH_2Cl_2, 80:20); **^{1}H NMR** (400 MHz, $CDCl_3$) δ 8.01 (bs, 1H), 7.63 (d, *J* = 7.8 Hz,1H), 7.40 (d, *J* = 8.1 Hz, 1H), 7.30 – 7.23 (m, 1H), 7.21 – 7.17 (m, 1H), 7.09 (d, *J* = 2.3 Hz, 1H), 3.69 (tt, J_1 = 7.50 Hz, J_2 = 4.0 Hz, 2H), 3.14 (t, *J* = 7.4 Hz, 2H); **^{13}C NMR** (101 MHz, $CDCl_3$) δ 136.32, 127.23, 122.39, 122.33, 119.67, 118.57, 112.27, 111.39, 46.69, 27.05 (t, *J* = 1.5 Hz); **^{19}F NMR** (377 MHz, $CDCl_3$) δ 47.51 (t, *J* = 3.7, 2F);

These data are in agreement with literature data. [233]

(2-chloro-6-fluorobenzyl)sulfurimidoyl difluoride 9.3p;

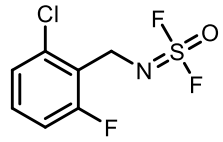

Following the general procedure **C** (0.23 mmol scale), **9.3p** was obtained as a **colorless liquid** (47 mg, 84% yield); R_f = 0.43 (Pentane); **^{1}H NMR** (400 MHz, $CDCl_3$) δ 7.35 – 7.23 (m, 2H), 7.10 – 7.02 (m, 1H), 4.00 (td, J_1 = 4.1 Hz, J_2 = 1.9 Hz, 2H); **^{13}C NMR** (101 MHz, $CDCl_3$) δ 161.67 (d, *J* = 251.2 Hz), 135.84 (d, *J* = 4.8 Hz), 130.73 (d, *J* = 9.8 Hz), 125.74 (d, *J* = 3.4 Hz), 122.50 (d, *J* = 17.6 Hz), 114.52 (d, *J* = 22.3 Hz), 40.31 (d, *J* = 4.4 Hz).; **^{19}F NMR** (377 MHz, $CDCl_3$) δ 47.70 – 47.65 (m, 2F), -113.78 – -113.83 (m, 1F); ASAP-MS m/z: Calcd [M]+: 243.0, found: 242.9

N-((5S)-5-(((benzyloxy)carbonyl)amino)-6-methoxy-6-oxohexyl)sulfurimidoyl difluoride 9.3q;

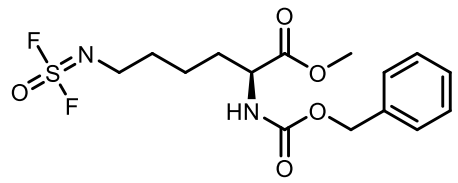

Following the general procedure **D** (0.2 mmol scale), **9.3q** was obtained as a **white solid** (g, % yield); R_f = 0.42 (isohexane:EtOAc 7:3); **^{1}H NMR** (400 MHz, $CDCl_3$) δ 7.38 – 7.31 (m, 5H), 5.30 (d, *J* = 7.7 Hz, 1H), 5.10 (s, 2H), 4.41 – 4.36 (m, 1H), 3.74 (s, 3H), 3.34 – 3.30 (m, 2H), 1.91 – 1.82 (m, 1H), 1.73 – 1.57 (m, 3H), 1.49 – 1.36 (m, 2H), ; **^{13}C NMR** (101 MHz, $CDCl_3$) δ 172.86, 155.97, 136.31, 128.69, 128.37, 128.27, 67.20, 53.72, 52.59, 45.87, 32.25, 30.19, 22.24; **^{19}F NMR** (377 MHz, $CDCl_3$) δ 47.01 (t, *J* = 3.8 Hz, 2F); ASAP-MS m/z: Calcd [M+H]+: 379.1, found: 379.0

(1-phenylethyl)sulfurimidoyl difluoride 9.3r;

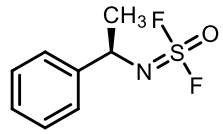

Following the general procedure **C** (0.27 mmol scale), **9.3r** was obtained as a **colorless liquid** (50 mg, 90% yield); R_f = 0.80 (Pentane); **^{1}H NMR** (400 MHz, $CDCl_3$) δ 7.39 – 7.30 (m, 5H), 4.90 – 4.70 (m, 1H), 1.60 (d, *J* = 6.7 Hz, 3H); **^{13}C NMR** (101 MHz, $CDCl_3$) δ 142.51, 128.85, 128.01, 125.88, 57.47, 25.60 (d, *J* = 2.8 Hz); **^{19}F NMR** (377 MHz, $CDCl_3$) δ 49.91 – 48.51 (m, 2F);

These data are in agreement with literature data. [76]

N-(3,4-dichlorophenyl)-1,1,1-trifluoromethanesulfonimidoyl fluoride 9.4a;

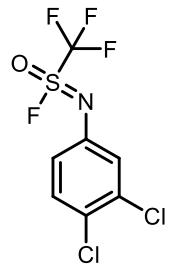

Following the general procedure **E** (0.3 mmol scale), **9.4a** was obtained as a **colorless liquid** (81 mg, 91% yield); R_f = 0.81 (Pentane); **^{1}H NMR** (400 MHz, $CDCl_3$) δ 7.40 (d, *J* = 8.6 Hz, 1H),

7.27 (dd, J_1 = 2.6 Hz, J_2 = 0.82 Hz, 1H), 7.00 – 6.99 (ddd, J_1 = 8.60 Hz, J_2 = 2.50 Hz, J_3 = 0.80 Hz, 1H); **^{13}C NMR** (101 MHz, $CDCl_3$) δ 135.20 (d, J = 6.40 Hz), 133.57, 131.24, 130.16 (d, J = 1.5 Hz), 125.83 (d, J = 5.2 Hz), 123.28 (d, J = 4.9 Hz), 118.14 (qd, J_1 = 320.1, J_2 = 61.2, CF_3); **^{19}F NMR** (377 MHz, $CDCl_3$) δ 60.20 (q, J = 16.6 Hz, 1F), -72.31 (d, J = 16.6 Hz, 3F); ASAP-MS m/z: Calcd [M]+: 294.9, found: 294.8

1,1,1-trifluoro-N-(4-methoxyphenyl)methanesulfonimidoyl fluoride 9.4b;

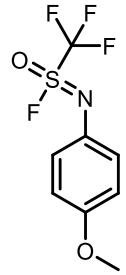

Following the general procedure **E** (0.2 mmol scale), **9.4b** was obtained as a **colorless liquid** (44 mg, 86% yield); R_f = 0.45 (Pentane); **^{1}H NMR** (400 MHz, $CDCl_3$) δ 7.10 – 7.05 (m, 2H), 6.89 – 6.83 (m, 2H), 3.79 (s, 3H); **^{13}C NMR** (101 MHz, $CDCl_3$) δ 157.67 (d, J = 1.2 Hz), 128.70 (d, J = 6.7 Hz), 124.81 (d, J = 4.9 Hz), 118.15 (qd, J_1 = 320.5, J_2 = 64.0 Hz, CF_3); 114.92, 55.64; **^{19}F NMR** (377 MHz, $CDCl_3$) δ 61.47 (q, J = 16.1 Hz, 1F), -72.43 (d, J = 16.1 Hz, 3F); ASAP-MS m/z: Calcd [M]+: 257.0, found: 256.9

N-(4-bromophenyl)-1,1,1-trifluoromethanesulfonimidoyl fluoride 9.4c;

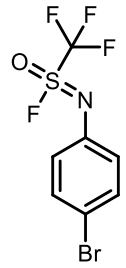

Following the general procedure **E** (0.25 mmol scale), **9.4c** was obtained as a **pale yellow liquid** (63 mg, 82% yield); R_f = 0.90 (Pentane); **^{1}H NMR** (400 MHz, $CDCl_3$) δ 7.46 (d, J = 8.6 Hz, 2H), 7.02 (d, J = 8.5 Hz, 2H); **^{13}C NMR** (101 MHz, $CDCl_3$) δ 135.02 (d, J = 6.4 Hz), 132.83, 125.50 (d, J = 5.0 Hz), 119.35 (d, J = 1.6 Hz), 118.23 (qd, J_1 = 381.2, J_2 = 62.6 Hz, CF_3); **^{19}F NMR** (377 MHz, $CDCl_3$) δ 60.50 (q, J = 16.4 Hz, 1F), -72.46 (d, J = 16.4 Hz, 3F);

These data are in agreement with literature data.[232]

1,1,1-trifluoro-N-(4-nitrophenyl)methanesulfonimidoyl fluoride 9.4d;

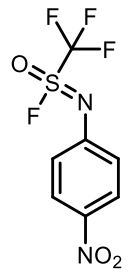

Following the general procedure **E** (0.25 mmol scale), **9.4d** was obtained as a **pale yellow liquid** (56 mg, 82% yield); R_f = 0.33 (Pentane); **^{1}H NMR** (400 MHz, $CDCl_3$) δ 8.30 – 8.22 (m, 2H), 7.34 – 7.28 (m, 2H); **^{13}C NMR** (101 MHz, $CDCl_3$) δ 145.52, 141.98 (d, *J* = 6.4 Hz), 125.47, 124.53 (d, *J* = 4.8 Hz), 118.00 (qd, J_1 = 319.8, J_2 = 61.6 Hz, CF_3); **^{19}F NMR** (377 MHz, $CDCl_3$) δ 59.43 (q, *J* = 16.4 Hz, 1F), -72.31 (d, *J* = 16.4 Hz, 3F);

These data are in agreement with literature data.[232]

1,1,1-trifluoro-N-(((1R,4aS,10aR)-7-isopropyl-1,4a-dimethyl-1,2,3,4,4a,9,10,10a-octahydrophenanthren-1-yl)methyl)methanesulfonimidoyl fluoride 9.4e;

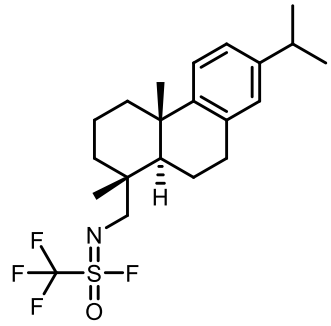

Following the general procedure **E** (0.3 mmol scale), **9.4e** was obtained as a **white solid** (107 mg, 85% yield); R_f = 0.80 (Pentane); **^{1}H NMR** (400 MHz, $CDCl_3$) δ 7.19 (d, *J* = 8.1 Hz, 1H), 7.01 (dd, J_1 = 8.1 Hz, J_2 = 1.5 Hz, 1H), 6.90 (s, 1H), 3.47 – 3.33 (m, 1H), 3.24 – 3.12 (m, 1H), 2.95 - 2.78 (m, 3H), 2.31 (dt, J_1 = 12.8 Hz, J_2 = 3.2 Hz, 1H), 1.80 - 1.59 (m, 5H), 1.45 - 1.36 (m, 3H), 1.25 (s, 3H), 1.23 (s, 6H), 0.96 (d, *J* = 1.7 Hz 3H); **^{13}C NMR** (101 MHz, $CDCl_3$) δ 147.08, 145.72, 134.74 (d, *J* = 1.9 Hz), 127.00, 124.49, 124.05, 118.10 (qd, J_1 = 319.7, J_1 = 69.50 Hz, CF_3), 55.28 (t, *J* = 3.8 Hz), 44.99, 38.38, 37.63, 37.47, (d, *J* = 3.4 Hz), 35.86 (d, *J* = 1.4 Hz), 33.57, 30.35, 30.27, 25.49, 24.10 (d, *J* = 1.2 Hz), 18.98 (d, *J* = 3.8 Hz), 18.79 (d, *J* = 2.1 Hz), 18.45 (d, *J* = 6.8 Hz); **^{19}F NMR** (377 MHz, $CDCl_3$) δ 64.70 (m, 1F), -72.84 (m, 3F); ASAP-MS m/z: Calcd [M]+: 419.2, found: 419.2

N-(2,2-diphenylethyl)-1,1,1-trifluoromethanesulfonimidoyl fluoride 9.4f:

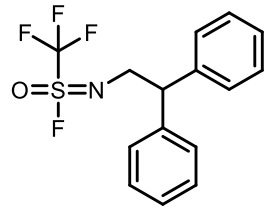

Following the general procedure **E** (0.25 mmol scale), **9.4f** was obtained as a **colorless liquid** (66 mg, 80% yield); R_f = 0.43 (Pentane); **^{1}H NMR** (400 MHz, $CDCl_3$) δ 7.40 – 7.33 (m, 4H), 7.32 – 7.24 (m, 6H), 4.29 (t, *J* = 7.7 Hz, 1H), 4.15 – 4.07 (m, 2H); **^{13}C NMR** (101 MHz, $CDCl_3$) δ 141.28 (d, *J* = 2.4 Hz), 128.78 (d, *J* = 4.4 Hz), 128.19 (d, *J* = 9.9 Hz), 127.12 (d, *J* = 8.8 Hz), 117.88 (qd, J_1 = 319.4, J_2 = 69.0 Hz, CF_3), 52.45 (d, *J* = 5.2 Hz), 48.73 (d, *J* = 4.8 Hz); **^{19}F NMR** (377 MHz, $CDCl_3$) δ 65.88 (q, *J* = 16.4 Hz, 1F), -73.35 (d, *J* = 17.0 Hz, 3F);

Phenyl N-(3,4-dichlorophenyl)trifluoromethanesulfonimidate 9.5;

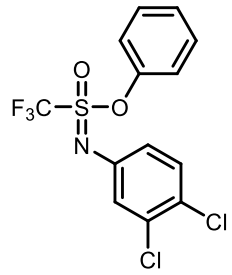

Following the general procedure **F** (0.2 mmol scale), **9.5** was obtained as a **pale yellow liquid** (59 mg, 80% yield); R_f = 0.44 (Pentane); **^{1}H NMR** (400 MHz, $CDCl_3$) δ 7.50 – 7.43 (m, 2H), 7.42 – 7.37 (m, 1H), 7.32 (d, *J* = 8.6 Hz, 1H), 7.28 – 7.25 (m, 2H), 7.13 (d, *J* = 2.5 Hz, 1H), 6.89 (dd, J_1 = 8.6 Hz, J_2 = 2.5 Hz, 1H); **^{13}C NMR** (101 MHz, $CDCl_3$) δ 149.08, 138.26, 133.00, 130.84, 130.33, 128.44, 128.30, 125.73, 123.29, 122.27, 119.23 (q, *J* = 323.5, CF_3); **^{19}F NMR** (377 MHz, $CDCl_3$) δ -73.54 (s, 3F); ASAP-MS m/z: Calcd [M]+: 369.0, found: 368.9

((3,4-dichlorophenyl)imino)(phenyl)(trifluoromethyl)-λ^6-sulfanone 9.6;

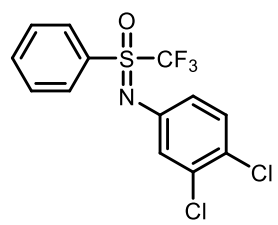

Following the general procedure **G** (0.2 mmol scale), **9.6** was obtained as a **colorless liquid** (56 mg, 79% yield); R_f = 0.54 (Pentane); **^{1}H NMR** (400 MHz, $CDCl_3$) δ 8.18 (d, *J* = 7.5 Hz, 2H), 7.82 (tt, J_1 = 7.5 Hz, J_1 = 1.2 Hz, 1H), 7.71 – 7.65 (m, 2H), 7.35 (d, *J* = 2.5 Hz, 1H), 7.33 (d, *J* = 8.7 Hz, 1H), 7.10 (dd, J_1 = 8.6 Hz, J_2 = 2.5 Hz, 1H); **^{13}C NMR** (101 MHz, $CDCl_3$) δ 141.11, 135.93, 132.84, 131.18, 130.76, 130.65, 129.87, 127.60, 125.88, 123.49, 121.42 (q, *J* = 339.7, CF_3); **^{19}F NMR** (377 MHz, $CDCl_3$) δ -72.23 (s, 3F); ASAP-MS m/z: Calcd [M]+: 353.0, found: 352.9

11.8 General procedures and Characterization of Chapter 10

^{19}F NMR quantification experiments

In order to have reproducible and reliable results from our ^{19}F NMR experiments, certain aspects were consistently taken into account.

- In order to minimize the integration error in quantitative NMR caused by the inherent excitation profile of ^{19}F nuclei, the transmitter frequency (i.e. the middle of the spectrum, O1P) was set close to a value in the middle of the chemical shift of the internal standard and that of the intended peak.
- For the calibration – as well as for quantification purposes – of the acquired ^{19}F NMR spectra, an internal standard - either α,α,α-trifluorotoluene (to be set at -63.72 ppm) or (trifluoromethoxy)benzene (to be set at -58.00 ppm) - was used. It should be noted that the internal standard was added at the end of the reaction time.
- It should be taken into account that for crude ^{19}F NMR analyses, typically 0.2 ml filtered aliquot of the mixture was mixed with 0.3 ml of the deuterated solvent (to facilitate locking and shimming).
- Concerning the processing of the acquired spectra, the baseline and phase corrections of the acquired spectra were done by the automatic phase and baseline correction command available on TopSpin 4.1.3 software (apbk -n).

Optimization of the reaction conditions

The reaction conditions for the selected model reaction shown in Scheme S1 were optimized. The results are given in Table S1.

Procedure for the optimization process: In an oven- and Schlenk-dried two-chamber reactor equipped with magnetic stirring bars in both chambers, calcium hypochlorite was added to the gas-generating chamber (A) and the main chamber (B) was charged with finely-crushed oven-dried anhydrous potassium fluoride. After sealing the two-chamber carefully, vacuum-N_2 cycles were performed and the reactor was filled with nitrogen gas. Subsequently, anhydrous acetonitrile and phenyl iodide (1 equiv) were injected into the gas-consumption chamber (B) via a syringe through the septum and without opening the cap. Then, the gas-generation chamber (A) was immersed in an ice bath for 15 minutes. This was followed by the gentle injection of concentrated sulfuric acid into the gas-generation chamber (A) using a syringe through the septum and without opening the cap. The temperature of the gas-generation chamber (A) was allowed to rise back to room temperature. The reaction was stirred. Subsequently, the remaining chlorine gas was slowly neutralized by ventilating the atmosphere of the reactor with a slow flow of nitrogen gas into a concentrated solution of sodium hydroxide. In order to measure the ^{19}F NMR yield, a known amount of an internal standard -either (trifluoromethoxy)benzene or α,α,α-trifluorotoluene- was introduced to the reaction mixture. After mixing for about 5 minutes, an aliquot of the reaction mixture was taken with a syringe and filtered (0.2 mL) via a PTFE syringe filter straight into an NMR tube. The filtered aliquot was mixed with deuterated acetonitrile (0.3 mL).

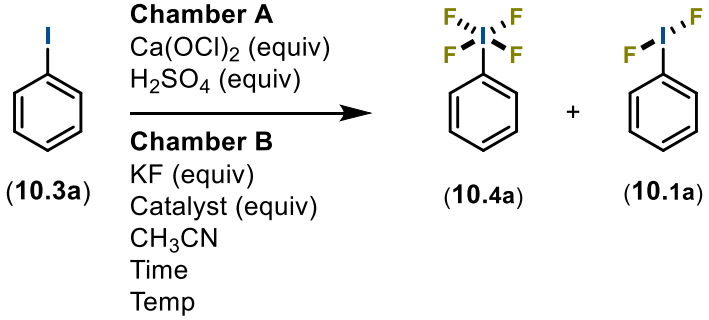

Scheme S1. Selected model reaction for the optimization of the conditions

Table S1. Optimization of the reaction conditions

Entry	$Ca(OCl)_2$ (equiv)	H_2SO_4 (equiv)	KF (equiv)	CH_3CN (mL)	Time (h)	Temp. Chamber B (°C)	Catalyst (equiv)	**10.4a** yield (%)[a]	**10.1a** yield (%)[a]
1	1	51.4	4	2	16	25	-	0	0
2	2	51.4	4	2	16	25	-	3	11

3	4	51.4	4	2	16	25	-	22	5
4	1	51.4	6	2	16	25	-	0	27
5	2	51.4	6	2	16	25	-	0	34
6	4	51.4	6	2	16	25	-	48	7
7	8	51.4	6	2	16	25	-	70	3
8	16	51.4	6	2	16	25	-	55	0
9	8	25.7	6	2	16	25	-	56	6
10	8	38.6	6	2	16	25	-	59	3
11	8	64.3	6	2	16	25	-	38	8
12	8	77.1	6	2	16	25	-	61	6
13	8	51.4	2	2	16	25	-	17	9
14	8	51.4	4	2	16	25	-	56	9
15	8	51.4	8	2	16	25	-	55	9
16	8	51.4	10	2	16	25	-	51	6
17	8	51.4	6	1	16	25	-	76	2
18	8	51.4	6	4	16	25	-	39	13
19	8	51.4	6	1	48	25	-	79	0
20	8	51.4	6	1	32	25	-	73	0
21	8	51.4	6	1	24	25	-	74	0
22	8	51.4	6	1	8	25	-	24	4
23	8	51.4	6	1	4	25	-	9	8
24	**8**	**51.4**	**6**	**1**	**16**	**25**	**TFA (0.1)**	**90**	**0**
25	8	51.4	6	1	16	40	TFA (0.1)	86	0
26	8	51.4	6	2	16	25	-	0	0
27	8	51.4	6	2	16	25	-	7	7

[a] Yields are determined using ^{19}F NMR spectroscopy; [b] No moisture precautions taken; non-anhydrous reagents were used without drying. The glassware was not dried. The atmosphere of the vial was normal air. The yields are to be compared with entry 7. [c] No moisture precautions taken; non-anhydrous reagents were used without drying. The KF was taken from an anhydrous

bottle but without oven- or Schlenk-drying. The glassware was not dried. The atmosphere of the vial was normal air. The yields are to be compared with entry 7.

Practical and safety aspects

We strongly advise that a risk assessment is made before the reaction is performed. This file must be shared with all the parties that are involved. In case of any incidents exposing the user to the chemicals, immediate medical support should be sought.

Other practical points that should be taken into consideration are:

- The equipment that was meant to be used to set up reactions requiring anhydrous conditions (such as two-chamber reactors, glass funnels, etc.) was first kept in the oven at 150 °C overnight.
- In order to neutralized the atmosphere inside the vessels (e.g. two-chamber reactors), before the reaction and apply the nitrogen atmosphere inside, the vessels were taken out of the oven, well-sealed, vacuumed for 15 minutes and vacuum-inert gas cycles were performed at least 3 times using a Schlenk line. Finally, the vessels is filled with nitrogen gas. Throughout the text, this is referred to as “oven- and Schlenk-dried” vessels.

- Anhydrous KF was crushed with a mortar and a pestle and transferred to a glass petri dish to be oven-dried overnight at 150 °C prior to loading.
- To prevent the potassium fluoride loaded in the two-chamber reactor from absorbing moisture from the air, the two-chamber reactor is immediately sealed and attached to the Schlenk line to be vacuumed for about 15 minutes
- Commercial extra-dry solvents (i.e. MeCN) over molecular sieves were used to carry out the reactions.
- At the end of reactions in two-chamber reactors, the atmosphere of the reactor was carefully flushed via a slow flow of nitrogen gas into a solution of sodium hydroxide to neutralize the possible remainder of chlorine gas. This must be done using needles and without opening the caps as shown in Figure **S1**. After this, the NMR analyses can be carried out.

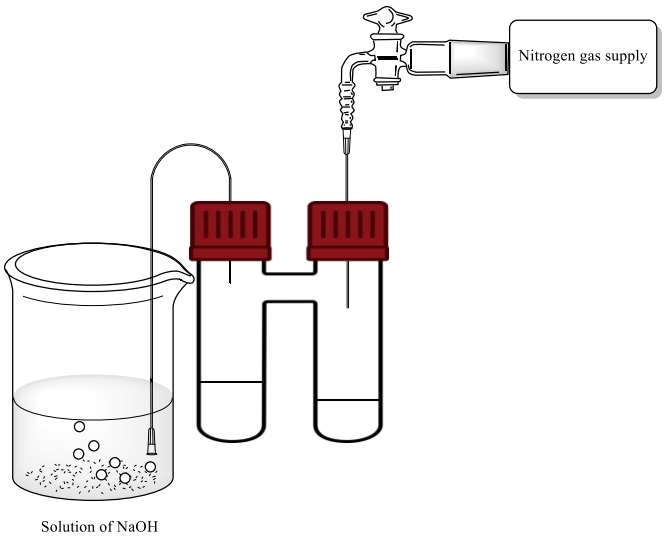

Figure S1. Neutralization of the two-chamber reactor atmosphere after the reaction

Tetrafluoro(phenyl)-λ^5-iodane, 9.4a [218]

^{19}F NMR yield= 90%. **^{19}F NMR** (376 MHz, CH_3CN/CD_3CN) δ -28.01

Tetrafluoro(p-tolyl)-λ^5-iodane, 9.4b [218]

^{19}F NMR yield= 64%. **^{19}F NMR** (376 MHz, CH_3CN/CD_3CN) δ -27.99

(4-(Tert-butyl)phenyl)tetrafluoro-λ^5-iodane, 9.4c

^{19}F NMR yield= 76%. **^{19}F NMR** (376 MHz, CH_3CN/CD_3CN) δ -27.35

(3-(Tert-butyl)phenyl)tetrafluoro-λ^5-iodane, 9.4d

^{19}F NMR yield= 88%. **^{19}F NMR** (376 MHz, CH_3CN/CD_3CN) δ -27.95

(4-(Bromomethyl)phenyl)tetrafluoro-λ^5-iodane, 9.4e

^{19}F NMR yield= 59%. **^{19}F NMR** (376 MHz, CH_3CN/CD_3CN) δ -27.25

(3-Bromophenyl)tetrafluoro-λ^5-iodane, 9.4f

^{19}F NMR yield= 86%. **^{19}F NMR** (376 MHz, CH_3CN/CD_3CN) δ -26.48

(4-Bromophenyl)tetrafluoro-λ^5-iodane, 9.4g [218]

^{19}F NMR yield= 91%. **^{19}F NMR** (376 MHz, CH_3CN/CD_3CN) δ -26.90

(3-Chlorophenyl)tetrafluoro-λ^5-iodane, 9.4h

^{19}F NMR yield= 96%. **^{19}F NMR** (376 MHz, CH_3CN/CD_3CN) δ -26.72

4-(Tetrafluoro-λ^5-iodaneyl)benzonitrile), 9.4i

^{19}F NMR yield= 31%. **^{19}F NMR** (376 MHz, CH_3CN/CD_3CN) δ -27.05

3-(Tetrafluoro-λ^5-iodaneyl)benzonitrile), 9.4j

^{19}F NMR yield= 21%. **^{19}F NMR** (376 MHz, CH_3CN/CD_3CN) δ -26.05

(2-Chlorophenyl)difluoro-λ^3-iodane, 9.1k

^{19}F NMR yield= 88%. **^{19}F NMR** (376 MHz, CH_3CN/CD_3CN) δ -165.05

(2-Bromophenyl)difluoro-λ^3-iodane, 9.1l

^{19}F NMR yield= 81%. **^{19}F NMR** (376 MHz, CH_3CN/CD_3CN) δ -163.10

(3-Bromo-4-methylphenyl)tetrafluoro-λ^5-iodane, 9.4m

^{19}F NMR yield= 42%. **^{19}F NMR** (376 MHz, CH_3CN/CD_3CN) δ -26.95

(Tetrafluoro(3-phenoxyphenyl)-λ^5-iodane, 9.4n

^{19}F NMR yield= 44%. **^{19}F NMR** (376 MHz, CH_3CN/CD_3CN) δ -26.60

[1,1'-Biphenyl]-4-yltetrafluoro-λ^5-iodane, 9.4o

^{19}F NMR yield= 56%. **^{19}F NMR** (376 MHz, CH_3CN/CD_3CN) δ -27.48

References

[1] K. Mori, T. Mizoroki, A. Ozaki, *Bulletin of the chemical society of Japan* **1973**, *46*, 1505-1508.

[2] a) R. F. Heck, *Journal of the American Chemical Society* **1968**, *90*, 5518-5526; b) H. Dieck, R.-F. Heck, *Journal of the American Chemical Society* **1974**, *96*, 1133-1136; c) R. F. Heck, J. Nolley Jr, *The Journal of organic chemistry* **1972**, *37*, 2320-2322.

[3] K. Sonogashira, *Journal of organometallic chemistry* **2002**, *653*, 46-49.

[4] J. K. Stille, *Angewandte Chemie International Edition in English* **1986**, *25*, 508-524.

[5] E.-i. Negishi, *Journal of organometallic chemistry* **2002**, *653*, 34-40.

[6] K. Tamao, K. Sumitani, M. Kumada, *Journal of the American Chemical Society* **1972**, *94*, 4374-4376.

[7] V. Grignard, *Synthesis* **1900**, *130*, 1322.

[8] a) N. Miyaura, K. Yamada, A. Suzuki, *Tetrahedron Letters* **1979**, *20*, 3437-3440; b) N. Miyaura, A. Suzuki, *Journal of the Chemical Society, Chemical Communications* **1979**, 866-867.

[9] A. F. Littke, G. C. Fu, *Angewandte Chemie International Edition* **1998**, *37*, 3387-3388.

[10] A. F. Littke, C. Dai, G. C. Fu, *Journal of the American Chemical Society* **2000**, *122*, 4020-4028.

[11] E.-i. Negishi.

[12] R. Heck, Academic Press, London, **1985**.

[13] Q.-Y. Chen, Z.-Y. Yang, *Tetrahedron letters* **1986**, *27*, 1171-1174.

[14] W. Cabri, I. Candiani, A. Bedeschi, R. Santi, *The Journal of Organic Chemistry* **1993**, *58*, 7421-7426.

[15] A. B. Dounay, L. E. Overman, *Chemical reviews* **2003**, *103*, 2945-2964.

[16] A. Dounay, Wiley, Chichester, **2009**.

[17] J. Link, *Organic Reactions* **2004**, *60*, 157-561.

[18] a) Y. Sato, M. Sodeoka, M. Shibasaki, *The Journal of Organic Chemistry* **1989**, *54*, 4738-4739; b) N. E. Carpenter, D. J. Kucera, L. E. Overman, *The Journal of Organic Chemistry* **1989**, *54*, 5846-5848.

[19] K. Sonogashira, Y. Tohda, N. Hagihara, *Tetrahedron letters* **1975**, *16*, 4467-4470.

[20] I. Paterson, R. D. Davies, R. Marquez, *Angewandte Chemie* **2001**, *113*, 623-627.

[21] a) B. P. Carrow, J. F. Hartwig, *Journal of the American Chemical Society* **2011**, *133*, 2116-2119; b) A. J. Lennox, G. C. Lloyd‐Jones, *Israel Journal of Chemistry* **2010**, *50*, 664-674.

[22] a) J. Uenishi, J. M. Beau, R. W. Armstrong, Y. Kishi, *Journal of the American Chemical Society* **1987**, *109*, 4756-4758; b) R. W. Armstrong, J. M. Beau, S. H. Cheon, W. J. Christ, H. Fujioka, W. H. Ham, L. D. Hawkins, H. Jin, S. H. Kang, *Journal of the American Chemical Society* **1989**, *111*, 7530-7533.

[23] J. Tsuji, H. Takahashi, M. Morikawa, *Tetrahedron Letters* **1965**, *6*, 4387-4388.

[24] a) R. Tamura, L. S. Hegedus, *Journal of the American Chemical Society* **1982**, *104*, 3727-3729; b) N. One, I. Hamamoto, A. Kaji, *Journal of the Chemical Society, Chemical Communications* **1982**, 821-822.

[25] a) B. M. Trost, N. R. Schmuff, M. J. Miller, *Journal of the American Chemical Society* **1980**, *102*, 5979-5981; b) H. Kotake, T. Yamamoto, H. Kinoshita, *Chemistry Letters* **1982**, *11*, 1331-1334; c) T. Cuvigny, M. Julia, C. Rolando, *Journal of organometallic chemistry* **1985**, *285*, 395-413.

[26] a) B. M. Trost, L. Weber, P. E. Strege, T. J. Fullerton, T. J. Dietsche, *Journal of the American Chemical Society* **1978**, *100*, 3416-3426; b) T. Hayashi, T. Hagihara, M. Konishi, M. Kumada, *Journal of the American Chemical Society* **1983**, *105*, 7767-7768;

c) B. Akermark, J.-E. Bäckvall, A. Löwenborg, K. Zetterberg, *Journal of Organometallic Chemistry* **1979**, *166*, C33-C36.
[27] B. M. Trost, P. E. Strege, *Journal of the American Chemical Society* **1977**, *99*, 1649-1651.
[28] B. M. Trost, D. L. Van Vranken, C. Bingel, *Journal of the American Chemical Society* **1992**, *114*, 9327-9343.
[29] G. Helmchen, A. Pfaltz, *Accounts of Chemical Research* **2000**, *33*, 336-345.
[30] T. Hayashi, *Pure and Applied Chemistry* **1988**, *60*, 7-12.
[31] B. M. Trost, G. M. Schroeder, *The Journal of Organic Chemistry* **2000**, *65*, 1569-1573.
[32] B. M. Trost, J. D. Oslob, *Journal of the American Chemical Society* **1999**, *121*, 3057-3064.
[33] M. Nakanishi, M. Mori, *Angewandte Chemie* **2002**, *114*, 2014-2016.
[34] B. M. Trost, Z. Shi, *Journal of the American Chemical Society* **1996**, *118*, 3037-3038.
[35] B. M. Trost, M. G. Organ, G. A. O'Doherty, *Journal of the American Chemical Society* **1995**, *117*, 9662-9670.
[36] a) V. Ritleng, C. Sirlin, M. Pfeffer, *Chemical Reviews* **2002**, *102*, 1731-1770; b) F. Kakiuchi, N. Chatani, *Advanced Synthesis & Catalysis* **2003**, *345*, 1077-1101; c) D. Alberico, *Chem. Rev* **2007**, *107*, 174-238.
[37] a) N. Lebrasseur, I. Larrosa, *Journal of the American Chemical Society* **2008**, *130*, 2926-2927; b) Y. Zhang, J. Feng, C.-J. Li, *Journal of the American Chemical Society* **2008**, *130*, 2900-2901.
[38] a) J. M. Murphy, X. Liao, J. F. Hartwig, *Journal of the American Chemical Society* **2007**, *129*, 15434-15435; b) M. S. Chen, M. C. White, *Science* **2007**, *318*, 783-787.
[39] R. Li, L. Jiang, W. Lu, *Organometallics* **2006**, *25*, 5973-5975.
[40] J.-B. Xia, S.-L. You, *Organometallics* **2007**, *26*, 4869-4871.
[41] D. R. Stuart, E. Villemure, K. Fagnou, *Journal of the American Chemical Society* **2007**, *129*, 12072-12073.
[42] B. Liégault, D. Lee, M. P. Huestis, D. R. Stuart, K. Fagnou, *The Journal of Organic Chemistry* **2008**, *73*, 5022-5028.
[43] H. C. Kolb, M. Finn, K. B. Sharpless, *Angewandte Chemie International Edition* **2001**, *40*, 2004-2021.
[44] a) M. Breugst, H. U. Reissig, *Angewandte Chemie International Edition* **2020**, *59*, 12293-12307; b) R. Huisgen, G. Szeimies, L. Möbius, *Chemische Berichte* **1967**, *100*, 2494-2507.
[45] C. W. Tornøe, M. Meldal, in *Peptides: The Wave of the Future: Proceedings of the Second International and the Seventeenth American Peptide Symposium, June 9–14, 2001, San Diego, California, USA*, Springer, **2001**, pp. 263-264.
[46] R. V. G. L. F. VV, K. Sharpless, *Angew. Chem* **2002**, *114*, 2708-2711.
[47] F. Himo, T. Lovell, R. Hilgraf, V. V. Rostovtsev, L. Noodleman, K. B. Sharpless, V. V. Fokin, *Journal of the American Chemical Society* **2005**, *127*, 210-216.
[48] B. T. Worrell, J. Malik, V. V. Fokin, *Science* **2013**, *340*, 457-460.
[49] I. E. Valverde, A. Bauman, C. A. Kluba, S. Vomstein, M. A. Walter, T. L. Mindt, *Angewandte Chemie International Edition* **2013**, *34*, 8957-8960.
[50] E. Bonandi, M. S. Christodoulou, G. Fumagalli, D. Perdicchia, G. Rastelli, D. Passarella, *Drug Discovery Today* **2017**, *22*, 1572-1581.
[51] M. Xu, Y. Peng, L. Zhu, S. Wang, J. Ji, K. Rakesh, *European journal of medicinal chemistry* **2019**, *180*, 656-672.
[52] J. Thomas, W. Dehaen, J. John, *Molecules* **2023**, *28*, 308.
[53] H. Kumar, M. Dhameja, M. Rizvi, P. Gupta, *ChemistrySelect* **2021**, *6*, 4889-4947.
[54] J. Deng, Y.-M. Wu, Q.-Y. Chen, *Synthesis* **2005**, *2005*, 2730-2738.

[55] a) T. Jeffery, *Tetrahedron letters* **1985**, *26*, 2667-2670; b) T. Jeffery, *Tetrahedron letters* **1991**, *32*, 2121-2124.
[56] S. Chuprakov, N. Chernyak, A. S. Dudnik, V. Gevorgyan, *Organic letters* **2007**, *9*, 2333-2336.
[57] L. Ackermann, H. K. Potukuchi, D. Landsberg, R. Vicente, *Organic letters* **2008**, *10*, 3081-3084.
[58] L. Ackermann, R. Jeyachandran, H. K. Potukuchi, P. Novak, L. Büttner, *Organic Letters* **2010**, *12*, 2056-2059.
[59] A. S. Jadhav, Y. A. Pankhade, R. V. Anand, *The Journal of Organic Chemistry* **2018**, *83*, 8596-8606.
[60] C. Xu, S.-F. Jiang, Y.-D. Wu, F.-C. Jia, A.-X. Wu, *The Journal of Organic Chemistry* **2018**, *83*, 14802-14810.
[61] a) M. A. Subbaiah, N. A. Meanwell, *Journal of Medicinal Chemistry* **2021**, *64*, 14046-14128; b) S. Kumari, A. V. Carmona, A. K. Tiwari, P. C. Trippier, *Journal of medicinal chemistry* **2020**, *63*, 12290-12358.
[62] a) A. Qin, J. W. Lam, B. Z. Tang, *Chemical Society Reviews* **2010**, *39*, 2522-2544; bZ. Xu, S.-J. Zhao, Y. Liu, *European journal of medicinal chemistry* **2019**, *183*, 111700.
[63] a) D. Sharma, R. Dandela, V. Dhayalan, *Chemistry (Weinheim an der Bergstrasse, Germany)* **2023**, e202302106-e202302106; b) D. Yadagiri, P. Anbarasan, *The Chemical Record* **2021**, *21*, 3872-3883.
[64]) aC. Laurence, K. A. Brameld, J. Graton, J.-Y. Le Questel, E. Renault, *Journal of medicinal chemistry* **2009**, *52*, 4073-4086; b) L. Mao, Y. Wang, Y. Liu, X. Hu, *Journal of molecular biology* **2004**, *336*, 787-807.
[65] a) R. D. Taylor, M. MacCoss, A. D. Lawson, *Journal of medicinal chemistry* **2014**, *57*, 5845-5859; b) E. Vitaku, D. T. Smith, J. T. Njardarson, *Journal of medicinal chemistry* **2014**, *57*, 10257-10274.
[66] J. Shearer, J. L. Castro, A. D. Lawson, M. MacCoss, R. D. Taylor, *Journal of Medicinal Chemistry* **2022**, *65*, 8699-8712.
[67] C. Knox, M. Wilson, C. M. Klinger, M. Franklin, E. Oler, A. Wilson, A. Pon, J. Cox, N. E. Chin, S. A. Strawbridge, *Nucleic Acids Research* **2024**, *52*, D1265-D1275.
[68] a) N. H. Amin, M. T. El-Saadi, A. A. Ibrahim, H. M. Abdel-Rahman, *Bioorganic chemistry* **2021**, *111*, 104841; b) R. Kaur, A. Ranjan Dwivedi, B. Kumar, V. Kumar, *Anti-Cancer Agents in Medicinal Chemistry (Formerly Current Medicinal Chemistry-Anti-Cancer Agents)* **2016**, *16*, 465-489.
[69] a) C. Brotschi, M. H. Bolli, J. Gatfield, B. Heidmann, F. Jenck, C. Roch, T. Sifferlen, A. Treiber, J. T. Williams, C. Boss, *ChemMedChem* **2020**, *15*, 430-448; b) C. Brotschi, C. Roch, J. Gatfield, A. Treiber, J. T. Williams, T. Sifferlen, B. Heidmann, F. Jenck, M. H. Bolli, C. Boss, *ChemMedChem* **2019**, *14*, 1257-1270.
[70] a) J. Dai, S. Tian, X. Yang, Z. Liu, *Frontiers in Chemistry* **2022**, *10*, 891484; b) D. Dheer, V. Singh, R. Shankar, *Bioorganic Chemistry* **2017**, *71*, 30-54.
[71] a) L. Wang, X. Shao, T. Zhong, Y. Wu, A. Xu, X. Sun, H. Gao, Y. Liu, T. Lan, Y. Tong, *Nature Chemical Biology* **2021**, *17*, 567-575; b) S. Xie, F. Zhan, J. Zhu, Y. Sun, H. Zhu, J. Liu, J. Chen, Z. Zhu, D. H. Yang, Z. S. Chen, *Angewandte Chemie International Edition* **2023**, *62*, e202217246.
[72] J. Dong, L. Krasnova, M. Finn, K. B. Sharpless, *Angewandte Chemie International Edition* **2014**, *53*, 9430-9448.
[73] G. A. Takacs, *Journal of Chemical and Engineering Data* **1978**, *23*, 174-175.
[74] K. L. Wray, E. V. Feldman, *The Journal of Chemical Physics* **1971**, *54*, 3445-3449.
[75] H. Wang, F. Zhou, G. Ren, Q. Zheng, H. Chen, B. Gao, L. Klivansky, Y. Liu, B. Wu, Q. Xu, *Angewandte Chemie* **2017**, *129*, 11355-11360.

[76] B. Gao, S. Li, P. Wu, J. E. Moses, K. B. Sharpless, *Angewandte Chemie* **2018**, *130*, 1957-1961.
[77] Q. Zheng, J. Dong, K. B. Sharpless, *The Journal of Organic Chemistry* **2016**, *81*, 11360-11362.
[78] B. Y. Li, K. Su, L. Van Meervelt, S. H. Verhelst, E. Ismalaj, W. M. De Borggraeve, J. Demaerel, *Angewandte Chemie* **2023**, *135*, e202305093.
[79] a) A. Barrow, C. Smedley, Q. Zheng, S. Li, J. Dong, J. Moses, *Chem. Soc. Rev.* **2019**, *48*, 4731-4758; b) D. Zeng, W. P. Deng, X. Jiang, *Chemistry–A European Journal* **2023**, *29*, e202300536; c) T. S.-B. Lou, M. C. Willis, *Nature Reviews Chemistry* **2022**, *6*, 146-162; d) R. Lekkala, R. Lekkala, B. Moku, K. Rakesh, H.-L. Qin, *Organic Chemistry Frontiers* **2019**, *6*, 3490-3516; e) C. Veryser, J. Demaerel, V. Bieliūnas, P. Gilles, W. M. De Borggraeve, *Organic letters* **2017**, *19*, 5244-5247; f) C. Lee, N. D. Ball, G. M. Sammis, *Chemical Communications* **2019**, *55*, 14753-14756.
[80] J.-N. Luy, R. Tonner, *ACS omega* **2020**, *5*, 31432-31439.
[81] D. D. Liang, D. E. Streefkerk, D. Jordaan, J. Wagemakers, J. Baggerman, H. Zuilhof, *Angew. Chem.* **2020**, *132*, 7564-7570.
[82] a) M. Paranjothy, M. R. Siebert, W. L. Hase, S. M. Bachrach, *The Journal of Physical Chemistry A* **2012**, *116*, 11492-11499; b) T. A. Hamlin, M. Swart, F. M. Bickelhaupt, *ChemPhysChem* **2018**, *19*, 1315-1330; c) M. B. Smith, *March's advanced organic chemistry: reactions, mechanisms, and structure*, John Wiley & Sons, **2020**.
[83] a) V. Gembus, F. Marsais, V. Levacher, *Synlett* **2008**, *2008*, 1463-1466; b) C. Lee, A. J. Cook, J. E. Elisabeth, N. C. Friede, G. M. Sammis, N. D. Ball, *ACS catalysis* **2021**, *11*, 6578-6589.
[84] C. J. Smedley, J. A. Homer, T. L. Gialelis, A. S. Barrow, R. A. Koelln, J. E. Moses, *Angewandte Chemie* **2022**, *134*, e202112375.
[85] C. J. Smedley, Q. Zheng, B. Gao, S. Li, A. Molino, H. M. Duivenvoorden, B. S. Parker, D. J. Wilson, K. B. Sharpless, J. E. Moses, *Angewandte Chemie International Edition* **2019**, *58*, 4552-4556.
[86] S. Mahapatra, C. P. Woroch, T. W. Butler, S. N. Carneiro, S. C. Kwan, S. R. Khasnavis, J. Gu, J. K. Dutra, B. C. Vetelino, J. Bellenger, *Organic letters* **2020**, *22*, 4389-4394.
[87] M. Wei, D. Liang, X. Cao, W. Luo, G. Ma, Z. Liu, L. Li, *Angewandte Chemie* **2021**, *133*, 7473-7480.
[88] H. L. Qin, Q. Zheng, G. A. Bare, P. Wu, K. B. Sharpless, *Angewandte Chemie International Edition* **2016**, *55*, 14155-14158.
[89] M. K. Nielsen, C. R. Ugaz, W. Li, A. G. Doyle, *Journal of the American Chemical Society* **2015**, *137*, 9571-9574.
[90] a) D. Myers, A. Kemp, *Nature* **1954**, *173*, 33-34; b) A. Narayanan, L. Jones, *Sci* **2015**, *6*, 2650-2659.
[91] W. Chen, J. Dong, L. Plate, D. E. Mortenson, G. J. Brighty, S. Li, Y. Liu, A. Galmozzi, P. S. Lee, J. J. Hulce, *Journal of the American Chemical Society* **2016**, *138*, 7353-7364.
[92] M. Cheng, C. Guo, M. L. Gross, *Angewandte Chemie International Edition* **2020**, *59*, 5880-5889.
[93] a) H. Mukherjee, N. P. Grimster, *Current opinion in chemical biology* **2018**, *44*, 30-38; b) R. A. Ward, N. Grimster, *The design of covalent-based inhibitors*, Academic Press, **2021**.
[94] B. R. Baker, *Accounts of Chemical Research* **1969**, *2*, 129-136.
[95] a) J. Tam, M. Henault, L. Li, Z. Wang, A. W. Partridge, R. A. Melnyk, *Analytical biochemistry* **2011**, *414*, 254-260; b) D. Zhang, M. Lu, C. Chen, Y. Xu, T. Peng, *ChemBioChem* **2022**, *23*, e202100628.
[96] a) E. C. Hett, H. Xu, K. F. Geoghegan, A. Gopalsamy, R. E. Kyne Jr, C. A. Menard, A. Narayanan, M. D. Parikh, S. Liu, L. Roberts, *ACS Chemical Biology* **2015**, *10*, 1094-

1098; b) S. Liu, L. A. Dakin, L. Xing, J. M. Withka, P. V. Sahasrabudhe, W. Li, M. E. Banker, P. Balbo, S. Shanker, B. A. Chrunyk, *Scientific Reports* **2016**, *6*, 30859.
[97] J. Pettinger, K. Jones, M. D. Cheeseman, *Angewandte Chemie International Edition* **2017**, *56*, 15200-15209.
[98] G. J. Brighty, R. C. Botham, S. Li, L. Nelson, D. E. Mortenson, G. Li, C. Morisseau, H. Wang, B. D. Hammock, K. B. Sharpless, *Nature chemistry* **2020**, *12*, 906-913.
[99] Z. Liu, J. Li, S. Li, G. Li, K. B. Sharpless, P. Wu, *Journal of the American Chemical Society* **2018**, *140*, 2919-2925.
[100] Q. Zheng, J. Woehl, S. Kitamura, D. Santos-Martins, C. Smedley, G. Li, S. Forli, J. Moses, D. Wolan, K. Sharpless, **2019**.
[101] D. E. Mortenson, G. J. Brighty, L. Plate, G. Bare, W. Chen, S. Li, H. Wang, B. F. Cravatt, S. Forli, E. T. Powers, *Journal of the American Chemical Society* **2018**, *140*, 200-210.
[102] a) A. R. Katritzky, C. W. Rees, C. J. Drayton, *Comprehensive heterocyclic chemistry: the structure, reactions, synthesis and uses of heterocyclic compounds, Vol. 8*, Pergamon Oxford, **1984**; b) E. Scriven, *Comprehensive heterocyclic chemistry*, Pergamon Press, **1984**; c) A. R. Katritzky, C. A. Ramsden, E. F. Scriven, R. J. Taylor, in *V1 3-memb. Heterocycl., together with all Fused Syst. contain. a 3-memb. Heterocycl. Ring. V2 4-memb. Heterocycl. together with all Fused Syst. contain. a 4-memb. Heterocycl. Ring. V3 Five-memb. Rings with One Heteroat. together with their Benzo and other Carbocycl.-fused Deriv. V4 Five-memb. Rings with Two Heteroat., each with their Fused Carbocycl. Deriv.*, Elsevier, **2008**, pp. 1-13718; d) A. F. Pozharskii, A. T. Soldatenkov, A. R. Katritzky, *Heterocycles in life and society: an introduction to heterocyclic chemistry, biochemistry and applications*, John Wiley & Sons, **2011**; e) L. D. Quin, J. A. Tyrell, *Fundamentals of heterocyclic chemistry: importance in nature and in the synthesis of pharmaceuticals*, John Wiley & Sons, **2010**.
[103] J. J. Li, *Heterocyclic chemistry in drug discovery*, John Wiley & Sons, **2013**.
[104] P. Bhutani, G. Joshi, N. Raja, N. Bachhav, P. K. Rajanna, H. Bhutani, A. T. Paul, R. Kumar, *Journal of Medicinal Chemistry* **2021**, *64*, 2339-2381.
[105] M. D. Delost, D. T. Smith, B. J. Anderson, J. T. Njardarson, *Journal of Medicinal Chemistry* **2018**, *61*, 10996-11020.
[106] a) P. N. Kalaria, S. C. Karad, D. K. Raval, *European journal of medicinal chemistry* **2018**, *158*, 917-936; b) K. Passador, S. Thorimbert, C. Botuha, *Synthesis* **2019**, *51*, 384-398; cA. C. Ruberte, C. Sanmartin, C. Aydillo, A. K. Sharma, D. Plano, *Journal of Medicinal Chemistry* **2019**, *63*, 1473-1489; d) G. Grover, R. Nath, R. Bhatia, M. J. Akhtar, *Bioorganic & Medicinal Chemistry* **2020**, *28*, 115585; e) I. Muthukrishnan, V. Sridharan, J. C. Menendez, *Chemical reviews* **2019**, *119*, 5057-5191; fD. J. Newman, G. M. Cragg, *Journal of natural products* **2020**, *83*, 770-803.
[107] a) M. M. Heravi, V. Zadsirjan, *RSC advances* **2020**, *10*, 44247-44311; b) L. E. Rodriguez, C. H. House, K. E. Smith, M. R. Roberts, M. P. Callahan, *Scientific reports* **2019**, *9*, 9281; c) X.-F. Wu, H. Neumann, M. Beller, *Chemical Reviews* **2013**, *113*, 1-35; d) D. M. D'Souza, T. J. Mueller, *Chemical Society Reviews* **2007**, *36*, 1095-1108; e) Y. Shan, L. Su, Z. Zhao, D. Chen, *Advanced Synthesis & Catalysis* **2021**, *363*, 906-923.
[108] a) S. Kumar, S. Bawa, H. Gupta, *Mini reviews in medicinal chemistry* **2009**, *9*, 1648-1654; b) X.-M. Chu, C. Wang, W. Liu, L.-L. Liang, K.-K. Gong, C.-Y. Zhao, K.-L. Sun, *European journal of medicinal chemistry* **2019**, *161*, 101-117; c) L. M. Nainwal, S. Tasneem, W. Akhtar, G. Verma, M. F. Khan, S. Parvez, M. Shaquiquzzaman, M. Akhter, M. M. Alam, *European Journal of Medicinal Chemistry* **2019**, *164*, 121-170.
[109] a) L. Savegnago, A. I. Vieira, N. Seus, B. S. Goldani, M. R. Castro, E. J. Lenardão, D. Alves, *Tetrahedron Letters* **2013**, *54*, 40-44; b) S. M. Prajapati, K. D. Patel, R. H.

Vekariya, S. N. Panchal, H. D. Patel, *Rsc Advances* **2014**, *4*, 24463-24476; c) S. Jain, V. Chandra, P. K. Jain, K. Pathak, D. Pathak, A. Vaidya, *Arabian Journal of Chemistry* **2019**, *12*, 4920-4946.

[110] a) J. C. Jewett, C. R. Bertozzi, *Chemical Society Reviews* **2010**, *39*, 1272-1279; b) P. Thirumurugan, D. Matosiuk, K. Jozwiak, *Chemical reviews* **2013**, *113*, 4905-4979; cW. Song, N. Zheng, M. Li, J. He, J. Li, K. Dong, K. Ullah, Y. Zheng, *Advanced Synthesis & Catalysis* **2019**, *361*, 469-475; d) W. Song, N. Zheng, M. Li, K. Dong, J. Li, K. Ullah, Y. Zheng, *Organic letters* **2018**, *20*, 6705-6709.

[111] a) V. V. Rostovtsev, L. G. Green, V. V. Fokin, K. B. Sharpless, *Angewandte Chemie International Edition* **2002**, *41*, 2596-2599; b) C. W. Tornøe, C. Christensen, M. Meldal, *The Journal of organic chemistry* **2002**, *67*, 3057-3064.

[112] a) X. Yang, G. Zhou, W.-Y. Wong, *Chemical Society Reviews* **2015**, *44*, 8484-8575; b) L. Jacobs, C. de Kock, D. Taylor, S. C. Pelly, M. A. Blackie, *Bioorganic & medicinal chemistry* **2018**, *26*, 5730-5741; c) K. Mahesh, K. Ravi, P. K. Rathod, P. Leelavathi, *New Journal of Chemistry* **2020**, *44*, 2367-2373.

[113] a) D. Oehlrich, A. Peschiulli, G. Tresadern, M. Van Gool, J. A. Vega, A. I. De Lucas, S. A. Alonso de Diego, H. Prokopcova, N. Austin, S. Van Brandt, *ACS Medicinal Chemistry Letters* **2019**, *10*, 1159-1165; b) X. Cao, Z. Sun, Y. Cao, R. Wang, T. Cai, W. Chu, W. Hu, Y. Yang, *Journal of medicinal chemistry* **2014**, *57*, 3687-3706; c) G. Xiao, K. Wu, W. Zhou, Q. Cai, *Advanced Synthesis & Catalysis* **2021**, *363*, 4988-4991.

[114] D. K. Mohapatra, P. K. Maity, M. Shabab, M. Khan, *Bioorganic & medicinal chemistry letters* **2009**, *19*, 5241-5245.

[115] N. Sudhapriya, A. Nandakumar, Y. Arun, P. Perumal, C. Balachandran, N. Emi, *RSC advances* **2015**, *5*, 66260-66270.

[116] H. C. Shen, F.-X. Ding, Q. Deng, L. C. Wilsie, M. L. Krsmanovic, A. K. Taggart, E. Carballo-Jane, N. Ren, T.-Q. Cai, T.-J. Wu, *Journal of medicinal chemistry* **2009**, *52*, 2587-2602.

[117] B. Banerji, S. K. Pramanik, P. Sanphui, S. Nikhar, S. C. Biswas, *Chemical Biology & Drug Design* **2013**, *82*, 401-409.

[118] a) J. Yang, S. Xiong, Y. Ren, T. Xiao, Y. Jiang, *Organic & Biomolecular Chemistry* **2020**, *18*, 7174-7182; b) G. P. da Costa, M. F. Bach, M. C. de Moraes, T. Barcellos, E. J. Lenardão, M. S. Silva, D. Alves, *Advanced Synthesis & Catalysis* **2020**, *362*, 5044-5055.

[119] a) F. Roudesly, J. Oble, G. Poli, *Journal of Molecular Catalysis A: Chemical* **2017**, *426*, 275-296; b) G. Rouquet, N. Chatani, *Angewandte Chemie International Edition* **2013**, *52*, 11726-11743; c) O. Eisenstein, J. Milani, R. N. Perutz, *Chemical Reviews* **2017**, *117*, 8710-8753.

[120] a) C. Zhou, R. C. Larock, *The Journal of Organic Chemistry* **2006**, *71*, 3551-3558; b) T.-T. Wang, L. Zhao, Y.-J. Zhang, W.-W. Liao, *Organic letters* **2016**, *18*, 5002-5005.

[121] a) F. Teng, Y. Peng, X. Wang, W. Hu, H. Hu, Y. He, S. Luo, Q. Zhu, *Organic Letters* **2020**, *22*, 8188-8192; bP. Li, Q. Li, H. Weng, J. Diao, H. Yao, A. Lin, *Organic letters* **2019**, *21*, 6765-6769; c) A. Arcadi, S. Cacchi, G. Fabrizi, A. Fochetti, F. Ghirga, A. Goggiamani, A. Iazzetti, F. Marinelli, *Synthesis* **2019**, *51*, 3287-3294; d) A. Arcadi, S. Cacchi, G. Fabrizi, F. Ghirga, A. Goggiamani, A. Iazzetti, F. Marinelli, *Synthesis* **2018**, *50*, 1133-1140.

[122] a) A. Arcadi, G. Fabrizi, A. Fochetti, F. Ghirga, A. Goggiamani, A. Iazzetti, F. Marrone, G. Mazzoccanti, A. Serraiocco, *RSC advances* **2021**, *11*, 909-917; b) S. Cacchi, G. Fabrizi, A. Goggiamani, A. Iazzetti, R. Verdiglione, *Synthesis* **2017**, *49*, 4163-4172; c) A. Arcadi, F. Blesi, S. Cacchi, G. Fabrizi, A. Goggiamani, F. Marinelli, *The Journal of Organic Chemistry* **2013**, *78*, 4490-4498; d) S. Cacchi, E. Caponetti, M. A. Casadei, A. Di Giulio, G. Fabrizi, G. Forte, A. Goggiamani, S. Moreno, P. Paolicelli,

F. Petrucci, *Green chemistry* **2012**, *14*, 317-320; e) S. Cacchi, G. Fabrizi, A. Goggiamani, A. Iazzetti, *Organic & Biomolecular Chemistry* **2012**, *10*, 9142-9147.
[123] K. Li, J. Chen, J. Li, Y. Chen, J. Qu, X. Guo, C. Chen, B. Chen, *European Journal of Organic Chemistry* **2013**, *2013*, 6246-6248.
[124] D. Gangaprasad, J. P. Raj, K. Karthikeyan, R. Rengasamy, J. Elangovan, *Advanced Synthesis & Catalysis* **2018**, *360*, 4485-4490.
[125] N. Sun, H. Yang, K. Zheng, L. Jin, B. Hu, Z. Shen, X. Hu, *European Journal of Organic Chemistry* **2020**, *2020*, 6805-6812.
[126] a) C.-Y. Chen, C.-H. Yang, W.-P. Hu, J. K. Vandavasi, M.-I. Chung, J.-J. Wang, *RSC advances* **2013**, *3*, 2710-2719; b) A. Kumar, S. S. Shinde, D. K. Tiwari, B. Sridhar, P. R. Likhar, *RSC advances* **2016**, *6*, 43638-43647.
[127] a) S. Cacchi, G. Fabrizi, *Chemical reviews* **2005**, *105*, 2873-2920; b) M. Bandini, A. Eichholzer, *Angewandte Chemie International Edition* **2009**, *48*, 9608-9644; c) S. Cacchi, G. Fabrizi, A. Goggiamani, *Organic & biomolecular chemistry* **2011**, *9*, 641-652; d) K. Urbina, D. Tresp, K. Sipps, M. Szostak, *Advanced Synthesis & Catalysis* **2021**, *363*, 2723-2739; e) R. Dias do Espírito Santo, R. M. Capitão, P. Santos Barbosa, E. F. Simao dos Santos, C. Roque Duarte Correia, *Asian Journal of Organic Chemistry* **2021**, *10*, 1938-1957.
[128] a) E. Aguilar, J. Santamaría, *Organic Chemistry Frontiers* **2019**, *6*, 1513-1540; b) S. Nayak, B. Prabagar, A. K. Sahoo, *Organic & Biomolecular Chemistry* **2016**, *14*, 803-807; c) D. A. Horton, G. T. Bourne, M. L. Smythe, *Chemical reviews* **2003**, *103*, 893-930; d) M. E. Welsch, S. A. Snyder, B. R. Stockwell, *Current opinion in chemical biology* **2010**, *14*, 347-361; eY. Huang, Y. Yang, H. Song, Y. Liu, Q. Wang, *Scientific Reports* **2015**, *5*, 13516.
[129] a) L. Wang, X.-Q. Zhang, Z.-Q. Yin, Y. Wang, W.-C. Ye, *Chemical and pharmaceutical bulletin* **2009**, *57*, 610-611; b) Z. Jin, *Natural product reports* **2016**, *33*, 1318-1343.
[130] J. L. Stanton, M. H. Ackerman, *Journal of Medicinal Chemistry* **1983**, *26*, 986-989.
[131] M. Isaac, A. Slassi, A. O'Brien, L. Edwards, N. MacLean, D. Bueschkens, D. K. Lee, K. McCallum, I. De Lannoy, L. Demchyshyn, *Bioorganic & medicinal chemistry letters* **2000**, *10*, 919-921.
[132] K. D. Upadhyay, N. M. Dodia, R. C. Khunt, R. S. Chaniara, A. K. Shah, *ACS medicinal chemistry letters* **2018**, *9*, 283-288.
[133] A. Lauria, C. Patella, G. Dattolo, A. M. Almerico, *Journal of medicinal chemistry* **2008**, *51*, 2037-2046.
[134] Y. S. Yao, Q. X. Zhou, X. S. Wang, Y. Wang, B. W. Zhang, *Advanced Functional Materials* **2007**, *17*, 93-100.
[135] a) A. Brik, J. Muldoon, Y. C. Lin, J. H. Elder, D. S. Goodsell, A. J. Olson, V. V. Fokin, K. B. Sharpless, C. H. Wong, *ChemBioChem* **2003**, *4*, 1246-1248; b) C. He, J. n. M. Shreeve, *Angewandte Chemie* **2015**, *127*, 6358-6362; c) J. R. Johansson, T. Beke-Somfai, A. Said Stålsmeden, N. Kann, *Chemical Reviews* **2016**, *116*, 14726-14768; d) W. Song, N. Zheng, M. Li, K. Ullah, Y. Zheng, *Advanced Synthesis & Catalysis* **2018**, *360*, 2429-2434.
[136] a) K. R. Senwar, P. Sharma, T. S. Reddy, M. K. Jeengar, V. L. Nayak, V. Naidu, A. Kamal, N. Shankaraiah, *European Journal of Medicinal Chemistry* **2015**, *102*, 413-424; b) J. Yan, F. Zhou, D. Qin, T. Cai, K. Ding, Q. Cai, *Organic letters* **2012**, *14*, 1262-1265; c) G. C. Senadi, W. P. Hu, S. S. K. Boominathan, J. J. Wang, *Advanced Synthesis & Catalysis* **2013**, *355*, 3679-3693.
[137] C. Lu, D. Liu, J. Jin, H. Deokar, Y. Zhang, J. K. Buolamwini, X. Yu, C. Yan, X. Chen, *Biochemical pharmacology* **2013**, *85*, 1246-1256.

[138] a) C. Viegas-Junior, A. Danuello, V. da Silva Bolzani, E. J. Barreiro, C. A. M. Fraga, *Current medicinal chemistry* **2007**, *14*, 1829-1852; b) L. F. Tietze, H. P. Bell, S. Chandrasekhar, *Angewandte Chemie International Edition* **2003**, *42*, 3996-4028; c) F. Gao, L. Ye, Y. Wang, F. Kong, S. Zhao, J. Xiao, G. Huang, *European journal of medicinal chemistry* **2019**, *183*, 111678; d) G. Li, H. X. Lou, *Medicinal research reviews* **2018**, *38*, 1255-1294.

[139] a) L. Guillemard, N. Kaplaneris, L. Ackermann, M. J. Johansson, *Nature Reviews Chemistry* **2021**, *5*, 522-545; b) R. Jana, H. M. Begam, E. Dinda, *Chemical Communications* **2021**, *57*, 10842-10866; c) T. Rogge, N. Kaplaneris, N. Chatani, J. Kim, S. Chang, B. Punji, L. L. Schafer, D. G. Musaev, J. Wencel-Delord, C. A. Roberts, *Nature Reviews Methods Primers* **2021**, *1*, 43.

[140] R. Bernini, S. Cacchi, G. Fabrizi, G. Forte, F. Petrucci, A. Prastaro, S. Niembro, A. Shafir, A. Vallribera, *Green Chemistry* **2010**, *12*, 150-158.

[141] a) M.-Z. Zhang, Q. Chen, G.-F. Yang, *European journal of medicinal chemistry* **2015**, *89*, 421-441; bK. Nagaraju, D. Ma, *Chemical Society Reviews* **2018**, *47*, 8018-8029; c) J. L. Li, Q. Zhao, C. Gou, Q. Z. Li, H. J. Leng, Q. W. Huang, Y. Liu, *Advanced Synthesis & Catalysis* **2021**, *363*, 4497-4515.

[142] a) H. Ishikawa, D. A. Colby, D. L. Boger, *Journal of the American Chemical Society* **2008**, *130*, 420-421; b) M. Bian, Z. Wang, X. Xiong, Y. Sun, C. Matera, K. Nicolaou, A. Li, *Journal of the American Chemical Society* **2012**, *134*, 8078-8081; c) N. Chadha, O. Silakari, *European Journal of Medicinal Chemistry* **2017**, *134*, 159-184; d) M. A. Corsello, J. Kim, N. K. Garg, *Chemical science* **2017**, *8*, 5836-5844.

[143] a) E. Stempel, T. Gaich, *Accounts of chemical research* **2016**, *49*, 2390-2402; b) J. Li, H. Ni, W. Zhang, Z. Lai, H. Jin, L. Zeng, S. Cui, *Chemical Science* **2024**, *15*, 5211-5217; c) A. K. Singh, V. Raj, S. Saha, *European journal of medicinal chemistry* **2017**, *142*, 244-265.

[144] a) K. Ikegashira, T. Oka, S. Hirashima, S. Noji, H. Yamanaka, Y. Hara, T. Adachi, J.-I. Tsuruha, S. Doi, Y. Hase, *Journal of medicinal chemistry* **2006**, *49*, 6950-6953; b) J. Habermann, E. Capitò, M. d. R. R. Ferreira, U. Koch, F. Narjes, *Bioorganic & medicinal chemistry letters* **2009**, *19*, 633-638.

[145] R. Faust, P. J. Garratt, R. Jones, L.-K. Yeh, A. Tsotinis, M. Panoussopoulou, T. Calogeropoulou, M.-T. Teh, D. Sugden, *Journal of medicinal chemistry* **2000**, *43*, 1050-1061.

[146] C. Beaulieu, D. Guay, Z. Wang, Y. Leblanc, P. Roy, C. Dufresne, R. Zamboni, C. Berthelette, S. Day, N. Tsou, *Bioorganic & medicinal chemistry letters* **2008**, *18*, 2696-2700.

[147] a) D. Astruc, L. Liang, A. Rapakousiou, J. Ruiz, *Accounts of chemical research* **2012**, *45*, 630-640; b) P. L. Golas, K. Matyjaszewski, *Chemical Society Reviews* **2010**, *39*, 1338-1354.

[148] a) S. K. Mamidyala, M. Finn, *Chemical Society Reviews* **2010**, *39*, 1252-1261; b) H. C. Kolb, K. B. Sharpless, *Drug discovery today* **2003**, *8*, 1128-1137; c) A. H. El-Sagheer, T. Brown, *Chemical Society Reviews* **2010**, *39*, 1388-1405.

[149] a) J. E. Spangler, H. M. Davies, *Journal of the American Chemical Society* **2013**, *135*, 6802-6805; b) M. Zibinsky, V. V. Fokin, *Angewandte Chemie International Edition* **2013**, *52*; c) B. Chattopadhyay, V. Gevorgyan, *Angewandte Chemie International Edition* **2012**, *51*, 862-872.

[150] N. Y. Lam, K. Wu, J. Q. Yu, *Angewandte Chemie* **2021**, *133*, 15901-15924.

[151] J. E. Hein, V. V. Fokin, *Chemical Society Reviews* **2010**, *39*, 1302-1315.

[152] S. G. Agalave, S. R. Maujan, V. S. Pore, *Chemistry–An Asian Journal* **2011**, *6*, 2696-2718.

[153] I. Antonini, G. Santoni, R. Lucciarini, C. Amantini, S. Sparapani, A. Magnano, *Journal of medicinal chemistry* **2006**, *49*, 7198-7207.
[154] Y. S. Reddy, A. John Pal, P. Gupta, A. A. Ansari, Y. D. Vankar, *The Journal of Organic Chemistry* **2011**, *76*, 5972-5984.
[155] a) K. Majumdar, S. Samanta, B. Chattopadhyay, R. K. Nandi, *Synthesis* **2009**, 863-869; b) L. Min, B. Pan, Y. Gu, *Organic letters* **2016**, *18*, 364-367.
[156] a) K. S. Kumar, M. S. Ramulu, B. Rajesham, N. P. Kumar, V. Voora, R. K. Kancha, *Organic & Biomolecular Chemistry* **2017**, *15*, 4468-4476; b) M. Martín-Martínez, F. L. Perez-Gordillo, D. Alvarez de la Rosa, Y. Rodríguez, G. Gerona-Navarro, R. González-Muñiz, M.-M. Zhou, *Journal of Medicinal Chemistry* **2017**, *60*, 2629-2650.
[157] a) W. Gao, C. Nie, L. Xu, B. Zhao, Y. Li, *Heterocyclic Communications* **2014**, *20*, 161-166; b) H. V. Wikström, M. M. Mensonides-Harsema, T. I. Cremers, E. K. Moltzen, J. Arnt, *Journal of medicinal chemistry* **2002**, *45*, 3280-3285; c) N. Ait-Daoud, A. S. Hamby, S. Sharma, D. Blevins, *Journal of addiction medicine* **2018**, *12*, 4-10.
[158] K. L. Mikolajczak, C. R. Smith Jr, Google Patents, **1976**.
[159] K. Sprogøe, S. Manniche, T. O. Larsen, C. Christophersen, *Tetrahedron* **2005**, *61*, 8718-8721.
[160] a) D. H. Dethe, R. D. Erande, A. Ranjan, *The Journal of Organic Chemistry* **2013**, *78*, 10106-10120; b) R. Vallakati, J. A. May, *Journal of the American Chemical Society* **2012**, *134*, 6936-6939; c) S. Lucas, M. Negri, R. Heim, C. Zimmer, R. W. Hartmann, *Journal of Medicinal Chemistry* **2011**, *54*, 2307-2319.
[161] a) D. H. Dethe, R. D. Erande, A. Ranjan, *Journal of the American Chemical Society* **2011**, *133*, 2864-2867; b) R. M. Zeldin, F. D. Toste, *Chemical Science* **2011**, *2*, 1706-1709; c) L. S. Fernandez, M. S. Buchanan, A. R. Carroll, Y. J. Feng, R. J. Quinn, V. M. Avery, *Organic letters* **2009**, *11*, 329-332.
[162] a) U. Galm, M. H. Hager, S. G. Van Lanen, J. Ju, J. S. Thorson, B. Shen, *Chemical Reviews* **2005**, *105*, 739-758; b) S. E. Wolkenberg, D. L. Boger, *Chemical reviews* **2002**, *102*, 2477-2496.
[163] a) J.-F. Liu, Z.-Y. Jiang, R.-R. Wang, Y.-T. Zheng, J.-J. Chen, X.-M. Zhang, Y.-B. Ma, *Organic Letters* **2007**, *9*, 4127-4129; b) R. Dorow, P. M. Herrinton, R. A. Hohler, M. T. Maloney, M. A. Mauragis, W. E. McGhee, J. A. Moeslein, J. W. Strohbach, M. F. Veley, *Organic process research & development* **2006**, *10*, 493-499.
[164] G. A. Elmegeed, A. R. Baiuomy, O. M. Abdel-Salam, *European journal of medicinal chemistry* **2007**, *42*, 1285-1292.
[165] A. A. Protter, S. Chakravarty, Google Patents, **2014**.
[166] S. Danishefsky, E. Taniyama, *Tetrahedron Letters* **1983**, *24*, 15-18.
[167] a) X.-Y. Duan, Z. Tian, B. Liu, T. He, L.-L. Zhao, M. Dong, P. Zhang, J. Qi, *Organic Letters* **2021**, *23*, 3777-3781; b) W. L. Yang, Z. T. Sun, H. Sun, W. P. Deng, *Chinese Journal of Chemistry* **2019**, *37*, 216-220; c) Y.-J. Yang, Y. Ji, L. Qi, G. Wang, X.-P. Hui, *Organic letters* **2017**, *19*, 3271-3274; d) A. Ghosh, D. T. Bainbridge, L. M. Stanley, *The Journal of Organic Chemistry* **2016**, *81*, 7945-7951; e) H. Lu, J. B. Lin, J. Y. Liu, P. F. Xu, *Chemistry–A European Journal* **2014**, *20*, 11659-11663; f) H. Ikemoto, T. Yoshino, K. Sakata, S. Matsunaga, M. Kanai, *Journal of the American Chemical Society* **2014**, *136*, 5424-5431; g) Q. Ni, H. Zhang, A. Grossmann, C. C. Loh, C. Merkens, D. Enders, *Angewandte Chemie International Edition* **2013**, *52*.
[168] Y. Wang, H. Lu, P.-F. Xu, *Accounts of Chemical Research* **2015**, *48*, 1832-1844.
[169] a) A. Arcadi, S. Cacchi, G. Fabrizi, F. Ghirga, A. Goggiamani, A. Iazzetti, F. Marinelli, *Beilstein journal of organic chemistry* **2018**, *14*, 2411-2417; b) A. Arcadi, F. Blesi, S. Cacchi, G. Fabrizi, A. Goggiamani, F. Marinelli, *Tetrahedron* **2013**, *69*, 1857-1871; c) G. Cera, S. Piscitelli, M. Chiarucci, G. Fabrizi, A. Goggiamani, R. S. Ramon, S. P. Nolan, M. Bandini, *Angewandte Chemie* **2012**, *124*, 10029-10033.

[170] L. Caruana, M. Mondatori, V. Corti, S. Morales, A. Mazzanti, M. Fochi, L. Bernardi, *Chemistry–A European Journal* **2015**, *21*, 6037-6041.
[171] A. Arcadi, A. Calcaterra, G. Fabrizi, A. Fochetti, A. Goggiamani, A. Iazzetti, F. Marrone, G. Mazzoccanti, A. Serraiocco, *Organic & Biomolecular Chemistry* **2022**, *20*, 3160-3173.
[172] a) J. Ouyang, R. Maji, M. Leutzsch, B. Mitschke, B. List, *Journal of the American Chemical Society* **2022**, *144*, 8460-8466; b) W. Tan, F. Shi, *Chem. Synth* **2022**, *2*; c) K. Bera, C. Schneider, *Organic letters* **2016**, *18*, 5660-5663; d) K. Bera, C. Schneider, *Chemistry–A European Journal* **2016**, *22*, 7074-7078.
[173] A. Arcadi, G. Berden, A. Ciogli, D. Corinti, M. E. Crestoni, M. De Angelis, G. Fabrizi, A. Goggiamani, A. Iazzetti, F. Marrone, *European Journal of Organic Chemistry* **2022**, *2022*, e202201166.
[174] A. Arcadi, A. Calcaterra, M. Chiarini, G. Fabrizi, A. Fochetti, A. Goggiamani, A. Iazzetti, F. Marrone, V. Marsicano, A. Serraiocco, *Synthesis* **2022**, *54*, 741-753.
[175] R. Kuwano, Y. Kondo, T. Shirahama, *Organic Letters* **2005**, *7*, 2973-2975.
[176] E. Rossi, A. Arcadi, G. Abbiati, O. A. Attanasi, L. De Crescentini, *ANGEWANDTE CHEMIE. INTERNATIONAL EDITION* **2002**, *41*, 1400-1402.
[177] T. E. Muller, K. C. Hultzsch, M. Yus, F. Foubelo, M. Tada, *Chemical reviews* **2008**, *108*, 3795-3892.
[178] a) A. Arcadi, *Au-Catalyzed Synthesis and Functionalization of Heterocycles* **2016**, 53-85; b) R. A. Widenhoefer, X. Han, *European journal of organic chemistry* **2006**, *2006*, 4555-4563; c) J. F. Hartwig, J. P. Collman, *Organotransition metal chemistry: from bonding to catalysis, Vol. 1*, Springer, **2010**.
[179] S. Cacchi, G. Fabrizi, A. Goggiamani, A. Iazzetti, *Organic letters* **2016**, *18*, 3511-3513.
[180] S. Cacchi, G. Fabrizi, A. Fochetti, F. Ghirga, A. Goggiamani, A. Iazzetti, *Organic & Biomolecular Chemistry* **2019**, *17*, 527-532.
[181] a) A. Grinev, Y. I. Trofimkin, E. Lomanova, N. Andreeva, M. Mashkovskii, *Pharmaceutical Chemistry Journal* **1978**, *12*, 895-898; b) R. Nagata, N. Tanno, T. Kodo, N. Ae, H. Yamaguchi, T. Nishimura, F. Antoku, T. Tatsuno, T. Kato, *Journal of medicinal chemistry* **1994**, *37*, 3956-3968.
[182] G. Campiani, F. Aiello, M. Fabbrini, E. Morelli, A. Ramunno, S. Armaroli, V. Nacci, A. Garofalo, G. Greco, E. Novellino, *Journal of medicinal chemistry* **2001**, *44*, 305-315.
[183] a) J. Guillon, P. Grellier, M. Labaied, P. Sonnet, J.-M. Léger, R. Déprez-Poulain, I. Forfar-Bares, P. Dallemagne, N. Lemaître, F. Péhourcq, *Journal of medicinal chemistry* **2004**, *47*, 1997-2009; b) J. Guillon, E. Mouray, S. Moreau, C. Mullié, I. Forfar, V. Desplat, S. Belisle-Fabre, N. Pinaud, F. Ravanello, A. Le-Naour, *European journal of medicinal chemistry* **2011**, *46*, 2310-2326; c) J. Guillon, S. Nim, S. Moreau, L. Ronga, S. Savrimoutou, E. Thivet, M. Marchivie, A. Di Pietro, R. Prasad, M. Le Borgne, *RSC advances* **2020**, *10*, 2915-2931; dF. Grande, F. Aiello, O. De Grazia, A. Brizzi, A. Garofalo, N. Neamati, *Bioorganic & medicinal chemistry* **2007**, *15*, 288-294.
[184] C. H. Leung, M. Baron, A. Biffis, *Catalysts* **2020**, *10*, 1210.
[185] A. Richardson Jr, *The Journal of Organic Chemistry* **1965**, *30*, 2589-2593.
[186] J. P. Burke, Z. Bian, S. Shaw, B. Zhao, C. M. Goodwin, J. Belmar, C. F. Browning, D. Vigil, A. Friberg, D. V. Camper, *Journal of medicinal chemistry* **2015**, *58*, 3794-3805.
[187] a) M. Magre, S. Ni, J. Cornella, *Angew. Chem. Int. Ed.* **2022**; b) N. D. Ball, in *Emerging Fluorinated Motifs*, **2020**, pp. 621-674.
[188] a) M. C. Giel, C. J. Smedley, J. E. Moses, in *Click Chemistry, Vol. 2021/4* (Ed.: F. P. J. T. Rutjes), Thieme Verlag, Stuttgart, **2022**; b) C. Lee, A. J. Cook, J. E. Elisabeth, N. C. Friede, G. M. Sammis, N. D. Ball, *ACS Catal.* **2021**, 6578-6589.
[189] a) F. Liu, C. Wang, S. Li, G. A. L. Bare, X. Chen, C. Wang, J. E. Moses, P. Wu, K. B. Sharpless, *Angew. Chem. Int. Ed.* **2019**, *58*, 8029-8033; b) B. Gao, S. Li, P. Wu, J. E.

Moses, K. B. Sharpless, *Angew. Chem. Int. Ed.* **2018**, *57*, 1939-1943; c) S. Li, P. Wu, J. E. Moses, K. B. Sharpless, *Angew. Chem. Int. Ed.* **2017**, *56*, 2903-2908.
[190] B.-Y. Li, K. Su, L. Van Meervelt, S. H. L. Verhelst, E. Ismalaj, W. M. De Borggraeve, J. Demaerel, *Angew. Chem. Int. Ed.* **2023**, *62*, e202305093.
[191] a) S. Greed, E. L. Briggs, F. I. M. Idiris, A. J. P. White, U. Lücking, J. A. Bull, *Chem. Eur. J.* **2020**, *26*, 12533-12538; bZ.-X. Zhang, M. C. Willis, *Chem* **2022**, *8*, 1137-1146; c) S. Greed, O. Symes, J. A. Bull, *Chem. Commun.* **2022**, *58*, 5387-5390.
[192] a) S. Kitamura, Q. Zheng, J. L. Woehl, A. Solania, E. Chen, N. Dillon, M. V. Hull, M. Kotaniguchi, J. R. Cappiello, S. Kitamura, V. Nizet, K. B. Sharpless, D. W. Wolan, *J. Am. Chem. Soc.* **2020**, *142*, 10899-10904; b) G. J. Brighty, R. C. Botham, S. Li, L. Nelson, D. E. Mortenson, G. Li, C. Morisseau, H. Wang, B. D. Hammock, K. B. Sharpless, J. W. Kelly, *Nat. Chem.* **2020**, *12*, 906-913; c) H. Mukherjee, J. Debreczeni, J. Breed, S. Tentarelli, B. Aquila, J. E. Dowling, A. Whitty, N. P. Grimster, *Org. Biomol. Chem.* **2017**, *15*, 9685-9695.
[193] a) Y. Chao, M. Subramaniam, K. Namitharan, Y. Zhu, V. Koolma, Z. Hao, S. Li, Y. Wang, I. Hudoynazarov, F. M. Miloserdov, H. Zuilhof, *J. Org. Chem.* **2023**, *88*, 15658-15665; b) D.-D. Liang, S. P. Pujari, M. Subramaniam, M. Besten, H. Zuilhof, *Angew. Chem. Int. Ed.* **2022**, *61*, e202116158; c) S. Li, G. Li, B. Gao, S. P. Pujari, X. Chen, H. Kim, F. Zhou, L. M. Klivansky, Y. Liu, H. Driss, D.-D. Liang, J. Lu, P. Wu, H. Zuilhof, J. Moses, K. B. Sharpless, *Nat. Chem.* **2021**, *13*, 858-867.
[194] R. Cramer, D. D. Coffman, *J. Org. Chem.* **1961**, *26*, 4010-4014.
[195] K. Seppelt, W. Sundermeyer, *Angew. Chem. Int. Ed.* **1970**, *9*, 905.
[196] C. J. Smedley, Q. Zheng, B. Gao, S. Li, A. Molino, H. M. Duivenvoorden, B. S. Parker, D. J. D. Wilson, K. B. Sharpless, J. E. Moses, *Angew. Chem. Int. Ed.* **2019**, *58*, 4552-4556.
[197] A gas bottle can be purchased from SynQuest Labs at 795 USD/10 g (checked 16/01/2024), being the only provider globally.
[198] W. C. Smith, V. A. Engelhardt, *J. Am. Chem. Soc.* **1960**, *82*, 3838-3840.
[199] K. Seppelt, *Angewandte Chemie International Edition in English* **1982**, *21*, 877-888.
[200] a) F. Sladky, *Angew. Chem. Int. Ed.* **1969**, *8*, 523-523; b) K. Seppelt, *Chem. Ber.* **1972**, *105*, 2431-2436; c) F. Sladky, H. Kropshofer, O. Leitzke, *J. Chem. Soc., Chem. Commun.* **1973**, 134-135; d) H. Kropshofer, O. Leitzke, P. Peringer, F. Sladky, *Chem. Ber.* **1981**, *114*, 2644-2648; eK. Seppelt, *Phosphorus, Sulfur, Silicon Relat. Elem.* **1998**, *136*, 107-122; f) A. Wiesner, T. W. Gries, S. Steinhauer, H. Beckers, S. Riedel, *Angew. Chem. Int. Ed.* **2017**, *56*, 8263-8266.
[201] K. Seppelt, *Z. Anorg. Allg. Chem.* **1977**, *428*, 35-42.
[202] a) J. K. Ruff, M. Lustig, *Inorganic Chemistry* **1964**, *3*, 1422-1425; b) M. Lustig, J. K. Ruff, *Inorganic Chemistry* **1967**, *6*, 2115-2117.
[203] a) W. Heilemann, R. Mews, S. Pohl, W. Saak, *Chem. Ber.* **1989**, *122*, 427-432; bP. Kirsch, W. Hierse, E. Claus, M. Kleineidam, G.-V. Röschenthaler, N. Kalinovich, *Vol. DE102011114650A1*, Merck Patent GmbH, Germany, **2012**; c) R. G. Syvret, G. S. Lal, K. E. Minnich, *Vol. US7771611B2*, Air Products and Chemicals Inc, United States, **2010**.
[204] A. Haupt, D. Duvinage, E. Lork, M. Ponomarenko, G. V. Röschenthaler, *Angewandte Chemie International Edition* **2021**, *60*, 17866-17870.
[205] T. Gatzenmeier, Y. Liu, M. Akamatsu, T. Okazoe, K. Nozaki, **2023**.
[206] J. Demaerel, C. Veryser, W. M. De Borggraeve, *React. Chem. Eng.* **2020**, *5*, 615-631.
[207] a) R. Mews, P. Kricke, I. Stahl, *Z. Naturforsch. B* **1981**, *36*, 1093-1098; b) S.-L. Yu, J. M. Shreeve, *J. Fluor. Chem.* **1976**, *7*, 85-94; c) R. Y. Garlyauskayte, A. V. Bezdudny, C. Michot, M. Armand, Y. L. Yagupolskii, L. M. Yagupolskii, *J. Chem. Soc. Perkin Trans. 1* **2002**, 1887-1889; dC. S. Richards-Taylor, C. Martínez-Lamenca, J. E.

Leenaerts, A. A. Trabanco, D. Oehlrich, *J. Org. Chem.* **2017**, *82*, 9898-9904; e) M. Wright, C. Martínez-Lamenca, J. E. Leenaerts, P. E. Brennan, A. A. Trabanco, D. Oehlrich, *J. Org. Chem.* **2018**, *83*, 9510-9516; f) B.-Y. Li, L. Voets, R. Van Lommel, F. Hoppenbrouwers, M. Alonso, S. H. L. Verhelst, W. M. De Borggraeve, J. Demaerel, *Chem. Sci.* **2022**, *13*, 2270-2279.

[208] a) P. Jeschke, *ChemBioChem* **2004**, *5*, 570-589; b) C. Isanbor, D. O'Hagan, *J. Fluor. Chem.* **2006**, *127*, 303-319; c) K. Muller, C. Faeh, F. Diederich, *Science* **2007**, *317*, 1881-1886; d) W. K. Hagmann, *J. Med. Chem.* **2008**, *51*, 4359-4369; e) S. Purser, P. R. Moore, S. Swallow, V. Gouverneur, *Chem. Soc. Rev.* **2008**, *37*, 320-330; f) V. A. Petrov, *Fluorinated Heterocyclic Compounds: Synthesis, Chemistry, and Applications*, J. Wiley & Sons, Inc., Hoboken, NJ, USA, **2009**; g) D. O'Hagan, *J. Fluor. Chem.* **2010**, *131*, 1071-1081; h) P. Jeschke, *Pest Management Science: formerly Pesticide Science* **2010**, *66*, 10-27; i) R. Berger, G. Resnati, P. Metrangolo, E. Weber, J. Hulliger, *Chem. Soc. Rev.* **2011**, *40*, 3496-3508; j) T. Fujiwara, D. O'Hagan, *J. Fluor. Chem.* **2014**, *167*, 16-29; k) J. Wang, M. Sánchez-Roselló, J. L. Aceña, C. Del Pozo, A. E. Sorochinsky, S. Fustero, V. A. Soloshonok, H. Liu, *Chem. Rev.* **2014**, *114*, 2432-2506; l) E. P. Gillis, K. J. Eastman, M. D. Hill, D. J. Donnelly, N. A. Meanwell, *J. Med. Chem.* **2015**, *58*, 8315-8359; m) M. Inoue, Y. Sumii, N. Shibata, *ACS omega* **2020**, *5*, 10633-10640; n) Y. Ogawa, E. Tokunaga, O. Kobayashi, K. Hirai, N. Shibata, *Iscience* **2020**, *23*; o) J. Neufeld, R. Gilmour, *Emerging Fluorinated Motifs: Synthesis, Properties, and Applications. Edited by Dominique Cahard and Jun‐An Ma*, Copyright 2020 Wiley VCH Verlag GmbH & Co. KGaA, **2021**.

[209] a) P. Maienfisch, R. G. Hall, *Chimia* **2004**, *58*, 93-93; b) D. O'Hagan, *Chem. Soc. Rev.* **2008**, *37*, 308-319; c) P. Kirsch, *Modern fluoroorganic chemistry: synthesis, reactivity, applications*, John Wiley & Sons, **2013**; d) A. Tressaud, *Fluorine: A paradoxical element, Vol. 5*, Academic Press, **2018**; e) S. Dehnen, L. L. Schafer, T. Lectka, A. Togni, *Vol. 60*, ACS Publications, **2021**, pp. 17419-17425.

[210] a) W. Zhu, J. Wang, S. Wang, Z. Gu, J. L. Aceña, K. Izawa, H. Liu, V. A. Soloshonok, *J. Fluor. Chem.* **2014**, *167*, 37-54; b) X.-H. Xu, K. Matsuzaki, N. Shibata, *Chem. Rev.* **2015**, *115*, 731-764.

[211] a) S. Altomonte, M. Zanda, *J. Fluor. Chem.* **2012**, *143*, 57-93; b) P. R. Savoie, J. T. Welch, *Chem. Rev.* **2015**, *115*, 1130-1190; c) R. Kordnezhadian, B. Y. Li, A. Zogu, J. Demaerel, W. M. De Borggraeve, E. Ismalaj, *Chemistry–A European Journal* **2022**, *28*, e202201491.

[212] a) N. Yoneda, *J. Fluor. Chem.* **2004**, *125*, 7-17; b) S. V. Kohlhepp, T. Gulder, *Chem. Soc. Rev.* **2016**, *45*, 6270-6288; c) S. Meyer, J. Häfliger, R. Gilmour, *Chem. Sci.* **2021**, *12*, 10686-10695.

[213] S. Hara, M. Sekiguchi, A. Ohmori, T. Fukuhara, N. Yoneda, *Chem. Commun.* **1996**, 1899-1900.

[214] G. C. Geary, E. G. Hope, K. Singh, A. M. Stuart, *Chem. Commun.* **2013**, *49*, 9263-9265.

[215] a) A. Yoshimura, V. V. Zhdankin, *Chem. Rev.* **2016**, *116*, 3328-3435; b) J. C. Sarie, C. Thiehoff, R. J. Mudd, C. G. Daniliuc, G. Kehr, R. Gilmour, *J. Org. Chem.* **2017**, *82*, 11792-11798; c) M. Albayer, L. Sharp-Bucknall, N. Withanage, G. Armendariz-Vidales, C. F. Hogan, J. L. Dutton, *Inorg. Chem.* **2020**, *59*, 2765-2770; d) C. Hou, P. Chen, G. Liu, *Angew. Chem., Int. Ed. Engl.* **2020**, *59*, 2735-2739; e) B. Winterson, T. Rennigholtz, T. Wirth, *Chem. Sci.* **2021**, *12*, 9053-9059.

[216] H. Frohn, *Chem-Ztg* **1984**, *108*, 146-147.

[217] V. V. L. L.M. Yagupol'skii, L.A. Alekseyeva, *Zh. Obshch. Khim.* **1968**, *38*, 2813.

[218] J. Häfliger, C. R. Pitts, D. Bornemann, R. Käser, N. Santschi, J. Charpentier, E. Otth, N. Trapp, R. Verel, H. P. Lüthi, *Chem. Sci.* **2019**, *10*, 7251-7259.

[219] a) R. Kordnezhadian, A. Zogu, C. Borgarelli, R. Van Lommel, J. Demaerel, W. M. De Borggraeve, E. Ismalaj, *Chem. Eur. J.* **2023**, e202300361; b) R. Kordnezhadian, T. De Bels, K. Su, L. Van Meervelt, E. Ismalaj, J. Demaerel, W. M. De Borggraeve, *Org. Lett.* **2023**, *25*, 8947-8951.
[220] a) D. C. Powers, T. Ritter, *Nat. Chem.* **2009**, *1*, 302-309; b) D. C. Powers, D. Benitez, E. Tkatchouk, W. A. Goddard III, T. Ritter, *J. Am. Chem. Soc.* **2010**, *132*, 14092-14103.
[221] M. Sawaguchi, S. Ayuba, S. Hara, *Synthesis* **2002**, *2002*, 1802-1803.
[222] D. Zhu, Z. Wu, B. Luo, Y. Du, P. Liu, Y. Chen, Y. Hu, P. Huang, S. Wen, *Organic letters* **2018**, *20*, 4815-4818.
[223] I. Wilkening, G. del Signore, C. P. Hackenberger, *Chemical communications* **2011**, *47*, 349-351.
[224] C. R. Pitts, N. Santschi, A. Togni, *Vol. WO2019229103A1*, **2019**.
[225] a) F. Neese, F. Wennmohs, U. Becker, C. Riplinger, *J. Chem. Phys.* **2020**, *152*; b) F. Neese, *WIREs Comput. Mol. Sci.* **2012**, *2*, 73-78.
[226] a) E. Caldeweyher, S. Ehlert, A. Hansen, H. Neugebauer, S. Spicher, C. Bannwarth, S. Grimme, *J. Chem. Phys.* **2019**, *150*; b) E. Caldeweyher, C. Bannwarth, S. Grimme, *J. Chem. Phys.* **2017**, *147*.
[227] F. Weigend, R. Ahlrichs, *Phys. Chem. Chem. Phys.* **2005**, *7*, 3297-3305.
[228] F. Weigend, *Phys. Chem. Chem. Phys.* **2006**, *8*, 1057-1065.
[229] a) S. Kozuch, J. M. L. Martin, *Phys. Chem. Chem. Phys.* **2011**, *13*, 20104-20107; b) F. Jensen, *Journal of Chemical Theory and Computation* **2015**, *11*, 132-138.
[230] a) F. Weigend, A. Köhn, C. Hättig, *J. Chem. Phys.* **2002**, *116*, 3175-3183; b) C. Hättig, *Phys. Chem. Chem. Phys.* **2005**, *7*, 59-66.
[231] T. R. Lex, M. I. Swasy, S. Panda, B. R. Brummel, L. N. Giambalvo, K. G. Gross, C. D. McMillen, K. Kobra, W. T. Pennington, D. C. Whitehead, *Tetrahedron Letters* **2020**, *61*, 151723.
[232] B.-Y. Li, L. Voets, R. Van Lommel, F. Hoppenbrouwers, M. Alonso, S. H. Verhelst, W. M. De Borggraeve, J. Demaerel, *Chemical science* **2022**, *13*, 2270-2279.
[233] S. Li, P. Wu, J. E. Moses, K. B. Sharpless, *Angewandte Chemie* **2017**, *129*, 2949-2954.